

Aspects of Metallacyclic Chemistry



A thesis submitted in partial fulfilment of
the requirements for the degree of
Doctor of Philosophy in Chemistry at
The University of Waikato
by

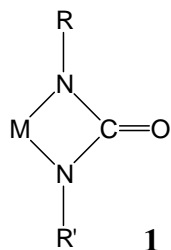
Maarten Dinger

February 1998

Abstract

A range of silver(I) oxide mediated reactions of metal halide complexes with various organic substrates have been investigated. The reaction of $[\text{PtCl}_2(\text{COD})]$ or *cis*- $[\text{PtCl}_2(\text{PPh}_3)_2]$ with disubstituted ureas $[\text{RNHC}(\text{O})\text{NHR}']$ ($\text{R} = \text{Ph}, \text{Ac}, \text{H}$; $\text{R}' = \text{Ph}, \text{Me}, \text{Py}, \text{Me}, \text{Ac}, \text{H}$), in the presence of silver(I) oxide, gave the corresponding ureylene complexes (**1**) (Chapter Two). Similarly, the reaction of the gold(III) dichloride $[\text{Au}\{\text{C}_6\text{H}_3(\text{CH}_2\text{NMe}_2)\text{-2-(OMe)-5}\}\text{Cl}_2]$ with *N,N'*-diphenylurea or *N,N'*-diacetylurea gave the expected aurauylene complexes (Chapter Five).

The reactions of the platinum-group metal halide complexes $[\text{PtCl}_2(\text{COD})]$, $[\text{Cp}^*\text{RhCl}_2(\text{PPh}_3)]$ ($\text{Cp}^* = \eta^5\text{-C}_5\text{Me}_5$), $[\text{Cp}^*\text{IrCl}_2(\text{PPh}_3)]$, $[(\eta^6\text{-}p\text{-cymene})\text{RuCl}_2(\text{PPh}_3)]$ and $[(\eta^6\text{-}p\text{-cymene})\text{OsCl}_2(\text{PPh}_3)]$ with symmetrically trisubstituted guanidines $[\text{RNHC}(\text{NR})\text{NHR}]$ ($\text{R} = \text{Ph}, \text{Ac}$), mediated by silver(I) oxide, gives a general synthetic route into platinum-group metal complexes (**2**) derived from the guanidine dianion, formally containing a triazatrimethylenemethane ligand. Crystal structures of both the ureylene and triazatrimethylenemethane complexes show planar metallacycles, indicative of an η^2 -bonding mode (Chapter Three).

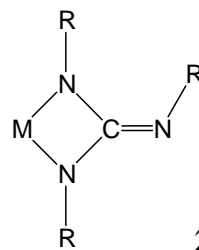
**1**

Ureylene complexes

$\text{M} = \text{Pt}$; $\text{R} = \text{Ph}$; $\text{R}' = \text{Ph}, \text{Me}, \text{Py}, \text{Ad}, \text{H}$

$\text{M} = \text{Pt}$; $\text{R} = \text{Ac}$; $\text{R}' = \text{Ac}, \text{Me}$

$\text{M} = \text{Au}$; $\text{R} = \text{R}' = \text{Ph}$; $\text{R} = \text{R}' = \text{Ac}$

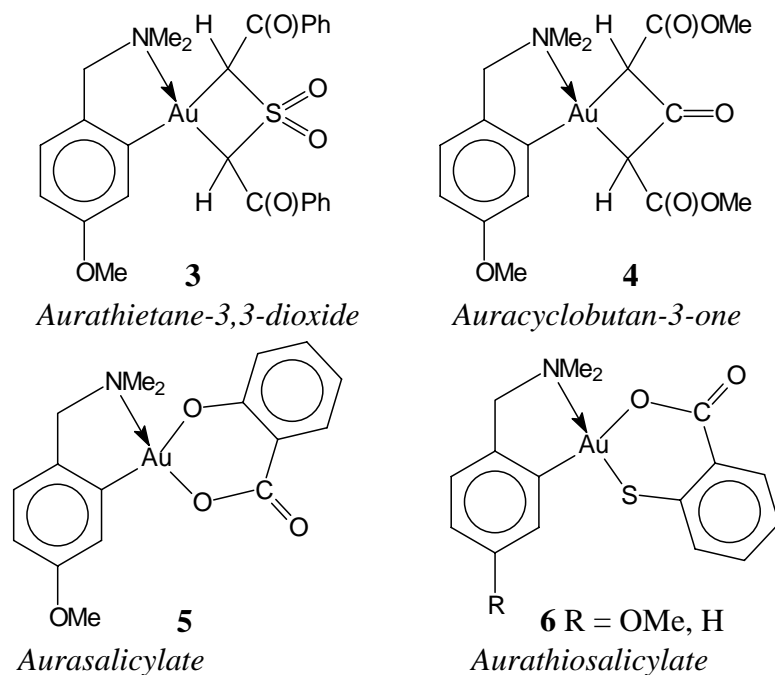
**2**

Guanidine dianion complexes

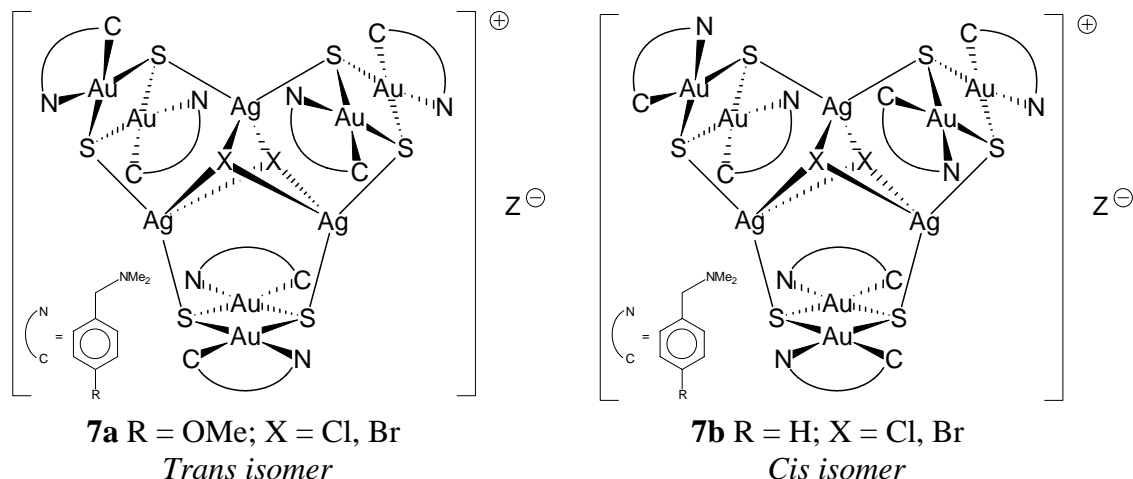
$\text{M} = \text{Pt}, \text{Rh}$; $\text{R} = \text{Ph}$

$\text{M} = \text{Ru}, \text{Os}, \text{Rh}, \text{Ir}$; $\text{R} = \text{Ac}$

The silver(I) oxide mediated reactions of $[\text{Au}\{\text{C}_6\text{H}_3(\text{CH}_2\text{NMe}_2)\text{-2-(OMe)-5}\}\text{Cl}_2]$ with diphenacyl sulfone $[\{\text{PhC}(\text{O})\text{CH}_2\}_2\text{S}(\text{O})_2]$ or dimethyl 1,3-acetonedicarboxylate $[\{\text{MeOC}(\text{O})\text{CH}_2\}_2\text{C}(\text{O})]$, gave the predicted gold(III) aurathietane-3,3-dioxide (**3**) and auracyclobutan-3-one (**4**) complexes respectively. The X-ray structural analysis of the former, showed a puckered metallacycle with a fold angle similar to that previously observed for the analogous platinum(II) system. Similarly, when $[\text{Au}\{\text{C}_6\text{H}_3(\text{CH}_2\text{NMe}_2)\text{-2-R-5}\}\text{Cl}_2]$ ($\text{R} = \text{OMe}, \text{H}$) was reacted with salicylic or thiosalicylic acids, the respective gold(III) salicylate (**5**) and thiosalicylate (**6**) complexes were formed. X-ray structures revealed a contrast in the orientation of the co-ordinated ligands for the two systems, with the carboxyl group *trans* to N in the salicylate case, but *trans* to C in the thiosalicylate system. Both structures revealed puckered metallacycles (Chapter Seven).

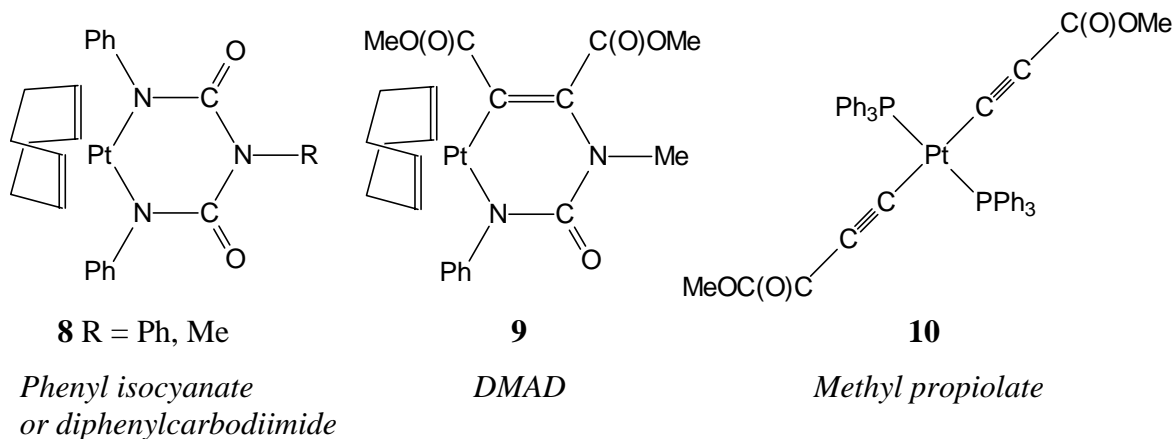


In contrast to the reactions described above, when the gold(III) dihalide precursors $[\text{Au}\{\text{C}_6\text{H}_3(\text{CH}_2\text{NMe}_2)\text{-2-R-5}\}\text{X}_2]$ ($\text{X} = \text{Cl}, \text{Br}$; $\text{R} = \text{OMe}, \text{H}$) were reacted with *N,N*-dimethylthiourea, the unexpected nonmetallic gold(III)-sulfide-silver(I)-halide aggregates (**7**) resulted by desulfurisation of the thiourea. X-ray studies on two derivatives show that both *trans* (**7a**) and *cis* (**7b**) isomers (with respect to the orientation of the opposing *N,N*-dimethylbenzylamine ligands on either side of the Au_2S_2 group) form, although only one isomer was isolated in each case (Chapter Six).

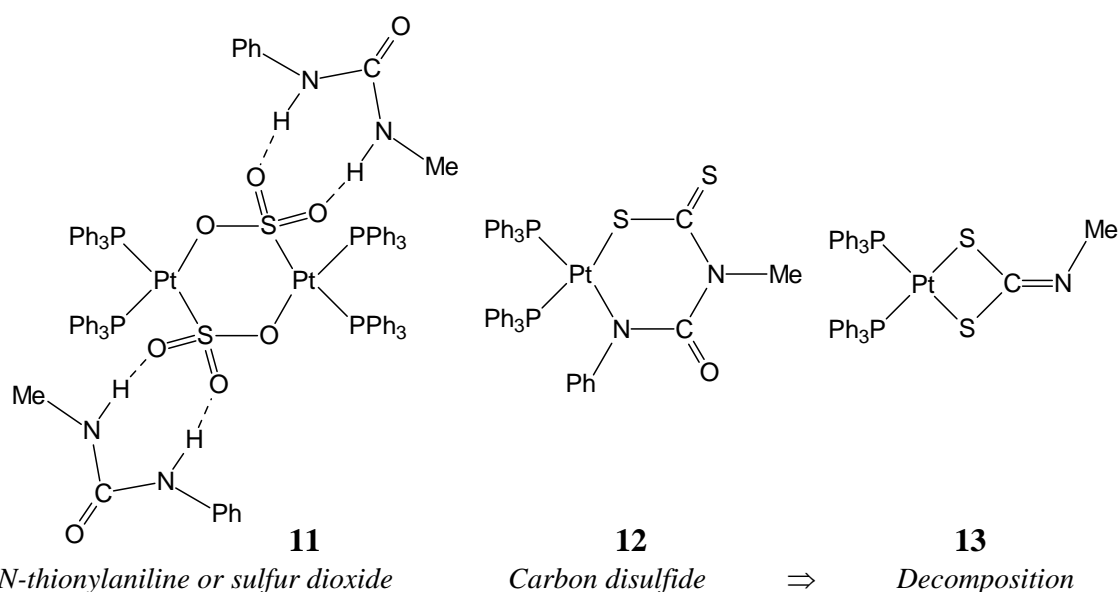


The reactivity of platinum(II) ureylene complexes towards various unsaturated molecules has been investigated (Chapter Four). The complexes $[\text{Pt}\{\text{NPhC}(\text{O})\text{NPh}\}(\text{COD})]$ and $[\text{Pt}\{\text{NPhC}(\text{O})\text{NMe}\}(\text{COD})]$ readily insert phenyl isocyanate to give biureto complexes (**8**), with insertion taking place solely at the Pt-NMe linkage for the latter. When $[\text{Pt}\{\text{NPhC}(\text{O})\text{NMe}\}(\text{COD})]$ was reacted with the isoelectronic diphenyl carbodiimide, the biureto complex $[\text{Pt}\{\text{NPhC}(\text{O})\text{NMeC}(\text{O})\text{NPh}\}(\text{COD})]$ (**8** R = Me) was again isolated,

presumably the result of hydrolysis. Dimethyl acetylenedicarboxylate (DMAD) also rapidly inserted into the Pt-NMe bond of $[\text{Pt}\{\text{NMeC}(\text{O})\text{NPh}\}(\text{COD})]$ to generate (**9**), thus forming a new Pt-C bond. Reaction of the platinaureylene $[\text{Pt}\{\text{NMeC}(\text{O})\text{NPh}\}(\text{PPh}_3)_2]$ with methyl propiolate displaced the urea dianion to give the diacetylide complex (**10**).



When the compound $[\text{Pt}\{\text{NMeC}(\text{O})\text{NPh}\}(\text{PPh}_3)_2]$ was reacted with N-thionylaniline (PhNSO) or sulfur dioxide, the ureylene ligand was displaced to give a dimeric platinum sulfito complex (**11**), that was shown crystallographically to contain co-crystallised N-methyl-N'-phenylurea, hydrogen-bonded from the NH moieties to the S(O)₂ groups. However, $[\text{Pt}\{\text{NMeC}(\text{O})\text{NPh}\}(\text{PPh}_3)_2]$ did insert carbon disulfide to give (**12**). This complex was fully characterised by a single crystal X-ray study, which shows the complex contains a highly puckered six-membered ring. In solution, the complex slowly decomposed by loss of phenyl isocyanate to give the dithiocarbimato complex (**13**), also fully characterised by an X-ray crystallographic study.



Where possible, all new complexes reported in this thesis were fully characterised by multinuclear (¹H, ¹³C and ³¹P) NMR and IR spectroscopies, electrospray mass spectrometry and elemental analyses.

Acknowledgements

During the course of the last three years, a number of people have provided valuable contributions, whom I would like to acknowledge. First, I thank my supervisor Dr. Bill Henderson, for his seemingly boundless enthusiasm and dedication toward this research. Second, I wish to extend gratitude towards Professor Brian Nicholson, primarily for the much needed help in unlocking the secrets of X-ray crystallography, but also for the interest and occasional advice concerning this work. Third, I would like to thank Professor Alistair Wilkins for teaching me more or less everything I know about NMR spectroscopy.

I also wish to acknowledge the following people: G. Ellis (University of Canterbury, biological assays); W. Jackson (electrospray mass spectrometry); various lab colleagues (miscellaneous items); A. G. Oliver (collection of X-ray data sets, Ag₂O advice, and proof-reading); Assoc. Prof. C. E. F. Rickard (University of Auckland, collection of X-ray data sets); Prof. W. T. Robinson (University of Canterbury, collection of X-ray data sets); Dr. R. A. Thomson (NMR spectroscopy); and A. Upreti (lab technician and safety consultant).

A special thanks goes to colleague and friend Craig Depree, who continued to provide the much needed therapeutic distractions over the last three years.

Finally, I would like to thank the William Georgetti Trust and the University of Waikato, for providing financial support in the way of scholarships.

Ik moet natuurlijk ook mijn ouders bedanken voor alles dat ze hebben gedaan voor mij (voor wat weten ze zelf wel) over de laatste drie jaren.

Table of Contents

<i>Abstract</i>	<i>iii</i>
<i>Acknowledgements</i>	<i>vii</i>
<i>List of Tables</i>	<i>xv</i>
<i>List of Selected Figures</i>	<i>xvi</i>
<i>List of Abbreviations</i>	<i>xviii</i>

Chapter One: Introduction to Metallacyclic Chemistry and Silver(I) Oxide Mediated Synthesis 1

1.1 Introduction	1
1.2 Syntheses of Metallacycles	2
1.2.1 Metallacycles containing two M-C bonds	2
1.2.1.1 Metallacyclobutanes	3
1.2.1.2 Metallacyclobutanones	5
1.2.1.3 Metallacyclobutane derivatives containing a heteroatom in the 3-position	7
1.2.2 Metallacycles containing one M-C bond	10
2-Oxametallacyclobutanes (includes metallalactones)	10
1.2.2.2 2-Azametallacyclobutanes	13
1.2.2.3 Metallacyclobutanes containing two heteroatoms in the 2- and 3-positions	14
1.2.2.4 Cyclometallated complexes with a neutral donor	15
1.2.3 Metallacycles containing no M-C bonds	16
1.2.3.1 $\overline{\text{M-O-C-O}}$ complexes	16
1.2.3.2 $\overline{\text{M-S-X-S}}$ (X = C, S, P) complexes	18
1.2.3.3 $\overline{\text{M-N-X-N}}$ (X = C, S) complexes	21
1.2.3.4 Other metallacycles containing two metal-bonded non-carbon heteroatoms	21
1.3 Synthesis of Metallacycles using Silver(I) Oxide	24
1.3.1 Metallacyclobutanone (oxatrimethylenemethane complex)	25
1.3.2 Metallathietanes and metallaphosphetanes	26
1.3.3 Metallalactones	27
1.3.4 Metallalactams	28
1.3.5 Metallacycles containing no M-C bonds	29
References	32

Chapter Two: Syntheses and characterisation of platinum(II) ureylene complexes 37

2.1 Introduction	37
2.1.1 Ureylene formation from organic azides	37
2.1.2 Ureylene formation from isocyanates	38
2.1.3 Ureylene formation from ureas	41
2.2 Results and Discussion	42
2.2.1 Syntheses of ureylene complexes	42
2.2.1.1 Silver(I) oxide mediated synthesis	42
2.2.1.2 Sodium hydride mediated synthesis	44
2.2.2 X-ray structure of [Pt{NPhC(O)NAd}(COD)] 2.22d dichloromethane solvate	45
2.2.3 Spectroscopic and mass spectrometric characterisation	50
2.2.3.1 NMR spectroscopy	50
2.2.3.2 IR spectroscopy	52
2.2.3.3 Electrospray mass spectrometry (ESMS)	54
2.2.4 Platinum hydroxide impurity	55
2.2.5 Conclusions	56
2.3 Experimental Section	56
2.3.1 Preparation and analysis of N,N'-disubstituted aromatic ureas	57
2.3.2 Preparation of acetylureas	59
2.3.3 Preparation of the platinum(II) ureylene complexes 2.22a-2.23	59
2.3.4 X-ray structure of [Pt{NPhC(O)NAd}(COD)] 2.22d dichloromethane solvate	68
References	70

Chapter Three: Synthesis and Characterisation of Guanidine Dianion Complexes 73

3.1 Introduction	73
3.2 Results and Discussion	77
3.2.1 Syntheses of platinum(II) guanidine dianion complexes	77
3.2.2 Syntheses of ruthenium(II), osmium(II), rhodium(III) and iridium(III) guanidine dianion complexes	78
3.2.3 X-ray structure of [Pt{NPhC(NPh)NPh}(COD)] 3.17a diethyl ether solvate	82
3.2.4 X-ray structure of [(η^6 - <i>p</i> -cymene)Ru{NAcC(NAc)NAc}(PPh ₃)] 3.21a	86
3.2.5 Spectroscopic and mass spectrometric characterisation	88
3.2.5.1 NMR spectroscopy	88
3.2.5.2 Electrospray mass spectrometry (ESMS)	93
3.2.6 Conclusions	93
3.3 Experimental	94
3.3.1 Preparation of the free guanidines	94
3.3.2 Preparation of the triazatrimethylenemethane complexes	96
3.3.3 X-ray structure of [Pt{NPhC(NPh)NPh}(COD)] 3.17a diethyl ether solvate	104
3.3.4 X-ray structure of [(η^6 - <i>p</i> -cymene)Ru{NAcC(NAc)NAc}(PPh ₃)] 3.21a	105
References	108

Chapter Four: Insertion Reactions of Platinum(II) Ureylene Complexes 111

4.1 Introduction	111
4.2 Results and Discussion	114
4.2.1 Insertion reactions with phenyl isocyanate and diphenylcarbodiimide	114
4.2.1.1 Spectroscopic and mass spectrometric characterisation	116
4.2.1.1.1 NMR spectroscopy	116
4.2.1.1.2 IR spectroscopy	117
4.2.1.1.3 Electrospray mass spectrometry (ESMS)	117
4.2.2 Reaction with acetylenes	117
4.2.2.1 Spectroscopic and mass spectrometric characterisation	119
4.2.2.1.1 NMR spectroscopy	119
4.2.2.1.2 Electrospray mass spectrometry	119
4.2.3 Reactions with N-thionylaniline and sulfur dioxide	120
4.2.3.1 X-ray structure of $[\{\text{Pt}(\text{SO}_3)(\text{PPh}_3)_2\}_2 \cdot 2\text{PhNHC}(\text{O})\text{NHMe}]$ chloroform solvate 4.23	121
4.2.3.2 Spectroscopic and mass spectrometric characterisation	125
4.2.3.2.1 NMR spectroscopy	125
4.2.3.2.2 IR spectroscopy	125
4.2.4 Insertion reaction with <u>carbon disulfide</u>	126
4.2.4.1 X-ray structure of $[\text{Pt}\{\text{SC}(\text{S})\text{NMeC}(\text{O})\text{NPh}\}(\text{PPh}_3)_2]$ chloroform solvate 4.28	127
4.2.4.2 Spectroscopic and mass spectrometric characterisation	131
4.2.4.2.1 NMR spectroscopy	131
4.2.4.2.2 IR spectroscopy	131
4.2.4.2.3 Electrospray mass spectrometry	132
4.2.5 Decomposition of complex 4.28	132
4.2.5.1 X-ray structure of $[\text{Pt}\{\text{S}_2\text{C}=\text{NMe}\}(\text{PPh}_3)_2]$ 4.29a	133
4.2.5.2 Spectroscopic and mass spectrometric characterisation	136
4.2.5.2.1 NMR spectroscopy	136
4.2.5.2.2 Electrospray mass spectrometry	136
4.2.6 Conclusions	137
4.3 Experimental	137
4.3.1 X-ray structure of $[\{\text{Pt}(\text{SO}_3)(\text{PPh}_3)_2\}_2 \cdot 2\text{PhNHC}(\text{O})\text{NHMe}]$ chloroform solvate 4.23	146
4.3.2 X-ray structure of $[\text{Pt}\{\text{SC}(\text{S})\text{NMeC}(\text{O})\text{NPh}\}(\text{PPh}_3)_2]$ chloroform solvate 4.28	147
4.3.3 X-ray structure $[\text{Pt}\{\text{S}_2\text{C}=\text{NMe}\}(\text{PPh}_3)_2]$ 4.29a	148
References	149

Chapter Five: Syntheses, Characterisation, Insertion Reactions and Biological Activity of Gold(III) Ureylene Complexes 151

5.1 Introduction	151
5.2 Results and Discussion	153
5.2.1 X-ray structures of $[\{\text{C}_6\text{H}_3(\text{CH}_2\text{NMe}_2)-2-(\text{OMe})-5\}\text{Au}\{\text{NRC}(\text{O})\text{NR}\}]$ 5.8a (R = Ph) and 5.8b water solvate (R = Ac)	154
5.2.2 Spectroscopic and mass spectrometric characterisation	160

5.2.2.1	NMR spectroscopy	160
5.2.2.2	IR spectroscopy	161
5.2.2.3	Electrospray mass spectrometry (ESMS)	162
5.2.3	Reaction with phenyl isocyanate and DMAD	162
5.2.3.1	Spectroscopic and mass spectrometric characterisation	163
5.2.4	Biological Activity	165
5.2.5	Conclusions	166
5.3	Experimental	166
5.3.1	X-ray structure of [$\{C_6H_3(CH_2NMe_2)-2-(OMe)-5\}Au\{NPhC(O)NPh\}$] 5.8a	170
5.3.2	X-ray structure of [$\{C_6H_3(CH_2NMe_2)-2-(OMe)-5\}Au\{NAcC(O)NAc\}$] 5.8b water solvate	171
References		173

Chapter Six: Reactions of Gold(III) Dihalide Complexes with Thioureas 175

6.1	Introduction	175
6.2	Results and Discussion	176
6.2.1	X-ray structure of [$\{(\{C_6H_3(CH_2NMe_2)-2-(OMe)-5\}Au\{\mu-S\})_2\}_6Ag_3Cl_2]Z$ 6.5a	180
6.2.2	X-ray structure of [$\{(\{C_6H_4(CH_2NMe_2)-2\}Au\{\mu-S\})_2\}_3Ag_3Br_2]Z$ 6.5d	185
6.2.3	Spectroscopic and mass spectrometric characterisation	188
6.2.3.1	NMR characteristics	188
6.2.3.2	Electrospray mass spectrometry (ESMS)	189
6.2.4	Additional synthetic studies	192
6.2.4.1	Aggregate synthesis using silver(I) sulfide	192
6.2.4.2	Attempted synthesis of [$\{C_6H_3(CH_2NMe_2)-2-R-5\}Au(\mu-S)_2$] monomer	192
6.2.4.3	Attempted synthesis of gold(III)-selenide-silver(I)-halide analogues	192
6.2.5	Conclusions	193
6.3	Experimental	193
6.3.1	X-ray structure determination of 6.5a	197
6.3.2	X-ray structure determination of 6.5d	198
References		200

Chapter Seven: Synthesis and Characterisation of Auracyclobutan-3-one and Aurathietane-3,3-dioxide Complexes 205

7.1	Introduction	205
7.2	Results and Discussion	207
7.2.1	X-ray structure of 7.9 [$\{C_6H_3(CH_2NMe_2)-2-(OMe)-5\}Au\{CH(COPh)S(O)_2CH(COPh)\}$] benzene solvate	207
7.2.2	Spectroscopic and mass spectrometric characterisation	212
7.2.2.1	NMR spectroscopy	212

7.2.2.2	Electrospray mass spectrometry (ESMS)	214
7.2.3	Conclusions	214
7.3	Experimental	215
7.3.1	X-ray structure of 7.9 $[\{C_6H_3(CH_2NMe_2)-2-(OMe)-5\}Au\{CH(COPh)S(O)_2CH(COPh)\}]$ benzene solvate	218
	References	220

Chapter Eight: Synthesis, Characterisation and Biological Activity of Gold(III) Salicylate and Thiosalicylate Complexes 221

	Introduction	221
8.2	Results and Discussion	223
8.2.1	Synthesis of gold(III) thiosalicylate complexes	223
8.2.2	X-ray structure of $[\{C_6H_4(CH_2NMe_2)-2\}Au\{SC_6H_4(COO)-2\}]$ 8.10b	224
8.2.3	Synthesis of a gold(III) salicylate complex	228
8.2.4	X-ray structure of $[\{C_6H_3(CH_2NMe_2)-2-(OMe)-5\}Au\{OC_6H_4(COO)-2\}]$ 8.15b dichloromethane solvate	229
8.2.5	Spectroscopic and mass spectrometric characterisation	232
8.2.5.1	NMR spectroscopy	232
8.2.5.2	Electrospray mass spectrometry (ESMS)	233
8.2.6	Attempted reaction of 8.10a with mercury(II) iodide	234
8.2.7	Biological activity of the gold(III) thiosalicylate and salicylate complexes 8.10a , 8.10b and 8.15b	234
8.2.8	Attempted synthesis and characterisation of the cation $[Au\{C_6H_3(CH_2NMe_2)-2-(OMe)-5\}_2]^+$ 8.16	235
8.2.9	Conclusions	237
8.3	Experimental	237
8.3.1	X-ray structure of $[\{C_6H_4(CH_2NMe_2)-2\}Au\{SC_6H_4(COO)-2\}]$ 8.10b	241
8.3.2	X-ray structure of $[\{C_6H_3(CH_2NMe_2)-2-(OMe)-5\}Au\{OC_6H_4(COO)-2\}]$ 8.15b dichloromethane solvate	242
	References	243

Appendix I: General Experimental Procedure and Preparation of Inorganic and Organometallic Precursors 247

	A.I.1 General Experimental Procedure	247
	A.I.2 Preparation of Inorganic and Organometallic Precursors	248
	References	255

Appendix II: Instrumentation and Analyses 256

	A.II.1 NMR spectroscopy	256
	A.II.2 X-ray diffractometer methodology and configuration	262

A.II.3 Electrospray mass spectrometry (ESMS)	263
A.II.4 Elemental microanalysis and biological assays	263
A.II.5 IR spectroscopy	263
A.II.6 Melting points	263
References	264
Appendix III: X-ray data for 2.22d	265
Appendix IV: X-ray data for 3.17a	269
Appendix V: X-ray data for 3.21a	273
Appendix VI: X-ray data for 4.23	278
Appendix VII: X-ray data for 4.28	284
Appendix VIII: X-ray data for 4.29a	289
Appendix IX: X-ray data for 5.8a	293
Appendix X: X-ray data for 5.8b	296
Appendix XI: X-ray data for 6.5a	299
Appendix XII: X-ray data for 6.5d	303
Appendix XIII: X-ray data for 7.5	313
Appendix XIV: X-ray data for 8.10b	317
Appendix XV: X-ray data for 8.15b	320
Appendix XVI: List of publications	323

List of Tables

2.1: Selected bond lengths (Å) and angles (°) of the platinum(II) ureylene complex 2.22d ·CH ₂ Cl ₂ .	47
2.2: Comparison of M-N bond lengths and N-M-N and N-C-N bond angles of 2.22d ·CH ₂ Cl ₂ with related ureylene complexes.	49
2.3: A comparison of cyclo-octadiene olefinic ¹ H and ¹³ C resonances and coupling constants for the various ureylene complexes [Pt{NRC(O)NR'}(COD)]	50
2.4: A comparison of triphenylphosphine ³¹ P resonances and coupling constants for the various ureylene complexes [Pt{NRC(O)NR'}(PPh ₃) ₂] 2.22	52
3.1: Selected bond lengths (Å) and angles (°) of the platinum(II) N,N',N''-triphenylguanidine dianion complex 3.17a ·½C ₄ H ₁₀ O.	84
3.2: Selected bond lengths (Å) and angles (°) of the ruthenium(II) N,N',N''-triacetylguanidine dianion complex 3.21a .	88
3.3: A comparison of significant NMR spectroscopic properties of the guanidine dianion complexes, together with those of the starting materials and related complexes.	89
4.1: Selected bond lengths (Å) and bond angles (°) for 4.23 ·2CHCl ₃ .	123
4.2: Comparison of ¹ H and ¹³ C NMR chemical shifts of the hydrogen-bonded urea fragment of 4.23 and free N-methyl-N'-phenylurea.	126
4.3: Selected bond lengths (Å) and bond angles (°) for 4.28 ·CHCl ₃	130
4.4: Selected bond lengths (Å) and bond angles (°) for 4.29a .	135
5.1: Selected bond lengths (Å) and angles (°) of the gold(III) ureylene complex 5.8a .	157
5.2: Selected bond lengths (Å) and angles (°) ureylene complex 5.8b ·½H ₂ O.	159
5.3: Comparison of ¹³ C chemical shifts (ppm) of 5.8a and 5.8b compared to the respective urea starting materials.	161
5.4: Biological assay results for the gold(III) ureylene complex 5.8b .	165
6.1: Selected bond lengths (Å) and angles (°) of the gold(III) aggregate cation 6.5a .	183
6.2: Selected bond lengths (Å) and angles (°) for 6.5d .	187
7.1: Selected bond lengths (Å) and angles (°) for 7.9 ·C ₆ H ₆ .	210
8.1: Selected bond lengths (Å) and angles (°) for the gold(III) thiosalicylate complex 8.10b (molecule 2).	226
8.2: Selected bond lengths (Å) and angles (°) for the gold(III) salicylate complex 8.15b ·CH ₂ Cl ₂ .	231
8.3: Comparison of selected ¹³ C NMR chemical shifts of 8.10a , 8.10b and 8.15b compared to the respective thiosalicylic acid and salicylic acid starting materials.	233
8.4: Biological assay results for the gold(III)thiosalicylate complexes 8.10a , 8.10b and the salicylate complex 8.15b .	235

List of Selected Figures

2.12:	Perspective view of the X-ray crystal structure of the ureylene complex [Pt{NPhC(O)NAd}(COD)]·CH ₂ Cl ₂ 2.22d .	46
2.13:	Side view of the structure of the ureylene complex [Pt{NPhC(O)NAd}(COD)]·CH ₂ Cl ₂ 2.22d .	47
2.15:	³¹ P NMR of the ureylene complex [Pt{NHC(O)NH}(PPh ₃) ₂] 2.22k illustrating decomposition at various stages.	53
2.16:	Electrospray mass spectrum of [Pt{NPhC(O)NPh}(COD)] 2.22d	55
3.13:	ORTEP perspective view of the structure of the platinum(II) triazatri-methylenemethane complex [Pt{NPhC(NPh)NPh}(COD)]·½C ₄ H ₁₀ O 3.17a .	83
3.14:	ORTEP side view of the structure of the platinum(II) triazatri-methylenemethane complex [Pt{NPhC(NPh)NPh}(COD)]·½C ₄ H ₁₀ O 3.17a .	84
3.15:	PLUTO perspective view of the structure of ruthenium(II) triazatri-methylenemethane complex [(<i>η</i> ⁶ -p-cymene)Ru{NAcC(NAc)NAc}(PPh ₃) ₂] 3.21a .	87
3.16:	¹ H NMR (300.13 MHz) spectra of the complex [Pt{NPhC(NPh)NPh}(COD)] 3.17a at temperatures of 300, 280, 260 and 240 K (as indicated).	91
3.17:	¹³ C NMR (75.47 MHz) spectra of the complex [Pt{NPhC(NPh)NPh}(COD)] 3.17a at temperatures of 300, 280, 260 and 240 K.	92
4.9:	ORTEP representation of [{Pt(SO ₃ (PPh ₃) ₂) ₂ ·2PhNHC(O)NHMe]·2CHCl ₃ 4.23 .	122
4.13:	Perspective view of the structure of [Pt{SC(S)NMeC(O)NPh}(PPh ₃) ₂]·CHCl ₃ 4.28	128
4.14:	Side view of the structure of [Pt{SC(S)NMeC(O)NPh}(PPh ₃) ₂]·CHCl ₃ 4.28 .	129
4.16:	Perspective view of the structure of [Pt{S ₂ C=NMe}(PPh ₃) ₂] 4.29a .	134
4.17:	Side view of the structure of [Pt{S ₂ C=NMe}(PPh ₃) ₂] 4.29a .	134
5.7:	Perspective view of the X-ray crystal structure of the gold(III) ureylene complex [{C ₆ H ₃ (CH ₂ NMe ₂)-2-(OMe)-5}Au{NPhC(O)NPh}] 5.8a .	156
5.8:	Side view of the X-ray crystal structure of the gold(III) ureylene complex [{C ₆ H ₃ (CH ₂ NMe ₂)-2-(OMe)-5}Au{NPhC(O)NPh}] 5.8a .	157
5.9:	Perspective view of the X-ray crystal structure of the gold(III) ureylene complex [{C ₆ H ₃ (CH ₂ NMe ₂)-2-(OMe)-5}Au{NAcC(O)NAc}]·½H ₂ O 5.8b .	158
5.10:	Side view of the X-ray crystal structure of the gold(III) ureylene complex [{C ₆ H ₃ (CH ₂ NMe ₂)-2-(OMe)-5}Au{NAcC(O)NAc}]·½H ₂ O 5.8b .	159
5.12:	Positive-ion electrospray mass spectra of [{C ₆ H ₃ (CH ₂ NMe ₂)-2-(OMe)-5}Au{NPhC(O)NPhC(O)NPh}] 5.11 .	164
6.10:	ORTEP representation of the structure of the core of the cationic aggregate 6.5a .	181
6.12:	ORTEP representation of “monomer 1” from 6.5a , illustrating the <i>trans</i> configuration of the opposing N,N-dimethylbenzylamine ligands.	182
6.13:	ORTEP representation of the structure of the core of the cationic aggregate 6.5d .	186

6.14:	ORTEP representation of one of the monomer units from 6.5d , illustrating the <i>cis</i> configuration of the opposing N,N-dimethylbenzylamine ligands.	186
6.15:	Positive-ion electrospray mass spectrum of the complex 6.5a , recorded in methanol, at a cone voltage of 20 V.	191
7.5:	ORTEP perspective view of the structure of $[\{C_6H_3(CH_2NMe_2)-2-(OMe)-5\}Au\{CH(COPh)S(O)_2CH(COPh)\}] \cdot C_6H_6$ 7.9 .	208
7.6:	ORTEP side view of the structure of $[\{C_6H_3(CH_2NMe_2)-2-(OMe)-5\}Au\{CH(COPh)S(O)_2CH(COPh)\}] \cdot C_6H_6$ 7.9 .	209
8.6:	PLUTO perspective view of the X-ray structure of the gold(III) thiosalicylate complex $[\{C_6H_4(CH_2NMe_2)-2\}Au\{SC_6H_4(COO)-2\}]$ 8.10b .	225
8.7:	PLUTO side view of the X-ray structure of molecule 2 of the gold(III) thiosalicylate complex $[\{C_6H_4(CH_2NMe_2)-2\}Au\{SC_6H_4(COO)-2\}]$ 8.10b .	225
8.12:	ORTEP perspective view of the molecular structure of the gold(III) salicylate complex $[\{C_6H_3(CH_2NMe_2)-2-(OMe)-5\}Au\{OC_6H_4(COO)-2\}] \cdot CH_2Cl_2$ 8.15b .	230
8.13:	ORTEP side view of the molecular structure of the gold(III) salicylate complex $[\{C_6H_3(CH_2NMe_2)-2-(OMe)-5\}Au\{OC_6H_4(COO)-2\}] \cdot CH_2Cl_2$ 8.15b .	230
A.II.2:	1H NMR of the aromatic region of the gold(III) complex 5.11 .	258
A.II.3:	HOHAHA spectrum of the gold(III) complex 5.11 , showing the slices used to generate the corresponding 1H spectra shown in Figure A.II.4.	258
A.II.4:	Resolved 1H NMR slices (for the gold(III) complex 5.11) corresponding to those shown on the HOHAHA spectrum given in Figure A.II.3.	259
A.II.5:	ROESY spectrum of the gold(III) complex 7.5 .	260

Abbreviations

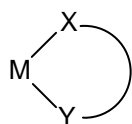
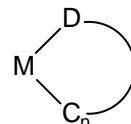
Ac	-	acetyl
Ad	-	1-adamantyl
br	-	broad
bipy	-	2,2'-bipyridyl
b.p.	-	boiling point
Bu	-	butyl
Bu ^t	-	tertiary butyl
δ	-	chemical shift (ppm)
COD	-	1,5-cyclo-octadiene
Cp	-	cyclopentadienyl (η^5 -C ₅ H ₅)
Cp*	-	pentamethylcyclopentadienyl (η^5 -C ₅ Me ₅)
DMAD	-	dimethyl acetylenedicarboxylate
DMSO	-	dimethyl sulfoxide
dppe	-	1,2 bis(diphenylphosphine)ethane
dppm	-	1,2 bis(diphenylphosphine)methane
<i>d</i>	-	doublet (NMR)
Et	-	ethyl
IR	-	infrared
J	-	coupling constant in Hz (NMR)
m	-	medium (IR)
<i>m</i>	-	multiplet (NMR)
Me	-	methyl
m.p.	-	melting point
ESMS	-	electrospray mass spectrometry
NMR	-	nuclear magnetic resonance
Ph	-	phenyl
phen	-	1,10-phenanthroline
Pr ⁱ	-	isopropyl
Py	-	pyridyl
<i>q</i>	-	quartet (NMR)
s	-	strong (IR)
<i>s</i>	-	singlet (NMR)
<i>t</i>	-	triplet (NMR)
THF	-	tetrahydrofuran
v	-	stretching frequency (IR)
vs	-	very strong (IR)
w	-	weak (IR)

Chapter One

Introduction to Metallacyclic Chemistry and Silver(I) Oxide Mediated Synthesis

1.1 Introduction

Metallacycles **1.1** (Figure 1.1), usually defined as a ring containing at least one metal centre, form an important class of inorganic and organometallic compounds. The relevance of metallacyclic transition-metal complexes in organic synthesis has been greatly studied, and has been summarised in a number of reviews.^{1,2} Traditionally, the term “metallacycle” referred only to compounds containing two metal-carbon bonds as part of the ring,³ but is now commonly used to refer to any ring system incorporating a metal, provided both ring M-X bonds are not neutral donor ligands (these being more typically referred to as “chelate complexes”). The ring system can thus be derived from formally monoanionic or dianionic ligands, and thereby the term “metallacycle” includes cyclometallated complexes **1.2** (which often contain a “chelating” neutral donor atom, D) (Figure 1.1). Since it is such a diverse class of compounds, used to refer to rings of any size, comprising of multiple atoms of any element, a vast number of complexes containing metallacycles are possible, and indeed a huge number of such complexes have been prepared.

**1.1****1.2** D = O, S, Se, N etc.**Figure 1.1**

Due to the sheer volume of metallacyclic complexes that have been reported over the years, the author makes no attempt at providing a complete summary of their chemistry. Representative examples only are presented, restricted to mononuclear four-membered ring systems of the platinum group metals, with a particular emphasis on platinum(II) systems, these being especially relevant to the work presented in this thesis.

1.2 Syntheses of Metallacycles

Due to the very large scope of the field, comprehensive reviews concerning the syntheses of metallacycles are unfortunately unavailable. The purpose of this chapter is primarily to give the reader a taste of the diverse range of metallacycles that have been prepared, and the diverse range of chemistry that results in these complexes.

Subsequent discussion on metallacycles has been divided into three sections, those containing two metal-carbon bonds, those containing one, and those devoid of metal-carbon bonds. Metallacycles formed by the silver(I) oxide route are excluded here, but are discussed in detail in Section 1.3.

1.2.1 Metallacycles containing two M-C bonds

By far the most widely studied class of metallacycles are those containing metal-carbon linkages, especially the metallacyclobutanes (Section 1.2.1.1). The interest in these systems largely stems from their relevance as intermediates in catalytic cycles, especially in olefin (metallacyclobutane) and acetylene (metallacyclobutene) metathesis reactions,⁴⁻⁶ but also due to their ready formation. Chappel and Cole-Hamilton describe five main routes to traditional “metallacycles” containing two metal-carbon bonds.³ These are insertion into C-C bonds, dilithio and diGrignard reagents, via cyclometallation reactions (C-H bond cleavage), coupling reactions of alkenes and alkynes, and polyalkene and polyalkyne reactions. The latter method leads almost exclusively to five-membered ring complexes and so fall outside the scope of this discussion. There are of course numerous other routes to metallacyclobutane synthesis, but the methods listed cover the majority of complexes.

Focussing on four-membered ring metallacycles with two M-C bonds, three main classes are evident. These are unsubstituted metallacyclobutanes **1.3**, metallacyclobutanones **1.4**, and those containing a heteroatom as part of the metallacyclic ring, such as metallaoxetanes **1.5** and metallaazetidines **1.6** (Figure 1.2), and these are discussed in some detail in the following sections, with a focus on platinum(II) systems.

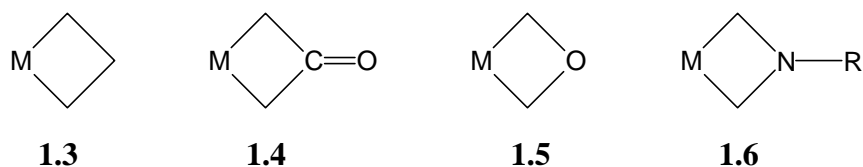
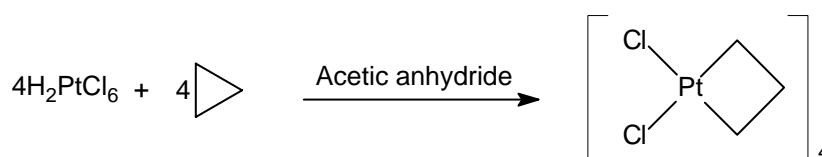


Figure 1.2

1.2.1.1 Metallacyclobutanes

As already mentioned, metallacyclobutanes have been exhaustively studied, and are the subject of three major reviews,^{3,7,8} with the latter citation devoted solely to platinacyclobutanes.

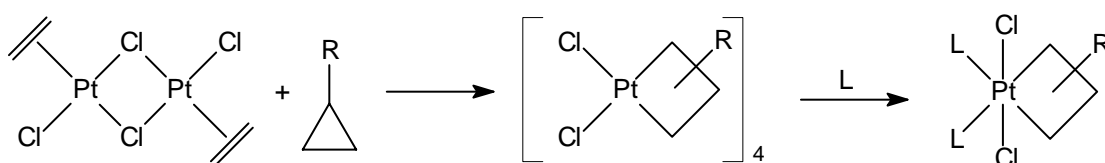
The first reported metallacyclobutane (and possibly the first metallacycle in general) was the platinum(IV) complex **1.7**, synthesised by Tipper in 1955 by the reaction of cyclopropane and hexachloroplatinic acid (H_2PtCl_6) (Equation 1.1),⁹ and characterised some years later.¹⁰



1.7

Equation 1.1

Tipper's reaction, an example of C-C bond cleavage, is surprisingly ineffective at activating most other cyclopropane systems. Zeise's dimer **1.8** provides a better, more general reagent, reacting with many cyclopropanes to give corresponding platina(IV)cyclobutane tetramers **1.9** (Equation 1.2).¹¹ These can then subsequently be reacted with neutral donor ligands to give the mononuclear complexes **1.10** (Equation 1.2).¹¹ Formation of a range of M(II) (M = Pt, Pd) cyclobutanes are also possible if platinum(0) or palladium(0) precursors such as $[\text{ML}_4]$ (L = tertiary phosphine) are used.^{12,13}



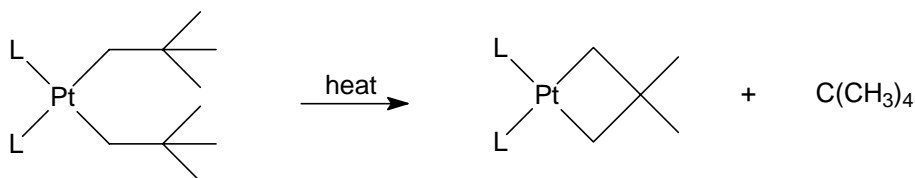
1.8

1.9 R = alkyl, aryl groups

1.10 L = Py, phen etc.

Equation 1.2

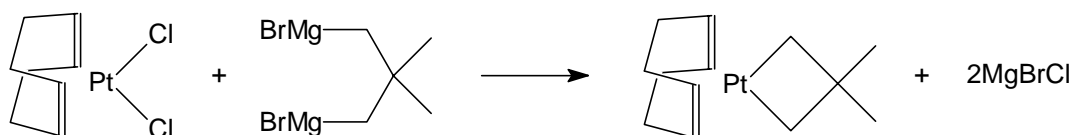
Carbon-hydrogen bond cleavage by oxidative addition to a central metal atom, otherwise known as cyclometallation, has also been used to synthesise metallacyclobutanes.⁷ Typically, a metal dihalide is treated with neopentylmagnesium bromide (or other suitable compound) to give a dineopentylmetal complex, which undergoes cyclometallation when heated, to give a metallacyclobutane system. A representative platinum(II) example is shown in Equation 1.3.¹⁴



L = tertiary phosphine

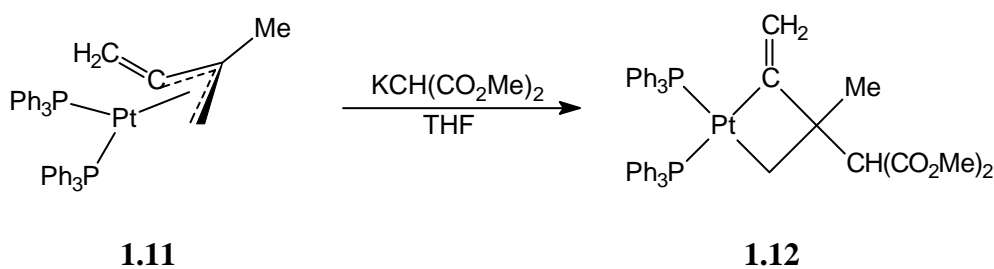
Equation 1.3

Dilithio and diGrignard reagents are also an effective means of forming metallacyclobutanes, and indeed many other metallacycles, and the methodology is probably the most general.³ A metal dihalide is reacted with the 1,3-dimetallic organometallic species to give the metallacyclobutane complex directly (e.g. Equation 1.4).¹⁵



Equation 1.4

Nucleophilic addition to the central carbon of a η^3 -allyl (π -allyl) transition-metal complexes can lead to metallacyclobutanes, and a range of complexes have been prepared by this route.⁷ Again, a representative example of a platinum(II) system is shown (Equation 1.5). The isolated η^3 -allyl complex **1.11** was reacted with $\text{KCH}(\text{CO}_2\text{Me})_2$ in THF, resulting in nucleophilic attack to give a ring-closed product **1.12**, containing a metallacyclobutane moiety.¹⁶

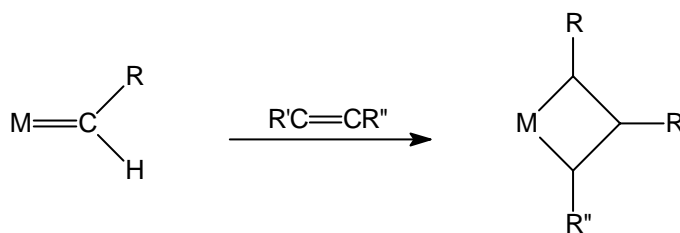


1.11

1.12

Equation 1.5

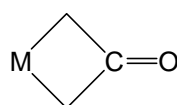
Finally, and perhaps the most intensively researched, is the formation of metallacyclobutane complexes by reaction of alkenes (or alkynes) with metal-carbene complexes (Equation 1.6), primarily due to their high relevance in the industrially-important olefin metathesis reaction, in which metallacyclobutanes are considered to be intermediates in the catalytic cycle.^{3,6}



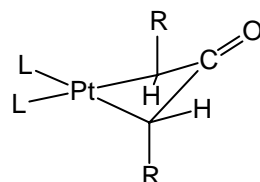
R, R', R'' = various alkyl or aryl groups

Equation 1.6

1.2.1.2 Metallacyclobutanones



Reaction of various platinum(0) and palladium(0) species, $[\text{Pt}(\text{PR}_3)_4]$, $[\text{Pt}(\text{AsPh}_3)_4]$, $[\text{Pt}(\text{CO})_3(\text{PR}_3)_2]$, *cis*- $[\text{Pt}(\text{OC}(\text{O})\text{Ph})_2]$, $[\text{Pd}(\text{PR}_3)_2]$ and $[\text{Pd}_2(\text{dba})_3]$ (dba = dibenzylideneacetone) with esters of 3-oxopentanedioic acid or 2,4,6-heptanetrione, under a range of reaction conditions, gives pallada(II)- and platina(II)cyclobutan-3-ones **1.13** (Figure 1.3), also known as oxatrimethylenemethane complexes, and these have been the subject of a review.¹⁷

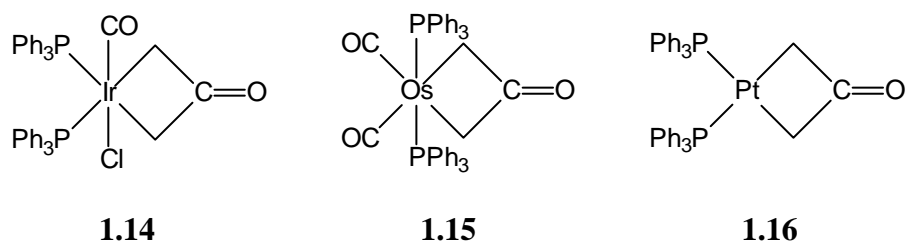


1.13 L = various tertiary phosphines, AsPh_3 , $\frac{1}{2}(\text{bipy})$;

R = CO_2Me , CO_2Et , $\text{CO}_2\text{-}n\text{-Pr}$, COMe

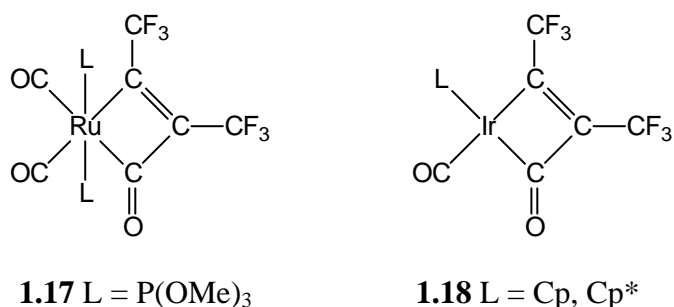
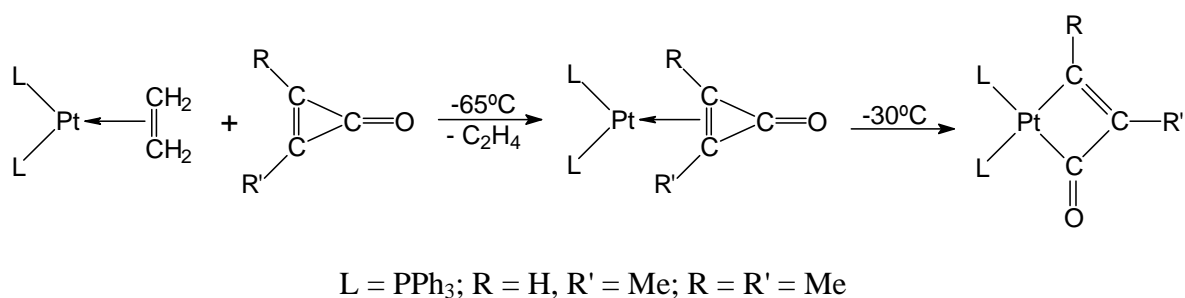
Figure 1.3

Similarly, the oxidative addition of 3-chloro-1-(trimethylsilyl)propan-2-one $[\text{H}_2\text{C}=\text{C}(\text{OSiMe}_3)\text{CH}_2\text{Cl}]$ to the complexes *trans*- $[\text{IrCl}(\text{CO})(\text{PPh}_3)_2]$, $[\text{Os}(\text{CO})_2(\text{PPh}_3)_2]$ and $[\text{Pt}\{\eta^2\text{-(PhC}\equiv\text{CPh)}\}(\text{PPh}_3)_2]$ gave the respective metallabutan-3-one complexes **1.14-1.16** (Figure 1.4).¹⁸

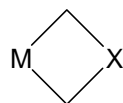
**Figure 1.4**

In contrast to the unsubstituted metallacyclobutanes (which are typically planar and the metal-carbon bonding is considered predominantly as σ -like),⁷ the metallacyclobutan-3-one systems have been found to be highly puckered, with fold angles ranging from 41-56.7°, and this is believed to be attributable to η^3 -allylic contributions to the bonding.¹⁷ The effect is discussed in greater detail in Chapter Seven (Section 7.2.1).

Finally, metallabuten-2-one rings with the carbonyl group in the 2-position, have been prepared by the reaction of highly electron-deficient alkynes containing CF_3 groups, with $[\text{Ru}(\text{CO})_3\{\text{P}(\text{OMe})_3\}_2]$ or $[\text{Ir}(\text{CO})_2\text{L}]$ ($\text{L} = \text{Cp}$ or Cp^*), to give the complexes **1.17** and **1.18** (Figure 1.5) respectively.¹⁹ A second synthesis of metallabuten-2-ones involved the reaction of substituted cyclopropenes with $\text{cis-}[\text{Pt}(\eta^2\text{-CH}_2\text{=CH}_2)\text{L}_2]$ (Equation 1.7).²⁰ Especially important in this reaction, was that in one case ($\text{R} = \text{H}$, $\text{R}' = \text{Me}$), at low temperatures, a cyclopropenone intermediate could be isolated.²⁰

**Figure 1.5****Equation 1.7**

1.2.1.3 Metallacyclobutane derivatives containing a heteroatom in the 3-position



As already mentioned, most investigations have focussed on all-carbon metallacycles, although recently there has been interest in generating metallacyclic rings incorporating synthetically interesting heteroatoms, such as nitrogen and oxygen. However, these heteroatoms are almost invariably bound directly to metal (the 2-position) (see Section 1.2.2). Nonetheless, a number of complexes with the heteroatom in the 3-position have been prepared.

The 3-oxametallacyclobutane (metallaioxetane) complexes **1.19** (Figure 1.6) were prepared from intramolecular dehydrative cyclisation of the platinum(II) complex **1.20**, using triphenylphosphine and diethyl azodicarboxylate ($\text{EtO}_2\text{CN}=\text{NCO}_2\text{Et}$) in THF.²¹ The subsequent reaction of the trimethylphosphine derivative of **1.19** with methyl iodide, gave the 3-oxaplatina(IV)cyclobutanone complex **1.21** (Figure 1.6).²²

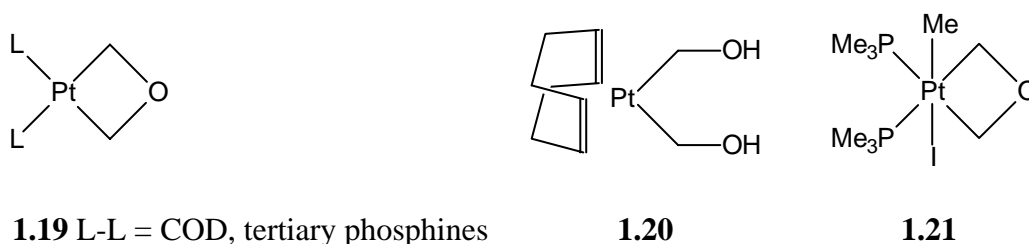


Figure 1.6

Equally rare are complexes incorporating a nitrogen in the 3-position. The cationic complex **1.22** (Figure 1.7), containing a 3-metalla-azetidinium ring, was unexpectedly prepared from the reaction of **1.23** and dimethylformamide dimethylacetal [$\text{Me}_2\text{NCH}(\text{OMe})_2$] in methanol.²³ The neutral 3-platina-azetidine complex **1.24** (Figure 1.7) was subsequently prepared by reacting **1.23** with excess isopropylamine in chlorobenzene.²³

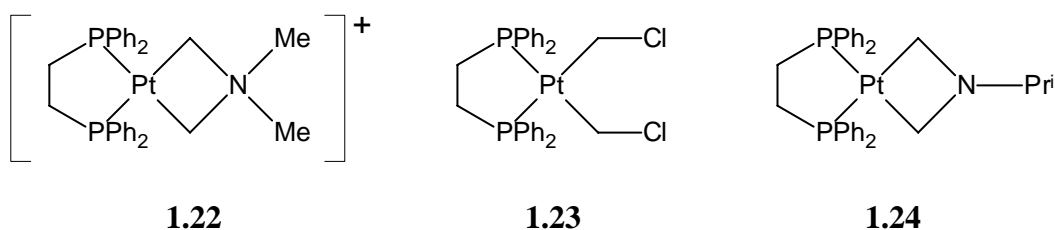
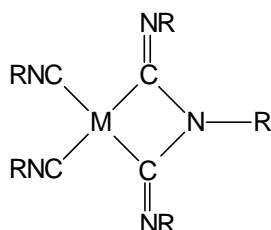


Figure 1.7

The reaction of the platinum(II) and palladium(II) isocyanide complexes $[\text{MCl}_2(\text{RNC})_2]$ ($\text{M} = \text{Pt}, \text{Pd}$; $\text{R} = 2,6\text{-xylyl}$) with 2,6-xylyl isocyanide in the presence of sodium amalgam in THF gave, amongst various reduction products, the respective platina- and pallada-3-azacyclobutane derivatives **1.25a** and **1.25b** (Figure 1.8), which also incorporate a nitrogen into the four-membered metallacycles.²⁴

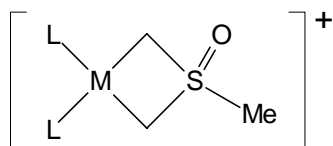


1.25a $\text{M} = \text{Pt}$; $\text{R} = 2,6\text{-Me}_2\text{C}_6\text{H}_3$

1.25b $\text{M} = \text{Pd}$; $\text{R} = 2,6\text{-Me}_2\text{C}_6\text{H}_3$

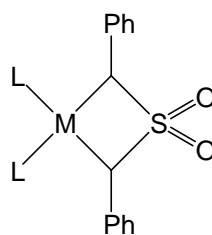
Figure 1.8

Metallacycles containing the $\text{S}=\text{O}$ moiety (metallathietanes) have also been synthesised. The complexes $[\text{MCl}_2\text{L}_2]$ ($\text{M} = \text{Pt}, \text{Pd}$; $\text{L} =$ tertiary phosphines) when reacted with trimethylsulfoxonium iodide in the presence of base (NaOH) and a phase transfer catalyst $[(n\text{-Bu})_4\text{N}]\text{I}$, gives the complexes **1.26** (Figure 1.9) in high yield.²⁵ A more typical preparation of metallathietanes involves reaction of the appropriate dihalide precursor $[\text{MCl}_2\text{L}_2]$ ($\text{M} = \text{Pt}, \text{Pd}$; $\text{L} =$ neutral donor ligand) with the dilithium salt of dibenzyl sulfone $[\text{PhCHLiS}(\text{O})_2\text{CHLiPh}]$, to give the corresponding complexes **1.27**.²⁶



1.26a $\text{M} = \text{Pt}$; $\text{L} =$ tertiary phosphine

1.26b $\text{M} = \text{Pd}$; $\text{L} =$ tertiary phosphine



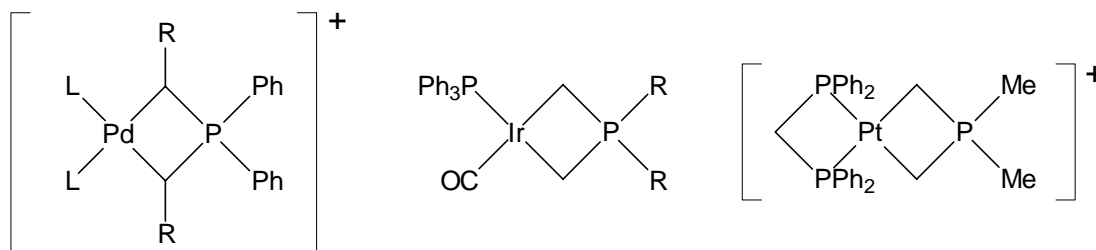
1.27a $\text{M} = \text{Pt}$; $\text{L} =$ neutral donor ligand

1.27b $\text{M} = \text{Pd}$; $\text{L} =$ neutral donor ligand

Figure 1.9

The palladium complexes **1.28** (Figure 1.9), with a phosphorus in the 3-position, could be obtained by reaction of $[\text{Ag}_2(\mu\text{-(CHCO}_2\text{R)}_2\text{PPh}_2)_2]$ ($\text{R} = \text{Me}, \text{Et}$) with PdCl_2 to initially give the complex $[\text{Pd}\{(\text{CHCO}_2\text{R)}_2\text{PPh}_2\}_2]$, which subsequently reacts with neutral ligands to give the cationic complexes (**1.28**) (isolated as perchlorate salts).²⁷ The iridium analogues **1.29** (Figure 1.10) have also been reported, and were prepared by reaction of the appropriate ylides

anions $[\text{R}_2\text{P}(\text{CH}_2)_2\text{Li}]$ ($\text{R} = \text{Me}, \text{Ph}$) with Vaska's complex $[\text{IrCl}(\text{CO})(\text{PPh}_3)_2]$.²⁸ The X-ray crystal structure of **1.29** showed a non-planar metallacycle with a fold angle of $\sim 36^\circ$. An analogous cationic platinum(II) complex **1.30** (Figure 1.10) was similarly prepared.²⁹



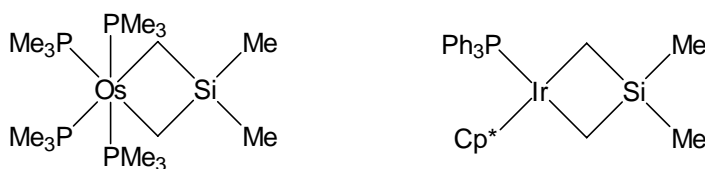
1.28 L-L = bipy, L = Py, dppe
R = CO₂Me, CO₂Et

1.29 R = Me, Ph

1.30

Figure 1.10

Finally, a few complexes with silicon as the heteroatom have been reported. The osmium acetato-complex $[\text{Os}\{\text{O}_2\text{CMe}\}_2(\text{PMe}_3)_4]$ when reacted with the alkylating agent $[\text{Mg}(\text{CH}_2\text{SiMe}_3)_2]$ gave, amongst other products, the metallacyclic complex **1.31** (Figure 1.11), resulting from C-H bond activation.³⁰ Contrary to the phosphorus ylide derivative **1.29**, **1.31** was shown to have an extremely planar ring system.³⁰ Similarly, the reaction of $[\text{Cp}^*\text{IrCl}_2(\text{PPh}_3)]$ and $[\text{Mg}(\text{CH}_2\text{SiMe}_3)_2]$, after thermolysis, gave the analogous iridium complex **1.32** (Figure 1.11).³¹

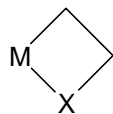


1.31

1.32

Figure 1.11

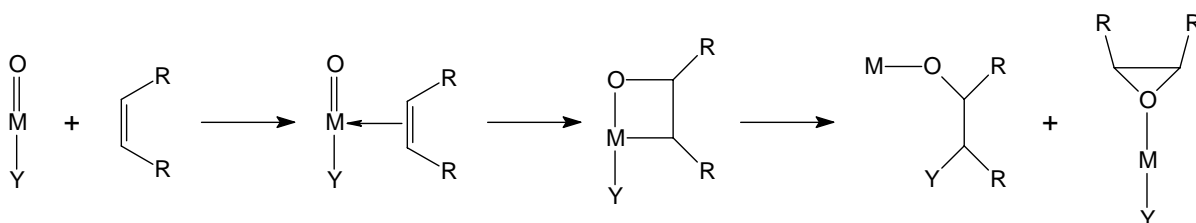
1.2.2 Metallacycles containing one M-C bond



Metallacyclobutanes with a heteroatom in the 2-position, thus bound directly to the metal centre, are much more common than in the 3-position (Section 1.2.1.3). The major classes of these systems are the 2-oxametallacyclobutanes and 2-azametallacyclobutanes.

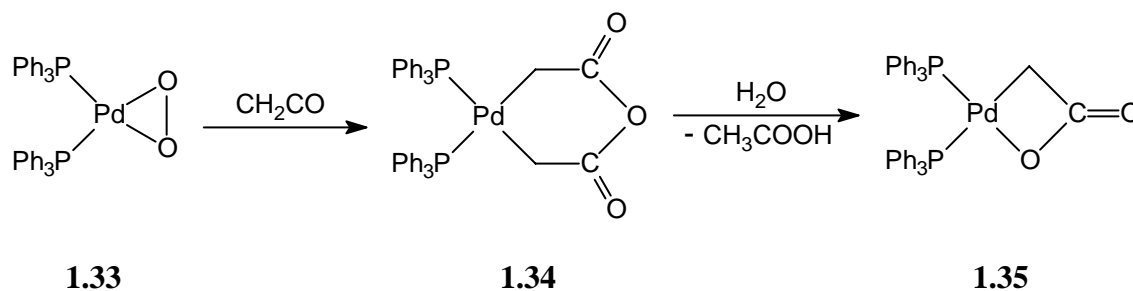
1.2.2.1 2-Oxametallacyclobutanes (includes metallalactones)

Metallalactones $[\overline{\text{M-C-C(O)-O}}]$ and 2-oxametallacyclobutanes $[\overline{\text{M-C-CRR'-O}}]$ are the most thoroughly researched of the $\overline{\text{M-C-C-X}}$ ring systems, and are the basis of a review regarding oxygen-transfer reactions, in which they may be an intermediate species (Scheme 1.1).³² Oxametallacyclobutanes have also been invoked as intermediates in several other reactions mediated by transition-metal complexes that have found widespread utility. Examples of this include carbonyl methylenation reactions,³³ asymmetric epoxidation of allylic alcohols,³³ and the metal-catalysed oxidation of olefins.³⁴

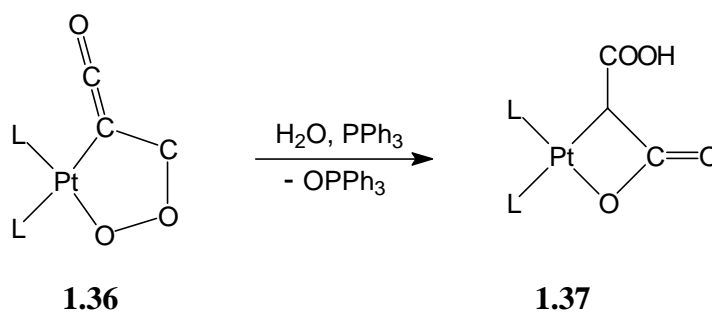


Scheme 1.1

Probably the first reported metallalactone (1972) was prepared from the reaction of the peroxopalladium complex **1.33** and ketene (CH_2CO) to give the complex **1.34**, which subsequently underwent hydrolysis to give the palladalactone system **1.35** and acetic acid (Equation 1.8).³⁵ A platinum analogue was synthesised from the dioxometallic adduct **1.36**, which, when reacted with water and triphenylphosphine, gave the platinalactone **1.37** (Equation 1.9).³⁶

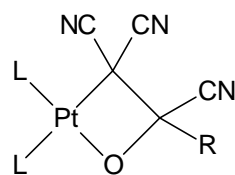


Equation 1.8

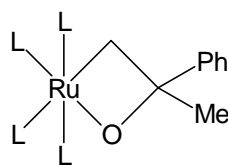


Equation 1.9

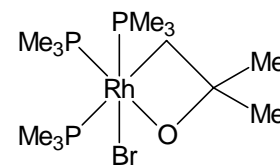
The 2-oxametallabutanes **1.38** (Figure 1.12) were prepared by the oxidative addition of tetra- and tricyano-substituted ethylene oxides (epoxides) to $[\text{PtL}_4]$ [$\text{L} = \text{PPh}_3, \text{P}(p\text{-MeC}_6\text{H}_4)_3, \text{AsPh}_3$].³⁷ The ruthenium oxametallacyclobutane **1.39** was prepared from the reaction of $[(\eta^2\text{-C}_6\text{H}_4)\text{RuL}_4]$ ($\text{L} =$ tertiary phosphines) with acetone, and the reactivity of this complex has been extensively explored.³³ A rhodium system has been formed by oxidative addition of 2-hydroxy-2-methyl-bromopropane ($\text{HO}(\text{CMe}_2\text{CH}_2\text{Br})$) to $[\text{RhCl}(\text{PMe}_3)_3]$ to give the β -hydroxy complex $[(\text{PMe}_3)_3\text{RhBrCl}\{\text{CH}_2\text{CMe}_2\text{OH}\}]$ which, when deprotonated with $[(\text{Me}_3\text{Si})_2\text{N}]\text{K}$, gave the rhodaoxacyclobutane complex **1.40**.³⁸



1.38 [$\text{L} = \text{PPh}_3, \text{P}(p\text{-MeC}_6\text{H}_4)_3, \text{AsPh}_3$; $\text{R} = \text{H}, \text{CN}$]



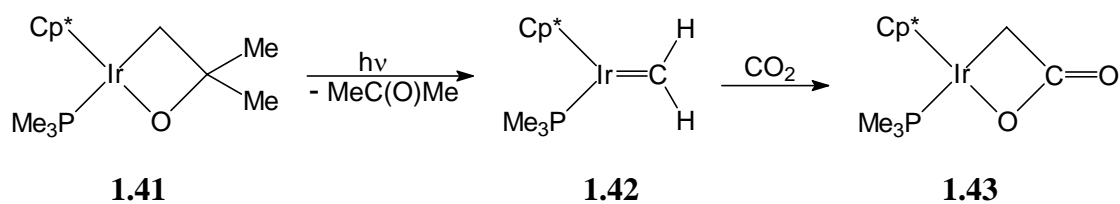
1.39 $\text{L} =$ tertiary phosphines



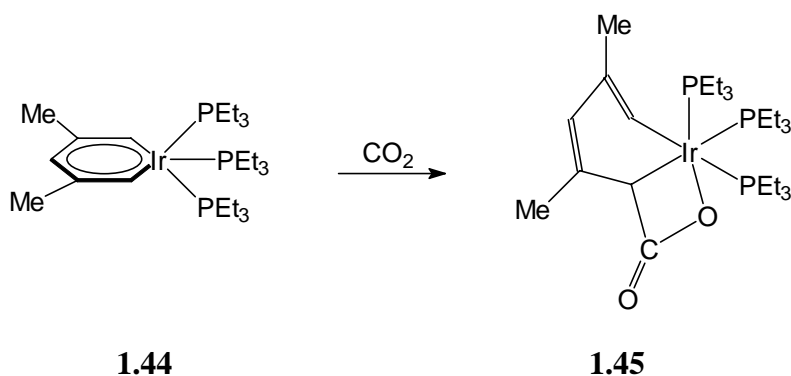
1.40

Figure 1.12

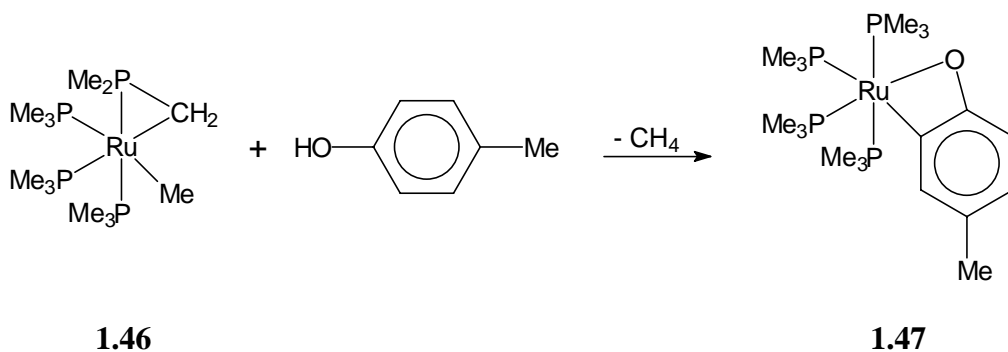
The iridium derivative **1.41**, containing the iridaoxetane ring, was synthesised by the UV irradiation of $[\text{Cp}^*(\text{PMe}_3)\text{IrH}_2]$ and butanol, followed by treatment with chloroform and a base.³⁹ The reactivity of this system was also ascertained, and UV exposure of **1.39** led to the carbene complex **1.42** which, when treated with carbon dioxide, resulted in the iridalactone complex **1.43** (Equation 1.10).⁴⁰

*Equation 1.10*

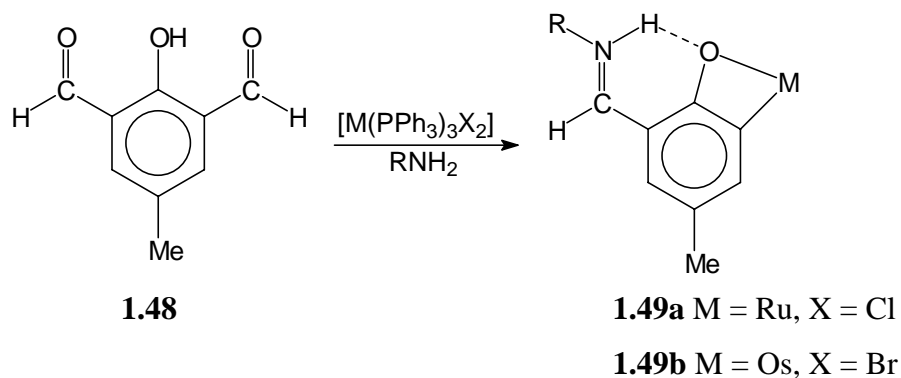
Treatment of the iridium-based metallabenzene complex **1.44** with carbon dioxide, led to the derivative **1.45**, also containing a iridalactone ring (Equation 1.11).⁴¹

*Equation 1.11*

The complexes are not restricted only to metallacyclobutane derived systems, and orthometallated-type complexes, also containing $\overline{\text{M-C-C-O}}$ rings, have been reported. The reaction of the cyclometallated ruthenium complex **1.46** with *p*-cresol resulted in orthometallation, to give **1.47** and methane (Equation 1.12).⁴² The reactivity of **1.47** towards carbon monoxide and dioxide has been investigated, and both were found to insert into the Ru-C bond as opposed to Ru-O.⁴³

*Equation 1.12*

Lastly, ruthenium(II) and osmium(II) systems derived from **1.48** (Equation 1.13) have been extensively researched.⁴⁴⁻⁴⁶ Reaction of $[\text{RuCl}_2(\text{PPh}_3)_3]$ or $[\text{OsBr}_2(\text{PPh}_3)_3]$ with **1.48** in the presence of a primary amine, gives the respective zwitterionic complexes **1.49a** and **1.49b**, via an aldehyde decarbonylation process (Equation 1.13).

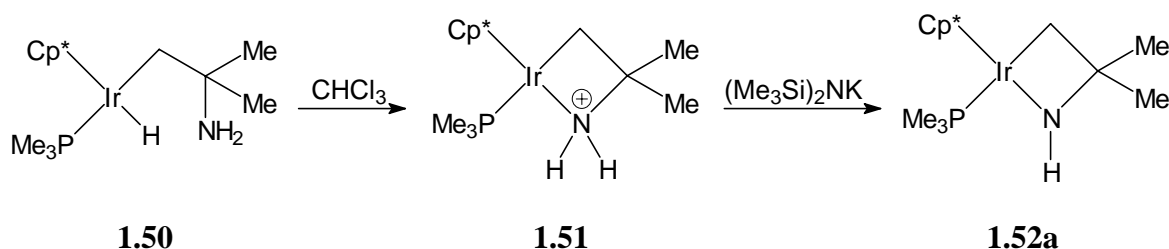
*Equation 1.13*

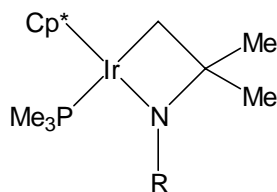
Unlike the isoelectronic metallacyclobutan-3-one complexes, the metallacycles in all the metallalactones and oxametallacyclobutanes reported to date have been planar, and show no unusual bond lengths or angles, indicating that the bonding in these systems is primarily σ -like.

1.2.2.2 2-Azametallacyclobutanes

2-Azametallacyclobutane complexes, incorporating a nitrogen atom in the 2-position of the metallacycle, are even more scarce than their isoelectronic oxygen counterparts. Nevertheless, a few of examples have been reported.

In a preparation analogous to **1.41**, $[\text{Cp}^*(\text{PMe}_3)\text{IrH}_2]$, when exposed to UV light in the presence of *tert*-butylamine, gives the complex **1.50**. Treatment of this complex with chloroform gave the ammonium salt **1.51** (isolated as the chloride salt) which, after reaction with base $[(\text{Me}_3\text{Si})_2\text{N}]\text{K}$, gave the neutral 2-azairidacyclobutane complex **1.52a** (Equation 1.14).⁴⁷ This complex, when reacted with carbon dioxide or *tert*-butyl isocyanate, gave the azametallacyclobutane derivatives **1.52b** or **1.52c** respectively (Figure 1.13).⁴⁷

*Equation 1.14*



1.52b R = C(O)OH; **1.52c** C(O)NHBu^t

Figure 1.13

The preparation described in Section 1.2.2.1 for the synthesis of the ruthenium complex **1.47** can also be applied for the formation of the analogous amide complex. Thus, reaction of **1.46** with aniline gives the corresponding orthometallated derivative (Figure 1.14).⁴⁸ The reactivity of this complex has also been investigated (see also Chapter Four, Section 4.1).

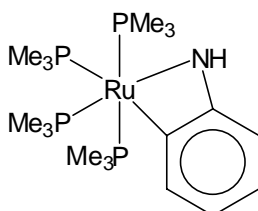
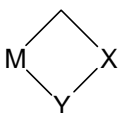
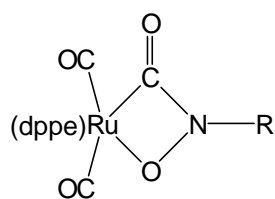


Figure 1.14

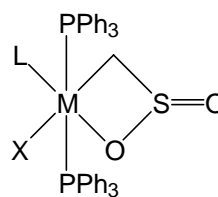
1.2.2.3 Metallacyclobutanes containing two heteroatoms in the 2- and 3-positions



Surprisingly few examples of four-membered ring systems of the type $\overline{\text{M-C-X-Y}}$ [where X and Y are any non-carbon (and non-transition-metal) atoms], have been synthesised. The ruthenium complexes **1.53** (Figure 1.15) were formed from the reaction of $[(\text{dppe})\text{Ru}(\text{CO})_3]$ and aromatic nitroso-compounds $[\text{RNO}$ (R = *o*-tolyl, *p*-chlorophenyl, 2,5-dimethylphenyl)].⁴⁹ The metallacyclic ring of this complex is planar. The reaction of the osmium(III) and iridium(III) carbene complexes $[(\text{ON})\text{OsCl}(=\text{CH}_2)(\text{PPh}_3)_2]$ and $[(\text{ON})\text{IrCl}(=\text{CH}_2)(\text{PPh}_3)_2]$ with sulfur dioxide gave **1.54a** and **1.54b**, respectively.⁵⁰



1.53 R = *o*-tolyl, *p*-chlorophenyl,
2,5-dimethylphenyl

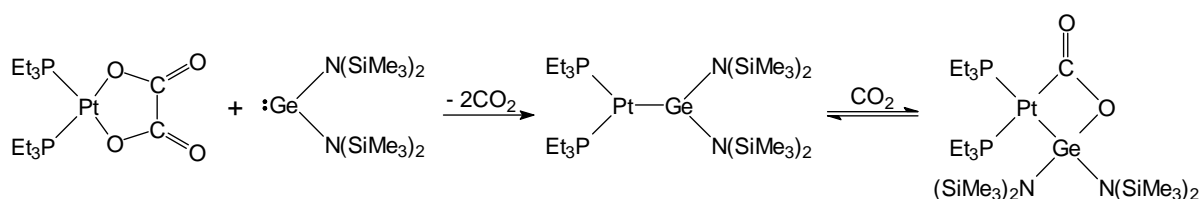


1.54a M = Os; L = NO; X = Cl

1.54b M = Ir; L = CO; X = I

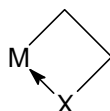
Figure 1.15

A metallacycle containing germanium has also been synthesised (and characterised crystallographically), as described by Equation 1.15.⁵¹



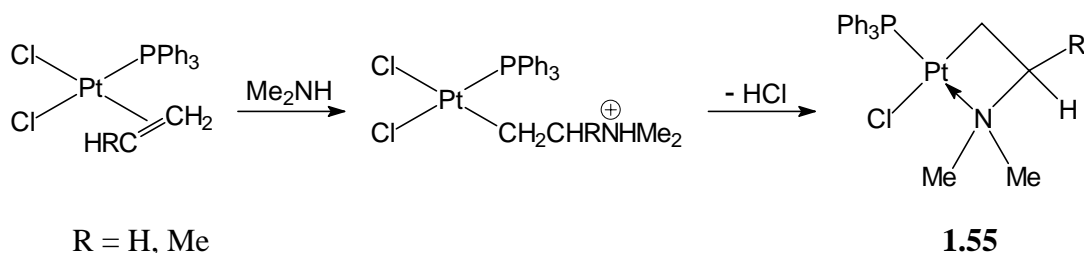
Equation 1.15

1.2.2.4 Cyclometallated complexes with a neutral donor

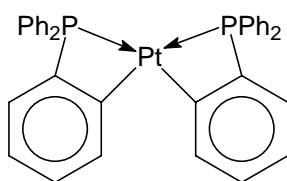


A number of monoanionic four-membered ring cyclometallated complexes with a neutral donor group have been described, and all are derived from nitrogen or phosphorus. Although these complexes are not directly relevant to the work presented in this thesis, they strictly are metallacycles, and thus warrant some discussion, although this is restricted to platinum(II) examples.

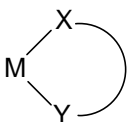
The cycloplatinated complexes **1.55** (R = H, Me), containing a nitrogen donor atom, were prepared from the amination of platinum complexes containing co-ordinated mono-olefins according to Equation 1.16.⁵² Four-membered nitrogen-donor cyclometallated complexes of the platinum-group metals are extremely scarce, with possibly only two other examples reported to date (both palladium systems).^{53,54}

**Equation 1.16**

Much more numerous are cyclometallated complexes incorporating a phosphorus donor. A representative example containing two such metallacycles is shown in Figure 1.16, prepared from $[\text{PtCl}_2(\text{SEt}_2)_2]$ and *ortho*-lithiated triphenylphosphine (*o*- $\text{LiC}_6\text{H}_4\text{PPh}_2$) in diethyl ether.⁵⁵

**Figure 1.16**

1.2.3 Metallacycles containing no M-C bonds



Four-membered metallacyclic complexes, of the type shown above, where X and Y are any non-transition-metal element excluding carbon, initially seem numerous. However the majority are those where $X = Y = \text{S, O or N}$, and surprisingly few examples where $X \neq Y$. A discussion of this class of compound follows, although neutral donor and monoanionic metallacyclic complexes, of which there are many examples, have been excluded for brevity.

1.2.3.1 $\overline{\text{M-O-C-O}}$ complexes

Complexes formally derived from the carbonate dianion (CO_3^{2-}) are probably the most extensively described system for the four-membered $\overline{\text{M-X-E-Y}}$ complexes ($X, Y \neq \text{C}$). Indeed, the first example was (inadvertently) prepared in 1961 by reaction of $[\text{Pt}(\text{PPh}_3)_4]$ and hydrogen gas(!).⁵⁶ The white precipitated complex was initially thought to be the hydrido complex $[\text{PtH}_2(\text{PPh}_3)_2]$, but was later characterised (crystallographically) as the carbonato complex (Figure 1.17), presumably formed from adventitious oxygen and carbon dioxide in

the hydrogen gas used.⁵⁷ The latter was a known impurity in commercial hydrogen gas of the time.

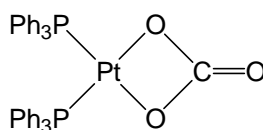
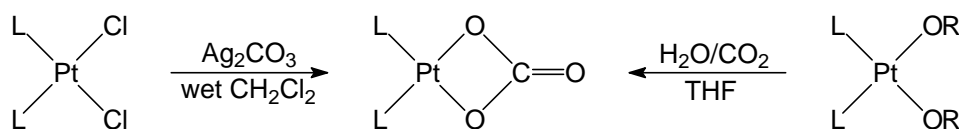


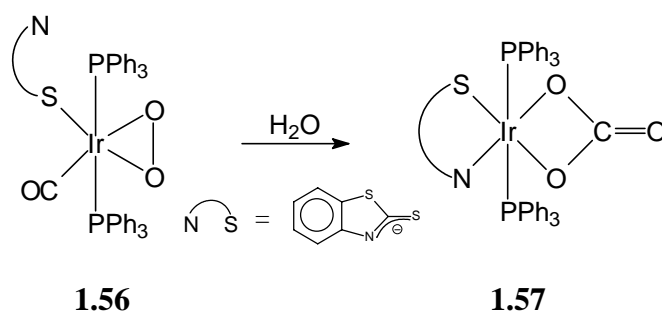
Figure 1.17

More common and general preparative methods involve either the reaction of a metal dihalide complex with silver(I) carbonate (Ag_2CO_3) [which simultaneously acts a halide abstracting agent (see also Section 1.3) and the source for carbonate dianions], or by treating the corresponding dioxygen complex with carbon dioxide (Equation 1.17).⁵⁸ The methodology has also been successfully applied to give palladium analogues.⁵⁸ Surprisingly, for the other platinum(II) group metals, carbonato complexes appear to be much rarer. An iridium example has been prepared from an $\eta^2\text{-O}_2$ complex **1.56**, which, when exposed to water, migrates the carbonyl ligand to form the carbonato complex **1.57** (Equation 1.17).⁵⁹



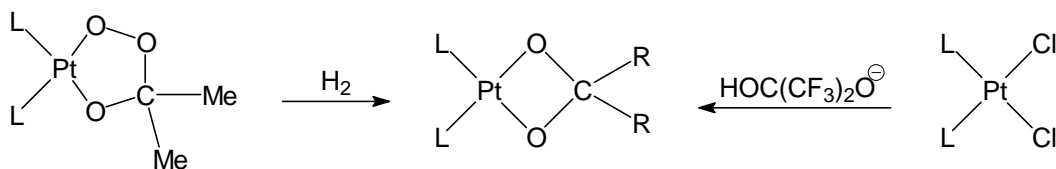
L = various tertiary phosphines

Equation 1.17

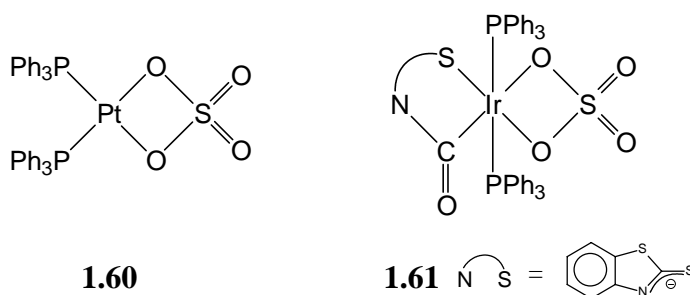
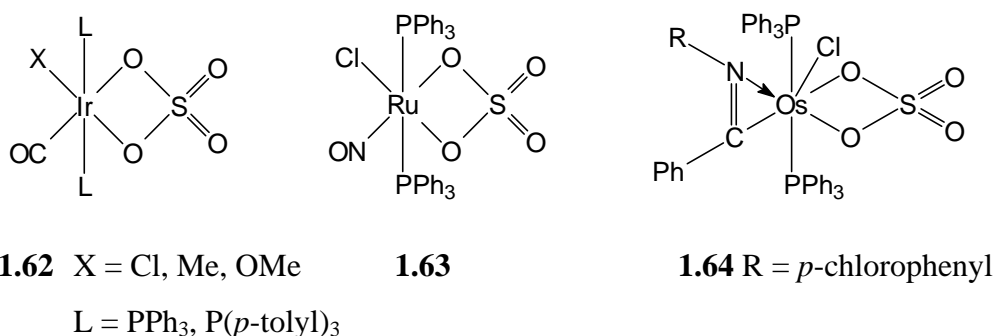


Equation 1.18

Diolato complexes of the type $\overline{\text{M-O-CR}_2\text{-O}}$ have been synthesised by two routes. Reduction of the peroxo ring complex **1.58** with hydrogen gives the complex **1.59a** (Equation 1.19),⁶⁰ whereas the trifluoromethyl analogue **1.59b** was prepared by reaction of hexafluoroacetone hemiacetal [$\text{HO}(\text{CF}_3)_2\text{O}^-$] with L_2PtCl_2 (L = tertiary phosphine).⁶¹

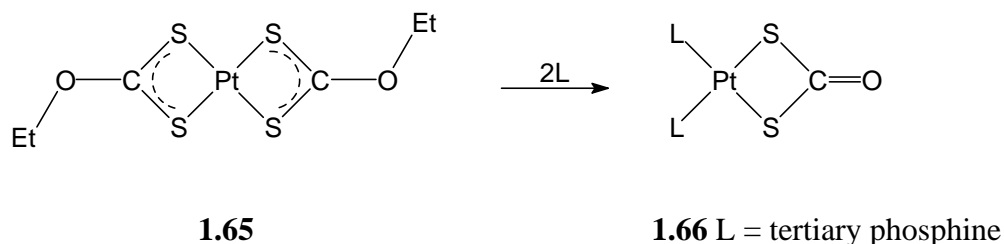
**1.58****1.59a** R = Me; L = tertiary phosphines**1.59b** R = CF₃; L = tertiary phosphines**Equation 1.19**

The other major class of $\overline{\text{M-O-X-O}}$ metallacycles are the η^2 -sulfato complexes, and a large number of such complexes have been reported. Like the platinum carbonato system, the analogous reaction of silver(I) sulfate (Ag_2SO_4) with *cis*-[PtCl₂(PPh₃)₂] readily yields the sulfato complex **1.60** (Figure 1.18).⁶² Sulfato complexes are also common for the other platinum group metals, and a common synthesis is via the apparently quite general reaction of η^2 -O₂-complexes with sulfur dioxide. The compounds **1.61-1.64** (Figure 1.19) were prepared using this methodology.^{59,63-66}

**1.60****1.61** N S = **Figure 1.18****1.62** X = Cl, Me, OMe**1.63****1.64** R = *p*-chlorophenylL = PPh₃, P(*p*-tolyl)₃**Figure 1.19****1.2.3.2 $\overline{\text{M-S-X-S}}$ (X = C, S, P) complexes**

Complexes derived from the dithiocarbonate dianion (S_2CO^{2-}), isoelectronic with the carbonato and sulfato complexes described above, are well known. The reaction of the

bis(dithiocarbonate) complex **1.65** with at least two mole equivalents of a tertiary phosphine, yields the corresponding dithiocarbonate derivative **1.66** (Equation 1.20).^{67,68}



Equation 1.20

The related dithiocarbimato systems $\overline{\text{M-S-C(NR)-S}}$ have also been described. The complex **1.67** (Figure 1.20) can, unsurprisingly, be prepared in an analogous fashion to the dithiocarbonate complex **1.66** above, by treating the bis(carbamate) complex $[\text{Pt}(\text{S}_2\text{CNEt}_2)_2]$ with excess tertiary phosphine.⁶⁷ An alternative method involving reaction of $[\text{MCl}_2\text{L}_2]$ (M = Pt, Pd; L = tertiary phosphines) with a primary amine and carbon disulfide has also been reported,⁶⁹ and is described in more detail in Chapter Four (Section 4.2.5). The reaction of palladium(0) complexes such as L_2Pd (L = tertiary phosphines) with ethoxycarbonyl isothiocyanate $[\text{EtOC(O)NCS}]$ also reportedly gives dithiocarbimato complexes **1.68**.⁷⁰

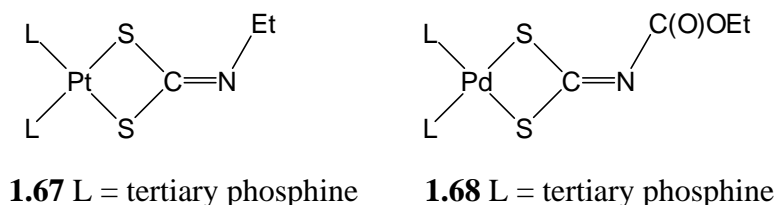


Figure 1.20

A more direct systematic synthesis of an $\overline{\text{M-S-C-S}}$ ring system was achieved by reacting the salt $\text{K}_2[\text{S}_2\text{CC}(\text{CO}_2\text{Et})(\text{CN})]$ with $[\text{PtCl}_2(\text{COD})]$, to yield the complex **1.69** (Figure 1.21).⁷¹ Similarly, $[\text{MCl}_2\text{L}_2]$ (M = Pt, Pd; L = tertiary phosphines), when reacted with HSC(S)CH=C(OH)Ph in the presence of base (sodium acetate), gave the complexes **1.70**.⁷²

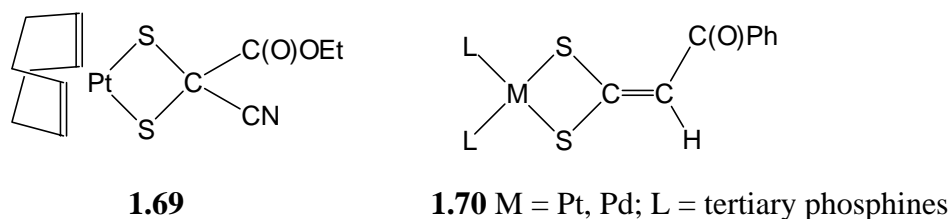
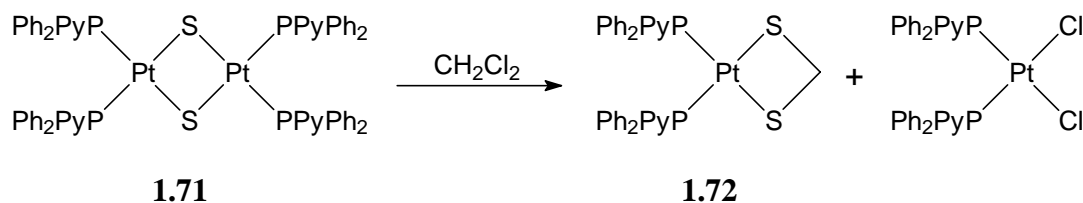


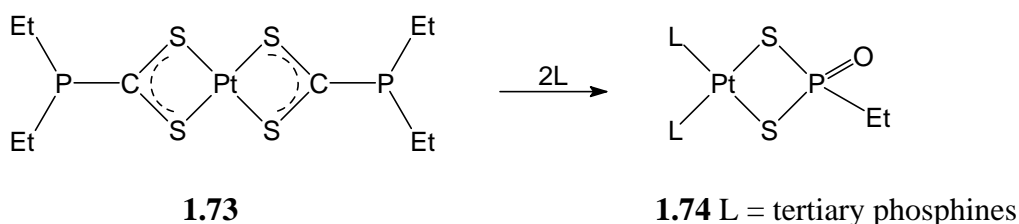
Figure 1.21

The first example of a completely unsubstituted dithiolato complex was surprisingly not reported until recently, from the unexpected reaction of the platinum sulfide dimer complex **1.71** with dichloromethane, to give **1.72** and the platinum(II) dihalide (Equation 1.21).



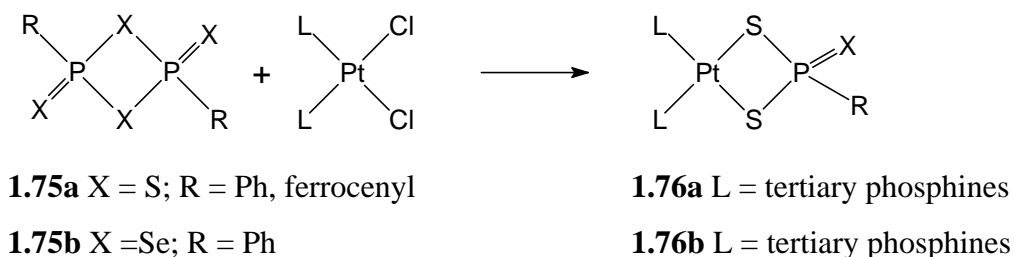
Equation 1.21

Much rarer are complexes involving a heteroatom other than carbon in the 3-position. An example prepared by a reaction analogous to that for the dithiocarbonate **1.66** described above, but using the phosphorus precursor **1.73**, gives the corresponding dithioplatingphosphetane complexes **1.74** (Equation 1.22).⁶⁸



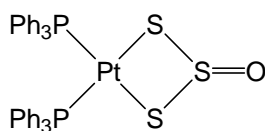
Equation 1.22

An interesting reaction involving the asymmetric cleavage of the $\overline{\text{P-S-P-S}}$ ring of **1.75a** with *cis*-[PtCl₂L₂] (L = various phosphines) also gives phosphetane complexes, **1.76a** (Equation 1.23).⁷³ The chemistry also works for the analogous selenium system **1.75b** to give **1.76b**.⁷⁴



Equation 1.23

Lastly, an example of a metallacycle incorporating three sulfur atoms has been reported. Treatment of *cis*-[Pt(SH)₂(PPh₃)₂] with sulfur dioxide gave the 3-oxotrisulfido complex **1.77** (Figure 1.22) and water.⁷⁵ In contrast to most of the other examples of $\overline{\text{M-S-X-S}}$ metallacycles, which are planar, the ring in **1.77** is puckered with a fold angle of 22.3°.⁷⁵

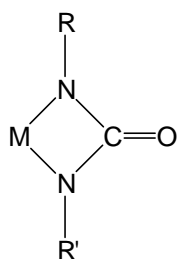


1.77

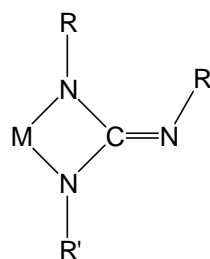
Figure 1.22

1.2.3.3 $\overline{\text{M-N-X-N}}$ (X = C, S) complexes

Complexes derived from the urea **1.78** or guanidine **1.79** dianions (Figure 1.23), incorporating the $\overline{\text{M-N-C-N}}$ metallacycle, are the basis of Chapters Two and Three respectively, and will not be further discussed in this chapter.



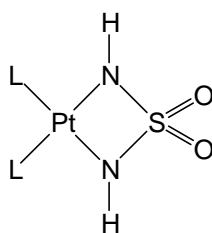
1.78



1.79

Figure 1.23

Excluding **1.78** and **1.79**, very few other instances of $\overline{\text{M-N-X-N}}$ rings systems have been reported. A rare example is the reaction of sulfamide [$\text{SO}_2(\text{NH}_2)_2$], liquid ammonia, and *cis*- $[\text{PtCl}_2\text{L}_2]$, which resulted in the (planar) platinacycle **1.80** (Figure 1.24).^{76,77}



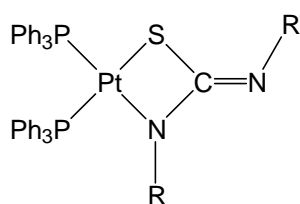
1.80

Figure 1.24

1.2.3.4 Other metallacycles containing two metal-bonded non-carbon heteroatoms

Included in this class are complexes formally derived from the thiourea dianion, and these are discussed in more detail in Chapter Six (Section 6.1). For the platinum-group metals, only

examples of platinum(II) derivatives are known. The diethylthioureaato complex **1.81a** (Figure 1.25) was prepared from the reaction of $[\text{Pt}(\text{hfac})(\text{PPh}_3)_2]$ (hfac = 1,1,1,5,5,5-hexafluoro-2,4-pentanedionate) with diethylthiourea.⁷⁸ The sodium salt of N-methyl-N'-cyanothiourea $[\text{MeNHC}(\text{S})\text{N}(\text{CN})]\text{Na}$, and base (triethylamine), has also been used to give the analogous complex **1.81b**.⁷⁹ A third example, **1.81c**, was formed directly from the 1,3-dianion of N,N'-diphenylthiourea (thiocarbanilide), by treating *cis*- $[\text{PtCl}_2(\text{PPh}_3)_2]$ with $[\text{PhNC}(\text{S})\text{NPh}]\text{Li}_2$ in THF.⁸⁰ In contrast to the complexes derived from urea dianions (**1.78**, see Chapter Two), for these complexes the softer sulfur, a better match for the soft metal centre, directs the coordination mode.



1.81a R = R' = Et

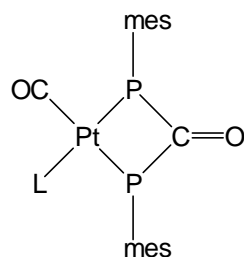
1.81b R = Me, R' = CN

1.81c R = R' = Ph

Figure 1.25

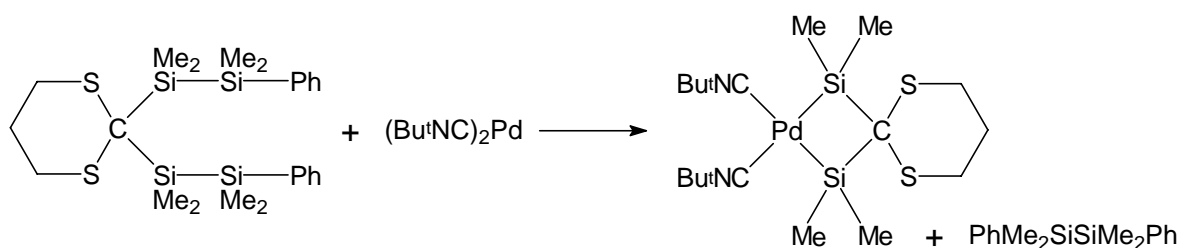
Complexes incorporating two metal-phosphorus bonds in a four-membered fashion as neutral donor complexes are, of course, extremely common, and countless systems involving the dppm [bis(diphenylphosphine)methane], $\text{Ph}_2\text{PCH}_2\text{PPh}_2$ ligand have been prepared. However, complexes formally derived from phosphorus *anions* are rare. Reaction of the platinum(0) complexes L_2Pt (L = various tertiary phosphines) with the phosphaketene mes-P=C=O (mes = 2,4,6-*tert*-butylphenyl), gave **1.82**, hitherto the only examples of mononuclear diphosphaureylene complexes.⁸¹ The compound is believed to be formed by decarbonylation of the phosphaketene by the neutral metal complex to give a phosphinimide fragment, which subsequently couples with a second cumulene to generate the diphosphaureylene ligand.

Equally novel is the dimethylsilano derivative **1.83**, formed as described by Equation 1.24.⁸² Also, Vaska's complex $[\text{IrCl}(\text{CO})(\text{PPh}_3)_2]$ readily reacts with tetramethyldisiloxane ($\text{Me}_2\text{HSiOSiHMe}_2$) to give **1.84** (Figure 1.27).⁸³



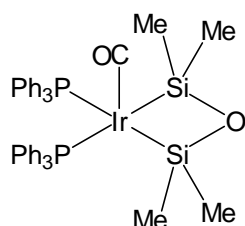
1.82 L = tertiary phosphine; mes = 2,4,6-Bu^t-C₆H₂

Figure 1.26



1.83

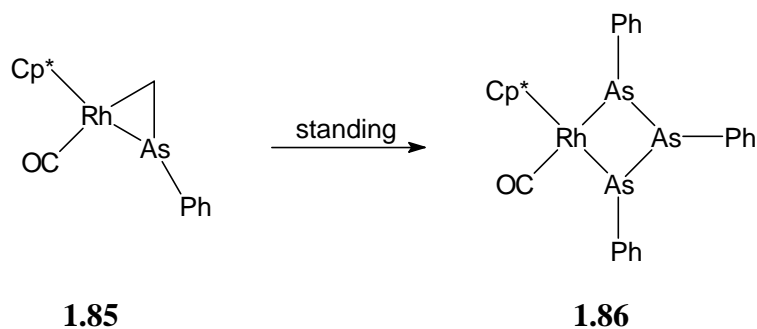
Equation 1.24



1.84

Figure 1.27

Finally, a very rare example of an $\overline{\text{M-As-As-As}}$ ring was formed by standing a solution of the cyclometallated rhodium complex **1.85**, which remarkably (and unexpectedly) gave **1.86** (Equation 1.25). No mechanism for its formation has been formulated. An X-ray study, showed the metallacycle is non-planar, with a fold-angle of 23.1°.



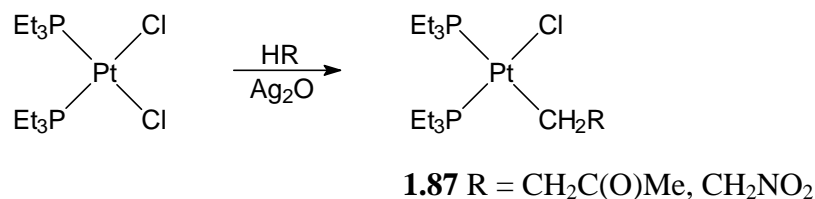
1.85

1.86

Equation 1.25

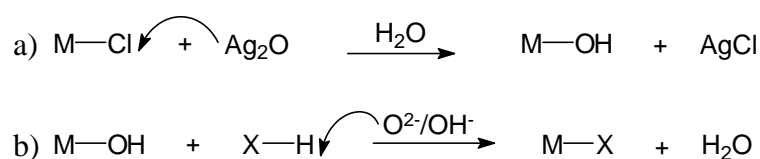
1.3 Synthesis of Metallacycles using Silver(I) Oxide

The first reported silver(I) oxide (Ag_2O) mediated synthesis was for the formation of the complexes **1.87** containing a Pt-C bond, by reaction of a platinum(II) dihalide $[\text{PtCl}_2(\text{PEt}_3)_2]$ with acetone or nitromethane (doubling as the solvents), in the presence of silver(I) oxide (Equation 1.26).⁸⁴ The diacetylide complex $[\text{Pt}\{\text{C}\equiv\text{CPh}\}_2(\text{PEt}_3)_3]$ was similarly prepared by reaction of $[\text{PtCl}_2(\text{PEt}_3)_2]$ and phenylacetylene in benzene.⁸⁴



Equation 1.26

The rationale for the development of the silver(I) oxide methodology, was that it was found that hydroxoplatinum complexes such as $[\text{PtMe}(\text{OH})(\text{dppe})]$ and *cis*- $[\text{Pt}(\text{OH})(\text{C}_6\text{F}_5)(\text{PPh}_3)_2]$ react with compounds containing acidic C-H groups, such as acetone, acetylacetone, acetonitrile or nitromethane,⁸⁵ and a method was sought to produce hydroxide complexes *in situ*. Silver(I) oxide is considered to simultaneously serve as a halide abstracting agent (since it is a source of Ag^+), and as a strong base (since it is source of O^{2-} and/or OH^-).⁸⁴ A tentative mechanism is given in Scheme 1.2, although this is almost certainly an oversimplification of the actual processes involved.



Scheme 1.2

Silver(I) oxide reactions are typically carried out in air without exclusion of water, indeed (as shown in Scheme 1.2) water is a reaction by-product. The only other by-product is silver(I) chloride, and this is concomitantly removed on filtration of the excess silver(I) oxide on work-up. These features render product isolation extremely convenient.

Most of the syntheses of the metallacyclic complexes reported in this thesis were achieved by use of silver(I) oxide. Compared with the vast range of metallacycles synthesised by alternative routes (described in Section 1.2), only a limited number compounds have been prepared using silver(I) oxide. This is somewhat surprising, since the silver(I) oxide route is

both extremely mild and moderately general. Only two groups have been actively involved in the utilisation of silver(I) oxide for the generation of metallacycles, these being Kemmitt *et al.*, and our own laboratory.

Almost all silver(I) oxide chemistry that has been carried out to date has been using platinum(II) and palladium(II) halide precursors, although there is no evidence suggesting other transition-metal dihalides would fail. Indeed, the research presented in Chapters Three and Five-Eight goes some way to demonstrate the wide applicability of the method. The solvent used for silver(I) oxide mediated synthesis is almost invariably dichloromethane, although again, there is no reason to assume that this is the only solvent for which the reactions work. The principle limitation of the method is the requirement of sufficiently acidic X-H groups on the organic precursor, which must eventually be deprotonated.

A review of the four-membered ring metallacycles successfully synthesised previously using the silver(I) oxide method follows.

1.3.1 Metallacyclobutanone (oxatrimethylenemethane complex)

The first instance (1984) of the application of silver(I) oxide to form metallacycles, was from the reaction of dimethyl acetonedicarboxylate $[(\text{MeO}_2\text{CCH}_2)_2\text{C}(\text{O})]$ with *cis*- $[\text{PtCl}_2(\text{PPh}_3)_2]$ in the presence of excess of silver(I) oxide, which readily afforded the platinum(II)cyclobutanone complex **1.88** (Figure 1.28) (also one of the complexes **1.13**, Section 1.2.1.2), in a 62% yield.⁸⁶ In spite of the success of this reaction, the analogous reaction of 1,5-diphenylpentane-1,3,5-trione $[\{\text{PhC}(\text{O})\text{CH}_2\}_2\text{C}(\text{O})]$ with *cis*- $[\text{PtCl}_2(\text{PPh}_3)_2]$ unexpectedly gave the dienediolate complex **1.89**.⁸⁷ The formation of this complex has been attributed to the extra stability imparted by the conjugation present in **1.89**, relative to the formation of a strained four-membered metallacycle.⁸⁷

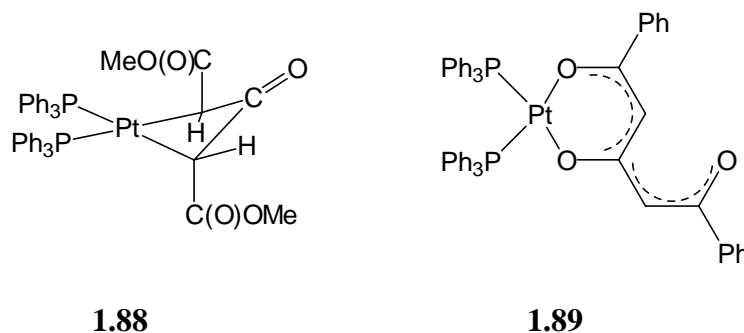
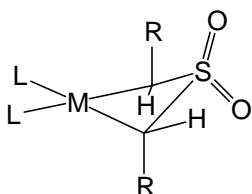


Figure 1.28

Thus, previous to the work in this thesis (Chapter Seven), **1.88** was the only example of a metallacyclobutanone derivative synthesised by the silver(I) oxide route.

1.3.2 Metallathietanes and metallaphosphetanes

A number of platina- and palladathietane-3,3-dioxide complexes (see also Section 1.2.1.3) have been prepared using the silver(I) oxide method. Treatment of the complexes *cis*-[PtCl₂L₂] or *trans*-[PdCl₂L₂] (L = various tertiary phosphines) with one equivalent of diphenacyl sulfone [$\{\text{PhC(O)CH}_2\}_2\text{S(O)}_2$] or bis(methyl carboxyl) sulfone [(MeCO₂CH₂)₂C(O)] and an excess of silver(I) oxide gave the platinum and palladium(II) complexes **1.90a** and **1.90b** respectively.^{87,88}

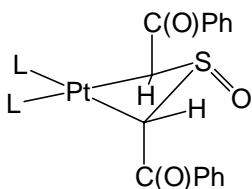


1.90a M = Pt; L = tertiary phosphine; R = PhC(O), MeCO₂

1.90b M = Pd; L = tertiary phosphine; R = PhC(O), MeCO₂

Figure 1.29

Examples of metallathietaneoxide complexes have also been prepared via the silver(I) oxide route. Reaction of diphenacyl sulfoxide [$\{\text{PhC(O)CH}_2\}_2\text{S(O)}$], *cis*-[PtCl₂L₂] (L = PPh₃, PMePh₂ or PMe₂Ph) and silver(I) oxide, affords high yields of the platinathietane-3-oxide complexes **1.91** (Figure 1.30).⁸⁹

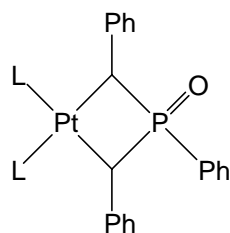


1.91 L = PPh₃, PMePh₂ or PMe₂Ph

Figure 1.30

Phosphorus analogues of the metallathietanes have also been synthesised. The silver(I) oxide mediated reaction of *cis*-[PtCl₂L₂] (L = tertiary phosphines, L₂ = COD) and the phosphine oxide [PhC(O)CH₂]₂P(O)(Ph) gives the expected platina-3-phenylphosphetane-3-oxide complexes (Figure 1.31).⁹⁰ X-ray analysis shows the metallacycle, as expected, is puckered,

with a fold-angle of 31.1° . This is only slightly less than that of the platinathietane complex **1.91** ($L = PPh_3$), for which a fold-angle of 36.7° was measured.⁸⁹



$L =$ tertiary phosphines, $L_2 =$ COD

Figure 1.31

1.3.3 Metallalactones

Metallalactones (see Section 1.2.2.1) can also be synthesised by silver(I) oxide mediated reactions, although via a somewhat unexpected route. The reaction of *cis*-[PtCl₂(PPh₃)₂], silver(I) oxide and dimethyl malonate or diethyl malonate [RO₂CCH₂CO₂R (R = Me, Et)] affords the platinolactone complexes **1.92**.⁹¹ The mechanism for the synthesis is unclear, although it is speculated that the initial formation of a platinum C-malonato species **1.93** may be involved. Alternatively, an initial oxide promoted hydrolysis of one of the ester groups, followed by platinum carboxylate formation and subsequent cyclisation, is also plausible.⁹¹

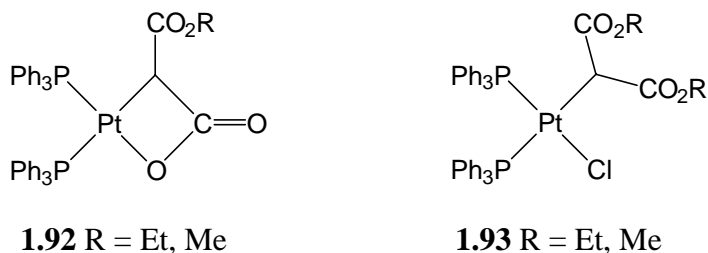
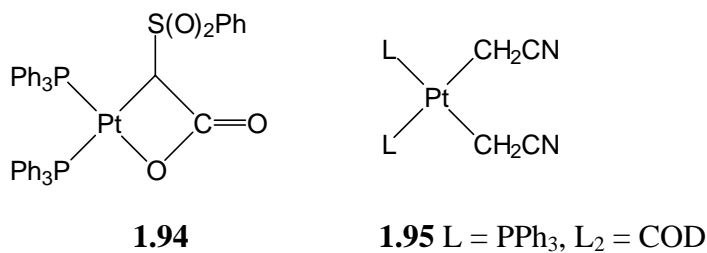


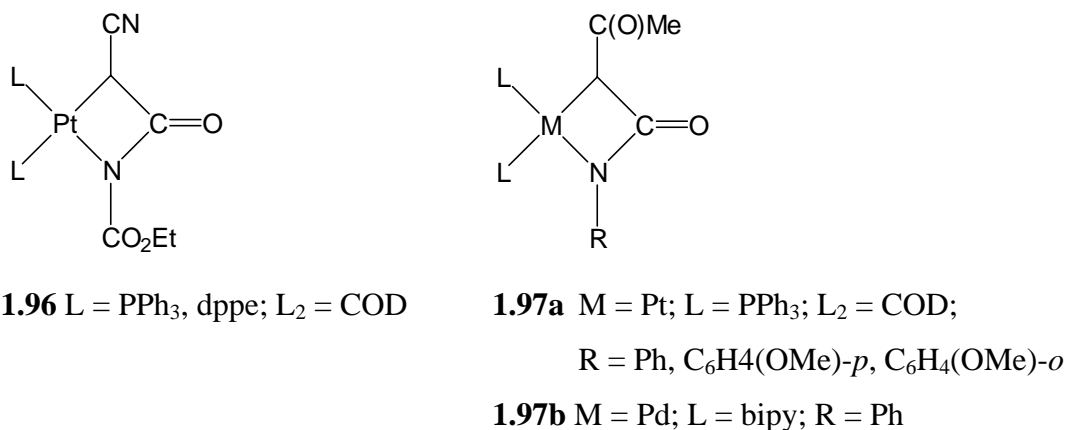
Figure 1.32

A more systematic synthesis of metallalactones has (and still is) being pursued, although this has hitherto met with only limited success. (Phenylsulfonyl)acetic acid [PhS(O)₂CH₂C(O)OH], *cis*-[PtCl₂(PPh₃)₂] and silver(I) oxide were refluxed for in dichloromethane for 16 hours and stirred at room temperature for an additional 72 hours. Analysis of the crude reaction mixture revealed ~50% of the platinolactone **1.94** (Figure 1.33), but also three other unidentified species.⁹¹ Remarkably, the reaction of cyanoacetic acid [NCCH₂C(O)H], *cis*-[PtCl₂L₂] ($L = PPh_3$, $L_2 = COD$) and silver(I) oxide results in decarboxylation of the cyanoacetic acid, and formation of the complexes **1.95**.⁹²

*Figure 1.33*

1.3.4 Metallalactams

Four-membered metallalactams, with metallacycles analogous to **1.52** (Section 1.2.2.2), are extremely rare for the platinum-group metals. Nonetheless, they can be readily prepared by the silver(I) oxide mediated reaction of N-cyanoacetylurethane [EtOC(O)NHC(O)CH₂(CN)] and *cis*-[PtCl₂L₂] (L = PPh₃; L₂ = COD, dppe) to give the corresponding platinalactams **1.96** (Figure 1.34).⁹³ The success of this work spurred further research, and the pallada- and platinalactams **1.97** derived from acetacetanilide [PhNHC(O)CH₂C(O)Me] and *o*- and *p*-acetoacetanilide [(MeO)C₆H₄NHC(O)CH₂C(O)Me] were synthesised analogously.⁹⁴

*Figure 1.34*

Interestingly, X-ray structural determinations for **1.96** (L₂ = COD) and the palladium system **1.97b**, show somewhat contrasting results regarding the puckering of the metallacycles. The complex **1.96** (L₂ = COD) shows an essentially planar metallacycle (fold-angle 2.5°),⁹³ whereas **1.97b** showed significant puckering (fold-angle 17.5°).⁹⁴ The discrepancy between the two systems suggests the puckering in **1.97b** is probably not from a η^3 -allylic contribution to the bonding (as invoked for the metallacyclobutanones, see Section 1.2.1.2), but rather to relieve steric strain caused by the interaction of the metallacycle C(O)Me and N-phenyl substituents.⁹⁴

Some evidence as to the nature of the intermediates involved in the formation of the metallalactams emerged from studies of palladium complexes analogous to the platinum system **1.96**. When $[\text{PdCl}_2(\text{dppe})]$, N-cyanoacetylurethane $[\text{EtOC(O)NHC(O)CH}_2(\text{CN})]$ and silver(I) oxide were reacted, the expected four-membered palladalactam **1.98** (Figure 1.35) resulted.⁹⁵ However, when $[\text{PdCl}_2(\text{PPh}_3)_2]$ was used (in place of $[\text{PdCl}_2(\text{dppe})]$), the monodentate amide complex **1.99** was isolated in high yield.⁹⁵ The latter was fully characterised by an X-ray structural analysis, which showed the N-bonded cyanoacetylurethane ligand was virtually perpendicular to the (square-planar) palladium coordination sphere.

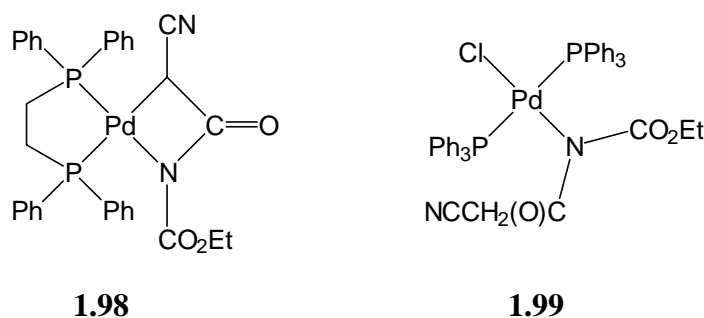
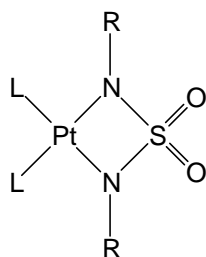


Figure 1.35

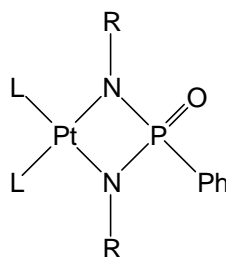
1.3.5 Metallacycles containing no M-C bonds

More unusual metallacycles, that do not contain metal-carbon linkages, have also been synthesised using the silver(I) oxide method. Previous to the work presented in this thesis, only two types of metallacycles containing two metal-nitrogen bonds had been synthesised by the silver(I) oxide route. The complexes **1.100** and **1.101** (Figure 1.36) were prepared from *cis*- $[\text{PtCl}_2\text{L}_2]$ (L, L₂ = tertiary phosphines, COD) and, respectively, the sulfamides $[\text{RNHS(O)}_2\text{NHR}]$ (R = H, Ph) or the phenylphosphonic diamides $[\text{RNHP(O)(Ph)NHR}]$ (R = H, Ph, *p*-nitrophenyl).^{90,96}

X-ray structure determinations have been carried out on both systems. Complex **1.100** (L₂ = COD) has a two-fold rotation axis about the Pt...S bond, and thus the metallacycle is, necessarily, absolutely planar.⁹⁶ This result is contrary to structural studies of analogous metallathietane complexes **1.90**, which show markedly puckered metallacyclic rings.⁸⁷ Similarly, the four-membered metallacycle of **1.101** (L = PPh₃) is also almost planar, with a fold-angle of only 6.2°.⁹⁶



1.100 L, L₂ = tertiary phosphines, COD;
R = H, Ph

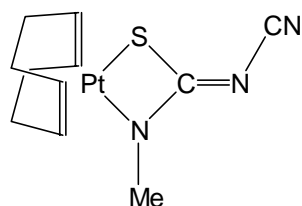


1.101 L, L₂ = tertiary phosphines, COD
R = H, Ph, *p*-nitrophenyl

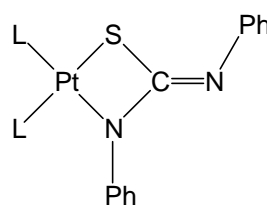
Figure 1.36

Preliminary studies showed the complexes **1.100** and **1.101** display quite a high degree of reactivity towards dimethyl acetylenedicarboxylate,⁹⁰ which readily singly insert into the metallacycles to give the six-membered ring insertion products. Chapter Four describes this work in more detail. Further papers expanding on this research have not yet appeared.

The cyclo-octa-1,5-diene analogue of the complex **1.81b**, could be synthesised using the silver(I) oxide method, from [PtCl₂(COD)] and the sodium salt of N-methyl-N'-cyanothiourea to give complex **1.81d** (Figure 1.37).⁷⁹ A number of additional derivatives of **1.81c** were prepared by simple displacement of the COD ligand by various tertiary phosphines. The complexes **1.81e**, which includes **1.81d**, could be formed from *cis*-[PtCl₂L₂] (L = tertiary phosphines), free N,N'-diphenylthiourea (thiocarbanilide) [PhNHC(S)NPh], and silver(I) oxide.⁸⁰ Although isoelectronic to the oxatrimethylenemethane complexes **1.13** and **1.88** (which show a high degree of puckering), these “thiadiazatrimethylenemethane” ring systems have been shown crystallographically to be planar.^{79,80}



1.81d

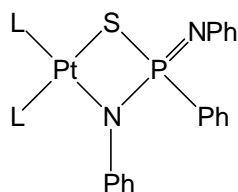


1.81e L = tertiary phosphines

Figure 1.37

Metallacycles related to **1.81**, containing a phosphorus atom in place of carbon, could be prepared using *cis*-[PtCl₂L₂] (L = tertiary phosphines), N,N',P-triphenylphosphonothioic diamide [PhNHP(S)(Ph)NHP] (a sulfur analogue of the precursor used for the synthesis of **1.101**) and silver(I) oxide, to give the species **1.102** (Figure 1.38).⁸⁰ As observed for the

thiourea derivatives (see Section 1.2.3.4), the softer sulfur directs the co-ordination mode (cf. complex **1.101**).



1.102

Figure 1.38

The reactivity of **1.102** was tested with various unsaturated molecules (such as phenyl isocyanate, carbon dioxide, carbon disulfide), and although reactions did occur, none of the reagents were observed to insert into either the platinum-sulfur or -nitrogen linkages.⁸⁰

Obviously the silver(I) oxide methodology is not limited only to the formation of four-membered ring metallacycles, and a number of complexes with larger (> four-membered) ring systems have been prepared by the silver(I) oxide route. Although these lie somewhat outside of the scope of this introductory review, Chapter Eight demonstrates the formation of six-membered ring systems formally derived from salicylate and thiosalicylate dianions.

References

- 1 *The Chemistry of the Metal-Carbon Bond*, Ed. F.R. Hartley, Wiley, New York, (1987), Vol. 4, Chapters 7-9.
- 2 *Principles and Applications of Organotransition Metal Chemistry*, Ed. A. Kelly, University Science, Mill Valley CA, (1987), Chapters 9 and 16.
- 3 S.D. Chappell and D.J. Cole-Hamilton, *Polyhedron*, 11-12 (1982) 739.
- 4 T.J. Katz, *Adv. Organomet. Chem.*, 16 (1977) 283.
- 5 R.H. Grubbs in *Comprehensive Organometallic Chemistry*, Ed. G. Wilkinson, F.G.A. Stone, E.W. Abel, Pergamon Press, New York (1982), Vol. 8, 499-551.
- 6 K.J. Ivin, *Olefin Metathesis*, Academic Press, New York, (1983).
- 7 P.W. Jennings and L.L. Johnson, *Chem. Rev.*, 94 (1994) 2241.
- 8 R.J. Puddephatt, *Coord. Chem. Rev.*, 33 (1980) 149.
- 9 C.F.H. Tipper, *J. Chem. Soc.*, (1955) 2045.
- 10 S.E. Binns, R.H. Cragg, R.D. Gillard, B.T. Heaton and M.F. Pilbrow, *J. Chem. Soc. (A)*, (1969) 1227.
- 11 G.W. Littlecott, F.J. McQuillin and K.G. Powell, *Inorg. Synth.*, 16 (1976) 113.
- 12 M. Lenarda, R. Ros, M. Graziani and U. Belluco, *J. Organomet. Chem.*, 65 (1974) 407.
- 13 G. Pellizer, M. Graziani, M. Lenarda and R. Ganzerla, *Inorg. Chim. Acta*, 145 (1988) 219.
- 14 P. Foley, R. Dicosimo and G.M. Whitesides, *J. Am. Chem. Soc.*, 102 (1980) 6713.
- 15 R. Dicosimo and G.M. Whitesides, *J. Am. Chem. Soc.*, 104 (1982) 3601.
- 16 S.A. Benyunes, L. Brandt, M. Green and A. Parkins, *Organometallics*, 10 (1991) 57.
- 17 R.D.W. Kemmitt and M.R. Moore, *Transition Met. Chem.*, 18 (1993) 348.
- 18 M.D. Jones, R.D.W. Kemmitt, J. Fawcett and D.R. Russell, *J. Chem. Soc., Chem. Commun.*, (1986) 427.
- 19 P.A. Corrigan and R.S. Dickson, *Aust. J. Chem.*, 32 (1979) 2147.
- 20 J.P. Visser and J.E. Ramakers-Blom, *J. Organomet. Chem.*, 44 (1972) C63.
- 21 J.F. Hoover and J.M. Stryker, *J. Am. Chem. Soc.*, 111 (1989) 6466.
- 22 J.F. Hoover and J.M. Stryker, *Organometallics*, 8 (1989) 2973.
- 23 R. McCrindle, G. Ferguson and A.J. McAlees, *J. Chem. Soc., Chem. Commun.*, (1990) 1524.
- 24 Y. Yamamoto and H. Yamazaki, *J. Chem. Soc., Dalton Trans.*, (1989) 2161.
- 25 J.S. Lai, R.F. Wu, I.J.B. Lin, M.C. Cheng and Y. Wang, *J. Organomet. Chem.*, 393 (1990) 431.

-
- 26 K.W. Chiu, J. Fawcett, W. Henderson, R.D.W. Kemmitt and D.R. Russell, *J. Chem. Soc., Dalton Trans.*, (1987) 733.
- 27 J. Vicente, M-T. Chicote, I. Saura-Llamas, M-J. López-Muñoz and P.G. Jones, *J. Chem. Soc., Dalton Trans.*, (1990) 3683.
- 28 M.J. Hostetler, M.D. Butts and R.G. Bergman, *Inorg. Chim. Acta*, 198 (1992) 377.
- 29 *Chem. Ber.*, 113 (1980) 1145.
- 30 T. Behling, G.S. Girolami, G. Wilkinson, R.G. Somerville and M.B. Hursthouse, *J. Chem. Soc., Dalton Trans.*, (1984) 877.
- 31 L. Andreucci, P. Diversi, G. Ingrosso, A. Lucherini, F. Marchetti, V. Adovasio and M. Nardelli, *J. Chem. Soc., Dalton Trans.*, (1986) 477.
- 32 K.A. Jørgenson and B. Schiøtt, *Chem. Rev.*, 90 (1990) 1483.
- 33 J.F. Hartwig, R.G. Bergman and R.A. Anderson, *Organometallics*, 10 (1991) 3344, and references therein.
- 34 B. de Bruin, M.J. Boerakker, J.J.J.M. Domers, B.E.C. Christiaans, P.P.J. Schlebos, R. de Gebler, J.M.M. Smits, A.L. Spek and A.W. Gal, *Angew. Chem., Int. Ed. Engl.*, 36 (1997) 2063.
- 35 S. Baba, T. Ogura, S. Kawaguchi, H. Tokunan, Y. Kai and N. Kashi, *J. Chem. Soc., Chem. Commun.*, (1972) 910.
- 36 L. Pandolfo, G. Paiaro, G. Valle and P. Ganis, *Gazz. Chim. Ital.*, 115 (1985) 65.
- 37 M. Lenarda, N.B. Pahor, M. Calligaris, M. Graziani and L. Randaccio, *J. Chem. Soc., Dalton Trans.*, (1978) 279.
- 38 M.J. Calhorda, A.M. Galvao, C. Unaleraglu, A.A. Zlota, F. Frolow and D. Milstein, *Organometallics*, 12 (1993) 3316.
- 39 D.P. Klein, J.C. Hayes and R.G. Bergman, *J. Am. Chem. Soc.*, 110 (1988) 3704.
- 40 D.P. Klein and R.G. Bergman, *J. Am. Chem. Soc.*, 111 (1989) 3079.
- 41 J.R. Bleeker, R. Behm, Y-F. Xie, T.W. Clayton, K.D. Robinson, *J. Am. Chem. Soc.*, 116 (1994) 4093.
- 42 J.F. Hartwig, R.G. Bergman and R.A. Andersen, *J. Organomet. Chem.*, 394 (1990) 417.
- 43 J.F. Hartwig, R.G. Bergman and R.A. Andersen, *J. Am. Chem. Soc.*, 113 (1991) 6499.
- 44 N. Bag, S.B. Choudhury, A. Pramanik, G.K. Lahari and A. Chakravorty, *Inorg. Chem.*, 29 (1990) 5013.
- 45 N. Bag, S.B. Choudhury, G.K. Lahari and A. Chakravorty, *J. Chem. Soc., Chem. Commun.*, (1990) 1626.

- 46 P. Ghosh, N. Bag and A. Chakravorty, *Organometallics*, 15 (1996) 3042.
- 47 E.N. Jacobson, K.I. Goldberg and R.G. Bergman, *J. Am. Chem. Soc.*, 110 (1988) 3706.
- 48 J.F. Hartwig, R.G. Bergman and R.A. Andersen, *J. Am. Chem. Soc.*, 113 (1991) 3404.
- 49 J.D. Gargulak, A.J. Berry, M.D. Noirot and W.L. Gladfelter, *J. Am. Chem. Soc.*, 114 (1992) 8933.
- 50 W.R. Roper, J.M. Waters and A.H. Wright, *J. Organomet. Chem.*, 275 (1984) C13.
- 51 K.E. Litz, K. Henderson, R.W. Gourley and M.N.B. Holl, *Organometallics*, 14 (1995) 5008.
- 52 A. de Renzi, B. di Blasio, G. Morelli and A. Vitagliano, *Inorg. Chim. Acta*, 63 (1982) 233.
- 53 R. Arnek and K. Zetterberg, *Organometallics*, 6 (1987) 1230.
- 54 Y. Angnus, M. Gross, M. Labarelle, R. Louis and B. Metz, *J. Chem. Soc., Chem. Commun.*, (1994) 939.
- 55 M.A. Bennett, D.E. Berry, S.K. Bhargava, E.J. Ditzel, G.B. Robertson and A.C. Willis, *J. Chem. Soc., Chem. Commun.*, (1987) 1613.
- 56 I.A. Chopoorian, J. Lewis and R.S. Nyholm, *Nature*, 190 (1961) 528.
- 57 F. Cariati, R. Mason, G.B. Robertson and R. Ugo, *Chem. Commun.*, (1967) 408.
- 58 M.A. Andrews, G.L. Gould, W.T. Klooster, K.S. Koenig and E.J. Voss, *Inorg. Chem.*, 35 (1996) 5478.
- 59 M.A. Ciriano, J.A. Lopez, L.A. Oro, J.J. Perez-Torrente, M. Lanfranchi, A. Tiripicchio and M.T. Camellini, *Organometallics*, 14 (1995) 4764.
- 60 P.J. Hayward, D.M. Blake, G. Wilkinson and C.J. Nyman, *J. Am. Chem. Soc.*, 92 (1970) 5873.
- 61 P. Bradford, R.C. Hynes, N.C. Payne and C.J. Willis, *J. Am. Chem. Soc.*, 112 (1990) 2647.
- 62 C.D. Cook and G.S. Jauhal, *J. Am. Chem. Soc.*, 89 (1967) 3066.
- 63 J.C. Fettinger, M.R. Churchill, K.A. Bernard and J.D. Atwood, *J. Organomet. Chem.*, 340 (1988) 377.
- 64 S.L. Randall, C.A. Miller, T.S. Janik, M.R. Churchill and J.D. Atwood, *Organometallics*, 13 (1994) 141.
- 65 J. Reed, S.L. Soled and R. Eisenberg, *Inorg. Chem.*, 13 (1974) 3001.
- 66 S.M. Maddock, C.E.F. Rickard, W.R. Roper and L.J. Wright, *J. Organomet. Chem.*, 510 (1996) 267.
- 67 I.J.B. Lin, H.W. Chen and J.P. Fackler Junior, *Inorg. Chem.*, 17 (1978) 394.

-
- 68 R. Contreras, M. Valderrama, O. Riveros and R. Moscoso, *Polyhedron*, *15* (1996) 183.
- 69 R. Schierl, U. Nagel and W. Beck, *Z. Naturforsch., Teil B*, *39* (1984) 649.
- 70 J. Ahmed, K. Itoh, I. Matsuda, F. Ueda, Y. Ishii and J.A. Ibers, *Inorg. Chem.*, *16* (1977) 620.
- 71 J.M. Bevilacqua, J.A. Zuleta and R. Eisenberg, *Inorg. Chem.*, *32* (1993) 3689.
- 72 W. Weigand, G. Bosl and K. Polborn, *Chem. Ber.*, *123* (1990) 1339.
- 73 M.R.St.J. Foreman, A.M.Z. Slawin and J.D. Woollins, *J. Chem. Soc., Dalton Trans.*, (1996) 3653.
- 74 I.P. Parkin, M.J. Pilkington, A.M.Z. Slawin, D.J. Williams and J.D. Woollins, *Polyhedron*, *9* (1990) 987.
- 75 A. Shaver, M. El-khateeb and A.-M. Lebuis, *Angew. Chem., Int. Ed. Engl.*, *35* (1996) 2362.
- 76 I.P. Parkin, A.M.Z. Slawin, D.J. Williams and J.D. Woollins, *J. Chem. Soc., Chem. Commun.*, (1989) 1060.
- 77 I.P. Parkin and J.D. Woollins, *J. Chem. Soc., Dalton Trans.*, (1990) 519.
- 78 S. Okeya, Y. Fujiwara, S. Kawashima, Y. Hayashi, K. Isobe, Y. Nakamura, H. Shimomura and Y. Kushi, *Chem. Lett.*, (1992) 1823.
- 79 W. Henderson and B.K. Nicholson, *Polyhedron*, *15* (1996) 4015.
- 80 W. Henderson, R.D.W. Kemmitt, S. Mason, M.R. Moore, J. Fawcett and D.R. Russell, *J. Chem. Soc., Dalton Trans.*, (1992) 59.
- 81 M.-A. David, D.S. Glueck, G.P.A. Yap and A.L. Rheingold, *Organometallics*, *14* (1995) 4040.
- 82 M. Suginome, H. Oike and Y. Ito, *Organometallics*, *13* (1994) 4148.
- 83 M.D. Curtis, J. Greene and W.M. Butler, *J. Organomet. Chem.*, *164* (1979) 371.
- 84 M.A. Cairns, K.R. Dixon and M.A.R. Smith, *J. Organomet. Chem.*, *135* (1977) C33.
- 85 T.G. Appleton and M.A. Bennett, *J. Organomet. Chem.*, *55* (1973) C88.
- 86 D.A. Clarke, R.D.W. Kemmitt, M.A. Mazid, P. McKenna, D.R. Russell, M.D. Schilling and L.J.S. Sherry, *J. Chem. Soc., Dalton Trans.*, (1984) 1993.
- 87 W. Henderson, R.D.W. Kemmitt, L.J.S. Prouse and D.R. Russell, *J. Chem. Soc., Dalton Trans.*, (1989) 259.
- 88 W. Henderson, R.D.W. Kemmitt, J. Fawcett, L.J.S. Prouse and D.R. Russell, *J. Chem. Soc., Chem. Commun.*, (1986) 1791.

- 89 W. Henderson, R.D.W. Kemmitt, L.J.S. Prouse and D.R. Russell, *J. Chem. Soc., Dalton Trans.*, (1990) 1853.
- 90 R.D.W. Kemmitt, S. Mason, M.R. Moore, J. Fawcett and D.R. Russell, *J. Chem. Soc., Chem. Commun.*, (1990) 1535.
- 91 W. Henderson, R.D.W. Kemmitt and A.L. Davis, *J. Chem. Soc., Dalton Trans.*, (1993) 2247.
- 92 A.G. Oliver and W. Henderson, unpublished results.
- 93 W. Henderson, B.K. Nicholson and A.G. Oliver, *J. Chem. Soc., Dalton Trans.*, (1994) 1831.
- 94 W. Henderson, J. Fawcett, R.D.W. Kemmitt, C. Proctor and D.R. Russell, *J. Chem. Soc., Dalton Trans.*, (1994) 3085.
- 95 W. Henderson, B.K. Nicholson and A.G. Oliver, *Polyhedron*, 13 (1994) 3099.
- 96 R.D.W. Kemmitt, S. Mason, M.R. Moore and D.R. Russell, *J. Chem. Soc., Dalton Trans.*, (1992) 409.

Chapter Two

Syntheses and Characterisation of Platinum(II) Ureylene Complexes

2.1 Introduction

A very wide range of complexes derived from ureas have been prepared over the years. Since ureas can co-ordinate through nitrogen and/or oxygen, and act either as a neutral donor, monoanion (ureato) or dianion (ureylene) ligand, they have proved to be extremely versatile systems. The work presented in this chapter is primarily concerned with complexes derived from the urea dianion, and discussion will be restricted to these structures only.

Ureylene complexes incorporate the four-membered ring system $\overline{\text{M-N-C(O)-N}}$ (Figure 2.1), and have been known since at least 1967, when the dinuclear iron carbonyl ureylene **2.1a** (Figure 2.2) was first formulated.¹ Since then, a substantial number of complexes have been prepared from a variety of routes, and these have been a subject in two reviews.^{2,3} The main methods are summarised in the following sections.

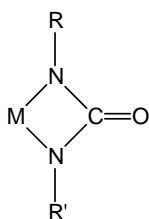
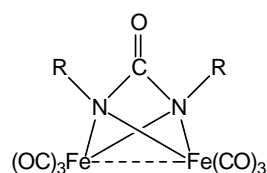


Figure 2.1

2.1.1 Ureylene formation from organic azides

The reactions of organic azides (RN_3) with metal carbonyl complexes typically result in the formation of ureylene complexes. Ureylene complexes prepared by this method can be both dinuclear or mononuclear. Reaction of either $[\text{Fe}_2(\text{CO})_9]$ or $[\text{Fe}_3(\text{CO})_{12}]$ with the appropriate organic azide leads to the complexes **2.1a-2.1c** (Figure 2.2).^{4,6}



2.1a-2.1c R = Ph, Me, *p*-(MeO)C₆H₄

Figure 2.2

Similarly, when [Ru(CO)₃(PPh₃)₂], [M(NO)(CO)(PPh₃)₂] (M = Rh, Ir) and [Pd(PPh₃)₃(CO)] were reacted with *p*-tolylsulfonyl azide [*p*-MeC₆H₄S(O)₂N₃] the respective ureylene compounds **2.2**^{3,7} and **2.3-2.4**⁸ (Figure 2.3) were isolated. Furthermore, the ureylene ligand in these complexes could be readily displaced from the complexes by the addition of a halic acid, to give the disubstituted urea, and the dihalide of the metal precursor.⁸

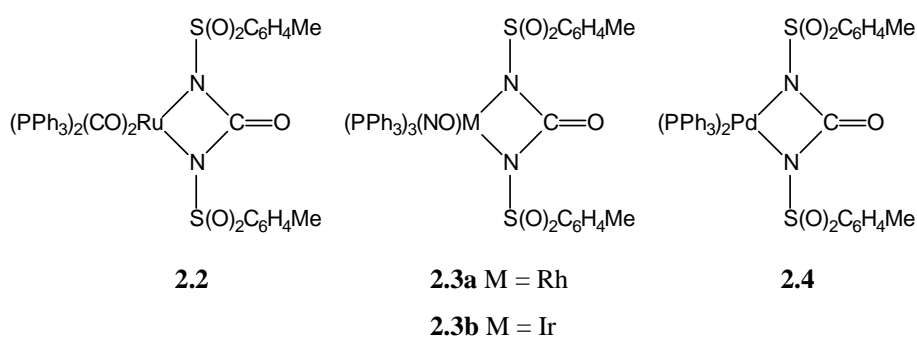
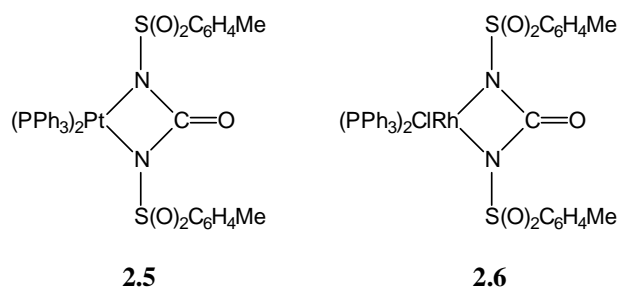
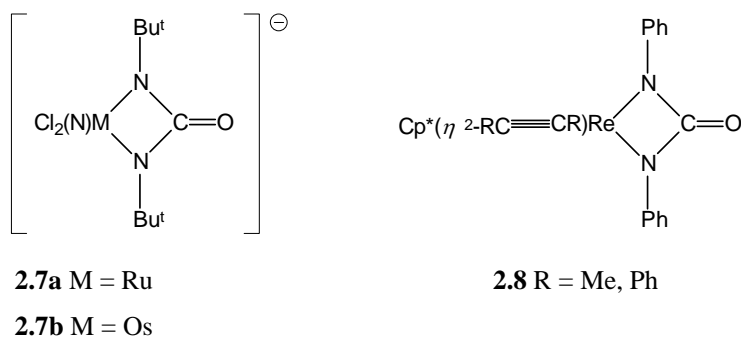


Figure 2.3

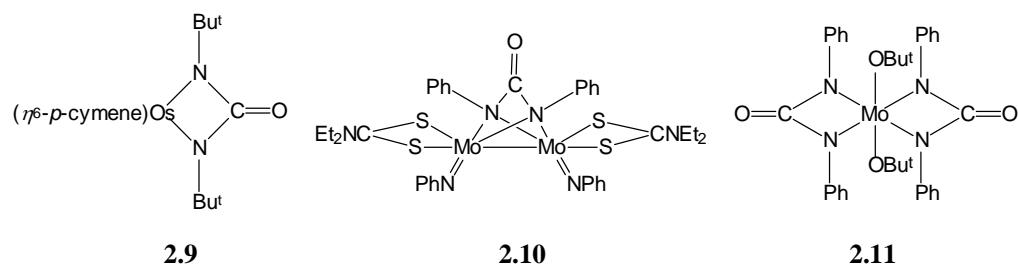
2.1.2 Ureylene formation from isocyanates

The reactions of a wide range of inorganic complexes with isocyanates results in the formation of ureylene complexes. When *p*-tolylsulfonyl isocyanate was reacted with the low valent complexes [Ru(CO)₃(PPh₃)₂], [Rh(NO)(PPh₃)₃], [Ir(NO)(PPh₃)₃], [Pd(PPh₃)₄], [Pt(PPh₃)₄] or [RhCl(PPh₃)₃] in dry benzene, the ureylene derivatives **2.2**^{3,7} and **2.3-2.6**⁸ (Figure 2.4), were formed. The interaction of *tert*-butyl isocyanate with the ruthenium(VI) and osmium(VI) oxo-complexes [RuO₂Cl_n]⁽ⁿ⁻²⁾⁻ and [OsO₂Cl₄]²⁻ (as tetraphenylphosphonium salts) in refluxing acetonitrile, gave the ureylene complexes **2.7a** and **2.7b** (Figure 2.5) respectively.⁹ Similarly, the rhenium(III) oxo-complex [Cp*ReO(η²-RC≡CR)] (Cp* = η⁵-C₅Me₅; R = Me, Ph) was reacted with phenyl isocyanate, and the ureylenes **2.8** (Figure 2.5) resulted.¹⁰

Comment:

**Figure 2.4****Figure 2.5**

When the osmium(II) imido complex $[(p\text{-cymene})\text{OsN}^t\text{Bu}]$ was reacted with *tert*-butyl isocyanate the complex **2.9** (Figure 2.6) formed.^{11,12} The molybdenum imido complexes $[\{\text{Mo}\{\text{NPh}\}(\text{S}_2\text{CNEt}_2)(\mu\text{-NPh})\}_2]$ and $[\text{Mo}\{\text{NC}_6\text{H}_3\text{Pr}^i_{2-2,6}\}_2(\text{OBu}^t)]$ similarly react with phenyl isocyanate to give the ureylenes **2.10**¹³ and **2.11**,¹⁴ although the formulation of the latter was not conclusively proven.

**Figure 2.6**

The tungsten ureylene complex **2.12**¹⁵ and the sterically protected iridium and ruthenium ureylene compounds **2.13** and **2.14**¹⁶ (Figure 2.7) were prepared by the action of the appropriate isocyanate with the imido complexes $[\text{Cp}^*\text{W}(\text{NC}_6\text{H}_4\text{-}p\text{-Me})_2(\text{CH}_2\text{SiMe}_3)]$ (*p*-

tolyl isocyanate), $[\text{Cp}^*\text{Ir}\{\text{NC}_6\text{H}_3(2,6\text{-Pr}_2^i)\}]$ (mesityl isocyanate) and $[(p\text{-cymene})\text{Ru}\{\text{NC}_6\text{H}_3(2,4,6\text{-Bu}^t_3)\}]$ (mesityl isocyanate).

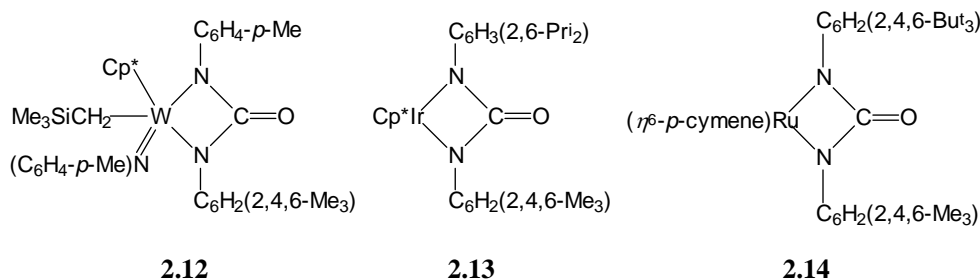
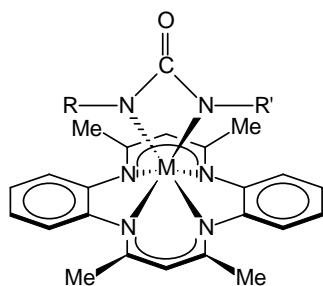


Figure 2.7

Tetraazamacrocycle-stabilised imido titanium(IV) and zirconium(IV) complexes also react with isocyanates, and the complexes **2.15a**, **2.15b** and **2.16** (Figure 2.8) have been characterised from reactions involving phenyl isocyanate, *p*-tolyl isocyanate, and *tert*-butyl isocyanate.¹⁷



2.15a M = Ti, R = R' = Ph

2.15b M = Ti, R = Ph, R' = *p*-tolyl

2.16 M = Zr, R = $[\text{C}_6\text{H}_3(2,6\text{-Pr}_2^i)]$, R' = Bu^t

Figure 2.8

The palladaureylene **2.17** was prepared by reaction of $[\text{Pd}\{\text{C}(\text{O})\text{NPhOC}(\text{O})\}(\text{phen})]$ (phen = 1,10-phenanthroline) with phenyl isocyanate,¹⁸ and the more complex ureylene **2.18** was isolated from the reaction of a cyclophosphazene rhenium oxide with 2,6-diisopropylphenyl isocyanate.¹⁹ Finally, the dinuclear ureylene complex **2.19** was prepared from the reaction of the cobalt hydride $[\text{Cp}^*_3\text{Co}_3(\mu_2\text{-H})_3(\mu_3\text{-H})]$ with phenyl isocyanate, and was characterised structurally.²⁰

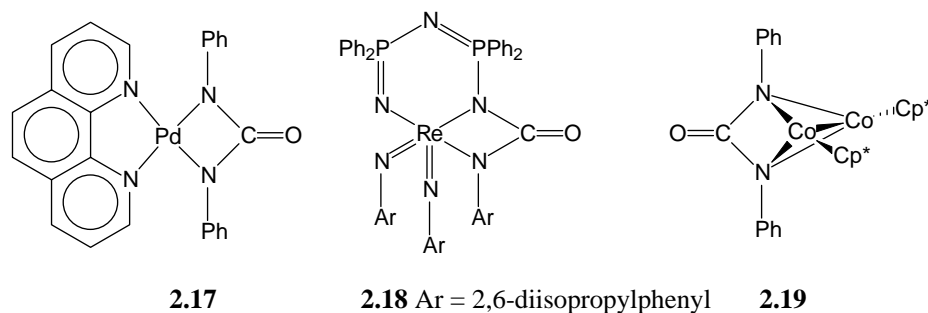


Figure 2.9

2.1.3 Ureylene formation from ureas

Ureylene complexes can also be prepared directly from the parent ureas. The oxidative addition of *N,N'*-ditolyl-*p*-sulfonylurea to the low valent metal complexes $[\text{Ru}(\text{CO})_3(\text{PPh}_3)_2]$, $[\text{Pt}(\text{PPh}_3)_4]$ and $[\text{Rh}(\text{PPh}_3)_3\text{Cl}]$, gave the ureylenes **2.2**^{3,7}, **2.5**⁸ and **2.6**⁸ respectively.

The complex **2.17** (already described) could also be prepared by reacting $[\text{Pd}(\text{OAc})_2(\text{phen})]$ with the dilithio salt of *N,N'*-diphenylurea.¹⁸ The reaction of $[\text{Pd}(\text{hfac})_2]$ (Hhfac = hexafluoroacetylacetonate) with ureas in methanol gave the novel tri- and tetra-nuclear palladium(II) complexes containing ureylene ligand(s), **2.20** and **2.21** (Figure 2.10).²¹

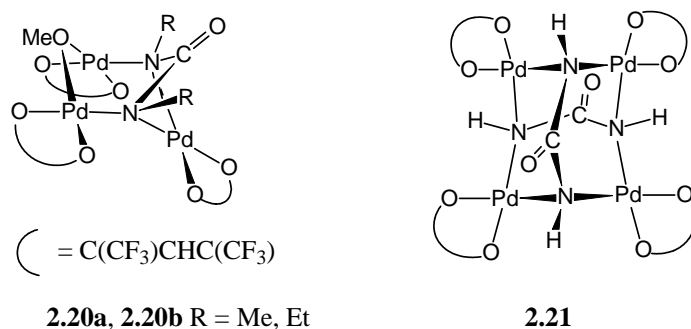


Figure 2.10

We wished to develop a more systematic approach for the synthesis of ureylene complexes directly from ureas. In light of the success of previous silver(I) oxide studies to prepare related compounds (as detailed in Chapter One, Section 1.3), the silver(I) oxide route seemed a promising method for their preparation, and had not been applied previously. This chapter reports detailed investigations on the applicability of silver(I) oxide for the preparation of platinum(II) ureylene complexes.

2.2 Results and Discussion

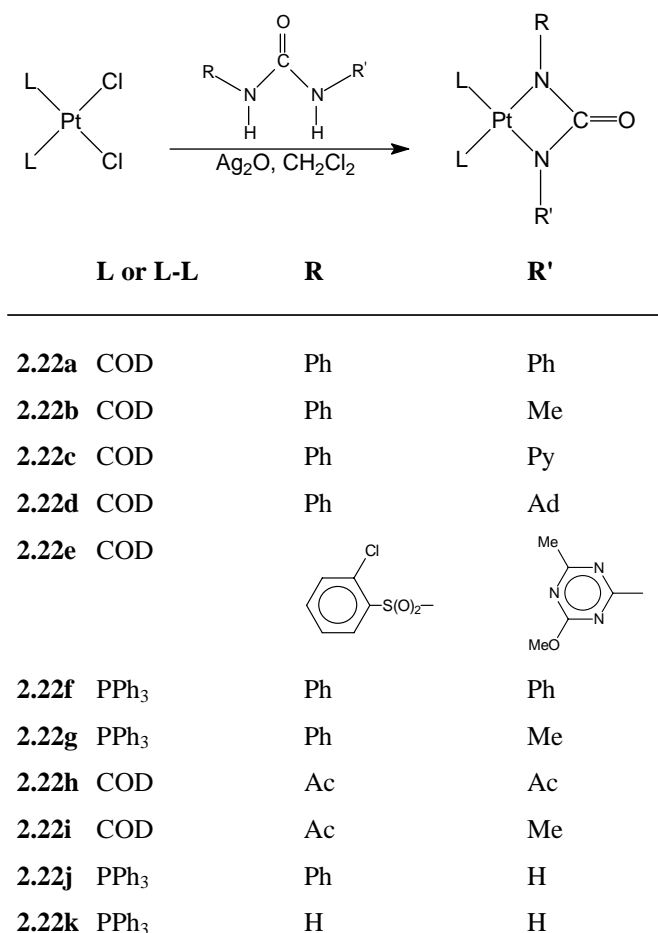
2.2.1 Syntheses of ureylene complexes

2.2.1.1 Silver(I) oxide mediated synthesis

The reaction of platinum(II) chloride complexes with ureas in the presence of silver(I) oxide has been studied as a general method for preparing ureylene complexes. A wide range of ureas have been investigated to demonstrate the general utility of the method, and the resulting ureylene complexes have been characterised by a combination of ^1H , ^{13}C and (where appropriate) ^{31}P NMR spectroscopy, IR spectroscopy, electrospray mass spectrometry (ESMS) and elemental analysis. One derivative was also fully characterised by a single-crystal X-ray structure determination.

When $[\text{PtCl}_2(\text{COD})]$ (COD = 1,5-cyclo-octadiene) with 1 mole equivalent of the appropriate arylurea ($\text{PhNHC}(\text{O})\text{NHR}$, R = phenyl, methyl, 2-pyridyl, 1-adamantyl) were refluxed in dichloromethane in the presence of silver(I) oxide, the platinum(II) ureylene complexes **2.22a-2.22e** (Scheme 2.1) were isolated in good yield. Additionally, the novel sulfonylurea herbicide Chlorsulfuron reacted smoothly under the same conditions and gave the expected ureylene complex **2.22f**. The triphenylphosphine analogues of **2.22a** and **2.22b** were readily prepared directly from the silver(I) oxide-mediated reaction of *cis*- $[\text{PtCl}_2(\text{PPh}_3)_2]$ and N,N'-diphenylurea or N-methyl-N'-phenylurea to give the respective complexes **2.22f** and **2.22g**. The former was also prepared by the conventional ligand displacement of the COD group by the addition of two equivalents of triphenylphosphine.

Hitherto, only ureas containing at least one aromatic group had been tried, and so other ureas were attempted. Thus, when N,N'-diacetylurea or N-acetyl-N'-methylurea were reacted in the presence of silver(I) oxide, the respective acetylureylene products **2.22h** and **2.22i** could also be obtained. The latter formed as an oil that did not crystallise, despite repeated attempts. Furthermore **2.22i** decomposed to a range of uncharacterised products when dichloromethane or chloroform solutions were left standing.



COD = cyclo-octa-1,5-diene, Ad = 1-adamantyl, Py = 2-pyridyl, Ac = acetyl

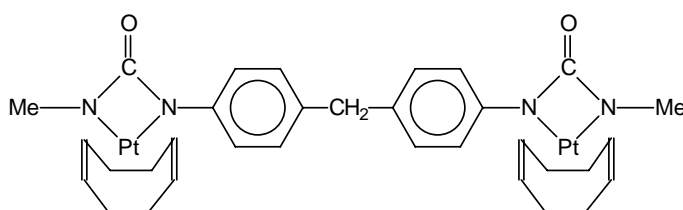
Scheme 2.1

The presence of one sufficiently electron withdrawing group appeared to be essential, with no detectable reaction occurring between [PtCl₂(COD)] and N,N'-dimethylurea, even after refluxing for two days. This is almost certainly a consequence of the reduced acidity of the NH group in aliphatic-substituted ureas compared to their aromatic and acetyl counterparts. The requirement of only one acidic group can be rationalised by the rapid reaction rates associated with the intramolecular cyclisation reaction after co-ordination of the first urea nitrogen.

Phenylurea and unsubstituted urea proved reactive, and tentatively gave the platinaureylenes **2.22j** and **2.22k** respectively, characterised by NMR and ESMS. However, both were found to be unstable and slowly decomposed over a few days, evidenced by ³¹P NMR (see Section

2.2.3.1). This decreased stability is in contrast with the related systems $[\text{Pt}\{\overline{\text{NHXNH}}\}(\text{PPh}_3)_2]$ **1.100** [$\text{X} = \text{S}(\text{O})_2$] or **1.101** [$\text{X} = \text{P}(\text{O})\text{Ph}$] which were reported to be stable.²²⁻²⁵ This is possibly due to the greater electron-withdrawing capabilities of $\text{S}(\text{O})_2$ and $\text{P}(\text{O})\text{Ph}$ [relative to $\text{C}(\text{O})$], thus stabilising the Pt-N bond.

Finally, the silver(I) oxide route was applied to the synthesis of a dinuclear ureylene complex. The bis(urea) $\{\text{MeNHC}(\text{O})\text{NH}(p\text{-C}_6\text{H}_4)\}_2\text{CH}_2$, synthesised from diphenylmethane-4,4'-diisocyanate and excess methylamine, was reacted with two equivalents of $[\text{PtCl}_2(\text{COD})]$ to give the dinuclear complex **2.23** (Figure 2.11). The reaction proceeded readily, and no mononuclear complex was detected.



2.23

Figure 2.11

2.2.1.2 Sodium hydride mediated synthesis

Recently we have begun an exploration of using sodium hydride for the syntheses of various metallacycles. The hydride anion (H^-) is a stronger base than the oxide dianion (O^{2-}), so sodium hydride could potentially facilitate faster reaction rates and be more general than silver(I) oxide. Although the method has to date proved less reliable than silver(I) oxide for these reactions, it was nonetheless of interest to examine its possible application for the synthesis of ureylene complexes.

When $[\text{PtCl}_2(\text{COD})]$, *N,N'*-diphenylurea and excess sodium hydride (freshly powdered) were stirred together in THF, a bright yellow precipitate rapidly formed. The complex **2.22a** could be isolated from this reaction in 56% yield (compared with 84% for the silver(I) oxide route). The method failed for the synthesis of **2.22b**, with only small quantities of product detected by NMR spectroscopy. Increased reaction times induced extensive decomposition of the product. However the method was applicable for the syntheses of **2.22g** from the more robust starting material *cis*- $[\text{PtCl}_2(\text{PPh}_3)_2]$, which is apparently more resilient to the longer reaction

times (2 hours) required. The reaction times in this case proved critical, with reaction times greater than 2 hours resulting in decomposition of **2.22g**, evidenced by triphenylphosphine oxide ($\text{Ph}_3\text{P}=\text{O}$) formation in the ^{31}P NMR spectra of the crude reaction residue.

2.2.2 X-ray structure of $[\text{Pt}\{\overline{\text{NPhC(O)NAd}}\}(\text{COD})]$ **2.22d** dichloromethane solvate

The crystal structure of **2.22d** was determined to fully characterise the reaction product of $[\text{PtCl}_2(\text{COD})]$ and N-adamantyl-N'-phenylurea, to examine the absolute geometry of the compound, and for comparison with related systems. The complex **2.22d** was chosen, since it is asymmetrically substituted, containing two electronically and sterically different substituents. Previous to our study, only one other asymmetrical ureylene had been structurally characterised (the novel rhenium complex **2.18**),¹⁹ although more recently the structure of the zirconium ureylene **2.16** was elucidated.¹⁷ Nonetheless, this is the first reported structure of a platinum ureylene complex.

ORTEP perspective and side views of the final structure are shown in Figures 2.12 and 2.13 respectively, illustrating the atom numbering scheme. Selected bond lengths and angles are given in Table 2.1, and tables containing complete bond lengths and angles, final positional parameters, thermal parameters and calculated H-atom positions are presented in Appendix III.

The structure confirms the expected cycloplatinated product **2.22d**. The metallacycle is analogous to the structures reported for iron,^{4,6} cobalt,^{20,26} molybdenum,^{13,14} ruthenium,¹⁶ palladium,^{18,21} tungsten,¹⁵ rhenium,¹⁹ zirconium,¹⁷ iridium,¹⁶ and osmium ureylene complexes.⁹ The ureylene ligand is co-ordinated in the expected N,N'-bonded configuration, in contrast to the N,S-chelating mode found for structures of the platinum(II) complexes **1.81** (Figure 2.14),²⁷⁻²⁹ derived from the thiourea dianion (see also Chapter One, Section 1.2.3.4).

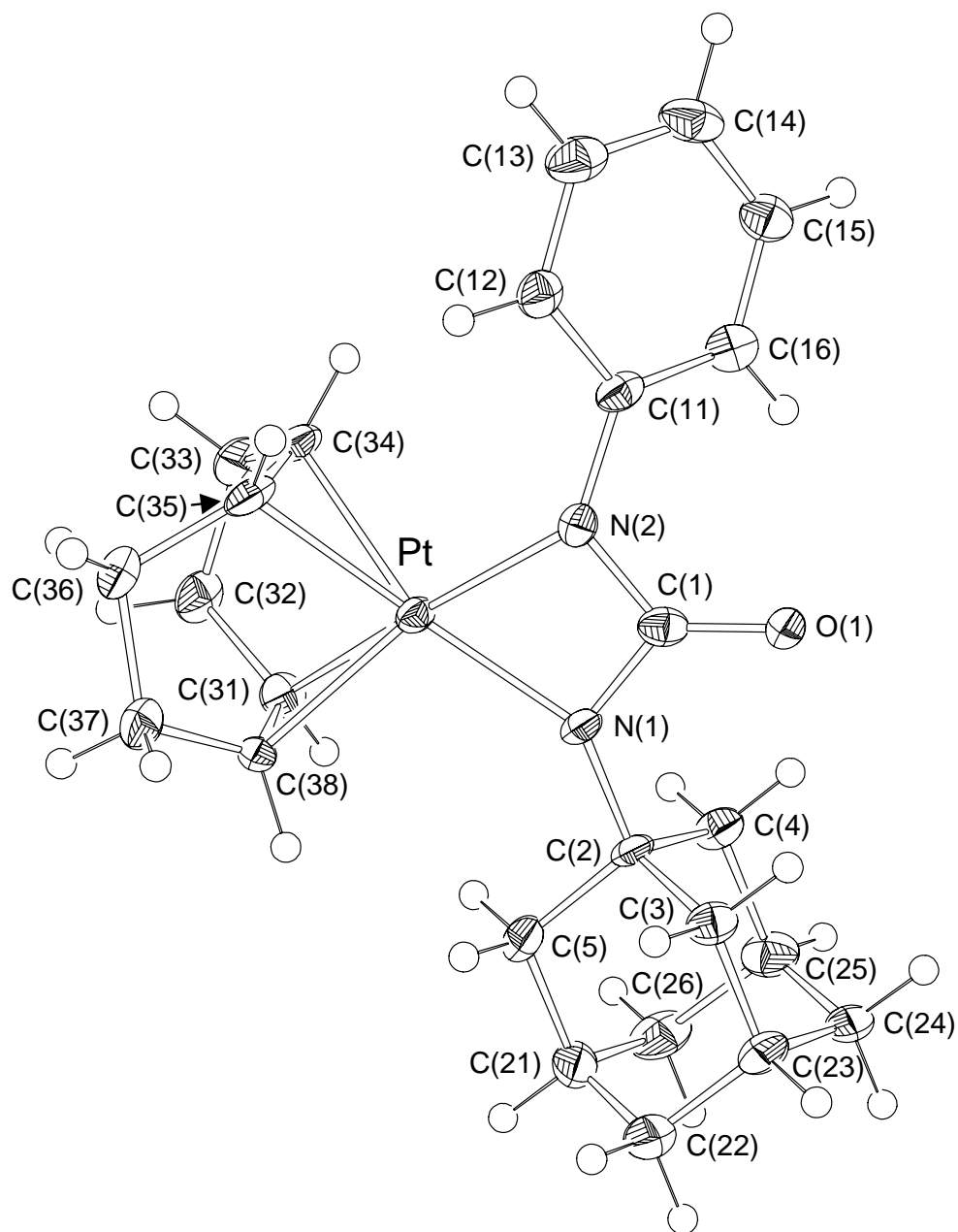


Figure 2.12: *Perspective view of the X-ray crystal structure of the ureylene complex [Pt{NPhC(O)NAd}(COD)]·CH₂Cl₂ 2.22d, showing the atom labelling scheme. CH₂Cl₂ and possible Et₂O (see text) solvates are omitted. Thermal ellipsoids are shown at the 50% probability level.*

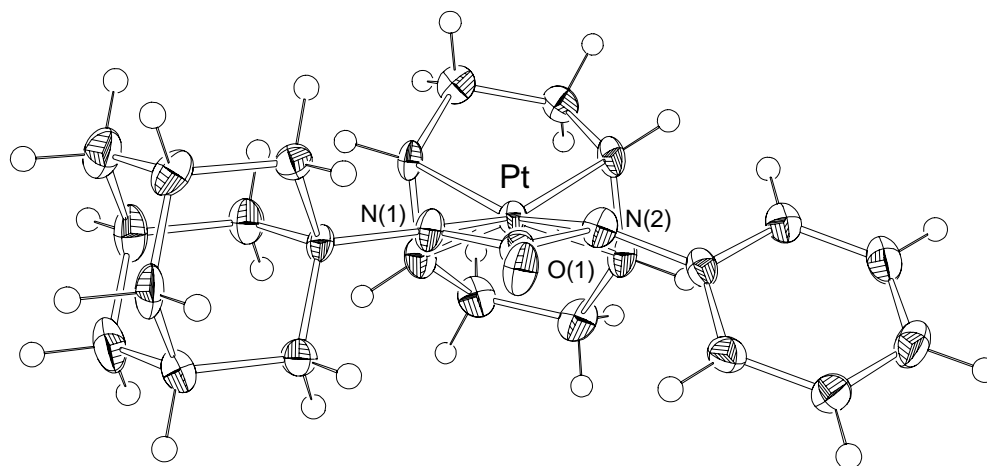
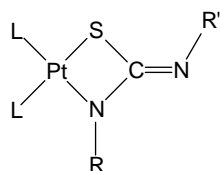


Figure 2.13: Side view of the structure of the ureylene complex $[Pt\{NPhC(O)NAd\}(COD)] \cdot CH_2Cl_2$ **2.22d**. CH_2Cl_2 and possible Et_2O (see text) solvates are omitted. Thermal ellipsoids are shown at the 50% probability level.

Table 2.1: Selected bond lengths (\AA) and angles ($^\circ$) (estimated standard deviations in parentheses) of the platinum(II) ureylene complex **2.22d**· CH_2Cl_2 .

Bond	Length	Bonds	Angle
Pt-N(1)	2.048(8)	N(1)-Pt-N(2)	64.7(3)
Pt-N(2)	2.021(8)	Pt-N(1)-C(1)	94.7(5)
Pt-C(31)	2.177(9)	Pt-N(2)-C(1)	95.5(5)
Pt-C(38)	2.178(9)	Pt-N(2)-C(11)	133.2(6)
Pt-C(34)	2.185(9)	Pt-N(1)-C(2)	142.4(6)
Pt-C(35)	2.191(9)		
Pt...C(1)	2.56(1)		
Ureylene and COD ligands			
N(1)-C(1)	1.37(1)	N(1)-C(1)-N(2)	104.1(7)
N(2)-C(1)	1.39(1)	N(1)-C(1)-O(1)	128.4(8)
C(1)-O(1)	1.24(1)	N(2)-C(1)-O(1)	127.3(8)
N(1)-C(2)	1.47(1)	C(1)-N(1)-C(2)	121.7(7)
N(2)-C(11)	1.41(1)	C(1)-N(2)-C(11)	121.6(7)
C(31)-C(38)	1.38(1)		
C(34)-C(35)	1.39(1)		



1.81a L = PPh₃, R = R' = Et

1.81b L₂ = COD, R = Me, R' = CN

1.81c L = PPh₃, R = R' = Ph

Figure 2.14

As is normal with four-membered platina(II)cyclic compounds, the central metal is coordinated in a distorted square-planar arrangement, with the bidentate ureylene and η^4 -coordinated COD ligands lying in the plane. The main distortion is the N-Pt-N bite angle, which in this case is 64.7(3)°, so deviating by 25.3° from a regular square plane. This is due to the geometrical constraint set by the ligand, whose bonds have insufficient flexibility to adopt the 90° angle required for a regular square planar arrangement. Table 2.2 illustrates this constraint, showing metal N-M-N and ligand N-C-N angles ranging from (for the accurate data) 62-66° and 102-108° respectively. Comparing key features of the structure of **2.22d** with structures previously reported for other mononuclear ureylene complexes (Table 2.2), it is clear the parameters of **2.22d** lie well within the limits shown by the known examples, especially resembling those of the platinum group metals (**2.7a**, **2.7b** and **2.13**).

Since the ureylene is an unsymmetrical ligand, the Pt-N(1) and Pt-N(2) bond distances are not expected to be equal. Unfortunately the standard deviations are too high for an accurate comparison to be made, but the Pt-NAd [Pt-N(1)] linkage is possibly slightly [0.027(8) Å] longer than the Pt-NPh bond [Pt-N(2)]. Although the differing *trans*-influences³⁰ of the two inequivalent nitrogen atoms has a substantial effect on the ¹H and ¹³C NMR spectra of the CH=CH groups of the COD ligand (see Section 2.2.3.1), the Pt- $\{\eta^2\}$ -(CH=CH) bond distances do not vary significantly [2.178(9) compared with 2.188(9) Å], although more accurate data should show a difference.

Table 2.2: Comparison of M-N bond lengths and N-M-N and N-C-N bond angles of **2.22d**·CH₂Cl₂ with related ureylene complexes.

Complex	M-N bond lengths (Å)	N-M-N angle (°)	N-C-N angle (°)
M = Pt 2.22d	2.048(8), 2.021(8)	64.7(3)	104.1(7)
M = Zr 2.16	2.155(4), 2.168(4)	62.0(2)	107.5(5)
M = Ru 2.7a	1.973(6), 1.974(6)	66.2(3)	102.9(4)
M = Ru 2.14	1.998(4), 2.023(4)	66.1(2)	102.8(4)
M = Pd 2.17	1.992(3), 2.001(3)	65.6(1)	103.9(3)
M = W 2.12	2.22(1), 2.12(1)	57.9(5)	101(2)
M = Re 2.18	2.199(3), 2.048(3)	61.0(1)	103.1(3)
M = Os 2.7b	1.980(7), 1.977(6)	66.1(3)	102.2(5)
M = Ir 2.13	1.92(2), 2.03(2)	68.0(7)	96(2)

The metallacycle in **2.22d** is essentially planar, with no atom deviating from the least squares-plane drawn through Pt, N(1), C(1) and N(2) by more than 0.068(5) Å, for C(1), with the carbonyl group also lying in plane. The dihedral angle between the ureylene metallacycle and the phenyl ring is 42.0(3)°. The alkene moieties of the COD ligand are almost perpendicular to the metallacycle, forming an angle of 87.0(4)° between the planes C(31), C(34), C(35) and C(38), and Pt, N(1), C(1) and N(2).

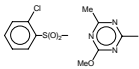
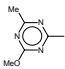
The ureylene four-membered ring is formally isoelectronic with the $\overline{\text{M-CH}_2\text{-C(O)-CH}_2}$ (oxodimethylenemethane) ring system (e.g. **1.13-1.16**, Chapter One, Section 1.2.1.2), and can indeed be considered as oxadiazatrimethylenemethane complexes. However, structural studies^{31,32} have shown the $\overline{\text{M-CH}_2\text{-C(O)-CH}_2}$ four-membered ring, unlike those of the ureylene compounds (which are planar), to be highly puckered. This phenomenon is discussed in more detail in Chapter Seven, Section 7.2.1. Ureylene complexes thus much more closely resemble the isoelectronic carbonato complexes containing the $\overline{\text{M-O-C(O)-O}}$ ring system (see Chapter One, Section 1.2.3.1), which have also been shown to have planar metallacyclic rings.³³⁻³⁵

2.2.3 Spectroscopic and mass spectrometric characterisation

2.2.3.1 NMR spectroscopy

The most diagnostic NMR spectroscopic feature of the COD derivatives (**2.22a-2.22e**, **2.22h**, **2.22i**) are the proton and carbon olefinic resonances. These are summarised for all the prepared COD-derived complexes in Table 2.3. It is evident from the table that there is no obvious trend in either the ^1H or ^{13}C NMR chemical shifts, which range from 4.7 to 6.5 ppm and from 91 to 99 ppm respectively, regardless of the nature of the substituents of the nitrogen *trans* to it. For the unsymmetrical species studied, if the ^1H chemical shift for any particular group was larger, then the ^{13}C chemical shift was also greater, although this is of little diagnostic value. However, the associated ^2J ($^{195}\text{Pt}-^1\text{H}$) and ^1J ($^{195}\text{Pt}-^{13}\text{C}$) coupling constants seem to show a trend. The more strongly electron-withdrawing groups (i.e. phenyl and acetyl) show a *higher* ^2J ($^{195}\text{Pt}-^1\text{H}$) but *lower* ^1J ($^{195}\text{Pt}-^{13}\text{C}$) value for the co-ordinated COD ligand than their respective lesser electron-withdrawing counterparts, with the exception of **2.22d**, for which the coupling constants were identical within the experimental accuracy of the spectrometer.

Table 2.3: A comparison of cyclo-octadiene olefinic ^1H and ^{13}C resonances and coupling constants for the various ureylene complexes $[\text{Pt}\{\text{NRC}(\text{O})\text{NR}'\}(\text{COD})]$

Substituent		Pt-CH group <i>trans</i> R				Pt-CH group <i>trans</i> R'				
R	R'	δ (ppm)		J (Hz)		δ (ppm)		J (Hz)		
		^1H	^{13}C	$^1\text{H}-^{195}\text{Pt}$	$^{13}\text{C}-^{195}\text{Pt}$	^1H	^{13}C	$^1\text{H}-^{195}\text{Pt}$	$^{13}\text{C}-^{195}\text{Pt}$	
Ph	Ph	2.22a	5.20	94.1	59.4	141.7	5.20	94.1	59.4	141.7
Ph	Me	2.22b	5.08	93.7 ^a	- ^b	133.1	5.13	92.1	53.9	143.5
Ph	Py	2.22c	6.48	95.2	64.6	131.6	5.21	94.1	63.1	145.5
Ph	Ad	2.22d	4.73	90.7	60.8	128.6	5.63	93.8	61.0	142.8
Ac	Ac	2.22h	6.17	96.7	64.0	132.7	6.17	96.7	64.0	132.7
Ac	Me	2.22i	5.17	93.5	62.4	128.7	6.08	93.9	61.3	141.1
		2.22e	6.41	98.6	68.2	139.1	6.33	97.1	61.0	153.8

^a Assigned following the basic trend in coupling constants observed for related species.

^b Not resolved.

In addition to the COD resonances, a number of other diagnostic features are noteworthy. In the ^{13}C NMR the central carbonyl resonance of the parent ureas appeared in the range 151.0 (for to N,N'-diacetylurea) to 163.5 ppm (for Chlorsulfuron). On co-ordination to platinum, a large downfield shift (~ 20 ppm) associated with ring formation was observed for these signals, now ranging from 165.3 (for **2.22h**) to 178.7 ppm (for **2.23**). However the signal, being a quaternary carbon with long relaxation times, was typically extremely weak, and required long acquisition times for its elucidation. For the poorly soluble ureylene **2.22a**, the carbonyl signal could not be resolved, even after two days of acquisition on a 300 MHz spectrometer.

For the ureylene complexes with an NMe group, **2.22b**, **2.22g** and **2.22i**, the ^1H and ^{13}C NMR spectra showed the expected splitting due to coupling to ^{195}Pt . For the complexes **2.22b** and **2.22g** the methyl showed ^3J (^{195}Pt - ^1H) and ^2J (^{195}Pt - ^{13}C) values of ~ 35 and ~ 30 Hz respectively, and the acetyl derivative **2.22i** showed slightly higher values of 40.0 and 41.5 Hz.

The ^{31}P NMR data for the triphenylphosphine derived species are presented in Table 2.4. The symmetrical N,N'-diphenylureylene **2.22f** shows the expected single resonance, with a ^1J (^{195}Pt - ^{31}P) coupling constant of 3337 Hz, in line with that expected for the moderate *trans*-influence nitrogen.³⁰ Similar values are observed for other amide complexes, such as $[\text{Pt}\{\text{NPhS}(\text{O})_2\text{NPh}\}(\text{PPh}_3)]$ **1.100** and $[\text{Pt}\{\text{NPhP}(\text{O})(\text{Ph})\text{NPh}\}(\text{PPh}_3)_2]$ **1.101** which have ^1J (^{195}Pt - ^{31}P) values of 3501 and 3401 Hz respectively. The *trans*-influence of the NPh group in the ureylene complexes is clearly lower than the NPh in the platinalactam complex $[\text{Pt}\{\text{CH}(\text{COMe})\text{C}(\text{O})\text{NPh}\}(\text{PPh}_3)_2]$ **1.97a** which has the high ^1J (^{195}Pt - ^{31}P) value of 3709 Hz (in this case the Pt-C has a high *cis*-influence,³⁰ so weakens the Pt-N bond further). The unsubstituted ureylene **2.22k** showed a surprisingly high value of 3291 Hz, higher than PPh_3 *trans* NMe. The values for the mixed ureylene **2.22j** are outside the range defined by the two corresponding symmetrical ureylenes **2.22f** and **2.22k**.

Table 2.4: A comparison of triphenylphosphine ^{31}P resonances and coupling constants for the various ureylene complexes $[\text{Pt}\{\text{NRC}(\text{O})\text{NR}'\}(\text{PPh}_3)_2]$ **2.22**

Substituent			Pt-P group <i>trans</i> R		Pt-P group <i>trans</i> R'	
R	R'		δ (ppm)	^1J (^{195}Pt - ^{31}P)	δ (ppm)	^1J (^{195}Pt - ^{31}P)
Ph	Ph	2.22f	10.0	3337	10.0	3337
Ph	Me	2.22g	13.5	3329	11.2	3249
Ph	H	2.22j	11.7	3423	12.7	3174
H	H	2.22k	12.3	3291	12.3	3291

The decomposition of the unsubstituted ureylene complex **2.22k** could be readily followed by ^{31}P NMR, and the resulting spectra recorded over three days are shown together in Figure 2.15. Two of the decomposition products still clearly possess the *cis*- $[\text{PtX}_2(\text{PPh}_3)_2]$ pattern, with signals appearing at 11.7 and 7.5 ppm showing ^1J (^{195}Pt - ^{31}P) coupling values of 3096 and 3567 Hz respectively, however their identity remains unknown. The remaining signal at 27.5 ppm is attributable to triphenylphosphine oxide, a typical feature in spectra of decomposed Ph_3P -Pt compounds. The figure also shows a signal at 6.8 ppm present from the outset that remains steady over time, and this is discussed in Section 2.2.4.

2.2.3.2 IR spectroscopy

The IR spectra of the ureylene complexes show two strong bands in the carbonyl region (1580-1700 cm^{-1}), although obviously only one can be from the C=O itself. The values range from 1637 to 1662 cm^{-1} for the first band, and 1548 to 1605 cm^{-1} for the second, and these positions are generally very similar to those of the starting ureas and consequently of little diagnostic utility. Other mononuclear ureylene complexes have been reported as showing the ν (C=O) band between 1608-1698 cm^{-1} ,¹² with a value of 1615 cm^{-1} for palladaureylene **2.17**¹⁸ and 1693 cm^{-1} for the only previously reported platinaureylene **2.5**.⁸

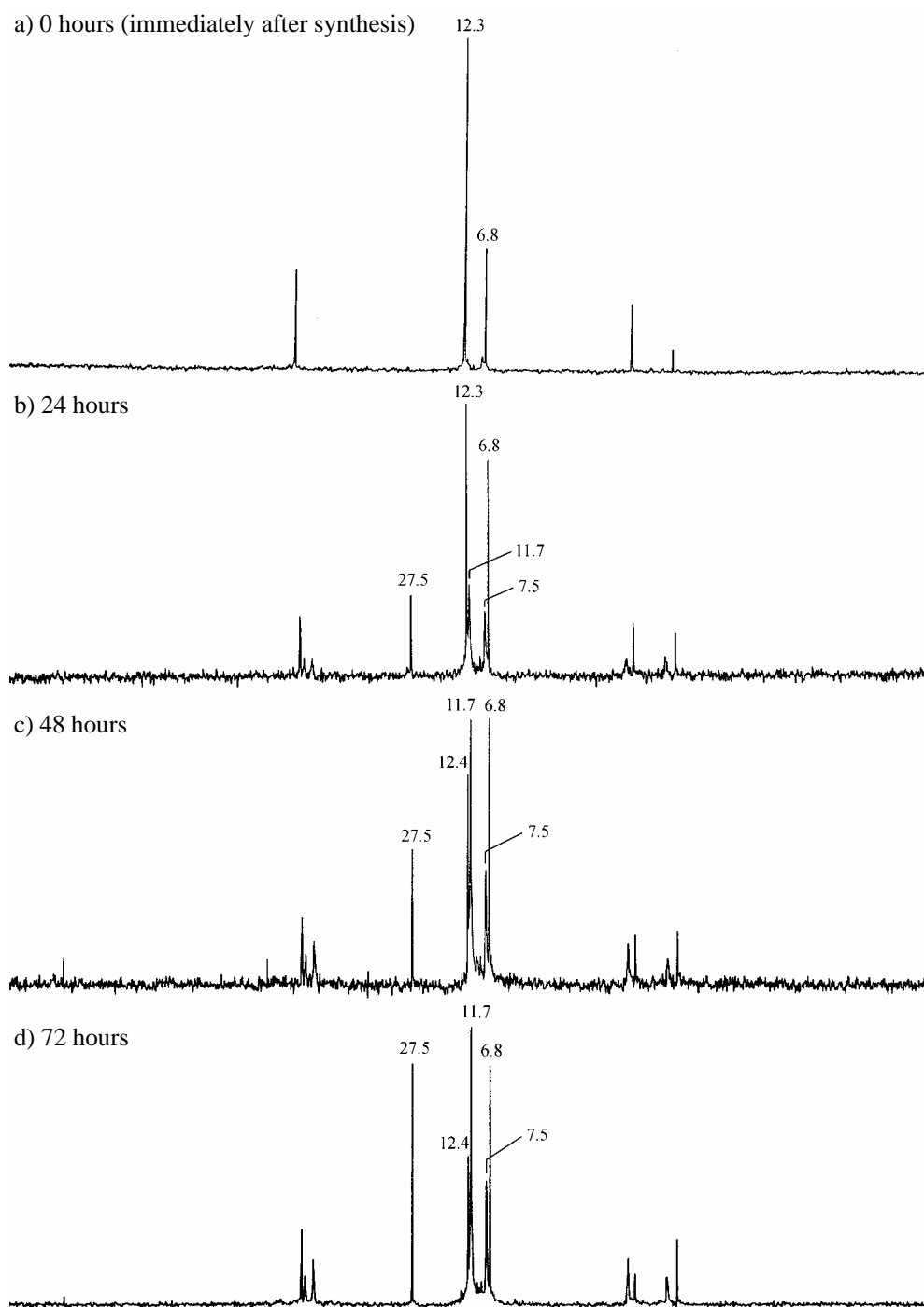


Figure 2.15: ^{31}P NMR (36.23 MHz) of the ureylene complex $[\text{Pt}\{\overline{\text{NHC}(\text{O})\text{NH}}\}(\text{PPh}_3)_2]$ 2.22k illustrating decomposition at various stages. The labelled peaks denote chemical shifts (ppm). a) recorded immediately after reaction completion; b) – d) recorded after standing for the time stated.

2.2.3.3 Electrospray mass spectrometry (ESMS)

Although a relatively new ionisation technique and developed primarily for the mass determination of large bio-molecules, ESMS is becoming increasingly popular for mass spectral analysis of inorganic and organometallic compounds, for which it is apparently equally well suited.

The ureylene complexes generally showed the strong $[M + H]^+$ or $[M + NH_4]^+$ parent ions typical of ESMS. Although parent ions were seen at a wide range of different cone voltages, optimum intensity was generally achieved with a cone voltage of around 50 V. Despite ESMS being extremely successful for most of the ureylene complexes, analysis of the disubstituted complexes incorporating an alkyl substituent (**2.22b**, **2.22d**, **2.22g** and **2.23**), all resulted in uninterpretable spectra whose signals could not be assigned to chemically sensible species. The reason for this result is not obvious, since the complexes would not be expected to vary significantly from the other ureylene complexes analysed, as far as their ionisation properties are concerned.

A number of unusual ions assigned as $[Pt(OH)(COD)]^+$, alone, or with one or two molecules of acetonitrile (from the mobile phase) were also observed. These possibly arise from the incomplete reaction of the starting material $[PtCl_2(COD)]$. Abstraction of the chloride by Ag^+ , considered the first step in the synthesis of complexes from metal halide where silver(I) oxide is used (see Scheme 1.2, Chapter One, Section 1.3), could result in the formation of the hydroxide. Since the species may well be naturally cationic [of the type $[Pt(OH)(COD)L]^+$ (L = neutral ligand)], they will have very high ionisation efficiencies compared to the neutral ureylene complexes, and thus can give unrepresentatively large signals. The acetonitrile adducts decrease with increased cone voltage, as expected.

The ESMS spectra of the N,N'-diphenylureylene complex **2.22a** recorded with a cone voltage of 50 V is shown in Figure 2.16, together with the observed and calculated³⁶ isotope patterns for the parent ion $[M + H]^+$. The most striking feature of the spectrum is a signal attributable to the loss of phenyl isocyanate $[M + H - PhNCO]^+$. An analogous (selective) loss of chlorophenylsulfonyl isocyanate was also observed for the novel sulfonylurea-derived ureylene complex **2.22e**, and loss of acetyl isocyanate was observed for the N,N'-diacetylureylene **2.22h**. Loss of isocyanate was not observed for any of the other

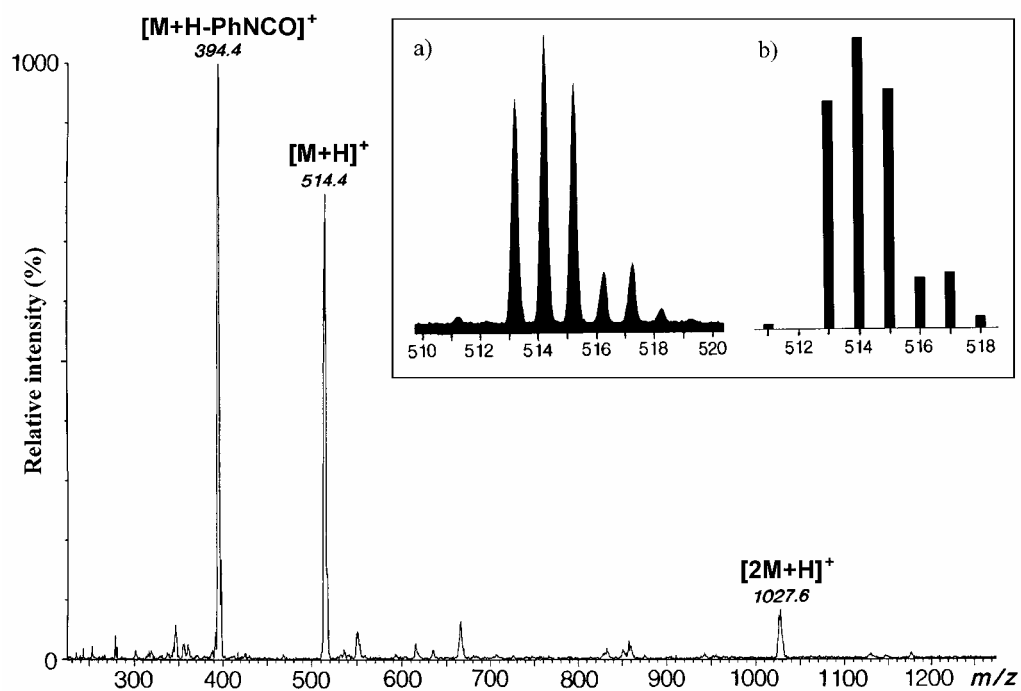


Figure 2.16: Positive-ion electrospray mass spectrum of $[\text{Pt}\{\overline{\text{NPhC(O)NPh}}\}(\text{COD})]$ **2.22d** ($= M$) recorded in MeCN/H₂O with cone = 50 V, showing peak assignments. The inset shows a comparison of the a) observed and b) calculated isotope distribution patterns for the $[M + H]^+$ parent ion at m/z 514.

complexes successfully analysed. Since isocyanates have been the principal source of ureylene complexes (as discussed in Section 2.1.2), ESMS potentially provides a rapid and convenient method for investigation of the decomposition pathway of these complexes.

2.2.4 Platinum hydroxide impurity

As seen earlier (Figure 2.15), a persistent peak at 6.8 ppm, with a 1J ($^{195}\text{Pt}-^{31}\text{P}$) coupling constant of 3700 Hz was evident. This species, present in many silver(I) oxide mediated reactions when *cis*-[PtCl₂(PPh₃)₂] is used as a starting material, has been isolated by fractional crystallisation from chloroform. The colourless crystals have been tentatively identified by ESMS, NMR and elemental analysis as the mononuclear platinum(II) hydroxide complex **2.24** (Figure 2.17). Mononuclear hydroxides are much less common than dinuclear complexes with bridging hydroxides (e.g. **2.25**), which have been characterised structurally.³⁷

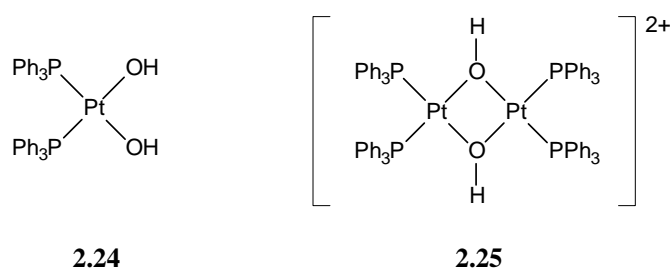


Figure 2.17

ESMS shows the expected signal at m/z 755 corresponding to the parent ion $[M + H]^+$. No signals associated with a dication, required for the dinuclear bridging species **2.25**, were detected. The isotope distribution pattern for **2.25** would clearly show the 2+ nature of a dication, with peaks separated by half mass units, and would be expected to be very strong since no aggregation with protons would be required for charge acquisition.

2.2.5 Conclusions

Silver(I) oxide provides an extremely convenient synthetic route to ureylene complexes, with the limitation of the necessary availability of at least one sufficiently acidic N-H hydrogen. Silver(I) oxide was found to be a milder method for forming ureylenes than sodium hydride, which, although proving significantly more rapid, decomposed the resulting complexes. The prepared ureylene complexes could be conveniently characterised both by ESMS and NMR spectroscopy, the latter by inspection of the resonances associated with the ancillary COD or triphenylphosphine ligands.

2.3 Experimental Section

General experimental procedures and the preparations of $[PtCl_2(COD)]$, *cis*- $[PtCl_2(PPh_3)_2]$ and silver(I) oxide are given in Appendix I. Details regarding the instrumentation used are given in Appendix II. ESMS spectra were recorded in MeCN/H₂O solvent. The sodium hydride (Koch-Light) used for the synthesis of **2.22a** and **2.22g** was oil-free and freshly powdered. Urea and N,N'-diphenylurea (BDH) were used as supplied from BDH.

All ¹H and ¹³C NMR spectra were recorded at 300.13 MHz and 75.47 MHz respectively, in CDCl₃ solvent. ³¹P NMR spectra were recorded at 36.23 MHz in CDCl₃ unless otherwise stated. ¹H and ¹³C spectra were unambiguously assigned by a combination of 1D NOE and 2D

^1H - ^{13}C COSY (short-range) and BIRDTRAP (long-range) experiments, and these are discussed in Appendix II.

2.3.1 Preparation and analysis of N,N' -disubstituted aromatic ureas

Unless otherwise stated, the disubstituted arylurea precursors were prepared via a minor modification of the literature procedure.³⁸ Excess phenyl isocyanate was carefully added to a stirred ethereal solution of the appropriate primary amine. The resulting white precipitate was filtered and thoroughly washed with diethyl ether to yield the product urea in near quantitative yields.

N,N'-diphenylurea

m.p. 239-240°C (lit.³⁹ 238°C).

IR: ν (CO region) 1648 (vs), 1594 (s), 1555 (s) cm^{-1} .

^1H NMR: ($\text{CD}_3\text{S}(\text{O})\text{CD}_3$) δ 8.75 (2H, s, br, NH), 7.56 (4H, d, $^3J_{2,3'} = 8.05$ Hz, H-2',6'), 7.36 (4H, t, $^3J_{3,2'} = 7.71$ Hz, H-3',5'), 7.05 (2H, t, $^3J_{4,3'} = 7.25$ Hz, H-4').

^{13}C NMR: ($\text{CD}_3\text{S}(\text{O})\text{CD}_3$) δ 154.3 (s, $\underline{\text{C}}=\text{O}$), 141.5 (s, C-1') 130.5 (d, C-3',5'), 123.6 (d, C-4'), 120.0 (d, C-2',6').

N-phenyl-*N'*-pyridylurea

m.p. 192-193°C (lit.³⁸ 194°C).

^1H NMR: δ 11.81 (1H, s, br, Ph- NH), 9.23 (1H, s, br, Py- NH), 8.26 (1H, dd, $^3J_{5'',4''} = 5.07$ Hz, $^4J_{5'',3''} = 1.08$ Hz, H-5''), 7.65 (1H, td, $^3J_{3'',2''} = 7.34$ Hz, $^4J_{3'',5''} = 1.85$ Hz, H-3''), 7.63 (2H, dd, $^3J_{2,3'} = 7.88$ Hz, $^4J_{2,4'} = 1.08$ Hz, H-2',6'), 7.36 (2H, t, $^3J_{3,2'} = 7.92$, H-3',5'), 7.10 (1H, tt, $^3J_{4,3'} = 7.41$ Hz, $^4J_{4,2'} = 1.06$ Hz, H-4'), 6.98 (1H, d, $^3J_{2'',3''} = 8.39$ Hz, H-2''), 6.94 (1H, tt, $^3J_{4'',3''} = 6.11$ Hz, $^4J_{4'',2''} = 0.83$ Hz, H-4'').

^{13}C NMR: δ 154.0 (s, C=O), 153.2 (s, C-1''), 145.9 (d, C-5''), 138.7 (s, C-1'), 138.7 (d, C-3'), 129.0 (d, C-3',5'), 123.4 (d, C-4'), 120.3 (d, C-2',6'), 117.2 (d, C-4''), 112.4 (d, C-2'').

N-adamantyl-*N'*-phenylurea

m.p. 248°C.

IR: ν (CO region) 1642 (s), 1595 (m), 1552 (vs) cm^{-1} .

^1H NMR: δ 7.27 (4H, *m*, H-2',3',5',6'), 7.05 (1H, *tt*, $^3J_{4',3'} = 6.26$ Hz, $^4J_{4',2'} = 2.38$ Hz, H-4'), 6.22 (1H, *s*, Ph-NH), 4.57 (1H, *s*, Ad-NH), 2.08 (3H, *m*, CH₂-CH-CH₂), 2.00 (6H, *d*, C-CH₂-CH), 1.67 (6H, *t*, CH-CH₂-CH).

^{13}C NMR: δ 154.4 (*s*, C=O), 139.0 (*s*, C-1'), 129.3 (*d*, C-3',5'), 123.6 (*d*, C-4'), 120.9 (*d*, C-2',6'), 51.4 (*s*, N-C-CH₂), 42.3 (*t*, C-CH₂-CH), 36.4 (*t*, CH-CH₂-CH), 29.6 (CH₂-CH-CH₂).

N-methyl-N'-phenylurea

m.p. 178-179°C (lit.³⁹ 179°C).

^1H NMR: δ 7.32-7.26 (4H, *m*, H-2',3',5',6'), 7.09 (1H, *tt*, $^3J_{4',3'} = 6.48$ Hz, $^4J_{4',2'} = 2.21$ Hz, H-4'), 6.54 (1H, *s*, br, Ph-NH), 4.87 (1H, *s*, br, Me-NH) 2.82 (3H, *d*, $^3J_{\text{H,H}} = 4.76$ Hz, CH₃).

^{13}C NMR: δ 156.6 (*s*, C=O), 138.5 (*s*, C-1'), 129.4 (*d*, C-3',5'), 124.2 (*d*, C-4'), 121.6 (*d*, C-2',6'), 27.1 (*q*, CH₃).

Chlorsulfuron

Chlorsulfuron was obtained from D. McNaughton, AgResearch Ltd., Hamilton, New Zealand, and used as supplied.

^1H NMR: δ 12.69 (1H, *s*, br, S(O)₂-NH), 8.29 (1H, *dd*, $^3J_{\text{H,H}} = 7.76$ Hz, $^4J_{\text{H,H}} = 1.53$ Hz, H-Ar), 7.90 (1H, *s*, br, C₃N₃-NH), 7.59-7.44 (3H, *m*, H-Ar), 4.04 (3H, *s*, OCH₃), 2.57 (3H, *s*, CH₃).

^{13}C NMR: δ 163.5 (*s*, C=O), 148.1 (*s*), 136.0 (*s*), 134.9 (*d*), 133.0 (*d*), 131.9 (*s*), 131.7 (*d*), 127.3 (*d*), 55.8 (*q*, OCH₃), 25.5 (*q*, CH₃).

{MeNHC(O)NH(p-C₆H₄)}₂CH₂

Solid diphenylmethane-4,4'-diisocyanate (BDH) was dissolved in ether, and excess methylamine (33% in ethanol) was added. A white precipitate formed immediately, which was filtered and dried under vacuum. Although the compound is extremely insoluble in most organic solvents, the bis(urea) readily dissolved in dimethyl sulfoxide. The purity was checked by NMR, which revealed a symmetrical compound implying both isocyanate groups had reacted completely.

m.p. 280°C.

^1H NMR: ($\text{CD}_3\text{S}(\text{O})\text{CD}_3$) δ 8.44 (2H, *s*, br, $\text{C}_6\text{H}_4\text{-NH}$), 7.36 (4H, *d*, $^3J_{2,3'} = 8.49$ Hz, 2',6',2'',6''), 7.11 (4H, *d*, $^3J_{3,2'} = 8.47$ Hz, H-3',5',3'',5''), 6.01 (2H, *q*, $^3J_{\text{H,H}} = 4.66$ Hz, $\text{H}_3\text{C-NH}$), 3.82 (2H, *s*, CH_2), 2.70 (6H, *d*, $^3J_{\text{H,H}} = 4.63$ Hz, CH_3).

^{13}C NMR: ($\text{CD}_3\text{S}(\text{O})\text{CD}_3$) δ 159.9 (*s*, $\text{C}=\text{O}$), 142.4 (*s*, C-1'), 138.2 (*d*, C-4'), 132.6 (*d*, C-3',6'), 121.8 (*d*, C-2',6'), 43.7(*t*, CH_2) 30.1 (*q*, CH_3).

2.3.2 Preparation of acetylureas

N-acetyl-*N'*-methylurea

This was prepared by the literature procedure.⁴⁰

m.p. 178°C (lit.⁴⁰ 178-180°C).

^1H NMR: δ 10.33 (1H, *s*, $\text{CH}_3\text{CO-NH}$), 8.40 (1H, *s*, $\text{H}_3\text{C-NH}$), 2.84 (3H, *d*, $^3J_{\text{H,H}} = 5.49$ Hz, CO-CH_3), 2.10 (3H, *s*, CH_3).

^{13}C NMR: δ 172.6 (*s*, $\text{H}_3\text{C-C}=\text{O}$), 155.6 (*s*, $\text{C}=\text{O}$), 26.1 (*q*, NH-CH_3), 23.9 (*q*, CO-CH_3).

N,N'-diacetylurea

To a flask containing benzene (60 ml) were added acetyl chloride (10 ml, excess) and urea (5.0 g, 0.083 mol) and the mixture refluxed for 17 hours, during which time a solid precipitate had formed. The benzene was removed under reduced pressure, and the residue was repeatedly extracted with diethyl ether. The ether extracts were combined and the solvent removed, to leave a residue of pure *N,N'*-diacetylurea (8.5 g, 71%).

m.p. 153-155°C (lit.³⁹ 154-155°C).

^1H NMR: δ 10.10 (2H, *s*, NH), 2.30 (6H, *s*, CH_3).

^{13}C NMR: δ 172.0 (*s*, $\text{H}_3\text{C-C}=\text{O}$), 151.0 (*s*, $\text{C}=\text{O}$), 25.0 (*q*, CH_3).

2.3.3 Preparation of the platinum(II) ureylene complexes 2.22a-2.23

$[\text{Pt}\{\overline{\text{NPhC}(\text{O})\text{NPh}}\}(\text{COD})]$ 2.22a

$[\text{PtCl}_2(\text{COD})]$ (0.051 g, 0.136 mmol), *N,N'*-diphenylurea (0.029 g, 0.137 mmol) and silver(I) oxide (0.807 g, excess) were refluxed in dichloromethane (30 ml) for 18 hrs. Filtration to remove the silver salts gave a pale green/yellow solution. The solvent was removed by

evaporation, and subsequent recrystallisation of the residue from dichloromethane and diethyl ether gave a pale green powder of **2.22a** (0.059 g, 84%).

Alternatively, N,N'-diphenylurea (0.116 g, 0.547 mmol) and [PtCl₂COD] (0.201 g, 0.537 mmol) were added to a flask containing THF (30 ml). Sodium hydride (1 g, excess) was added, the flask stoppered, and the suspension stirred vigorously for 45 minutes, during which time the suspension becomes bright yellow. Dichloromethane (30 ml) was added to completely effect solution of the product, and the insoluble sodium salts were filtered off. The solvent was removed under reduced pressure, and the residue recrystallised by addition of diethyl ether to a dichloromethane solution. The micro-crystalline product was filtered and dried under vacuum to give **2.22a** (0.154 g, 56%), characterised by spectroscopic properties identical to an authentic sample of **2.22a** prepared by the silver(I) oxide route.

m.p. 150°C (decomposition point).

Found: C, 48.6; H, 4.6; N, 5.4%. Required for C₂₀H₂₂N₂O₂Pt: C, 49.1; H, 4.3; N, 5.5%.

IR: ν (CO region) 1648 (vs), 1594 (s) cm⁻¹.

ESMS: (Cone = 50V) m/z 1027 ([2M + H]⁺, 10%), 514 ([MH]⁺, 80%), 394 ([MH - PhNCO], 100%).

¹H NMR: δ 7.29-7.13 (8H, *m*, H-Ar), 6.91 (4H, *t*, ³J_{4,3'} = 7.13 Hz, H-4'), 5.20 (4H, (*t*, *br*), (*d*, ²J_{H,Pt} = 59.4 Hz), CH=CH), 2.61 (4H, *m*, CH-CH₂), 2.29 (4H, *m*, CH-CH₂).

¹³C NMR: δ 129.1 (*s*, C-3',5'), 128.9 (*s*, C-3',5'), 123.6 (*s*), 122.6 (*s*), 120.6 (*s*), 94.1 (*d*, (*d*, ¹J_{C,Pt} = 141.7 Hz), CH=CH), 30.2 (*t*, CH-CH₂).

[Pt{NPhC(O)NMe}(COD)] 2.22b

Similarly prepared to **2.22a** above, [PtCl₂(COD)] (0.052 g, 0.139 mmol), N-methyl-N'-phenylurea (0.016 g, 0.138 mmol) and silver(I) oxide (0.11 g, excess) were refluxed in dichloromethane for 5 hours. Work-up, and recrystallisation from dichloromethane and diethyl ether afforded pale yellow rosettes of **2.22b** (0.039 g, 81%).

m.p. 140°C.

Found: C, 42.7; H, 4.8; N, 6.1%. Required for C₁₆H₂₀N₂O₂Pt: C, 42.6; H, 4.5 ;N, 6.2%.

IR: ν (CO region) 1650 (vs), 1590 (s) cm⁻¹.

¹H NMR: δ 7.18-7.05 (4H, *m*, C-2',3',5',6'), 6.78 (1H, *t*, ³J_{4,3'} = 7.07 Hz, H-4'), 5.13 (2H, (*s*, *br*), (*d*, *br*), (*d*, *br*), ²J_{H,Pt} = 53.9 Hz), CH=CH *trans* NMe), 5.08 (2H, (*s*, *br*), (*d*, *br*), ²J_{H,Pt} = Hz),

$\underline{\text{CH}}=\text{CH}$ *trans* NPh), 2.94 (3H, *s*, (*d*, br, $^2J_{\text{H,Pt}} = 38.3$ Hz), $\underline{\text{CH}}_3$), 2.59 (4H, *m*, br, $\underline{\text{CH}}_2\text{-CH}$), 2.22 (4H, *m*, br, $\underline{\text{CH}}_2\text{-CH}$).

^{13}C NMR: δ 173.8 (*s*, $\underline{\text{C}}=\text{O}$), 147.3 (*s*, C-1'), 128.8 (*d*, C-3',5'), 120.9 (*d*, C-2',6'), 118.8 (*d*, C-4'), 93.7 (*d*, (*d*, $^1J_{\text{C,Pt}} = 133.1$ Hz), $\underline{\text{CH}}=\text{CH}$), 92.1 (*d*, (*d*, $^1J_{\text{C,Pt}} = 143.5$ Hz), $\underline{\text{CH}}=\text{CH}$), 31.7 (*q*, (*d*, $^2J_{\text{C,Pt}} = 30.5$ Hz), $\underline{\text{CH}}_3$), 30.4 (*t*, $\underline{\text{CH}}_2\text{-CH}$), 30.3 (*t*, $\underline{\text{CH}}_2\text{-CH}$).

$[\text{Pt}\{\overline{\text{NPhC(O)NPy}}\}(\text{COD})]$ **2.22c**

Similarly prepared to **2.22a** above, $[\text{PtCl}_2(\text{COD})]$ (0.100 g, 0.266 mmol), N-phenyl-N'-pyridylurea (0.056 g, 0.264 mmol) and silver(I) oxide (0.129 g, excess) were refluxed in dichloromethane for 24 hours. Work-up gave bright yellow crystals of **2.22c** (0.105 g, 77%).

m.p. 240°C (decomposed without melting).

Found: C, 46.7; H, 4.2; N, 8.1%. Required for $\text{C}_{19}\text{H}_{21}\text{N}_3\text{OPt}\cdot\frac{1}{4}(\text{CH}_3\text{CH}_2)_2\text{O}$: C, 46.1; H, 4.5; N, = 8.1%.

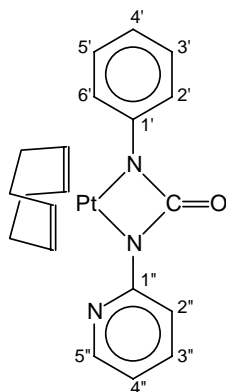
IR: ν (CO region) 1662 (vs), 1548 (s) cm^{-1} .

ESMS: (Cone 15 V) m/z 533 ($[\text{MNH}_4]^+$, 100%), 361 ($[\text{PtOH}(\text{COD}) + \text{CH}_3\text{CN}]^+$, 15%), 402 ($[\text{PtOH}(\text{COD}) + \text{CH}_3\text{CN}]^+$, 48%). (Cone 50 V) m/z 533 ($[\text{MNH}_4]^+$, 100%), 427 (undetermined, 36%), 361 ($[\text{PtOH}(\text{COD}) + \text{CH}_3\text{CN}]^+$, 72%), 320 ($[\text{PtOH}(\text{COD})]^+$, 77%).

^1H NMR: δ 7.98 (1H, *ddd*, $^3J_{2'',3''} = 6.05$ Hz, $^4J_{2'',4''} = 1.98$ Hz, $^5J_{2'',5''} = 0.84$ Hz, H-2''), 7.92 (1H, *dt*, $^3J_{5'',4''} = 8.51$ Hz, $^4J_{5'',3''} = 0.95$ Hz, H-5''), 7.41 (1H, *ddd*, $^3J_{4'',3''/5''} = 8.51$ Hz, $^3J_{4'',3''/5''} = 7.08$ Hz, $^4J_{4'',2''} = 2.02$ Hz, H-4''), 7.21 (2H, *tt*, $^3J_{3',2'} = 7.71$ Hz, $^4J_{3',5'} = 1.70$ Hz, H-3'), 7.12 (2H, *dt*, $^3J_{2',3'} = 9.2$ Hz, $^4J_{2',4'} = 1.79$ Hz, H-2'), 6.91 (1H, *tt*, $^3J_{4',3'} = 7.13$ Hz, $^4J_{4',2'} = 1.29$ Hz, H-4'), 6.50 (1H, *ddd*, $^3J_{3'',2''/4''} = 7.11$ Hz, $^3J_{3'',2''/4''} = 4.95$ Hz, $^4J_{3'',5''} = 0.98$ Hz, H-3''), 6.48 (2H, (*t*, $^3J_{\text{H,H}} = 2.81$ Hz), (*d*, $^2J_{\text{H,Pt}} = 64.6$ Hz), $\underline{\text{CH}}=\text{CH}$ *trans* NPh), 5.21 (2H, (*t*, $^3J_{\text{H,H}} = 2.52$ Hz), (*d*, $^2J_{\text{H,Pt}} = 63.1$ Hz), $\underline{\text{CH}}=\text{CH}$ *trans* NPy), 2.70-2.60 (4H, *m*, CH-CH_2), 2.40-2.14 (4H, *m*, CH-CH_2).

^{13}C NMR: δ 169.7 (*s*, C=O), 158.1 (*s*, C-1''), 147.5 (*d*, C-5''), 145.5 (*s*, C-1'), 136.9 (*d*, C-3''), 128.9 (*d*, C-3',5'), 122.6 (*d*, C-2',6'), 122.3 (*d*, C-4'), 115.6 (*d*, C-4''), 114.3 (*d*, ($^3J_{\text{C,Pt}} = 45.8$ Hz), C-2''), 95.2 (*d*, (*d*, $^1J_{\text{C,Pt}} = 131.6$ Hz), $\underline{\text{CH}}=\text{CH}$ *trans* NPh), 94.1 (*d*, (*d*, $^1J_{\text{C,Pt}} = 145.5$ Hz), $\underline{\text{CH}}=\text{CH}$ *trans* NPy), 30.7 (*d*, CH-CH_2), 30.0 (*d*, CH-CH_2).

NMR numbering scheme:



[Pt{NPhC(O)NAd}(COD)] 2.22d

Similarly prepared to **2.22a** above, [PtCl₂(COD)] (0.100 g, 0.266 mmol), N-phenyl-N'-1-adamantylurea (0.073 g, 0.270 mmol) and silver(I) oxide (0.126 g, excess) were refluxed in dichloromethane for 24 hours. Work-up and recrystallisation from dichloromethane and diethyl ether gave bright yellow crystals of **2.22d** (0.107 g, 70%).

m.p. 220°C (decomposition point).

Found: C, 50.2; H, 5.9; N, 4.4%. Required for C₂₅H₃₂N₂OPt.½CH₂Cl₂.½(CH₃CH₂)₂O (determined from the X-ray structure): C, 50.7; H, 5.9; N, 4.3%.

IR: ν (CO region) 1637 (vs), 1618 (s).

¹H NMR: δ 7.17 (2H, *dt*, ³J_{2,3'} = 6.52 Hz, ⁴J_{2,4'} = 1.79 Hz, H-2',6'), 7.11 (2H, *tt*, ³J_{3',2'} = 8.20 Hz, ⁴J_{3',5'} = 1.30 Hz, H-3',5'), 6.88 (1H, *tt*, ³J_{4',3'} = 7.10 Hz, ⁴J_{4',2'} = 1.48 Hz, H-4'), 5.63 (2H, (*t*, ³J_{H,H} = 2.77 Hz), (*d*, *br*, ²J_{H,Pt} = 61.0 Hz), CH=CH *trans* NAd), 4.73 (2H, (*t*, ³J_{H,H} = 2.79 Hz), (*d*, *br*, ²J_{H,Pt} = 60.8 Hz), CH=CH *trans* NPh), 2.54 (4H, *m*, CH₂-CH=CH), 2.26 (4H, *m*, CH₂-CH=CH), 2.01 (9H, *m*, *br*, H-Ad), 1.66 (6H, *m*, *br*, H-Ad).

¹³C NMR: δ 174.2 (*s*, C=O), 146.7 (*s*, C-1'), 128.5 (*d*, C-3',5'), 124.7 (*d*, C-2',6'), 122.6 (*d*, C-4'), 93.8 (*d*, (*d*, ¹J_{C,Pt} = 142.8 Hz), CH=CH₂), 90.7 (*d*, (*d*, ¹J_{C,Pt} = 128.6 Hz), CH=CH), 57.6 (*s*, N-C-CH₂), 44.2 (*t*, C-CH₂-CH), 36.8 (*t*, CH-CH₂-CH), 31.1 (*t*, CH₂-CH=CH), 30.3 (CH₂-CH-CH₂), 29.4 (*t*, CH₂-CH=CH).

[Pt{N(S(O)₂C₆H₄-2-Cl)C(O)NC₃N₃-2-(OMe)-4-Me}(COD)] 2.22e

Similarly prepared to **2.22a** above, [PtCl₂(COD)] (0.053 g, 0.142 mmol), Chlorsulfuron (0.51 g, 0.143 mmol) and silver(I) oxide (0.765 g, excess) were refluxed in dichloromethane for 5

hours. Work-up and recrystallisation from dichloromethane and diethyl ether gave **2.22e** as a cream solid (0.074 g, 79%).

m.p. 170°C (decomposition point).

Found: C, 35.8; H, 3.4; N, 10.2%. Required for $C_{20}H_{22}N_5OClPt \cdot 0.33CH_2Cl_2$: C, 35.5; H, 3.3; N, 10.2%.

IR: ν (CO region) 1725 (vs, br) cm^{-1} .

ESMS: (Cone 50 V) m/z 659 ($[MH]^+$, 100%). (Cone 100 V) m/z 659 ($[MH]^+$, 80%), 441 ($[MH - NSO_2C_6H_4Cl]^+$, 100%), 429 (undetermined, 63%). 1H NMR: δ 8.29 (1H, *d*, $^3J_{H,H} = 7.15$ Hz, Ar-H), 7.42-7.35 (3H, *m*, Ar-H), 6.41 (2H, (*s*, br), (*d*, br, $^2J_{H,Pt} = 68.2$ Hz), $\underline{CH=CH}$ *trans* N-S(O)₂), 6.33 (2H, (*s*, br), (*d*, br, $^2J_{H,Pt} = 61.0$ Hz), $\underline{CH=CH}$ *trans* N-triazene), 3.86 (3H, *s*, OCH₃), 2.65 (4H, *m*, br, $\underline{CH_2-CH}$), 2.42 (4H, *m*, br, $\underline{CH_2-CH}$), 2.32 (3H, *s*, CH₃)
 ^{13}C NMR: δ 178.7 (*s*, C=O), 171.5 (*s*), 168.1 (*s*), 161.3 (*s*), 139.0 (*s*), 133.6 (*d*), 133.0 (*d*), 131.5 (*s*), 131.3 (*d*), 127.2 (*d*), 98.6 (*d*, (*d*, br, $^1J_{C,Pt} = 139.1$ Hz), $\underline{CH=CH}$ *trans* N-chlorophenyl), 97.1 (*d*, (*d*, br, $^1J_{C,Pt} = 153.8$ Hz), $\underline{CH=CH}$ *trans* N-triazene), 54.6 (*q*, OCH₃), 30.9 (*t*, $\underline{CH_2-CH}$), 30.0 (*t*, $\underline{CH_2-CH}$), 25.6 (*q*, CH₃).

$[Pt\{NPhC(O)NPh\}(PPh_3)_2]$ **2.22f**

The compound **2.22f** was quantitatively prepared as a derivative of **2.22a** prepared above, by addition of two equivalents of triphenylphosphine to a dichloromethane solution of **2.22a**, and subsequent recrystallisation from dichloromethane and diethyl ether.

Alternatively, *cis*-[PtCl₂(PPh₃)₂] (0.106 g, 0.134 mmol), diphenylurea (0.029 g, 0.137 mmol) and silver(I) oxide (0.843 g, excess) were reacted as described for **2.22a** above. Work-up and recrystallisation from dichloromethane and diethyl ether gave **2.22f** as bright yellow crystals (0.107 g, 86%).

m.p. 240°C (decomposition point).

Found: C, 62.6; H, 4.0; N, 2.7%. Required for $C_{49}H_{40}N_2OP_2Pt$: C, 63.3; H, 4.3; N, = 3.0%.

IR: ν (CO region) 1639 (vs), 1589 (*m*) cm^{-1} .

ESMS: (Cone 50 V) m/z 957 (undetermined, 40%), 930 ($[MH]^+$, 70%), 772 (undetermined, 100%).

^{31}P NMR: δ 10.0 (*s*, (*d*, $^1J_{P,Pt} = 3337$ Hz), PPh₃).

^1H NMR: δ 7.47-7.32 (14H, *m*, PPh_3), 7.25-7.17 (8H, *m*, PPh_3), 7.09-7.04 (8H, *m*, PPh_3), 6.66 (2H, *d*, $^3J_{2,3'} = 7.24$ Hz, H-2',2''), 6.55 (2H, *t*, $^3J_{3',2'} = 7.29$ Hz, H-3',3''), 6.47 (1H, *t*, $^3J_{4',3'} = 6.97$ Hz, H-4',4'').

^{13}C NMR: δ 174.3 (*s*, $\text{C}=\text{O}$), 134.5-134.2 (*m*, PPh_3), 131.2 (*s*, PPh_3), 130.5 (*s*, PPh_3), 128.6-128.4 (*s*, PPh_3), 128.0-127.9 (*s*, PPh_3), 127.5 (*s*, C-2',6'), 127.2 (*s*, C-3',5'), 121.2 (*s*, C-4').

$[\text{Pt}\{\overline{\text{NPhC(O)NMe}}\}(\text{PPh}_3)_2]$ **2.22g**

To flask containing dichloromethane (30 ml) was added *cis*- $[\text{PtCl}_2(\text{PPh}_3)_2]$ (0.101 g, 0.128 mmol), N-methyl-N'-phenylurea (0.020 g, 0.133 mmol) and silver(I) oxide (0.12 g, excess) and the solution refluxed for 24 hours. The silver salts were removed by filtration and the dichloromethane removed under reduced pressure. The resulting bright yellow residue was dissolved in dichloromethane and diethyl ether slowly added, to give bright yellow crystals of **2.22g**, (0.071 g, 64%).

Alternatively, to a flask containing dry THF (30 ml) was added *cis*- $[\text{PtCl}_2(\text{PPh}_3)_2]$ (0.200 g, 0.253 mmol), N-methyl-N'-phenylurea (0.038 g, 0.253 mmol) and powdered sodium hydride (0.5 g, excess). The flask was stoppered and the suspension rapidly stirred at room temperature for 2 hours, during which time the solution became bright yellow. The insoluble matter was filtered off and the THF removed under reduced pressure. Dichloromethane (10 ml) was added to the residue and any remaining solids filtered off. Diethyl ether was slowly added to the supernatant to give yellow crystals of **2.22g** (0.160 g, 73%), and a cloudy suspension that could conveniently be separated from the crystals by decantation.

m.p. 231-232°C (melts with decomposition).

IR: ν (CO region) 1636 (*vs*), 1592 (*s*), 1571 (*w*) cm^{-1} .

Found: C, 60.0; H, 4.5; N, 3.2%. Required for $\text{C}_{44}\text{H}_{38}\text{N}_2\text{OP}_2\text{Pt}$: C, 60.9; H, 4.4; N, 3.2%.

^{31}P NMR: (121.49 MHz) δ 13.5 (*d*, $^2J_{\text{P,P}} = 21.9$ Hz, (*d*, $^1J_{\text{P,Pt}} = 3328.8$ Hz), PPh_3 *trans* NPh), 11.2 (*d*, $^2J_{\text{P,P}} = 21.9$ Hz, (*d*, $^1J_{\text{P,Pt}} = 3249.1$ Hz), PPh_3 *trans* NMe).

^1H NMR: δ 7.53-7.40 (12H, *m*, PPh_3), 7.33 (3H, *t*, $^3J_{\text{H,H}} = 7.01$ Hz, H-4 PPh_3), 7.18 (9H, *m*, PPh_3), 7.03 (6H, *t*, $^3J_{\text{H,H}} = 7.67$ Hz, PPh_3), 6.73 (2H, *d*, $^3J_{2,3'} = 7.84$ Hz, H-2',6'), 6.62 (2H, *t*, $^3J_{3',2'/4'} = 7.55$ Hz, H-3',5'), 6.53 (1H, *t*, $^3J_{4',3'} = 7.02$ Hz, H-4'), 2.21 (*s*, (*d*, $^3J_{\text{H,Pt}} = 34.64$ Hz), (*d*, $^4J_{\text{H,P}} = 5.45$ Hz), CH_3).

^{13}C NMR: δ 176.9 (*s*, $\text{C}=\text{O}$), 146.8 (*s*, C-1'), 134.6 (*d*, (*d*, $^3J_{\text{C,P}} = 11.1$ Hz), C-3,5 PPh_3), 134.0 (*d*, (*d*, $^3J_{\text{C,P}} = 11.2$ Hz), C-3,5 PPh_3), 130.8 (*d*, C-4 PPh_3), 130.3 (*s*, (*d*, $^1J_{\text{C,P}} = 45.1$ Hz), C-1

PPh₃), 130.0 (*s*, (*d*, ¹J_{C,P} = 34.9 Hz), C-1 PPh₃), 128.3 (*d*, (*d*, ²J_{C,P} = 10.8 Hz), C-2,6 PPh₃), 127.9 (*d*, (*d*, ²J_{C,P} = 10.9 Hz), C-2,6 PPh₃), 127.3 (*d*, C-2',6',3',5'), 121.0 (*d*, C-4'), 31.4 (*q*, (*d*, ²J_{C,Pt} = 27.3 Hz), (*d*, ³J_{C,P} = 3.3 Hz), CH₃).

[Pt{NAcC(O)NAc}(COD)] **2.22h**

Similarly prepared to **2.22a** above, [PtCl₂(COD)] (0.050 g, 0.134 mmol), N,N'-diacetylurea (0.020 g, 0.139 mmol) and silver(I) oxide (0.10 g, excess) were refluxed in dichloromethane for 6 hours. Work-up and recrystallisation from dichloromethane and diethyl ether afforded **2.22h** as cream crystals (0.047 g, 79%).

m.p = 264° (decomposes without melting).

Found: C, 35.1; H, 3.9; N, 6.2%. Required for C₁₅H₂₁N₃O₃Pt: C, 35.1; H, 4.1; N, 6.3%.

IR: ν(CO region) 1726 (*vs*), 1641 (*vs*, *br*) cm⁻¹.

ESMS: (Cone = 50 V) 446 ([MH]⁺, 100%), 361 ([Pt(OH)(COD) + CH₃CN]⁺, 28%).

¹H NMR: δ 6.17 (4H, (*s*, *br*), (*d*, *br*, ²J_{H,Pt} = 64.0 Hz), CH=CH), 2.50 (4H, *m*, CH-CH₂), 2.39 (6H, *s*, CH₃) 2.31 (4H, *m*, CH-CH₂).

¹³C NMR: δ 174.6 (*s*, C=O), 165.3 (*s*, C=N), 96.7 (*d*, (*d*, ¹J_{C,Pt} = 132.7 Hz), CH=CH), 30.4 (*t*, CH-CH₂), 26.7 (*q*, (*d*, ³J_{C,Pt} = 36.5 Hz), CH₃).

[Pt{NMeC(O)NAc}(COD)] **2.22i**

Similarly prepared to **2.22a** above, [PtCl₂(COD)] (0.052 g, 0.139 mmol), N-acetyl-N'-methylurea (0.016 g, 0.138 mmol) and silver(I) oxide (0.11 g, excess) were refluxed in dichloromethane for 5 hours. Work-up and recrystallisation from dichloromethane and diethyl ether afforded **2.22i** as a pale yellow oil [0.049 g, (~95% pure by ¹H NMR)], which slowly decomposed on standing.

¹H NMR: δ 6.08 (2H, (*t*, ³J_{H,H} = 2.65 Hz), (*d*, *br*, ²J_{H,Pt} = 61.3 Hz), CH=C *trans* NMe), 5.17 (2H, (*t*, ³J_{H,H} = 2.48 Hz), (*d*, *br*, ²J_{H,Pt} = 62.4 Hz), CH=CH *trans* NAc), 2.87 (3H, *s*, (*d*, *br*, ²J_{H,Pt} = 40.0 Hz), CH₃), 2.56 (4H, *m*, *br*, CH₂-CH), 2.37 (3H, *s*, N-CH₃), 2.32 (4H, *m*, *br*, CH₂-CH).

¹³C NMR: δ 172.7 (*s*, H₃C-C=O), 170.4 (*s*, C=O), 93.9 (*d*, (*d*, ¹J_{C,Pt} = 141.1 Hz), CH=CH), 93.5 (*d*, (*d*, ¹J_{C,Pt} = 128.7 Hz), CH=CH), 31.1 (*q*, CO-CH₃), 30.8 (*t*, CH₂-CH), 30.0 (*t*, CH₂-CH), 26.0 (*q*, (*d*, ¹J_{C,Pt} = 41.5 Hz), CH₃).

Attempted preparation of [Pt{NPhC(O)NH}(COD)]

Similarly, [PtCl₂(COD)] (0.101 g, 0.270 mmol), phenylurea (0.036 g, 0.264 mmol) and silver(I) oxide (0.164 g, excess) was refluxed in dichloromethane for 3 hours. Work-up gave a viscous orange oil which did not crystallise. NMR revealed a mixture of compounds, the major constituent being phenylurea.

[Pt{NPhC(O)NH}(PPh₃)₂] 2.22j

[PtCl₂(COD)] (0.050 g, 0.134 mmol), triphenylphosphine (0.071g, 0.270), phenylurea (0.018 g, 0.132 mmol) and silver(I) oxide (0.122 g, excess) were refluxed in dichloromethane for 5 hours. Work-up gave a pale orange oil which did not crystallise. On standing the solution became noticeably darker, indicating possible decomposition. This was later confirmed by ³¹P NMR. Decomposition in chloroform was also noted. ³¹P NMR revealed the oil contained considerable quantities of [Pt(OH)₂(PPh₃)₂], precluding further NMR studies and elemental analysis.

³¹P NMR: (36.23 MHz) (CH₂Cl₂, D₂O lock) δ 12.7 (*s*, (*d*, ²J_{P,P} = 22.0 Hz), (*d*, ¹J_{P,Pt} = 3174 Hz, Ph₃P *trans* NH), 11.7 (*s*, (*d*, ²J_{P,P} = 19.6 Hz), (*d*, ¹J_{P,Pt} = 3423 Hz, Ph₃P *trans* NPh), 6.82 (*s*, (¹J_{P,Pt} = 3699 Hz), impurity).

[Pt{NHC(O)NH}(PPh₃)₂] 2.22k

[PtCl₂(COD)] (0.052, 0.139 mmol), triphenylphosphine (0.074g, 0.282), urea (0.010 g, 0.167 mmol) and silver(I) oxide (0.113 g, excess) were refluxed in dichloromethane for 5 hours. Work-up gave a pale orange oil which did not crystallise. ³¹P NMR revealed the oil contained substantial quantities of [Pt(OH)₂(PPh₃)₂]. Additionally, on standing samples of the product in dichloromethane became dark orange, with ³¹P NMR indicating slow decomposition. For these reasons further analysis were not pursued.

³¹P NMR: (36.23 MHz) (CH₂Cl₂, D₂O lock) δ 12.3 (*s*, (*d*, ¹J_{P,Pt} = 3291 Hz), Ph₃P), 6.8 (*s*, (*d*, ¹J_{P,Pt} = 3704 Hz), [Pt(OH)₂(PPh₃)₂]).

On standing the following additional impurity resonances resulted: δ 27.5 (*s*, impurity), 11.7 (*s*, (*d*, ¹J_{P,Pt} = 3096 Hz), impurity), 7.5 (*s*, (*d*, ¹J_{P,Pt} = 3567 Hz), impurity),

Attempted preparation of $[\text{Pt}\{\overline{\text{NMeC(O)NMe}}\}(\text{COD})]$

Similarly, $[\text{PtCl}_2(\text{COD})]$ (0.053 g, 0.142 mmol), N,N'-dimethylurea (0.013 g, 0.148 mmol) and silver(I) oxide (0.832 g, excess) was refluxed in dichloromethane for 3 days (preliminary work revealed no reaction had occurred in 18 hours). Work-up gave a viscous orange oil which was analysed by ^1H and ^{13}C NMR as being a combination of starting materials and various decomposition products.

 $[(\text{COD})\text{Pt}\{\overline{\text{NMeC(O)N}}(p\text{-C}_6\text{H}_4)\}_2\text{CH}_2]$ 2.23

Similarly prepared to **2.22a** above, $[\text{PtCl}_2(\text{COD})]$ (0.052 g, 0.139 mmol), $\{\text{MeNHC(O)NH}(p\text{-C}_6\text{H}_4)\}_2\text{CH}_2$ (0.016 g, 0.138 mmol) and silver(I) oxide (0.11 g, excess) were refluxed in dichloromethane for 5 hours. Work-up and recrystallisation from dichloromethane and diethyl ether yielded bright yellow pellets of **2.23** (0.094 g, 75%).

m.p. 190°C (decomposition point).

Found: C, 43.6; H, 5.0; N, 6.2%. Required for $\text{C}_{33}\text{H}_{40}\text{N}_4\text{O}_2\text{Pt}_2$: C, 43.3; H, 4.4; N, 6.1%.

IR: ν (CO region) 1640 (vs, br), 1605 (s) cm^{-1} .

^1H NMR: δ 6.93 (4H, *d*, $^3J_{2,3'} = 8.52$ Hz, 2',6'), 6.88 (4H, *d*, $^3J_{3',2'} = 8.52$ Hz, H-3',5'), 4.98 (8H, (*s*, br), (*d*, br, $^2J_{\text{H,Pt}} = \text{Hz}$), $\underline{\text{CH}}=\text{CH}$), 3.68 (2H, *s*, CH_2), 2.87 (3H, *s*, (*d*, br, $^2J_{\text{H,Pt}} = 38.3$ Hz), $\underline{\text{CH}}_3$), 2.41 (4H, *m*, br, $\underline{\text{CH}}_2\text{-CH}$), 2.13 (4H, *m*, br, $\underline{\text{CH}}_2\text{-CH}$).

^{13}C NMR: δ 173.6 (*s*, $\underline{\text{C}}=\text{O}$), 145.1 (*s*, C-1'), 133.9 (*s*, C-4'), 128.9 (*d*, C-3',5'), 120.8 (*d*, C-2',6'), 93.6 (*d*, (*d*, br, $^1J_{\text{C,Pt}} = 127.5$ Hz), $\underline{\text{CH}}=\text{CH}$), 91.9 (*d*, (*d*, br, $^1J_{\text{C,Pt}} = 127.5$ Hz), $\underline{\text{CH}}=\text{CH}$), 40.6 (*t*, $\underline{\text{CH}}_2$), 31.5 (*q*, CH_3), 30.1 (*t*, $\underline{\text{CH}}_2\text{-CH}$), 30.0 (*t*, $\underline{\text{CH}}_2\text{-CH}$).

Isolation of the platinum(II) hydroxide *cis*- $[\text{Pt}(\text{OH})_2(\text{PPh}_3)_2]$ 2.24

On one occasion of the silver(I) oxide mediated preparation of **2.22g** described above, an unusually large quantity of the hydroxide complex **2.24** was detected by ^{31}P NMR. Slow fractional crystallisation from chloroform-ether eventually yielded pure **2.24** as colourless crystals.

m.p. 196-198°C.

ESMS: (Cone 20V) (MeOH) *m/z* 796 (undetermined, 33%), 765 (undetermined, 100%), 755 ($[\{\text{Pt}(\text{OH})_2(\text{PPh}_3)_2\}\text{H}]^+$, 30%). (Cone 50 V) *m/z* 755 ($[\{\text{Pt}(\text{OH})_2(\text{PPh}_3)_2\}\text{H}]^+$, 100%), 759 ($[\overline{\text{Pt}\{\text{C}_6\text{H}_4\text{PPh}_2\}}(\text{PPh}_3) + \text{MeCN}]^+$, 38%), 718 ($[\overline{\text{Pt}\{\text{C}_6\text{H}_4\text{PPh}_2\}}(\text{PPh}_3)]^+$, 52%).

Found: C, 49.9; H, 3.1; N, 0%. Required for $C_{36}H_{32}O_2P_2Pt \cdot CHCl_3$: C, 50.9; H, 3.8%.

^{31}P NMR: (121.49 MHz) δ 6.9 (*s*, (*d*, $^1J_{P,Pt} = 3706.3$ Hz), PPh_3).

1H NMR: δ 7.43-7.33 (18H, *m*, PPh_3), 7.20 (12H, *t*, $^3J_{H,H} = 7.79$, PPh_3).

^{13}C NMR: δ 134.2 (*d*, (*dd*, $^2J_{C,P} = 10.9$ Hz), C-2,6 PPh_3), 131.3 (*d*, C-4 PPh_3), 128.5 (*d*, (*dd*, $^3J_{C,P} = 11.2$ Hz), C-3,5 PPh_3), 127.9 (*d*, (*d*, $^2J_{C,P} = 10.9$ Hz), C-2,6 PPh_3). C-1 PPh_3 not resolved.

2.3.4 X-ray structure of $[Pt\{\overline{NPhC(O)NAd}\}(COD)]$ **2.22d** dichloromethane solvate

Results of preliminary studies

Yellow rectangular blocks of **2.22d** were obtained on crystallisation by vapour diffusion of diethyl ether into a saturated dichloromethane solution of **2.22d** at 4°C. Preliminary precession photography indicated triclinic symmetry, so the space group was assumed to be Pi (no. 2) which was confirmed by successful refinement.

Data collection

Accurate cell parameters and intensity data were collected on an Nicolet R3 automatic four-circle diffractometer at the University of Canterbury, using a crystal of dimensions 0.80 x 0.24 x 0.22 mm, with monochromated Mo-K α X-rays ($\lambda = 0.71073$ Å). A total of 3937 reflections in the range $2^\circ < \theta < 24^\circ$ were collected at 130(2) K, of which 3881 were unique. These were subsequently corrected for Lorentz effects, polarisation effects, and for linear absorption by a Ψ scan method ($T_{max, min} = 0.85, 0.40$).

Crystal Data: $C_{25}H_{32}N_2OPt \cdot CH_2Cl_2$, $M_r = 656.57$ (ignoring possible diethyl ether molecule of solvation), triclinic, space group Pi (no. 2), $a = 9.55(2)$, $b = 10.395(3)$, $c = 13.761$ Å, $\alpha = 90.54(3)$, $\beta = 91.21(7)$, $\gamma = 112.26(5)^\circ$, $U = 1263(2)$ Å³, $D_c = 1.726$ g cm⁻³, $Z = 2$, $F(000) = 648$, $\mu(Mo-K\alpha) = 5.79$ mm⁻¹.

Solution and refinement

The platinum atom position was located by the Patterson methods option of SHELXS-86⁴¹, and all other non-hydrogen atoms located routinely in subsequent full-matrix extended

automatic least-squares refinements based on F^2 (SHELXL-93).⁴² All non-hydrogen atoms were assigned anisotropic temperature factors, with all hydrogen atom positions determined by calculation.

A penultimate difference map showed some residual electron density, and this was modelled as three carbon atoms, with a tied occupancy factor which converged to 0.75. However these could not be assigned to any chemically-sensible species, although are most probably from a molecule of diethyl ether disordered across the inversion centre.

The refinement converged with $R_1 = 0.0397$ for 3474 data with $I \geq 2\sigma(I)$, 0.0449 for all data; $wR_2 = 0.1056$, and $\text{GoF} = 1.088$. No parameter shifted in the final cycle, and the final difference map showed no peaks or troughs of electron density greater than +1.88 and -1.69 e \AA^{-3} respectively (adjacent to the platinum atom).

References

- 1 W.T. Flannigan, G.R. Knox and P.L. Pauson, *Chem. and Ind.*, (1967) 1094.
- 2 P. Braunstein and D. Nobel, *Chem. Rev.*, 89 (1989) 1927.
- 3 S. Cenini and G. La Monica, *Inorg. Chim. Acta*, 18 (1976) 279.
- 4 J.A.J. Jarvis, B.E. Job, B.T. Kilbourn, R.H.B. Mais, P.G. Owston and P.F. Todd, *Chem. Commun.*, (1967) 1149.
- 5 P.C. Ellgen and J.N. Gerlach, *Inorg. Chem.*, 13 (1974) 1944.
- 6 R.J. Doedens, *Inorg. Chem.*, 7 (1968) 2323.
- 7 S. Cenini, M. Pizzotti, F. Porta and G. La Monica, *J. Organomet. Chem.*, 88 (1975), 237.
- 8 W. Beck, W. Rieber, S. Cenini, F. Porta and G. La Monica, *J. Chem. Soc. Dalton Trans.*, (1974) 298.
- 9 W-H. Leung, G. Wilkinson, B. Hussain-Bates and M.B. Hursthouse, *J. Chem. Soc. Dalton Trans.*, (1991) 2791.
- 10 W.A. Herrmann, G. Weichselbaumer, R.A. Paciello, R.A. Fischer, E. Herdtweck, J. Okuda and D.W. Marz, *Organometallics*, 9 (1990) 489.
- 11 R.I. Michelman, R.G. Bergman and R.A. Andersen, *J. Am. Chem. Soc.*, 113 (1991) 5100.
- 12 R.I. Michelman, R.G. Bergman and R.A. Andersen, *Organometallics*, 12 (1993) 2741.
- 13 G.D. Forster and G. Hogarth, *J. Chem. Soc., Dalton Trans.*, (1993) 2539.
- 14 M. Jolly, J.P. Mitchell and V.C. Gibson, *J. Chem. Soc., Dalton Trans.*, (1992) 1329.
- 15 P. Legzdins, E.C. Phillips, S.J. Rettig, J. Trotter, J.E. Veltheer and V.C. Yee, *Organometallics*, 11 (1992) 3104.
- 16 A.A. Danopoulos, G. Wilkinson, T.K.N. Sweet and M.B. Hursthouse, *J. Chem. Soc., Dalton Trans.*, (1996) 3771.
- 17 A.J. Blake, P. Mountford, G.I. Nikonov and D. Swallow, *J. Chem. Soc., Chem. Commun.*, (1996) 1835.
- 18 F. Paul, J. Fischer, P. Oschenbein and J.A. Osborn, *Angew. Chem. Int. Ed. Engl.*, 32 (1993) 1638.
- 19 R. Hasselbring, H.W. Roesky and M. Noltemeyer, *Angew. Chem. Int. Ed. Engl.*, 31 (1992) 601.
- 20 C.P. Casey, R.A. Widenhoefer and R.K. Hayashi, *Inorg. Chem.* 34 (1995) 1138.
- 21 S. Okeya, S. Koshino, M. Namie, I. Nagasawa and Y. Kushi, *J. Chem. Soc., Chem. Commun.*, (1995) 2123.

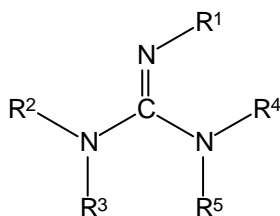
- 22 R.D.W. Kemmitt, S. Mason, M.R. Moore, J. Fawcett and D.R. Russell, *J. Chem. Soc., Dalton Trans.*, (1992) 409.
- 23 R.D.W. Kemmitt, S. Mason, M.R. Moore, J. Fawcett and D.R. Russell, *J. Chem. Soc., Chem. Commun.*, (1990) 1535.
- 24 I.P. Parkin and J.D. Woollins, *J. Chem. Soc., Dalton Trans.*, (1990) 519.
- 25 I.P. Parkin, A.M.Z. Slawin, D.J. Williams and J.D. Woollins, *J. Chem. Soc., Chem. Commun.*, (1989) 1060.
- 26 Y. Matsuura, N. Yasuoka, T. Ueki, N. Kasai and M. Kakudo, *Bull. Chem. Soc. Japan*, *42* (1969) 881.
- 27 W. Henderson, R.D.W. Kemmitt, S. Mason, M.R. Moore, J. Fawcett and D.R. Russell, *J. Chem. Soc., Dalton Trans.*, (1992) 59.
- 28 S. Okeya, Y. Fujiwara, S. Kawashima, Y. Hayashi, K. Isobe, Y. Nakamura, H. Shimomura and Y. Kushi, *Chem. Lett.*, (1992) 1823.
- 29 W. Henderson and B.K. Nicholson, *Polyhedron*, *15* (1996) 4015.
- 30 T.G. Appleton, H.C. Clark and L.E. Manzer, *Coord. Chem. Rev.*, *10* (1973) 335.
- 31 R.D.W. Kemmitt and M.R. Moore, *Transition Met. Chem.*, *18* (1993) 348.
- 32 A. Ohsuka, T. Hirao, H. Kurosawa and I. Ikeda, *Organometallics*, *14* (1995) 2538.
- 33 M.R. Gregg, J. Powell and J.F. Sawyer, *Acta Cryst. Sect. C*, *44* (1988) 43.
- 34 M.A. Andrews, G.L. Gould, W.T. Klooster, K.S. Koenig and E.J. Voss, *Inorg. Chem.*, *35* (1996) 5478.
- 35 T.K. Miyamoto, Y. Suzuki and H. Ichida, *Bull. Chem. Soc. Japan*, *65* (1992) 3386.
- 36 L.J. Arnold, *J. Chem. Educ.*, *69* (1992) 811.
- 37 J.J. Li, W. Li and P.R. Sharp, *Inorg. Chem.*, *35* (1996) 604.
- 38 A. Hocquet, J. Tohier and J. Fournier, *J. Chem. Educ.*, *71* (1994) 1092.
- 39 R.C. Weast, *CRC Handbook of Chemistry and Physics*, 59th Edition, CRC Press, West Palm Beach, Florida, (1978).
- 40 A.I. Vogel, *Practical Organic Chemistry*, 3rd Edn., Longman, London, (1972) 969.
- 41 G.M. Sheldrick, SHELXS-86, Program for Solving X-Ray Crystal Structures, University of Göttingen, Germany, (1986).
- 42 G.M. Sheldrick, SHELXL-93, Program for Refining X-Ray Crystal Structures, University of Göttingen, Germany, (1993).

Chapter Three

Synthesis and Characterisation of Guanidine Dianion (Triazatrimethylenemethane) Complexes

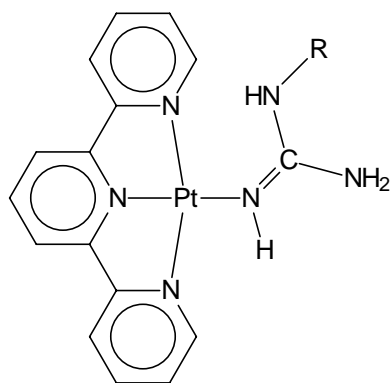
3.1 Introduction

Like ureas (Chapter Two), the guanidine group **3.1** (Figure 3.1) is a versatile ligand, capable of bonding to metal centres in variety of co-ordination modes. The most common of these is as neutral-donor ligands or monoanions.¹ The former has over the years attracted some interest, due its presence in the biologically relevant arginine system, which is frequently found in the active site of enzymes.² The complexes **3.2-3.4** (Figure 3.2) were thus prepared,^{2,3} and represent some examples of guanidines acting as neutral donor ligands.

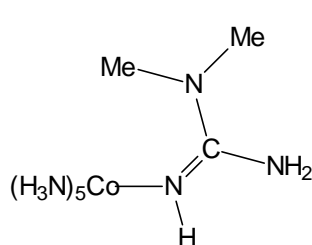


3.1

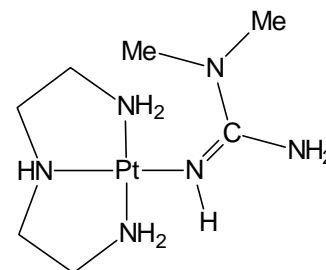
Figure 3.1



3.2 R = H, various alkyl groups



3.3



3.4

Figure 3.2

For the monoanions, both mono and bidentate systems have been prepared, although surprisingly the latter were until recently unknown. Bailey *et al.*, have synthesised a number of guanidine complexes containing chelating deprotonated N,N',N''-triphenylguanidine. The mononuclear rhodium and ruthenium complexes **3.5** and **3.6** (Figure 3.3) were prepared from the bridge-splitting of reaction of $[\{\text{Cp}^*\text{RhCl}_2\}_2]$ ($\text{Cp}^* = \eta^5\text{-pentamethylcyclopentadienyl}$, $\eta^5\text{-C}_5\text{Me}_5$) and $[(\eta^6\text{-}p\text{-cymene})\text{RuCl}_2]_2$ ($p\text{-cymene} = p\text{-isopropyltoluene}$, $p\text{-MeC}_6\text{H}_4\text{CHMe}_2$) using four equivalents of N,N',N''-triphenylguanidine.⁴ Very recently, the reaction of N,N'-diphenyl and N,N',N''-triphenylguanidine with $[\text{MnBr}(\text{CO})_5]$ was reported, to give the manganese complexes **3.7** (Figure 3.4).⁵ Subsequent reaction of **3.7** with $[\text{MoCl}(\text{Cp})(\text{CO})_3]$ ($\text{Cp} = \eta^5\text{-cyclopentadienyl}$, $\eta^5\text{-C}_5\text{H}_5$) gave the molybdenum derivatives **3.8** (Figure 3.4), also containing chelating guanidine monoanions.⁵

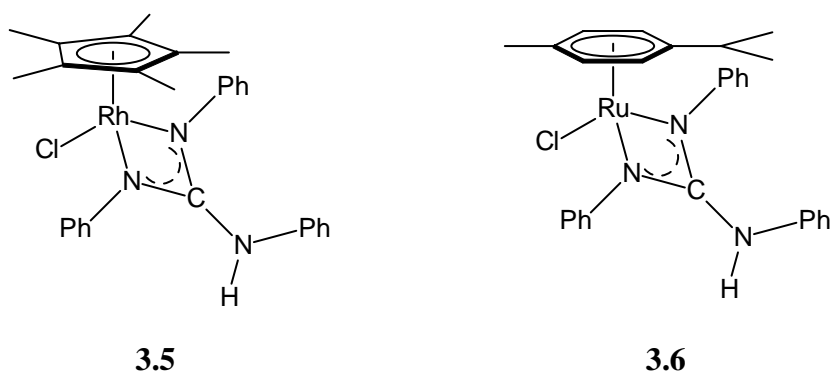


Figure 3.3

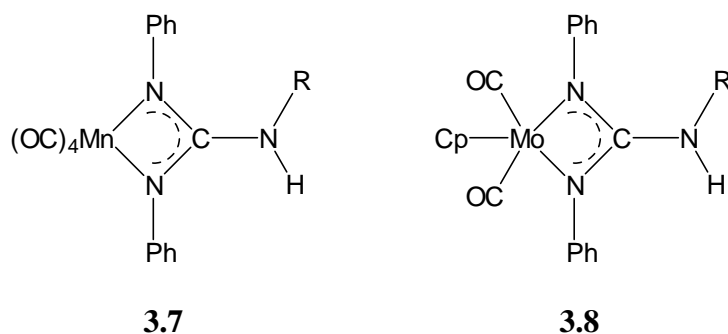
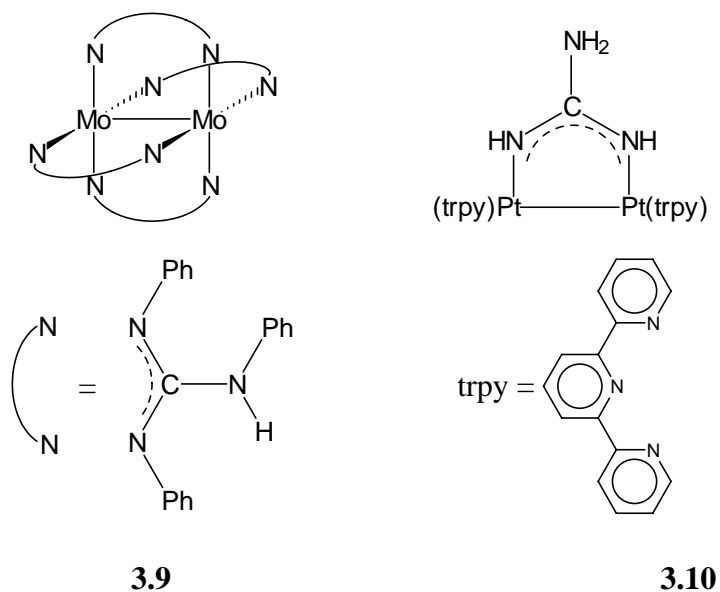
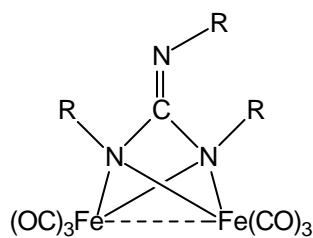


Figure 3.4

The dinuclear molybdenum complex **3.9** (Figure 3.5) incorporating four bridging guanidino groups was synthesised by the action of N,N',N''-triphenylguanidine on $[\text{Mo}(\text{CO})_6]$, and **3.9** could be readily oxidised by addition of AgBF_4 to give the monocationic analogue of **3.9**.⁶ The reaction of $[\text{Pt}(\text{trpy})\text{Cl}]\text{Cl}$ ($\text{trpy} = 2,2':6'\text{-terpyridine}$) with guanidine carbonate gave the dinuclear platinum complex **3.10** (Figure 3.5).⁷

*Figure 3.5*

The work described in this chapter is largely concerned with the derivatives of the much rarer guanidine dianion $[C(NR)_3]^{2-}$ (which could be described as a triazatrimethylenemethane dianion), closely related to the urea dianions detailed in Chapter Two. The first reported examples of systems containing the guanidine dianion were the dinuclear iron complexes **3.11a** (Figure 3.6) and **3.11b** (characterised crystallographically) reported in 1971, formed by the reaction of the appropriate dialkylcarbodiimides with $Fe(CO)_5$.⁸ The complexes **3.11** were found to be very similar to the isoelectronic tricarbonyl iron ureylene complexes **2.1** discussed in Chapter Two (Section 2.1.1).



3.11a R = *iso*-propyl

3.11b R = cyclohexyl

Figure 3.6

Further examples of systems containing the guanidine dianion were not reported until twenty-four years later, when the dilithio salt of *N,N',N''*-triphenylguanidine **3.12** (Figure 3.7), synthesised from *N,N',N''*-triphenylguanidine and *n*-butyllithium, was reported by Bailey *et al.*⁹ The resurgence of interest was primarily spawned by the possible synthesis of complexes containing the triazatrimethylenemethane dianion, formally isoelectronic with the widely

known, and greatly studied, trimethylenemethane ligand $[\text{C}(\text{CH}_2)_3]^{2-}$ systems. The trimethylenemethane dianion forms complexes with co-ordination in the η^4 -mode, and it was questioned if the guanidine dianion could co-ordinate in an analogous fashion. A number of isoelectronic monoazatri-methylenemethane complexes **3.13** (Figure 3.7) that have been prepared, were found to co-ordinate in an η^3 -configuration.¹⁰⁻¹⁴

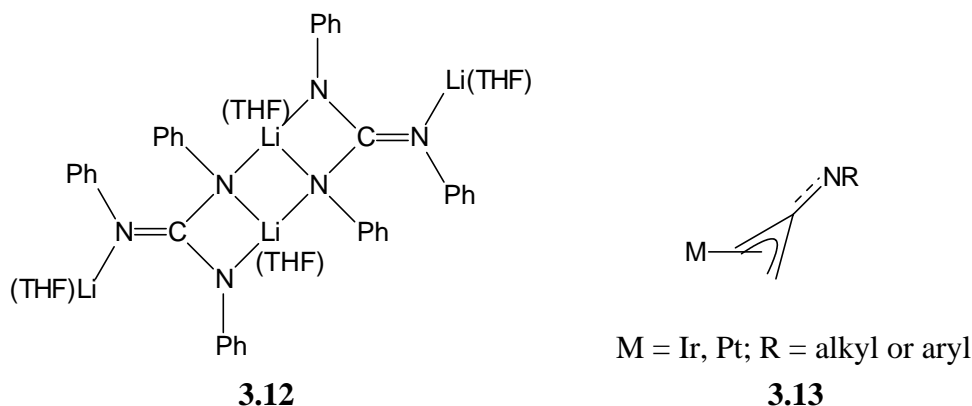


Figure 3.7

Indeed, **3.12** should potentially provide a useful route for the synthesis of transition-metal complexes, although hitherto Bailey has reported only one compound derived from **3.12**, the novel cadmium complex **3.14** (Figure 3.8), formed from the reaction of **3.12** with $[\text{Cd}\{\text{N}(\text{SiMe}_3)_2\}]$.¹⁵ Very recently the titanium triazatri-methylenemethane complex **3.15** (Figure 3.8), formed from the reaction of $[\text{Ti}\{=\text{N}(p\text{-tolyl})\}(\text{Me}_4\text{taa})]$ ($\text{H}_2\text{Me}_4\text{taa} =$ tetramethyldibenzotetraaza[14]annulene) with phenyl isocyanate,¹⁶ has been reported and is extremely similar to the isoelectronic ureylene complexes **2.15** (Chapter Two). Finally, the antimony complex **3.16**, in which the Sb(III) centre is formally chelated by monoanionic and dianionic N,N',N'' -triisopropylguanidine ligands, was synthesised from the reaction of $[\text{Sb}(\text{NMe}_2)_3]$ and N,N',N'' -triisopropylguanidine.¹⁷

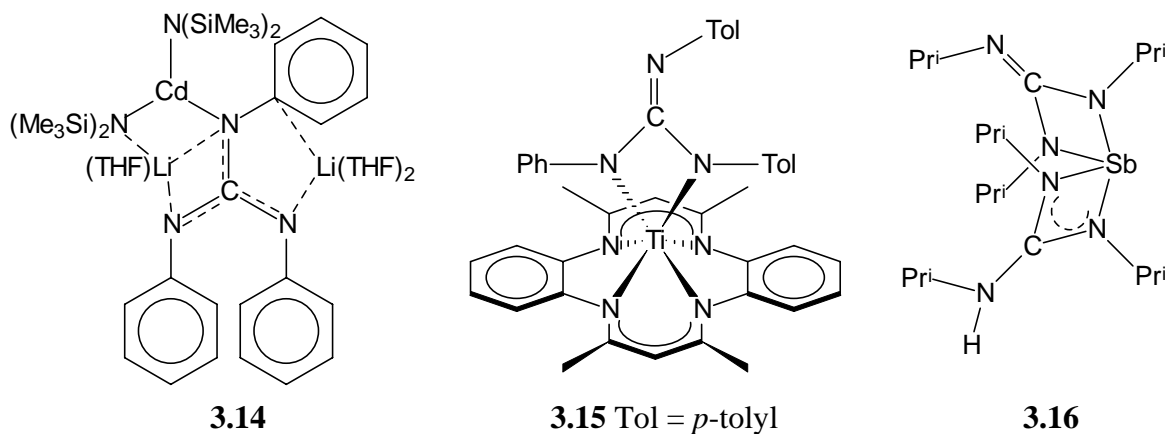


Figure 3.8

Our interest in the guanidine dianion stemmed from their similarity with the ureylene dianion, on which a considerable quantity of research had been carried out. It was reasoned that the silver(I) oxide mediated syntheses that proved extremely applicable to formation of ureylene complexes from ureas, could also be applied to guanidines. This chapter reports what were the first reported examples of mononuclear transition-metal complexes containing the guanidine dianion.

3.2 Results and Discussion

3.2.1 Syntheses of platinum(II) guanidine dianion complexes

Since both N,N',N''-triphenylguanidine and N,N',N''-triacetylguanidine could be readily prepared, the former from the reaction of diphenylcarbodiimide and aniline, the latter from the acetylation of free guanidine, they seemed to provide useful precursors for our studies.

When N,N',N''-triphenylguanidine was refluxed in dichloromethane with [PtCl₂(COD)] in the presence of silver(I) oxide for three hours, the solution became bright yellow. ¹H and ¹³C NMR of the crude reaction products revealed the reaction proceeded smoothly to produce only one major product, the η^2 -triazatrimethylenemethane complex **3.17a** (Figure 3.9), characterised spectroscopically, by electrospray mass spectrometry, elemental analysis and by a single crystal X-ray structure. In marked contrast, the triphenylphosphine analogue **3.17b** did not form readily, and only very little product was detected by ³¹P NMR even after 24 hours reaction. Even less successful was the attempted syntheses of **3.17b** from **3.17a** by simple ligand substitution of COD for triphenylphosphine, which surprisingly led only to recovery of starting materials. Since the triphenylphosphine N,N'-diphenylureylene complex **2.22f** (Chapter Two) formed readily under the same conditions, the resistance to the formation of **3.17b** was unexpected. Possibly the increased crowding from the extra phenyl ring in the guanidine system (C=NPh), in addition to the bulky rings from both N,N',N''-triphenylguanidine and triphenylphosphine, precludes the formation of **3.17b** on steric grounds.

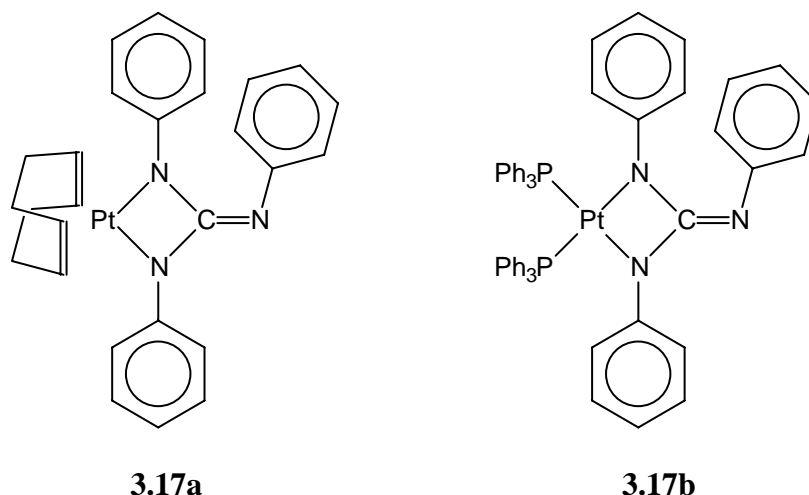


Figure 3.9

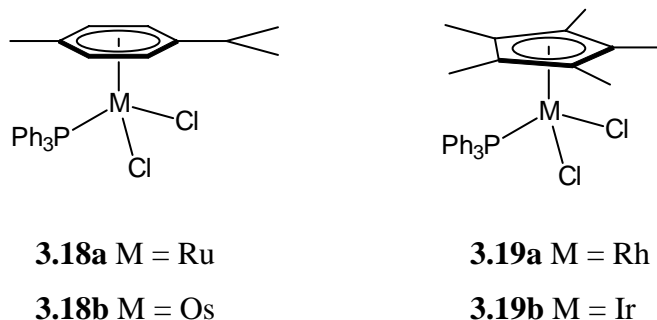
Despite the ready formation of **3.17a**, the analogous triacetylguanidine dianion complex could surprisingly not be prepared using *N,N,N''*-triacetylguanidine. In this case only the *N,N'*-diacetylureylene complex **2.22h** (Chapter Two) could be isolated (in an 87% yield), presumably the result of hydrolysis of the ligand (discussed later).

As for the ureas, the presence of sufficiently acidic nitrogen atoms seems to be essential, and like *N,N''*-dimethylurea, the reaction of *N,N',N''*-trimethylguanidine with $[\text{PtCl}_2(\text{COD})]$ and silver(I) oxide failed, and only starting materials were identified from the crude reaction mix.

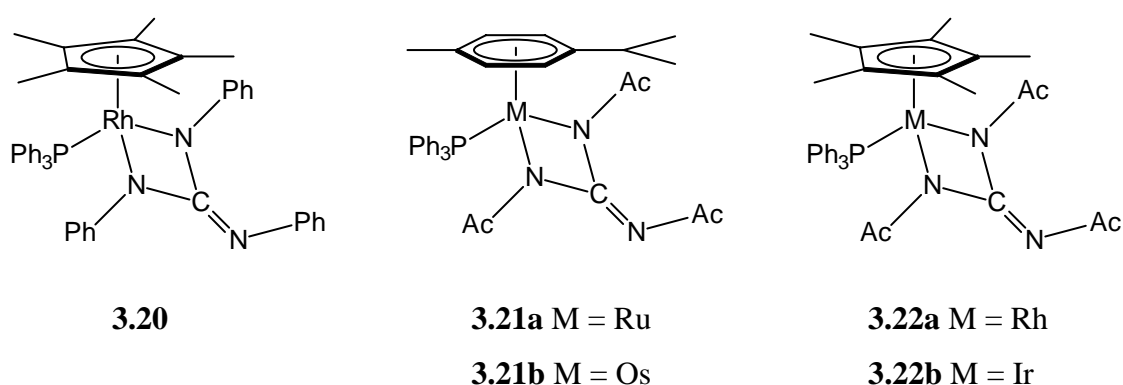
Perhaps more surprisingly, the reaction of *N,N'*-diphenyl-*N''*-methylguanidine and $[\text{PtCl}_2(\text{COD})]$ also failed to give a metal complex, although in this case a reaction did take place, but resulted only in decomposition of both the $[\text{PtCl}_2(\text{COD})]$ and the guanidine.

3.2.2 Syntheses of ruthenium(II), osmium(II), rhodium(III) and iridium(III) guanidine dianion complexes

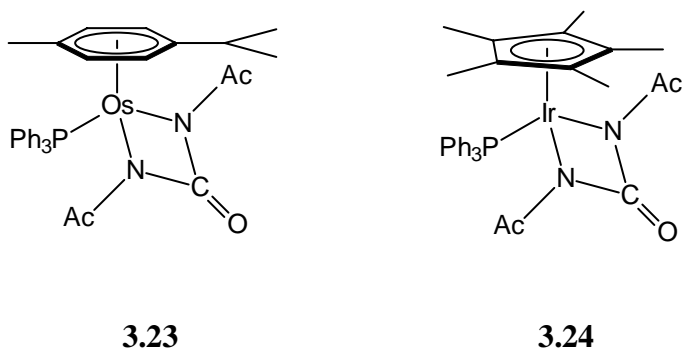
The contrasting reaction outcomes of *N,N',N''*-triphenylguanidine and *N,N',N''*-triacetylguanidine and the paucity of transition-metal guanidine dianion complexes in the literature, led us to investigate their chemistry with a range of alternative metal complexes. Since the ruthenium(II) and osmium(II) η^6 -*p*-cymene complexes **3.18a** and **3.18b** and the rhodium(III) and iridium(III) η^5 -pentamethylcyclopentadienyl complexes **3.19a** and **3.19b** (Figure 3.10) are, like *cis*- $[\text{PtCl}_2\text{L}_2]$, dihalide complexes, it was reasoned they may make suitable precursors.

**Figure 3.10**

When N,N',N''-triphenylguanidine and the complex **3.19a** were refluxed in dichloromethane using a nitrogen atmosphere, in the presence of silver(I) oxide, the complex **3.20** (Figure 3.11) was detected, although could not be isolated. When N,N',N''-triacetylguanidine was reacted with **3.18** and **3.19** the complexes **3.21** and **3.22** (Figure 3.11) containing the N,N',N''-triacetylguanidine dianion were characterised, although in varying yield. The nitrogen atmosphere appears to be essential, with only decomposition occurring in its absence.

**Figure 3.11**

The ruthenium and rhodium complexes **3.21a** and **3.22a** formed smoothly, and only these species were detected (by NMR spectroscopy) in crude reaction mixtures. However the reaction mixtures of the osmium and iridium systems **3.21b** and **3.22b** proved to contain the respective N,N'-diacetylureylene complexes **3.23** and **3.24** (Figure 3.12), analogous to **2.22h**. For the iridium system, the ureylene impurity constituted ~25% by ^{31}P NMR, and pure **3.22b** could be obtained by fractional crystallisation. For the osmium complex the ratio of **3.21b**:**3.23** was found to ~50:50 and efforts at purification proved futile. Chromatography was unsuccessful, since the complexes were found to bind irreversibly to all the supports trialed (silica, neutral alumina and florisil).

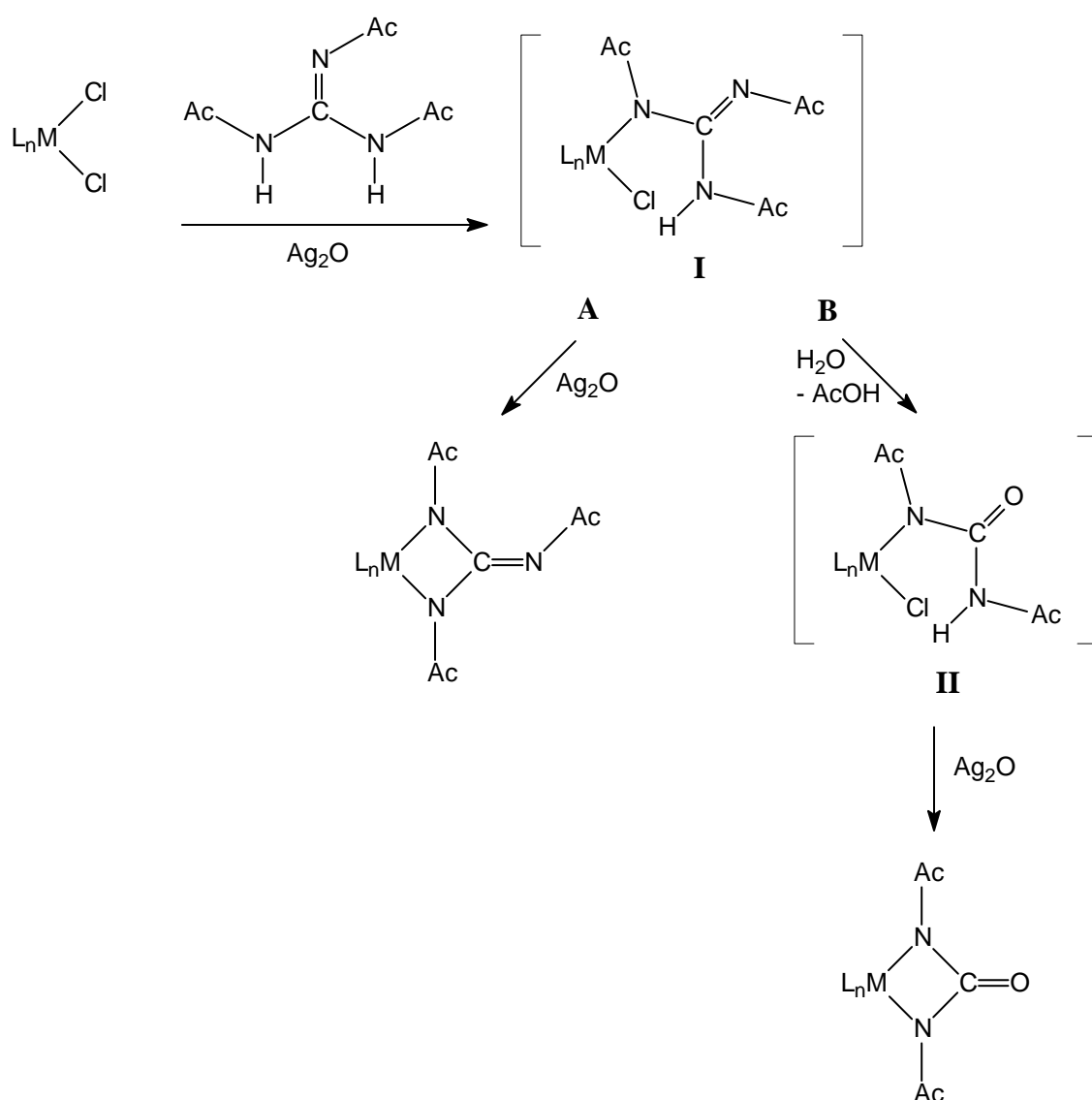
*Figure 3.12*

Nonetheless, all the complexes could be identified spectroscopically, by ESMS, and the ruthenium guanidine dianion derivative **3.21a** was additionally characterised by a single crystal X-ray study. Spectroscopic characterisation of the osmium and iridium complexes was aided by the ready formation of the ureylene complexes **3.23** and **3.24** prepared directly from the silver(I) oxide mediated reaction of N,N'-diacetylurea with **3.18b** and **3.19b**.

The formation of the N,N'-diacetylureylene complexes clearly arises as a result of hydrolysis of the N,N',N''-triacetylguanidine ligand. The hydrolysis appears to occur to variable extents, depending on the metal centre, with the ureylene complex being the sole product for the platinum, ~50% for the osmium, ~25% for the iridium, and not at all for the ruthenium and rhodium systems. Studies with the osmium system (in an effort to obtain higher concentrations of **3.21b**) revealed hydrolysis probably occurs in some intermediate species, and is facilitated by the metal centre. The relative amounts of **3.21b** and **3.23** remained constant when N,N',N''-triacetylguanidine and silver(I) oxide were refluxed in dichloromethane for 18 hours, with and without added water, prior to the addition of a stoichiometric quantity of **3.18b**. Additionally, extending the reflux time from 2 to 20 hours had little bearing on the ratio, with a 42:58 ratio in favour of the ureylene complex obtained in this case. These observations imply that both the free guanidine and the guanidine dianion product **3.21b** resist hydrolysis in the reaction conditions used.

A possible mechanism to account for these observations is presented in Scheme 3.1. The initial reaction of the metal-dichloride complex with N,N',N''-triacetylguanidine mediated by silver(I) oxide gives the monodentate guanidine intermediate **I**, which can subsequently react in one of two ways, represented by pathways **A** and **B**. Pathway **A** gives the guanidine dianion complex by simple cyclisation. However if the intermediate **I** hydrolyses as in pathway **B**, a second intermediate **II** could result, which could then, by silver(I) oxide mediated cyclisation,

give the ureylene complex. The greater lability of the second-row metals, ruthenium and rhodium, over their third-row counterparts results in pathway **A** being rapid, and so no ureylene complexes are formed. For platinum, osmium and iridium, the slower cyclisation makes pathway **B** competitive with **A**, and irreversible metal-promoted hydrolysis occurs to give intermediate **II**. It is unlikely that the active group in the hydrolysis process is a metal hydroxide ($M-OH$ could result from $M-Cl + Ag_2O$). Formation of such a group could provide a driving force for the hydrolysis, however, if this was the case, the rhodium and ruthenium systems would be expected to react (hydrolyse) more rapidly, and this was not observed experimentally.



Scheme 3.1

3.2.3 X-ray structure of $[\text{Pt}\{\overline{\text{NPhC(NPh)NPh}}\}(\text{COD})]$ **3.17a** diethyl ether solvate

The crystal structure of **3.17a** was determined to fully characterise the reaction product of $[\text{PtCl}_2(\text{COD})]$ and triphenylguanidine, to examine the absolute geometry of the compound, and for comparison with related systems. This is the first reported mononuclear structure of a transition-metal complex derived from a guanidine dianion.

ORTEP perspective and side views of the final structure, illustrating the atom labelling scheme, are shown in Figures 3.13 and 3.14 respectively, and selected bond lengths and angles are given in Table 3.1. Tables containing complete bond lengths and angles, final positional parameters, thermal parameters and calculated H-atom positions are presented in Appendix IV.

The structure confirms the expected cycloplatinated product **3.17a**, containing an η^2 -triazatrimethylenemethane ligand, co-ordinating to the platinum *via* two nitrogen atoms, thus forming an $\overline{\text{Pt-N-C-N}}$ metallacycle. The metallacycle is essentially planar, with no atom deviating from the least-squares plane by more than 0.05(1) Å, for N(2), with the imino group N(3) also lying in the plane. The C(1)-N(3) bond length [1.30(1) Å] is significantly shorter than both the C(1)-N(1) and C(1)-N(2) bond distances [both 1.40(1) Å], indicating localised single and double bonds. This contrasts with the structure of dilithio-triphenylguanidine dimer $[\{(\text{PhN})_3\text{C}\}_2\text{Li}_4(\text{THF})_6]$ **3.12**, which shows all C-N bond lengths to be approximately equal averaging 1.36(1) Å.⁹ The structure of free N,N',N''-triphenylguanidine has also been reported, and also shows delocalised bonding, with all C-N bonds ~ 1.34 Å.¹⁸ Thus, like the structure of ureylene complex **2.22d** (see Chapter Two, Section 2.2.2.4), the N,N',N''-triphenylguanidine dianion in **3.17a** overall bears a strong resemblance to the isoelectronic carbonato complexes (see Chapter One, Section 1.2.3.1).

As observed for **2.22d**, the central metal is co-ordinated in a distorted square planar arrangement, with the bidentate ligand and the η^4 -co-ordinated COD lying in the plane. For reasons discussed for **2.22d**, the main distortion is the N(1)-Pt-N(2) bite angle, which in this case is 65.9(3)°, thus deviating by 24.1° from a regular square-plane. The COD ligand is almost coplanar with the ureylene ring, deviating by only 6.9(3)°, and the ethylene moieties are almost perpendicular to the metallacycle with a dihedral angle of 85.9(4)°.

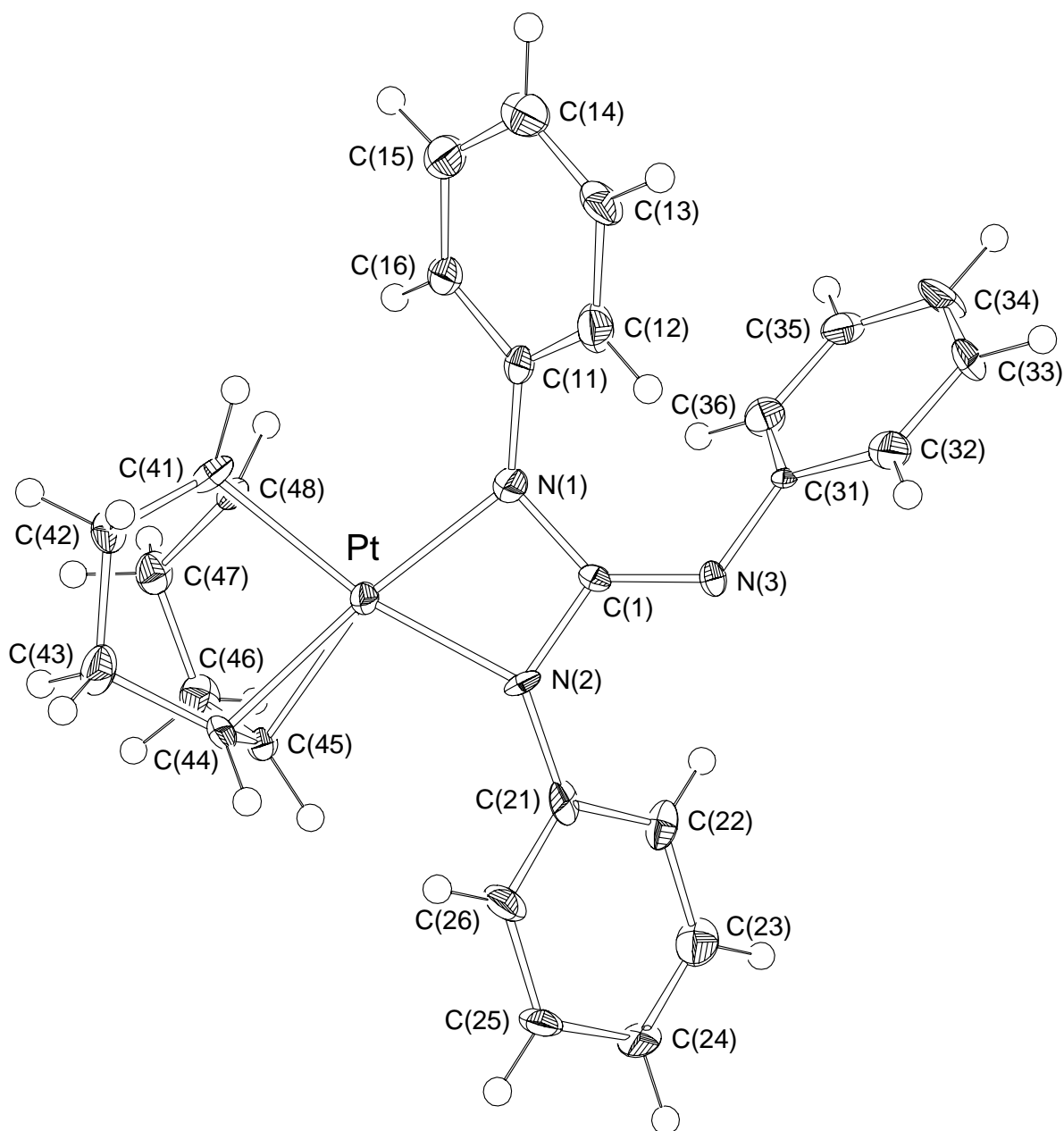


Figure 3.13: ORTEP perspective view of the structure of the platinum(II) triazatrimethylene-methane complex $[\text{Pt}\{\text{NPhC}(\text{NPh})\text{NPh}\}(\text{COD})]\cdot\frac{1}{2}\text{C}_4\text{H}_{10}\text{O}$ **3.17a**. The disordered diethyl ether solvate has been omitted for clarity. Thermal ellipsoids are shown at the 50% probability level.

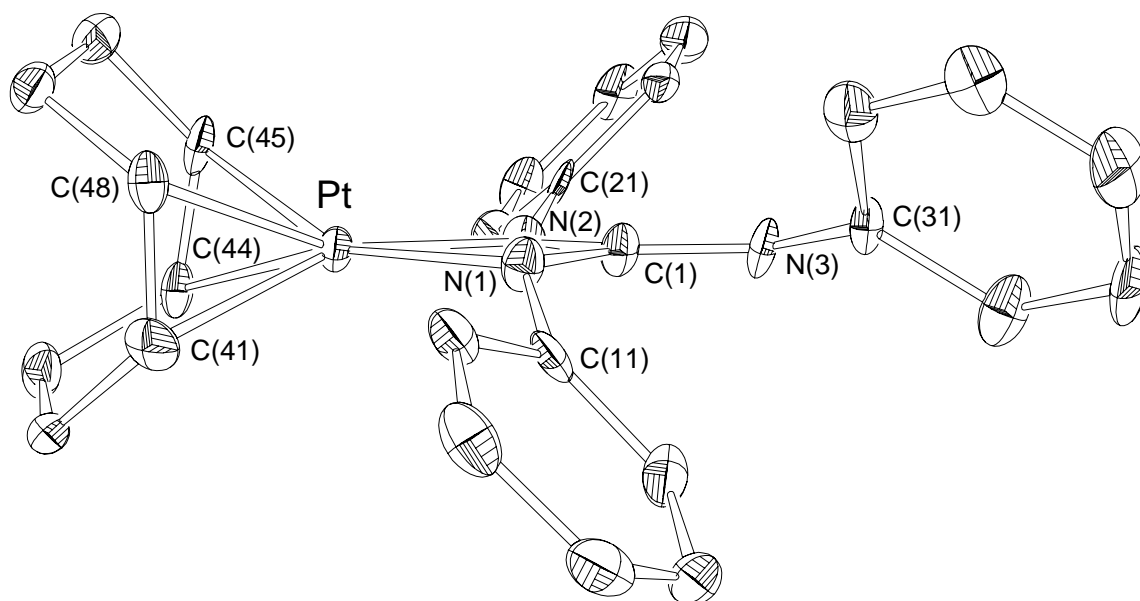


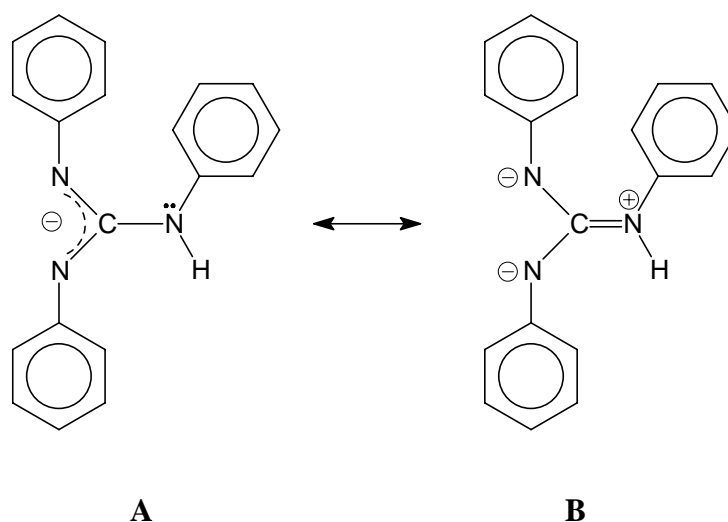
Figure 3.14: ORTEP side view of the structure of the platinum(II) triazatrimethylenemethane complex $[Pt\{NPhC(NPh)NPh\}(COD)] \cdot \frac{1}{2}C_4H_{10}O$ **3.17a**. The disordered diethyl ether solvate and all hydrogen atoms have been omitted for clarity. Thermal ellipsoids are shown at the 50% probability level.

Table 3.1: Selected bond lengths (Å) and angles (°) (estimated standard deviations in parentheses) of the platinum(II) *N,N',N''*-triphenylguanidine dianion complex **3.17a**·½C₄H₁₀O.

Bond	Length	Bonds	Angle
Pt-N(1)	2.034(8)	N(1)-Pt-N(2)	65.9(3)
Pt-N(2)	2.002(7)	Pt-N(1)-C(1)	94.7(5)
Pt-C(41)	2.173(9)	Pt-N(2)-C(1)	96.0(5)
Pt-C(48)	2.183(9)	Pt-N(1)-C(11)	129.2(6)
Pt-C(44)	2.188(9)	Pt-N(2)-C(21)	133.5(6)
Pt-C(45)	2.155(9)		
Pt...C(1)	2.561(9)		
Guanidine dianion and COD ligands			
N(1)-C(1)	1.398(11)	N(1)-C(1)-N(2)	103.3(7)
N(2)-C(1)	1.402(11)	N(1)-C(1)-N(3)	133.0(8)
N(3)-C(1)	1.298(11)	N(2)-C(1)-N(3)	123.7(8)
N(1)-C(11)	1.402(12)	C(1)-N(1)-C(11)	125.1(8)
N(2)-C(21)	1.406(12)	C(1)-N(2)-C(21)	124.8(7)
N(3)-C(31)	1.406(12)	C(1)-N(3)-C(31)	122.1(8)
C(41)-C(48)	1.407(13)		
C(44)-C(45)	1.379(13)		

The Pt-N(1) and Pt-N(2) bond distances are not the same length, with the Pt-N(1) bond being slightly [0.032(8) Å] longer. This is probably due to steric influence of the imino phenyl ring, whose orientation exerts some steric interaction on the N(1) phenyl substituent, having the observed effect of allowing a closer approach of N(2) to the platinum centre. This is further demonstrated by the inequivalent Pt-N-C bond angles which differ by 4.3(6)°, lower as expected for N(1)-Ph. Additionally the phenyl rings are tipped out of the metallacyclic plane, with C(11), C(21) and C(31) being respectively 0.84(1) Å above, 0.62(1) Å below, and 0.34(1) Å below the plane, as depicted in Figure 3.14. The dihedral angles of the planar phenyl rings with respect to the metallacycle are 45.8(2)° for N(1)-Ph, 44.6° for N(2)-Ph and 50.7(3)° for N(3)-Ph. As expected, the Pt- $\{\eta^2\text{-(CH=CH)}\}$ bond distances do not vary significantly [2.178(9) compared with 2.172(9) Å].

Comparing **3.17a** with the rhodium and ruthenium mononuclear monoanionic N,N',N''-triphenylguanidine derivatives **3.5** and **3.6**, the key difference is the C(1)-N(3) bond length. In contrast to **3.17a**, for these complexes this is the longest C(1)-N bond length at 1.38(1) Å and 1.374(5) Å for **3.5** and **3.6** respectively.⁴ Additionally the metallacycles are not planar, with a slight puckering of the chelate ring. Two possible modes of bonding were suggested for these complexes, **A** and **B** (Scheme 3.2), with the observations best rationalised as the former providing the predominant bonding contribution.



Scheme 3.2

3.2.4 X-ray structure of $[(\eta^6\text{-}p\text{-cymene})\text{Ru}\{\overline{\text{NAcC(NAc)NAc}}\}(\text{PPh}_3)]$ **3.21a**

For comparison with the platinum(II) complex **3.17a**, an X-ray structure determination of the ruthenium(II) derivative **3.21a** incorporating the N,N',N''-triacetylguanidine dianion was also undertaken.

A PLUTO perspective view of the final structure, with partial deletion of the disordered groups, is shown in Figure 3.15 along with the atom labelling scheme. Selected bond lengths and angles are given in Table 3.2, and tables containing complete bond lengths and angles, final positional parameters, thermal parameters and calculated H-atom positions are presented in Appendix V.

Despite the substantial amount of disorder in guanidine dianion ligand (see Section 3.3.4.3) and possibly unresolved twinning which led to the high R_1 factor (0.1439), the structure confirms the formation of the ruthenium η^2 -triazatrimethylenemethane complex **3.21a**. The analysis can only be taken to confirm the atom connectivity and the overall conformation, and a detailed discussion and comparisons of bond lengths and angles is not justified (as seen by the high estimated standard deviations in Table 3.2).

A few structural features, however, can be discussed. The overall conformation is a distorted “piano stool” arrangement, with the guanidine dianion ligand constraining the N(1)-Ru-N(2) bite angle of $62.3(7)^\circ$. A least-squares plane drawn through the metallacycle indicates the $\overline{\text{Ru-N-C-N}}$ ring is, like **3.17a**, planar with a maximum deviation of $0.01(2)$ Å [for C(1)].

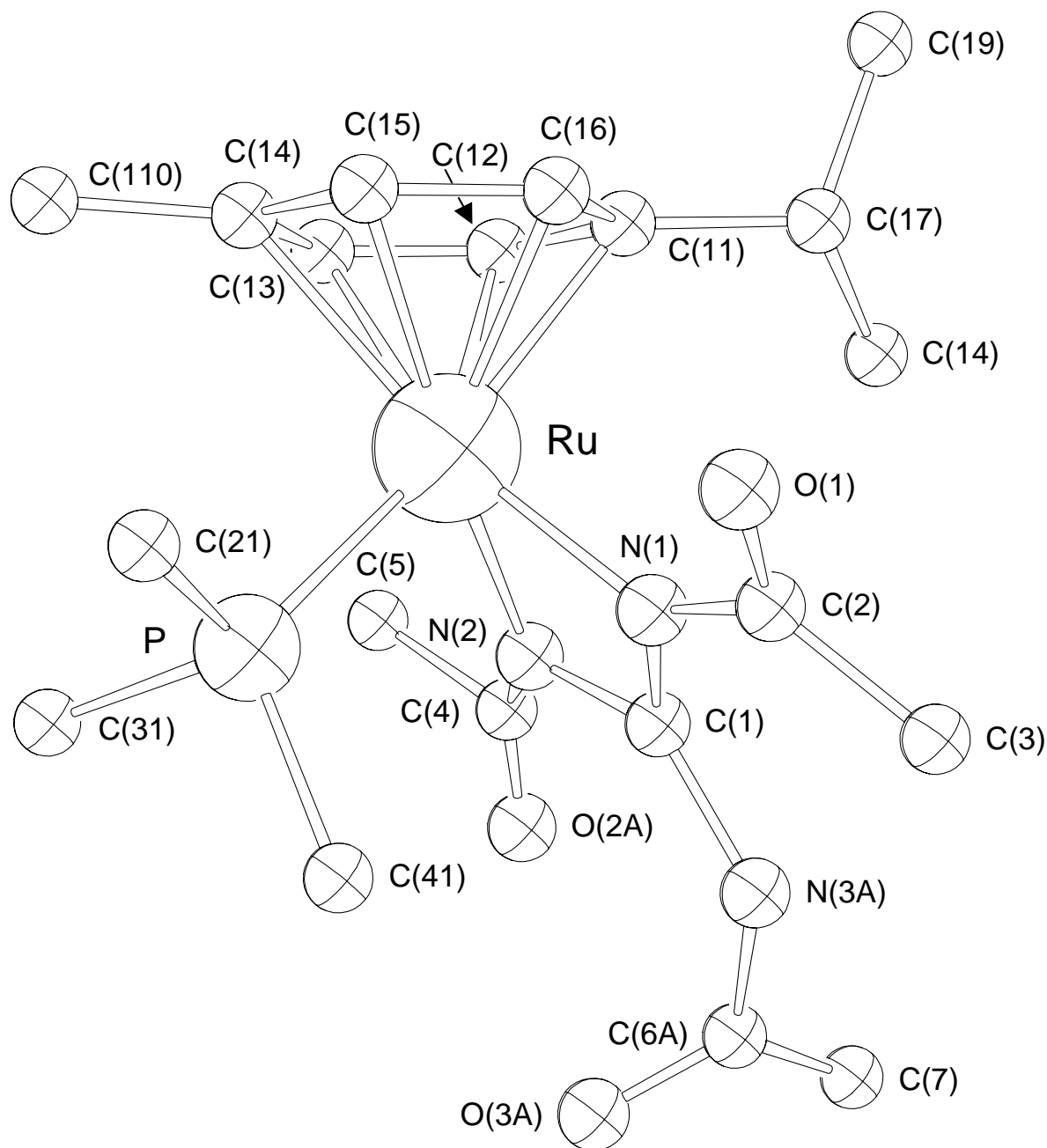


Figure 3.15: PLUTO perspective view of the structure of ruthenium(II) triazatrimethylene-methane complex $[(\eta^6\text{-}p\text{-cymene})\text{Ru}\{\text{N}(\text{Ac})\text{C}(\text{N}(\text{Ac})\text{N}(\text{Ac})\text{C}\{\text{P}(\text{Ph})_3\}_2\}]$ **3.21a**. Only the P-bonded carbons of triphenylphosphine phenyl rings are shown, and some of the disordered acetyl moieties have been omitted for clarity.

Table 3.2: *Selected bond lengths (Å) and angles (°) (estimated standard deviations in parentheses) of the ruthenium(II) N,N',N''-triacylguanidine dianion complex 3.21a.*

Bond	Length	Bonds	Angle
Ru-N(1)	2.04(2)	N(1)-Ru-N(2)	62.4(6)
Ru-N(2)	2.10(2)	P-Ru-N(1)	85.2(5)
Ru-P	2.347(5)	P-Ru-N(2)	90.3(5)
Ru...C(1)	2.63(1)	Ru-N(1)-C(1)	99(2)
		Ru-N(2)-C(1)	96(1)
		Ru-N(1)-C(2)	133(1)
		Ru-N(2)-C(4)	140(2)
Guanidine dianion ligand			
N(1)-C(1)	1.36(3)	N(1)-C(1)-N(2)	103(2)
N(2)-C(1)	1.39(3)	C(1)-N(1)-C(2)	127(2)
N(1)-C(2)	1.37(2)	C(1)-N(2)-C(4)	124(2)
N(2)-C(4)	1.36(3)		

3.2.5 Spectroscopic and mass spectrometric characterisation

3.2.5.1 NMR spectroscopy

Since most of the starting materials, and consequently the products, contained the triphenylphosphine ligand, ^{31}P NMR could conveniently be used to monitor reaction outcomes. Significant and diagnostic NMR features of the complexes, together with the corresponding starting materials and related complexes, are presented in Table 3.3, and complete NMR assignments are given in the experimental section (Section 3.3).

From these data a number of trends are clear. In the ^{31}P NMR, a downfield shift of the PPh_3 resonance, relative to the starting material, is observed on formation of the guanidine dianion complexes. This is consistent with a notion of decreased electron density about the metal centre, which in turn results in decreased density (and consequent magnetic shielding) at the phosphorus. Similarly, a downfield shift (relative to the starting material) of the ^{13}C NMR resonance of the central guanidine carbon ($\text{C}=\text{N}$) is observed on co-ordination for all the complexes, and for the N,N',N'' -triacylguanidine dianion systems studied, is largely independent of the metal. The ^{13}C NMR $\underline{\text{C}}=\text{N}$ resonance for the guanidine dianion complexes

Table 3.3: *A comparison of significant NMR spectroscopic properties of the guanidine dianion complexes, together with those of the starting materials and related complexes.*

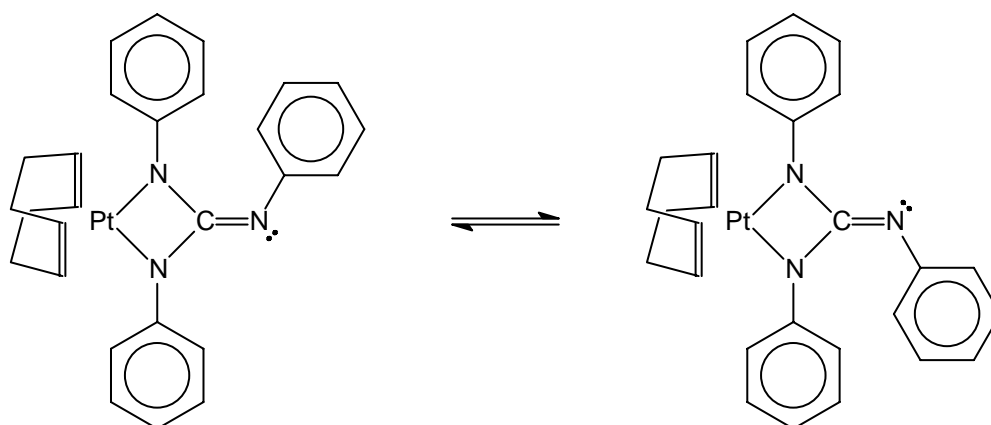
Compound	$^{13}\text{C}=\text{N}$ (ppm)	Product	Starting Material
	$[\text{}^2\text{J}_{\text{P,M}}]$ (Hz)	$^{31}\text{PPh}_3$ (ppm) $[\text{}^1\text{J}_{\text{P,M}}]$ (Hz)	$^{31}\text{PPh}_3$ (ppm) $[\text{}^1\text{J}_{\text{P,M}}]$ (Hz)
Free PhNHC(NPh)NHPPh	145.2	-	-
$[\{(\text{PhN})_3\text{C}\}_2\text{Li}_4(\text{THF})_6]$ 3.12	169.4	-	-
3.17a (M = Pt)	166.4	-	-
3.17b (M = Pt)	not observed	8.1 [3344]	14.0 [3750]
3.20 (M = Rh)	not observed	35.6 [158.7]	30.0 [144.0]
3.5 (M = Rh, monoanionic)	154.4 [4]	-	-
3.6 (M = Ru, monoanionic)	152.9	-	-
Free AcNHC(NPh)NHPPh	150.3	-	-
3.21a (M = Ru)	161.9	44.2	24.9
3.21b (M = Os)	164.0	11.6 [301.5]	-12.4 [281.8]
3.22a (M = Rh)	164.8	40.9 [150.2]	30.0 [144.0]
3.22b (M = Ir)	166.0	15.4	2.2

is significantly higher than the monoanionic rhodium and ruthenium N,N',N''-triphenylguanidine systems **3.5** and **3.6**, indicating more electron deficient C=N carbons in the dianion systems.

For the metal centres with NMR active isotopes (^{195}Pt , ^{103}Rh and ^{187}Os) additional diagnostic information provided by the different electronic properties of the ligands is available. For the triphenylphosphine platinum derivative **3.17b**, a lowering of $\sim 400\text{Hz}$ of the ^1J ($^{195}\text{Pt}-^{31}\text{P}$) coupling constant relative to the starting material *cis*- $[\text{PtCl}_2(\text{PPh}_3)_2]$ is observed on co-ordination of the guanidine dianion, as expected on *trans*-influence grounds.¹⁹ For the rhodium and osmium systems the ^1J ($^{103}\text{Rh}-^{31}\text{P}$) and ^1J ($^{187}\text{Os}-^{31}\text{P}$) value is raised slightly relative to the starting material by 16.2 and 19.7 Hz respectively.

The most significant feature of the ^1H and ^{13}C NMR studies however, was that the substituents on the metal co-ordinated nitrogen atoms were always equivalent, despite the expected inequivalence that should arise from the *syn*- or *anti*-arrangements of the

substituents on the imino nitrogen, as indeed is observed in the X-ray crystal structures of **3.17a** and **3.21a**. For this reason a variable temperature ^1H and ^{13}C NMR was undertaken on the COD complex **3.17a**. The ^1H and ^{13}C NMR spectra at four temperatures ranging from 300–240 K are shown in Figure 3.16 and Figure 3.17 respectively. At room temperature, a single slightly broadened COD CH=CH resonance is observed at 4.92 ppm, which broadens as the temperature was lowered, before eventually splitting into two resonances at 260 K, which subsequently sharpen at 240 K (the lowest temperature examined). In the ^{13}C NMR spectrum, a similar trend was observed, with the single room temperature COD signals at 93.8 and 30.1 ppm eventually forming two discrete signals at 240 K. As seen in the figures, all resonances associated with the complex are effected by temperature change, although most cannot be easily rationalised since their identity is not certain (lower solubilities and unavailability of prolonged low temperature work precluded assignment experiments). The observations are fully consistent with a room-temperature fluxional process (as shown in Scheme 3.3), which serves to interchange the lone pair and the phenyl substituent on the imino nitrogen. At low temperatures this process is frozen out, producing the structure observed in the solid state, with the fixed orientation of the imino phenyl group rendering the two sides of the COD ligand inequivalent. Unfortunately the ^2J (^{195}Pt - ^1H) and ^1J (^{195}Pt - ^{13}C) couplings associated with COD CH=CH resonances were not resolved (the former due to their poor resolution, the latter because of the limited time-scale for the experiments), although small differences would be expected from the slightly different *trans*-influence nitrogen atoms.



Scheme 3.3

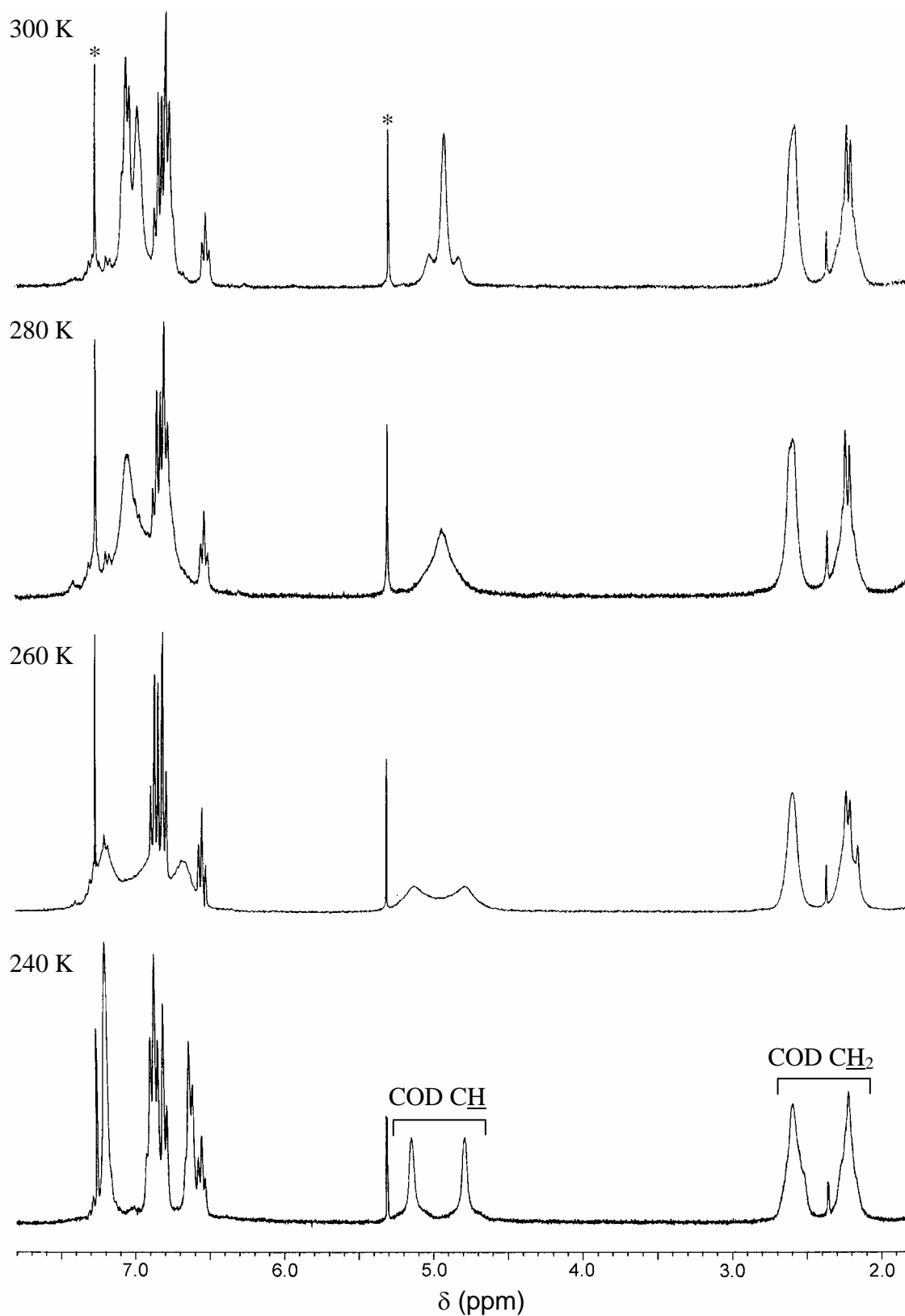


Figure 3.16: ^1H NMR (300.13 MHz) spectra of the complex $[\text{Pt}\{\overline{\text{NPhC(NPh)NPh}}\}(\text{COD})]$ 3.17a at temperatures of 300, 280, 260 and 240 K (as indicated), in CDCl_3 solution. The peaks marked * are due to CHCl_3 (δ 7.26) and residual CH_2Cl_2 (δ 7.26) respectively.

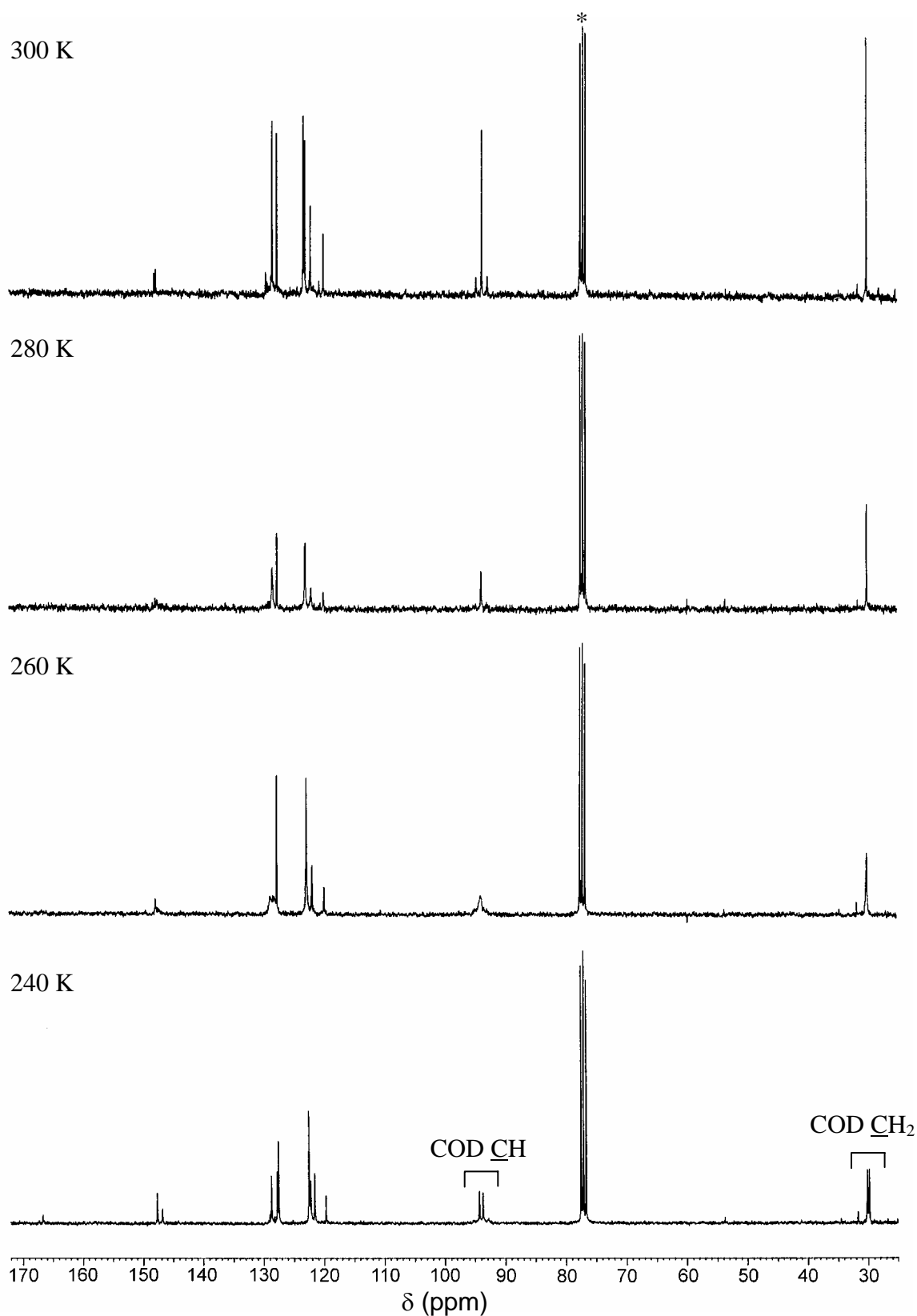
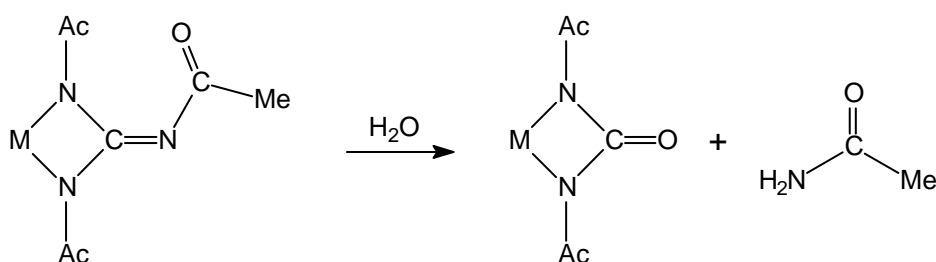


Figure 3.17: ^{13}C NMR (75.47 MHz) spectra of the complex $[\text{Pt}\{\overline{\text{NPhC(NPh)NPh}}\}(\text{COD})]$ **3.17a** at temperatures of 300, 280, 260 and 240 K (as indicated), in CDCl_3 solution. The peak marked * is due to the CDCl_3 solvent.

3.2.5.2 Electrospray mass spectrometry (ESMS)

As for the ureylene complexes reported in Chapter Two, ESMS could successfully be used as an additional method for the characterisation of the triazatrimethylenemethane complexes. The complexes typically show strong $[M + H]^+$ ions, this being the base peak at low to moderate cone voltages (20 – 50 V). For the rhodium, iridium, ruthenium and osmium complexes **3.20-3.22**, which contain a co-ordinated triphenylphosphine ligand, ions corresponding to $[M - PPh_3 + H]^+$ and $[M - PPh_3 + MeCN + H]^+$ were also generally observed. These species presumably arise from the sterically crowded environment around the metal centre, thus labilising the phosphine ligand. This behaviour has been previously noted in a series of pentamethylcyclopentadienyl rhodium(III) oxolene complexes with triphenylphosphine ligands.²⁰

Also of note is the observed nett loss of acetonitrile in all the triacetylguanidine derived complexes. This corresponds to the formation of ureylene complexes, and is interpreted in terms of a hydrolysis reaction occurring in the mass spectrometer (Scheme 3.4), since no ureylene complexes were formed in reactions involving rhodium and ruthenium.



Scheme 3.4

3.2.6 Conclusions

A number of platinum-group metal complexes containing guanidine dianion (triazatrimethylenemethane) ligands were successfully synthesised using the silver(I) oxide method. X-ray crystallographic studies revealed that the ligands bond in a planar η^2 -type configuration, analogous to the bonding found for ureylene (Chapter Two) and carbonate complexes.

3.3 Experimental

General experimental procedures, instrumentation used and the preparations of [PtCl₂(COD)], [(η^6 -*p*-cymene)RuCl₂(PPh₃)], [(η^6 -*p*-cymene)RuCl₂)₂ [(η^6 -*p*-cymene)OsCl₂(PPh₃)], [Cp*RhCl₂(PPh₃)], [Cp*IrCl₂(PPh₃)] and silver(I) oxide are given in Appendices I and II. ESMS spectra were recorded in MeCN/H₂O solvent. Unless otherwise stated, all ¹H, ¹³C and ³¹P NMR spectra were recorded at 300.13, 75.47 and 121.49 MHz respectively, in CDCl₃. ¹H and ¹³C spectra were unambiguously assigned by a combination of 1D NOE and 2D ¹H-¹³C COSY (short-range) and BIRDTRAP (long-range) experiments, and these are discussed in Appendix II.

3.3.1 Preparation of the free guanidines

N,N',N''-Triphenylguanidine

Aniline (0.50 g, 5.37 mmol) was added to a THF (20 ml) solution of diphenylcarbodiimide (prepared by literature methods²¹ from the desulfurisation of N,N'-diphenylthiourea with yellow mercurous oxide) (1.01 g, 5.20 mmol), and stirred at room temperature for 1 hour. The THF was removed under reduced pressure, and the resulting residue was recrystallised from hot ethanol to give N,N',N''-triphenylguanidine as large colourless crystals (1.17 g, 78%).

m.p. 144-145° (lit.²² 144°).

ESMS: (Cone = 10V) *m/z* 288 ([MH]⁺, 100). (Cone = 100V) *m/z* 288 ([MH]⁺, 3%), 195 (MH – PhNH₂)⁺, 100%).

IR: ν (CO region) 1643 (m), 1627 (m), 1592 (s), 1680 (vs), 1571 (m), 1542 (s) cm⁻¹.

¹H NMR: 300K δ 7.34-7.29 (6H, *m*, H-Ar), 7.22-7.20 (6H, *m*, br, H-Ar), 7.05 (3H, *t*, br, 4',4'').

¹³C NMR: 300K δ 145.2 (*s*, C=N), 129.5 (*d*, C-3',3''), 123.3 (*d*, br, C-4',4''), 121.6 (*d*, br, C-2',2''). C-1',1'' not observed at this temp. 325K δ 145.1 (*s*, C=N), 129.4 (*d*, C-3',3''), 142.8 (*d*, v. br, C-1',1''), 123.3 (*d*, br, C-4',4''), 121.7 (*d*, br, C-2',2'').

N,N'-Diphenyl-N'-methylguanidine

Methylamine (extracted into 25 ml of ether from a 33% H₂O solution, excess) was added to diphenylcarbodiimide (0.05 g, 0.257 mmol), and stirred at room temperature for 1 hour. The

ether was removed under reduced pressure to give a colourless oil which slowly crystallised. The residue was recrystallised from refluxing ethanol to give N,N'-diphenyl-N''-methylguanidine as white crystals (0.040 g, 69%).

^1H NMR: δ 7.30 (4H, *t*, $^3J_{3',2'} = 7.82$ Hz, C-3'), 7.06-7.03 (6H, *m*, 2',4'), 2.90 (3H, *s*, $\underline{\text{CH}}_3$).

^{13}C NMR: δ 149.1 (*s*, C=N), 129.5 (*d*, C-3'), 123.3 (*d*, C-2',4'), 28.7 (*q*, $\underline{\text{CH}}_3$). C-1', 1'' not observed.

N,N',N''-Triacetylguanidine

Following literature procedure,²² sodium hydroxide (0.72 g, 0.18 mol) was dissolved in hot methanol (5 ml), and guanidine nitrate (2.0 g, 0.018 mol) was added and the resulting mixture refluxed with stirring for 15 minutes. The solution was cooled and the sodium nitrate precipitate was filtered off and washed with methanol. The methanol was removed under reduced pressure to give free guanidine as a colourless viscous oil. Further sodium nitrate precipitation was removed by filtering through a sintered glass funnel with a Buchner flask. Acetic acid was added dropwise to the free guanidine until no further precipitation was induced. The solid was filtered and washed with ether and recrystallised from refluxing ethanol/ether to give guanidine acetate as white crystals.

N,N',N''-triacetylguanidine was subsequently prepared as described.²³ Guanidine acetate (1.0 g, 8.39 mmol) was heated for 1 hour in a water bath (80°C) with acetic anhydride (5 ml). The solution was taken to dryness under vacuum to give a colourless oil which slowly crystallised. The compound was recrystallised from acetone to give N,N',N''-triacetylguanidine (1.2 g, 77%) as cream needles.

m.p. 112°C (lit.²³ 110-112°C).

ESMS: (Cone = 10V) *m/z* 186 ($[\text{MH}]^+$, 100%), 163 ($[\{(\text{AcNH})_2\text{C}=\text{NH}_2\}\text{NH}_4]^+$, 30%), 145 ($[\{(\text{AcNH})_2\text{C}=\text{NH}_2\}\text{H}]^+$, 45%).

IR: ν (CO region) 1720 (*m*), 1698 (*s*), 1638 (*s*), 1601 (*vs*), 1528 (*m*) cm^{-1} .

^1H NMR: δ 11.77 (2H, *s*, br, N-H), 2.28 (9H, *s*, $\underline{\text{CH}}_3$).

^{13}C NMR: δ 172.0 (*s*, $\underline{\text{C}}=\text{O}$), 150.3 (*s*, $\underline{\text{C}}=\text{N}$), 27.0 (*q*, $\underline{\text{CH}}_3$).

N,N',N''-Trimethylguanidine

N,N'-Dimethylurea (2.5 g, 0.028 mol) was added to phosphorus oxychloride (13.3 ml, excess) in pyridine (15 ml) and heated at 70°C for 2 hours. The reaction mixture was poured onto crushed ice, extracted with petroleum spirits (b.p. 60-80°C) and subsequently dried over anhydrous sodium sulfate. To this, excess methylamine (extracted with ether from a 33% solution in water) was added. The solvent was removed under reduced pressure to give a clear oil, which slowly crystallised under vacuum to give N,N',N''-trimethylguanidine (0.7 g, 24%) as an amorphous hygroscopic solid.

ESMS: (Cone = 15V) m/z 120 ($[MH + H_2O]^+$, 68%), 102 ($[MH]^+$, 43%), 94 (undetermined, 100%), 89 ($[MeNHC(O)NHMe]H^+$, 47%).

1H NMR: $[CD_3S(O)CD_3]$ δ 8.10 (2H, *s*, *v. br.*, N-H), 2.40 (9H, *s*, $\underline{CH_3}$).

^{13}C NMR: $[CD_3S(O)CD_3]$ δ 131.6 (*s*, *br.*, $\underline{C=N}$), 28.0 (*q*, *br.*, $\underline{CH_3}$).

3.3.2 Preparation of the triazatrimethylenemethane complexes

$[Pt\{\overline{NPhC(NPh)NPh}\}(COD)]$ **3.17a**

$[PtCl_2(COD)]$ (0.050 g, 0.134 mmol), N,N',N''-triphenylguanidine (0.039 g, 0.136 mmol) and silver(I) oxide (0.103 g, excess) were refluxed in dichloromethane (20 ml) for 3 hours. Filtration to remove the silver salts gave a bright yellow solution. The solvent was removed by evaporation, and subsequent recrystallisation of the residue from dichloromethane and diethyl ether gave bright yellow crystals of **3.17a** (0.074 g, 94%).

m.p. = 175°C (melted with decomposition).

Found: C, 54.4; H, 5.1; N, 6.8%. Required for $C_{27}H_{27}N_3Pt \cdot \frac{1}{2}(C_2H_5)_2O \cdot \frac{1}{4}CH_2Cl_2$: C, 54.3; H, 5.1; N, 6.5%.

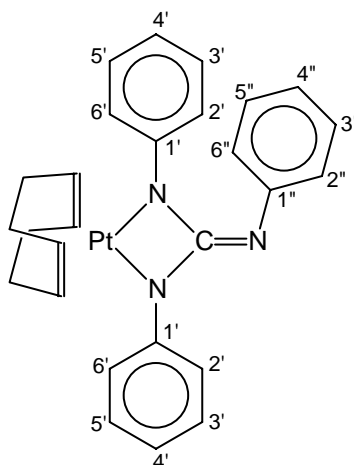
ESMS: (Cone = 50V) m/z 589 ($[MH]^+$, 100%).

IR: ν (CO region) 1609 (*s*), 1590 (*s*), 1574 (*s*), 1565 (*vs*) cm^{-1} .

1H NMR: δ 7.05 (4H, *t*, *br.*, $^3J_{3,2'} = 7.33$ Hz, H-3',5'), 6.97 (4H, *s*, *br.*, H-2',6'), 6.86-6.73 (6H, *m*, H-Ar), 6.51 (1H, *tt*, $^3J_{4'',3''} = 7.01$ Hz, $^4J_{4'',2''} = 1.48$ Hz, H-4''), 4.92 (4H, (*s*, *br.*), (*d*, $^2J_{H,Pt} = 57.3$ Hz), $\underline{CH=CH}$), 2.59 (4H, *m*, $\underline{CH-CH_2}$), 2.21 (4H, *m*, $\underline{CH-CH_2}$).

^{13}C NMR: δ 166.4 (*s*, C=N), 148.0 (*s*, 1''), 147.7 (*s*, C-1'), 129.4 (*d*, C-3',5'), 128.3 (*d*, C-3'',5''), 123.2 (*d*, C-2',6'), 123.0 (*d*, C-2'',6''), 122.0 (*s*, C-4'), 119.9 (*s*, C-4''), 93.8 (*d*, (d , $^1J_{\text{C,Pt}} = 140.5$ Hz), $\underline{\text{C}}\text{H}=\text{CH}$), 30.1 (*t*, $\text{CH}-\underline{\text{C}}\text{H}_2$).

NMR numbering scheme:



$[\text{Pt}\{\overline{\text{NPhC}(\text{NPh})\text{NPh}}\}(\text{PPh}_3)_2]$ **3.17b**

Similarly, $[\text{PtCl}_2(\text{COD})]$ (0.052, 0.139 mmol), *N,N',N''*-triphenylguanidine (0.082 g, 0.139 mmol), triphenylphosphine (0.073 g, 0.278 mmol), and silver(I) oxide (0.987 g, excess) were refluxed in dichloromethane (20 ml) for 4 hours. Filtration to remove the silver salts gave a dark orange solution. The solvent was removed by evaporation, to give a solid residue that failed to crystallise. NMR studies revealed the reaction does not proceed smoothly, with considerable quantities of both starting materials and the hydroxide complex *cis*- $[\text{Pt}(\text{OH})_2(\text{PPh}_3)_2]$ **2.24** (see Chapter Two, 2.2.4).

ESMS: (Cone = 10V) m/z 1019 (undetermined, 39%), 1005 ($[\text{MH}]^+$, 88%), 771 ($[\text{Pt}(\text{OH})_2(\text{Ph}_3\text{P})_2 + \text{NH}_4]^+$, 100%), 755 ($[\{\text{Pt}(\text{OH})_2(\text{Ph}_3\text{P})_2\}\text{H}]^+$, 20%).

^{31}P NMR: (36.23 MHz) δ 8.14 (*s*, (d , $^1J_{\text{P,Pt}} = 3344$ Hz), Ph_3P), 6.06 (*s*, (d , $^1J_{\text{P,Pt}} = 3709$ Hz), $[\text{Pt}(\text{OH})_2(\text{Ph}_3\text{P})_2]$).

^1H NMR: δ 7.42-7.07 (45H, *m*, H-Ar).

^{13}C NMR: δ 134.2 (*m*), 132.2 (*s*), 132.1 (*s*), 131.3 (*d*), 130.9 (*d*), 129.6-127.3 (*m*). C=N not observed.

An alternative synthesis by ligand substitution of the COD complex **3.17a** was also attempted. **3.17a** (0.035 g, 0.059 mmol) and triphenylphosphine (0.032 g, 0.122 mmol) were refluxed in

dichloromethane (25 ml) for 3 hours. No colour change was noted, and upon removing the solvent under reduced pressure, the distinctive smell of free cyclo-octa-1,5-diene was not detected. ^1H and ^{31}P NMR showed only starting materials, indicating no reaction had taken place.

Attempted preparation of $[\text{Pt}\{\overline{\text{NPhC(NMe)NPh}}\}(\text{COD})]$

$[\text{PtCl}_2(\text{COD})]$ (0.103 g, 0.275 mmol), N,N'-diphenyl-N''-methylguanidine (0.062 g, 0.275 mmol) and silver(I) oxide (0.13 g, excess) were refluxed in dichloromethane (30 ml) for 3 hours. Filtration to remove the silver salts gave a bright yellow solution. The solvent was removed under reduced pressure to give a yellow oil which did not crystallise. Preliminary ^{13}C NMR revealed a number resonances associated with the COD ligand indicating numerous reaction products, and for this reason the reaction was abandoned.

Reaction of $[\text{PtCl}_2(\text{COD})]$ with N,N',N''-triacetylguanidine

$[\text{PtCl}_2(\text{COD})]$ (0.050 g, 0.134 mmol), N,N',N''-triacetylguanidine (0.025 g, 0.135 mmol) and silver(I) oxide (0.08 g, excess) were refluxed in dichloromethane (20 ml) for 2 hours. Filtration to remove the silver salts gave a colourless solution. The solvent was removed by evaporation, and subsequent recrystallisation of the residue from dichloromethane and diethyl ether gave white crystals of $[\text{Pt}\{\overline{\text{NAcC(O)NAc}}\}(\text{COD})]$ **2.22h** (0.052 g, 87%), with spectroscopic properties identical to those of an authentic sample (Chapter Two, 2.3.3).

Attempted preparation of $[\text{Pt}\{\overline{\text{NMeC(NMe)NMe}}\}(\text{COD})]$

$[\text{PtCl}_2(\text{COD})]$ (0.050 g, 0.134 mmol), N,N',N''-trimethylguanidine (0.014 g, 0.138 mmol) and silver(I) oxide (0.7 g, excess) were refluxed in dichloromethane for 17 hours. The solution was filtered and the solvent removed under vacuum to leave a pale yellow solid. NMR showed only starting materials, indicating no reaction had taken place.

$[\text{Cp}^*\text{Rh}\{\overline{\text{NPhC(NPh)NPh}}\}(\text{PPh}_3)]$ 3.20

Similarly, $[\text{Cp}^*\text{RhCl}_2(\text{PPh}_3)]$ (0.050 g, 0.088 mmol), N,N',N''-triphenylguanidine (0.026 g, 0.091 mmol) and silver(I) oxide (0.06 g, excess) were added to dichloromethane (25 ml), which had previously been degassed and flushed with nitrogen. The mixture was refluxed under nitrogen for 1 hour, during which time no colour change was noted. An inert

atmosphere appeared to be essential, with attempts of carrying out the reaction in air proving unsuccessful. At completion, with no further efforts at excluding air, the silver salts were filtered off and the solvent removed under reduced pressure, to give a bright yellow oil which did not crystallise. ^{31}P NMR revealed less than 50% purity, with a very broad (>100 Hz) singlet at 9.6 ppm indicating substantial decomposition.

ESMS: (Cone = 20V) m/z 978 (undetermined, 8%), 937 (undetermined, 10%), 834 (undetermined, 20%), 787 ($[\text{MH}]^+$, 100%), 566 ($[\text{M} - \text{PPh}_3 + \text{MeCN}]^+$, 32%).

^{31}P NMR: (36.23 MHz) δ 35.6 (*d*, $^1J_{\text{P,Rh}} = 158.7$ Hz, $\underline{\text{PPh}}_3$), 9.6 (*s*, br, impurity).

^1H NMR: δ 7.48-6.64 (*m*, Ar-H), 1.61 (15H, *s*, Cp- $\underline{\text{CH}}_3$).

^{13}C NMR: δ 144.9 (*s*, C-1"), 138.3 (*s*, C-1'''), 134.1 (*d*, (*d*, $^3J_{\text{C,P}} = 16.45$ Hz), C-3',5'), 132.0 (*s*, $^1J_{\text{C,P}} = 29.51$ Hz, C-1'), 130.3 (*d*, C-4'), 129.3 (*d*), 128.8 (*d*, $^2J_{\text{C,P}} = 10.04$ Hz, C-2',6'), 128.6 (*d*, C-3''), 128.2 (*d*), 124.2 (*d*, C-2''), 122.3 (*d*), 120.9 (*d*), 99.9 (*s*, (*d*, $^2J_{\text{C,P}} = 8.53$ Hz), Cp), 9.2 (*q*, Cp- $\underline{\text{CH}}_3$).

$[(\eta^6\text{-}p\text{-cymene})\text{Ru}\{\overline{\text{N}(\text{Ac})\text{C}(\text{N}(\text{Ac})\text{N}(\text{Ac}))}\}(\text{PPh}_3)]$ **3.21a**

To a Schlenk flask containing dichloromethane (20 ml) (which had previously been degassed and flushed with nitrogen) was added $[(\eta^6\text{-}p\text{-cymene})\text{RuCl}_2]_2$ (0.30 g, 0.049 mmol) and triphenylphosphine (0.026 g, 0.099 mmol) and refluxed for 15 minutes. To this was added N,N',N''-triacetylguanidine (0.018 g, 0.097 mmol) and silver(I) oxide (0.07 g, excess) and the mixture refluxed under nitrogen for a further 1½ hours, during which time a marked colour change from bright orange to pale yellow was observed. Without further regard to exclude air, the silver salts were filtered off and solvent was evaporated under reduced pressure, to leave a yellow oil. Recrystallisation by vapour diffusion of pentane/ether into dichloromethane over three months gave bright orange blocks of **3.21a** (0.040 g, 60%). A highly coloured dark green ruthenium complex that formed in small quantities from freshly prepared bright yellow-orange solutions of **3.21a**, was visibly observed. NMR studies only showed resonances attributable to **3.21a**, so the green compound(s) presumably result from the decomposition of a minor impurity. The orange crystals of **3.21a** were stable, and did not form green solutions when redissolved.

m.p. = 188-189°C.

Found: C, 58.8; H, 5.6; N, 5.9%. Required for $\text{C}_{35}\text{H}_{38}\text{N}_3\text{O}_3\text{PRu} \cdot \frac{1}{2}\text{CH}_2\text{Cl}_2$: C, 59.0; H, 5.4; N, 5.8%.

IR: ν (CO region) 1673 (m), 1651 (m), 1590 (m), 1577 (m), 1569 (m) cm^{-1} .

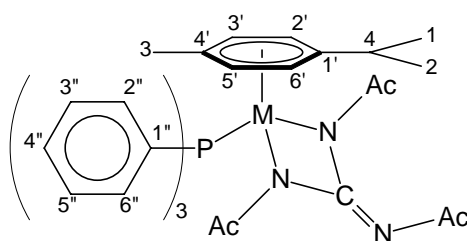
ESMS: (Cone = 20V) m/z 682 ($[\text{MH}]^+$, 100%). (Cone = 50V) m/z 682 ($[\text{MH}]^+$, 70%), 419 ($[\text{M} - \text{PPh}_3]^+$, 100%). (Cone = 80V) m/z 419 ($[\text{M} - \text{PPh}_3]^+$, 22%), 335 ($[(\eta^6\text{-}p\text{-cymene})\text{Ru} + 2\text{MeCN} + \text{H}_2\text{O}]^+$, 100%), 294 ($[(\eta^6\text{-}p\text{-cymene})\text{Ru} + \text{MeCN} + \text{H}_2\text{O}]^+$, 80%).

^{31}P NMR: δ 44.2 (s, $\underline{\text{PPh}}_3$)

^1H NMR: δ 7.56 (6H, t, $^3J_{3''} = 8.63$ Hz, C-3''), 7.43-7.35 (9H, m, C-2''), 5.95 (2H, d, $^3J_{2',3'} = 6.12$ Hz, C-2',6'), 5.05 (2H, d, $^3J_{3',2'} = 5.98$ Hz, C-3',5'), 2.74 (1H, *quintet*, $^3J_{4,1} = 6.87$ Hz, C-4), 1.93 (6H, s, $\text{RuNC}(\text{O})\underline{\text{CH}}_3$), 1.82 (3H, s, $\text{C}=\text{NC}(\text{O})\underline{\text{CH}}_3$), 1.68 (3H, s, C-3), 1.16 (3H, d, $^3J_{1,4} = 6.90$ Hz, C-1,2).

^{13}C NMR: δ 177.9 (s, $\text{RuNC}(\text{O})\underline{\text{CH}}_3$), 174.4 (s, $\text{C}=\text{NC}(\text{O})\underline{\text{CH}}_3$), 161.9 (s, $\underline{\text{C}}=\text{N}$), 134.6 (d, (d, $^3J_{\text{C,P}} = 10.94$ Hz), C-3''), 131.8 (s, (d, $^1J_{\text{C,P}} = 45.58$ Hz), C-1''), 130.5 (d, C-4''), 128.2 (d, (d, $^2J_{\text{C,P}} = 9.96$ Hz), C-2''), 112.4 (s, (d, $^2J_{\text{C,P}} = 8.75$ Hz), C-1'), 102.6 (s, C-4'), 88.4 (d, C-2',6'), 86.8 (d, C-3',5'), 30.9 (d, C-4), 26.4 (q, $\text{C}=\text{NC}(\text{O})\underline{\text{CH}}_3$), 25.8 (q, $\text{RuNC}(\text{O})\underline{\text{CH}}_3$), 22.5 (q, C-1,2), 18.7 (q, C-3).

NMR numbering scheme:



$[(\eta^6\text{-}p\text{-cymene})\text{Os}\{\overline{\text{NacC}(\text{Nac})\text{Nac}}\}(\text{PPh}_3)]$ **3.21b (not isolated)**

To a Schlenk flask containing dichloromethane (20 ml) (which had previously been degassed and flushed with nitrogen) was added $[(\eta^6\text{-}p\text{-cymene})\text{OsCl}_2(\text{PPh}_3)]$ (0.050 g, 0.076 mmol), N,N',N'' -triacetylguanidine (0.014 g, 0.076 mmol) and silver(I) oxide (0.10 g, excess) and refluxed under nitrogen for 2 hours, during which time a marked colour change from bright yellow to almost colourless was observed. Without further regard to exclude air, the silver salts were filtered off and solvent was evaporated under reduced pressure to give a pale yellow oil which, despite repeated efforts, did not crystallise. ^{31}P NMR of the residue showed two products in ~50:50 distribution. These were characterised as being the desired product **3.21b**, and the ureylene complex **3.23**. Attempts at varying the product distribution by either

refluxing the ligand in silver(I) oxide for 18 hours, with and without the addition of water, followed by stoichiometric quantities of $[(\eta^6\text{-}p\text{-cymene})\text{OsCl}_2(\text{PPh}_3)]$, were unsuccessful.

ESMS (reaction mixture): m/z (Cone = 15V) 772 ($[\text{MH}]^+$, 100%), 731 ($[\text{M} - \text{MeCN}]\text{H}^+$, 28%). (Cone = 50V) m/z 772 ($[\text{MH}]^+$, 100%), 731 ($[\text{M} - \text{MeCN}]\text{H}^+$, 15%), 510 ($[\text{M} - \text{PPh}_3]^+$, 27), 469 ($[\text{M} - \text{MeCN} - \text{PPh}_3]^+$, 28%).

^{31}P NMR: δ 11.6 (*s*, *d*, $^1J_{\text{P,Os}} = 301.5$ Hz), $\underline{\text{PPh}_3}$.

^1H NMR: δ 7.60 (6H, *m*, Ar-H), 7.38-7.33 (9H, *m*, Ar-H), 5.99 (2H, *d*, $^3J_{2',3'} = 5.58$ Hz, C-2',6'), 5.13 (2H, *d*, $^3J_{3',2'} = 5.58$ Hz, C-3',5'), 2.61 (1H, *quintet*, $^3J_{4,1} = 6.87$ Hz, C-4), 1.92 (6H, *s*, $\text{OsNC}(\text{O})\underline{\text{CH}_3}$), 1.84 (3H, *s*, C-3), 1.81 (3H, *s*, $\text{C}=\text{NC}(\text{O})\underline{\text{CH}_3}$), 1.12 (6H, *d*, $^3J_{1,4} = 6.89$ Hz, C-1,2).

^{13}C NMR: δ 177.0 (*s*, $\text{OsNC}(\text{O})\underline{\text{CH}_3}$), 174.6 (*s*, $\text{C}=\text{NC}(\text{O})\underline{\text{CH}_3}$), 164.0 (*s*, $\underline{\text{C}}=\text{NC}(\text{O})\underline{\text{CH}_3}$), 134.9 (*d*, (*d*, $^3J_{\text{C,P}} = 10.72$ Hz), C-3"), 131.4 (*s*, (*d*, $^1J_{\text{C,P}} = 52.45$ Hz), C-1"), 130.6 (*d*, C-4"), 128.1 (*d*, (*d*, $^2J_{\text{C,P}} = 9.58$ Hz), C-2"), 105.5 (*s*, (*d*, $^2J_{\text{C,P}} = 8.98$ Hz), C-1'), 94.7 (*s*, C-4'), 80.0 (*d*, C-2',6'), 77.8 (*d*, C-3',5'), 31.0 (*d*, C-4), 25.2 (*q*, $\text{OsNC}(\text{O})\underline{\text{CH}_3}$), 22.6 (*q*, C-1,2), 22.1 (*q*, $\text{C}=\text{NC}(\text{O})\underline{\text{CH}_3}$), 18.4 (*q*, C-3).

$[(\eta^6\text{-}p\text{-cymene})\text{Os}\{\overline{\text{NAC}(\text{O})\text{NAC}}\}(\text{PPh}_3)]$ **3.23**

Similarly, $[(\eta^6\text{-}p\text{-cymene})\text{OsCl}_2(\text{PPh}_3)]$ (0.052 g, 0.079 mmol), N,N'-diacetylurea (0.012 g, 0.083 mmol) and silver(I) oxide (0.13 g, excess) were refluxed in dichloromethane (25 ml) under nitrogen for 2 hours. Work-up gave a very pale yellow oil that resisted crystallisation. However, removal of all solvent under vacuum gave **3.23** as a pale yellow solid of high purity (0.055 g, 95%).

m.p. 235-238°C.

Found: C, 53.6; H, 5.0; N, 4.0%. Required for $\text{C}_{33}\text{H}_{35}\text{N}_2\text{O}_3\text{POs}$: C, 54.4; H, 4.8; N, 3.8%.

IR: ν (CO region) 1692 (*s*), 1616 (*s*), 1599 (*s*) cm^{-1} .

ESMS: (Cone = 20V) m/z 731 ($[\text{MH}]^+$, 100%). (Cone = 50V) m/z 731 ($[\text{MH}]^+$, 100%), 510 ($[\text{MH} - \text{PPh}_3 + \text{MeCN}]^+$, 3%), 469 ($[\text{MH} - \text{PPh}_3]^+$, 10%), 263 ($[\text{PPh}_3\text{H}]^+$, 22%). (Cone = 80V) m/z 731 ($[\text{MH}]^+$, 20%), 510 ($[\text{MH} - \text{PPh}_3 + \text{MeCN}]^+$, 22%), 469 ($[\text{MH} - \text{PPh}_3]^+$, 48%), 425 ($[\text{MH} - \text{CH}_3\text{C}(\text{O}) - \text{PPh}_3]^+$, 48%), 384 (unidentified, 80%), 263 ($[\text{PPh}_3\text{H}]^+$, 100%).

^{31}P NMR: δ 13.9 (*s*, (*d*, $^1J_{\text{P,Os}} = 301.1$ Hz), $\underline{\text{PPh}_3}$).

^1H NMR: δ 7.62-7.55 (6H, *m*, Ar-H), 7.42-7.33 (9H, *m*, Ar-H), 6.03 (2H, *d*, $^3J_{2,3'} = 5.77$ Hz, C-2',6'), 5.15 (2H, *d*, $^3J_{3',2'} = 5.73$ Hz, C-3',5'), 2.53 (1H, *quintet*, $^3J_{4,1} = 6.90$ Hz, C-4), 2.10 (6H, *s*, OsNC(O)CH₃), 1.80 (3H, *s*, C-3), 1.04 (6H, *d*, $^3J_{1,4} = 6.93$ Hz, C-1,2).

^{13}C NMR: δ 176.7 (*s*, OsNC(O)CH₃), 164.6 (*s*, C=O), 134.9 (*d*, (*d*, $^3J_{\text{C,P}} = 10.64$ Hz), C-3"), 131.3 (*s*, (*d*, $^1J_{\text{C,P}} = 52.15$ Hz), C-1"), 130.5 (*d*, C-4"), 128.4 (*d*, (*d*, $^2J_{\text{C,P}} = 9.58$ Hz), C-2"), 104.0 (*s*, (*d*, $^2J_{\text{C,P}} = 9.89$ Hz), C-1'), 94.2 (*s*, C-4'), 79.8 (*d*, C-2',6'), 76.7 (*d*, C-3',5'), 31.2 (*d*, C-4), 26.6 (*q*, OsNC(O)CH₃), 22.6 (*q*, C-1,2), 18.4 (*q*, C-3).

[Cp*Rh{NAcC(NAc)NAc}(PPh₃)] 3.22a

Similarly, [Cp*RhCl₂(PPh₃)] (0.051 g, 0.089 mmol), N,N',N''-triacetylguanidine (0.017 g, 0.092 mmol) and silver(I) oxide (0.05 g, excess) were added to dichloromethane (25 ml). The resulting mixture was refluxed under nitrogen for 1 hour, during which time a marked colour change from orange to bright yellow was observed. At completion, with no further efforts at excluding air, the silver salts were filtered off and the solvent removed under reduced pressure. Recrystallisation from dichloromethane-pentane gave **3.22a** as bright yellow crystals (0.051 g, 85%).

m.p. = 153-155°C.

Found: C, 59.7; H, 5.6; N, 5.7%. Required for C₃₅H₃₈N₃O₃PRh: C, 61.7; H, 5.6; N, 6.1%.

IR: ν (CO region) 1669 (w), 1610 (m) cm⁻¹.

ESMS: (Cone = 15V) m/z 1368 ([2M + H]⁺, 3%), 684 ([MH]⁺, 100%). (Cone = 50V) m/z 684 ([MH]⁺, 90%), 643 ([MH - MeCN]⁺, 30%), 422 ([MH - PPh₃]⁺, 100%).

^{31}P NMR: δ 40.9 (*d*, $^1J_{\text{P,Rh}} = 150.2$ Hz, PPh₃).

^1H NMR: δ 7.53 (6H, *t*, $^3J_{3',2'} = 8.88$, C-3',5'), 7.43-7.35 (9H, *m*, br, C-2',4',6'), 1.97 (6H, *s*, RhNC(O)CH₃), 1.83 (3H, *s*, C=NC(O)CH₃), 1.56 (15H, *d*, $^4J_{\text{H,P}} = 3.17$ Hz, Cp-CH₃).

^{13}C NMR: δ 177.8 (*s*, RhNC(O)CH₃), 174.1 (*s*, C=NC(O)CH₃), 164.8 (*s*, C=N), 134.7 (*d*, (*d*, $^3J_{\text{C,P}} = 11.17$ Hz), C-3',5'), 131.3 (*d*, C-4'), 130.1 (*s*, $^1J_{\text{C,P}} = 45.35$ Hz, C-1'), 128.2 (*d*, (*d*, $^2J_{\text{C,P}} = 10.49$ Hz), C-2',6'), 99.9 (*s*, Cp), 26.7 (*q*, RhNC(O)CH₃), 26.1 (*q*, C=NC(O)CH₃), 8.8 (*q*, Cp-CH₃).

[Cp*Ir{NAcC(NAc)NAc}(PPh₃)] 3.22b

Similarly, [Cp*IrCl₂(PPh₃)] (0.050 g, 0.076 mmol), N,N',N''-triacetylguanidine (0.014 g, 0.076 mmol) and silver(I) oxide (0.05 g, excess) were added to dichloromethane (20 ml)

(which had previously been degassed and flushed with nitrogen), and refluxed under nitrogen for 6 hours. At completion, with no further efforts at excluding air, the silver salts were filtered off and the solvent removed under reduced pressure to give a yellow oil. Preliminary NMR studies indicated 25% of the ureylene complex **3.24**. Recrystallisation from dichloromethane and pentane gave **3.22b** as bright yellow crystals (0.036 g, 61%). The ureylene complex could not be satisfactorily purified, but could be synthesised directly from $[\text{Cp}^*\text{IrCl}_2(\text{PPh}_3)]$ and *N,N'*-diacetylurea.

m.p. = 224-226°.

Found: C, 51.2; H, 4.8; N, 5.1%. Required for $\text{C}_{35}\text{H}_{39}\text{N}_3\text{O}_3\text{PIr}\cdot\frac{1}{2}\text{CH}_2\text{Cl}_2$: C, 52.3; H, 4.9; N, 5.2%.

IR: ν (CO region) 1616 (m), 1590 (w), 1525 (s, br) cm^{-1} .

ESMS: (Cone = 15V) m/z 774 ($[\text{MH}]^+$, 100%), 732 ($[\text{MH} - \text{MeCN}]\text{H}^+$, 10%). (Cone = 50V) m/z 774 ($[\text{MH}]^+$, 100%), 732 ($[\text{MH} - \text{MeCN}]\text{H}^+$, 5%), 512 ($[\text{MH} - \text{PPh}_3]^+$, 20%).

^{31}P NMR: δ 15.4 (s, $\underline{\text{PPh}}_3$).

^1H NMR: δ 7.51 (6H, *m*, Ar-H), 7.43-7.26 (9H, *m*, Ar-H), 1.96 (6H, *s*, $\text{IrNC}(\text{O})\underline{\text{CH}}_3$), 1.83 (3H, *s*, $\text{C}=\text{NC}(\text{O})\underline{\text{CH}}_3$), 1.56 (15H, *s*, (*d*, $^4J_{\text{H,P}} = 1.51$ Hz), $\text{Cp}-\underline{\text{CH}}_3$).

^{13}C NMR: δ 176.3 (*s*, $\text{IrNC}(\text{O})\underline{\text{CH}}_3$), 174.4 (*s*, $\text{C}=\text{NC}(\text{O})\underline{\text{CH}}_3$), 166.0 (*s*, $\underline{\text{C}}=\text{N}$), 134.9 (*d*, (*d*, $^3J_{\text{C,P}} = 10.79$ Hz), C-3',5'), 130.8 (*d*, C-4'), 130.0 (*s*, (*d*, $^1J_{\text{C,P}} = 54.72$ Hz), C-1'), 128.1 (*d*, (*d*, $^2J_{\text{C,P}} = 10.49$ Hz), C-2',6'), 93.6 (*s*, Cp), 26.3 (*q*, $\text{C}=\text{NC}(\text{O})\underline{\text{CH}}_3$), 26.1 (*q*, $\text{IrNC}(\text{O})\underline{\text{CH}}_3$), 9.3 (*q*, $\text{Cp}-\underline{\text{CH}}_3$).

$[\text{Cp}^*\text{Ir}\{\overline{\text{NAcC}(\text{O})\text{N}\text{Ac}}\}(\text{PPh}_3)]$ **3.24**

Similarly, $[\text{Cp}^*\text{IrCl}_2(\text{PPh}_3)]$ (0.051 g, 0.077 mmol), *N,N'*-diacetylurea (0.011 g, 0.076 mmol) and silver(I) oxide (0.08 g, excess) were refluxed in dichloromethane (25 ml) under nitrogen for 2 hours. Work-up gave a yellow oil that readily crystallised from a vapour diffusion of pentane into a saturated chloroform solution at room temperature, to give large yellow blocks of **3.24** (0.047 g, 84%).

m.p. 200°C (decomposed without melting).

Found: C, 48.3; H, 4.5; N, 3.4%. Required for $\text{C}_{33}\text{H}_{36}\text{N}_2\text{O}_3\text{PIr}\cdot\text{CHCl}_3$: C, 48.0; H, 4.4; N, 3.3%.

IR: ν (CO region) 1694 (s), 1616 (s), 1600 (s) cm^{-1} .

ESMS: (Cone = 20V) m/z 733 ($[\text{MH}]^+$, 100%). (Cone = 50V) m/z 731 ($[\text{MH}]^+$, 100%), 471 ($[\text{MH} - \text{PPh}_3]^+$, 22%), 263 ($[\text{PPh}_3\text{H}]^+$, 12%). (Cone = 80V) m/z 733 ($[\text{MH}]^+$, 20%), 493 ($[\text{MNa} - \text{PPh}_3]^+$, 22%), 471 ($[\text{MH} - \text{PPh}_3]^+$, 100%), 427 ($[\text{M} - \text{CH}_3\text{C}(\text{O}) - \text{PPh}_3]^+$, 12%), 386 (unidentified, 80%), 263 ($[\text{PPh}_3\text{H}]^+$, 38%).

^{31}P NMR: δ 17.6 (*s*, PPh_3)

^1H NMR: δ 7.61 (6H, *m*, br, Ar-H), 7.41-7.37 (9H, *m*, Ar-H), 2.16 (6H, *s*, $\text{IrNC}(\text{O})\underline{\text{C}}\text{H}_3$), 1.56 (15H, *s*, (*d*, $^4\text{J}_{\text{H,P}} = 1.51$ Hz), $\text{Cp}-\underline{\text{C}}\text{H}_3$).

^{13}C NMR: δ 175.9 (*s*, $\text{IrNC}(\text{O})\underline{\text{C}}\text{H}_3$), 165.0 (*s*, $\underline{\text{C}}=\text{O}$), 134.9 (*d*, (*d*, $^3\text{J}_{\text{C,P}} = 10.79$ Hz), C-3',5'), 130.7 (*d*, C-4'), 130.0 (*s*, (*d*, $^1\text{J}_{\text{C,P}} = 54.72$ Hz), C-1'), 127.9 (*d*, (*d*, $^2\text{J}_{\text{C,P}} = 10.49$ Hz), C-2',6'), 92.9 (*s*, Cp), 27.5 (*q*, $\text{IrNC}(\text{O})\underline{\text{C}}\text{H}_3$), 9.3 (*q*, $\text{Cp}-\underline{\text{C}}\text{H}_3$).

3.3.3 X-ray structure of $[\text{Pt}\{\overline{\text{NPhC}(\text{NPh})\text{NPh}}\}(\text{COD})]$ **3.17a** diethyl ether solvate

Results of preliminary studies

Yellow rectangular blocks of **3.17a** were obtained on crystallisation by vapour diffusion of diethyl ether into a saturated dichloromethane solution of **3.17a** at 4°C. Preliminary precession photography indicated monoclinic symmetry, so the space group was assumed to be $\text{P}2_1/\text{c}$ which was confirmed by successful refinement.

Data collection

Accurate cell parameters and intensity data were collected on an Nicolet R3 automatic four-circle diffractometer at the University of Canterbury, using a crystal of dimensions 0.80 x 0.24 x 0.22 mm, with monochromated Mo- $\text{K}\alpha$ X-rays ($\lambda = 0.71073$ Å). A total of 4291 reflections in the range $2^\circ < \theta < 25^\circ$ were collected at 130(2) K, of which 4270 were unique. These were subsequently corrected for Lorentz effects, polarisation effects, and for linear absorption by a Ψ scan method ($T_{\text{max.}, \text{min.}} = 0.18, 0.49$).

Crystal Data: $\text{C}_{27}\text{H}_{27}\text{N}_3\text{Pt}\cdot\frac{1}{2}\text{C}_4\text{H}_{10}\text{O}$, $M_r = 625.67$, monoclinic, space group $\text{P}2_1/\text{c}$, $a = 9.862(1)$ Å, $b = 14.497(3)$ Å, $c = 17.436(3)$ Å, $\beta = 103.02(1)^\circ$, $U = 2428.7(6)$ Å³, $D_c = 1.711$ g cm^{-3} , $Z = 4$, $F(000) = 1236$, $\mu(\text{Mo}-\text{K}\alpha) = 5.80$ mm^{-1} .

Solution and refinement

The platinum atom position was located by the Patterson methods option of SHELXS-86,²⁴ with the remaining non-hydrogen atoms were located in subsequent full-matrix extended automatic least-squares refinements based on F^2 using SHELXL-93.²⁵ The penultimate difference map revealed residual electron density which was attributed to a disordered diethyl ether molecule lying across an inversion centre in the lattice, with 50% occupancy. All non-hydrogen atoms were assigned anisotropic temperature factors, with all hydrogen atom positions determined by calculation. The refinement converged with $R_1 = 0.0456$ for 3197 data with $I \geq 2\sigma(I)$, 0.0612 for all data; $wR_2 = 0.1147$, and $GoF = 0.933$. No parameter shifted in the final cycle, and the final difference map showed no peaks or troughs of electron density greater than +2.58 and -1.97 e \AA^{-3} respectively (attributable to stray density about the platinum atom).

3.3.4 X-ray structure of $[(\eta^6\text{-}p\text{-cymene})\text{Ru}\{\overline{\text{NAcC(NAc)NAc}}\}(\text{PPh}_3)]$ **3.21a**

Results of preliminary studies

An orange rosette of **3.21a** was obtained on crystallisation by vapour diffusion of diethyl ether/pentane into a saturated dichloromethane solution of **3.21a** at 4°C, from which a rectangular block suitable for X-ray analysis was removed. Preliminary precession photography indicated orthorhombic symmetry, with the space group deduced as being Pbcn. This was later confirmed by successful refinement.

Data collection

Accurate cell parameters and intensity data were collected on an Nicolet R3 automatic four-circle diffractometer at the University of Canterbury, using a crystal of dimension 0.88 x 0.34 x 0.14 mm, with monochromatic Mo-K α X-rays ($\lambda = 0.71073 \text{ \AA}$).

Crystal Data: $\text{C}_{35}\text{H}_{38}\text{N}_3\text{O}_3\text{PRu}$, $M_r = 680.72$, orthorhombic, space group Pbcn, $a = 25.174(4)$, $b = 14.497(3) \text{ \AA}$, $c = 16.913(9) \text{ \AA}$, $U = 6322(4) \text{ \AA}^3$, $D_c = 1.431 \text{ g cm}^{-3}$, $Z = 8$, $F(000) = 2816$, $\mu(\text{Mo-K}\alpha) = 0.59 \text{ mm}^{-1}$.

A total of 5445 reflections in the range $2.41^\circ < \theta < 22.50^\circ$ were collected at 130(2)K, of which 4131 were unique. These were subsequently corrected for Lorentz and polarisation effects, and for linear absorption by a Ψ scan method ($T_{\max., \min.} = 0.32, 0.35$).

Solution and refinement

The structure was solved by the direct methods option of SHELXS-86²⁴ and some of the non-hydrogen atoms located. The remaining non-hydrogen atoms were located in subsequent refinements using SHELXL-93,²⁵ in which all non-hydrogen atoms were assigned anisotropic temperature factors. Although the data set itself was of reasonable quality (with an internal R factor of 0.0556) indicating a satisfactory crystal, it was immediately obvious the structure contained significant disorder, and this was modelled as follows. N(3) and the carbonyl group bound to it, are disordered over two positions with 50% occupancy for each, and the terminal methyl moiety, C(7), is shared by both to complete the acetyl group. The two resulting NC(O) groups are labelled A and B as shown in Figure 3.18. Additional disorder was observed for the oxygen bound to C(4) which again was disordered over two positions, each with 50% occupancy, labelled O(2A) and O(2B). For the acetyl groups, the oxygen atoms were distinguished from the methyl carbons predominantly on bond length criteria.

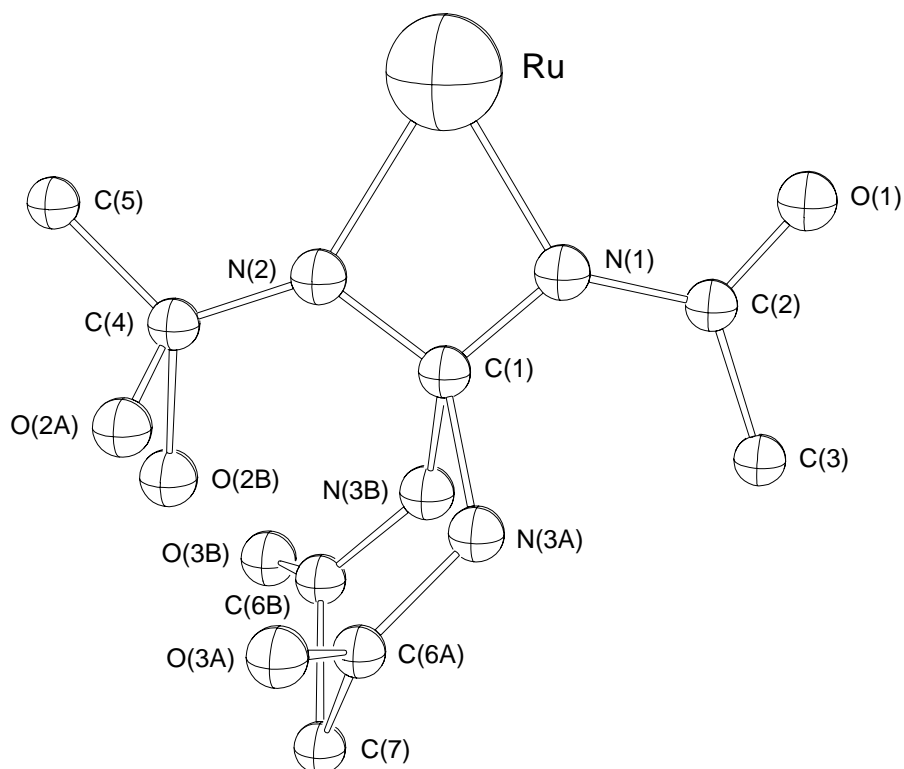


Figure 3.18: *The metallacycle of 3.21a showing the observed disorder and atom numbering scheme.*

The triphenylphosphine aromatic rings were modelled as rigid hexagons (all bond lengths 1.390 Å, all bond angles 120°) with the *ipso* carbons providing the pivot points. Residual electron density clearly associated with hydrogen atoms was located in the penultimate difference map, so all hydrogen atom positions were included in calculated positions, with the exception of those associated with C(7). The refinement converged with $R_1 = 0.1439$ for 2821 data with $I \geq 2\sigma(I)$, 0.1890 for all data; $wR_2 = 0.2969$, and $\text{GoF} = 1.316$. No parameter shifted in the final cycle, and the final difference map showed no peaks or troughs of electron density greater than +1.70 and -2.80 e Å⁻³ respectively, both near O(1).

References

- 1 R.C. Mehrotra in *Comprehensive Coordination Chemistry*, Ed. in Chief G. Wilkinson, Pergamon Press, Oxford, Section 13.8 (1987) 281.
- 2 D.P. Fairlie, W.G. Jackson, B.W. Skelton, H. Wen, A.H. White, W.A. Wickramasinghe, T.C. Woon and H. Taube, *Inorg. Chem.*, *36* (1997) 1020.
- 3 E.M.A. Ratilla and N.M. Kostic, *J. Am. Chem. Soc.*, *110* (1988) 4427.
- 4 P.J. Bailey, L.A. Mitchell and S. Parsons, *J. Chem. Soc., Dalton Trans.*, (1996) 2839.
- 5 J.R.S. Maia, P.A. Gazard, M. Kilner, A.S. Batsanov and J.A.K. Howard, *J. Chem. Soc., Dalton Trans.*, (1997) 4625.
- 6 P.J. Bailey, S.F. Bone, L.A. Mitchell, S. Parsons, K.J. Taylor and L.J. Yellowlees, *Inorg. Chem.*, *36* (1997) 867.
- 7 H-K. Yip, C-M. Che, Z-Y. Zhou and T.C.W. Mak, *J. Chem. Soc., Chem. Commun.*, (1992) 1369.
- 8 N.J. Bremer, A.B. Cutcliffe, M.F. Faroni and W.G. Kofron, *J. Chem. Soc. (A)*, (1971) 3264.
- 9 P.J. Bailey, A.J. Blake, M. Kryszczuk, S. Parsons and D. Reed, *J. Chem. Soc., Chem. Commun.*, (1995) 1647.
- 10 J-T. Chen, Y-K. Chen, J-B. Chu, G.H. Lee and Y. Wang, *Organometallics*, *16* (1997) 1476.
- 11 M.W. Baize, V. Plantevin, J.C. Gallucci and A. Wojcicki, *Inorg. Chim. Acta*, *235* (1995) 1.
- 12 T-M. Huang, R.H. Hsu, C-S. Yang, J-T. Chen, G-H. Lee and Y. Wang, *Organometallics*, *13* (1994) 3657.
- 13 K. Ohe, H. Matsuda, T. Morimoto, S. Ogoshi, N. Chatani and S. Murai, *J. Am. Chem. Soc.*, *116* (1994) 4125.
- 14 J-T. Chen, T-M. Huang, M-C. Cheng, Y-C. Lin and Y. Wang, *Organometallics*, *11* (1992) 1761.
- 15 P.J. Bailey, L.A. Mitchell, P.R. Raithby, M-A. Rennie, K. Verhorevoort and D.S. Wright, *Chem. Commun.*, (1996) 1351.
- 16 P. Mounford, *Chem. Commun.*, (1997) 2127.
- 17 P.J. Bailey, R.O. Gould, C.N. Harmer, S. Pace, A. Steiner and D.S. Wright, *Chem. Commun.*, (1997) 1161.

- 18 A. Kemme, M. Rutkis and J. Eiduss, *Latv.PSR Zinat. Akad. Vestis, Khim. Ser.*, (1988) 595.
- 19 T.G. Appleton, H.C. Clark and L.E. Manzer, *Coord. Chem. Rev.*, 10 (1973) 335.
- 20 W. Henderson, J. Fawcett, R.D.W. Kemmitt and D.R. Russell, *J. Chem. Soc., Dalton Trans.*, (1995) 3007.
- 21 *Organic Functional Group Preparations Vol. II*, Ed. S. R. Sandler and W. Karo, Academic Press, London (1971)
- 22 A.I. Vogel, *Practical Organic Chemistry*, 3rd Edn., Longman, London, (1972) 969.
- 23 R. Greenhalgh and A.A.B. Bannard, *Can. J. Chem.*, 37 (1959) 1810.
- 24 G.M. Sheldrick, SHELXS-86, Program for Solving X-Ray Crystal Structures, University of Göttingen, Germany, (1986).
- 25 G.M. Sheldrick, SHELXL-93, Program for Refining X-Ray Crystal Structures, University of Göttingen, Germany, (1993).

Chapter Four

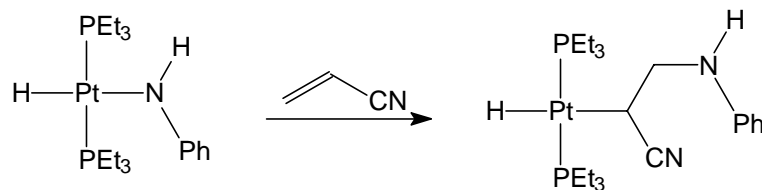
Insertion Reactions of Platinum(II) Ureylene Complexes

4.1 Introduction

Insertion reactions into late transition metal-carbon bonds form a fundamental aspect of organometallic chemistry, and these important reactions and their applications to catalysis have been intensely studied over the years. Despite this, the analogous chemistry of metal-nitrogen (and, to a lesser extent, metal-oxygen) complexes has been left largely unexplored, principally due to relative scarcity and lower stability of precursor metal-amide (and metal-alkoxide) complexes compared with alkyl and aryl compounds.¹ The lower stability of these complexes is attributed to the mismatch of hard, basic ligands, with the soft late transition-metal centres.²

Recently however, research involving the insertion reactions of metal-amide complexes has been steadily increasing, and some work describing this potentially important area of chemistry has now been described. Some representative examples are presented below, demonstrating the reactive nature of the M-N bond.

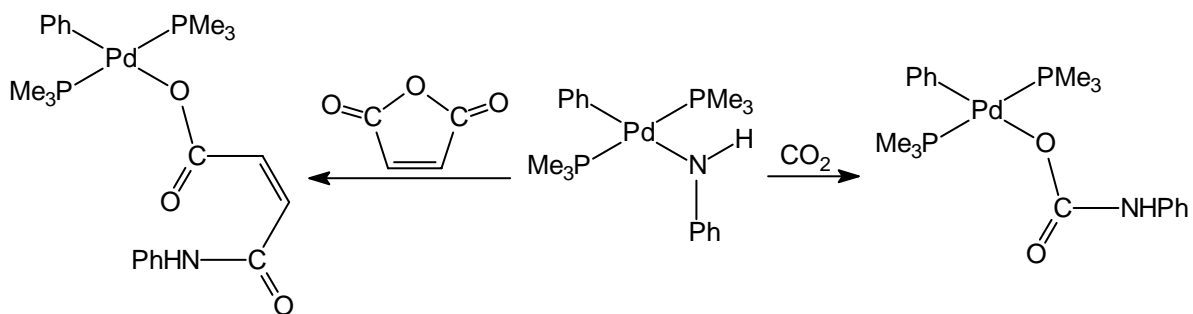
The platinum amide **4.1** readily and cleanly inserts acrylonitrile into the Pt-N bond to give the adduct **4.2** (Equation 4.1).³ Similarly, the palladium amide complex **4.3** inserts both carbon dioxide and maleic anhydride into the Pd-N bond to form the complexes **4.4** and **4.5** respectively (Equation 4.2),⁴ and the iridium complex **4.6** inserts carbon monoxide to give **4.7**, with subsequent cyclometallation to give **4.8** (Equation 4.3).⁵ Interestingly, the reactions of **4.3** with diphenyl ketene and various isocyanates showed only addition into the N-H linkage.⁴



4.1

4.2

Equation 4.1

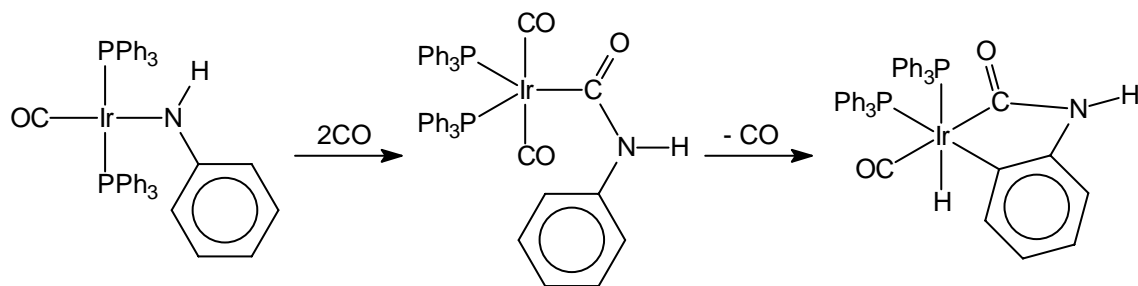


4.4

4.3

4.5

Equation 4.2



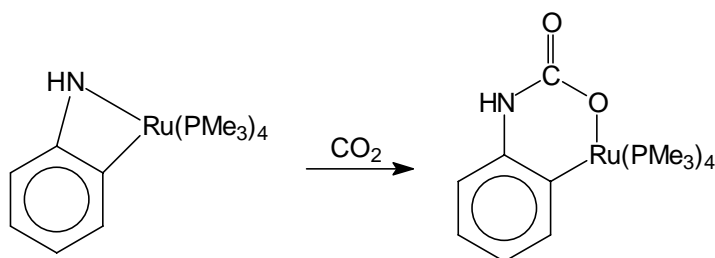
4.6

4.7

4.8

Equation 4.3

The cyclometallated ruthenium amide **4.9** (see Chapter One, Section 1.2.2.2) proved reactive to carbon dioxide and gave the carbamate complex **4.10** (Equation 4.4).⁶



4.9

4.10

Equation 4.4

More relevant to the work described in this chapter are the reactions of metallacyclic complexes containing two metal-nitrogen bonds, and a number of insertion reactions involving these complexes have been published. The previously reported palladium(II) ureylene complex $[\text{Pd}\{\overline{\text{NPhC(O)NPh}}\}(\text{phen})]$ (phen = *o*-phenanthroline) **2.17** readily undergoes insertion of phenyl isocyanate and carbon monoxide to give complexes **4.11** and **4.12** respectively (Figure 4.1).⁷ Additionally the reaction of dimethyl acetylenedicarboxylate $[\text{MeO(O)CC}\equiv\text{CC(O)OMe}]$, DMAD] with $[\text{Pt}\{\overline{\text{NHS(O)}_2\text{NH}}\}(\text{PMePh}_2)]$ **1.100** and $[\text{Pt}\{\overline{\text{NHP(O)PhNH}}\}\text{L}_2]$ **1.101** (L = tertiary phosphines) gave the respective inserted products **4.13** and **4.14** (Figure 4.2).⁸

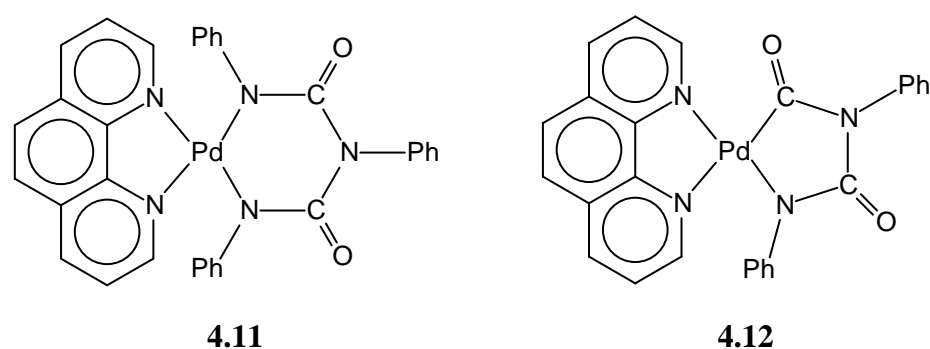


Figure 4.1

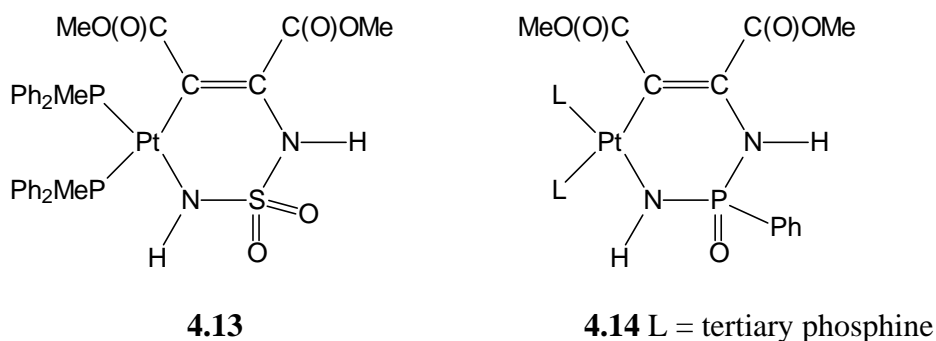


Figure 4.2

The appreciable reactivity of these M-N systems, and the ready availability of platinum(II) ureylene complexes $[\text{Pt}\{\overline{\text{NRC(O)NR}'}\}\text{L}_2]$ ($\text{L}_2 = \text{COD}$, $\text{L} = \text{PPh}_3$) **2.22** (Chapter Two), led us to investigate the reactivity of the platinaureylene complexes towards phenyl isocyanate, diphenylcarbodiimide, acetylenes, N-thionylaniline, sulfur dioxide, and carbon disulfide. The results of these reactions are described in this chapter.

4.2 Results and Discussion

4.2.1 Insertion reactions with phenyl isocyanate and diphenylcarbodiimide

When a bright-yellow dichloromethane solution of the complex $[\text{Pt}\{\overline{\text{NPhC(O)NPh}}\}(\text{COD})]$ **2.22a** was reacted with phenyl isocyanate at room temperature overnight, the solution became almost colourless. Characterisation using NMR and IR spectroscopy, electrospray mass spectrometry (ESMS) and elemental analysis confirmed the product as **4.15a** (Figure 4.3), analogous to the palladium(II) complex **4.11**⁷ and to the nickel(II) and chromium(VI) biureto complexes **4.16**⁹ and **4.17**¹⁰ (Figure 4.3) respectively.

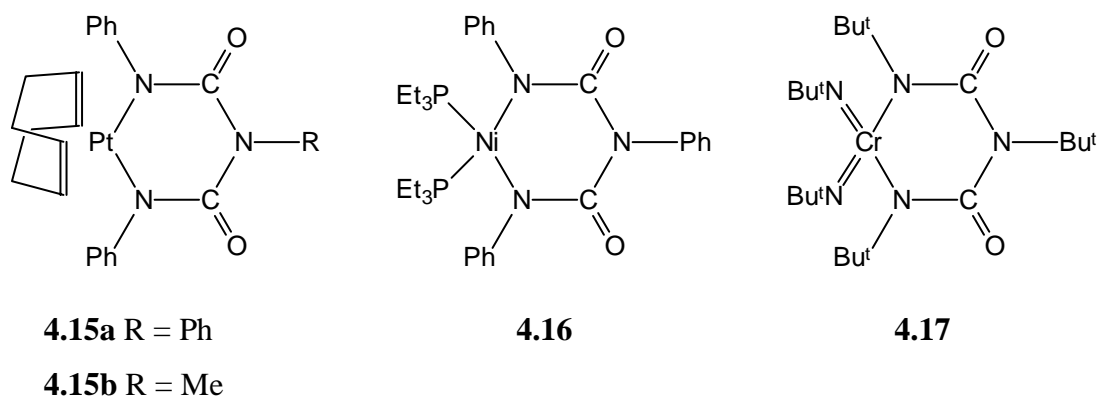


Figure 4.3

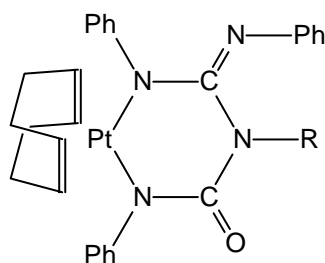
The ready formation of **4.15a** led us to examine the effect of using an unsymmetrical ureylene complex, introducing the possibility of two isomers forming. When the complex $[\text{Pt}\{\overline{\text{NPhC(O)NMe}}\}(\text{COD})]$ **2.22b** was reacted with phenyl isocyanate in dichloromethane, the solution decolourised rapidly from bright yellow to almost colourless. Completion was typically achieved in less than a minute. Both ¹H and ¹³C NMR of the crude reaction product showed the presence of only one CH=CH cyclo-octa-1,5-diene (COD) resonance indicating reaction had taken place *exclusively* at the Pt-NMe linkage (reaction at Pt-NPh would result in two inequivalent COD CH=CH groups). Further evidence could be seen in the ¹H NMR where the absence of ³J (¹⁹⁵Pt-¹H) coupling to the methyl group indicated the methyl group was now further removed from the platinum. The product was characterised as the biureto complex **4.15b** (Figure 4.3) also on the basis of NMR analysis, ESMS and elemental analysis.

The very rapid and exclusive insertion of phenyl isocyanate into only the Pt-NMe bond, gives an indication of the relative reactivities of the Pt-NPh versus Pt-NMe linkages. The increase

in reactivity of **2.22b** indicates the Pt-N alkyl linkage is apparently weaker, also tentatively evidenced in the crystal structure of $[\text{Pt}\{\overline{\text{NPhC(O)NAd}}\}(\text{COD})]$ **2.22d**, where the Pt-NAd bond length was slightly longer [2.048(8) Å] than Pt-NPh [2.021(8) Å] (Chapter Two, Section 2.2.2) although steric influences could be responsible in part.

In light of the successful “one pot” insertion reactions (using DMAD) described by Kemmitt *et al.*,⁸ we decided to determine if this was also applicable to our isocyanate insertion reactions. When $[\text{PtCl}_2(\text{COD})]$, N-methyl-N'-phenylurea, excess phenyl isocyanate and silver(I) oxide were reacted in dichloromethane, **4.15b** was formed in good yield. The only reaction by-product appeared to be **4.15a**, formed presumably by the hydrolysis of phenyl isocyanate to diphenylurea, which subsequently reacted with any unreacted $[\text{PtCl}_2(\text{COD})]$ to give **2.22a**, which in turn inserted phenyl isocyanate. This “one-pot” synthesis provides an easy synthetic route (see later) to trisubstituted biurets $\text{RNHC(O)NR}'\text{C(O)NHR}''$ [with (potentially) $\text{R} \neq \text{R}' \neq \text{R}''$], although other isocyanates were not tested.

When **2.22b** was reacted with the closely related compound diphenylcarbodiimide ($\text{PhN}=\text{C}=\text{NPh}$), the biureto complex **4.15b** was still the only reaction product. This is presumably the result of the hydrolysis of either diphenylcarbodiimide or of the presumed guanidine intermediate derivative **4.18a** (Figure 4.4). To investigate when the hydrolysis occurred, the moisture stable guanidine complex **3.17a** (Chapter Three) was reacted with phenyl isocyanate. The product was characterised as the triphenylbiureto complex **4.15a**, by identical ^1H and ^{13}C NMR. No detectable quantity of the expected complex **4.18b** was observed. This result suggests hydrolysis occurs *after* insertion. The apparent relative high moisture sensitivity of **4.18** compared with that of **4.15a**, both of which contain the NPhC(=NPh)NPh groups, is not clear.



4.18a R = Me

4.18b R = Ph

Figure 4.4

In the absence of excess phenyl isocyanate, deinsertion of the complexes **4.15a** and **4.15b** took place on standing, to regenerate the respective starting complexes **2.22a** and **2.22b** and phenyl isocyanate, evidenced by NMR. This typically occurred over a few days, and for spectroscopic characterisation excess phenyl isocyanate was not necessary. However, a few drops of phenyl isocyanate were added to solutions of **4.15a** or **4.15b** prior to crystallisation, to inhibit formation of crystals from the starting materials (**2.22a** or **2.22b**).

To examine possible synthetic utility of the insertion reaction, a dichloromethane solution of **4.15b** was treated with concentrated hydrochloric acid. The diethyl ether extract of the residue contained pure N,N''-diphenyl-N'-methylbiuret, characterised by ^1H and ^{13}C NMR spectroscopy, elemental analysis and ESMS. Integration of the ^1H NMR showed the expected phenyl:methyl and NH:methyl ratios of 2:1. Additionally, the methyl signal contained no splitting, indicating the absence of adjacent methyl and NH moieties that are present in N-methyl-N'-phenylurea. The ether insoluble residue was characterised by NMR as almost pure $[\text{PtCl}_2(\text{COD})]$.

4.2.1.1 Spectroscopic and mass spectrometric characterisation

4.2.1.1.1 NMR spectroscopy

In addition to the ^1H and ^{13}C NMR already discussed, a few additional features are noteworthy. Upon insertion of phenyl isocyanate, the carbonyl carbon resonance undergoes a large upfield shift. For the complex **4.15b**, a chemical shift of 156.4 ppm was noted, which compares with a value of 173.8 ppm for the starting material **2.22b**. This is consistent with a release of steric strain on going from a four-membered to a six-membered ring system; indeed the platinum centre appears to have little bearing on the position of the carbonyl resonance in **4.15b**, since free N,N''-diphenyl-N'-methylbiuret shows the signal at 154.2 ppm.

The $^2\text{J} (^{195}\text{Pt}-^1\text{H})$ and $^1\text{J} (^{195}\text{Pt}-^{13}\text{C})$ coupling constants from the CH=CH part of the COD ligand are only slightly different from those of the starting materials (**2.22a** and **2.22b**). For the complex **4.15a** a $^2\text{J} (^{195}\text{Pt}-^1\text{H})$ value of 53.2 Hz and $^1\text{J} (^{195}\text{Pt}-^{13}\text{C})$ of 145.2 Hz compare with respective values of 59.4 Hz and 141.7 Hz for **2.22a**. Unsurprisingly, **4.15b** shows similar $^2\text{J} (^{195}\text{Pt}-^1\text{H})$ and $^1\text{J} (^{195}\text{Pt}-^{13}\text{C})$ coupling constants, with values of 56.1 and 143.1 Hz respectively.

4.2.1.1.2 IR spectroscopy

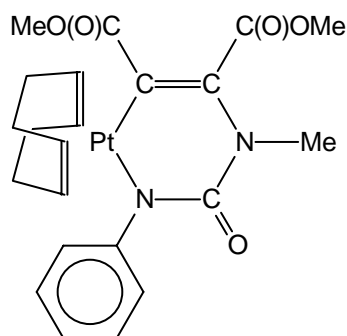
The carbonyl region ($1700\text{-}1550\text{ cm}^{-1}$) of the IR spectrum is the only area of diagnostic value. Upon insertion, the expected complication of bands arising from the addition of a carbonyl group was observed. For the complex **4.15b**, five bands [1641 , 1632 , 1611 , 1600 and 1584 cm^{-1}] are seen, compared to only two for the starting material **2.22b** [1650 and 1590 cm^{-1}].

4.2.1.1.3 Electrospray mass spectrometry (ESMS)

Positive-ion electrospray mass spectra of the complexes **4.15a** and **4.15b** show very strong parent ions at low cone voltages ($\sim 20\text{ V}$), with increased fragmentation at higher voltages. The fragmentation pathway at moderate cone voltages ($\sim 50\text{ V}$) shows solely loss of phenyl isocyanate. Whether this process results in the four-membered ring system $[\text{Pt}\{\overline{\text{NPhC(O)NR}}\}\text{COD} + \text{H}]^+$ ($\text{R} = \text{Ph, Me}$) i.e. $[\mathbf{2.22} + \text{H}]^+$, or a ring-opened structure $[\text{Pt}^+\{\text{NPhC(O)NHR}\}\text{COD}]$, can not be determined, although the ready deinsertion of phenyl isocyanate to regenerate starting materials in solution suggests the former as the most probable. In this case the most likely site for the protonation is the carbonyl group, as opposed to the NR moieties which are not expected to be sufficiently basic (sp^2 hybridised and conjugated).

4.2.2 Reaction with acetylenes

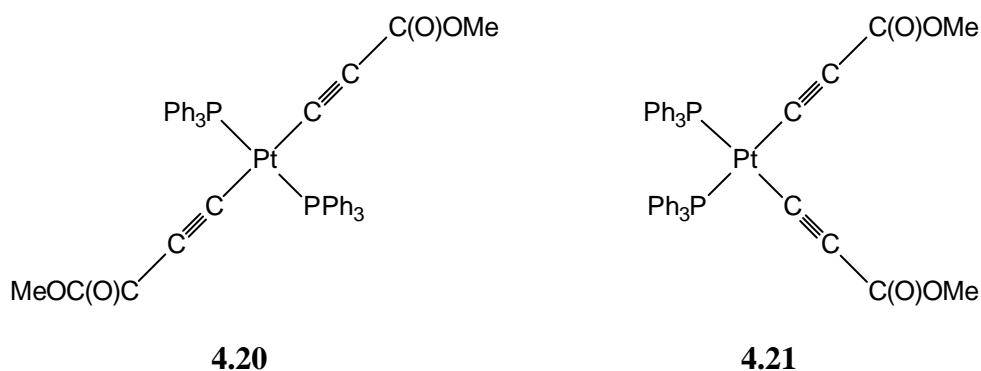
When DMAD was added to a dichloromethane solution of the complex **2.22a** no visible reaction occurred, so reflux was commenced and maintained for 24 hours. NMR analysis of the crude reaction residue revealed no reaction had occurred. However when complex **2.22b** was treated with DMAD, rapid decolourisation of the solution was noted. Recrystallisation produced flaky pale yellow crystals, which were characterised spectroscopically and by elemental analysis as the DMAD inserted product **4.19** (Figure 4.5). The ready formation of complex **4.19** is analogous to the that reported for complexes **4.13** and **4.14**.⁸ However, complex **2.22b** failed to react to any detectable extent with the more electron-rich diphenylacetylene, even after two days reflux.



4.19

Figure 4.5

In an attempt to examine the favoured orientation of an unsymmetrical acetylene upon insertion into a Pt-N of the ureylene ring, methyl propiolate [HC≡CC(O)OMe] was reacted with complex **2.22b**. ^1H NMR of the crude reaction mixture showed no signals attributable to the COD-Pt moiety, indicating its complete decomposition. For this reason the more robust triphenylphosphine derivative [$\text{Pt}\{\overline{\text{NPhC(O)NMe}}\}(\text{PPh}_3)_2$] **2.22g** was used. However, methyl propiolate proved too acidic and when the acetylene was added to a solution of **2.22g**, rather than insert into the Pt-N bond, loss of the ureylene ligand resulted, to give the diacetylide complex **4.20** (Figure 4.6). This formulation was strongly supported by ^{31}P NMR (see Section 4.2.2.1.1) and elemental analysis which showed zero nitrogen content, proving ureylene displacement.



4.20

4.21

Figure 4.6

Acetylide complexes are well known in the literature and are found for most of the transition metals.¹¹ A number of platinum(II) examples have been structurally characterised.¹²⁻¹⁴ Unsurprisingly, **4.20** could be readily synthesised from *cis*-[PtCl₂(PPh₃)₂], methyl propiolate and silver(I) oxide. NMR analysis of the crude reaction mixture from both the direct synthesis and by displacement of the ureylene ligand in **2.22g**, show the expected¹² initial *cis* isomer

4.21 (see previous figure), which slowly converts to the *trans* isomer **4.20** on standing, with **4.20** being the only product isolated on crystallisation.

4.2.2.1 Spectroscopic and mass spectrometric characterisation

4.2.2.1.1 NMR spectroscopy

Unlike the phenyl isocyanate insertion products, the DMAD-inserted complex remains unsymmetrical, thus giving rise to two COD CH=CH resonances. 2J (^{195}Pt - ^1H) coupling of 58.3 and 36.2 Hz was observed for the signals at 5.06 and 4.77 ppm, and assigned as CH=CH *trans* to N and C respectively, on the basis of their relative *trans*-influences.²⁴ The ^{13}C NMR similarly showed 1J (^{195}Pt - ^{13}C) couplings of 155.8 and 67.2 Hz for the respective signals at 90.4 and 112.6 ppm. Like the phenyl isocyanate reactions, insertion took place solely at the Pt-NMe bond, readily witnessed by loss of 3J (^{195}Pt - ^1H) coupling on the methyl resonance. A 1J (^{195}Pt - ^{13}C) value of 982.0 Hz in the ^{13}C NMR spectrum of **4.19** unambiguously confirms formation of a Pt-C bond. As seen for complexes **4.15a** and **4.15b**, a large upfield shift in the ureylene carbonyl is observed going from 173.8 ppm in **2.22b**, to 154.3 ppm in **4.19**.

The acetylide complex **4.20** was readily characterised from ^{31}P NMR, which showed a single ^{31}P resonance at 18.1 ppm, consistent with a symmetrical complex. The 1J (^{195}Pt - ^{31}P) value of 2533 Hz is indicative of P *trans* to P. Spectra of the crude reaction residue from both the ureylene route and from direct synthesis show predominantly the *cis* isomer **4.21** at 15.7 ppm with the expected lower 1J (^{195}Pt - ^{31}P) value of 2365 Hz, consistent with P *trans* to C.

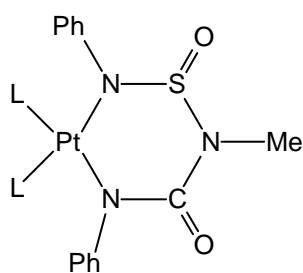
4.2.2.1.2 Electrospray mass spectrometry

Like complexes **4.15a** and **4.15b**, **4.19** shows a very strong parent ion in its positive ion ES mass spectrum. Higher cone voltages induced fragmentation, which in this system could be expected to proceed via either loss of phenyl isocyanate, or by deinsertion of DMAD. Examination of the spectrum of **4.19** at a cone voltage of 50 V, only the former was observed, with no ions attributable to loss of DMAD. This is not unexpected, since platinum prefers to bond to the softer carbon atom, and the electron-withdrawing groups on the alkene linkage should further enhance the Pt-C bond stability. At a higher cone voltage of 80 V, fragmentation of the ester units following loss of phenyl isocyanate yielded the principal ions $[\text{M} - \text{PhNCO} - \text{MeO}]^+$ and $[\text{M} - \text{PhNCO} - \text{MeOC(O)}]^+$.

4.2.3 Reactions with N-thionylaniline and sulfur dioxide

Chemically similar to isocyanates, insertion reactions with thionylamines (RNSO) have attracted relatively little attention, with the isoelectronic sulfur dioxide^{15,16} dominating the literature. Nonetheless, work describing thionylamines inserting into metal-carbon σ -bonds¹⁷ or giving co-ordination complexes from various ruthenium, osmium, rhodium and iridium compounds,¹⁸⁻²¹ has been published.

In a reaction analogous to the phenyl isocyanate insertions described in Section 4.2.1, reaction with N-thionylaniline was attempted, with the goal of forming insertion products of the type **4.22** (Figure 4.7). In contrast to phenyl isocyanate, the COD complex **2.22b** was decomposed by N-thionylaniline, although this is not surprising since N-thionylaniline contains a soft sulfur atom, which would be expected to displace the labile COD ligand.

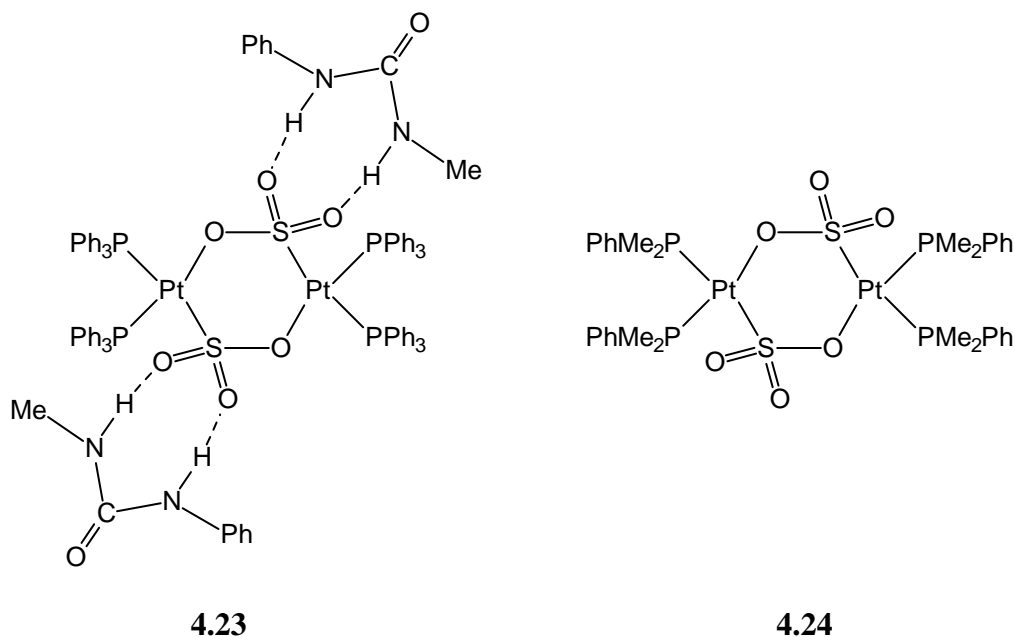


4.22

Figure 4.7

When N-thionylaniline was reacted with the ureylene complex $[\text{Pt}\{\overline{\text{NPhC(O)NMe}}\}(\text{PPh}_3)_2]$ **2.22g**, a pure white powder was isolated. The connectivity of the product was initially not obvious, due to the continuing presence of resonances associated with a ureylene-type moiety in the ¹H and ¹³C NMR spectra. Additionally when the complex **2.22g** was dissolved in liquid sulfur dioxide, the same product was isolated, by similarity of ³¹P, ¹H and ¹³C NMR spectra.

The complex was eventually characterised as **4.23** (Figure 4.8), and this formulation is consistent with NMR and IR spectroscopies and elemental analysis. The absolute connectivity was determined by an X-ray crystallographic study. Compounds containing the $\overline{\text{M-S-O-M-S-O}}$ unit have been previously reported for palladium,²² and the structure has been determined for the very closely related platinum(II) compound **4.24** (Figure 4.8).²³ The latter was formed by the hydrolysis of $[\text{Pt}(\text{NSO})_2(\text{PMe}_2\text{Ph})_2]$, and did not form in dry conditions even under an oxygen atmosphere.

**Figure 4.8**

We believe it is unlikely the formation of **4.23** resulted from the *in situ* hydrolysis of N-thionylaniline. This could conceivably give sulfur dioxide, providing a source for the sulfite dianion which could subsequently displace the ureylene ligand. Although no insertion products were detected, simple attack of the ureylene ligand by free SO_3^{2-} would probably result in the formation of $[\text{Pt}\{\overline{\text{O-S(O)-O}}\}(\text{PPh}_3)_2]$, the reported reaction product of *cis*- $[\text{PtCl}_2(\text{PPh}_3)_2]$ and silver(I) sulfite.²³ Additionally, the reaction of **2.22g** with sodium sulfite in methanol also did not give **4.23**. We speculate the formation of **4.23** is the result of an initial insertion of N-thionylaniline or sulfur dioxide into the Pt-N bond, followed by metal activated hydrolysis [similar to that suspected to occur for the formation of **4.15b** from **2.22b** and diphenylcarbodiimide (see Section 4.2.1)], with the eventual extrusion of N-methyl-N'-phenylurea. Although a rigorously anhydrous protocol was not followed, even when freshly dried and distilled solvents were used, **4.23** was still the only significant reaction product.

4.2.3.1 X-ray structure of $[\{\text{Pt}(\text{SO}_3)(\text{PPh}_3)_2\}_2 \cdot 2\text{PhNHC(O)NHMe}]$ chloroform solvate **4.23**

An ORTEP perspective view of the structure is shown in Figure 4.9 together with the atom numbering scheme (the complex is centrosymmetric and ' denotes symmetry related atoms). Selected bond lengths and angles are presented in Table 4.1, with tables of complete bond lengths and angles, final positional parameters, thermal parameters and calculated H-atom positions presented in Appendix VI.

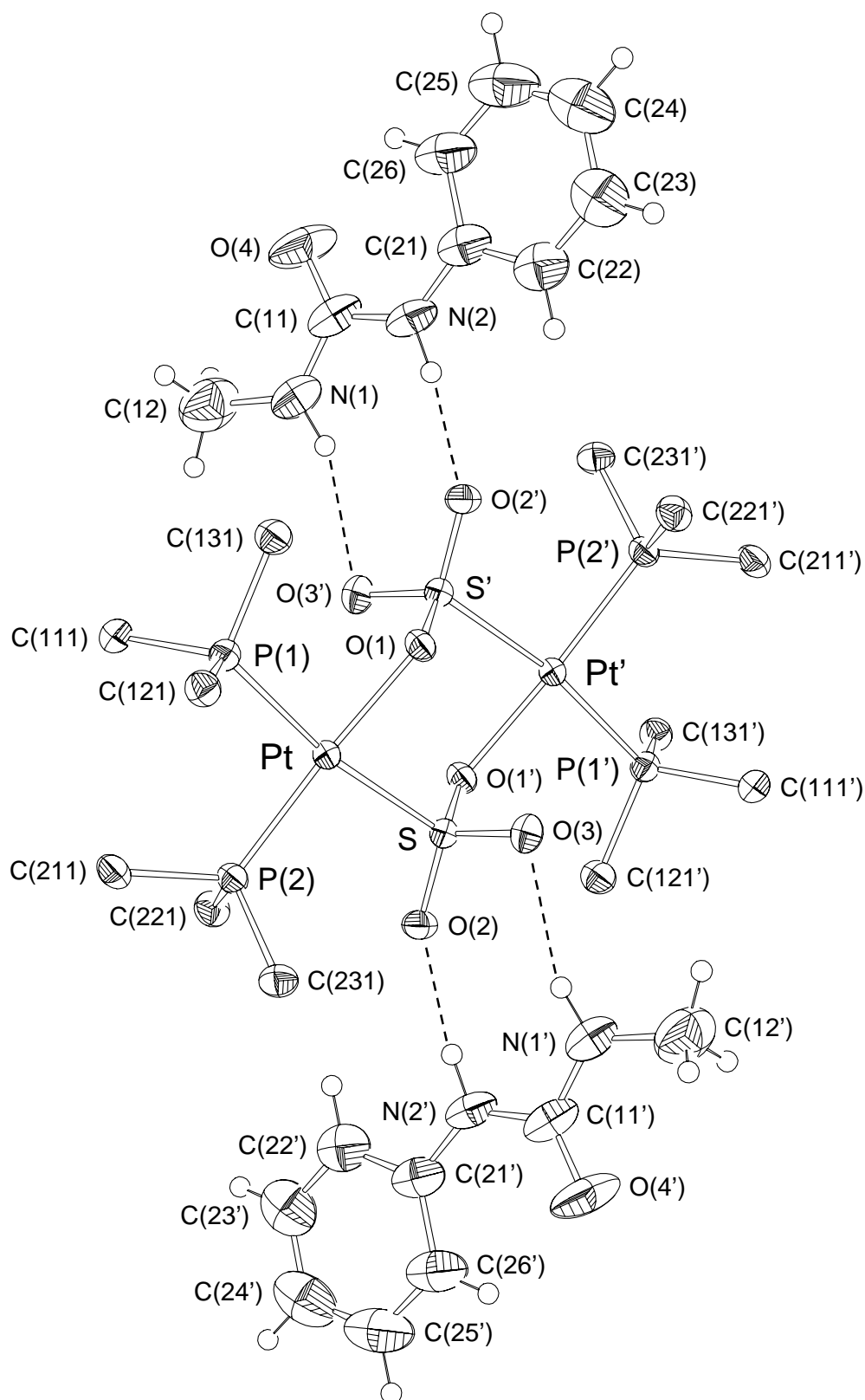


Figure 4.9: ORTEP representation of $[\{\text{Pt}(\text{SO}_3)(\text{PPh}_3)_2\}_2 \cdot 2\text{PhNHC}(\text{O})\text{NHMe}] \cdot 2\text{CHCl}_3$ **4.23**, showing the atom numbering scheme (the ' denotes symmetry related atoms). Only P-bonded carbons of the triphenylphosphine aromatic rings are shown, and the two chloroforms of crystallisation have been omitted for clarity. Atoms are shown as thermal ellipsoids at the 50% probability level.

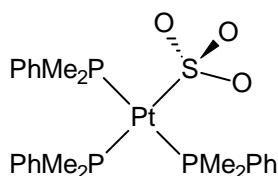
Table 4.1: Selected bond lengths (Å) and bond angles (°) (estimated standard deviations in parentheses) for **4.23**·2CHCl₃.

Bond	Length	Bonds	Angle
Pt-P(1)	2.3404(7)	P(1)-Pt-P(2)	97.37(3)
Pt-P(2)	2.2506(8)	S-Pt-O(1)	83.73(6)
Pt-O(1)	2.084(2)	P(1)-Pt-O(1)	87.01(6)
Pt-S	2.3273(7)	P(2)-Pt-S	91.93(3)
S-O(1)	1.534(2)	Pt-O(1)-S	121.82(12)
S-O(2)	1.474(2)	Pt-S-O(1)	104.95(8)
S-O(3)	1.463(2)	Pt-S-O(2)	114.70(9)
O(2)...N(2)	2.860(5)	Pt-S-O(3)	108.91(9)
O(3)...N(1)	3.118(5)	O(1)-S-O(2)	106.59(12)
Pt...Pt'	4.287(3)	O(1)-S-O(3)	109.41(12)
S...S'	3.547(3)	O(2)-S-O(3)	111.93(13)
Co-crystallised PhNHC(O)NHMe			
C(11)-O(4)	1.233(5)	N(1)-C(11)-N(2)	114.3(3)
C(11)-N(1)	1.355(6)	N(1)-C(11)-O(4)	121.8(4)
C(11)-N(2)	1.367(5)	N(2)-C(11)-O(4)	123.9(4)
N(1)-C(12)	1.446(6)	C(11)-N(1)-C(12)	121.6(4)
N(2)-C(21)	1.395(6)	C(11)-N(2)-C(21)	128.7(3)

The structure shows the six-membered $\overline{\text{Pt-S-O-Pt-S-O}}$ ring system, identical to that previously reported for **4.24**·5CHCl₃.²³ The platinum atom has the typical distorted square-planar arrangement, with the maximum deviations for the least-square plane drawn through P(1), P(2), Pt, S and O(1) being 0.038(1) Å above and 0.034(1) Å below for S(1) and O(1) respectively. The core of the molecule has geometrical parameters almost identical to **4.24**. The chair conformation of the $\overline{\text{Pt-S-O-Pt-S-O}}$ ring is inclined 123.1(1)° between the S(1), O(1), S(1') and O(1') plane and the Pt, O(1) and S(1) plane; **4.24** shows a corresponding angle of 124°. The P-Pt bond lengths are not equal, as expected on *trans*-influence considerations,²⁴ with P *trans* to the higher *trans*-influence S being significantly longer [2.3404(7) Å] than P *trans* O [2.2506(8) Å]. Additional detail and discussion regarding the geometry of this six-membered ring has been reported by Woollins *et al.*²³

The most structurally interesting feature of **4.23** is the hydrogen-bonded co-crystallised N-methyl-N'-phenylurea molecule. The hydrogen-bonding occurs through the urea N-H groups and the S(O)₂ groups of the sulfite, as depicted in Figure 4.9. The N...O contacts are markedly different in length, with N(2)...O(2) being significantly shorter [2.860(5) Å] than N(1)...O(3) [3.118(5) Å]. This is probably not due to geometric incompatibility of the urea and S(O)₂ groups, since the angles between N(1)-C(11)-N(2) [114.3(3)°] and O(2)-S-O(3) [111.9(1)°] would suggest a good match. Rather, steric hindrance from the bulky triphenylphosphine ligands possibly restricts more optimised hydrogen-bonding. Ureas hydrogen-bonded to S(O)₂ groups (the majority being sulfate dianions) in this way have been observed previously.²⁵ Additionally, hydrogen-bonding between diarylureas and various co-crystallised hydrogen-bond acceptors,²⁶ and also between molecules of platinum(II) complexes with various amide ligands,^{27,28} have attracted interest as model complexes exhibiting “molecular recognition”.

Remarkably, for the crystal structure of **4.25**·H₂O²³ (Figure 4.10), also containing a sulfite group, the authors report the structure displays no hydrogen-bonding between the SO₃ and the water of crystallisation.



4.25

Figure 4.10

The N-methyl-N'-phenylurea of crystallisation is almost planar, with no atom deviating from a least-squares plane drawn through every non-hydrogen atom of the molecule by more than 0.201(5) Å above for C(12) and 0.116(4) Å below the plane for O(4). Attempts at removing the co-crystallised urea from **4.23** by repeated recrystallisation proved futile, and neither N-methyl-N'-phenylurea or [$\text{Pt}(\text{SO}_3)(\text{PPh}_3)_2$]₂ could be isolated separately, indicating the hydrogen-bonding has a substantial effect for this compound, persisting in solution and directing the crystallisation.

One of the two chloroforms of crystallisation also forms a convincing hydrogen-bond to O(3), with a C...O contact of 3.086(6) Å.

4.2.3.2 Spectroscopic and mass spectrometric characterisation

4.2.3.2.1 NMR spectroscopy

The ^{31}P NMR spectrum of **4.23** shows the expected AB pattern, with chemical shifts of 21.3 and 10.5 ppm showing ^{195}Pt - ^{31}P coupling of 2459 and 4331 Hz. These were assigned as P *trans* to S and P *trans* to O respectively, on the basis of the *trans*-influences associated with these atoms.²⁴ The related compound **4.24** shows similar coupling constants of 2329 and 3986 Hz, the discrepancy due to the electronically different phosphine moieties (PPh_3 and PMe_2Ph).

Interestingly, the N-methyl-N'-phenylurea present in solution shows different chemical shift values to the free urea (Table 4.2), indicating the persistence of the hydrogen-bonding interactions with the $\text{S}(\text{O})_2$ unit in solution. The NH resonances are the most affected, as expected, with downfield differences in their chemical shifts of 0.86 and 0.73 ppm for the NH groups adjacent to the phenyl and methyl moieties respectively. This is consistent with the notion of decreased shielding of protons caused by a lowering of electron density associated with hydrogen-bond formation. Unexpectedly, the carbonyl carbon appears to be unaffected, showing a value of 156.7 ppm for both **4.23** and free N-methyl-N'-phenylurea.

4.2.3.2.2 IR spectroscopy

The IR stretching frequencies for **4.23** are significantly different to those reported for **4.24**, presumably due to the hydrogen-bonding present in **4.23** only. Significant bands in the SO_3 stretching region ($1200\text{-}900\text{ cm}^{-1}$) appear at 1177, 1096, 1063 and 923 cm^{-1} , compared with values of 1168, 1156, 1048 and 1004 cm^{-1} given for **4.24**.²³ In the NH stretching region ($3500\text{-}3000\text{ cm}^{-1}$) bands are observed at 3082 and 3056 cm^{-1} , compared with bands at 3360 and 3316 cm^{-1} for free N-methyl-N'-phenylurea, thus showing a lowering in stretching frequency, as expected for hydrogen-bonded NH groups.²⁹

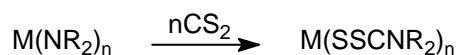
Table 4.2: Comparison of ^1H and ^{13}C NMR chemical shifts[†] of the hydrogen-bonded urea fragment of **4.23** and free *N*-methyl-*N'*-phenylurea.

Group	δ ^1H (ppm)		δ ^{13}C (ppm)	
	4.23	free <i>N</i> -phenyl- <i>N'</i> -methylurea	4.23	free <i>N</i> -phenyl- <i>N'</i> -methylurea
Ph-NH	7.37	6.51	-	-
Me-NH	5.59	4.86	-	-
Me	2.45	2.82	26.2	27.1
C=O	-	-	156.7	156.7
Ipsso Ph	-	-	141.2	138.5
Ortho Ph	7.09	7.28	118.2	121.6
Meta Ph	7.19	7.32	128.1	129.4
Para Ph	6.80	7.09	120.0	124.1

[†] All data acquired in CDCl_3 solvent and referenced to SiMe_4 (δ 0.0 ppm)

4.2.4 Insertion reaction with carbon disulfide

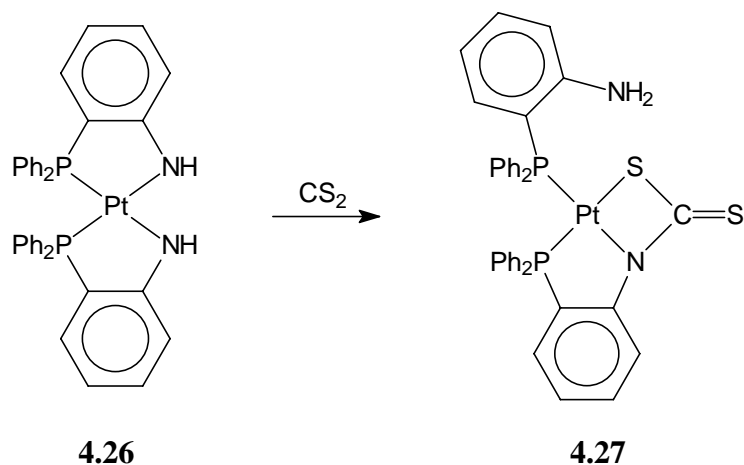
The insertion chemistry of carbon disulfide with transition-metal-nitrogen bonds has only been relatively poorly explored. Typically, the reaction of CS_2 with early transition-metal amides, specifically complexes of Ti(IV), V(IV) Zr(IV), Nb(V) and Ta(V) give tetrakis(*N,N*-dialkyldithiocarbamato) complexes (Equation 4.5).³⁰ The reaction of the five-membered ring platinum(II) co-ordination complex **4.26** with carbon disulfide resulted only in displacement of the amino group to give **4.27** (Figure 4.11). To the best of our knowledge no previous reactions of carbon disulfide with ureylene complexes, or indeed four-membered ring metallacycles in general, had been attempted.



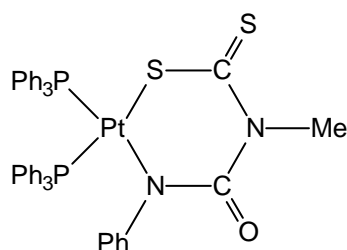
M = Ti, Zr; R = Me, Et, n-Pr; n = 4

M = V, R; R = Me, Et; n = 5

Equation 4.5

*Figure 4.11*

When carbon disulfide was added to a dichloromethane solution of **2.22g**, and stirred for 3 minutes, the carbon disulfide inserted product **4.28** (Figure 4.12) was produced in quantitative yield by ^{31}P NMR analysis of the residue. Large yellow blocks could be obtained on addition of diethyl ether to a dichloromethane solution. The compound was fully characterised by ^{31}P , ^1H and ^{13}C NMR, ESMS, elemental analysis and a single crystal X-ray crystallographic study was undertaken. Solutions of the complex **4.28** slowly decomposed to produce, in high yield, a second product, discussed later in Section 4.2.5. As for the reaction involving N-thionylaniline, carbon disulfide readily decomposed the COD complex **2.22b**.

**4.28***Figure 4.12*

4.2.4.1 X-ray structure of $\text{[Pt}\{\text{SC(S)NMeC(O)NPh}\}\text{(PPh}_3\text{)}_2\text{]}$ chloroform solvate **4.28**

ORTEP representations of perspective and side views are shown in Figures 4.13 and 4.14 respectively. Selected bond lengths and angles are presented in Table 4.3, with tables of complete bond lengths and angles, final positional parameters, thermal parameters and calculated H-atom positions presented in Appendix VII.

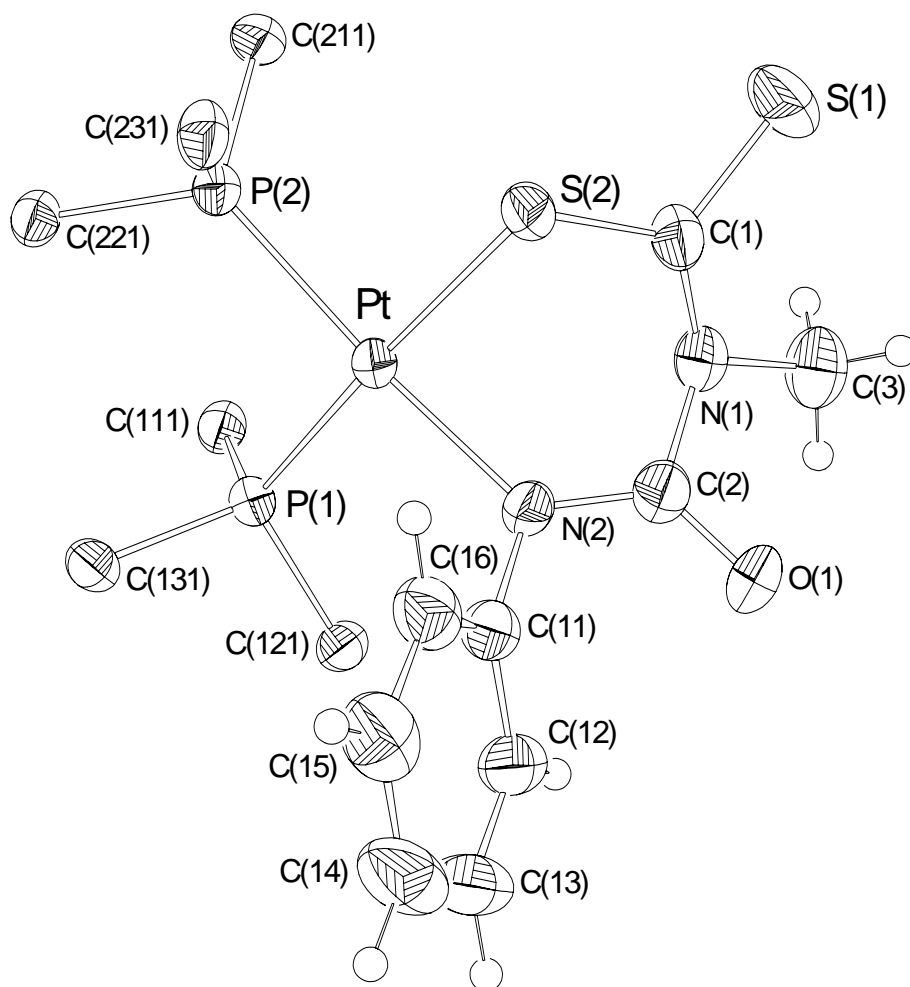


Figure 4.13: Perspective view of the structure of $[Pt\{SC(S)NMeC(O)NPh\}(PPh_3)_2] \cdot CHCl_3$ **4.28**, showing the atom numbering scheme. For clarity, only the P-bonded carbon atoms of the triphenylphosphine aromatic rings are shown, and the chloroform of crystallisation has been omitted. Atoms are shown as thermal ellipsoids at the 50% probability level.

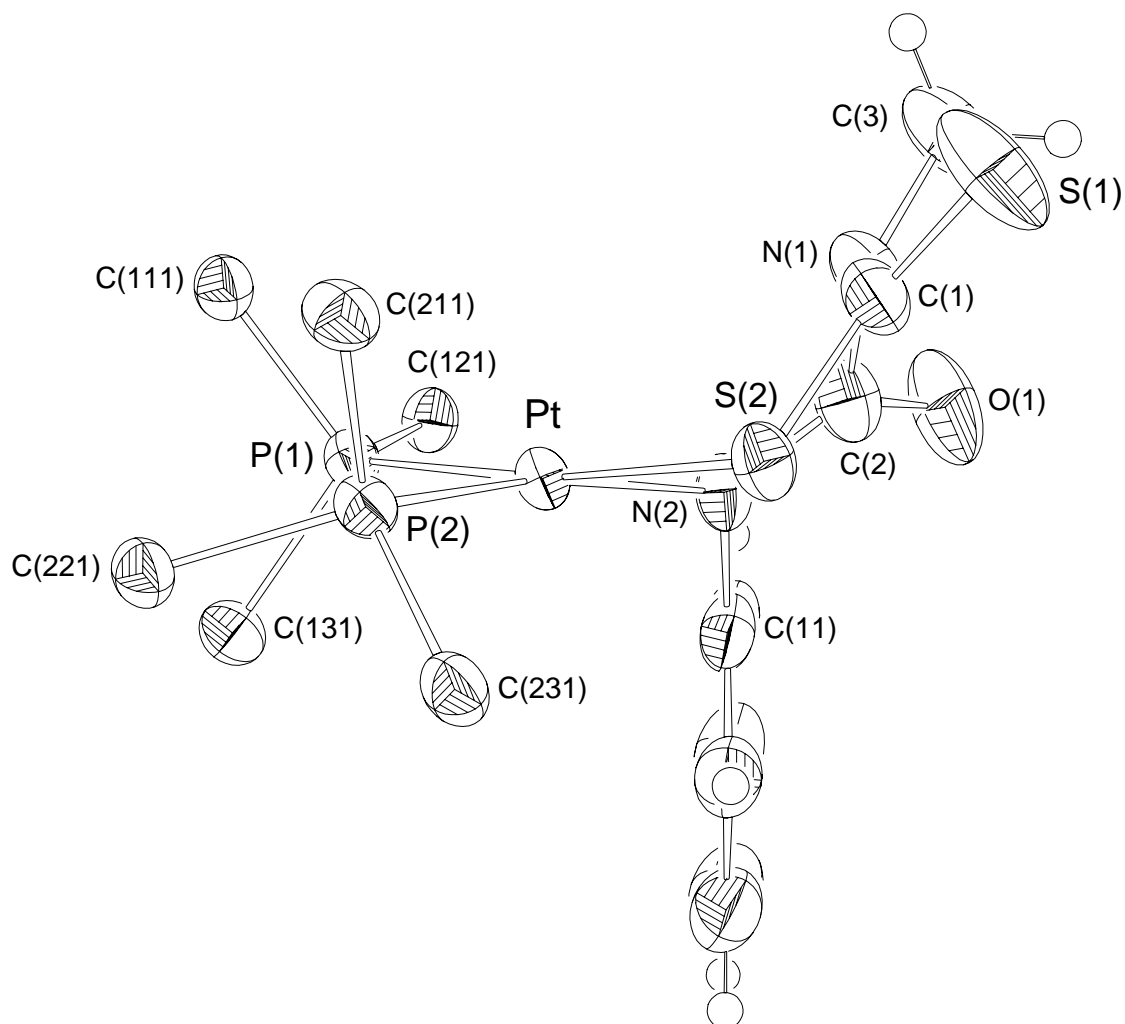


Figure 4.14: Side view of the structure of $[\text{Pt}\{\overline{\text{SC}(\text{S})\text{NMeC}(\text{O})\text{NPh}}\}(\text{PPh}_3)_2]\cdot\text{CHCl}_3$ **4.28**, showing the atom numbering scheme. For clarity, only the P-bonded carbon atoms of the triphenylphosphine aromatic rings are shown, and the chloroform of crystallisation has been omitted. Atoms are shown as thermal ellipsoids at the 50% probability level.

Table 4.3: Selected bond lengths (Å) and bond angles (°) (estimated standard deviations in parentheses) for **4.28**·CHCl₃

Bond	Length	Bonds	Angle
Pt-P(1)	2.2921(10)	P(1)-Pt-P(2)	97.21(4)
Pt-P(2)	2.2686(10)	S(2)-Pt-N(2)	83.53(10)
Pt-N(2)	2.066(3)	P(1)-Pt-N(2)	94.20(10)
Pt-S(2)	2.3358(10)	P(2)-Pt-S(2)	86.17(4)
		Pt-S(2)-C(1)	101.15(16)
		Pt-N(2)-C(2)	126.5(3)
		Pt-N(2)-C(11)	115.5(3)
S ₂ CNMeC(O)NPh ligand			
C(1)-S(2)	1.736(5)	S(2)-C(1)-S(1)	116.3(3)
C(1)-S(1)	1.672(5)	S(2)-C(1)-N(1)	121.7(3)
C(1)-N(1)	1.360(6)	S(1)-C(1)-N(1)	122.0(3)
N(1)-C(3)	1.470(6)	C(1)-N(1)-C(2)	122.0(4)
N(1)-C(2)	1.454(6)	C(1)-N(1)-C(3)	118.9(4)
C(2)-O(1)	1.232(6)	C(3)-N(1)-C(2)	113.0(4)
C(2)-N(2)	1.323(6)	N(1)-C(2)-N(2)	116.6(4)
N(2)-C(11)	1.441(6)	N(1)-C(2)-O(1)	116.8(4)
		O(1)-C(2)-N(2)	126.6(5)
		C(2)-N(2)-C(11)	116.6(4)

The structure confirms the insertion of carbon disulfide into the Pt-NMe bond of **2.22g**. The most striking feature of the structure is the highly puckered six-membered metallacyclic ring, as depicted in Figure 4.14. The butterfly angle between the least squares-planes drawn through Pt, S(2), N(2) and N(2), S(2), N(1) is 58.6(1)°. The reason for the puckering of the metallacycle is not entirely clear, but high fold angles have been observed previously for the $\overline{\text{M-S-C-C-C(O)-O}}$ six-membered ring in the platinum(II) and gold(III) thiosalicylate complexes $[\text{Pt}\{\overline{\text{SC}_6\text{H}_4(\text{COO})-2}\}(\text{PPh}_3)_2]$ **8.7**³¹ and $[\{\text{C}_6\text{H}_4(\text{CH}_2\overline{\text{NMe}_2}-2)\}\text{Au}\{\overline{\text{SC}_6\text{H}_4(\text{COO})-2}\}]$ **8.10** (see Chapter Eight for greater detail). The planes Pt, S(2), N(2) and the phenyl ring [C(11)...C(16)] are almost at right angles [88.8(1)°].

The platinum has a distorted square-planar geometry. A least-squares plane drawn through P(1), P(2), Pt, S(2) and N(2) shows maximum deviations of 0.166(1) Å for S(2) above and 0.168(1) below the plane for N(2). The six-membered metallacyclic ring allows the platinum

to adopt an N-Pt-S angle of $83.5(1)^\circ$, much closer to ideal square-planar geometry. For comparison, the N-Pt-N angle for **2.22d** (Chapter Two, Section 2.2.2) with a four-membered ring is $64.7(3)^\circ$.

The N(1)-C(2)-N(2) angle of $116.6(4)^\circ$ is larger than that of **2.22d** [$104.1(7)^\circ$] as expected for a less constrained ligand. Indeed the angle is only marginally larger than the analogous N(1)-C(11)-N(2) angle of the free N-methyl-N'-phenylurea ligand present in **4.23**, which has an angle $114.3(3)^\circ$.

The Pt-P bonds are not equal [$2.2921(10)$ and $2.2686(10)$ Å for Pt-P(1) and Pt-P(2) respectively], as expected for a non-symmetrical structure. The longer bond is *trans* to the higher *trans*-influence sulfur as predicted,²⁴ although the difference here is not as marked as that in the structure of **4.23**. The C-S bond lengths are also not equal [$1.672(5)$ Å for C(1)=S(1) and $1.736(5)$ Å for C(1)-S(2)], and the difference [$0.064(7)$ Å] is that expected for formally single and double bonds, with sp^2 hybridised C=S bond lengths averaging $1.67(2)$ Å and C-S averaging $1.76(2)$ Å.³²

4.2.4.2 Spectroscopic and mass spectrometric characterisation

4.2.4.2.1 NMR spectroscopy

The ^{31}P NMR of **4.28** shows the expected AB spin pattern with signals at 18.0 and 5.3 ppm with ^1J (^{195}Pt - ^{31}P) coupling constants of 3098 Hz and 3211 Hz, corresponding to PPh_3 *trans* to sulfur and nitrogen respectively. As for the phenyl isocyanate (Section 4.2.1) and DMAD (Section 4.2.2) reactions, insertion took place only at the Pt-NMe bond, readily deduced from the ^1H NMR spectrum, with the methyl signal devoid of ^{195}Pt and ^{31}P coupling. In the ^{13}C NMR, the carbonyl carbon again moved upfield from 176.9 to 155.0 ppm, consistent with the shifts observed for the inserted products **4.15b** (phenyl isocyanate) and **4.19** (DMAD). The C=S carbon, at 205.1 ppm, is more deshielded than free carbon disulfide, which appears at 192.6 ppm.

4.2.4.2.2 IR spectroscopy

The infrared spectrum of **4.28** shows a number of bands in the carbonyl region (1700 - 1550 cm^{-1}) with absorbances at 1646 , 1632 and 1586 cm^{-1} , and these have slightly higher energies than the starting ureylene complex **2.22g** (1636 , 1592 and 1571 cm^{-1}). The vibrations

associated with the CS₂ group cannot be readily identified because of coupling and overlap with other peaks, but are probably found among the bands at 1265, 1096 and 1069 cm⁻¹.

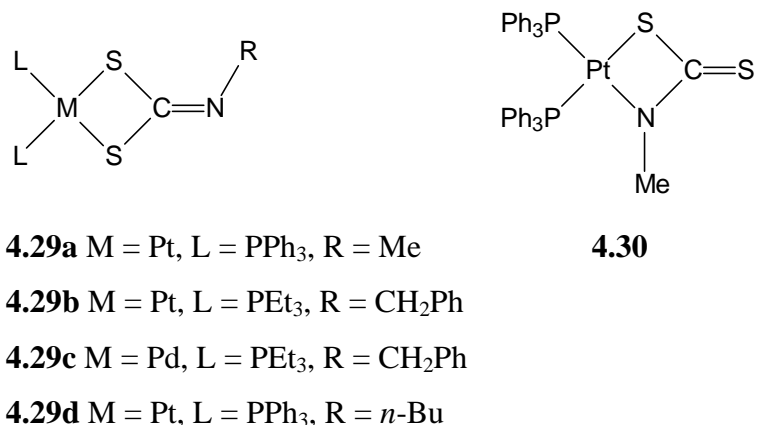
4.2.4.2.3 Electropray mass spectrometry

The ESMS spectrum of **4.28** at a cone voltage of 20 V shows a very strong peak at m/z 945 attributable to the parent ion $[M + H]^+$. A number of other signals were also observed. At m/z 1434 a signal assigned as $[3M + 2NH_4]^{2+}$ is seen, its dicationic nature confirmed by a higher resolution acquisition showing an isotope peak spacing of 0.5 mass units. Loss of phenyl isocyanate was also observed, even at low cone voltages, with a peak at m/z 825. Loss of carbon disulfide was detected only at higher voltages (50 V), and only as additional fragmentation of the $[M + H - PhNCO]^+$ ion, to give m/z 751 assigned as $[M + H - PhNCO - CS_2]^+$, with $[M + H - CS_2]^+$ not observed. This result is consistent with the high relative stability of the Pt-S bond.

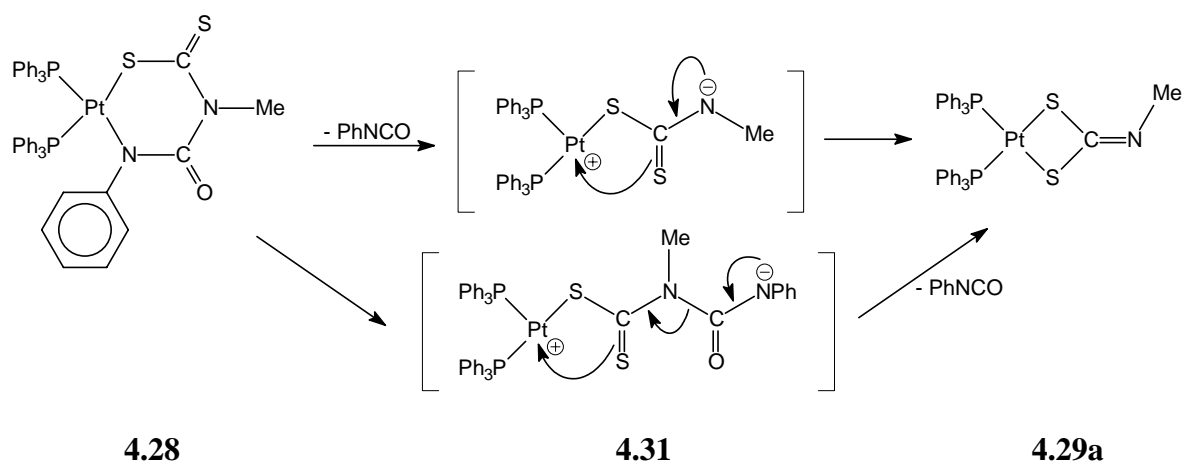
4.2.5 Decomposition of complex **4.28**

When dichloromethane or chloroform solutions of **4.28** were left overnight, ³¹P NMR spectra showed the complex was slowly decomposing to a second compound. Complete decomposition was effected after a week, during which time the solution became noticeably paler. Crystallisation of the yellow residue from chloroform gave colourless crystals, and an X-ray crystallographic study revealed the compound to be the bidentate dithiocarbamate complex **4.29a** (Figure 4.15). Although **4.29a** has not been reported previously, a range of complexes of this type have been prepared by reaction of *cis*-[PtCl₂L₂] (L = PPh₃, PEt₃) with primary amines RNH₂ [R = Ph, CH₂Ph, *n*-Bu, Bu^t, *c*-pentyl, CH₂CO₂H, CH₂CO₂Et, CH₂CH₂OH, CH(Me)CO₂Et] and carbon disulfide in dichloromethane to give [Pt{S₂C=NR}L₂].³³ Not surprisingly, **4.29a** could be readily prepared in high yield by this method from the reaction of *cis*-[PtCl₂(PPh₃)₂], methylamine and carbon disulfide.

Starting from **4.28**, the compound **4.29a** could arise either by loss of phenyl isocyanate to initially give intermediate **4.30** (Figure 4.15) (analogous to the loss of phenyl isocyanate seen for the biureto systems both synthetically and in ES mass spectra), which could then rearrange to **4.29a** because of the relatively high lability of the Pt-NMe bond and the affinity of platinum(II) for the softer sulfur atom.

*Figure 4.15*

However, more likely, the loss of phenyl isocyanate or simple ring opening of **4.28**, could give either of the intermediate species **4.31** which, by a one-step process, could rearrange to give **4.29a** (Scheme 4.1). In any case, the reaction by-product, phenyl isocyanate, was unsurprisingly converted to diphenylurea by adventitious water, and characterised by ¹H and ¹³C NMR of the crude residue. It was not isolated.

*Scheme 4.1*

4.2.5.1 X-ray structure of [Pt{S₂C=NMe}(PPh₃)₂] **4.29a**

ORTEP perspective and side views of the structure are shown in Figures 4.16 and 4.17, together with the atom numbering scheme. Selected bond lengths and angles are presented in Table 4.4, with tables of complete bond lengths and angles, final positional parameters, thermal parameters and calculated H-atom positions presented in Appendix VIII.

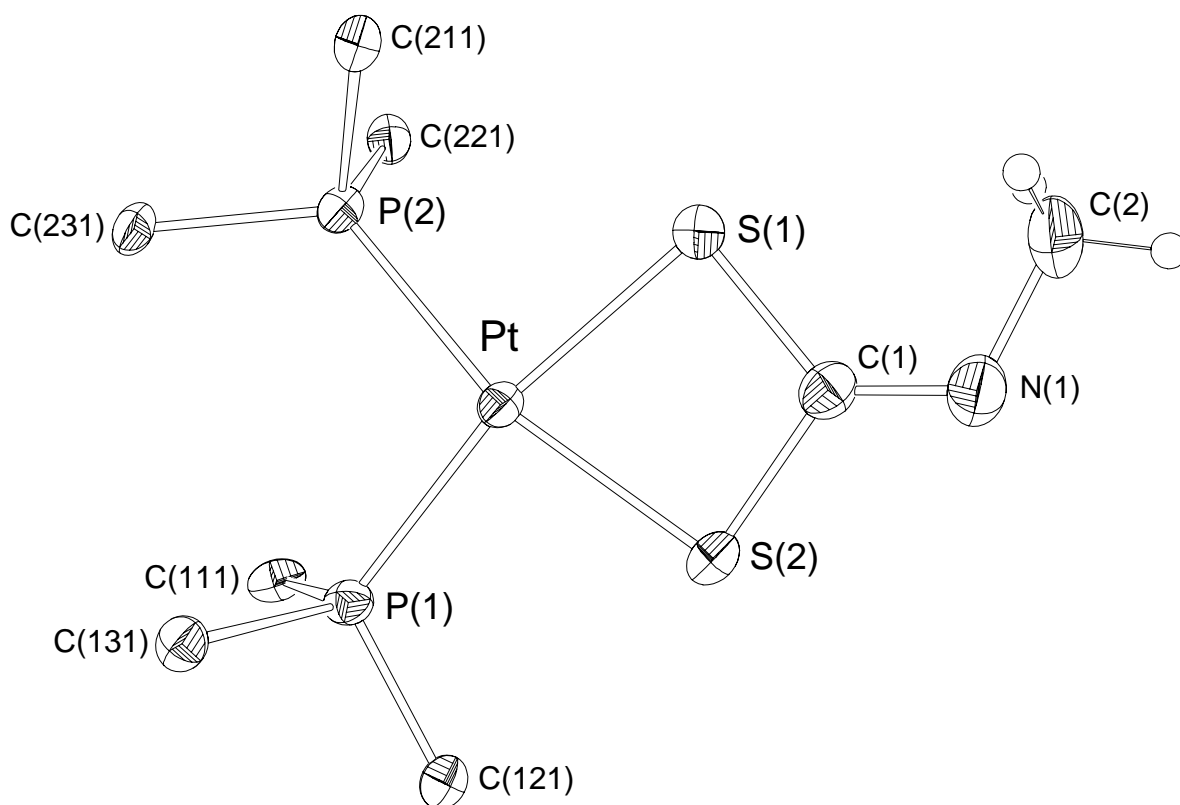


Figure 4.16: Perspective view of the structure of $[\text{Pt}\{\text{S}_2\text{C}=\text{NMe}\}(\text{PPh}_3)_2]$ **4.29a**, showing the atom numbering scheme. For clarity, only the P-bonded carbon atoms of the triphenylphosphine aromatic rings are shown. Atoms are shown as thermal ellipsoids at the 50% probability level

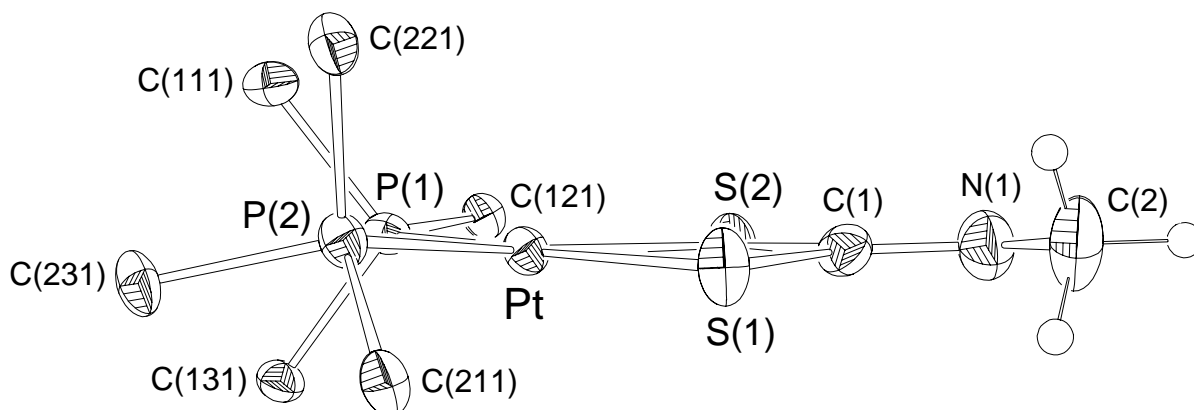


Figure 4.17: Side view of the structure of $[\text{Pt}\{\text{S}_2\text{C}=\text{NMe}\}(\text{PPh}_3)_2]$ **4.29a**, showing the atom numbering scheme. For clarity, only the P-bonded carbon atoms of the triphenylphosphine aromatic rings are shown. Atoms are shown as thermal ellipsoids at the 50% probability level.

Table 4.4: Selected bond lengths (Å) and bond angles (°) (estimated standard deviations in parentheses) for **4.29a**.

Bond	Length	Bonds	Angle
Pt-P(1)	2.280(2)	P(1)-Pt-P(2)	100.59(6)
Pt-P(2)	2.298(2)	S(1)-Pt-S(2)	75.46(6)
Pt-S(1)	2.342(2)	P(2)-Pt-S(1)	90.55(6)
Pt-S(2)	2.321(2)	P(1)-Pt-S(2)	93.34(3)
Pt...C(1)	2.902(2)	Pt-S(1)-C(1)	88.7(2)
		Pt-S(2)-C(1)	89.2(2)
N-Methyl dithiocarbamate ligand			
S(1)-C(1)	1.775(7)	S(1)-C(1)-S(2)	106.6(4)
S(2)-C(1)	1.783(7)	S(1)-C(1)-N(1)	129.0(6)
C(1)-N(1)	1.285(9)	S(2)-C(1)-N(1)	124.4(6)
N(1)-C(2)	1.483(11)	C(1)-N(1)-C(2)	116.9(7)

The structure is analogous to those previously reported for the platinum and palladium complexes [Pt{S₂C=NCH₂Ph}(PEt₃)₂] **4.29b** and [Pd{S₂C=NCH₂Ph}(PEt₃)₂] **4.29c**.³³

Because of the restricted rotation about the C=N double bond, the molecule is asymmetrical, giving rise to non-equivalent Pt-P bond lengths. Pt-P(2) (phosphorus *cis* to Me) is slightly longer than Pt-P(1), although the difference [0.018(2) Å] is only small, since the locale of the asymmetry is quite removed from the metal centre. This is also witnessed in ³¹P NMR, which shows very similar chemical shifts and ³¹P-¹⁹⁵Pt coupling constants for the two phosphorus atoms (Section 4.2.5.2.1). Similarly, the Pt-S bond lengths are not equal, with Pt-S(1) [2.342(2) Å] longer than Pt-S(2) [2.321(2) Å].

As seen in Figure 4.17, the molecule (excluding the phenyl rings) is essentially planar, and least-squares analysis reveals the P(1), P(2), Pt, S(1) and S(2) plane to have maximum deviations of 0.046(1) Å [P(2)] above, and 0.051(1) Å [S(2)] below the plane. For the plane drawn through the metallacycle and ligand [Pt, S(1), S(2), C(1), N(1) and C(2)] the largest deviations are 0.056(2) Å for Pt, and 0.060(3) Å for S(1). Since the metallacycle is four-membered, the S(1)-Pt-S(2) angle is only 75.46(6)°. However, the two co-ordinating sulfur atoms, being larger, are somewhat more accommodating than the nitrogen atoms in the ureylene complex **2.22d**, which has a N-Pt-N angle of 64.7(3)°.

A comparison of the structure of **4.29a** with that of the previously reported structure of **4.29b**,³³ reveals them, as expected, to be very similar. The respective Pt-S, C=N and N-C bond lengths and P-Pt-P, S-Pt-S, S-C-S and Pt-S-C bond angles are essentially identical. However, the structure of **4.29a** is very accurate (*R* factor 0.024) and allows, tentatively at least, determination of the relative *trans*-influences of the two inequivalent sulfur atoms. Using bond length criteria [Pt-P(1) is 2.280(2) Å and Pt-P(2) is 2.298(2) Å], the sulfur [S(2)] *trans* to the methyl group has the higher *trans*-influence, thus lengthening the Pt-P bond. This is consistent with the notion of Pt-S(2) being shorter than Pt-S(1) since S(1), being in a less sterically crowded position, can make a closer approach to the metal centre, thus acting as a slightly higher *trans*-influence ligand.

4.2.5.2 Spectroscopic and mass spectrometric characterisation

4.2.5.2.1 NMR spectroscopy

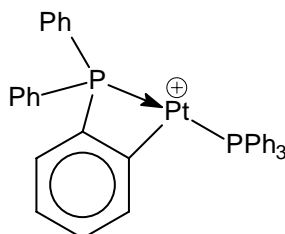
The ³¹P NMR shows the expected AB pattern fully consistent with two phosphorus atoms occupying very similar chemical environments, both *trans* to sulfur. On the basis of the *trans*-influences suggested crystallographically, the resonances at 19.6 [¹J (¹⁹⁵Pt-³¹P) 3107 Hz] and 18.8 ppm [¹J (¹⁹⁵Pt-³¹P) 3086 Hz] tentatively correspond to phosphorus atoms *trans* to S(1) and S(2) respectively (numbering scheme of X-ray structure). These chemical shifts and the ¹J (¹⁹⁵Pt-³¹P) coupling are very similar to those reported for the most closely related complex [Pt{S₂C=N(*n*-Bu)}(PPh₃)₂] **4.29d**, which shows resonances at 20.9 [¹J (¹⁹⁵Pt-³¹P) 3133 Hz] and 19.4 ppm [¹J (¹⁹⁵Pt-³¹P) 3103 Hz].

The central C=N carbon resonates at 171.5 ppm, significantly lower than in the S₂CN carbon in **4.28** with a chemical shift of 205.1 ppm, in the absence of the highly electronegative thiocarbonyl group. The value compares with 176.2 ppm recorded for complex **4.29d**.

4.2.5.2.2 Electrospray mass spectrometry

The ESMS spectrum of **4.29a** is completely consistent with that expected for [Pt{S₂C=NMe}(PPh₃)₂]. At low cone voltages the parent ion [M + H]⁺ at *m/z* 826 is the only observed species. Significant fragmentation was not detected until a moderately high cone voltage of 80 V was used, when loss of triphenylphosphine was observed. This is not a typical fragmentation pathway for triphenylphosphine platinum derivatives, with (non-triphenylphosphine) ligand loss and subsequent cyclometallation to give **4.32** (Figure 4.18)

(as seen for the acetylide complex **4.20**) more usual. This result suggests a high stability for the dithiocarbamate platinum ring system in **4.29a**. More extensive fragmentation could only be induced with very high voltages (>120 V).

**4.32***Figure 4.18*

4.2.6 Conclusions

The platinum(II) ureylene complexes investigated appear to be quite reactive compounds, readily inserting phenyl isocyanate, DMAD and carbon disulfide. The Pt-NMe linkage displays much higher reactivity than Pt-NPh in the unsymmetrical ureylene systems **2.22b** and **2.22g**, with insertion taking place exclusively in the Pt-NMe bond. In electrospray spectra of all the successful insertions, loss of phenyl isocyanate was the major decomposition pathway, and this was also observed synthetically in the decomposition of **4.15a**, **4.15b** and **4.28**.

4.3 Experimental

General experimental procedures and the instrumentation used are described in Appendices I and II. The precursors $[\text{Pt}\{\overline{\text{PhNC(O)NPh}}\}(\text{COD})]$ **2.22a**, $[\text{Pt}\{\overline{\text{PhNC(O)NMe}}\}(\text{COD})]$ **2.22b** and $[\text{Pt}\{\overline{\text{PhNC(O)NMe}}\}(\text{PPh}_3)_2]$ **2.22g** (Chapter Two, Section 2.3.3), $[\text{Pt}\{\overline{\text{PhNC(=NPh)NPh}}\}(\text{COD})]$ **3.17a** (Chapter Three, Section 3.3.2) and *cis*- $[\text{PtCl}_2(\text{PPh}_3)_2]$ (Appendix I) were prepared as described. ESMS spectra were recorded in MeCN/H₂O solvent. Unless otherwise stated, all ¹H, ¹³C and ³¹P NMR spectra were recorded at 300.13, 75.47 and 121.49 MHz respectively, in CDCl₃. ¹H and ¹³C spectra were unambiguously assigned by a combination of 1D NOE and 2D ¹H-¹³C COSY (short-range) and BIRDTRAP (long-range) experiments. Additional inverse 2D experiments (HMQC, HMBC, NOESY and HOHAHA) were recorded on a Bruker DRX 400 spectrometer at 400.13 MHz and 100.61 MHz for the proton and carbon channels. The experiments are discussed in more detail in Appendix II.

Dimethyl acetylenedicarboxylate (Aldrich), methyl propiolate (Aldrich), diphenylacetylene (Aldrich), phenyl isocyanate (BDH), sulfur dioxide (BDH), methyl amine (33% w/w in ethanol) (BDH) and carbon disulfide (May and Baker) were obtained from commercial sources, and used as received. N-thionylaniline (N-sulfinylaniline)³⁴ and diphenyl carbodiimide³⁵ were prepared by literature methods, distilled, and their purity checked by NMR.

Reaction of 2.22a with phenyl isocyanate

To a dichloromethane (20 ml) solution of **2.22a** (0.050 g, 0.097 mmol) was added phenyl isocyanate (5 drops, excess) and the mixture refluxed for 2 hours, during which time it became markedly paler. Evaporation of the dichloromethane and recrystallisation of the residue (by vapour diffusion of diethyl ether into a chloroform solution) gave **4.15a** as colourless crystals (0.055 g, 90%).

m.p. 140°C (decomposes without melting).

Found: C, 47.0; H, 3.7; N, 5.6%; $C_{28}H_{27}N_3O_2Pt \cdot CHCl_3$ requires: C, 46.4; H, 3.8; N, 5.6%.

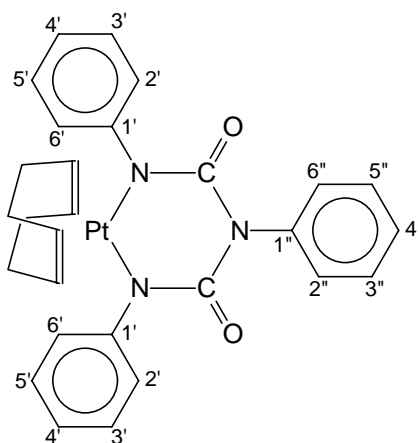
IR: ν (CO region) 1642 (vs), 1610 (s), 1588 (m) cm^{-1} .

ESMS: (Cone voltage = 20V) m/z 1288 ($[2MNa]^+$, 32%), 1169 ($[2MNa - PhNCO]^+$, 9%), 971 ($[3MNa + H]^{2+}$, 23%), 868 ($[4MNa + 2H]^{3+}$, 14%), 696 ($[MNa + MeCN]^+$, 23%), 655 ($[MNa]^+$, 100%), 634 ($[MH]^+$, 23%), 536 ($[MNa - PhNCO]^+$, 10%), 354 ($[PhNHC(O)NPhC(O)NPh + Na]^+$, 16%). (Cone voltage = 50V) m/z 1288 ($[2MNa]^+$, 30%), 1169 ($[2MNa - PhNCO]^+$, 33%), 1050 ($[2MNa - 2PhNCO]^+$, 56%), 971 ($[3MNa + H]^{2+}$, 5%), 868 ($[4MNa + 2H]^{3+}$, 29%), 634 ($[MH]^+$, 3%), 577 ($[MNa - PhNCO + MeCN]^+$, 27%), 536 ($[MNa - PhNCO]^+$, 100%), 514 ($[MH - PhNCO]^+$, 11%). (Cone voltage = 80V) m/z 1050 ($[2MNa - 2PhNCO]^+$, 10%), 536 ($[MNa - PhNCO]^+$, 100%), 354 ($[PhNHC(O)NPhC(O)NPh + Na]^+$, 6%).

1H NMR: δ 7.35-7.30 (12H, *m*, H-2',6',3',5',2'',6'',3'',5''), 6.74 (1H, *t*, $^3J_{4'',3''} = 6.74$ Hz, H-4''), 7.13 (2H, *t*, $^3J_{4',3'} = 6.81$ Hz, H-4'), 4.61 (4H, (*s*, *br*), (*d*, *br*, $^2J_{H,Pt} = 53.15$ Hz), $\underline{CH=CH}$), 2.50 (4H, *m*, *br*, $\underline{CH_2-CH}$), 2.12 (4H, *m*, *br*, $\underline{CH_2-CH}$).

^{13}C NMR: δ 155.9 (*s*, $\underline{C=O}$), 147.3 (*s*, C-1'), 140.9 (*s*, C-1''), 130.0 (*d*, C-2''), 129.3 (*d*, C-2',6'), 128.4 (*d*, C-3',5'), 128.1 (*d*, C-3''), 126.7 (*d*, C-4''), 125.7 (*d*, C-4'), 100.3 (*d*, (*d*, $^1J_{C,Pt} = 145.2$ Hz), $\underline{CH=CH}$), 29.6 (*t*, $\underline{CH_2-CH}$).

NMR numbering scheme:



Reaction of 3.17 with phenyl isocyanate

To a dichloromethane (20 ml) solution of the triphenylguanidine dianion complex **3.17** (0.025 g, 0.042 mmol) was added phenyl isocyanate (5 drops, excess) and the mixture refluxed for 2 hours. During this time the solution became noticeably paler. The solvent was removed under reduced pressure, and the residue crystallised by vapour diffusion of diethyl ether into a dichloromethane solution, to give colourless crystals, characterised as **4.15a** (0.024 g, 89%) by identical NMR and ESMS spectra.

Reaction of 2.22b with phenyl isocyanate

To a dichloromethane solution of **2.22b** (0.032 g, 0.071 mmol) was added phenyl isocyanate (4 drops, excess), and stirred for two minutes. The solution became almost immediately paler upon addition of the isocyanate. Evaporation of the solvent and crystallisation of the residue by vapour diffusion of diethyl ether into a dichloromethane solution containing two drops of phenyl isocyanate, gave **4.15b** as almost colourless crystals (0.033 g, 82%). Slow deinsertion of phenyl isocyanate to regenerate **2.22b** was observed on standing solutions of **4.15b**, in the absence of free isocyanate.

Alternatively, to dichloromethane (50 ml) was added successively [PtCl₂(COD)] (0.102 g, 0.273 mmol), N-methyl-N'-phenylurea (0.042 g, 0.280 mmol), silver(I) oxide (0.12 g, excess) and phenyl isocyanate (10 drops excess) and the mixture refluxed, with a drying tube fitted to the condenser, for 18 hours. The silver salts were filtered off, and the solvent removed from the supernatant under reduced pressure. To the oily orange residue was added ether, to give a brown powder, revealed by NMR spectrometry to be a mixture of **4.15a** and **4.15b**, in a 1:6

ratio respectively. Pure **4.15b** could be readily achieved by the recrystallisation process detailed above (0.113 g, 74%).

m.p. 167-168°C.

Found: C, 45.8; H, 4.2; N, 6.4%; $C_{23}H_{25}N_3O_2Pt \cdot \frac{1}{2}CH_2Cl_2$ requires: C, 46.1; H, 4.3; N, 6.9%.

IR: ν (CO region) 1641 (vs), 1632 (vs), 1611 (s), 1600 (s), 1584 (s) cm^{-1} .

ESMS: (Cone voltage = 20V) m/z 633 ($[MNa + MeCN]^+$, 8%), 588 ($[MNH_4]^+$, 5%), 571 ($[MH]^+$, 100%). (Cone voltage = 50V) m/z 633 ($[MNa + MeCN]^+$, 3%), 571 ($[MH]^+$, 91%), 514 ($[MNa - PhNCO + MeCN]^+$, 10%), 473 ($[MNa - PhNCO]^+$, 14%), 452 ($[MH - PhNCO]^+$, 100%).

1H NMR: δ 7.34 (4H, *t*, $^3J_{3',2'/4'}$ = 7.55 Hz, H-3',5'), 7.27 (4H, *d*, $^3J_{2',3'}$ = 8.92 Hz, H-2',6'), 7.15 (2H, *t*, $^3J_{4',3'}$ = 7.08 Hz, H-4'), 5.29 (1H, *s*, $\underline{CH_2}Cl_2$ of crystallisation), 4.53 (4H, (*s*, *br*), (*d*, *br*, $^2J_{H,Pt}$ = 56.13 Hz), $\underline{CH=CH}$), 3.14 (3H, *s*, $\underline{CH_3}$), 2.48 (4H, *m*, *br*, $\underline{CH_2-CH}$), 2.10 (4H, *m*, *br*, $\underline{CH_2-CH}$).

^{13}C NMR: δ 156.4 (*s*, $\underline{C=O}$), 147.7 (*s*, C-1'), 129.2 (*d*, C-3',5'), 128.5 (*d*, C-2',6'), 125.7 (*d*, C-4'), 99.9 (*d*, (*d*, $^1J_{C,Pt}$ = 143.1 Hz), $\underline{CH=CH}$), 32.6 (*q*, $\underline{CH_3}$), 29.5 (*t*, $\underline{CH_2-CH}$).

Reaction of 4.15b with HCl

The complex **4.15b** (0.025 g, 0.044 mmol) was dissolved in dichloromethane (5 ml) and three drops of concentrated hydrochloric acid added. The solution immediately became paler. After 5 minutes of stirring, the volatiles were removed under vacuum. The residue was dissolved in the minimum quantity of dichloromethane, and excess diethyl ether was added. The white precipitate, characterised spectroscopically as $[PtCl_2(COD)]$ (0.014 g, 88%), was removed by filtration. The solvent was removed from the supernatant to give a colourless residue. This was recrystallised from chloroform and pentane to give large colourless blocks of N,N"-diphenyl-N'-methylbiuret (0.009 g, 76%).

m.p. 54-55°C.

Found: C, 66.6; H, 5.5; N, 15.7%; $C_{15}H_{15}N_3O_2$ requires: C, 66.9; H, 5.6; N, 15.6%.

ESMS: (Cone voltage = 20V) m/z 561 ($[2MNa]^+$, 50%), 556 ($[2MNH_4]^+$, 35%), 333 ($[MNa + MeCN]^+$, 11%), 292 ($[MNa]^+$, 12%), 287 ($[MNH_4]^+$, 39%), 270 ($[MH]^+$, 100%). (Cone voltage = 50V) m/z 561 ($[2MNa]^+$, 50%), 424 (unidentified, 11%), 333 ($[MNa + MeCN]^+$, 26%), 292 ($[MNa]^+$, 56%), 270 ($[MH]^+$, 100%), 151 ($[MH - PhNCO]^+$, 60%).

^1H NMR: δ 9.20 (2H, s, NH), 7.46 (4H, d, $^3J_{2',3'} = 7.94$ Hz, H-2',6'), 7.34 (4H, t, $^3J_{3',2'/4'} = 7.74$ Hz, H-3',5'), 7.13 (2H, t, $^3J_{4',3'} = 7.30$ Hz, H-4'), 3.46 (3H, s, NCH₃).

^{13}C NMR: (75.47 MHz) (CDCl₃) δ 154.2 (s, NC=O), 137.5 (s, C-1'), 129.1 (d, C-3',5'), 124.6 (d, C-2',6'), 121.3 (d, C-4'), 30.6 (q, NCH₃).

Reaction of 2.22b with diphenylcarbodiimide

To a dichloromethane (20 ml) solution of **2.22b** (0.025 g, 0.055 mmol) was added N,N'-diphenylcarbodiimide (0.2 ml, excess) and the mixture refluxed for 15 hours. During this time the solution became darker in colour. Evaporation of the solvent gave an orange residue. This was dissolved in a small amount of dichloromethane and a 1:1 mixture of diethyl ether and pentane added. Filtration of the resulting precipitate yielded a beige powder which upon recrystallisation from dichloromethane and diethyl ether gave almost colourless crystals, characterised as **4.15b** (0.018 g, 57%) by identical NMR and ESMS spectra.

Reaction of 2.22a with DMAD

To a dichloromethane (20 ml) solution of **2.22b** (0.025 g, 0.055 mmol) was added DMAD (0.058 g, 50 μl , excess) and the resulting mixture refluxed for 24 hours. During this time no colour change was noted. Subsequent evaporation of the solvent and examination of the ^1H and ^{13}C NMR of the residue, showed no reaction had taken place.

Reaction of 2.22b with DMAD

To a dichloromethane (20 ml) solution of **2.22b** (0.030 g, 0.066 mmol) was added DMAD (0.058 g, 50 μl , excess) and the resulting mixture refluxed for 2 hours. During this time the solution became noticeably paler. Evaporation of the solvent and crystallisation of the residue by vapour diffusion of diethyl ether into a dichloromethane solution gave **4.19** as pale yellow plates (0.032 g, 81%).

m.p. 200-204°C.

Found: C, 44.2; H, 4.6; N, 4.6%. C₂₃H₂₅N₃O₂Pt requires: C, 44.5; H, 4.4; N, 4.7%.

IR: ν (CO region) 1722 (s), 1698 (m), 1691 (s), 1616 (vs), 1584 (m) cm⁻¹.

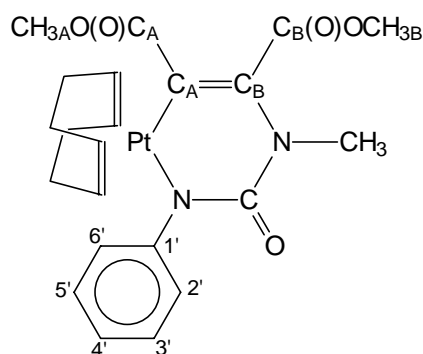
ESMS: (Cone voltage = 20V) m/z 616 ([MNa]⁺, 10%), 594 ([MH]⁺, 100%). (Cone voltage = 50V) m/z 616 ([MNa]⁺, 8%), 594 ([MH]⁺, 100%), 475 ([MH - PhNCO]⁺, 28%). (Cone

voltage = 80V) m/z 616 ($[\text{MNa}]^+$, 8%), 594 ($[\text{MH}]^+$, 40%), 475 ($[\text{MH} - \text{PhNCO}]^+$, 38%), 443 ($[\text{M} - \text{PhNCO} - \text{MeO}]^+$, 100%), 415 ($[\text{M} - \text{PhNCO} - \text{MeOC(O)}]^+$, 95%).

^1H NMR: δ 7.28 (2H, t , $^3J_{3',2'/4'} = 7.44$ Hz, H-3',5'), 7.21 (2H, d , $^3J_{2',3'} = 7.38$ Hz, H-2',6'), 7.07 (1H, t , $^3J_{4',3'} = 7.04$ Hz, H-4'), 5.06 (2H, (t , $^3J_{\text{H,H}} = 2.74$ Hz), (d , br , $^2J_{\text{H,Pt}} = 58.3$ Hz), $\text{CH}=\text{CH}$ *trans* N), 4.77 (2H, (t , $^3J_{\text{H,H}} = 2.71$ Hz), (d , br , $^2J_{\text{H,Pt}} = 36.2$ Hz), $\text{CH}=\text{CH}$ *trans* C), 3.78 (3H, s , $\text{CH}_{3\text{B}}$), 3.67 (3H, s , $\text{CH}_{3\text{A}}$), 3.09 (3H, s , NCH_3), 2.55-2.11 (8H, m , $\text{CH}_2\text{-CH}$).

^{13}C NMR: δ 172.9 (s , $\text{C}_\text{A}=\text{O}$), 165.1 (s , $\text{C}_\text{B}=\text{O}$), 154.3 (s , $\text{NC}=\text{O}$), 149.9 (s , C-1'), 138.7 (s , $\text{PtC}=\text{C}_\text{B}$), 129.3 (d , C-3',5'), 127.9 (d , C-2',6'), 125.3 (d , C-4'), 114.5 (s , (d , $^1J_{\text{C,Pt}} = 982.0$ Hz), $\text{PtC}=\text{C}_\text{A}$), 112.6 (d , (d , $^1J_{\text{C,Pt}} = 67.2$ Hz), $\text{CH}=\text{CH}$ *trans* C), 90.4 (d , (d , $^1J_{\text{C,Pt}} = 155.8$ Hz), $\text{CH}=\text{CH}$ *trans* N), 52.4 (q , $\text{CH}_{3\text{B}}$), 52.0 (q , $\text{CH}_{3\text{A}}$), 36.3 (q , NCH_3), 31.4 (t , $\text{CH}_2\text{-CH}$ *trans* N), 27.8 (t , $\text{CH}_2\text{-CH}$ *trans* C).

NMR numbering scheme:



Reaction of 2.22b with diphenylacetylene

To a dichloromethane (20 ml) solution of **2.22b** (0.025 g, 0.055 mmol) was added diphenylacetylene (0.010 g, 0.056 mmol) and the resulting mixture refluxed for 48 hours. During this no colour change was noted. Evaporation of the solvent and examination of the ^1H and ^{13}C NMR of the residue, showed no reaction had taken place.

Reaction of 2.22g with methyl propiolate

Methyl propiolate (5 drops, excess) was added to a dichloromethane solution of **2.22g** (0.035 g, 0.040 mmol) and refluxed for 2 hours. During this time the solution became almost colourless. Removal of the solvent, and crystallisation of the residue from dichloromethane and diethyl ether gave **4.20** as large colourless blocks.

m.p. 235-238°C (melts with decomposition).

Found: C, 60.0 ; H, 3.9; N, 0%; C₂₃H₂₅N₃O₂Pt requires: C, 59.7; H, 4.1%.

IR: ν (C≡C region) 2116 (vs) cm⁻¹. ν (CO region) 1687 (vs) cm⁻¹.

ESMS: (Cone voltage = 20V) m/z 1789 ([2MNH₄]⁺, 75%), 904 ([MNH₄]⁺, 100%), 886 ([MH]⁺, 33%). (Cone voltage = 50V) m/z 1789 ([2MNH₄]⁺, 33%), 908 ([MNa]⁺, 29%), 886 ([MH]⁺, 100%). (Cone voltage = 80V) m/z 1789 ([2MNH₄]⁺, 10%), 908 ([MNa]⁺, 32%), 886 ([MH]⁺, 100%), 802 (Unidentified, 12%), 759 ([Pt{C₆H₄PPh₂}(PPh₃) + MeCN]⁺, 22%), 718 ([Pt{C₆H₄PPh₂}(PPh₃)]⁺, 22%).

³¹P NMR: δ 18.1 (*s*, (*d*, ¹J_{P,Pt} = 2535.6 Hz), PPh₃ *trans* P). *Initial cis isomer (see main text)*: δ 15.7 (*s*, (*d*, ¹J_{P,Pt} = 2364.6 Hz), PPh₃ *trans* C).

¹H NMR: δ 7.72-7.65 (12H, *m*, PPh₃), 7.43-7.35 (18H, *m*, PPh₃), 2.45 (6H, *s*, CH₃).

¹³C NMR: δ 154.2 (*s*, C=O), 134.8 (*d*, (*t*, ³J_{C,P} = 12.15 Hz), C-3,5 PPh₃), 130.8 (*d*, C-4 PPh₃), 134.5 (*d*, (*t*, ³J_{C,P} = 10.88 Hz), C-3,5 PPh₃), 129.9 (*s*, (*t*, ¹J_{C,P} = 59.85 Hz), C-1 PPh₃), 116.0 (*s*, (*t*, ²J_{C,P} = 29.2 Hz), (*d*, ¹J_{C,Pt} = 988.6 Hz), Pt-C≡C), 104.6 (*s*, (*d*, ²J_{C,Pt} = 259.4 Hz), Pt-C≡C), 51.2 (*q*, CH₃).

Reaction of 2.22g with N-thionylaniline

To a dichloromethane (25 ml) solution of **2.22g** (0.050 g, 0.058 mmol) was added N-thionylaniline (0.0087 g, 7.0 μ l, 0.062 mmol) and refluxed for 2 hours. During this time a noticeable colour change from bright to pale yellow was observed. The dichloromethane was removed under reduced pressure, and the residue dissolved in chloroform. This was slowly evaporated from a tube to give large colourless crystals of **4.23** (0.028 g, 51%).

m.p. 202-206°C.

Found: C, 56.1; H, 4.5; N, 3.8%; C₈₈H₈₀N₄O₈P₄Pt₂ requires: C, 55.6; H, 4.3; N, 3.0%.

IR: ν (NH region) 3082 (w), 3056 (m). ν (CO region) 1693 (m), 1677 (w), 1609 (w), 1697 (w), 1554 (s), 1500 (s) cm⁻¹. ν (SO₃ region) 1177 (br, w), 1096 (s), 1063 (vs), 999 (w), 923 (br, vs) cm⁻¹. ³¹P NMR: δ 21.3 (*d*, ²J_{P,P} = 18.7 Hz, (*d*, ¹J_{P,Pt} = 2458.9 Hz), PPh₃ *trans* S(O)₂-O), 10.5 (*d*, ²J_{P,P} = 19.0 Hz, (*d*, ¹J_{P,Pt} = 4330.6 Hz), PPh₃ *trans* O-S(O)₂).

¹H NMR: δ 7.50-7.43 (24H, *m*, PPh₃), 7.37 (2H, *s*, br, PhNH), 7.19 (4H, *t*, ³J_{3',2'/4'} = 7.39 Hz, H-3',5'), 7.09 (4H, *d*, ³J_{2',3'} = 6.93 Hz, H-2',6'), 7.04-6.95 (36H, *m*, PPh₃), 6.80 (2H, *t*, ³J_{4',3'} = 7.14 Hz, H-4'), 5.59 (2H, *s*, br, MeNH), 2.45 (6H, *d*, ³J_{H,H} = 4.26 Hz, CH₃).

^{13}C NMR: δ 156.7 (s, $\underline{\text{C}}=\text{O}$), 141.2 (s, C-1'), 134.8 (d, (d, $^3\text{J}_{\text{C,P}} = 10.79$ Hz), C-3,5 PPh₃), 134.5 (d, (d, $^3\text{J}_{\text{C,P}} = 11.32$ Hz), C-3,5 PPh₃), 130.6 (s, (d, $^1\text{J}_{\text{C,P}} = 67.09$ Hz), C-1 PPh₃), 130.1 (d, C-4 PPh₃), 130.1 (d, C-4 PPh₃), 128.4 (s, (d, $^1\text{J}_{\text{C,P}}$ not resolved), C-1 PPh₃), 128.14 (d, (d, $^2\text{J}_{\text{C,P}} = 10.41$ Hz), C-2,6 PPh₃), 128.07 (d, C-3',5'), 127.5 (s, (d, $^2\text{J}_{\text{C,P}} = 11.39$ Hz), C-2,6 PPh₃), 120.0 (d, C-4'), 118.2 (d, C-2',6'), 26.2 (q, $\underline{\text{C}}\text{H}_3$).

Reaction of 2.22g with sulfur dioxide

The complex **2.22g** (0.025 g, 0.029 mmol) was placed in a glass ampoule, evacuated and sulfur dioxide (~10 ml), which had previously been degassed by two cycles of freeze-pump-thawing, was condensed inside using standard vacuum line techniques. The ampoule was sealed, and placed in a Carius tube maintained at 55°C for 16 hours. At completion a white precipitate had formed. The sulfur dioxide was frozen, the ampoule opened, and the solvent slowly allowed to evaporate at room temperature. Recrystallisation of the residue from chloroform gave small crystals, characterised as **4.23** above by identical NMR and IR spectra (0.012 g, 44%).

Reaction of 2.22g with carbon disulfide

To a dichloromethane (15 ml) solution of **2.22g** (0.025 g, 0.029 mmol) was added three drops of carbon disulfide, and the resulting mixture was stirred for 3 minutes. The volatiles were removed under reduced pressure to give a yellow oil. Large yellow crystals of **4.28** were grown by liquid-liquid diffusion of ether layered on a saturated chloroform solution of the residue (0.026 g, 96%).

m.p. 129-130°C.

Found: C, 52.1; H, 3.4; N, 2.7%; C₄₅H₃₈N₂OS₂P₂Pt.CHCl₃ requires: C, 52.0; H, 3.7; N, 2.6%.

IR: ν (CO region) 1646 (vs), 1632 (s), 1586 (m) cm⁻¹. ν (C=S region) 1265 (s), 1096 (s), 1069 (s), 749 (m), 727 (s), 693 (vs) cm⁻¹.

ESMS: (Cone voltage = 20V) m/z 1434 ([3M + 2NH₄]²⁺, 12%), 961 ([MNH₄]⁺, 29%), 945 ([MH]⁺, 100%), 825 ([MH - PhNCO]⁺, 34%). (Cone voltage = 50V) m/z 945 ([MH]⁺, 100%), 825 ([MH - PhNCO]⁺, 30%), 751 ([MH - PhNCO - CS₂]⁺, 13%).

^{31}P NMR: δ 18.0 (d, $^2\text{J}_{\text{P,P}} = 24.3$ Hz, (d, $^1\text{J}_{\text{P,Pt}} = 3097.6$ Hz), PPh₃ *trans* S), 5.3 (d, $^2\text{J}_{\text{P,P}} = 24.3$ Hz, (d, $^1\text{J}_{\text{P,Pt}} = 3210.5$ Hz), PPh₃ *trans* N).

^1H NMR: δ 7.39-6.96 (33H, *m*, PPh_3 , C-3',5',4'), 6.81 (2H, *d*, $^3J_{2,3'} = 7.33$ Hz, H-2',6'), 3.66 (3H, *s*, CH_3).

^{13}C NMR: δ 205.1 (*s*, $\text{C}=\text{S}$), 155.0 (*s*, $\text{C}=\text{O}$), 147.8 (*s*, C-1'), 134.6 (*d*, (*d*, $^3J_{\text{C,P}} = 10.04$ Hz), C-3,5 PPh_3), 133.6 (*d*, (*d*, $^3J_{\text{C,P}} = 11.09$ Hz), C-3,5 PPh_3), 131.1 (*d*, C-4 PPh_3), 130.8 (*d*, C-4 PPh_3), 128.9 (*s*, (*d*, $^1J_{\text{C,P}} = 54.41$ Hz), C-1 PPh_3), 128.8 (*s*, (*d*, $^1J_{\text{C,P}}$ not resolved), C-1 PPh_3), 128.4 (*d*, C-3',5'), 128.3 (*d*, (*d*, $^2J_{\text{C,P}} = 10.64$ Hz), C-2,6 PPh_3), 127.5 (*d*, C-2',6'), 124.3 (*d*, C-4'), 40.4 (*q*, CH_3).

Decomposition of 4.28 and preparation of [Pt{S₂C(NMe)}(PPh₃)₂] 4.29a

Dichloromethane and chloroform solutions of **4.28** prepared above were left standing for 1 week in the presence of excess carbon disulfide. During this time, the solutions continually became paler. ^{31}P NMR showed the gradual formation of a new species, which was recrystallised by slow evaporation of a chloroform solution to yield colourless crystals. This was characterised as **4.29a** on the basis of an X-ray crystallographic study (0.021 g, 88% based on 0.025 g of **2.22g**). N,N'-diphenylurea was detected by ^1H and ^{13}C NMR, but was not isolated.

Alternatively, in a preparation analogous to literature procedure,³³ to a dichloromethane solution (20 ml) of *cis*-[PtCl₂(PPh₃)₂] (0.098 g, 0.124 mmol) was added methylamine (0.046 ml, 33% in ethanol, 0.012 g, 0.380 mmol) and the solution stirred for two minutes. Carbon disulfide (0.0095 g, 7.6 μl , 0.125 mmol) was added, and after a few minutes a precipitate of methylamine hydrochloride formed. The mixture was stirred for four hours, filtered, and solvent removed under reduced pressure. The residue was recrystallised from chloroform, to give **4.29a** (0.087 g, 85%), characterised by identical ^{31}P and ^1H NMR spectra to that observed for the previous preparation.

m.p. 220°C (decomposes without melting).

Found: C, 53.8; H, 3.4; N, 1.5%; C₃₈H₃₃NS₂P₂Pt.0.33CHCl₃ requires: C, 53.3; H, 3.9; N, 1.6%.

IR: ν (C=N region) 1583 (vs) cm^{-1} .

ESMS: (Cone voltage = 20V) m/z 826 ([MH]⁺, 100%). (Cone voltage = 50V) m/z 826 ([MH]⁺, 100%), 563 ([MH - PPh₃]⁺, 4%). (Cone voltage = 80V) m/z 826 ([MH]⁺, 100%), 563 ([MH - PPh₃]⁺, 38%). (Cone voltage = 100V) m/z 826 ([MH]⁺, 20%), 563 ([MH - PPh₃]⁺, 100%).

^{31}P NMR: δ 19.6 (*d*, $^2J_{\text{P,P}} = 23.1$ Hz, (*d*, $^1J_{\text{P,Pt}} = 3107.2$ Hz), PPh_3 *trans* S), 18.8 (*d*, $^2J_{\text{P,P}} = 23.2$ Hz, (*d*, $^1J_{\text{P,Pt}} = 3086.2$ Hz), PPh_3 *trans* S).

^1H NMR: δ 7.46-7.11 (30H, *m*, PPh_3), 3.15 (3H, *s*, CH_3).

^{13}C NMR: δ 171.5 (*s*, $\underline{\text{C}}=\text{N}$), 134.5 (*d*, (*d*, $^3J_{\text{C,P}} = 10.79$ Hz), C-3,5 PPh_3), 130.7 (*d*, C-4 PPh_3), 130.8 (*d*, C-4 PPh_3), 130.1 (*s*, (*d*, $^1J_{\text{C,P}} = 54.34$ Hz), C-1 PPh_3), 129.7 (*s*, (*d*, $^1J_{\text{C,P}} = 54.26$), C-1 PPh_3), 128.04 (*d*, (*d*, $^2J_{\text{C,P}} = 10.64$ Hz), C-2,6 PPh_3), 128.01 (*d*, (*d*, $^2J_{\text{C,P}} = 10.26$ Hz), C-2,6 PPh_3), 34.5 (*q*, $\underline{\text{C}}\text{H}_3$).

N,N'-diphenylurea signals: ^1H NMR δ 8.93 (2H, *s*, NH), 7.53 (4H, *d*, $^3J_{2',3'} = 7.96$ Hz, H-2',6'), 6.86 (2H, *t*, $^3J_{4',3'} = 7.01$ Hz, H-4'). ^{13}C NMR δ 153.8 (*s*, C=O), 140.2 (*s*, C-1'), 128.5 (*d*, C-3'), 121.5 (*d*, C-2'), 119.1 (*d*, C-4').

4.3.1 X-ray structure of $[\{\text{Pt}(\text{SO}_3)(\text{PPh}_3)_2\}_2 \cdot 2\text{PhNHC}(\text{O})\text{NHMe}]$ chloroform solvate 4.23

Crystals were grown by the slow evaporation of a chloroform solution of **4.23** in a narrow tube at 4°C.

Data collection

Accurate cell parameters and intensity data were collected on Siemens SMART CCD diffractometer at Auckland University. Details regarding the collection methodology and configuration are described in Appendix II.

Collection Data: crystal size = 0.40 x 0.11 x 0.10 mm, unique reflections = 10569, range = $1.47 < \theta < 28.11^\circ$, absorption correction $T_{\text{max.}, \text{min.}} = 0.67, 0.57$.

Crystal Data: $\text{C}_{36}\text{H}_{28}\text{O}_3\text{P}_2\text{SPt} \cdot \text{C}_8\text{H}_{10}\text{N}_2\text{O} \cdot 2\text{CHCl}_3$, $M_r = 1186.59$, triclinic, space group $P\bar{1}$ (no. 2), $a = 14.0378(2)$, $b = 14.0731(2)$, $c = 14.2127(2)$ Å, $\alpha = 119.487(1)$, $\beta = 94.800(1)$, $\gamma = 93.597(1)^\circ$, $U = 2417.98(6)$ Å³, $D_c = 1.630$ g cm⁻³, $Z = 2$, $F(000) = 1176$, $\mu(\text{Mo-K}\alpha) = 3.387$ mm⁻¹.

Solution and refinement

The structure was solved by the Patterson methods option of SHELXS-96,³⁶ and the platinum position determined. The remaining non-hydrogen atoms were located routinely in subsequent

full-matrix least-squares refinements based on F^2 (SHELXL-96).³⁷ All non-hydrogen atoms were assigned anisotropic temperature factors, and all hydrogen atom positions determined by calculation. The refinement converged with $R_1 = 0.0251$ for 9733 data with $I \geq 2\sigma(I)$, 0.0294 for all data; $wR_2 = 0.0617$ $\{w = 1/[\sigma^2(F_o^2) + (0.0246P)^2 + 4.4280P]$ where $P = (F_o^2 + 2F_c^2)/3\}$, and $GoF = 1.030$. No parameter shifted in the final cycle. The final difference map showed no peaks or troughs of electron density greater than +1.65 and $-1.20 \text{ e } \text{Å}^{-3}$ respectively [adjacent to Cl(3)].

4.3.2 X-ray structure of $[\text{Pt}\{\overline{\text{SC}(\text{S})\text{NMeC}(\text{O})\text{NPh}}\}(\text{PPh}_3)_2]$ chloroform solvate **4.28**

Crystals were grown by liquid-liquid diffusion of ether layered on a dichloromethane solution of **4.28** at 4°C.

Data collection

Accurate cell parameters and intensity data were collected on Siemens Smart CCD diffractometer at Auckland University. Details regarding collection methodology and configuration are described in Appendix II.

Collection Data: crystal size = 0.56 x 0.40 x 0.20 mm, unique reflections = 9725, range = $1.58 < \theta < 28.22^\circ$, absorption correction $T_{\text{max.}, \text{min.}} = 0.61, 0.39$. *Crystal Data:* $\text{C}_{45}\text{H}_{38}\text{N}_2\text{OS}_2\text{P}_2\text{Pt}\cdot\text{CHCl}_3$, $M_r = 1063.29$, monoclinic, space group $\text{P}2_1/c$, $a = 12.7698(2)$, $b = 16.7061(2)$, $c = 20.4585(2) \text{ Å}$, $\beta = 94.620(1)^\circ$, $U = 4350.30(10) \text{ Å}^3$, $D_c = 1.623 \text{ g cm}^{-3}$, $Z = 4$, $F(000) = 2112$, $\mu(\text{Mo-K}\alpha) = 3.617 \text{ mm}^{-1}$.

Solution and refinement

The structure was solved by the Patterson methods option of SHELXS-96,³⁶ and the platinum position determined. The remaining non-hydrogen atoms were located routinely in subsequent refinements (SHELXL-96).³⁷ All non-hydrogen atoms were assigned anisotropic temperature factors, and all hydrogen atom positions determined by calculation. The refinement converged with $R_1 = 0.0322$ for 8327 data with $I \geq 2\sigma(I)$, 0.0418 for all data; $wR_2 = 0.0860$ $\{w = 1/[\sigma^2(F_o^2) + (0.0359P)^2 + 12.3925P]$ where $P = (F_o^2 + 2F_c^2)/3\}$, and $GoF = 1.051$. No parameter shifted in the final cycle. The final difference map showed no peaks or troughs of

electron density greater than +2.27 and $-1.99 \text{ e } \text{\AA}^{-3}$ respectively, both adjacent to the platinum atom.

4.3.3 X-ray structure [Pt{S₂C=NMe}(PPh₃)₂] 4.29a

Crystals of **4.29a** were grown by the slow evaporation of a chloroform solution of **4.29a** at 4°C.

Data collection

Accurate cell parameters and intensity data were collected on Siemens Smart CCD diffractometer at Auckland University. Details regarding collection methodology and configuration are described in Appendix II.

Collection Data: crystal size = 0.30 × 0.11 × 0.08 mm, unique reflections = 6285, range = $1.13 < \theta < 28.22^\circ$, absorption correction $T_{\text{max.}, \text{min.}} = 0.70, 0.51$. *Crystal Data:* C₃₈H₃₃NS₂P₂Pt, $M_r = 824.80$, monoclinic, space group P2₁, $a = 9.8358(1)$, $b = 9.3356(1)$, $c = 18.2494(1) \text{ \AA}$, $\beta = 99.008(1)^\circ$, $U = 1655.05(2) \text{ \AA}^3$, $D_c = 1.655 \text{ g cm}^{-3}$, $Z = 2$, $F(000) = 816$, $\mu(\text{Mo-K}\alpha) = 4.491 \text{ mm}^{-1}$.

Solution and refinement

The structure was solved by the Patterson methods option of SHELXS-96,³⁶ and the platinum position determined. The remaining non-hydrogen atoms were located routinely in subsequent refinements (SHELXL-96).³⁷ All non-hydrogen atoms were assigned anisotropic temperature factors, and all hydrogen atom positions determined by calculation. The refinement converged with $R_1 = 0.0242$ for 5841 data with $I \geq 2\sigma(I)$, 0.0279 for all data; $wR_2 = 0.0821$ $\{w = 1/[\sigma^2(F_o^2) + (0.0300P)^2 + 0.0000P]$ where $P = (F_o^2 + 2F_c^2)/3\}$, and $\text{GoF} = 1.074$. The Flack x parameter refined to a value of 0.016(7), showing the correct polarity of the space group had been chosen. No parameter shifted in the final cycle, and the final difference map showed no peaks or troughs of electron density greater than +0.73 and $-1.25 \text{ e } \text{\AA}^{-3}$ respectively, the latter adjacent to the platinum atom.

References

- 1 H.E. Bryndza and W. Tam, *Chem. Rev.*, 88 (1988) 1163.
- 2 M.F. Lappert, P.P. Power, A.R. Sanger and R.C. Srivastava, *Metal and Metalloid Amides*, Ellis Horwood, Chichester (1980).
- 3 W.C. Trogler and R.L. Cowen, *Organometallics*, 6 (1987) 2451.
- 4 J.M. Boncella and A. Villanueva, *J. Organomet. Chem.*, 465 (1994) 297.
- 5 M. Rahim, C.H. Bushweller and K.J. Ahmed, *Organometallics* 13 (1994) 4952.
- 6 J.F. Hartwig, R.G. Bergman and R.A. Anderson, *J. Am. Chem. Soc.*, 113 (1991) 6499.
- 7 F. Paul, J. Fischer, P. Oschenbein and J.A. Osborn, *Angew. Chem. Int. Ed. Engl.*, 32 (1993) 1638.
- 8 R.D.W. Kemmitt, S. Mason, M.R. Moore, J. Fawcett and D.R. Russell, *J. Chem. Soc., Chem. Commun.*, (1990) 1535.
- 9 H. Hoberg, B.W. Oster, C. Krüger and Y.H. Tsay, *J. Organomet. Chem.*, 252 (1983) 365.
- 10 H-W. Lam, G. Wilkinson, B. Hussain-Bates and M.B. Hursthouse, *J. Chem. Soc., Dalton Trans.*, (1993) 781.
- 11 R. Nast, *Coord. Chem. Rev.*, 47 (1982) 89.
- 12 A. Furlani, S. Licoccia and M.V. Russo, *J. Chem. Soc. Dalton Trans.*, (1984) 2197.
- 13 J.R. Phillips, G.A. Miller and W.C. Trogler, *Acta Cryst.*, C46 (1990) 1648.
- 14 M. Bonamico, G. Dessy, V. Fares, M.V. Russo and L. Scaramuzza, *Cryst. Struct. Commun.*, 6 (1977) 39.
- 15 A. Wojcicki, *Adv. Organomet. Chem.*, 12 (1974) 31.
- 16 G.J. Kubas, *Acc. Chem. Res.*, 27 (1994) 183.
- 17 A.F. Hill, *Adv. Organomet. Chem.*, 36 (1994) 159.
- 18 M. Heberhold and A.F. Hill, *J. Organomet. Chem.*, 395 (1990) 315.
- 19 A.F. Hill, G.R. Clark, C.E.F. Rickard, W.R. Roper and M. Herberhold, *J. Organomet. Chem.*, 401 (1991) 357.
- 20 W.-Y Yeh, C.L. Stern and D.F. Shriver, *Inorg. Chem.* 36 (1997) 4408.
- 21 W.-Y Yeh, C.L. Stern and D.F. Shriver, *Inorg. Chem.* 35 (1996) 7857.
- 22 R. Eskenzai, J. Raskovan and R. Levitus, *J. Inorg. Nucl. Chem.*, 27 (1965) 371.
- 23 V.C. Ginn, P.F. Kelly, C. Papadimitriou, A.M.Z. Slawin, D.J. Williams and J.D. Woollins, *J. Chem. Soc. Dalton Trans.*, (1993) 1805.
- 24 T.G. Appleton, H.C. Clark and L.E. Manzer, *Coord. Chem. Rev.*, 10 (1973) 335.

- 25 For recent examples see J. Habash and R.L. Beddoes, *Acta Cryst. C47* (1991) 1595; H.E. Wages, K.L. Taft and S.J. Lippard, *Inorg. Chem.*, **32** (1993) 4985.
- 26 M.C. Etter, Z. Urbańczyk-Lipkowska, M. Zia-Ebrahimi and T.W. Panunto, *J. Am. Chem. Soc.* **112** (1990) 8415.
- 27 A.D. Burrows, D.M.P. Mingos, A.J.P. White and D.J. Williams, *J. Chem. Soc. Dalton Trans.*, (1996) 149.
- 28 A.D. Burrows, D.M.P. Mingos, A.J.P. White and D.J. Williams, *J. Chem. Soc. Dalton Trans.*, (1996) 3805.
- 29 N.B. Colthup, L.H. Daly and S.E. Wiberley, *Introduction to Infrared and Raman Spectroscopy*, Academic Press, New York, 1964.
- 30 I.S. Butler and A.E. Fenster, *J. Organomet. Chem.*, **66** (1974) 161.
- 31 L.J. McCaffrey, W. Henderson, B.K. Nicholson, J.E. Mackay, and M.B. Dinger, *J. Chem. Soc., Dalton Trans.*, (1997) 2577.
- 32 F.H. Allen, O. Kennard, D.G. Watson, L. Brammer, A.G. Orpen and R. Taylor, *J. Chem. Soc. Perkin Tran. II*, (1987) S1.
- 33 R. Schierl, U. Nagel and W. Beck, *Z. Naturforsch., Teil B*, **39** (1984) 649.
- 34 P. Rajagopalan, B.G. Advani and C.N. Talaty, *Organic Synthesis, Collect. Vol. V*, Wiley, New York, (1973) 504.
- 35 S.R. Sandler and W. Karo, *Organic Functional Group Preparations, Vol. II*, Academic Press, New York, (1971) 205.
- 36 G.M. Sheldrick, SHELXS-96, Program for Solving X-Ray Crystal Structures, University of Göttingen, Germany, (1996).
- 37 G.M. Sheldrick, SHELXL-96, Program for Refining X-Ray Crystal Structures, University of Göttingen, Germany, (1996).

Chapter Five

Syntheses, Characterisation, Insertion Reactions and Biological Activity of Gold(III) Ureylene Complexes

5.1 Introduction

Four-membered ring metallacycles are involved in a wide range of metal-catalysed reactions of organic molecules, and are of fundamental interest for their structures and reactivities. The interest in the field is exemplified by the very large number of platinum(II) metallacycles which have been described over the years (Chapter One). However, the metallacyclic chemistry of gold(III), despite being isoelectronic (d^8) with platinum(II) (although more electronegative and more strongly oxidising), has been left essentially unexplored. Furthermore, of the handful of gold(III) metallacycles that have been reported, the vast majority are dithiolato type complexes, a result of the strong affinity of gold for sulfur. Additionally, recent publications¹⁻³ regarding the biological activity of gold(III) compounds, which often rival those of platinum, have further enhanced gold(III) organometallic complexes as lucrative systems, demanding closer investigation.

The paucity of gold(III) metallacycles led us to examine the possibility of gold forming metallacycles analogous to the numerous platinum(II) examples. There has been some recent interest in cyclometallated gold(III) complexes,^{4,5} and the ready accessibility of the compounds **5.1a**⁶ and **5.1b**⁷ (Figure 5.1) suggested that these could be ideal precursors for the study of organogold(III) metallacycles.

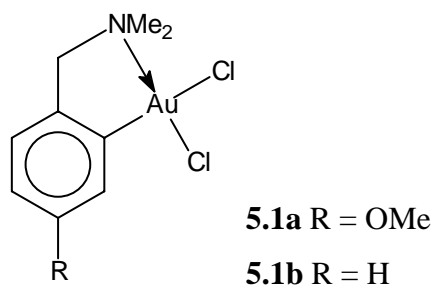
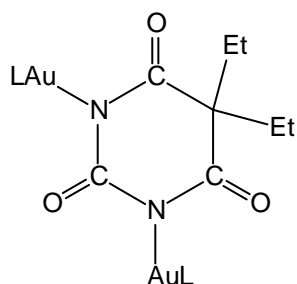
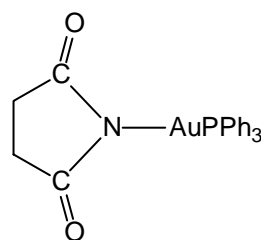


Figure 5.1

Gold amide complexes are relatively sparse in the literature, but gold(I) compounds derived for example from barbituric acid **5.2**,⁸ succinimide **5.3**,⁹ purines **5.4**,¹⁰ and phthalimide **5.5**¹¹ (Figures 5.2 and 5.3) have been reported. Fewer still have been reported for gold(III), despite the ability of amide ligands to stabilise high oxidation states [e.g. copper(III)],^{12,13} but examples derived from the binaphthyl bis-amide to give **5.6**¹⁴ and the peptide glycylglycyl-L-histidine to give **5.7**¹ (Figure 5.4) have been reported.

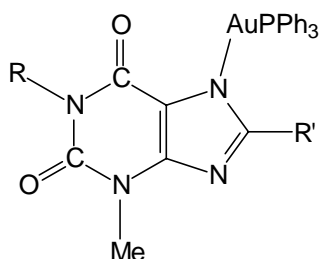


5.2 L = tertiary phosphines

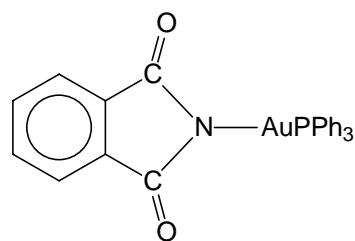


5.3

Figure 5.2

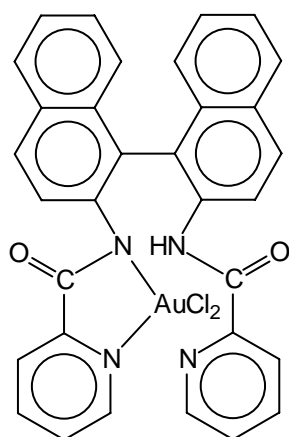


5.4 R = H, Me; R' = H, Et

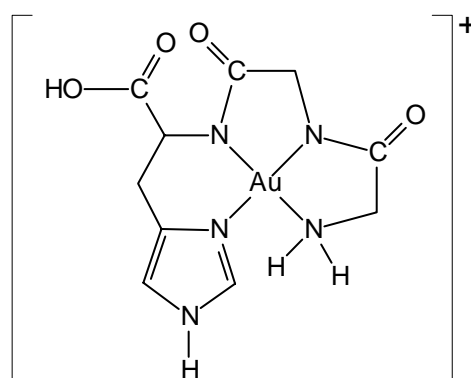


5.5

Figure 5.3



5.6



5.7

Figure 5.4

As demonstrated in Chapter Two, a range of platinum(II) ureylene complexes **2.22** $[\text{Pt}\{\overline{\text{NRC(O)NR}'}\text{L}_2]$ (R = Ph, Ac; R' = Ph, Me, 2-Py, 1-Ad, Ac; L-L = COD, L = PPh₃) can also be synthesised, in good yield, by reaction of platinum(II) chloride complexes with the appropriate parent urea in the presence of silver(I) oxide. Ureylene complexes were also (inadvertently) synthesised by the reaction of $[\text{PtCl}_2(\text{COD})]$ with N,N',N''-triacetylguanidine in the presence of silver(I) oxide, during the studies into the synthesis of guanidine dianion complexes (Chapter Three). The platinum ureylene complexes also display a high reactivity toward various unsaturated molecules (e.g. phenyl isocyanate and dimethyl acetylenedicarboxylate, which readily inserted into the platinum-nitrogen bond (Chapter Four).

This chapter details the silver(I) oxide and sodium hydride mediated syntheses of the first gold ureylene complexes, and their reactivity toward dimethyl acetylenedicarboxylate (DMAD) and phenyl isocyanate. The biological activity of one derivative was also determined.

5.2 Results and Discussion

The silver(I) oxide mediated reactions of **5.1a** with either N,N'-diphenylurea or N,N'-diacetylurea in refluxing dichloromethane for two hours, afforded in good yields the ureylene complexes **5.8a** and **5.8b** (Figure 5.5) respectively. These reactions proceeded markedly faster than for the synthesis of the analogous platinum(II) ureylene complexes ($[\text{Pt}\{\overline{\text{NRC(O)NR}'}\text{COD}]$ **2.22a** [R = Ph] and **2.22h** [R = Ac]), for which a reaction time of 24 hours was typically required for completion. The compound **5.8a** formed bright orange needles, whereas **5.8b** was isolated as cream-coloured blocks. This striking colour difference can be attributed to the conjugation imparted by the phenyl rings of the ureylene ligand present in **5.8a**, and was also noted for the platinum phenylureylene systems **2.22a-2.22d**.

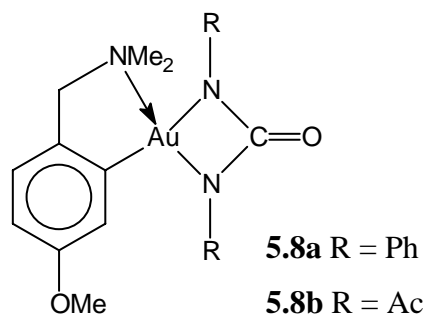


Figure 5.5

As for **2.22a** (Chapter Two, Section 2.2.1.2), the synthesis of **5.8a** could also be readily achieved using sodium hydride (as the base) in THF at room temperature. The complexes **5.8a** and **5.8b** were unambiguously characterised on the basis of elemental microanalysis, NMR spectroscopy, electrospray mass spectrometry, and single crystal X-ray crystallographic studies.

5.2.1 X-ray structures of

$[\{C_6H_3(CH_2NMe_2)-2-(OMe)-5\}Au\{NRC(O)NR\}]$ **5.8a** (R = Ph) and **5.8b** water solvate (R = Ac)

The crystal structures of both complexes were carried out in order to fully characterise the reaction product of both N,N'-diphenylurea and N,N'-diacetylurea dianions with **5.1a**, the geometry of the compounds, and for comparison with the ureylene structures previously determined for platinum (**2.22d**, Chapter Two, Section 2.2.2) and palladium (**2.17**¹⁵). Additionally, complex **5.8b** showed a very strong $[2M + H]^+$ ion in the electrospray mass spectrum (see Section 5.2.2.3), and a possible dimerisation of the complex was considered. It has been shown in our laboratory that the reaction of N-cyanoacetylurethane $[NCCH_2C(O)NHC(O)OEt]$ with **5.1a** gives initially the monomer complex **5.9**, but eventually crystallises as the poorly soluble dimer **5.10**, thus forming an eight-membered ring (Figure 5.6).¹⁶ Diagnostic distinction between monomer or dimer systems is not readily achievable by spectroscopic methods. Also, the determination of the structures of both **5.8a** and **5.8b** allows a direct comparison of two electronically different ureylene substituents.

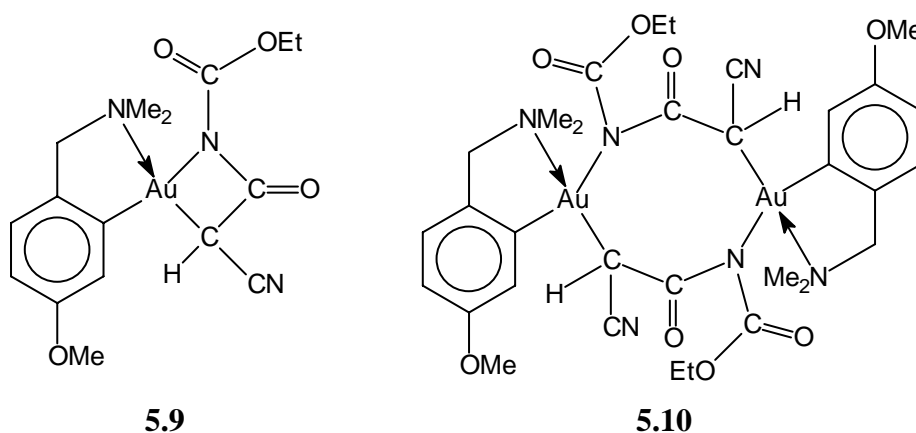


Figure 5.6

ORTEP perspective and side views of the structure of **5.8a** are shown in Figures 5.7 and 5.8 respectively, together with the atom numbering scheme. Selected bond lengths and angles are presented in Table 5.1, with tables of complete bond lengths and angles, final positional parameters, thermal parameters and calculated H-atom positions presented in Appendix IX.

Likewise, ORTEP perspective and side views of the structure of **5.8b** are shown in Figures 5.9 and 5.10. Selected bond lengths and angles are shown in Table 5.2, with tables of complete bond lengths and angles, final positional parameters, thermal parameters and calculated H-atom positions presented in Appendix X.

The structures confirm the expected monomeric reaction products, and are analogous to the structures of ureylene complexes observed for platinum(II) (Chapter Two, Section 2.2.2) and palladium(II).¹⁵ The equivalent bond lengths and angles for **5.8a** and **5.8b** are remarkably similar, with the majority being identical within two standard deviations. This shows that the complexes formed by the N,N'-diphenylurea and the N,N'-diacetylurea dianions, despite being somewhat electronically different, nonetheless give extremely similar structures.

As seen in Figure 5.8, the geometry about the gold atom of complex **5.8a** is, as expected, almost planar with no atom deviating from a least-squares plane defined by N(1), N(2), Au, N(3) and C(31) by more than 0.065(3) Å, for N(1). Similarly (Figure 5.10), for **5.8b** the analogous plane drawn through N(1), N(2), Au, N(3) and C(11) has no atom deviating by more than 0.120(3) Å, for N(2). The four-membered ureylene rings formed by Au, N(1), N(2) and C(1) are also planar, with the largest deviation being 0.014(4) Å and 0.031(4) Å [for C(1)] for **5.8a** and **5.8b** respectively. The carbonyl groups also lie in this plane, as expected. Thus the gold ureylene structures, as for platinum, closely resemble the isoelectronic carbonato complexes¹⁷ (see also Chapter One, Section 1.2.3.1), rather than the puckered ring system observed for the gold(III) aurathietane-3,3-dioxide complex (see Chapter Seven). The major distortion from a regular square-planar arrangement is the N(1)-Au-N(2) bite angle, which is 64.3(2)° for **5.8a** and 64.1(2)° for **5.8b**, a geometrical constraint imposed by the ureylene ligand. These are comparable to those already discussed (Chapter Two, Section 2.2.2.4) for the platinum and palladium(II) complexes **2.22d** and **2.17**, which have bite angles of 64.7(3)° and 65.6(1)° respectively for the ureylene ligands.

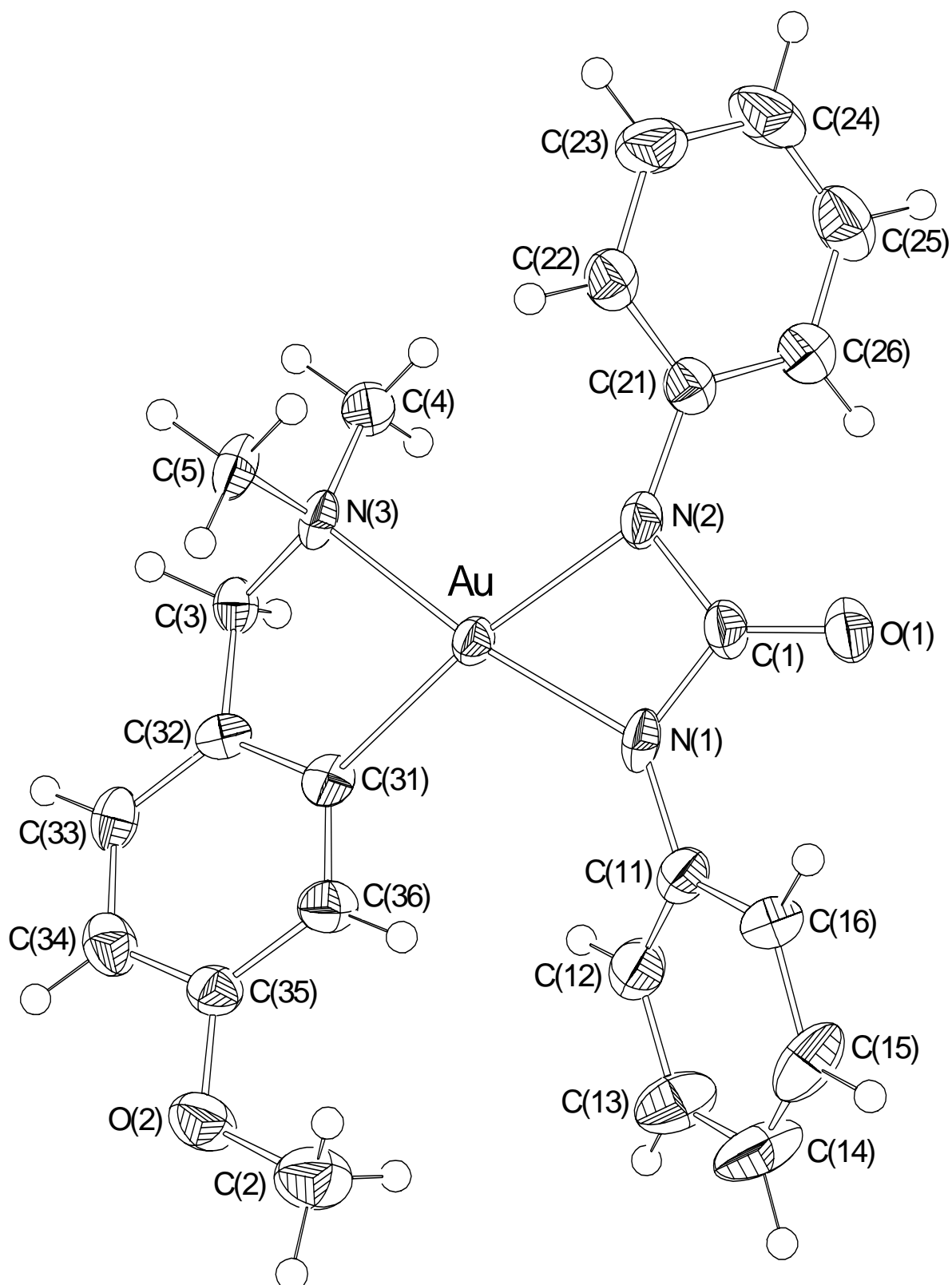


Figure 5.7: Perspective view of the X-ray crystal structure of the gold(III) ureylene complex $[\{C_6H_3(CH_2NMe_2)_2-2-(OMe)-5\}Au\{NPhC(O)NPh\}]$ **5.8a**, showing the atom numbering scheme. Thermal ellipsoids are shown at the 50% probability level.

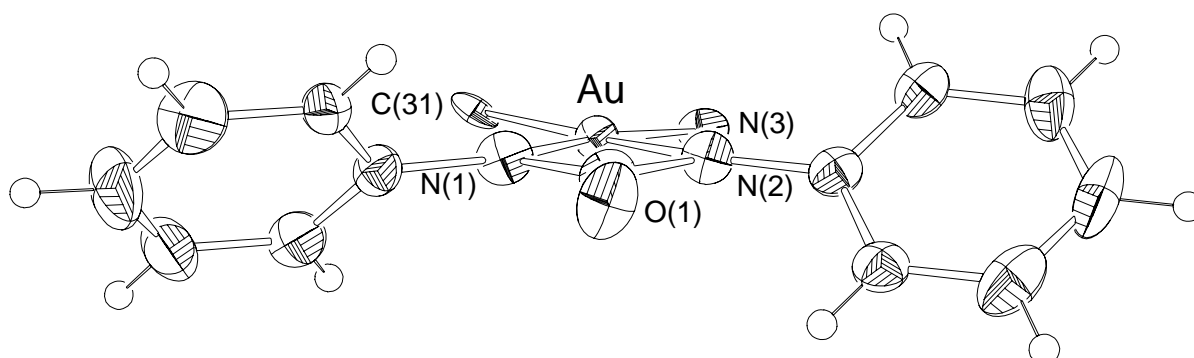


Figure 5.8: Side view of the X-ray crystal structure of the gold(III) ureylene complex $[\{C_6H_3(CH_2NMe_2)-2-(OMe)-5\}Au\{NPhC(O)NPh\}]$ **5.8a**. For clarity, only the Au-bonded atoms of the *N,N*-dimethylbenzylamine ligand are shown. Thermal ellipsoids are shown at the 50% probability level.

Table 5.1: Selected bond lengths (Å) and angles (°) (estimated standard deviations in parentheses) of the gold(III) ureylene complex **5.8a**.

Bond	Length	Bonds	Angle
Au-N(1)	2.003(6)	N(1)-Au-N(2)	64.3(2)
Au-N(2)	2.092(6)	N(2)-Au-N(3)	108.6(2)
Au-N(3)	2.088(6)	N(1)-Au-C(31)	106.3(3)
Au-C(31)	2.025(7)	N(3)-Au-C(31)	80.9(3)
Au...C(1)	2.584(8)	Au-N(1)-C(1)	97.7(5)
		Au-N(2)-C(1)	93.9(5)
		Au-N(1)-C(11)	137.3(5)
		Au-N(2)-C(21)	143.1(5)
PhNC(O)NPh ligand			
C(1)-O(1)	1.219(8)	N(1)-C(1)-N(2)	103.9(6)
C(1)-N(1)	1.387(10)	N(1)-C(1)-O(1)	127.1(7)
C(1)-N(2)	1.383(9)	N(2)-C(1)-O(1)	128.9(8)
N(1)-C(11)	1.404(9)	C(1)-N(1)-C(11)	124.6(6)
N(2)-C(21)	1.421(9)	C(1)-N(2)-C(21)	122.5(6)

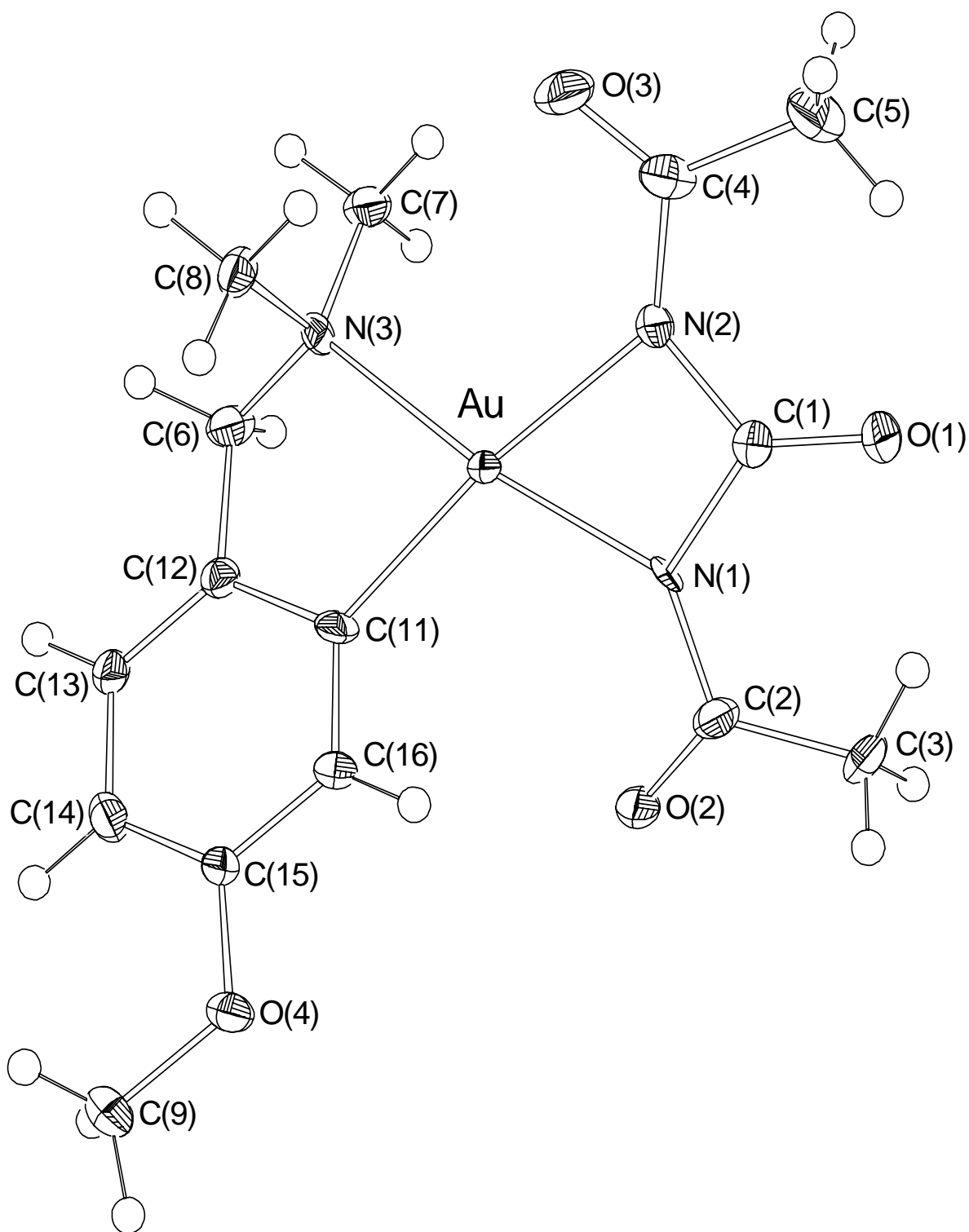


Figure 5.9: Perspective view of the X-ray crystal structure of the gold(III) ureylene complex $[[C_6H_3(CH_2NMe_2)-2-(OMe)-5]Au\{N\text{Ac}C(O)N\text{Ac}\}] \cdot \frac{1}{2}H_2O$ **5.8b**, showing the atom numbering scheme. The water of crystallisation has been omitted. Thermal ellipsoids are shown at the 50% probability level.

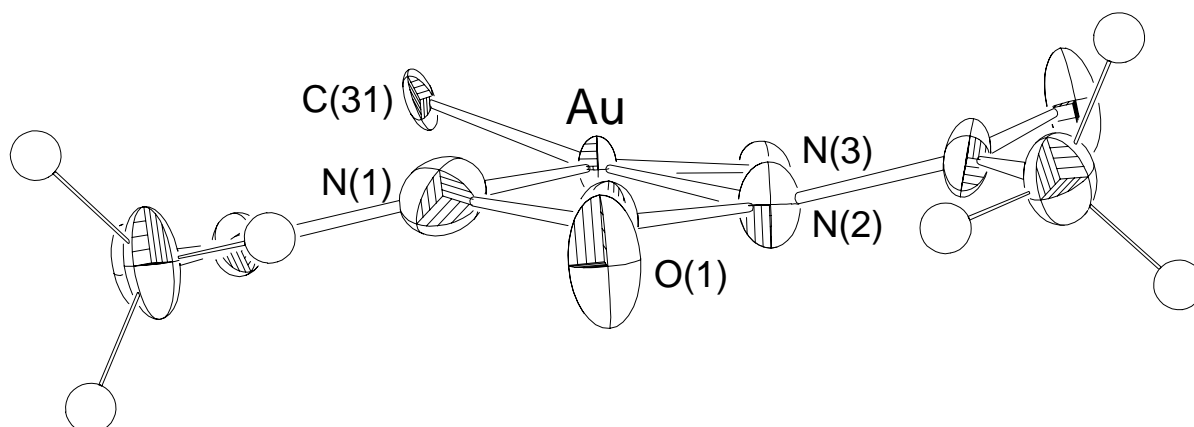


Figure 5.10: Side view of the X-ray crystal structure of the gold(III) ureylene complex $[\{C_6H_3(CH_2NMe_2)-2-(OMe)-5\}Au\{NACC(O)NAC\}] \cdot \frac{1}{2}H_2O$ **5.8b**. For clarity, only the Au-bonded atoms of the *N,N*-dimethylbenzylamine ligand are shown, and the water of crystallisation has been omitted. Thermal ellipsoids are shown at the 50% probability level.

Table 5.2: Selected bond lengths (Å) and angles (°) (estimated standard deviations in parentheses) of the gold(III) ureylene complex **5.8b**·½H₂O.

Bond	Length	Bonds	Angle
Au-N(1)	2.014(5)	N(1)-Au-N(2)	64.1(2)
Au-N(2)	2.092(6)	N(2)-Au-N(3)	108.9(2)
Au-N(3)	2.090(5)	N(1)-Au-C(11)	107.0(2)
Au-C(11)	2.021(6)	N(3)-Au-C(11)	80.7(2)
Au...C(1)	2.622(7)	Au-N(1)-C(1)	98.2(4)
		Au-N(2)-C(1)	95.6(4)
		Au-N(1)-C(2)	133.8(4)
		Au-N(2)-C(4)	133.4(5)
AcNC(O)NAC ligand			
C(1)-O(1)	1.222(9)	N(1)-C(1)-N(2)	102.0(6)
C(1)-N(1)	1.415(8)	N(1)-C(1)-O(1)	128.8(6)
C(1)-N(2)	1.392(9)	N(2)-C(1)-O(1)	129.1(7)
N(1)-C(2)	1.390(9)	C(1)-N(1)-C(2)	125.2(6)
N(2)-C(4)	1.371(8)	C(1)-N(2)-C(4)	127.1(6)
C(2)-O(2)	1.230(8)	N(1)-C(2)-O(2)	119.7(6)
C(4)-O(3)	1.218(9)	N(2)-C(4)-O(3)	121.4(7)

Due to the non-symmetrical nature of the five-membered cyclometallated ring, the bond lengths from the gold atom to the ureylene nitrogen atoms, N(1) and N(2), are not equal. Since the *ortho*-carbon on the cyclometallated ring has a higher *trans*-influence¹⁸ than coordinated nitrogen, the Au-N(2) distances are significantly longer [2.092(6) Å for both **5.8a** and **5.8b**] than Au-N(1) [2.003(6) Å for **5.8a** and 2.014(6) Å for **5.8b**]. Comparing these lengths to the platinum(II) ureylene complex **2.22d**, which has Pt-N distances of 2.048(8) Å for Pt-NAd and 2.021(8) Å for Pt-NPh, it is clear the average Au-NPh lengths for **5.8a** and **5.8b** [$\sim 2.05(1)$ Å] are very much consistent with the platinum ureylene system.

It is evident from Figures 5.7 and 5.9 that the OMe groups for **5.8a** and **5.8b** point in opposite directions, with the Me group orientated towards the ureylene ligand for **5.8a** and away for **5.8b**. The water of crystallisation [O(5)] in **5.8b** [which is hydrogen-bonded to O(3) (O...O contact 2.813(9) Å)] is 3.627(9) and 4.424(9) Å from O(2) and O(4) (in adjacent molecules) respectively, so the orientation of the OMe group is probably not directed by hydrogen-bonding interactions. Additionally, the phenyl group in **5.8a** is bulkier than the C(O)Me in **5.8b**, so steric effects are also unlikely. For these reasons the most probable explanation for the observation is crystal-packing forces.

The two carbonyl groups C(2)-O(2) and C(4)-O(3) both point towards the cyclometallated ligand, thus minimising steric interactions of the bulkier methyl groups C(3) and C(5). The torsion angles of the ureylene phenyl rings of **5.8a** are 39.1(2) and 49.2(2)° for C(26)-C(21)-N(2)-C(1) and C(16)-C(11)-N(1)-C(1) respectively. For **5.8b** the torsion angles are 11.4(2) and 22.3(2)° for C(5)-C(4)-N(2)-C(1) and C(3)-C(2)-N(1)-C(1).

5.2.2 Spectroscopic and mass spectrometric characterisation

5.2.2.1 NMR spectroscopy

A combination of 2D experiments [HMQC, HMBC, COSY and NOESY (See Appendix II)] were used to unambiguously assign the ¹H and ¹³C NMR spectra of **5.8a** and **5.8b**. Due to the differing *trans*-influence groups on the orthometallated ligand, the ureylene ligand, despite being symmetrical itself, gives two sets of resonances for its substituents. These could be readily assigned by 1D NOE difference or 2D NOESY experiments, which show clear through-space correlation to either the *para*-methoxy group, or the NMe groups.

Table 5.3 shows a comparison of the relevant ^{13}C chemical shifts of starting materials and products. A large downfield shift of the central carbonyl resonance is observed upon coordination. This is probably due to the deshielding of this moiety by the electronegative metal centre [the electronegativity of gold(III) is quite high],¹⁹ and with the formation of the strained four-membered ring. The data compares with values for platinum(II) complex $[\text{Pt}\{\text{NPhC}(\text{O})\text{NPh}\}(\text{PPh}_3)_2]$ **2.22f** and $[\text{Pt}\{\text{NAcC}(\text{O})\text{NAc}\}(\text{COD})]$ **2.22h** of 174.3 and 165.3 ppm. Data for the carbonyl resonance for the COD N,N'-diphenylureylene complex **2.22a** is unfortunately not available, although trends from COD versus triphenylphosphine derivatives suggest the $\text{C}=\text{O}$ chemical shift would probably be 3-5 ppm lower than that for **2.22f**. Regardless, it is clear the gold(III) ureylene complexes have central carbonyl resonances in positions comparable to those of platinum(II).

Table 5.3: Comparison of ^{13}C chemical shifts (ppm) of **5.8a** and **5.8b** compared to the respective urea starting materials.

Group	5.8a ^a	free N,N'- diphenylurea ^b	5.8b ^a	free N,N'- diacetylurea ^a
Ring $\text{C}=\text{O}$	169.4	152.6	163.1	151.0
N- C <i>trans</i> C	144.2	139.7	176.5	171.8
N- C <i>trans</i> N	141.7	139.7	172.8	171.8
Au- C	145.0	-	143.0	-

^a Acquired in CDCl_3 solvent and referenced to SiMe_4 (0.0 ppm)

^b Acquired in $(\text{CD}_3)_2\text{SO}$ solvent and referenced to SiMe_4 (0.0 ppm)

A downfield shift was also noted, but to a lesser extent, for the remaining N-C groups, and those *trans* to the higher *trans*-influence C, are deshielded to a greater extent than those *trans* to N, as predicted. This information could possibly be used to unambiguously assign signals in these positions.

5.2.2.2 IR spectroscopy

The IR spectrum (in the $1580\text{-}1700\text{ cm}^{-1}$ region) of the diphenyl ureylene complex **5.8a** bears a remarkable similarity to the platinum ureylene complexes **2.22** (Chapter Two, Section 2.2.3.2), showing two bands at 1650 and 1592 cm^{-1} . This compares with values recorded for **2.22a** of 1648 and 1594 cm^{-1} . The spectrum recorded for **5.8b** is complicated by the presence of two additional carbonyl moieties, and is consequently of little diagnostic value.

5.2.2.3 Electrospray mass spectrometry (ESMS)

Electrospray mass spectrometry continues to provide excellent utility for the analysis of inorganic and organometallic compounds.²⁰ As expected for complexes containing oxygen and nitrogen atoms capable of association with protons [OMe, C=O], the complexes **5.8a** and **5.8b** gave strong parent ions $[M + H]^+$, with no observable fragmentation at low cone voltages (< 20 V). The complexes exhibited appreciable stability even at high cone voltages (~ 100 V), as evidenced by the persistence of significant parent ions. This contrasts with the platinum ureylene complexes **2.22**, which showed only fragmentation ions at high voltages. This is consistent with the notion of the extra stability imparted by two ring systems and has also been observed previously for platinum(II) complexes containing two rings.²¹

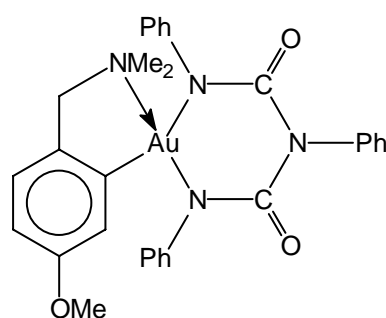
Fragmentation for **5.8a** and **5.8b** (cone voltage > 80 V), appears to proceed via different mechanisms. For **5.8a**, loss of both the gold and ureylene moieties is observed, giving rise to a strong peak at m/z 164, assigned as $[C_6H_3(CH_2NMe_2)-2-(OMe)-5]^+$. In contrast, **5.8b** shows loss of acetyl isocyanate to give $[Au\{C_6H_3(CH_2NMe_2)-2-(OMe)-5\}NHAc]^+$, analogous to the fragmentation of **2.22h** (Chapter Two, Section 2.2.3.3), which showed loss of phenyl isocyanate to give an ion assigned as $[Pt\{NHPh\}(COD)]^+$.

Also noteworthy is the propensity of **5.8b** to give very strong reproducible $[2M + H]^+$ ions, initially tentatively interpreted as solid state dimer formation. The reason for this is not fully clear, and was not observed for **5.8a**, but is most likely due to the presence of three carbonyl groups in **5.8b**.

5.2.3 Reaction with phenyl isocyanate and DMAD

As reported in Chapter Four, insertion of phenyl isocyanate into the four-membered $\overline{Pd-N-C(O)-N}$ ring of the diphenylureylene palladium complex $[Pd\{NPhC(O)NPh\}(phen)]$ **2.17** gave in high yield the triphenylbiureto derivative $[Pd\{NPhC(O)NPhC(O)NPh\}(phen)]$ **4.11**, and similarly, some platinum ureylene complexes also had a high reactivity toward unsaturated molecules, such as phenyl isocyanate, DMAD, and carbon disulfide, which rapidly inserted into the four membered ureylene metallacycles to give the expected six-membered ring insertion products (Chapter Four).

The insertion chemistry of **5.8a** with both DMAD and phenyl isocyanate was investigated. When DMAD was added to a stirred dichloromethane solution of **5.8a**, no reaction occurred, even after refluxing for 5 hours. Lack of reactivity towards DMAD insertion had also been noted for the platinum(II) diphenylureylene complex **2.22a** (Chapter Four, Section 4.2.1). However, when phenyl isocyanate was added to a solution of **5.8a**, a rapid colour change from bright orange to bright yellow was observed. The product was characterised as the expected insertion complex **5.11** (Figure 5.11) on the basis of elemental microanalysis, detailed NMR studies, and ESMS. The isolated crystalline compound was stable, but when dissolved in dichloromethane or chloroform, readily deinserted phenyl isocyanate to regenerate the starting material **5.8a**. For this reason NMR spectra of **5.11** were obtained in the presence of excess phenyl isocyanate.

**5.11***Figure 5.11*

5.2.3.1 Spectroscopic and mass spectrometric characterisation

Since complex **5.11** contains four inequivalent aromatic rings, the proton NMR contains many overlapping signals. For this reason the HOHAHA (Homonuclear Hartman-Hahn transfer) experiment was utilised (see Appendix II for details and spectra). This unambiguously verified the expected presence of three phenyl rings, and one trisubstituted aromatic ring. Coupled with the NOESY experiment, this allowed complete assignment of the ^1H NMR spectrum of **5.11**.

The complex **5.11** displays very broad NMe_2 and NCH_2 ^1H NMR signals, and lack of $^4J_{\text{H,H}}$ coupling on any of the three biureto phenyl rings, despite well resolved $^4J_{\text{H,H}}$ coupling observed on the orthometallated benzylamine ring. Additionally, the ^{13}C NMR spectrum shows four resolved signals corresponding to only two inequivalent $\text{C}=\text{O}$ groups. This is possibly the result of room temperature fluxionality, and is probably due the slow inversion of a non-planar six-membered $\text{Au-N-C(O)-N-C(O)-N}$ ring system present in **5.11**. Evidence in

support of this fluxionality was determined by the acquisition of a high temperature (55°C) ^1H NMR spectrum, which showed marked sharpening of the NMe_2 and NCH_2 resonances. Unfortunately the carbonyl signals could not be resolved in the high temperature ^{13}C NMR spectrum in the time-scale of the experiment, but could be expected to coalesce into two signals. The broadening and additional resonances are unlikely to be caused by rapid insertion/deinsertion of phenyl isocyanate, since no signal corresponding to the deinserted product **5.8a** is observed in the ESMS spectrum at low cone voltages. Indeed ESMS analysis of **5.11** shows solely strong parent ions ($[\text{M} + \text{H}]^+$ and $[2\text{M} + \text{H}]^+$) at cone voltage = 20V [Figure 5.12, a)], with the loss of phenyl isocyanate becoming the dominant ion only with higher voltages [Figure 5.12, b)]. The facile loss of phenyl isocyanate has been previously observed in the ESMS analysis of $[\text{Pt}\{\overline{\text{NPhC(O)NRC(O)NPh}}\}(\text{COD})]$ **4.15a** ($\text{R} = \text{Ph}$) and **4.15b** ($\text{R} = \text{Me}$) (see Chapter Four, Section 4.2.1.1.3), the reaction products of, respectively, **2.22a** and **2.22b** and phenyl isocyanate.

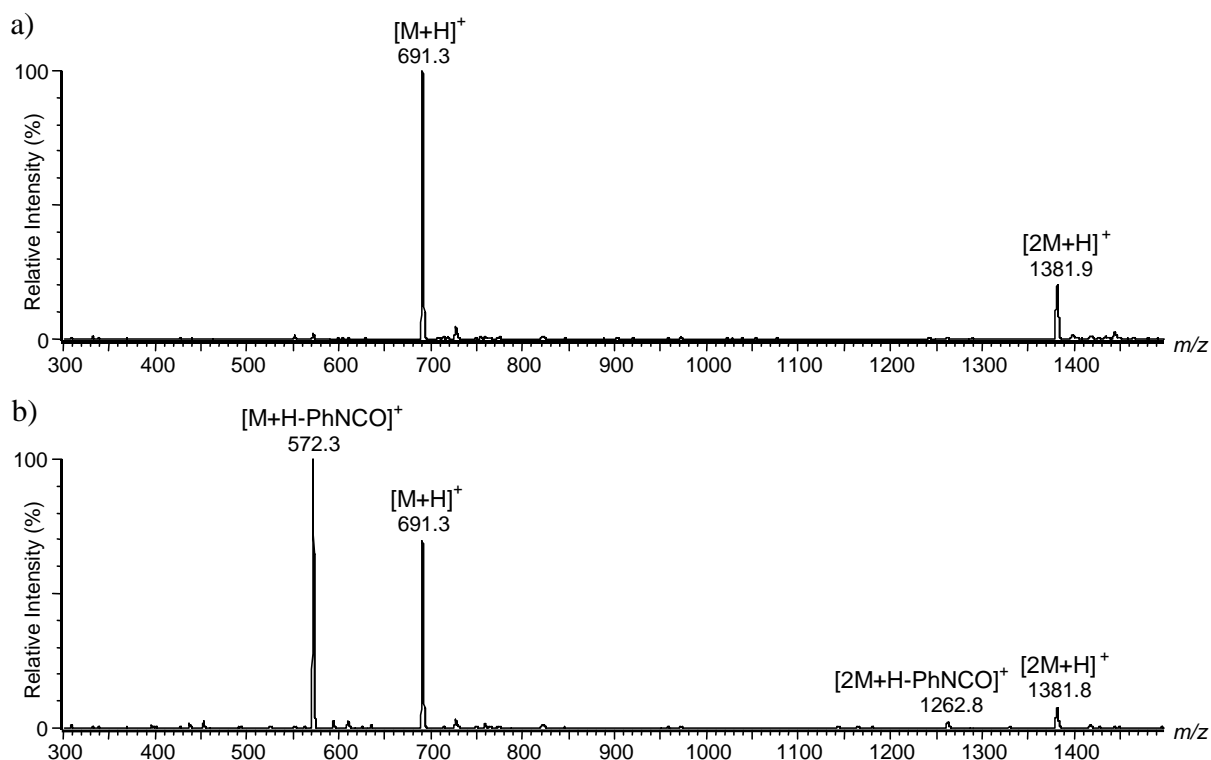
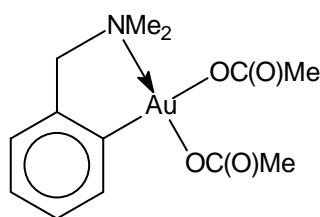


Figure 5.12: Positive-ion electrospray mass spectra of $[\{\text{C}_6\text{H}_3(\text{CH}_2\text{NMe}_2)\text{-2-(OMe)-5}\text{Au}\{\overline{\text{NPhC(O)NPhC(O)NPh}}\}]$ **5.11** ($= \text{M}$), showing peak assignments. a) cone voltage 20 V; b) cone voltage 50 V.

5.2.4 Biological Activity

The cyclometallated gold(III) complex **5.12** (Figure 5.13), containing water-solubilising acetate ligands, has generated interest since it shows both antibacterial activity, and activity against Chinese hamster ovary cells comparable to that of the well-established drug cisplatin.⁵ The dichloride complex **5.1a** also possesses activity against human breast tumour cells.⁷ Studies of the interaction of **5.12** with the thiol-containing compounds L-cysteine and glutathione indicated that cyclic thiolate complexes were formed.⁵



5.12

Figure 5.13

Assays for antimicrobial, antiviral and antitumour activities were determined for **5.8b**. The results are summarised in Table 5.4. The compound showed high cytotoxicity towards the bacteria (*Escherichia coli*, *Bacillus subtilis* and *Pseudomonas aeruginosa*) and fungi (*Candida albicans*, *Trichophyton mentagrophytes* and *Cladosporium resinae*) tested, and completely killed the BSC-1 cell line used for antiviral testing. Antitumour activity was moderate, requiring 7377 ng/ml to inhibit 50% of cell growth in P-388 tumour cells.

Table 5.4: Biological assay results for the gold(III) ureylene complex **5.8b** (2 µg loaded on disc in each case).

Antitumour (P-388) and antiviral/cytotoxicity				Antimicrobial/antifungal ^g activities ^h					
IC ₅₀ ^a	HSV1 ^b	PV1 ^c	Cyt ^d	Ec	Bs	Pa	Ca	Tm	Cr
7377	- ^e	- ^e	4+ ^f	9	14	9	8	10	6

^a The concentration of sample in ng/ml required to reduce the cell growth of the P-388 leukemia cell line (ATCC CCL 46) by 50%.

^b *Herpes simplex* type I virus (strain F, ATCC VR 733) grown on the BSC cell line (ATCC CCL 26).

^c *Polio* type I virus (Pfiser vaccine strain) grown on the BSC cell line.

^d cytotoxicity to BSC cells.

^e No data presented due to the high cytotoxicity of **5.8b** (killed the BSC cell line used for test).

^f 4+ denotes antiviral or cytotoxic zone over whole well (100% zone).

^g Ec = *Escherichia coli*, Bs = *Bacillus subtilis*, Pa = *Pseudomonas aeruginosa*, Ca = *Candida albicans*, Tm = *Trichophyton mentagrophytes*, Cr = *Cladosporium resinae*.

^h Inhibition zone as excess radius (mm) from a 6 mm (diameter) disc containing 2 µg of **5.8b**.

5.2.5 Conclusions

The gold(III) ureylene complexes reported here are analogous to those previously prepared for platinum(II) (**2.22**, Chapter Two), and the cyclometallated gold(III) compound **5.1a** apparently provides an excellent platinum(II) analogue. Although the silver(I) oxide mediated reactions used to prepare the ureylene complexes seem to proceed much more rapidly for the gold(III) system, reactivity of **5.8a** toward insertion of phenyl isocyanate and DMAD is comparable to the platinum(II) ureylene complex **2.22a**.

5.3 Experimental

General experimental procedures and the instrumentation used are given in Appendices I and II. The gold(III) precursor $[\text{Au}\{\overline{\text{C}_6\text{H}_3(\text{CH}_2\text{NMe}_2)\text{-2-(OMe)-5}}\}\text{Cl}_2]$ **5.1a** was prepared as described in Appendix I. ESMS spectra were recorded in MeCN/H₂O solvent.

Dimethyl acetylenedicarboxylate (Aldrich) and phenyl isocyanate (BDH) were obtained from commercial sources, and used as received. The sodium hydride (Koch-Light) used was oil-free and freshly powdered. N,N'-diphenylurea and N,N'-diacetylurea were prepared as described in Chapter Two (Section 2.3.1).

Proton and all inverse 2D NMR experiments [HMQC, HMBC, NOESY and HOHAHA (see Appendix II)] were recorded on a Bruker DRX 400 spectrometer at 400.13 MHz and 100.61 MHz for the proton and carbon channels respectively. The ¹³C NMR spectra were recorded a Bruker AC300 spectrometer at 75.47 MHz, with exception of **5.8b** which was recorded at 100.61 MHz on instrument above. All NMR analyses were carried out in CDCl₃, with the exception of the ¹³C NMR spectrum of N,N'-diphenylurea which was acquired in D₆-DMSO.

*Preparation of $[\{\overline{\text{C}_6\text{H}_3(\text{CH}_2\text{NMe}_2)\text{-2-(OMe)-5}}\}\text{Au}\{\underline{\text{NPhC(O)NPh}}\}]$ **5.8a***

To a Schlenk flask containing degassed dichloromethane (25 ml) was added **5.1a** (0.050 g, 0.116 mmol), N,N'-diphenylurea (0.025 g, 0.118 mmol) and silver(I) oxide (0.092 g, excess). The mixture was refluxed under nitrogen for 2 hours. The silver salts were filtered off and the solvent removed under reduced pressure, giving a bright orange oil. This was recrystallised by vapour diffusion of ether into a dichloromethane solution, to give bright orange needles of **5.8a** (0.034 g, 51%).

Alternatively, complex **5.1a** (0.050 g, 0.116 mmol), N,N'-diphenylurea (0.025 g, 0.118 mmol) and sodium hydride (0.5 g, excess) were added to a Schlenk flask containing freshly distilled degassed THF (25 ml), and stirred under nitrogen for 1 hour. The resulting bright orange solution was filtered, and the THF removed under reduced pressure. The residue was dissolved in dichloromethane and filtered again. Crystallisation by slow addition of diethyl ether gave **5.8a** (0.040 g, 60%).

M.p. 185-190 °C.

Found: C, 48.0; H, 4.4; N, 7.2%; C₂₃H₂₄N₃O₂Au requires: C, 48.3; H, 4.2; N, 7.4%.

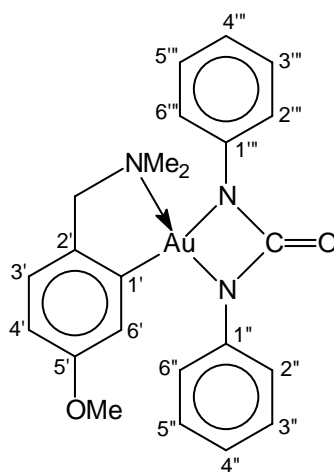
IR: ν (CO region) 1650 (vs), 1592 (m) cm⁻¹.

ESMS: (Cone voltage = 5V) m/z 588 ([MNH₄]⁺, 30%), 572 ([MH]⁺, 100%). (Cone voltage = 50V) m/z 588 ([MNH₄]⁺, 25%), 572 ([MH]⁺, 100%), 164 ([C₆H₃(CH₂NMe₂)-2-(OMe)-5]⁺, 17%). (Cone voltage = 100V) m/z 572 ([MH]⁺, 35%), 164 ([C₆H₃(CH₂NMe₂)-2-(OMe)-5]⁺, 100%).

¹H NMR: δ 7.38 (2H, *dd*, ³J_{2'',3''} = 8.09 Hz, ⁴J_{2'',4''} = 1.37 Hz, H-2'',6''), 7.33-7.25 (6H, *m*, H-3'',5'',2''',6''',3''',5'''), 7.13 (1H, *tt*, ³J_{4'',3''/5''} = 7.23 Hz, ⁴J_{4'',2''/6''} = 0.60 Hz, H-4''), 7.03 (1H, *d*, ³J_{3',4'} = 8.16 Hz, H-3'), 7.02 (1H, *t*, ³J_{4''',3'''/5'''} = 8.49 Hz, H-4'''), 6.68 (1H, *dd*, ³J_{4',3'} = 8.26 Hz, ⁴J_{4',6'} = 2.50 Hz, H-4'), 6.14 (1H, *d*, ⁴J_{6',4'} = 2.48 Hz, H-6'), 4.11 (2H, *s*, CH₂), 3.34 (3H, *s*, OCH₃), 2.95 (6H, *s*, NCH₃).

¹³C NMR: δ 169.4 (*s*, C=O), 157.8 (*s*, C-5'), 145.0 (*s*, C-1'), 144.2 (*s*, C-1'''), 141.7 (*s*, C-1''), 136.5 (*s*, C-2'), 129.0 (*d*, C-3'',5''), 128.7 (*d*, C-3''',5'''), 128.5 (*d*, C-2'',6''), 126.7 (*d*, C-2''',6'''), 124.9 (*d*, C-4''), 123.5 (*d*, C-4'''), 123.5 (*d*, C-3'), 115.2 (*d*, C-4'), 114.8 (*d*, C-6'), 73.9 (*t*, CH₂), 55.2 (*q*, OCH₃), 52.0 (*q*, NCH₃).

NMR numbering scheme:



Preparation of $[(C_6H_3(CH_2NMe_2)-2-(OMe)-5)Au\{NAcC(O)NAc\}]$ **5.8b**

In a similar fashion to the synthesis of **5.8a**, **5.1a** (0.050 g, 0.116 mmol), N,N'-diacetylurea (0.017 g, 0.118 mmol) and silver(I) oxide (0.088 g, excess) were refluxed under nitrogen for 2 hours. The silver salts were filtered off and the solvent removed under reduced pressure, giving a pale yellow oil. This was recrystallised by slow evaporation of an ether solution at -20°C , to give cream crystals of **5.8b** (0.044 g, 76%).

M.p. 168-171°C.

Found: C, 35.9; H, 4.0; N, 8.3%; $C_{15}H_{20}N_3O_4Au$ requires: C, 35.8; H, 4.0; N, 8.4%.

IR: ν (CO region) 1721 (vs), 1665 (m), 1641 (s), 1629 (s), 1596 (m) cm^{-1} .

ESMS: (Cone voltage = 20V) m/z 1007 ($[2MH]^+$, 33%), 504 ($[MH]^+$, 100%). (Cone voltage = 50V) m/z 1007 ($[2MH]^+$, 38%), 504 ($[MH]^+$, 100%), 419 ($[MH - AcNCO]^+$, 92%). (Cone voltage = 80V) m/z 1007 ($[2MH]^+$, 8%), 504 ($[MH]^+$, 70%), 419 ($[MH - AcNCO]^+$, 100%).

^1H NMR: δ 7.38 (1H, *d*, $^4J_{6,4'} = 2.49$ Hz, H-6'), 6.96 (1H, *d*, $^3J_{3',4'} = 8.27$ Hz, H-3'), 6.74 (1H, *dd*, $^3J_{4',3'} = 8.29$ Hz, $^4J_{4',6'} = 2.51$ Hz, H-4'), 4.17 (2H, *s*, $\underline{CH_2}$), 3.75 (3H, *s*, $\underline{OCH_3}$), 3.45 (6H, *s*, $\underline{NCH_3}$), 2.57 (3H, *s*, $\underline{NC(O)CH_3}$ *trans* N), 2.49 (3H, *s*, $\underline{NC(O)CH_3}$ *trans* C).

^{13}C NMR: δ 176.5 (*s*, $\underline{NC(O)CH_3}$ *trans* C), 172.8 (*s*, $\underline{NC(O)CH_3}$ *trans* N), 163.1 (*s*, C=O), 157.2 (*s*, C-5'), 143.0 (*s*, C-1'), 138.1 (*s*, C-2'), 122.9 (*d*, C-3'), 122.1 (*d*, C-6'), 114.7 (*d*, C-4'), 75.6 (*t*, $\underline{CH_2}$), 55.6 (*q*, $\underline{OCH_3}$), 53.8 (*q*, $\underline{NCH_3}$), 28.8 (*q*, $\underline{NC(O)CH_3}$ *trans* C), 28.1 (*q*, $\underline{NC(O)CH_3}$ *trans* N).

Reaction of 5.8a with DMAD

To a stirred solution of **5.8a** (0.025 g, 0.044 mmol) in dichloromethane (10 ml) was added two drops of dimethyl acetylenedicarboxylate. No immediate colour change occurred, so reflux was commenced for 24 hours after which time no visibly observable reaction had taken place. Evaporation of the solvent, and subsequent ^1H and ^{13}C NMR of the residue showed only starting materials, indicating no reaction had taken place.

Reaction of 5.8a with phenyl isocyanate

To a stirred solution of **5.8a** (0.025 g, 0.044 mmol) in dichloromethane (5 ml) was added two drops of phenyl isocyanate. A marked colour change from bright orange to bright yellow occurred almost immediately. Evaporation of the solvent, and recrystallisation of the residue

from dichloromethane and diethyl ether gave **5.11** as yellow rosettes (0.020 g, 67%). NMR studies revealed that gradual deinsertion of phenyl isocyanate (to regenerate **5.8a**) occurred over 24 hours, if an excess of the isocyanate was not present.

M.p. 175-176 °C.

Found: C, 50.5; H, 4.1; N, 7.6%; $C_{30}H_{29}N_4O_3Au \cdot \frac{1}{2}CH_2Cl_2$ requires: C, 50.0; H, 4.1; N, 7.6%.

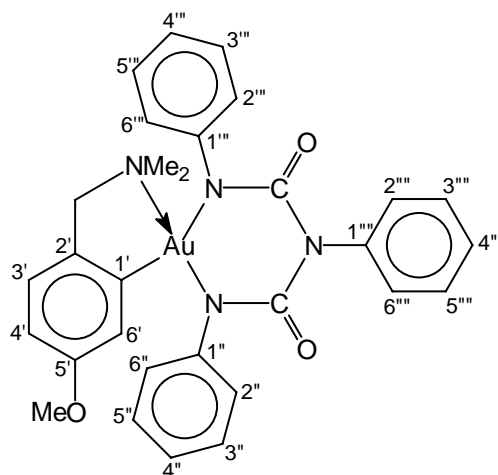
IR: ν (CO region) 1648 (vs), 1627 (s), 1592 (m) cm^{-1} .

ESMS: (Cone voltage = 20V) m/z 1382 ($[2MH]^+$, 22%), 691 ($[MH]^+$, 100%). (Cone voltage = 50V) m/z 1382 ($[2MH]^+$, 8%), 692 ($[MH]^+$, 69%), 572 ($[MH - PhNCO]^+$, 100%). (Cone voltage = 80V) m/z 1382 ($[2MH]^+$, 5%), 691 ($[MH]^+$, 72%), 572 ($[MH - PhNCO]^+$, 100%).

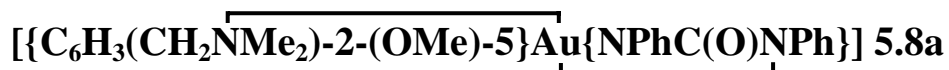
1H NMR: δ 8.01 (2H, *d*, $^3J_{2''',3'''} = 8.29$ Hz, H-2''',6'''), 7.86 (2H, *d*, $^3J_{2'',3''} = 8.29$ Hz, H-2'',6''), 7.44 (2H, *d*, $^3J_{2''',3'''} = 8.15$ Hz, H-2''',6'''), 7.39 (2H, *t*, $^3J_{3'',2''/4''} = 7.80$ Hz, H-3''), 7.38 (2H, *t*, $^3J_{3''',2'''/4'''} = 6.53$ Hz, H-3''',5'''), 7.34 (2H, *t*, $^3J_{3'',2''/4''} = 8.08$ Hz, H-3''/5''), 7.31 (1H, *t*, $^3J_{4''',3'''/5'''} = 8.15$ Hz, H-4'''), 7.11 (1H, *t*, $^3J_{4'',3''/5''} = 7.82$ Hz, H-4''), 7.11 (1H, *t*, $^3J_{4''',3'''/5'''} = 8.88$ Hz, H-4'''), 6.99 (1H, *t*, $^3J_{3',4'} = 8.33$ Hz, H-3'), 6.69 (1H, *dd*, $^3J_{4',3'} = 8.30$ Hz, $^4J_{4',6'} = 2.42$ Hz, H-4'), 6.20 (1H, *d*, $^4J_{6',4'} = 2.40$ Hz, H-6'), 5.25 (1H, *s*, CH_2Cl_2 of crystallisation), 4.22 (2H, *s*, br, $\underline{CH_2}$), 3.33 (3H, *s*, $\underline{OCH_3}$), 2.79 (6H, *s*, br, $\underline{NCH_3}$).

^{13}C NMR: δ 158.0 (*s*, C-5'), 156.5 (*s*, C=O), 156.2 (*s*, C=O), 153.43 (*s*, C=O), 153.36 (*s*, C=O), 145.2 (*s*, C-1''), 144.0 (*s*, C-1'''), 144.0 (*s*, C-1'), 139.9 (*s*, C-1'''), 135.9 (*s*, C-2'), 130.5 (*d*, C-2''',6'''), 129.1 (*d*, C-3'',5'' or C-3''',5'''), 128.5 (*d*, C-3''',5'''), 128.3 (*d*, C-3'',5'' or C-3''',5'''), 127.6 (*d*, C-4'''), 126.9 (*d*, C-2''',6'''), 125.8 (*d*, C-2'',6''), 124.6 (*d*, C-4'' or C-4'''), 124.3 (*d*, C-4'' or C-4'''), 123.4 (*d*, C-3'), 116.4 (*d*, C-4'), 114.7 (*d*, C-6'), 75.1 (*t*, $\underline{CH_2}$), 55.4 (*q*, $\underline{OCH_3}$), 52.4 (*q*, $\underline{NCH_3}$).

NMR numbering scheme:



5.3.1 X-ray structure of



An orange thin rectangular crystal suitable for an X-ray study was grown by vapour diffusion of diethyl ether into a dichloromethane solution of **5.8a** at 4°C.

Data collection

Accurate cell parameters and intensity data were collected on Siemens SMART CCD diffractometer at Auckland University. Details regarding the collection methodology and configuration are described in Appendix II.

Collection Data: crystal size = 0.23 × 0.09 × 0.03 mm, total reflections = 4909, unique reflections = 4751, range = 1.51 < θ < 28.14°, absorption correction $T_{\text{max.}, \text{min.}}$ = 0.86, 0.52.

Crystal Data: C₂₃H₂₄N₃O₂Au, M_r = 571.42, monoclinic, space group $P2_1/c$, a = 13.5099(5), b = 17.683(1), c = 9.028(1) Å, β = 92.37(1)°, U = 2154.7(1) Å³, D_c = 1.761 g cm⁻³, Z = 4, $F(000)$ = 1112, $\mu(\text{Mo-K}\alpha)$ = 6.851 mm⁻¹.

Solution and refinement

The structure was solved by the Patterson methods option of SHELXS-96,²² and the gold position determined. All further non-hydrogen atoms were located routinely in subsequent full-matrix least-squares refinements based on F^2 (SHELXL-96).²³ All non-hydrogen atoms were assigned anisotropic temperature factors, and all hydrogen atom positions determined by calculation. The refinement converged with R_1 = 0.0446 for 3233 data with $I \geq 2\sigma(I)$, 0.0882 for all data; wR_2 = 0.0937 { $w = 1/[\sigma^2(F_o^2) + (0.0339P)^2 + 0.0000P]$ where $P = (F_o^2 + 2F_c^2)/3$ }, and GoF = 1.010. No parameter shifted in the final cycle. The final difference map showed no peaks or troughs of electron density greater than +1.33 and -2.02 e Å⁻³ respectively, both adjacent to the gold atom.

5.3.2 X-ray structure of

$[\{\text{C}_6\text{H}_3(\text{CH}_2\text{NMe}_2)\text{-2-(OMe)-5}\}\text{Au}\{\text{NAcC(O)NAc}\}] \cdot \text{H}_2\text{O}$ **5.8b** water solvate

A cream crystal suitable for an X-ray diffraction was obtained by slow evaporation of a concentrated diethyl ether solution of **5.8b** at -20°C .

Data collection

Unit cell dimensions and intensity data were obtained on a Siemens CCD detector mounted on a P4 diffractometer at the University of Canterbury. Details regarding the collection methodology and configuration are described in Appendix II.

Collection Data: crystal size = 0.60 x 0.35 x 0.12 mm, total reflections = 5504, unique reflections = 4068, range = $1.89 < \theta < 30.48^\circ$, absorption correction $T_{\text{max.}, \text{min.}} = 1.00, 0.57$.

Crystal Data: $\text{C}_{15}\text{H}_{20}\text{N}_3\text{O}_4\text{Au}\cdot\frac{1}{2}\text{H}_2\text{O}$, $M_r = 513.32$, triclinic, space group $P\bar{1}$ (no. 2), $a = 8.890(1)$, $b = 8.983(1)$, $c = 11.201(1)$ Å, $\alpha = 74.78(1)$, $\beta = 89.77(1)$, $\gamma = 76.32(1)^\circ$, $U = 837.1(1)$ Å³, $D_c = 2.037$ g cm⁻³, $Z = 2$, $F(000) = 496$, $\mu(\text{Mo-K}\alpha) = 8.814$ mm⁻¹.

Solution and refinement

The structure was solved by the direct methods option of SHELXS-96,²² and the majority of the heavy atom positions determined. All further non-hydrogen atoms were located routinely in subsequent full-matrix least-squares refinements based on F^2 (SHELXL-96).²³ All non-hydrogen atoms were assigned anisotropic temperature factors, and all hydrogen atom positions determined by calculation. The refinement converged with $R_1 = 0.0396$ for 3592 data with $I \geq 2\sigma(I)$, 0.0427 for all data; $wR_2 = 0.0971$ $\{w = 1/[\sigma^2(F_o^2) + (0.0526P)^2 + 0.0000P]$ where $P = (F_o^2 + 2F_c^2)/3\}$, and $\text{GoF} = 1.006$. No parameter shifted in the final cycle. The final difference map showed significant peaks and troughs of electron density (maximum +3.24 and -3.94 e Å⁻³ respectively), adjacent to the gold atom, which can be attributed to poor absorption correction beyond our control.

After elucidation of the structure, an extra peak of electron density was present in the penultimate difference map that was clearly not part of the main molecule. This was successfully modelled as a lone oxygen atom with half occupancy, almost certainly therefore a water of crystallisation. The atom, O(5), is 2.813(8)Å from O(3), thus within hydrogen bonding distance. The associated hydrogen atoms could not be located in the final electron difference map.

References

- 1 S.L. Best, T.K. Chattopadhyay, M.I. Djuran, R.A. Palmer, P.J. Sadler, I. Sóvágó and K. Varnagy, *J. Chem. Soc., Dalton Trans.*, (1997) 2587.
- 2 R.V. Parish, J. Mack, L. Hargreaves, J.P. Wright, R.G. Buckley, A.M. Elsome, S.P. Fricker and B.R.C. Theobald, *J. Chem. Soc., Dalton Trans.*, (1996) 69.
- 3 R.V. Parish, B.P. Howe, J.P. Wright, J. Mack and R.G. Pritchard, *Inorg. Chem.*, 35 (1996) 1659.
- 4 J. Vicente, M. Bermudez, F. Carrion, P.G. Jones, *Chem. Ber.*, 129 (1996) 1301.
- 5 R.V. Parish, J. Mack, L. Hargreaves, J.P. Wright, R.G. Buckley, A.M. Elsome, S.P. Fricker, B.R.C. Theobald, *J. Chem. Soc., Dalton Trans.*, (1996) 69.
- 6 J. Vicente, M.T. Chicote, M.D. Bermúdez, *J. Organomet. Chem.*, 268 (1984) 191.
- 7 P.A. Bonnardel, R.V. Parish, R.G. Pritchard, *J. Chem. Soc., Dalton Trans.*, (1996) 3185.
- 8 F. Bonati, A. Burini and B.R. Pietroni, *J. Organomet. Chem.*, 317 (1986) 121.
- 9 D.M.L. Goodgame, C.A. O'Mahoney, S.D. Plank and D.J. Williams, *Polyhedron*, 12 (1993) 2705.
- 10 E. Colacio, A. Romerosa, J. Ruiz, P. Román, J.M. Gutiérrez-Zorrilla, and M. Martínez-Ripoll, *J. Chem. Soc., Dalton Trans.*, (1989) 2323.
- 11 P. Lange, A. Schier, J. Riede and H. Schmidbaur, *Z. Naturforsch.*, 49b (1994) 642.
- 12 J. Hanss and H.J. Krüger, *Angw. Chem. Int. Ed. Engl.*, 32 (1996) 2827.
- 13 R. Ruiz, C. Surville-Barland, A. Aukauloo, E. Anxolabehere-Mallart, Y. Journaux, J. Cano and M.C. Muñoz, *J. Chem. Soc., Dalton Trans.*, (1997) 745.
- 14 T. Cheung, T. Lai, C. Che, *Polyhedron*, 13 (1994) 2073.
- 15 F. Paul, J. Fischer, P. Oschenbein and J.A. Osborn, *Angw. Chem. Int. Ed. Engl.*, 32 (1993) 1638.
- 16 W. Henderson, A.G. Oliver and B.K. Nicholson, unpublished results.
- 17 M.R. Gregg, J. Powell and J.F. Sawyer, *Acta Crystallogr. Sect. C*, 44 (1988) 43.
- 18 T.G. Appleton, H.C. Clark and L.E. Manzer, *Coord. Chem. Rev.*, 10 (1973) 335.
- 19 K.M. Mackay, R.A. Mackay, *Introduction to Modern Inorganic Chemistry*, 4th Ed., Blackie, Glasgow and London, (1989).
- 20 R. Colton, A. D'Agostino and J.C. Traeger, *Mass Spectrom. Rev.*, 14 (1995) 79.

- 21 L.J. McCaffrey, W. Henderson, B.K. Nicholson, J.E. Mackay and M.B. Dinger, *J. Chem. Soc., Dalton Trans.*, (1997) 2577.
- 22 G.M. Sheldrick, SHELXS-96, Program for Solving X-Ray Crystal Structures, University of Göttingen, Germany, (1996).
- 23 G.M. Sheldrick, SHELXL-96, Program for Refining X-Ray Crystal Structures, University of Göttingen, Germany, (1996).

Chapter Six

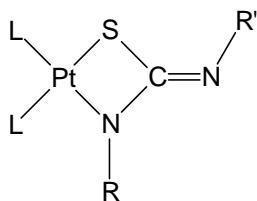
Reactions of Gold(III) Dihalide Complexes with Thioureas

6.1 Introduction

Thioureas and selenoureas, of the general formula $R^1R^2N-C(X)-NR^3R^4$, ($X = S, Se$) are interesting hybrid ligands, containing both hard (nitrogen) and soft (sulfur or selenium) donor atoms, and are therefore able to co-ordinate to a wide range of metal centres.¹ Such ligands are well-known to co-ordinate to metal centres either as neutral ligands¹⁻⁸ or as monoanions.^{1,9-15} In marked contrast however, complexes derived from thiourea dianions, containing the $\overline{M-NR-C(NR')-S}$ metallacycle, are much rarer.

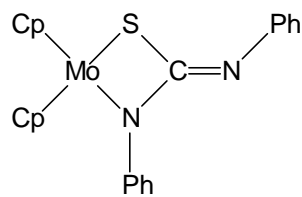
As already stated in Chapter One (Section 1.3.5), the platinum(II) complexes **1.81** (Figure 6.1) were readily formed from the silver(I) oxide mediated reactions of *cis*-[PtCl₂L₂] (L = tertiary phosphine) with N,N'-diphenylthiourea (thiocarbanilide)¹⁶ or the sodium salt of 1-cyano-3-methylisothiourea.¹⁷ The reaction of [Pt(hfac)(PPh₃)₂] (hfac = 1,1,1,5,5,5-hexafluoro-2,4-pentanedionate) with diethylthiourea also gave a thioureato complex.¹⁸

In addition to these platinum(II) examples, the molybdenum complex **6.1** could be synthesised from [Cp₂MoS₂] with di-*p*-tolylcarbodiimide in the presence of trimethylphosphine.¹⁹ Complexes derived from the cyclic thiourea 2-thiouracil (and related systems), also containing the $\overline{M-NR-C(NR')-S}$ metallacycle, have been synthesised. Numerous cobalt(II) derivatives of the type **6.2** (Figure 6.2) have been prepared,²⁰ and the tungsten(V) thiouracilate **6.3** has also been reported.²¹



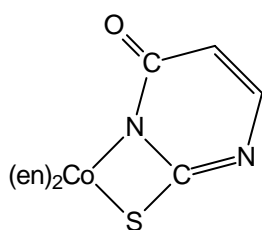
1.81 R = R' = Ph, Et; R = Me, R' = CN

L = tertiary phosphines

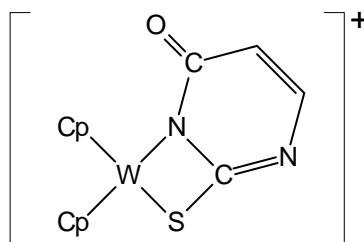


6.1

Figure 6.1



6.2 en = 1,2-diaminoethane



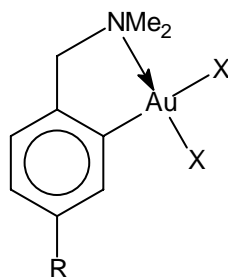
6.3

Figure 6.2

The ready formation of the gold(III) ureylene complexes **5.8a** and **5.8b** (Chapter Five), analogous to the respective platinum(II) ureylene complexes **2.22a/2.22b** and **2.22h** (Chapter Two), led us to investigate if the gold(III) dihalide complexes **5.1a** and **5.1b** could also form complexes derived from the thiourea dianion analogous to **1.81**. This chapter reports studies on the reactions of the cyclometallated complexes **5.1a**, **5.1b** and some related complexes, with disubstituted thioureas and with N,N'-diphenylselenourea, mediated by silver(I) oxide.

6.2 Results and Discussion

The reactions of the gold(III) dichloride **5.1a/5.1b** and dibromide **6.4a/6.4b** complexes (Figure 6.3) with N,N'-dimethylthiourea and an excess of silver(I) oxide in refluxing dichloromethane rapidly (*ca.* 5 minutes) led to bright yellow solutions. The mixtures were reacted for a further four hours from which bright yellow crystals could be obtained. From preliminary ^1H and ^{13}C NMR of the crude reaction residues, it was immediately obvious that



5.1a X = Cl, R = OMe

5.1b X = Cl, R = H

6.4a X = Br, R = OMe

6.4b X = Br, R = H

Figure 6.3

complexes derived from the thiourea dianion analogous to those of **1.81** and **6.1** had not formed, by the absence of the dual methyl resonances expected for the $\overline{\text{M-NMe-C(NMe)-S}}$ metallacycle.

The crystals were eventually fully characterised by ^1H and ^{13}C NMR, electrospray mass spectrometry (ESMS), elemental analysis, and single crystal X-ray diffraction studies, as the gold(III)-sulfide-silver(I)-halide aggregates **6.5a–6.5d** (Figure 6.4) from the respective starting materials **5.1a**, **5.1b**, **6.4a** and **6.4b**. The synthesis of the analogous diiodide-bridged aggregate was not attempted, because of the difficulty in the isolation and manipulation of the starting gold(III) diiodide (Figure 6.5) which was apparently exceedingly light-sensitive.

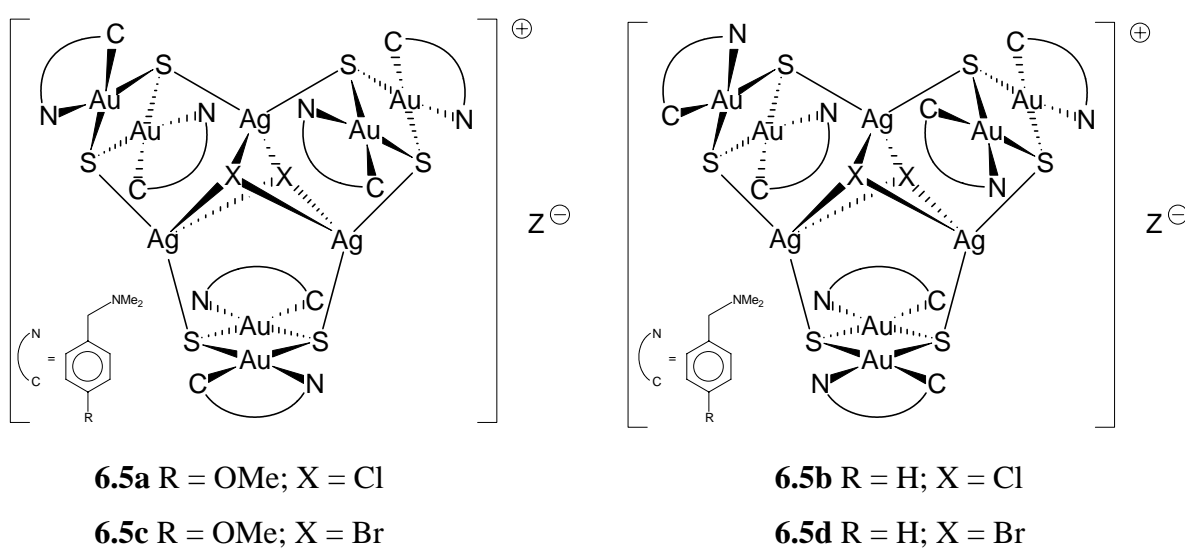


Figure 6.4

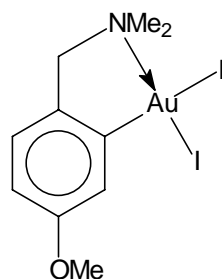
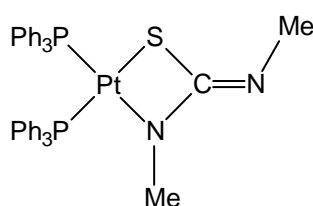


Figure 6.5

When N,N'-diphenylthiourea was reacted with **5.1a** in the presence of silver(I) oxide, the aggregate **6.5a** could also be successfully isolated. However, the reaction appeared to have poor reproducibility, with success in only one of four reaction attempts.

The synthesis of the sulfido-aggregates **6.5a-6.5d** clearly demonstrates markedly different behaviour between the formally isoelectronic platinum(II) and gold(III) centres towards thioureas; no analogous aggregate complexes have ever been observed in platinum(II) reactions with thioureas (specifically N,N'-diphenylthiourea), these always giving metallacycles of the type $\overline{\text{Pt-NR-C(NR')-S}}$. However, the silver(I) oxide mediated reaction of N,N'-dimethylthiourea with a platinum(II) halide had not been previously attempted. To verify the expected product **6.6** (Figure 6.6), the reaction of *cis*-[PtCl₂(PPh₃)₂], N,N'-dimethylthiourea and silver(I) oxide was undertaken and, as expected, **6.6** was only product formed. The ¹H NMR of complex **6.6** shows both the predicted ¹⁹⁵Pt-¹H and ³¹P-¹H couplings associated with the methyl group closest to the metal centre.

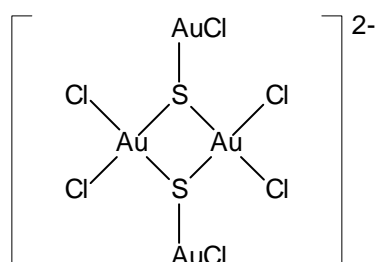


6.6

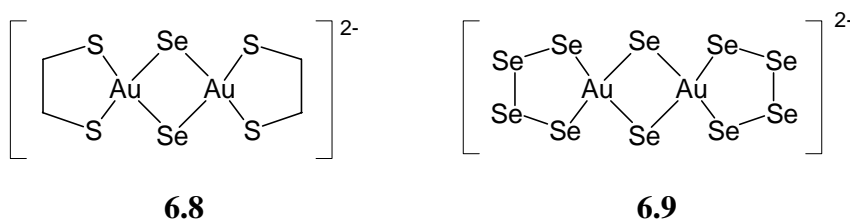
Figure 6.6

Complexes containing μ -sulfido and -selenido bridges between transition-metal centres have attracted considerable interest for their structures,²² nucleophilicity towards alkylation,²³ catalytic activities²⁴ and ability to act as “metallo-ligands” towards other metal centres, building up unusual sulfido-bridged co-ordination assemblies.²⁵⁻²⁷ A large number of complexes containing the dimeric metal(II)-sulfido/selenido unit $\text{M}(\mu\text{-X})_2\text{M}$ units (M = Pd or Pt; X= S, Se) are known,²⁸⁻³⁰ and these units have been employed in syntheses of a diverse

range of heterobimetallic complexes.³¹⁻⁴⁰ A review describing the chemistry of platinum sulfide polynuclear complexes has recently been published.⁴¹ To the best of our knowledge the isoelectronic gold(III) group, $\text{Au}(\mu\text{-S})_2\text{Au}$, has been described only once previously, in the mixed gold(I)-gold(III) anion $[\text{Au}_4\text{Cl}_6\text{S}_2]^{2-}$ **6.7** (Figure 6.7), isolated from the reaction between $[\text{AuCl}(\text{CO})]$, $\text{Na}(\text{SBU}^\dagger)$ and 15-crown-5 (1,4,7,10,13-pentaoxacyclopentadecane).⁴² The X-ray structure of **6.7** shows the gold(III) sulfide ring co-ordinating to two $-\text{AuCl}$ units.

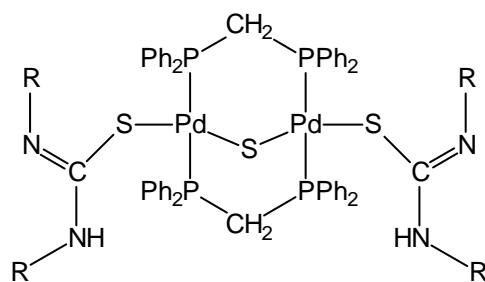
**6.7****Figure 6.7**

Additionally, two X-ray crystal structures of anions containing the related $\text{Au}(\mu\text{-Se})_2\text{Au}$ unit, in **6.8**⁴³ and **6.9**⁴⁴ have been reported, though full details on the former compound have not yet appeared. The complex **6.8** was isolated from an NaHSe , selenium, BH_4^- , and $[\text{Ph}_4\text{P}][\text{AuCl}_3\text{Br}]$ system, whereas the gold(III) polyselenide **6.9** was unexpectedly formed from Na_2Se_5 , Ph_4PCl and $[\text{AuCN}]$ in dimethylformamide solvent. Examples of gold(III) dimeric complexes containing bridging thiolate ligands, of the type $\text{Au}(\mu\text{-SR})_2\text{Au}$ are also known.^{45,46}

**6.8****6.9****Figure 6.8**

The formation of the sulfide aggregates from N,N'-dimethylthiourea presumably results in the formation of dimethyl carbodiimide as a by product, which would probably be hydrolysed under the reaction conditions to give N,N'-dimethylurea, though no attempts were made to identify any by-product(s) formed. Desulfurisation reactions of thioureas by metal aggregates are well-documented in the literature,⁴⁷⁻⁴⁹ though we are aware of only one related desulfurisation reaction of a thiourea by a mononuclear complex under mild reaction

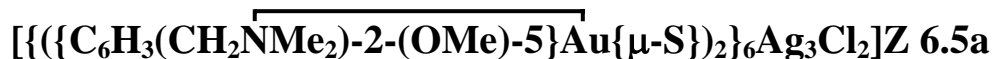
conditions. Okeya and co-workers recently reported the desulfurisation of a thiourea ligand by palladium(II), forming the sulfide-bridged dimeric complex **6.8** (Figure 6.9) which highlighted the difference between palladium and platinum systems.⁵⁰ Sulfide-bridged platinum and palladium dinuclear complexes have also been prepared by C-S bond fission reactions involving propylene sulfide⁵¹ or thiols⁵² respectively. Carbon-sulfur and carbon-selenium bond cleavage reactions have attracted interest for the formation of metal-sulfide and -selenide solid-state materials showing interesting optical and electronic properties.⁵³



6.8 R = *o*-tolyl

Figure 6.9

6.2.1 X-ray structure of



Crystals of compound **6.5a** suitable for an X-ray structure determination were obtained by layering benzene onto a chloroform solution of **6.5a** at 4°C. The compound crystallised in the rare cubic space group Pn-3n. The molecular structure of the core of the aggregate is shown in Figure 6.10 together with the atom numbering scheme. The cation lies on a two-fold axis, so there are effectively only two distinct gold “monomer” units, those formed by Au(1)/Au(2) and Au(3)/Au(3'), and these will be subsequently referred to as monomers 1 and 2 respectively. An ORTEP plot of monomer 1 is depicted in Figure 6.11, and selected bond lengths and angles are presented in Table 6.1. Tables of complete bond lengths and angles, final positional parameters and thermal parameters are presented in Appendix XI.

The aggregate consists of an assembly of three Au(μ -S)₂Au units (with each gold ligated by a cyclometallated N,N-dimethylbenzylamine ligand), with the two sulfur atoms co-ordinated to two of three silver(I) ions. The three silver ions are in turn bound by two μ_3 -chloride ligands, above and below the plane defined by the three silvers. The gold monomer units are pivoted at

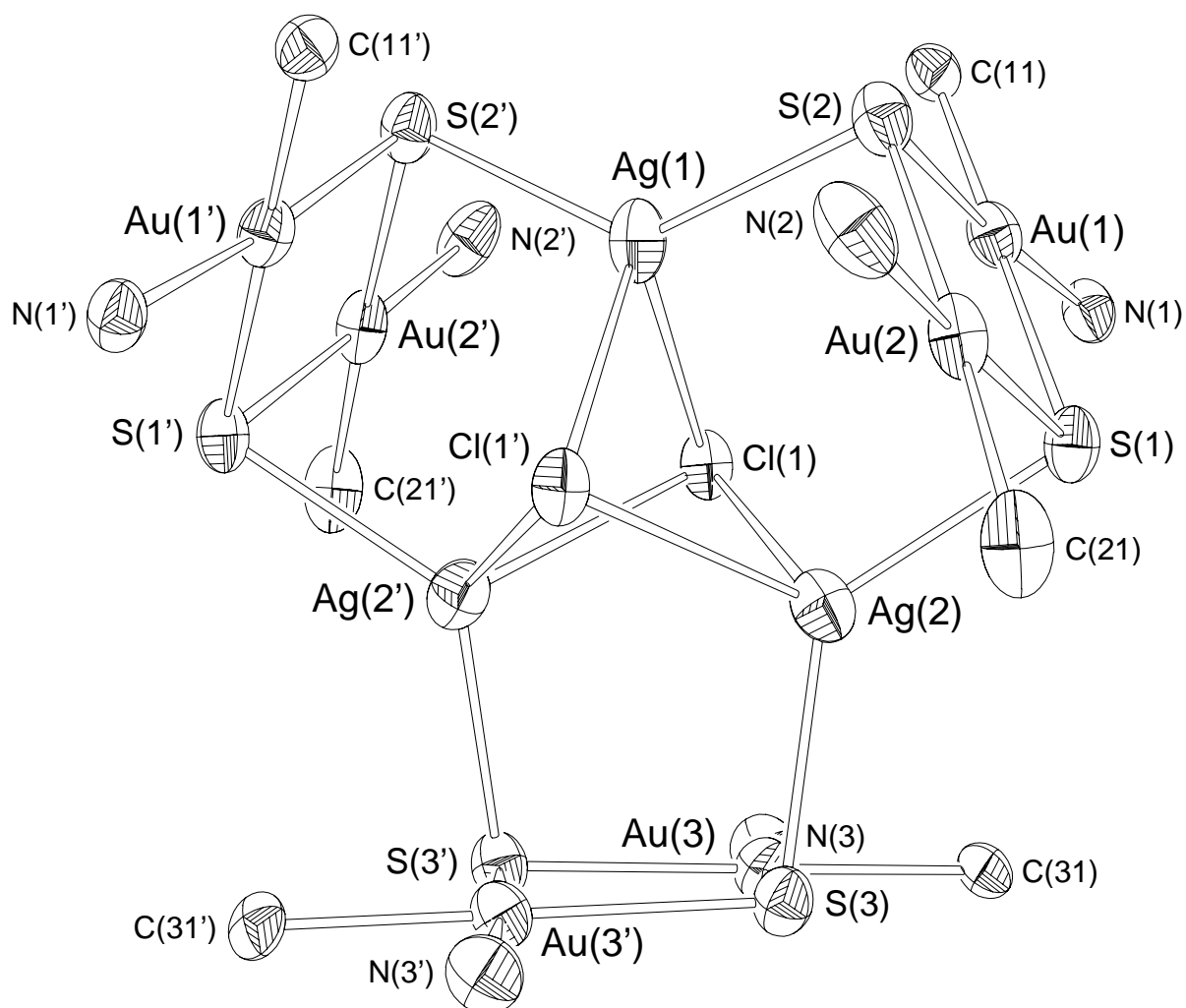


Figure 6.10: ORTEP representation of the structure of the core (only Au-bonded atoms of the *N,N*-dimethylbenzylamine ligand are shown) of the cationic aggregate **6.5a**, showing the atom numbering scheme (the ' denotes symmetry related atoms). Thermal ellipsoids are shown at the 30% probability level.

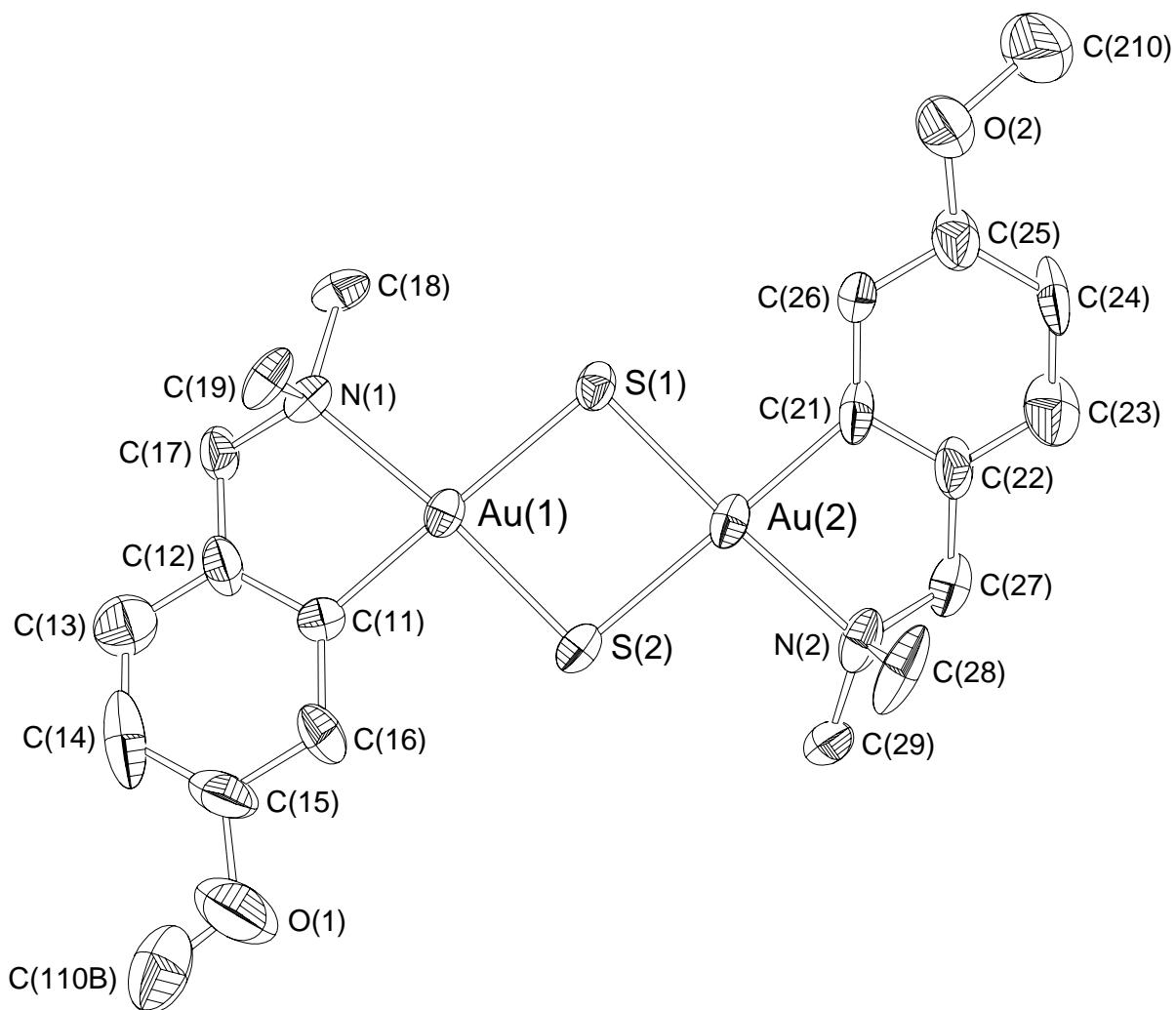


Figure 6.11: ORTEP representation of “monomer 1” (see text) from 6.5a, illustrating the trans configuration of the opposing *N,N*-dimethylbenzylamine ligands. Thermal ellipsoids are shown at the 30% probability level.

Table 6.1: Selected bond lengths (Å) and angles (°) (estimated standard deviations in parentheses) of the gold(III) aggregate cation **6.5a**.

Bond	Length	Bonds	Angle
Core			
Ag(1)-S(2)	2.512(6)	S(2)-Ag(1)-S(2')	132.9(3)
Ag(2)-S(1)	2.512(6)	S(1)-Ag(2)-S(3)	129.6(2)
Ag(2)-S(3)	2.520(7)	S(2)-Ag(1)-Cl(1)	113.1(2)
Ag(1)-Cl(1)	2.833(6)	S(2)-Ag(1)-Cl(1')	100.2(2)
Ag(2)-Cl(1)	2.854(6)	S(1)-Ag(2)-Cl(1)	98.1(2)
Ag(2)-Cl(1')	2.779(6)	S(1)-Ag(2)-Cl(1')	113.8(2)
Ag(1)...Ag(2)	3.523(4)	S(3)-Ag(2)-Cl(1)	117.9(2)
Ag(2)...Ag(2')	3.356(4)	S(3)-Ag(2)-Cl(1')	101.1(2)
Cl(1)...Cl(1')	3.976(6)	Ag(1)-Cl(1)-Ag(2)	76.5(2)
		Ag(1)-Cl(1)-Ag(2')	77.8(2)
		Ag(2)-Cl(1)-Ag(2')	73.1(2)
		Cl(1)-Ag(1)-Cl(1')	89.2(3)
		Cl(1)-Ag(2)-Cl(1')	89.8(2)
Gold sulfide monomers			
Au(1)-S(1)	2.389(6)	S(1)-Au(1)-S(2)	85.3(2)
Au(1)-S(2)	2.306(6)	S(1)-Au(2)-S(2)	85.4(2)
Au(2)-S(1)	2.302(6)	S(3)-Au(3)-S(3')	85.5(2)
Au(2)-S(2)	2.388(7)	N(1)-Au(1)-C(11)	80.8(6)
Au(3)-S(3)	2.293(6)	N(2)-Au(2)-C(21)	83.1(7)
Au(3)-S(3')	2.382(6)	N(3)-Au(3)-C(31)	80.9(6)
Au(1)-N(1)	2.15(2)	Au(1)-S(1)-Au(2)	94.7(2)
Au(2)-N(2)	2.14(2)	Au(1)-S(2)-Au(2)	94.6(2)
Au(3)-N(3)	2.13(2)	Au(3)-S(3)-Au(3')	94.4(2)
Au(1)-C(11)	1.973(11)		
Au(2)-C(21)	2.030(11)		
Au(3)-C(31)	2.034(8)		
Au(1)...Au(2)	3.451(6)		
Au(3)...Au(3')	3.432(6)		
S(1)...S(2)	3.181(6)		
S(3)...S(3')	3.174(6)		

right angles to the silver core, giving butterfly angles between least-squares planes drawn through Au(1), S(1), Au(2) and S(2) and Ag(1), S(2), S(1) and Ag(2) of $89.8(1)^\circ$ for monomer 1, and $90.0(1)^\circ$ for the analogous planes drawn through monomer 2. The silver atoms themselves are co-ordinated in a very distorted tetrahedral configuration, with an average S-Ag-S angle of $131.3(4)^\circ$, Cl-Ag-S angle of $107.4(5)^\circ$ and Cl-Ag-Cl averaging $89.5(4)^\circ$.

In contrast to the isoelectronic four-membered $\overline{\text{Pt-S-Pt-S}}$ ring systems with sulfido bridges, which have a strong propensity to adopt hinged structures,²² the monomer units in **6.5a** are essentially flat, with no atom deviating from the least-squares drawn through N(1), C(11), Au(1), S(1), S(2), Au(2), C(21) and N(2) by more than $0.080(9)$ Å above, and $0.08(1)$ Å below the plane, for C(21) and N(2) respectively. The analogous plane drawn through monomer 2 similarly shows maximum deviations of $0.10(2)$ Å for N(3) and $0.095(7)$ for S(3). This is consistent with the only related gold(III) sulfide complex **6.7**, which was found to be absolutely planar.⁴² Many of the platinum(II) bridging-sulfide complexes, where the sulfur is only two-co-ordinate, have been found to be bent. A theoretical study for these systems has suggested that the bending occurs in order to decrease through-ring antibonding interactions between in-plane sulfur *p*-orbitals.²² This is consistent with observation of sulfide-bridged systems being planar when the sulfur atoms are co-ordinated to a third moiety which presumably involves the sulfur *p*-orbitals, and explains the planarity of the gold-sulfide aggregate complexes **6a-6d**.

The N,N-dimethylbenzylamine ligands within the monomer units are co-ordinated in a *trans* configuration with respect to each other, as seen in Figure 6.11. The Au-S bond lengths [averaging $2.30(1)$ Å] *trans* to the N,N-dimethylamino group are, as expected on *trans*-influence grounds,⁵⁴ significantly shorter than those *trans* to the aryl carbons [$2.39(1)$ Å]. The S-Au-S angle in **6.5a** has an average value of $85.4(3)^\circ$, compared to $82.91(9)^\circ$ for **6.7**.⁴² Likewise the average Au-S-Au angles of **6.5a** [$94.6(3)^\circ$] resemble the Au-S-Au angle of **6.7** [$97.09(9)^\circ$]. The very different *trans*-influence groups of **6.5a** (N and C) and **6.7** (Cl), render bond-length comparisons unjustified.

While the identity of the aggregate cation in **6.5a** is unambiguous, also strongly supported by electrospray mass spectrometry (Section 6.2.3.2), the identity of the counter-anion (*Z*⁻) is not wholly certain. Residual electron density was located as a large peak and a smaller peak about a three-fold site. Although the larger peak could be modelled reasonably well as a chloride, a better model was to assign this peak as an Ag⁺ with partial occupancy, and the smaller peak as

a partial Cl^- . This then generates a trichloroargentate(I) $[\text{AgCl}_3]^{2-}$ ion which, although rare, has been reported previously,^{55,56} and the Ag-Cl distance of 2.54(2) Å is not unreasonable for this anion. However since there are 16 of these species in the unit cell versus 24 cations, either each anion site is only two-thirds occupied or there are equal numbers of $[\text{AgCl}_3]^{2-}$ and $[\text{AgCl}_2]^-$, so that total charge in the unit cell is 24-. Both options are consistent with the elemental analysis results, and are more desirable than a lone Cl^- anion, which would give an insufficient chlorine percentage. However, the quality of the data did not allow the nature of the anion to be unambiguously defined, and so the structural determination of the bromide analogue **6.5d** was also undertaken.

6.2.2 X-ray structure of $[\{(\text{C}_6\text{H}_4(\overline{\text{CH}_2\text{NMe}_2)-2\})\text{Au}\{\mu\text{-S}\}\}_2\text{Ag}_3\text{Br}_2]\text{Z}$ **6.5d**

Crystals suitable for the X-ray study of the bromide-bridged complex **6.5d** were grown from the slow diffusion of diethyl ether into a dichloromethane solution at -20°C . The structure revealed two independent cations in the unit cell (cations 1 and 2). The core of cation 1 is shown in Figure 6.12 with one of its constituent monomer units shown in Figure 6.13, illustrating the atom numbering scheme. Since the independent cations and their constituent monomer units show essentially the same structural parameters, only data from cation 1 (Figure 6.12) and the monomer shown in Figure 6.13 will be discussed; selected bond lengths and angles are presented in Table 6.2. Tables of complete bond lengths and angles, final positional parameters and thermal parameters are presented in Appendix XII.

Unfortunately the structure did not refine particularly well ($R_1 = 0.1090$), and once again the residual electron density could not be sensibly assigned to anions. In this case only relatively small peaks remained which probably preclude anions derived from Ag^+ or Br^- . The only sensible suggestion appears to be OH^- , although elemental analysis results suggest something heavier. For both these structures, **6.5a** and **6.5d**, it seems that the anion is determined by the packing of the very large cations. The associated anions are then accommodated within the gaps between the cations in poorly defined regions. The actual anions in any given preparation are those available in solution and could well vary from preparation to preparation. Some attempts were made to produce aggregate complexes with specific counter-anions such as BPh_4^- , but these did not lead to suitable single crystals.

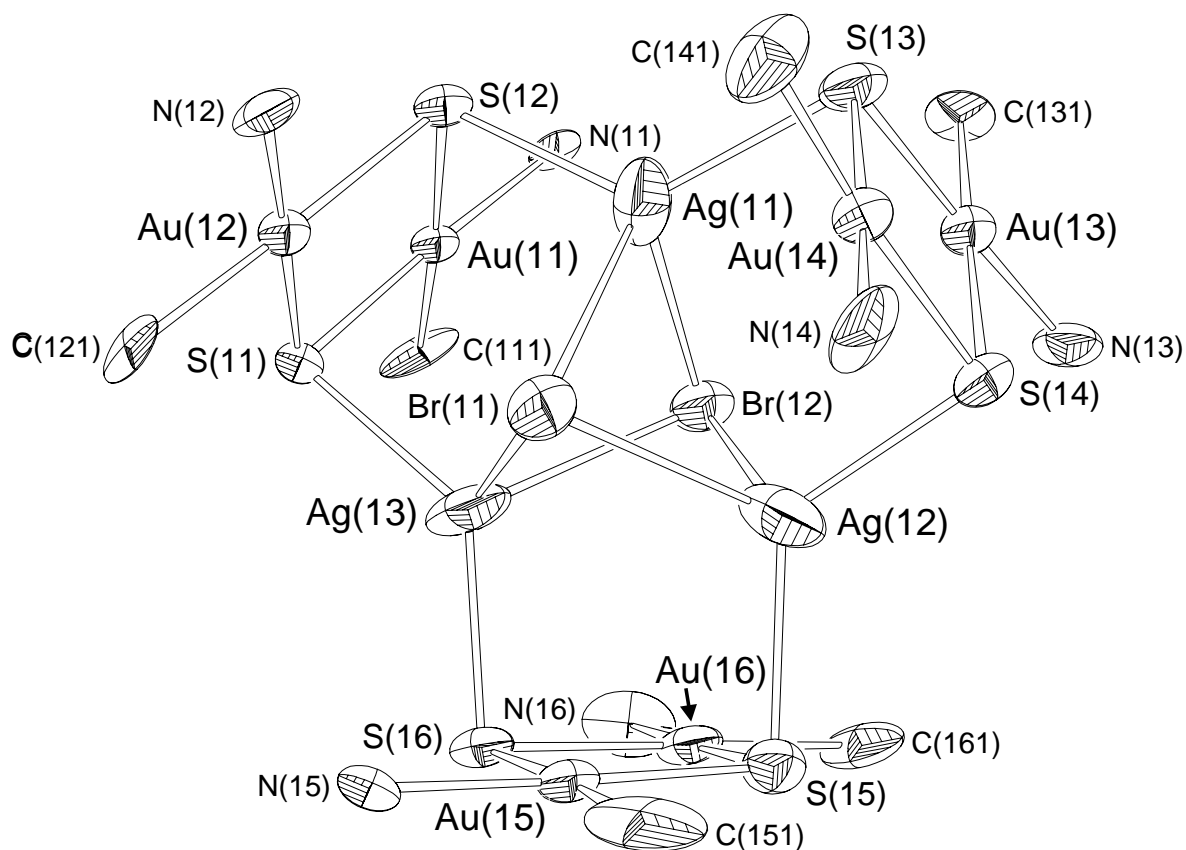


Figure 6.12: ORTEP representation of the structure of the core (only Au-bonded atoms of the *N,N*-dimethylbenzylamine ligand are shown) of the cationic aggregate **6.5d**, showing the atom numbering scheme. Thermal ellipsoids are shown at the 30% probability level.

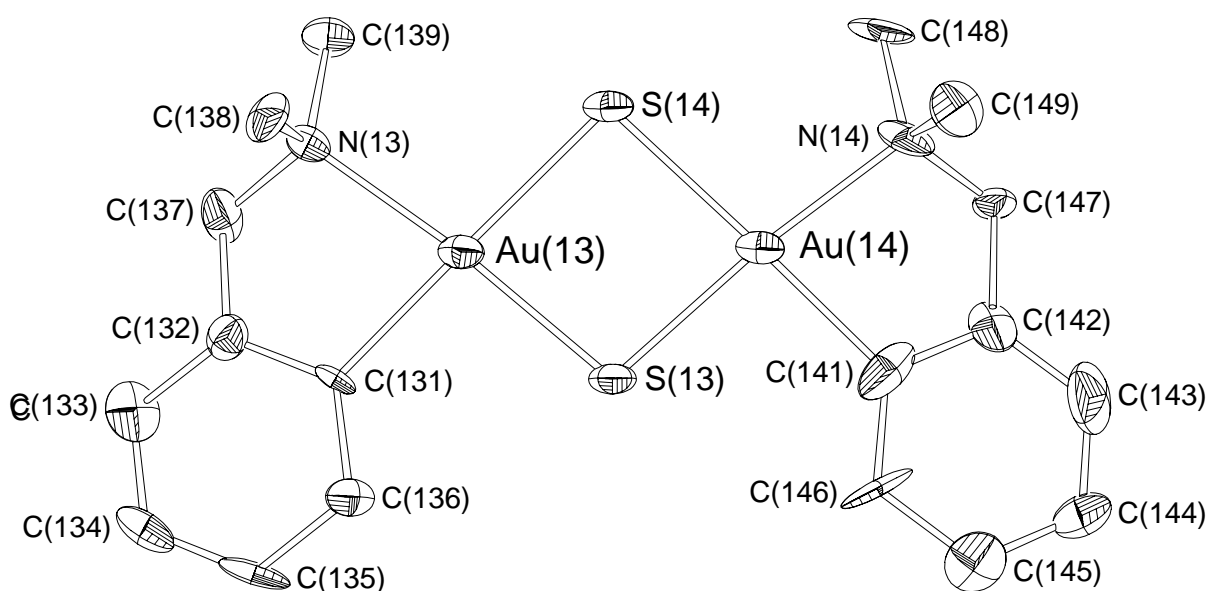


Figure 6.13: ORTEP representation of one of the monomer units from **6.5d**, illustrating the *cis* configuration of the opposing *N,N*-dimethylbenzylamine ligands. Thermal ellipsoids are shown at the 30% probability level.

Table 6.2: Selected bond lengths (Å) and angles (°) (estimated standard deviations in parentheses) for **6.5d**, specifically for cation **1** and for the monomer unit shown in Figure 6.11.

Bond	Length	Bonds	Angle
Core			
Ag(11)-S(12)	2.494(8)	S(12)-Ag(11)-S(13)	129.5(3)
Ag(11)-S(13)	2.520(10)	S(12)-Ag(11)-Br(11)	105.1(2)
Ag(11)-Br(11)	2.929(5)	S(12)-Ag(11)-Br(12)	103.3(2)
Ag(11)-Br(12)	2.952(5)	Ag(11)-Br(11)-Ag(12)	74.4(1)
Ag(11)...Ag(12)	3.502(5)	Ag(11)-Br(12)-Ag(12)	73.7(1)
Ag(11)...Ag(13)	3.708(5)	Br(11)-Ag(11)-Br(12)	89.4(1)
Ag(12)...Ag(13)	3.457(5)		
Br(11)...Br(12)	4.135(6)		
Gold sulfide monomer			
Au(13)-S(13)	2.304(8)	S(13)-Au(13)-S(14)	84.9(3)
Au(13)-S(14)	2.410(8)	S(13)-Au(14)-S(14)	84.8(3)
Au(14)-S(13)	2.304(8)	N(13)-Au(13)-C(131)	81.0(7)
Au(14)-S(14)	2.411(8)	N(14)-Au(14)-C(141)	81.3(9)
Au(13)-N(13)	2.17(3)	Au(13)-S(13)-Au(14)	97.9(3)
Au(14)-N(14)	2.12(3)	Au(13)-S(14)-Au(14)	92.3(3)
Au(13)-C(131)	2.08(1)		
Au(14)-C(141)	2.05(1)		
Au(13)...Au(14)	3.476(8)		
S(13)...S(14)	3.182(8)		

Despite the high *R* factor, the cation core is nonetheless well-defined, and a number of structural features are noteworthy. The core of the cation **6.5d** is directly analogous to **6.5a**, as predicted, with two triply-bridging bromides bonding the silver atoms. Similar to those in **6.5a**, the monomer gold sulfide units are co-ordinated at right angles with planes drawn through Au(13), S(13), Au(14) and S(14) and Ag(11), S(13), S(14) and Ag(12) forming an angle of 87.8(1)°. The monomer units themselves are essentially planar, exemplified by the least-squares plane drawn through N(13), Au(13), C(131), S(13), S(14), Au(14), C(141) and N(14) which shows maximum deviations of 0.10(1) Å above [for C(141)] or 0.10(1) Å below the plane [for S(13)].

The most structurally startling feature of **6.5d** is that the benzylamine ligands in the monomer units in this cation are co-ordinated *cis* with respect to each other (Figure 6.13), in contrast to those in **6.5a** which are *trans* (Figure 6.11). There is no obvious explanation for the difference, so presumably there is little preference for *cis* or *trans* configurations of the benzylamine ligands in the monomer formation. We believe that cations containing only *cis* and cations containing only *trans* monomer units both form in solution (evidenced by the detection of two species in the crude reaction mixture by NMR (Section 6.2.3.1), but only one **6.5** aggregate crystallises out in each case, presumably determined by their relative solubilities and concentrations (yields for **6.5a-6.5d** were less than 60%). Hence, during the aggregation process the nature (*cis* or *trans*) of the first monomer unit directs the “selection” of subsequent monomer units for the trimer formation.

Since the crystals of aggregate ions when dissolved in CDCl₃ are (and remain) pure, together with the observation that the complexes appear to be very stable in ESMS studies, the aggregation process is most likely essentially irreversible. The complete mechanism for their formation is not obvious.

Like those for **6.5a**, the Au-S bonds *trans* to N are significantly shorter than those *trans* C, with average lengths of 2.30(1) and 2.41(1) Å respectively, although in this case they are *cis* relative to each other. The remainder of the structural parameters (where justified) are comparable to those of **6.5a**.

6.2.3 Spectroscopic and mass spectrometric characterisation

6.2.3.1 NMR characteristics

As already mentioned, the ¹H and ¹³C NMR spectra of the isolated crystalline products, revealed them to be very pure. As expected, the presence of NMe groups and CH₂ protons pointing above and below the plane of the monomers (with respect to the silver-halide core) results in the inequivalence of these signals in the ¹H and ¹³C NMR spectra. For **6.5a** the N,N-dimethylamino protons are split by 0.44 ppm and the carbons by 1.1 ppm. Similarly, the methylene protons are split by 0.73 ppm, and show mutual ²J coupling of 13.22 Hz.

Analysis of the crude reaction products of **6.5a-6.5d** showed a second complex (*ca.* 30-50% NMR yield), with spectroscopic properties very similar to those of the isolated complexes. The structure of these complexes has not been confirmed, but in light of the structures of **6.5a**

and **6.5d**, probably arise from the corresponding aggregate (derived from all *cis* or all *trans* monomer units) not isolated in the recrystallisation process.

The elucidation of the structures **6.5a** and **6.5d** also allows tentative structural assignment of **6.5b** and **6.5c** by NMR. Since the bridging halides are probably too far removed (four bonds to Au-C, the nearest NMR active nucleus) from the benzylamine ligands, the chemical shifts in the ^1H and ^{13}C NMR are likely to be dominated by the *cis/trans* configurations of the ligands. The ^1H and ^{13}C spectra for the isolated crystalline aggregates **6.5a** and **6.5c** are virtually identical, as are the spectra for **6.5b** and **6.5d**. It is therefore proposed that the complex **6.5b** collected (like **6.5d**) is also a *cis* isomer, and the aggregate **6.5c** (like **6.5a**) is a *trans* isomer, as shown in Figure 6.4.

6.2.3.2 Electrospray mass spectrometry (ESMS)

ESMS is being increasingly used for the characterisation of a diverse range of co-ordination and organometallic compounds.^{57,58} A wide range of metal-sulfur bonded compounds have been analysed by the ESMS technique to date, including metal-chalcogenide-thiolate aggregates,⁵⁹⁻⁶² a polyoxo/thioanion⁶³ and complexes of thiourea dianions.¹⁷ ESMS is ideally suited for the analysis of charged species, since pre-existing ions present in solution are simply transferred to the gaseous phase for analysis. The soft ionisation process generally results in intact parent ions being observed.

Major ions observed in the ESMS spectra of the aggregates **6.5a-6.5d** are summarised in Table 6.3. For complex **6.5a**, at cone voltages of 20-100 V, the base peak was due to the aggregate cation $[\text{M}_3\text{Ag}_3\text{Cl}_2]^+$ ($\text{M} = [\text{Au}\{\text{C}_6\text{H}_3(\text{CH}_2\text{NMe}_2)\text{-2-(OMe)-5}\}\text{S}_2]$) (Figure 6.14), and even at a high cone voltage (150 V) this remained a major ion.

The presence of one or more elements possessing more than a single isotope provides substantial information in the form of isotope distribution patterns for the ions in question. In the case of the silver-gold aggregates described in this chapter, silver (^{107}Ag 51.8, ^{109}Ag 48.2%), chlorine (^{35}Cl 75.8, ^{37}Cl 24.2%) and bromine (^{79}Br 50.7, ^{81}Br 49.3%) all possess two isotopes in reasonable abundance, giving distinctive isotope patterns for all of the aggregate cations in the complexes **6.5a-6.5d**. Excellent agreement is observed between the experimental and calculated isotope distribution patterns (exemplified for the $[\text{M}_3\text{Ag}_3\text{Cl}_2]^+$ cation of **6.5a** shown in the inset of Figure 6.14) for all species observed in the spectra of the

Table 6.3: List of ions observed in the positive ion ESMS spectra of complexes **6.5a-6.5d**. All spectra were recorded using methanol as both the solvent and mobile phase. $M = [Au(C_6H_3(CH_2NMe_2)-2-R-5)S]_2$.

Complex	Cone Voltage (V)	Ions m/z [†] (identity, relative abundance (%))
6.5a (R = OMe)	20 V	2752 ($[M_3Ag_3Cl_2]^+$, 100%), 2357 ($[M_3H]^+$, 7%), 1824 ($[M_2Ag_2Cl]^+$, 10%), 1681 ($[M_2Ag]^+$, 2%), 894 ($[MAG]^+$, 15%), 814 (unidentified, 15%).
	50 V	2752 ($[M_3Ag_3Cl_2]^+$, 100%), 1968 ($[M_2Ag_3Cl_2]^+$, 6%), 1824 ($[M_2Ag_2Cl]^+$, 8%), 894 ($[MAG]^+$, 17%).
	150 V	2752 ($[M_3Ag_3Cl_2]^+$, 59%), 1968 ($[M_2Ag_3Cl_2]^+$, 27%), 1824 ($[M_2Ag_2Cl]^+$, 13%), 1681 ($[M_2Ag]^+$, 41%), 1288 (unidentified, 92%), 164 ($[C_6H_3(CH_2NMe_2)-2-(OMe)-5]^+$, 100%).
6.5b (R = H)	30 V	2573 ($[M_3Ag_3Cl_2]^+$, 100%), 1846 ($[M_2Ag_3Cl_2]^+$, 3%), 1704 ($[M_2Ag_2Cl]^+$, 59%), 1561 ($[M_2Ag]^+$, 97%).
	100 V	2573 ($[M_3Ag_3Cl_2]^+$, 100%), 1846 ($[M_2Ag_3Cl_2]^+$, 27%), 1704 ($[M_2Ag_2Cl]^+$, 13%), 1561 ($[M_2Ag]^+$, 17%).
6.5c (R = OMe)	20 V	2842 ($[M_3Ag_3Br_2]^+$, 10%), 1681 ($[M_2Ag]^+$, 40%), 661 (unidentified, 100%).
	100 V	2842 ($[M_3Ag_3Br_2]^+$, 100%), 2056 ($[M_2Ag_3Br_2]^+$, 8%), 1681 ($[M_2Ag]^+$, 39%).
6.5d (R = H)	50 V	2662 ($[M_3Ag_3Br_2]^+$, 100%), 1936 ($[M_2Ag_3Br_2]^+$, 6%), 1749 ($[M_2Ag_2Br]^+$, 17%), 1561 ($[M_2Ag]^+$, 13%).
	100 V	2662 ($[M_3Ag_3Br_2]^+$, 100%), 1936 ($[M_2Ag_3Br_2]^+$, 48%), 1749 ($[M_2Ag_2Br]^+$, 20%), 1561 ($[M_2Ag]^+$, 51%).

[†] m/z value refers to peak of greatest intensity in the isotope distribution pattern.

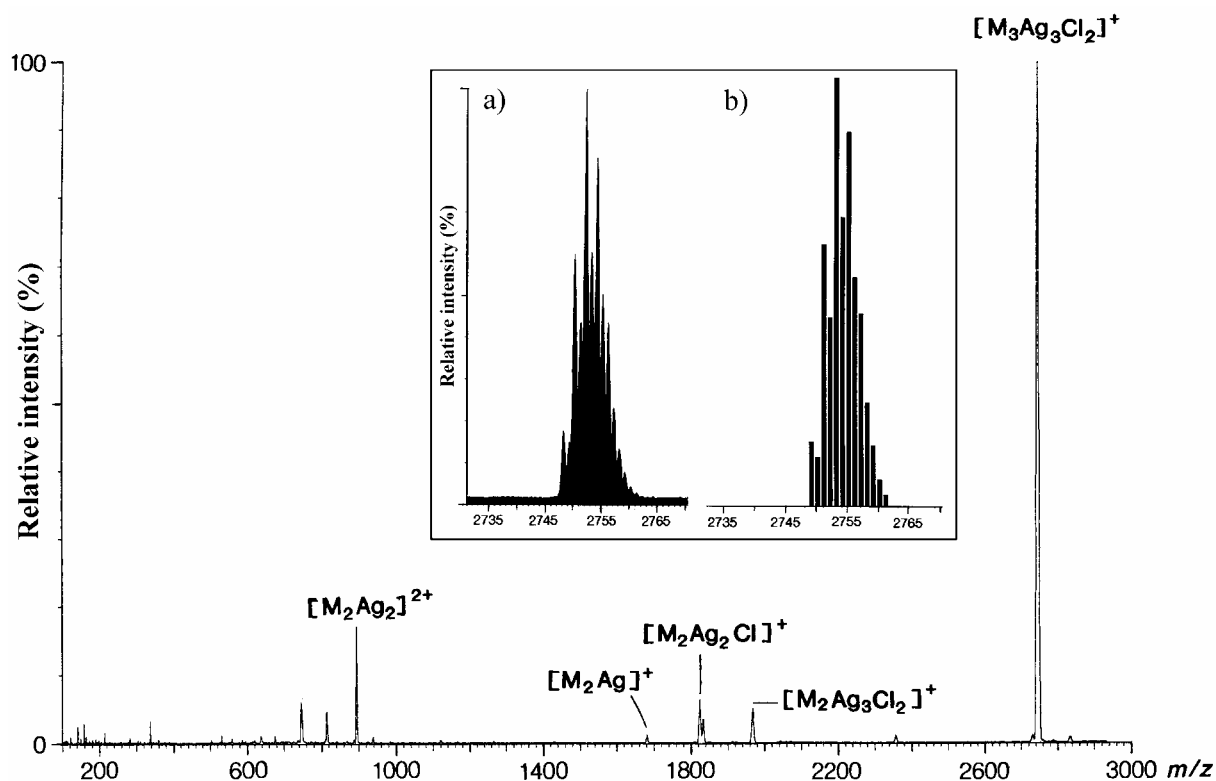


Figure 6.14: Positive-ion electrospray mass spectrum of the complex **6.5a**, recorded in methanol, at a cone voltage of 20 V. The inset shows a) the observed and b) the calculated isotope patterns of the parent ion $[M_3Ag_3Cl_2]^+$ ($M = [Au\{C_6H_3(CH_2NMe_2)-2-(OMe)-5\}S]_2$).

cations in **6.5a-6.5d**. These ESMS results indicate that the aggregate cations have very high stability. For complex **6.5a**, other easily identified minor fragment ions, such as $[M_2Ag_3Cl_2]^+$ and $[M_2Ag]^+$, which become significant only at higher cone voltages, additionally aid in characterisation, and are indicated in Figure 6.14.

Addition of lithium bromide to a solution of **6.5a** prior to injection into the mass spectrometer indicated ready displacement of the chloride ions by bromide, thereby generating the *trans* form (with respect to the opposing orientation of the benzylamine ligands) of **6.5c** *in situ*. No trace of any residual **6.5a** was detected.

6.2.4 Additional synthetic studies

6.2.4.1 Aggregate synthesis using silver(I) sulfide

To develop a more systematic synthesis of the gold-silver aggregates, it was reasoned that the reactions of the gold-dihalide complexes **5.1a**, **5.1b**, **6.4a** and **6.4b** with silver(I) sulfide might be successful. When **5.1a** and silver(I) sulfide were refluxed in dichloromethane for 28 hours, the isolated yellow residue contained at least five compounds by ^{13}C NMR, none of which corresponded to **6.5a**. Additionally ESMS showed only trace quantities of the aggregate **6.5a**, with the spectrum dominated by $[\text{M}_2\text{Ag}]^+$ (previously observed only as a fragment ion of **6.5a**). However, repeated recrystallisation of the residue by layering benzene on chloroform solutions at 4°C , eventually gave bright yellow crystals of **6.5a**, although in very low yield. A possible explanation for the relative success in forming the aggregates using the silver(I) oxide/thiourea methodology (compared to silver(I) sulfide) is the availability of solubilised silver(I) ions in the form of thiourea-silver adducts. Systems of this type have been reported previously,⁶⁴ and attempts at deprotonation with base resulted in their decomposition to silver(I) sulfide, *i.e.* thiourea desulfurisation. Analogous reactions could conceivably occur at the gold(III) metal centre, which is more electronegative than platinum(II).

6.2.4.2 Attempted synthesis of $[\{\text{C}_6\text{H}_3(\text{CH}_2\overline{\text{NMe}_2})\text{-2-R-5}\}\text{Au}(\mu\text{-S})]_2$ monomer

Since the uncomplexed $\overline{\text{Au-S-Au-S}}$ ring system could potentially provide a rich source of sulfide-bridged metal aggregates, we endeavoured to separate the Au_2S_2 monomer units from the silver-halide aggregates. Attempted abstraction/extrusion of silver from **6.5a** using sodium thiosulfate led only to decomposition of the complex to multiple compounds.

Attempts at direct synthesis of the monomer by the reaction of the dichloride complex **5.1a** with sodium sulfide (the standard preparation for the platinum(II) sulfide complexes),⁶⁵ did not afford the gold-sulfide monomer $[\{\text{C}_6\text{H}_3(\text{CH}_2\overline{\text{NMe}_2})\text{-2-(OMe)-5}\}\text{Au}(\mu\text{-S})]_2$, and resulted only in a plethora of unidentified decomposition products, observed by NMR.

6.2.4.3 Attempted synthesis of gold(III)-selenide-silver(I)-halide analogues

A preliminary investigation into the potential synthesis of gold-selenide bridged derivatives analogous to **6.5a** was undertaken. When N,N'-diphenylselenourea was refluxed with **5.1a** in the presence of silver(I) oxide, a wide range of compounds were detected, none of which

correlated with a selenium analogue (or even a fragment) of **6.5a**. Interestingly, when N,N'-diphenylselenourea was reacted with *cis*-[PtCl₂(PPh₃)₂] and silver(I) oxide in manner analogous to the preparation of **6.6**, no selenium metallacycle analogous to **1.81** formed, with ³¹P NMR showing the presence of at least seven compounds, including appreciable quantities of triphenylphosphine oxide, the latter indicative of decomposition.

6.2.5 Conclusions

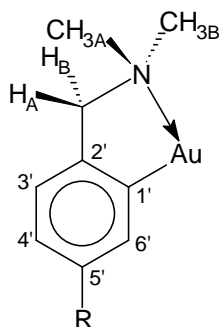
Unusual gold-sulfido-silver-halide aggregates have been synthesised by an unanticipated thiourea desulfurisation reaction. It is not unfeasible that related desulfurisation reactions from other transition metal (or main group) metal complexes might also provide new routes to heterobimetallic sulfido aggregates. Despite the ready formation of gold(III) metallacycles analogous to those formed by platinum(II) (Chapter Five), this work clearly demonstrates that the metallacyclic chemistry of gold(III) can, nonetheless, be significantly different and unpredictable. Further investigations are clearly warranted.

6.3 Experimental

General experimental procedures and the instrumentation used are given in Appendices I and II. The gold(III) precursors [$\overline{\text{Au}\{\text{C}_6\text{H}_3(\text{CH}_2\text{NMe}_2)\text{-2-R-5}\}}\text{Cl}_2$] **5.1a** (R = OMe), **5.1b** (R = H), [$\overline{\text{Au}\{\text{C}_6\text{H}_3(\text{CH}_2\text{NMe}_2)\text{-2-R-5}\}}\text{Br}_2$] **6.4a** (R = OMe) and **6.4b** (R = H) were prepared as described in Appendix I. N,N'-diphenylthiourea (BDH) was used as supplied. ESMS spectra were recorded in methanol solvent. Theoretical isotope patterns were calculated using the Isotope program.⁶⁶ Regarding elemental calculations, for the complexes **6.5a** and **6.5c** the counter-ions [AgCl₃]²⁻ and [AgBr₃]²⁻ are assumed, and for **6.5b** and **6.5d** Cl⁻ and Br⁻ have been (arbitrarily) used.

Proton and all inverse 2D NMR experiments (HMQC and HMBC) were recorded on a Bruker DRX 400 spectrometer at 400.13 MHz and 100.61 MHz for the proton and carbon channels respectively. The techniques are detailed in Appendix II. The ¹³C NMR spectra were recorded either on the instrument above at 100.61 MHz, or on a Bruker AC300 spectrometer at 75.47 MHz. All NMR analyses were carried out in CDCl₃, with the exception of the ¹³C NMR spectrum of N,N'-diphenylselenourea which was acquired in D₆-DMSO.

General NMR numbering scheme:



Preparation of *N,N'*-dimethylthiourea

Excess methylamine (BDH, 33% in ethanol) was added to an ether solution (20 ml) of methyl isothiocyanate (prepared from the reaction of methylamine, carbon disulfide and sodium hydroxide)⁶⁷ (1.0 g, 0.014 mol) and stirred at room temperature for 30 minutes. The solvents and excess methylamine were removed under reduced pressure to leave a pale yellow oil, which slowly solidified after several cycles of freeze drying. The crude product collected was pure by NMR.

¹H NMR: δ 6.61 (2H, *s*, NH), 2.84 (6H, *d*, ³J_{H,H} = 4.42 Hz, CH₃).

¹³C NMR: δ 182.1 (*s*, C=S), 30.6 (*q*, CH₃).

Preparation of *N,N'*-diphenylselenourea⁶⁸

In a Schlenk flask containing ethanol (60 ml) (which previously had been degassed and flushed with nitrogen), was added phenyl isonitrile (prepared from the reaction of aniline, bromoform and sodium hydride)⁶⁹ (2.0 g, 0.019 mol), finely powdered elemental selenium (1.84 g, 0.023 mol) and aniline (1.77g, 0.019 mol), and the mixture refluxed under nitrogen for 15 hours. Without further precautions at excluding air, the mixture was filtered to remove the excess selenium and the solvent removed under reduced pressure. The resulting residue was collected and thoroughly washed with diethyl ether to give pure *N,N'*-diphenylselenourea as a creamy grey powder (1.0 g, 19%).

m.p. 182-183°C (lit.⁶⁸ 185-186°C).

¹H NMR: δ 10.22 (2H, *s*, br, NH), 7.49 (4H, *d*, ³J_{2,3'} = 8.01 Hz, H-2',6'), 7.42 (4H, *t*, ³J_{3',2'} = 7.74 Hz, H-3',5'), 7.48 (2H, *t*, ³J_{4,3'} = 7.20 Hz, H-4').

^{13}C NMR: δ 178.6 (s, $\underline{\text{C}}=\text{Se}$), 139.7 (s, C-1'), 128.5 (d, C-2',6'), 125.2 (d, C-4'), 124.6 (d, C-3',5').

Preparation of 6.5a

To a nitrogen-flushed Schlenk flask containing dichloromethane (30 ml) was added **5.1a** (0.050 g, 0.116 mmol), N,N'-dimethylthiourea (0.013 g, 0.125 mmol), and silver(I) oxide (0.18 g, excess). The resulting mixture was stirred under reflux in dark conditions for 4 hours. Without further precautions to exclude air or light, the insoluble silver salts were filtered off, and the supernatant evaporated to dryness to give a yellow oil. This was recrystallised by liquid-liquid diffusion of benzene layered on dichloromethane at 4°C, to give bright yellow crystals of **6.5a** (0.032 g, 60%).

Alternatively, **5.1a** (0.050 g, 0.116 mmol) and silver(I) sulfide (0.15 g, excess) were refluxed in dichloromethane (30 ml) under nitrogen for 28 hours. Analysis of the crude reaction mixture by ^1H and ^{13}C NMR and ESMS indicated the presence of at least five compounds. Repeated recrystallisation from dichloromethane-benzene, eventually led to the isolation of the gold aggregate **6.5a** (0.011 g, 20%), characterised by identical NMR and ESMS spectra with an authentic sample of **6.5a**.

m.p. 155-157°C.

Found: C, 25.3; H, 3.1; N, 2.9; S, 6.5; Cl 4.9%; $[\text{C}_{60}\text{H}_{84}\text{N}_6\text{O}_6\text{S}_6\text{Au}_6\text{Cl}_2\text{Ag}_3]^{1/2}\text{AgCl}_3$ requires: C, 25.2; H, 3.0; N, 3.0; S, 6.7; Cl, 4.3%.

^1H NMR: δ 7.16 (6H, d, $^3\text{J}_{3',4'} = 8.23$ Hz, H-3'), 7.00 (6H, d, $^4\text{J}_{6',4'} = 2.49$ Hz, H-6'), 6.68 (6H, dd, $^3\text{J}_{4',3'} = 8.21$ Hz, $^4\text{J}_{4',6'} = 2.57$ Hz, H-4'), 4.41 (6H, d, $^2\text{J}_{\text{H}_\text{B},\text{H}_\text{A}} = 13.22$ Hz, NCH_B), 3.84 (18H, s, OCH₃), 3.68 (6H, d, $^2\text{J}_{\text{H}_\text{A},\text{H}_\text{B}} = 13.50$ Hz, NCH_A), 2.73 (18H, s, NCH_{3B}), 2.29 (18H, s, NCH_{3A}).

^{13}C NMR: δ 160.6 (s, C-5'), 157.6 (s, C-1'), 137.9 (s, C-2'), 124.8 (d, C-6'), 112.9 (d, C-4'), 112.2 (d, C-3'), 72.4 (t, NCH₂), 55.7 (q, OCH₃), 50.5 (q, NCH_{3B}), 49.4 (q, NCH_{3A}).

Preparation of 6.5b

In an analogous preparation to that of **6.5a**, **5.1b** (0.050 g, 0.124 mmol), N,N'-dimethylthiourea (0.013 g, 0.125 mmol), and silver(I) oxide (0.15 g, excess) were reacted for

4 hours. Subsequent work-up and recrystallisation from dichloromethane-ether, yielded **6.5b** as small yellow tetragonal shaped crystals (0.031 g, 57%).

m.p. 157-159°C.

Found: C, 24.0; H, 2.9; N, 3.3%; $[\text{C}_{54}\text{H}_{72}\text{N}_6\text{S}_6\text{Au}_6\text{Cl}_2\text{Ag}_3]\text{Cl}$ requires: C, 24.9; H, 2.8; N, 3.2%.

^1H NMR: δ 7.36 (6H, *d*, $^3J_{6',5'} = 8.00$ Hz, H-6'), 7.27 (6H, *d*, $^3J_{3',4'} = 6.11$ Hz, H-3'), 7.16 (6H, *t*, $^3J_{4',3'} = 7.19$ Hz, H-4'), 7.08 (6H, *t*, $^3J_{5',4'} = 6.53$ Hz, H-5'), 4.43 (6H, *d*, $^2J_{\text{H}_\text{B},\text{H}_\text{A}} = 13.50$ Hz, NCH_B), 3.54 (6H, *d*, $^2J_{\text{H}_\text{A},\text{H}_\text{B}} = 13.71$ Hz, NCH_A), 2.61 (18H, *s*, NCH_{3B}), 2.17 (18H, *s*, NCH_{3A}).

^{13}C NMR: δ 160.1 (*s*, C-1'), 145.7 (*s*, C-2'), 128.8 (*d*, C-6'), 127.4 (*d*, C-4'), 127.1 (*d*, C-5'), 124.3 (*d*, C-3'), 73.1 (*t*, NCH₂), 50.0 (*q*, NCH_{3B}), 48.4 (*q*, NCH_{3A}).

Preparation of 6.5c

In an analogous preparation to that of **6.5a**, **6.4a** (0.065 g, 0.125 mmol), N,N'-dimethylthiourea (0.014 g, 0.134 mmol), and silver(I) oxide (0.13 g, excess) were reacted for 4 hours. Recrystallisation from dichloromethane-ether yielded **6.5c** as thin yellow plates (0.040 g, 53%).

m.p. 178-180°C.

Found: C, 23.3; H, 2.9; N, 2.9%; $[\text{C}_{60}\text{H}_{84}\text{N}_6\text{O}_6\text{S}_6\text{Au}_6\text{Br}_2\text{Ag}_3]^{1/2}\text{AgBr}_3$ requires: C, 24.2; H, 2.9; N, 2.8%.

^1H NMR: δ 7.23 (6H, *d*, $^3J_{3',4'} = 8.19$ Hz, H-3'), 6.98 (6H, *d*, $^4J_{6',4'} = 2.40$ Hz, H-6'), 6.71 (6H, *dd*, $^3J_{4',3'} = 8.05$ Hz, $^4J_{4',6'} = 2.28$ Hz, H-4'), 4.43 (6H, *d*, $^2J_{\text{H}_\text{B},\text{H}_\text{A}} = 14.60$ Hz, NCH_B), 3.82 (18H, *s*, OCH₃), 3.51 (6H, *d*, $^2J_{\text{H}_\text{A},\text{H}_\text{B}} = 13.31$ Hz, NCH_A), 2.68 (18H, *s*, NCH_{3B}), 2.29 (18H, *s*, NCH_{3A}).

^{13}C NMR: δ 160.6 (*s*, C-5'), 157.5 (*s*, C-1'), 137.7 (*s*, C-2'), 124.8 (*d*, C-6'), 112.7 (*d*, C-4'), 112.1 (*d*, C-3'), 72.3 (*t*, NCH₂), 55.8 (*q*, OCH₃), 50.6 (*q*, NCH_{3B}), 49.1 (*q*, NCH_{3A}).

Preparation of 6.5d

In an preparation analogous to that of **6.5a**, **6.4b** (0.060 g, 0.122 mmol), N,N'-dimethylthiourea (0.013 g, 0.125 mmol), and silver(I) oxide (0.21 g, excess) were reacted for 4 hours. Subsequent work-up and recrystallisation from dichloromethane-benzene yielded **6.5d** as small yellow rectangular blocks (0.029 g, 52%).

m.p. 167-169°C.

Found: C, 22.6; H, 2.6; N, 3.2%; [C₅₄H₇₂N₆S₆Au₆Br₂Ag₃]Br requires: C, 23.7; H, 2.7; N, 3.1%.

¹H NMR: δ 7.40 (6H, *d*, ³J_{6,5'} = 7.53 Hz, H-6'), 7.25 (6H, *d*, ³J_{3',4'} = 8.30 Hz, H-3'), 7.17 (6H, *t*, ³J_{4',3'} = 6.73 Hz, H-4'), 7.09 (6H, *t*, ³J_{5',4'} = 7.16 Hz, H-5'), 4.49 (6H, *d*, ²J<sub>H_B,H_A} = 13.55 Hz, NCH_B), 3.55 (6H, *d*, ²J<sub>H_A,H_B} = 14.22 Hz, NCH_A), 2.68 (18H, *s*, NCH_{3B}), 2.24 (18H, *s*, NCH_{3A}).
¹³C NMR: δ 159.9 (*s*, C-1'), 145.6 (*s*, C-2'), 128.5 (*d*, C-6'), 127.3 (*d*, C-4'), 126.9 (*d*, C-5'), 124.3 (*d*, C-3'), 73.1 (*t*, NCH₂), 50.2 (*q*, NCH_{3B}), 48.4 (*q*, NCH_{3A}).</sub></sub>

Preparation of [Pt{SC(NMe)NMe}(PPh₃)₂] 6.6

To a flask containing dichloromethane (30 ml) was added *cis*-[PtCl₂(PPh₃)₂] (0.102 g, 0.129 mmol), N,N'-dimethylthiourea (0.014 g, 0.134 mmol) and silver(I) oxide (0.12 g, excess), and the solution refluxed for 4 hours. The silver salts were filtered off, giving a bright yellow solution. The dichloromethane was removed under reduced pressure to leave a residue which was slowly recrystallised by vapour diffusion of diethyl ether into a dichloromethane solution, to give bright yellow crystals of **6.6** (0.080 g, 75%).

Found: C, 55.6; H, 4.2; N, 3.3%. C₃₉H₃₆N₂SP₂Pt.½CH₂Cl₂ requires: C, 54.9; H, 4.3; N, 3.2%.

ESMS: (Cone voltage = 20V) *m/z* 823 ([MH]⁺, 100%). (Cone voltage = 50V) *m/z* 823 ([MH]⁺, 100%). (Cone voltage = 80V) *m/z* 823 ([MH]⁺, 100%), 759 ([Pt{C₆H₄PPh₂}(PPh₃) + MeCN]⁺, 33%), 718 ([Pt{C₆H₄PPh₂}(PPh₃)]⁺, 17%).

³¹P NMR: δ 17.0 (*d*, ²J_{P,P} = 21.2 Hz, (*d*, ¹J_{P,Pt} = 3216.8 Hz), PPh₃ *trans* S), 12.3 (*d*, ²J_{P,P} = 21.2 Hz, (*d*, ¹J_{P,Pt} = 3304.7 Hz), PPh₃ *trans* N).

¹H NMR: δ 7.45-7.15 (30H, *m*, PPh₃), 5.28 (1H, *s*, CH₂Cl₂), 2.76 (3H, *s*, C=NCH₃), 2.27 (3H, *s*, (*d*, ⁴J_{H,P} = 4.29 Hz, (*d*, ¹J_{P,Pt} = 31.21 Hz), PtNCH₃).

¹³C NMR: δ 177.0 (*s*, (*d*, ³J_{C,P} = 8.72 Hz), C=N), 134.4 (*d*, (*d*, ³J_{C,P} = 11.70 Hz), C-3,5 PPh₃), 133.8 (*d*, (*d*, ³J_{C,P} = 11.17 Hz), C-3,5 PPh₃), 131.8 (*d*, (*d*, ⁴J_{C,P} = 2.19 Hz), C-4 PPh₃), 131.5 (*d*, (*d*, ⁴J_{C,P} = 2.11 Hz), C-4 PPh₃), 128.8 (*d*, (*d*, ²J_{C,P} = 11.09 Hz), C-2,6 PPh₃), 128.6 (*s*, (*d*, ²J_{C,P} = 11.32 Hz), C-2,6 PPh₃), 36.4 (*q*, (*d*, ³J_{C,P} = 7.55 Hz), PtNCH₃), 26.5 (*q*, C=NCH₃).

6.3.1 X-ray structure determination of 6.5a

Yellow cubes suitable for X-ray crystallographic study were obtained by the slow liquid-liquid diffusion of benzene layered on a chloroform solution of **6.5a** at 4°C.

Data collection

Accurate cell parameters and intensity data were collected on Siemens SMART CCD diffractometer at Auckland University. Details regarding the collection methodology and configuration are described in Appendix II.

Collection Data: total reflections = 195914, unique reflections = 7500, range = $0.73 < \theta < 23.25^\circ$, absorption correction $T_{\text{max.}, \text{min.}} = 0.55, 0.34$.

Crystal Data: $\text{C}_{60}\text{H}_{74}\text{N}_6\text{O}_6\text{S}_6\text{Cl}_{2.83}\text{Ag}_{3.33}\text{Au}_6$, $M_r = 2809.42$, cubic, space group Pn-3n, $a = b = c = 39.6709(4) \text{ \AA}$, $U = 62433.3(11) \text{ \AA}^3$, $D_c = 1.793 \text{ g cm}^{-3}$, $Z = 24$, $F(000) = 31172$, $\mu(\text{Mo-K}\alpha) = 9.265 \text{ mm}^{-1}$.

Solution and refinement

The structure was solved by the Patterson methods option of SHELXS-96,⁷⁰ to give the gold atom positions. All further non-hydrogen atoms were located routinely (SHELXL-96)⁷¹ in subsequent difference maps, and during these full-matrix least-squares refinements based on F^2 , all non-hydrogen atoms were eventually assigned anisotropic temperature factors. All aromatic rings were modelled as rigid hexagons (bond distances 1.390 Å, bond angles 120°), with the carbon atoms attached to gold providing the pivot points. Hydrogen atoms were not included in the model. The anion was modelled as $[\text{AgCl}_3]^{2-}$, with site occupancy of 0.66 for overall neutrality. One of the methoxy groups [that bound to C(15)] was found to be disordered over two locations, each with half occupancy, and these have been denoted C(10A) and C(10B). The refinement converged with $R_1 = 0.0693$ for 5231 data with $I \geq 2\sigma(I)$, 0.1141 for all data; $wR_2 = 0.2189$ $\{w = 1/[\sigma^2(F_o^2) + (0.0891P)^2 + 2105.2412P]$ where $P = (F_o^2 + 2F_c^2)/3\}$, and $\text{GoF} = 1.160$. No parameter shifted in the final cycle. The final difference map showed no peaks or troughs of electron density greater than 2.75 and 1.22 e \AA^{-3} respectively, both adjacent to gold atoms.

6.3.2 X-ray structure determination of 6.5d

Small yellow crystals of **6.5d** suitable for an X-ray diffraction investigation were obtained by slow diffusion of diethyl ether into a dichloromethane solution of **6.5d** at -20°C .

Data collection

Accurate cell parameters and intensity data were collected on Siemens SMART CCD diffractometer at Auckland University. Details regarding the collection methodology and configuration are described in Appendix II.

Collection Data: crystal dimensions $0.52 \times 0.20 \times 0.08$, total reflections = 56055, unique reflections = 30904, range = $0.95 < \theta < 26.54^{\circ}$, absorption correction $T_{\text{max.}, \text{min.}} = 0.48, 0.27$.

Crystal Data: $\text{C}_{54}\text{H}_{72}\text{N}_6\text{S}_6\text{Br}_2\text{Ag}_3\text{Au}_6$ excluding anion, $M_r = 2662.77$, triclinic, space group $P\bar{1}$ (no. 2), $a = 12.1201(2)$, $b = 21.5804(2)$, $c = 32.6181(2)$ Å, $\alpha = 88.724(1)$, $\beta = 79.717(1)$, $\gamma = 82.704(1)^{\circ}$, $U = 8326.48(17)$ Å³, $D_c = 2.124$ g cm⁻³, $Z = 4$, $F(000) = 4876$, $\mu(\text{Mo-K}\alpha) = 12.358$ mm⁻¹.

Solution and refinement

The structure was solved by the Patterson methods option of SHELXS-96.⁷⁰ All further non-hydrogen atoms were located routinely (SHELXL-96).⁷¹ During full-matrix least-squares refinements based on F^2 , all non-hydrogen atoms were eventually assigned anisotropic temperature factors. All aromatic rings were modelled as rigid hexagons (bond distances 1.390 Å, bond angles 120°), with the carbon atoms attached to gold providing the pivot points. Hydrogen atoms were not included in the model. The refinement converged with $R_1 = 0.1090$ for 17991 data with $I \geq 2\sigma(I)$, 0.1706 for all data; $wR_2 = 0.3060$ $\{w = 1/[\sigma^2(F_o^2) + (0.1420P)^2 + 334.4861P]$ where $P = (F_o^2 + 2F_c^2)/3\}$, and $\text{GoF} = 1.029$. No parameter shifted in the final cycle. The final difference map showed a number of large peaks of electron density (maximum $7.11 \text{ e } \text{Å}^{-3}$) all of which were in close proximity to silver atoms, presumably the result of some disorder. These could not be modelled satisfactorily. The largest trough of electron density ($-3.25 \text{ e } \text{Å}^{-3}$) is adjacent to Au(15). The anions required for charge neutrality could not be located (see text).

References

- 1 *Comprehensive Coordination Chemistry*, Ed in Chief G. Wilkinson, Pergamon, Oxford, (1987) Ch. 16.6.
- 2 F.B. Stocker, M.A. Troester and D. Britton, *Inorg. Chem.*, **35** (1996) 3145.
- 3 R. Singh and S.K. Dikshit, *Acta Crystallogr.*, **C52** (1996) 635.
- 4 D. Fregona, R. Graziani, G. Faraglia, U. Caselato and S. Sitran, *Polyhedron*, **15** (1996) 2523.
- 5 C. Pakawatchai, K. Sivakumar and H.-K. Fun, *Acta Crystallogr.*, **C52** (1996) 1954.
- 6 R. Singh and S.K. Dikshit, *Polyhedron*, **14** (1995) 1799.
- 7 U. Bierbach and J. Reedijk, *Angew. Chem. Int. Ed. Engl.*, **33** (1994) 1632.
- 8 W. Eikens, P. G. Jones, J. Lautner and C. Thöne, *Z. Naturforsch.*, **49b** (1994) 21.
- 9 M. Lipowska, B. L. Hayes, L. Hansen, A. Taylor, Jr., and L.G. Marzilli, *Inorg. Chem.*, **35** (1996) 4227.
- 10 O. Seidelmann, L. Beyer, G. Zdobinsky, R. Kirmse, F. Dietze and R. Richte, *Z. anorg. allg. Chem.*, **622** (1996) 692.
- 11 I. Déchamps-Olivier, E. Guillon, A. Mohamadou and J.-P. Barbier, *Polyhedron*, **15** (1996) 3617.
- 12 A. Mohamadou, I. Déchamps-Olivier, and J.-P. Barbier, *Polyhedron*, **13** (1994) 3277.
- 13 E.W. Ainscough, A.M. Brodie, S.L. Ingham, T.G. Kotch, A.J. Lees, J. Lewis and J.M. Waters, *J. Chem. Soc., Dalton Trans.*, (1994) 1.
- 14 K.R. Koch, J. du Toit, M. R. Caira and C. Sacht, *J. Chem. Soc., Dalton Trans.*, (1994) 785.
- 15 U. Bodensieck, Y. Carraux, H. Stoeckli-Evans and G. Süss-Fink, *Inorg. Chim. Acta*, **195** (1992) 135.
- 16 W. Henderson, R.D.W. Kemmitt, S. Mason, M.R. Moore, J. Fawcett and D.R. Russell, *J. Chem. Soc., Dalton Trans.*, (1992) 59.
- 17 W. Henderson and B. K. Nicholson, *Polyhedron*, **15** (1996) 4015.
- 18 S. Okeya, Y. Fujiwara, S. Kawashima, Y. Hayashi, K. Isobe, Y. Nakamura, H. Shimomura and Y. Kushi, *Chem. Lett.*, (1992) 1823.
- 19 R.S. Pilato, K.A. Eriksen, E.I. Stiefel and A.L. Rheingold, *Inorg. Chem.*, **32** (1993) 3799.
- 20 K. Yamanari, K. Okusako, Y. Kushi and S. Kaizaki, *J. Chem. Soc., Dalton Trans.*, (1992) 1621.

- 21 A.R. Dias, M.T. Duarte, A.M. Galvão, M. Garcia, M. Marques and M.S. Salema, *Polyhedron*, *14* (1995) 675.
- 22 M. Capdevila, W. Clegg, P. González-Duarte, A. Jarid and A. Liedós, *Inorg. Chem.*, (1996) 35, 490. I. Dance and K. Fisher, *Prog. Inorg. Chem.*, *41* (1994) 637.
- 23 R.R. Gukathasan, R. H. Morris and A. Walker, *Can. J. Chem.*, *61* (1983) 2490.
- 24 M.R. Dubois, *Chem. Rev.*, *89* (1989) 1.
- 25 L.C. Roof and J. W. Kolis, *Chem. Rev.*, *93* (1993) 1037.
- 26 J. Wachter, *Angew. Chem. Int. Ed. Engl.*, *28* (1989) 1613.
- 27 B. Krebs and G. Henkel, *Angew. Chem. Int. Ed. Engl.*, *30* (1991) 769.
- 28 J. Chatt and D.M.P. Mingos, *J. Chem. Soc. A.*, (1970) 1243.
- 29 A. Bencini, M. Di Vaira, R. Morassi, P. Stoppioni and F. Mele, *Polyhedron*, *15* (1996) 2079.
- 30 V.W.-W. Yam, P. K.-Y. Yeung, and K.-K. Cheung, *J. Chem. Soc., Chem. Commun.*, (1995) 267.
- 31 L. Huang, A.L. Tan, K.F. Mok, T.C.W. Mak, A.S. Batsanov, J.A.K. Howard and T.S.A. Hor, *J. Am. Chem. Soc.*, *119* (1997) 11006.
- 32 M.S. Zhou, A.L. Tan, Y. Xu, C-F. Lam, P-H. Leung, K.F. Mok, L-L Koh and T.S.A. Hor, *Polyhedron*, *16* (1997) 2381.
- 33 H. Liu, A.L. Tan, Y. Xu, K.F. Mok, and T.S.A. Hor, *Polyhedron*, *16* (1997) 377.
- 34 M.S. Zhou, P-H. Leung, K.F. Mok and T. S. A. Hor, *Polyhedron*, *15* (1996) 1737.
- 35 G. Li, S. Li, A.L. Tan, W.-H. Yip, T.C.W. Mak, and T.S.A. Hor, *J. Chem. Soc., Dalton Trans.*, (1996) 4315.
- 36 H. Liu, A.L. Tan, K.F. Mok, and T.S.A. Hor, *J. Chem. Soc., Dalton Trans.*, (1996) 4023.
- 37 M. Zhou, P.-H. Leung, K.F. Mok, and T.S.A. Hor, *Polyhedron*, *15* (1996) 1737.
- 38 C.H. Chin and T.S.A. Hor, *J. Organomet. Chem.*, *509* (1996) 101.
- 39 M. Zhou, Y. Xu, A.-M. Tan, P.-H. Leung, K.F. Mok, L.-L. Koh and T.S.A. Hor, *Inorg. Chem.*, *34* (1995) 6425.
- 40 M. Zhou, Y. Xu, C.-F. Lam, P.-H. Leung, L.-L. Koh, K.F. Mok, and T.S.A. Hor, *Inorg. Chem.*, *33* (1994) 1572.
- 41 T.S.A. Hor, *J. Cluster Sci.*, *7* (1996) 263.
- 42 D.B. Dell'Amico, F. Calderazzo, N. Pasqualetti, R. Hübener, C. Maichle-Mössmer and J. Strähle, *J. Chem. Soc., Dalton Trans.*, (1995) 3917.

- 43 B. Krebs and G. Henkel, *Angew. Chem. Int. Engl.*, *30* (1991) 769.
- 44 M. Kanatzidis and S.-P. Huang, *Inorg. Chem.*, *28* (1989) 4667.
- 45 H.W. Chen, C. Pappas and J.P. Fackler, Jr., *Inorg. Chim. Acta*, *96* (1985) 137.
- 46 S. Wang and J.P. Fackler, Jr., *Inorg. Chem.*, *29* (1990) 4404.
- 47 L.A. Hoferkamp, G. Rheinwald, H. Stoeckli-Evans and G. Süss-Fink, *Organometallics*, *15* (1996) 704.
- 48 L. Hoferkamp, G. Rheinwald, H. Stoeckli-Evans and G. Süss-Fink, *Inorg. Chem.*, *34* (1995) 5786.
- 49 G. Süss-Fink, U. Bodensieck, L. Hoferkamp, G. Rheinwald and H. Stoeckli-Evans, *J. Cluster Sci.*, *3* (1992) 469.
- 50 S. Okeya, H. Kameda, H. Kawashima, H. Shimomura, T. Nishioka and K. Isobe, *Chem. Lett.*, (1995) 501.
- 51 A.L. Balch, L.S. Benner and M.M. Olmstead, *Inorg. Chem.*, *18* (1979) 2996.
- 52 N. Hadj-Bagheri, R.J. Puddephatt, L. Manojlović-Muir and A. Stefanović, *J. Chem. Soc., Dalton Trans.*, (1990) 535.
- 53 G. Kräuter, B. Neumüller, V.L. Goedken and W.S. Rees, Jr., *Chem. Mater.*, *8* (1996) 360.
- 54 T.G. Appleton, H.C. Clark and L.E. Manzer, *Coord. Chem. Rev.*, *10* (1973) 335.
- 55 G. Helgesson and S. Jagner, *Adv. Inorg. Chem.*, *35* (1991) 1.
- 56 G. Helgesson and S. Jagner, *J. Chem. Soc., Dalton Trans.*, (1993) 1069.
- 57 C.E.C.A. Hop and R. Bakhtiar, *J. Chem. Educ.*, *53* (1996) A162
- 58 R. Colton, A. D'Agostino and J. C. Traeger, *Mass Spectrom. Rev.*, *14* (1995) 79.
- 59 T. Løver, G. A. Bowmaker, W. Henderson, and R.P. Cooney, *Chem. Commun.*, (1996) 683.
- 60 T. Løver, G. A. Bowmaker, R. P. Cooney and W. Henderson, *Journal of Materials Chemistry*, *7* (1997) 647.
- 61 T. Løver, W. Henderson, G.A. Bowmaker, J. Seakins and R.P. Cooney, *Inorg. Chem.*, *36* (1997) 3711.
- 62 T. Løver, G.A. Bowmaker, J.M. Seakins, and R.P. Cooney, *Chem. Mater.*, *9* (1997) 1878.
- 63 R. Colton and J.C. Traeger, *Inorg. Chim. Acta*, *201* (1992) 153.
- 64 *Comprehensive Coordination Chemistry*, Ed in Chief G. Wilkinson, Pergamon, *5* (1987) 819.
- 65 R. Ugo, G. La Monica, S. Cenini, A. Serge, and F. Conti, *J. Chem. Soc. A*, (1971) 522.

-
- 66 L.J. Arnold, *J. Chem. Educ.*, (1992) 69, 811.
- 67 *Org. Synth. Coll. Vol. 3*, Ed. E. C. Horning, John Wiley & Sons, New York, (1967).
- 68 M. Lipp, F. Dallacker and I.M. zu Köcker, *Monatshefte für Chemie*, 90 (1959) 41.
- 69 *Organic Functional Group Preparations, Vol. III*, Ed. S.R. Sandler and W. Karo, Academic Press, London, (1989).
- 70 G.M. Sheldrick, SHELXS-96, Program for Solving X-Ray Crystal Structures, University of Göttingen, Germany, (1996).
- 71 G.M. Sheldrick, SHELXL-96, Program for Refining X-Ray Crystal Structures, University of Göttingen, Germany, (1996).

Chapter Seven

Synthesis and Characterisation of Auracyclobutan-3-one and Aurathietane-3,3-dioxide Complexes

7.1 Introduction

Four-membered ring metallacycles incorporating two metal-carbon linkages, of the type $\overline{\text{M-C-X-C}}$ (X = C, N, O, S), are abundant in the literature (see Chapter One, Section 1.2.1). Indeed these ring systems are known for the vast majority of transition-metals. The interest in the field is exemplified by the very large number of platinum(II) metallacycles which have been described over the years, including platinacyclobutanes (X = CRR') **7.1**,^{1,2} platinathietane derivatives (X = SO, SO₂) **7.2**,^{3,4} platinacyclobutanones⁵⁻⁷ (X = CO, also known as 1,3-oxodimethylenemethane complexes) **7.3** and platinaoxetanes (X = O) and azetanes (X = NR) **7.4**⁸ (Figure 7.1). Palladium(II) has a similar abundance of metallacycles.

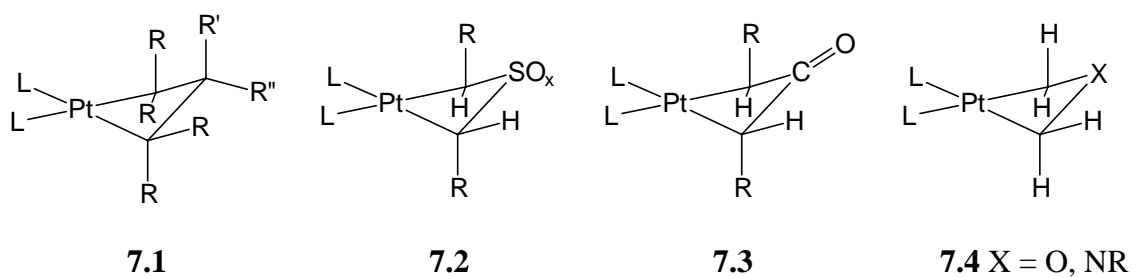
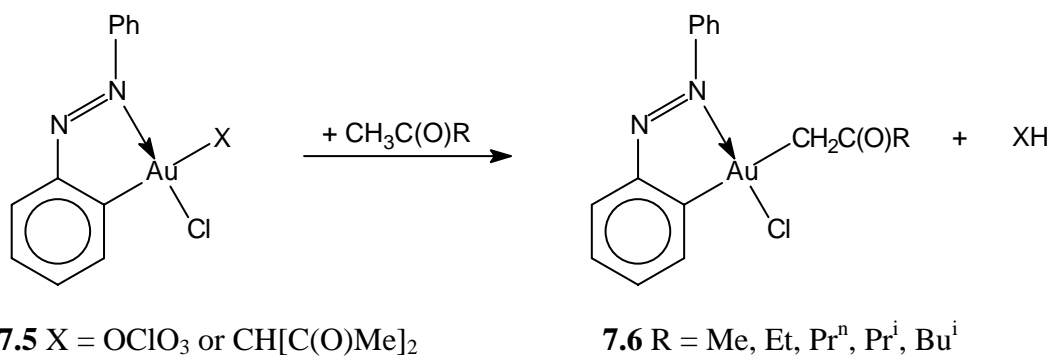


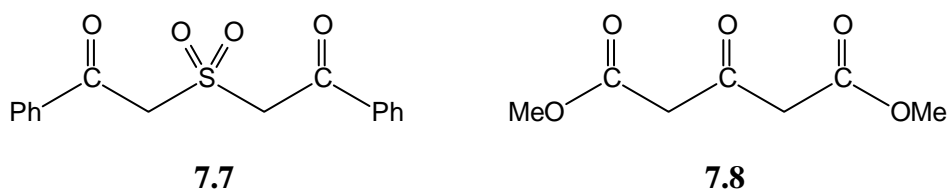
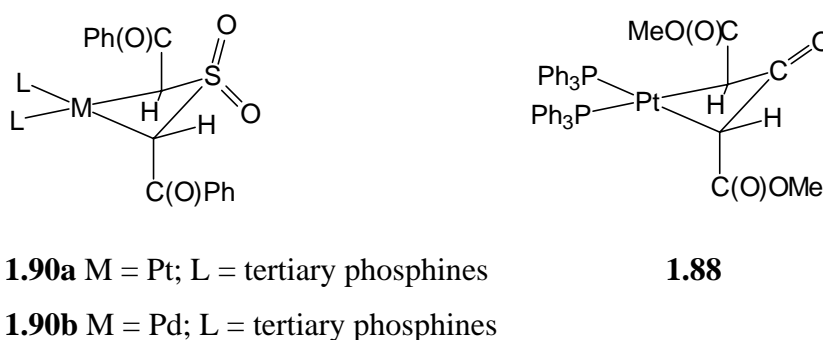
Figure 7.1

There is a paucity of information on similar gold metallacyclic complexes, indeed to the best of our knowledge no compounds containing the $\overline{\text{Au-C-X-C}}$ ring system had been previously reported. However, gold(III) has been shown to activate C-H bonds in ketones, with the orthometallated diazobenzene gold(III) complexes **7.5** reacting with a range of methyl ketones to give the ketonylgold(III) complexes **7.6** (Equation 7.1).⁹

**Equation 7.1**

The success in the syntheses of the gold(III) ureylene complexes **5.7a** and **5.7b** [using the gold(III) precursor $[\text{Au}\{\overline{\text{C}_6\text{H}_3(\text{CH}_2\text{NMe}_2)\text{-2-(OMe)-5}\}\text{Cl}_2]$ **5.1a**, as described in Chapter Five], analogous to the ureylenes found for platinum(II) (Chapter Two), suggested that this could also be an ideal precursor for the study of organogold(III) complexes containing the $\overline{\text{Au-C-X-C}}$ ring.

As detailed in Chapter One, the reaction of $[\text{MCl}_2\text{L}_2]$ (M = Pt, Pd; L = tertiary phosphines) with diphenacyl sulfone **7.7**, or *cis*- $[\text{PtCl}_2(\text{PPh}_3)_2]$ with dimethyl 1,3-acetonedicarboxylate **7.8** (Figure 7.2), in the presence of silver(I) oxide, readily gives the respective metallacyclic complexes **1.90a** and **1.88** (Figure 7.3). This chapter reports the silver(I) oxide mediated reaction of the gold(III) dihalide **5.1a** with **7.7** and **7.8**.

**Figure 7.2****Figure 7.3**

7.2 Results and Discussion

The reaction of **5.1a** with diphenacyl sulfone **7.7** in the presence of silver(I) oxide gave a white air-stable, but somewhat light-sensitive compound. This was characterised as the aurathietane-3,3-dioxide species **7.9**, on the basis of elemental microanalysis, NMR analysis, electrospray mass spectrometry, and an X-ray crystallographic study. Similarly, the reaction of **5.1a** and dimethyl 1,3-acetonedicarboxylate **7.8** afforded in high yield the auracyclobutan-3-one complex **7.10** as a pale yellow oil that resisted crystallisation. Attempted purification of **7.10** by chromatography using either silica plates or alumina columns proved futile, resulting only in substantial decomposition of the complex, evidenced by purple colloidal gold formation.

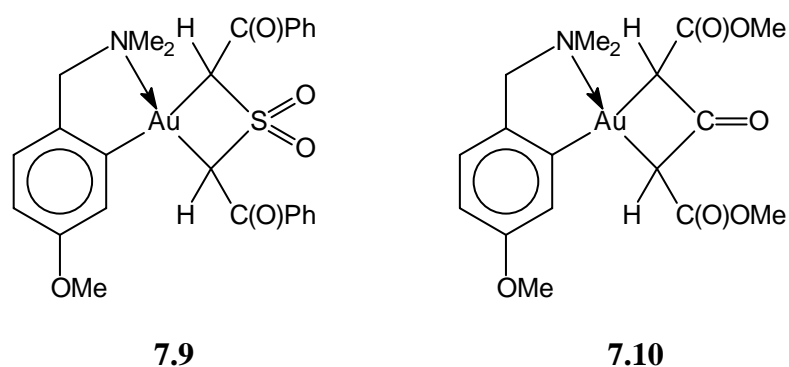
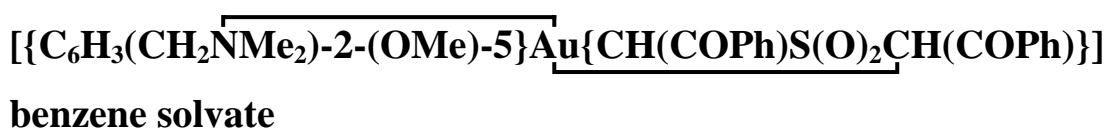


Figure 7.4

7.2.1 X-ray structure of **7.9**



The crystal structure of **7.9** was determined to fully characterise the reaction product of **5.1a** and diphenacyl sulfone **7.7**, to examine the absolute geometry of the compound, and for comparison with analogous platinum(II) and palladium(II) systems.

ORTEP perspective and side views of the final structure are shown in Figures 7.5 and 7.6 respectively, together with the atom labelling scheme. Selected bond lengths and angles for the structure are given in Table 7.1, with complete bond lengths and angles, final positional parameters, thermal parameters and calculated H-atom positions presented in Appendix XIII.

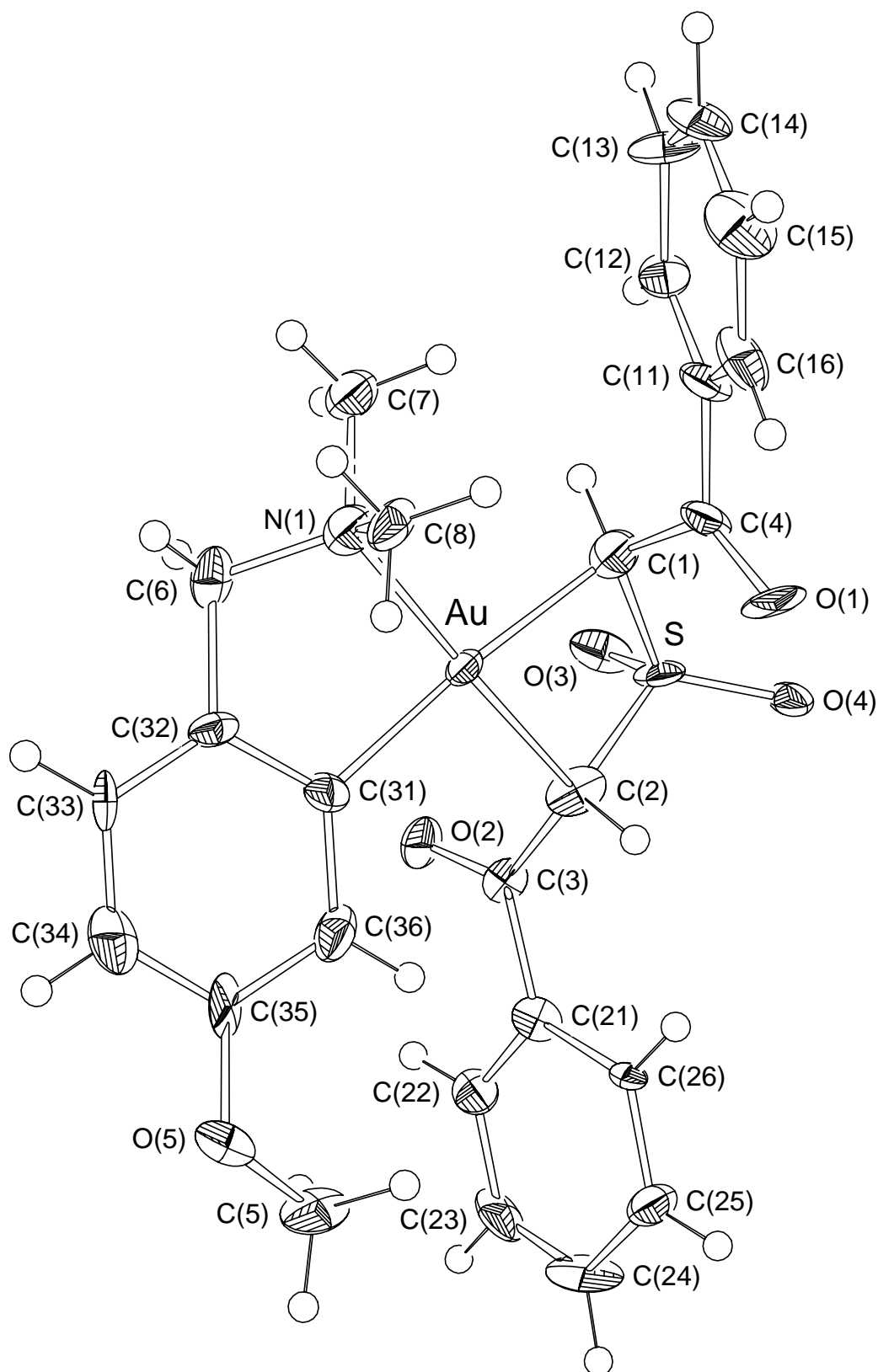


Figure 7.5: ORTEP perspective view of the structure of $[[\text{C}_6\text{H}_3(\text{CH}_2\text{NMe}_2)\text{-2-(OMe)-5}\}\text{Au}\{\text{CH(COPh)S(O)}_2\text{CH(COPh)}\}]\cdot\text{C}_6\text{H}_6$ **7.9**, showing the atom numbering scheme. Atoms are shown as thermal ellipsoids at the 50% probability level. The benzene of crystallisation has been omitted for clarity.

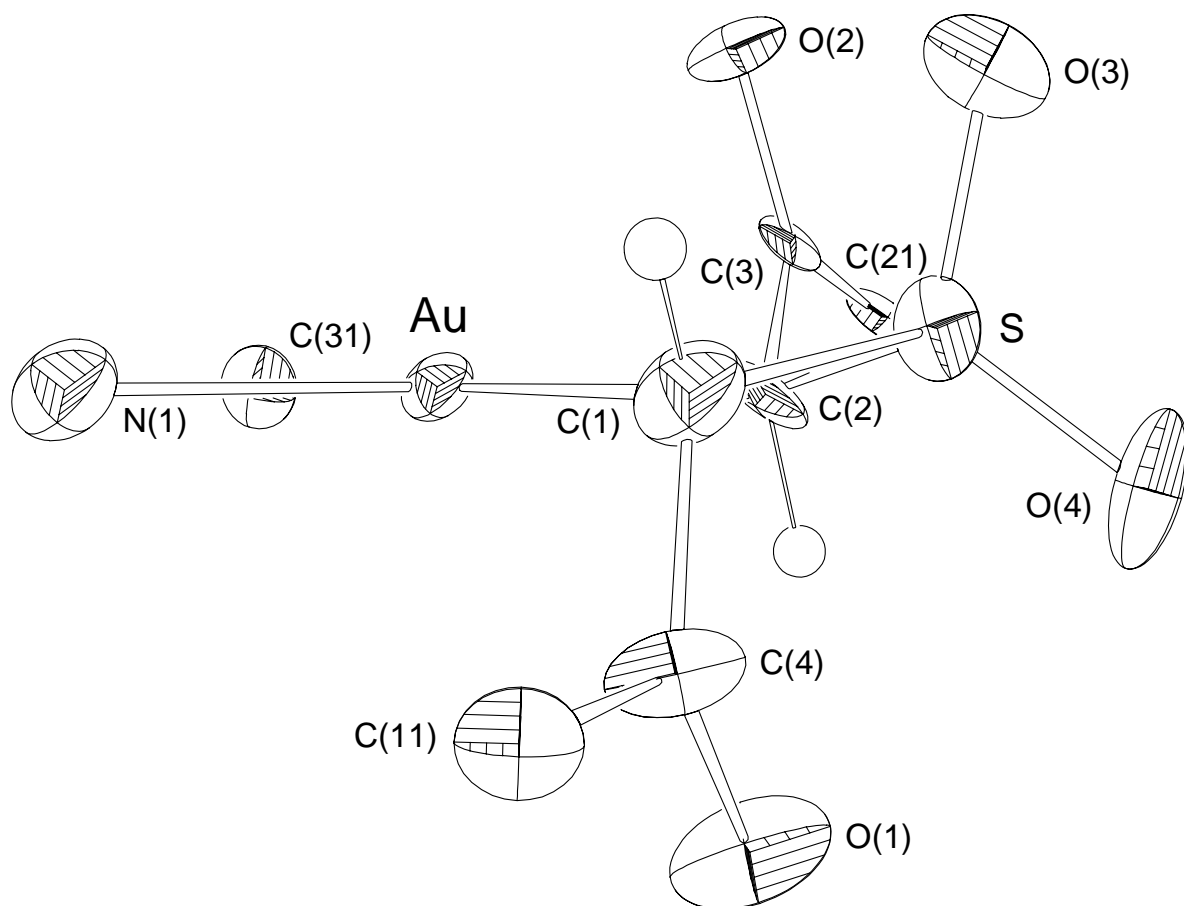


Figure 7.6: ORTEP side view of the structure of $[[\{C_6H_3(CH_2NMe_2)-2-(OMe)-5\}Au\{CH(COPh)S(O)_2CH(COPh)\}]\cdot C_6H_6$ **7.9**, illustrating the puckering of the metallacycle. For clarity, only the Au-bonded atoms of the *N,N*-dimethylbenzylamine ligand, and only the ipso-carbons of the thietane-3,3-dioxide phenyl rings are shown. The benzene of crystallisation has also been omitted. Atoms are shown as thermal ellipsoids at the 50% probability level.

Table 7.1: Selected bond lengths (Å) and angles (°) (estimated standard deviations in parentheses) for **7.9**·C₆H₆.

Bond	Length	Bonds	Angle
Au-C(1)	2.14(2)	C(1)-Au-C(2)	74.1(6)
Au-C(2)	2.05(2)	C(1)-Au-N(1)	104.4(5)
Au-C(31)	2.03(2)	C(2)-Au-C(31)	100.9(7)
Au-N(1)	2.14(1)	N(1)-Au-C(31)	80.6(6)
Au...S	2.833(4)	Au-C(2)-S	93.4(6)
		Au-C(1)-S	95.9(8)
		Au-C(1)-C(4)	105.7(11)
		Au-C(2)-C(3)	115.0(12)
CH(COPh)S(O) ₂ CH(COPh) ligand			
C(1)-S	1.73(2)	C(1)-S-O(3)	93.2(8)
C(2)-S	1.75(2)	C(1)-S-C(2)	108.1(7)
S-O(3)	1.44(1)	C(1)-S-O(4)	115.0(7)
S-O(4)	1.43(1)	C(2)-S-O(3)	109.7(8)
C(1)-C(4)	1.51(2)	C(2)-S-O(4)	111.0(8)
C(2)-C(3)	1.48(2)	C(1)-C(4)-O(1)	122(2)
C(3)-O(2)	1.24(2)	C(1)-C(4)-C(11)	119.2(14)
C(4)-C(11)	1.49(2)	C(2)-C(3)-O(2)	121(2)
C(3)-C(21)	1.52(2)	C(2)-C(3)-C(21)	122.5(14)

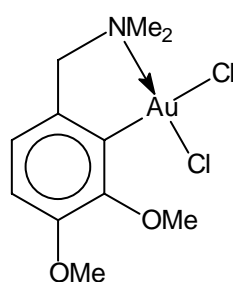
The structure confirms the expected product **7.9**, and overall bears a very strong similarity to the structures reported for the platinum(II) complex **1.90a**·2CH₂Cl₂ (L = PPh₃) and the palladium(II) complex **1.90b**·CH₂Cl₂·H₂O (L = PMePh₂) (Figure 7.3).³

As previously observed for the aurareylene complexes **5.8** (Chapter Five, Section 5.2.1), the gold atom is co-ordinated in a distorted square-planar arrangement, with the four- and five-membered rings in the plane. The main distortion is the C(1)-Au-C(2) bite angle of 74.1(6)°, not significantly different to bite angles of 75.4(4)° and 74.7(2)° reported for **1.90a** (L = PPh₃) and **1.90b** (L = PMePh₂) respectively. The geometry about the central gold atom is planar, with a maximum deviation from the least-squares plane drawn through N(1), C(31), Au, C(1) and C(2) being 0.018(6) Å, for the gold atom.

The four-membered aurathietane-3,3-dioxide ring itself is non-planar with the fold angle between the C(1)-Au-C(2) and C(1)-S-C(2) planes being $19(1)^\circ$. This is slightly higher than the angle observed for the platinum system **1.90a** [$15.3(6)^\circ$] but considerably lower than that reported for the palladium complex **1.90b** [$30.2(2)^\circ$]. The five-membered cyclometallated ring, as observed for the gold(III) complexes already discussed (Chapter Five and Six), incorporating an sp^2 hybridised carbon, is typically non-planar with deviations from the least-squares plane of $0.26(1)\text{\AA}$ above the plane for C(6) and $0.278(9)\text{\AA}$ below for N(1).

Additionally, the Au-C(1) and Au-C(2) bond lengths are not equal, as expected, with the former [$2.14(2)\text{\AA}$] longer than the latter [$2.05(2)\text{\AA}$]. As already mentioned, this is attributable to the higher *trans*-influence¹⁰ of C(31) relative to N(1). The average Au-CH bond distance of $2.10(2)\text{\AA}$ is not significantly different to the average Pt-CH and Pd-CH distances observed for **1.90a** (L = PPh₃) [$2.12(1)\text{\AA}$] and **1.90b** (L = PMePh₂) [$2.135(6)\text{\AA}$]. As for the analogous platinum and palladium(II) complexes, the two C(O)Ph groups in **7.9** are orientated *trans* with respect to each other (above and below the metallacyclic plane), as shown in Figure 7.6.

The Au-C(31) and Au-N(1) bond lengths of [$2.03(2)\text{\AA}$] and [$2.14(1)\text{\AA}$] respectively are, however, of comparable length to those of **7.11** (Figure 7.7)¹⁴ (a species closely related to **5.1a**), showing corresponding lengths of [$2.08(2)\text{\AA}$] and [$2.05(3)\text{\AA}$]. The presumably differing *trans*-influences of the C-C ligand versus the chloride anion apparently does not greatly influence bond lengths in this case.



7.11

Figure 7.7

The C-S bond lengths of $1.73(2)\text{\AA}$ and $1.75(2)\text{\AA}$ for C(1)-S and C(2)-S respectively, are also comparable to those reported for **1.90a** (L = PPh₃) and **1.90b** (L = PMePh₂), and are shorter than those measured in thietane-1,1-dioxides. A detailed comparison with starting materials and related compounds has been reported previously.³ The short C-S bond distances, together

with the puckering of the four-membered metallacycle, are best explained in terms of contributions from an η^3 -heteroallylic representation **7.12a** (resulting from a transannular attraction between the metal and the β -carbonyl group) (Figure 7.8) to the metallacyclic bonding **7.12b**, with a degree similar to that observed for the isoelectronic platinum(II) aurathietane-3,3-dioxide complex **1.90a** (L = PPh₃).

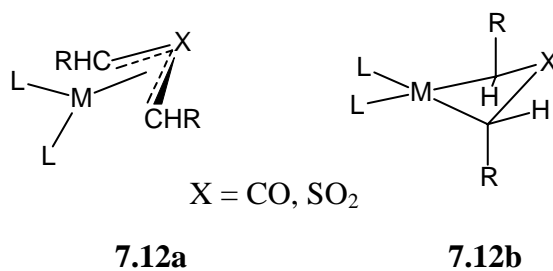


Figure 7.8

7.2.2 Spectroscopic and mass spectrometric characterisation

7.2.2.1 NMR spectroscopy

As expected, the differing *trans*-influences of the aryl carbon and nitrogen atoms markedly affects the environment of the methine proton and carbon atoms of both **7.9** and **7.10**. For **7.9**, 0.57 and 11.9 ppm differences in chemical shift are observed in the proton and carbon NMR spectra respectively. Similarly, 0.24 and 16.2 ppm differences are seen for the Au-CH groups of **7.10**. However, rationalisation in terms of *trans*-influences is not clear, since the higher chemical shift proton is bonded to the lower chemical shift carbon. In the carbon spectra the upfield ¹³C resonance is attributable to the CH *trans* to the lower *trans*-influence nitrogen.

The *average* ¹³C NMR Au-CH chemical shift of 62.1 ppm for **7.9** is significantly higher than that reported for analogous complexes **1.90a** (L = PPh₃) and **1.90b** (L = PPh₃), with shifts of 54.6 ppm and 52.2 ppm respectively. This is possibly due to the presence of a more electron-deficient central metal atom (respective Zhang electronegativity values for platinum(II) and gold(III) are 1.5 and 1.7),¹¹ although direct comparisons are difficult due to the complications arising from the electronically different groups *trans* to the ligand (triphenylphosphine for **1.90** versus N,N-dimethylbenzylamine for **7.9**). The starting material, diphenacyl sulfone **7.7**, shows the methylene carbon resonance at 60.0 ppm, this being slightly lower than that of the gold(III) derivative **7.9**, but higher than the platinum(II) derivative **1.90a** (L = PPh₃). A

similar trend is seen in the proton spectra, with **7.9** having an average methine resonance of 5.40 ppm, compared with a value of 4.86 ppm for **1.90a** (L = PPh₃), and 5.01 ppm for **7.7**.

The ¹³C chemical shift of the auracyclobutan-3-one ring C=O group of **7.10**, occurs at 185.9 ppm, indicating the carbon atom is deshielded to a significantly greater degree than that for **1.88** (Figure 7.3), where the resonance for this moiety is observed at 178.3 ppm.⁵ Again, this is possibly consistent with a more electronegative Au(III) centre [*cf.* Pt(II)], although the very similar data observed for the carbonyl chemical shifts of auraureylene complexes **5.8** compared with the platinaureylene complexes **2.22** (see Chapter Five, Section 5.2.2.1), suggest this may not be the case. It is conceivable, that if the auracyclobutan-3-one complex **7.10** was somewhat less puckered than the platinacyclobutan-3-one **1.88**, then the lower contribution from allylic bonding contribution **7.12a** (Figure 7.8) would result in a more localised central carbonyl (due to increased **7.12b** character). This would consequent in it being deshielded to a greater extent, and hence resonate further downfield. That said, and although no crystallographic data for **7.10** exist to support the hypothesis, additional NMR studies (see below) reveal **7.10** probably has similar η^3 -heteroallylic bonding to **1.88**.

It was of interest to investigate the applicability of NMR in measuring the putative η^3 -heteroallylic bonding contribution (Figure 7.8), which has been proposed to account for the non-planarity of the four-membered metallacyclic ring observed in X-ray crystal structure determinations.⁶ Referring to Figure 7.8, the arrangement **7.12a** would have predominantly *sp*² hybridised M-C carbons, whereas in **7.12b** the M-C's are *sp*³ hybridised. Therefore the ¹H coupled ¹³C NMR spectra for **7.9** and **7.10** were measured, since it has been shown that there is a clear correlation of the percentage *s* character of carbon atoms and their ¹J (¹³C-¹H) coupling constants,¹² with larger values observed for *sp* carbons (e.g. ~250 Hz for alkynes) than for *sp*² carbons (e.g. ~160 Hz for aromatics), which in turn are higher than *sp*³ carbons (e.g. ~125 Hz for alkanes).

For **7.9**, values of 147.5 Hz for Au-C *trans* to C and 149.9 Hz for Au-C *trans* to N, were recorded. Comparing these with a value of 137.9 Hz for the starting material, diphenacyl sulfone **7.7**, tentatively suggests that there is substantial *sp*² character in the Au-C ring carbon atoms, consistent with a heteroallylic bonding contribution. For **7.10**, values of 148.7 Hz and 151.3 Hz were recorded, these being very similar to those of **7.9**. However in this case the starting material **7.8** shows a ¹³C-¹H coupling constant of 131.2 Hz, so the nett *increase* is greater. This is important since the electronegativity of adjacent atoms (CO, SO₂ and the

metal centres themselves) also contribute to the magnitude of the ^1J value, with higher values observed for carbon atoms bound to electron-withdrawing groups.¹⁷ For the complex **1.88**, prepared by the literature procedure,⁵ a very similar value of 149.9 Hz was measured. It has been suggested that for sulfone derivatives **1.90a** η^3 -heteroallylic bonding is considered to be less than for oxodimethylenemethane complexes **1.88**, since the metallacycle is considerably more puckered in the latter [e.g. 50.4(4)° in the case of **1.88**].⁵ The new NMR evidence reported here further supports this notion.

7.2.2.2 Electrospray mass spectrometry (ESMS)

Electrospray mass spectrometric analyses of complexes **7.9** and **7.10** showed very strong parent ions ($[\text{MH}]^+$), with no observable fragmentation at low cone voltages (~20 V). Indeed, even when higher cone voltages (50-80 V) were used the complexes still showed the $[\text{MH}]^+$ ion as the predominant signal, indicating appreciable stability. This resistance to cone-voltage-induced fragmentation was also observed for the ureylene complexes **5.8a** and **5.8b** (Chapter Five, Section 5.2.2.3), and again is likely to be due to the extra stability imparted by the presence of two ring systems.

7.2.3 Conclusions

When combined with the results reported in Chapter Five (and Chapter Eight), it is clear the cyclometallated gold(III) complex **5.1a** provides an excellent precursor for the investigation of gold(III) metallacyclic chemistry. The compounds reported in this chapter are comparable to the previously reported isoelectronic platinum(II) analogues. Platinacyclobutane is an archetypical metallacycle (see Chapter One, Section 1.2.1),¹³ that was first prepared in 1955,¹⁴ and the work presented in this chapter clearly demonstrates a huge range of potential metallacycles derived from the precursors **5.1** could be synthesised, with no reason to suggest inaccessibility of the presently unknown auracyclobutane ring systems.

7.3 Experimental

General experimental procedures and the instrumentation used are given in Appendices I and II. The gold(III) precursor $[\text{Au}\{\overline{\text{C}_6\text{H}_3(\text{CH}_2\text{NMe}_2)\text{-2-(OMe)-5}\}\text{Cl}_2]$ **5.1a** was prepared as described in Appendix I. ESMS spectra were recorded in MeCN/H₂O solvent.

Proton and all inverse 2D NMR experiments (HSQC, HMBC and ROESY) were recorded on a Bruker DRX 400 spectrometer at 400.13 MHz and 100.61 MHz for the proton and carbon channels respectively. The NMR experiments are described in Appendix II, and the ROESY spectrum of **7.9** is presented. The ¹³C NMR spectra of **7.9** was recorded on instrument above and those of **7.8**, **7.9** and **7.10** on a Bruker AC300 spectrometer at 75.47 MHz. All NMR analyses were carried out in CDCl₃.

*Preparation of diphenacyl sulfone 7.7*¹⁵

Two equivalents of phenacyl chloride [PhC(O)CH₂Cl] were reacted with sodium sulfide in methanol/water, and the resulting precipitate collected. The solid (diphenacyl sulfide) was dissolved in acetone, and treated with acidified (H₂SO₄) potassium permanganate to give diphenacyl sulfone.

¹H NMR: 7.95 (4H, *d*, ³J_{2',3'} = 8.19 Hz, H-2',6'), 7.62 (2H, *t*, ³J_{4',3'} = 7.40 Hz, H-4'), 7.48 (4H, *t*, ³J_{3',2'/4'} = 7.70 Hz, H-3',5'), 5.01 (4H, *s*, CH₂).

¹³C NMR: 189.6 (*s*, C=O), 135.7 (*s*, C-1'), 129.1 (*d*, C-2',6' or C-3',5'), 128.9 (*d*, C-2',6' or C-3',5'), 60.0 (*t*, CH₂).

*Preparation of dimethyl 1,3-acetonedicarboxylate 7.8*¹⁶

Acetonedicarboxylic acid (readily synthesised from the reaction of citric acid and fuming sulfuric acid)¹⁷ (10 g, 0.068 mol) was reacted with methanol (15 ml) which had previously been treated with hydrogen chloride (synthesised *in situ* by reacting ammonium chloride with concentrated sulfuric acid). A drying tube was fitted to the reaction flask, and the mixture heated to 45°C in a water bath. After 20 minutes, the solution was slowly cooled to room temperature and left standing for 12 hours. The reaction contents were subsequently poured onto crushed ice (100 g), and the ester extracted with diethyl ether. The ether was washed with 10% sodium carbonate solution (50 ml) to remove any unreacted acid, followed by dilute

sulfuric acid and finally with water. The ethereal solution was dried with magnesium sulfate and the solvent removed under reduced pressure. The resulting residue was distilled under reduced pressure and the fraction that boiled at 131-136°C (10 mm) was collected, giving dimethyl 1,3-acetonedicarboxylate as a colourless oil (0.80 g, 7%).

$^1\text{H NMR}$: 3.69 (6H, *s*, CH_3), 3.57 (4H, *s*, CH_2).

$^{13}\text{C NMR}$: 195.2 (*s*, $(\text{CH}_2)_2\text{C}=\text{O}$), 167.1 (*s*, $\text{MeOC}=\text{O}$), 52.4 (*t*, CH_2), 48.7 (*q*, CH_3).

Preparation of $[\{\text{C}_6\text{H}_3(\text{CH}_2\text{NMe}_2)\text{-2-(OMe)-5}\}\text{Au}\{\text{CH(COPh)S(O)}_2\text{CH(COPh)}\}]$ **7.9**

To a nitrogen-flushed Schlenk flask containing dichloromethane (30 cm³) was added **5.1a** (0.051 g, 0.118 mmol), diphenacyl sulfone (0.035 g, 0.116 mmol), and silver(I) oxide (0.11 g, excess). The resulting mixture was stirred under reflux for 1 hour in dark conditions, during which time the initial yellow solution became noticeably paler. Without further precautions to exclude air or light, the insoluble silver salts were filtered off, giving an almost colourless solution. The solvent was removed under reduced pressure to give a colourless oil. This was subsequently recrystallised by vapour diffusion of ether into dichloromethane at 4°C to give colourless crystals which were dried *in vacuo* to yield **7.9** (0.054 g, 71%). The compound was air stable, but somewhat light sensitive, with slow decomposition occurring over several days as evidenced by purple colloidal gold formation on crystal surfaces.

m.p. 200-202°C (melted with decomposition).

Found: C, 47.1; H, 3.9; N, 2.2%; $\text{C}_{26}\text{H}_{26}\text{NO}_5\text{SAu}$ requires: C, 47.2; H, 4.0; N, 2.1%.

ESMS: (Cone voltage = 30V) 662 ($[\text{MH}]^+$, 100%); (Cone voltage = 80V) 684 ($[\text{MNa}]^+$, 18%), 662 ($[\text{MH}]^+$, 100%).

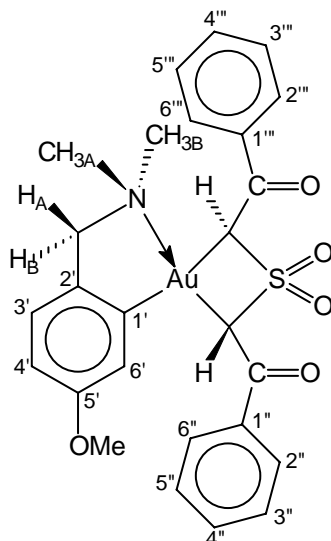
IR: $\nu(\text{CO region})$ 1668 (*s*), 1647 (*s*), 1592 (*s*) cm^{-1} ; $\nu(\text{SO}_2)$ 1276 (*s*), 1130 (*vs*) cm^{-1} .

$^1\text{H NMR}$: (400.13 MHz) δ 8.16 (2H, *d*, $^3\text{J}_{2'',3''} = 7.41$ Hz, H-2'',6''), 8.08 (2H, *d*, $^3\text{J}_{2''',3'''} = 7.39$ Hz, H-2''',6'''), 7.62-7.58 (2H, *m*, H-4'',4'''), 7.54-7.48 (4H, *m*, H-3'',3''',5'',5'''), 7.08 (1H, *d*, $^3\text{J}_{3',4'} = 8.28$ Hz, H-3'), 6.63 (1H, *dd*, $^3\text{J}_{4',3'} = 8.25$ Hz, $^4\text{J}_{4',6'}$ = 2.40 Hz, H-4'), 6.46 (1H, *d*, $^4\text{J}_{6',4'}$ = 2.40 Hz, H-6'), 5.68 (1H, *s*, AuCH *trans* N), 5.11 (1H, *s*, AuCH *trans* C), 4.42 (1H, *d*, $^2\text{J}_{\text{H}_\text{A},\text{H}_\text{A}}$ = 13.56 Hz, NCH_B), 3.78 (1H, *d*, $^2\text{J}_{\text{H}_\text{A},\text{H}_\text{B}}$ = 13.58 Hz, NCH_A), 3.32 (3H, *s*, OCH₃), 2.97 (3H, *s*, NCH_{3B}), 2.64 (3H, *s*, NCH_{3A}).

$^{13}\text{C NMR}$: (100.61 MHz) δ 193.6 (*s*, C=O *trans* C), 191.9 (*s*, C=O *trans* N), 158.2 (*s*, C-5'), 155.4 (*s*, C-1'), 139.0 (*s*, C-2'), 138.6 (*s*, C-1'''), 138.4 (*s*, C-1''), 133.8 (*d*, C-4'''), 133.6 (*d*, C-4''), 129.4 (*d*, C-3'''), 129.0-128.9 (*d*, C-2'',3'',2'''), 124.3 (*d*, C-3'), 117.9 (*d*, C-6'), 113.9 (*d*, C-

4'), 73.9 (*t*, NCH₂), 68.0 (*d*, AuCH *trans* C), 56.1 (*d*, AuCH *trans* N), 54.8 (*q*, OCH₃), 52.7 (*q*, NCH_{3B}), 50.6 (*q*, NCH_{3A}).

NMR numbering scheme:



Preparation of $[\{C_6H_3(CH_2NMe_2)-2-(OMe)-5\}Au\{CH(CO_2Me)C(O)CH(CO_2Me)\}]$ **7.10**

To a nitrogen-flushed Schlenk flask containing dichloromethane (30 cm³) was added **5.1a** (0.050 g, 0.116 mmol), dimethyl 1,3-acetonedicarboxylate (0.017 cm³, 0.020 g, 0.115 mmol), and silver(I) oxide (0.08 g, excess). The resulting mixture was stirred under reflux for 1 hour in dark conditions, during which time the initial yellow solution became noticeable paler. As described above, the insoluble silver salts were filtered off and subsequent evaporation of the filtrate gave a pale yellow oil which resisted crystallisation. ESMS and NMR revealed the product as **7.10** (~90% pure by NMR). Attempted purification by preparative layer or column chromatography resulted in substantial decomposition of the compound. The crude product was somewhat light and possibly air sensitive with decomposition occurring over several hours. This, and the difficulty in purification of the compound, rendered elemental analysis unfeasible.

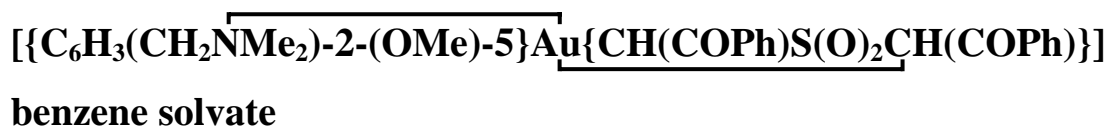
ESMS: (Cone voltage = 20V) 534 ([MH]⁺, 100%). (Cone voltage = 50V) 534 ([MH]⁺, 100%), 502 ([M - OMe]⁺, 52%), 402 (unidentified, 8%). (Cone voltage = 80V) 556 ([MNa]⁺, 19%), 534 ([MH]⁺, 100%), 502 ([M - OMe]⁺, 72%), 402 (unidentified, 40%), 164 ([C₆H₃CH₂NMe₂)MeO]⁺, 43%).

IR: ν(CO region) 1772-1636 (s) multiple signals, 1593 (vs) cm⁻¹.

^1H NMR: (400.13 MHz) δ 7.15 (1H, *d*, $^3J_{3',4'} = 8.27$ Hz, H-3'), 7.09 (1H, *d*, $^4J_{6',4'} = 2.55$ Hz, H-6'), 6.70 (1H, *dd*, $^3J_{4',3'} = 8.26$ Hz, $^4J_{4',6'} = 2.56$ Hz, H-4'), 4.23 (1H, *d*, $^2J_{\text{H}_\text{B},\text{H}_\text{A}} = 13.84$ Hz, NCH_B), 4.15 (1H, *s*, AuCH *trans* N), 3.96 (1H, *d*, $^2J_{\text{H}_\text{A},\text{H}_\text{B}} = 13.76$ Hz, NCH_A), 3.91 (1H, *s*, AuCH *trans* C), 3.77 (3H, *s*, OCH₃), 3.680 (3H, *s*, C(O)OCH₃) 3.678 (3H, *s*, C(O)OCH₃), 3.17 (3H, *s*, NCH_{3B}), 2.79 (3H, *s*, NCH_{3A}).

^{13}C NMR: (75.47 MHz) δ 185.9 (*s*, C=O) 170.7 (*s*, C(O)OCH₃ *trans* C), 169.6 (*s*, C(O)OCH₃ *trans* N), 158.3 (*s*, C-5'), 156.8 (*s*, C-1'), 139.1 (*s*, C-2'), 124.1 (*d*, C-3'), 118.3 (*d*, C-6'), 113.4 (*d*, C-4'), 73.0 (*t*, NCH₂), 61.6 (*d*, AuCH *trans* C), 55.3 (*q*, OCH₃), 52.3 (*s*, C(O)OCH₃), 52.2 (*q*, NCH_{3B}), 51.4 (*q*, NCH_{3A}), 51.0 (*s*, C(O)OCH₃), 45.4 (*d*, AuCH *trans* N).

7.3.1 X-ray structure of 7.9



Colourless rectangular blocks of **7.9**·C₆H₆ were obtained by liquid-liquid diffusion of benzene layered on a solution of **7.9** in chloroform, at 4°C.

Data collection

Cell parameters and intensity data were collected on an Nicolet R3 automatic four-circle diffractometer at the University of Canterbury, using a crystal of dimensions 0.35 x 0.30 x 0.16 mm, with monochromatic Mo-*K*α X-rays ($\lambda = 0.71073$ Å). A total of 3784 reflections in the range $2 < \theta < 25^\circ$ were collected at 130(2) K, of which 3745 were unique. These were subsequently corrected for Lorentz and polarisation effects, and for linear absorption by a Ψ scan method ($T_{\text{max.}, \text{min.}} = 0.55, 0.31$).

Crystal Data: C₂₆H₂₆NO₅SAu·C₆H₆, $M_r = 739.61$, monoclinic, space group P2₁/n, $a = 9.697(6)$, $b = 24.595(9)$, $c = 12.690(7)$ Å, $\beta = 107.84(4)^\circ$, $U = 2881(3)$ Å³, $D_c = 1.705$ g cm⁻³, $Z = 4$, $F(000) = 1464$, $\mu(\text{Mo-}K\alpha) = 5.22$ mm⁻¹.

Solution and refinement

The structure was solved by the Patterson methods option of SHELXS-86,¹⁸ and all further non-hydrogen atoms were located routinely (SHELXL-93),¹⁹ with all non-hydrogen atoms

assigned anisotropic temperature factors and all hydrogen atom positions determined by calculation. The refinement converged with $R_1 = 0.0624$ for data with $I \geq 2\sigma(I)$, 0.1071 for all data; $wR_2 = 0.1420$ $\{w = 1/[\sigma^2(F_o^2) + (0.0984P)^2 + 0.0000P]$ where $P = (F_o^2 + 2F_c^2)/3\}$, and $GoF = 1.065$. No parameter shifted in the final cycle, and the final difference map showed no peaks or troughs of electron density greater than +3.31 and -2.90 e \AA^{-3} respectively (adjacent to the gold atom). The benzene solvate [C(41)...C(46)] was partially disordered (largely over two positions), so was modelled as a single rigid hexagon (all bond lengths 1.390 \AA and bond angles 120°) with strongly anisotropic temperature factors.

References

- 1 R.J. Puddephatt, *Coord. Chem. Rev.*, **33** (1980) 149.
- 2 P.W. Jennings, L.L. Johnson, *Chem. Rev.*, **94** (1994) 2241.
- 3 W. Henderson, R.D.W. Kemmitt, L.J.S. Prouse, D.R. Russell, *J. Chem. Soc. Dalton Trans.*, (1989) 259; *Ibid*, (1990) 781.
- 4 W. Henderson, J. Fawcett, R.D.W. Kemmitt, L.J.S. Prouse, D.R. Russell, *J. Chem. Soc. Chem. Commun.*, (1986) 1791.
- 5 D.A. Clarke, R.D.W. Kemmitt, M.A. Mazid, P. McKenna, D.R. Russell, M.D. Schilling, L.J.S. Sherry, *J. Chem. Soc. Dalton Trans.*, (1984) 1993.
- 6 J. Fawcett, W. Henderson, M.D. Jones, R.D.W. Kemmitt, D.R. Russell, B. Lam, S.K. Kang, T.A. Albright, *Organometallics*, Vol. 8. No. 8, 1989.
- 7 R.D.W. Kemmitt, M.R. Moore, *Transition Met. Chem.*, **18** (1993) 348.
- 8 J.F. Hoover, J.M. Stryker, *J. Am. Chem. Soc.*, **111** (1989) 6466.
- 9 J. Vicente, M-D. Bermúdez, M-P. Carrillo and P.G. Jones, *J. Chem. Soc., Dalton Trans.*, (1992) 1975.
- 10 J.G. Appleton, H.C. Clark, L.E. Manzer, *Coord. Chem. Rev.*, **10** (1973) 335.
- 11 K.M. Mackay, R.A. Mackay, *Introduction to Modern Inorganic Chemistry*, 4th Ed., Blackie, Glasgow and London, (1989).
- 12 H. Kalinowski, S. Berger, S. Braun, *Carbon-13 NMR Spectroscopy*, John Wiley & Sons, Chichester, (1988) 495.
- 13 P.W. Jennings and L.L. Johnson, *Chem. Rev.*, **94** (1994) 2241.
- 14 C.F.H. Tipper, *J. Chem. Soc.*, (1955) 2045.
- 15 E. Fromm and J. Flaschen, *Liebigs Ann. Chem.*, **384** (1912) 310.
- 16 H. Gilman, A.H. Blatt, *Org. Synth., Coll. Vol. I*, 2nd Ed., John Wiley & Sons, (1967) 237.
- 17 H. Gilman, A.H. Blatt, *Org. Synth., Coll. Vol. I*, 2nd Ed., John Wiley & Sons, (1967) 10.
- 18 G.M. Sheldrick, *SHELXS-86, Program for Solving X-Ray Crystal Structures*, University of Göttingen, Germany, (1986).
- 19 G.M. Sheldrick, *SHELXL-93, Program for Refining X-Ray Crystal Structures*, University of Göttingen, Germany, (1993).

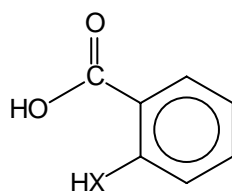
Chapter Eight

Synthesis, Characterisation and Biological Activity of Gold(III) Salicylate and Thiosalicylate Complexes

8.1 Introduction

The gold(III) halide complexes $[\text{Au}\{\overline{\text{C}_6\text{H}_3(\text{CH}_2\text{NMe}_2)\text{-2-R-5}}\}\text{Cl}_2]$ **5.1a** (R = OMe) and **5.1b** (R = H) have proved to be reasonably good analogues to platinum(II) halide complexes for the formation of metallacycles (Chapter Five and Seven), although failed to produce analogous metallacycles from thioureas (Chapter Six). Further work to develop gold(III) metallacyclic chemistry was thus pursued.

Thiosalicylic acid **8.1** (2-sulfanylbenzoic acid) and salicylic acid **8.2** are versatile heterodifunctional ligands capable of bonding to a range of metal centres as either mono- or dianions, co-ordinating in a range of bonding modes.



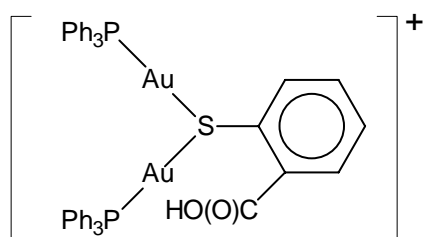
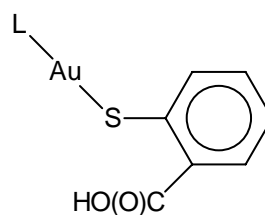
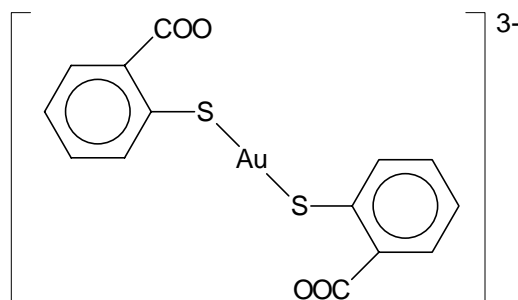
8.1 X = S

8.2 X = O

Figure 8.1

Gold complexes with thiolate ligands are an important class of co-ordination complex, finding various applications, including drugs for the treatment of rheumatoid arthritis¹⁻⁶ and nanotechnologies⁷ among others. The strong propensity of gold(I) to form stable thiolate complexes is well-known,⁸⁻¹³ and several gold(I)-thiosalicylate complexes have been described.

Schmidbaur and co-workers have recently reported a number of gold(I) complexes of thiosalicylic acid (and other mercapto-carboxylic acids), including the sulfonium salt **8.3**¹⁴ (Figure 8.2) and the isocyanide complexes **8.4a**.¹⁵ The related phosphine complex **8.4b** (Figure 8.2) has also been described, and its structure determined.¹⁶ A gold(I) bis(thiosalicylate) complex **8.5** (Figure 8.3) has also recently been synthesised (as a sodium salt) and characterised.¹⁷ The compounds **8.3-8.5** are of interest for their hydrogen-bonding as well as Au...Au interactions in the solid-state.

**8.3****8.4a** L = RNC (R = *tert*-butyl or mesityl)**8.4b** L = PPh₃**Figure 8.2****8.5****Figure 8.3**

Oligomeric and polymeric silver(I)-thiosalicylate complexes, with a 1:1 silver:thiosalicylate ratio, have also been described and found to display effective antimicrobial properties for yeast, bacteria and mould.¹⁸ Gold-thiosalicylate complexes have been studied as model complexes for the interaction of gold with sulfur donor groups in humic acid in natural systems.¹⁹ The gold salt of $[\text{Hg}\{\text{SC}_6\text{H}_4(\text{COO})-2\}_2]^{2-}$ **8.6** has been described,²⁰ and a gravimetric method using thiosalicylic acid for the determination of gold has also been reported.²¹

A number of platinum(II) complexes containing chelating thiosalicylate **8.7a-8.7c**,²² **8.8**²³ and salicylate **8.9**²² (Figure 8.4) dianion ligands have been prepared from *cis*-[PtCl₂L₂] and

thiosalicylic or salicylic acid in the presence of silver(I) oxide. This chapter reports the synthesis of analogous thiosalicylate and salicylate organo-gold(III) complexes.

Since the chelating binding mode of the thiosalicylate ligand in the gold(III) complexes would be very different to other previously characterised gold(I) thiosalicylate complexes, such complexes might display different biological activities, which could be of some interest given the medical importance of gold-thiolate complexes. Additionally, the biological activity of the gold(III) ureylene complex **5.8a** proved significant. For this reason biological assays for all the reported complexes have also been determined.

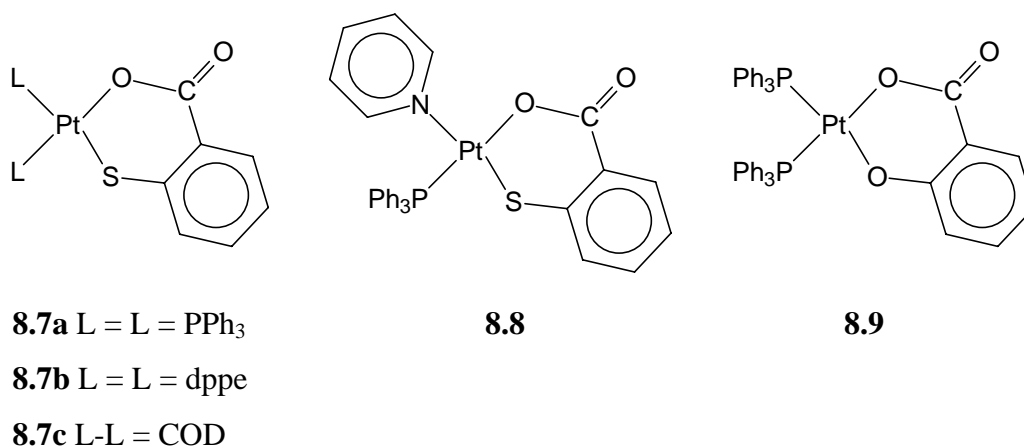


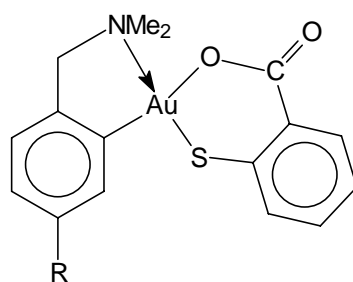
Figure 8.4

8.2 Results and Discussion

8.2.1 Synthesis of gold(III) thiosalicylate complexes

Reactions of the cycloaurated N,N-dimethylbenzylamine complexes $[\text{Au}\{\text{C}_6\text{H}_3(\text{CH}_2\text{NMe}_2)\text{-2-R-5}\}\text{Cl}_2]$ **5.1a** (R = OMe) and **5.1b** (R = H) with one molar equivalent of thiosalicylic acid and excess silver(I) oxide in refluxing dichloromethane gave the respective gold(III) thiosalicylate complexes **8.10a** and **8.10b**. Both complexes are air- and reasonably light-stable, bright yellow solids, with the methoxy-functionalised derivative **8.10a** showing a significantly higher solubility in organic solvents than the unsubstituted complex **8.10b**. The reactions proceeded in high yield, and NMR spectra of the crude reaction products (after removal of the silver salts and evaporation of the solvent) indicated that a single, pure product was formed in each case. However, unambiguous identification of the actual isomer formed was not possible using NMR spectroscopy, despite an attempt at correlating the chemical

shifts of the methylene and N,N-dimethylamino protons and carbons with the nature of the other groups co-ordinated to the gold(III) centre. Correlation and NOE experiments (see Appendix II) could also not distinguish between the two possible isomers, since the thiosalicylate ligand is too far removed from NMR active nuclei in the N,N-dimethylbenzylamine group. The unsubstituted complex **8.10b** gave crystals of suitable quality for an X-ray structure determination on recrystallisation from dichloromethane and diethyl ether, and the analysis was carried out in order to unequivocally determine which isomer had been formed.



8.10a R = OMe

8.10b R = H

Figure 8.5

8.2.2 X-ray structure of $[\{C_6H_4(CH_2NMe_2)-2\}Au\{SC_6H_4(COO)-2\}]$ **8.10b**

The data set was unfortunately of poor quality (R_1 0.156) which was primarily attributed to twinning present in the crystal, together with significant disorder. For these reasons the determined bond lengths and angles have high estimated standard deviations and are consequently indicative only. However, the overall connectivity and conformation of the compound is unambiguous, and the internal check provided by the presence of two independent molecules in the asymmetric unit, lends some additional credibility to the results of the study.

PLUTO plots of perspective and side views of the structure (molecule 2) are shown in Figures 8.6 and 8.7 respectively, showing the atom numbering scheme. Selected bond lengths and angles of molecule 2 are presented in Table 8.1, with tables of complete bond lengths and angles, final positional parameters and thermal parameters presented in Appendix XIV.

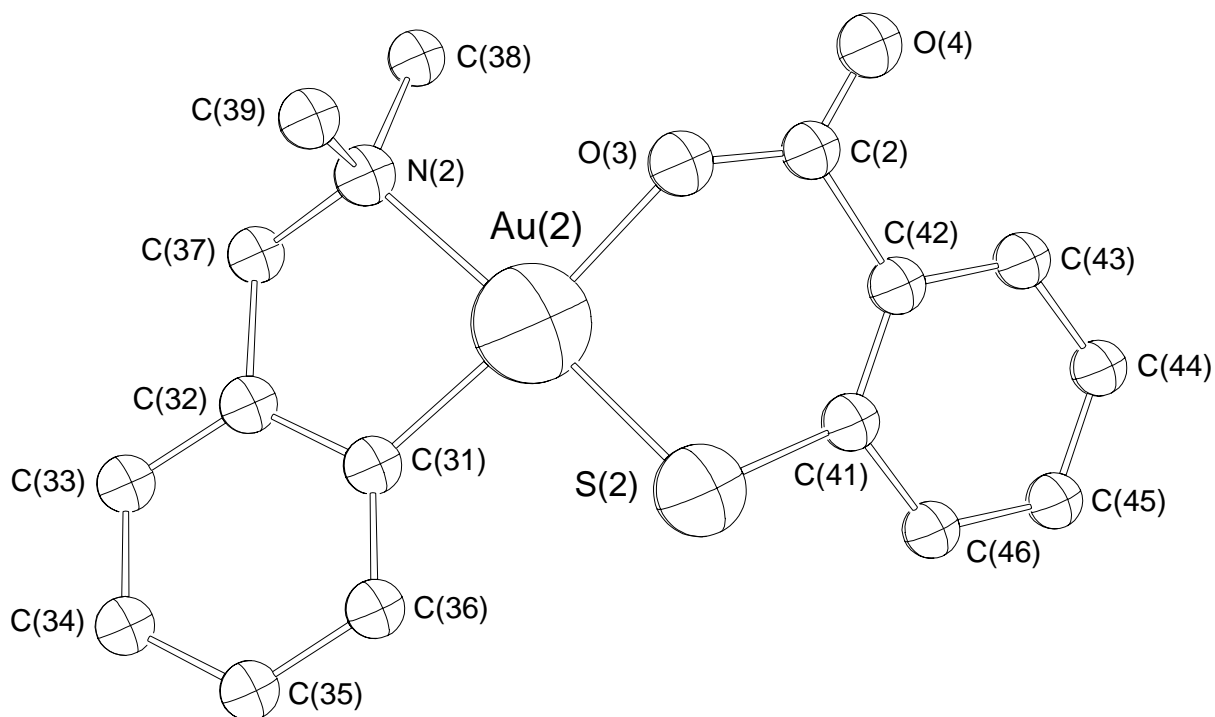


Figure 8.6: PLUTO perspective view of the X-ray structure of molecule 2 of the gold(III) thiosalicylate complex $[\{C_6H_4(CH_2NMe_2)-2\}Au\{SC_6H_4(COO)-2\}]$ **8.10b** showing the atom numbering scheme.

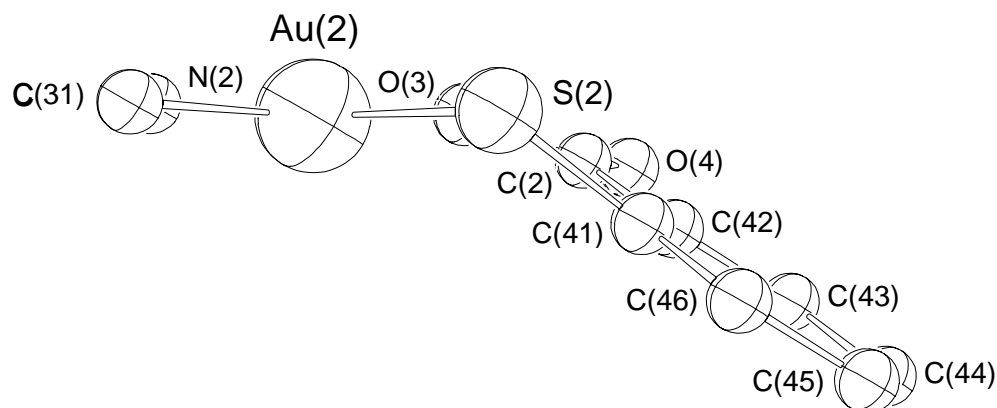


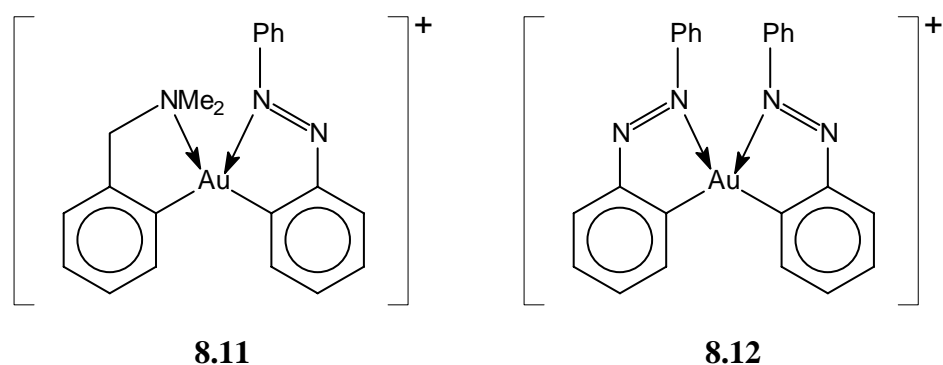
Figure 8.7: PLUTO side view of the X-ray structure of molecule 2 of the gold(III) thiosalicylate complex $[\{C_6H_4(CH_2NMe_2)-2\}Au\{SC_6H_4(COO)-2\}]$ **8.10b**, demonstrating the non-planarity of the gold-thiosalicylate moiety. For clarity, only the Au-bonded atoms of the *N,N*-dimethylbenzylamine ligand are shown.

Table 8.1: Selected bond lengths (Å) and angles (°) for the gold(III) thiosalicylate complex **8.10b** (molecule 2) with estimated standard deviations in parentheses.[†]

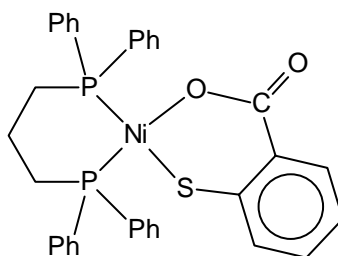
Bond	Length	Bonds	Angle
Au(2)-S(2)	2.28(2)	S(2)-Au(2)-O(3)	93.2(3)
Au(2)-O(3)	2.08(2)	N(2)-Au(2)-C(31)	83.4(4)
Au(2)-N(2)	2.20(2)	O(3)-Au(2)-N(2)	90.0(4)
Au(2)-C(31)	2.04(2)	S(2)-Au(2)-C(31)	93.3(4)
		Au(2)-S(2)-C(41)	101.1(3)
		Au(2)-O(3)-C(2)	128.1(5)
Thiosalicylate ligand			
S(2)-C(41)	1.81(1)	S(2)-C(41)-C(42)	128.9(6)
C(2)-O(3)	1.27(2)	C(41)-C(42)-C(2)	121.0(7)
C(2)-O(4)	1.25(2)	C(42)-C(2)-O(4)	112.8(6)
C(2)-C(42)	1.56(1)	C(42)-C(2)-O(3)	126.7(6)
		O(4)-C(2)-O(3)	120(2)

[†] The structure has a high *R* factor (R_1 0.1555), so data should be treated with caution.

The structure confirms the presence of the chelating dianionic thiosalicylate ligand, which is co-ordinated with the thiolate sulfur *trans* to the N,N-dimethylamino group of the cycloaurated benzylamine ligand. As a result, the two soft, strong σ -donor ligands (the aryl and thiolate moieties) are *cis* to each other. This effect, anti-symbiosis, is well known in gold(III) chemistry,^{24,25} and X-ray structures of the bis(cyclometallated)gold(III) complexes **8.11**²⁶ and **8.12**²⁷ (Figure 8.8) both show the high *trans*-influence aryl ligands in mutually *cis* positions. The platinum(II) thiosalicylate complex **8.8** (Figure 8.4) shows the same effect, with the poorer donor ligand (pyridine) *trans* to the sulfur atom.²³

**Figure 8.8**

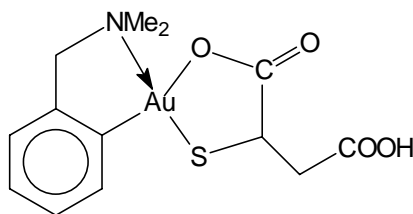
The most striking feature of the structures is that the gold-thiosalicylate moiety is markedly non-planar, with fold angles of $30.1(8)^\circ$ and $37.8(6)^\circ$ for molecules 1 and 2, between the planes defined by S(1), Au(1), O(1) and S(1), C(21), C(22), O(1), C(1) for molecule 1, and S(2), Au(2), O(3) and S(2), C(41), C(42), O(3), C(2) for molecule 2. These are significantly greater than that observed for the isoelectronic platinum(II) complex **8.8** [$10.3(4)^\circ$],²³ but considerably less than that of **8.7a** [45.9°].²² The reason for the different fold angles for **8.8** and **8.7a** is not clear, although presumably the conformation is readily influenced by crystal-packing forces. This notion is tentatively supported by the different fold angles measured for the independent molecules 1 and 2 in **8.10b**. The related nickel(II) complex **8.13** (Figure 8.9) was also found to be bent, but with a fold angle of only 9.4° .²²

**8.13***Figure 8.9*

In the case of the complex **8.10b**, steric factors are likely to play only a minor part in the puckering of the thiosalicylate ligand. It has been suggested previously that the puckering of the platinum(II) thiosalicylate moiety in **8.7a** compared to that in nickel(II) complex might be due to the bite of the thiosalicylate ligand which is better suited towards co-ordination of the smaller nickel(II).²² However, in light of the structural evidence from **8.8** and from the salicylate systems (see later) this interpretation is possibly oversimplified, and it is clear that more structure determinations are required for a more definitive picture to emerge.

The structure of **8.10b** bears a close resemblance to the recently reported gold complex involving the thiomalate ligand, **8.14**²⁸ (Figure 8.10), although the five-membered $\overline{\text{Au-S-C-C-O}}$ ring for this complex was found to be planar.

The quality of the data for **8.10b** does not warrant discussion of the remaining structural features, and comparisons of bond lengths and angles with those of the platinum and nickel thiosalicylate complexes or with **8.14**, **8.15b** (Section 8.2.4) can not be made with confidence.



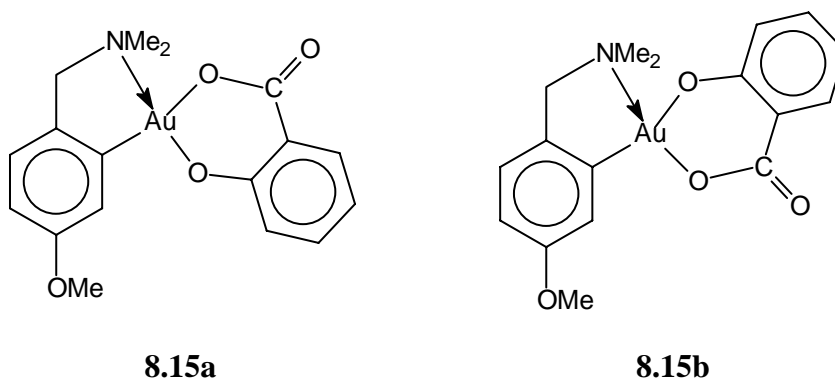
8.14

Figure 8.10

8.2.3 Synthesis of a gold(III) salicylate complex

Given the high regioselectivity of the reactions of the gold(III) halide complexes with thiosalicylic acid, it was of interest to see whether the same selectivity also existed in the reaction with salicylic acid, where the two donor groups are now both relatively low *trans*-influence oxygen atoms.

The reaction of complex **5.1a** with salicylic acid **8.2** was carried out in refluxing dichloromethane with silver(I) oxide, and NMR (^1H and ^{13}C) analysis of the crude reaction product indicated the expected mixture of isomers of the gold(III) salicylate complexes **8.15a** and **8.15b** (Figure 8.11) in an approximately 3:1 ratio. Confirmation of reaction completion was provided by ESMS which gave $[\text{M} + \text{H}]^+$ and $[2\text{M} + \text{H}]^+$ ions, obviously indistinguishable for **8.15a** and **8.15b**. However, upon standing the mixture of isomers in CDCl_3 overnight, complete conversion to a single isomer was effected. Light yellow crystals were obtained from the crude yellow solution by layering diethyl ether and pentane onto a solution of the complex in a dichloromethane-chloroform mixture.



8.15a

8.15b

Figure 8.11

The initially formed, kinetically favoured isomer **8.15a**, was tentatively assigned as the same isomer as for the gold(III) thiosalicylate complexes, *i.e.* with the phenolate group *trans* to the N,N-dimethylamino group. The phenolate group has a slightly higher *trans*-influence than the carboxylate group, as shown by values of 1J (^{195}Pt - ^{31}P) of 3549 and 3929 Hz for the triphenylphosphine ligands *trans* to O and O₂C moieties respectively, in the platinum-salicylate complex **8.9**.²² The corresponding 1J (^{195}Pt - ^{31}P) values for PPh₃ ligands *trans* to S and O₂C in **8.7a** are 2884 and 3899 Hz.

8.2.4 X-ray structure of

$[\{\text{C}_6\text{H}_3(\text{CH}_2\text{NMe}_2)\text{-2-(OMe)-5}\}\text{Au}\{\text{OC}_6\text{H}_4(\text{COO})\text{-2}\}]$ **8.15b** dichloromethane solvate

A single-crystal X-ray diffraction study was carried out on the salicylate complex **8.15b** in order to confirm the isomer assignment from NMR spectroscopy, and to compare the binding requirements of the gold-salicylate moiety with the gold and platinum thiosalicylate moieties. Additionally there is a paucity of structure determinations of salicylate complexes with platinum group metals and gold, so little is known about the detailed binding of the salicylate ligand towards these metals.

Perspective and side views of the structure are shown in Figures 8.12 and 8.13 respectively, together with the atom numbering scheme. Selected bond lengths and angles are given in Table 8.2, with tables of complete bond lengths and angles, final positional parameters, thermal parameters and calculated H-atom positions presented in Appendix XV.

The complex is the opposite isomer to that observed for the analogous thiosalicylate complex **8.10b**, in having the carboxylate group *trans* to the N,N-dimethylamino moiety. It appears that the geometric requirements of the salicylate ligand are a good match for the gold(III) centre, with the four donor atoms around the gold atom forming a very regular flat square plane. The maximum deviation from the least-squares plane defined by atoms Au, N(1), C(11), O(1), and O(2) is only 0.013(1) Å above the plane for N(1) and 0.012(1) Å below for Au. Additionally, the bite angle of the salicylate ligand at gold [O(1)-Au-O(2)] at 93.9(1)°, is close to the idealised 90°, and almost identical to that of the thiosalicylate complex **8.10b** [average 91.9(4)°].

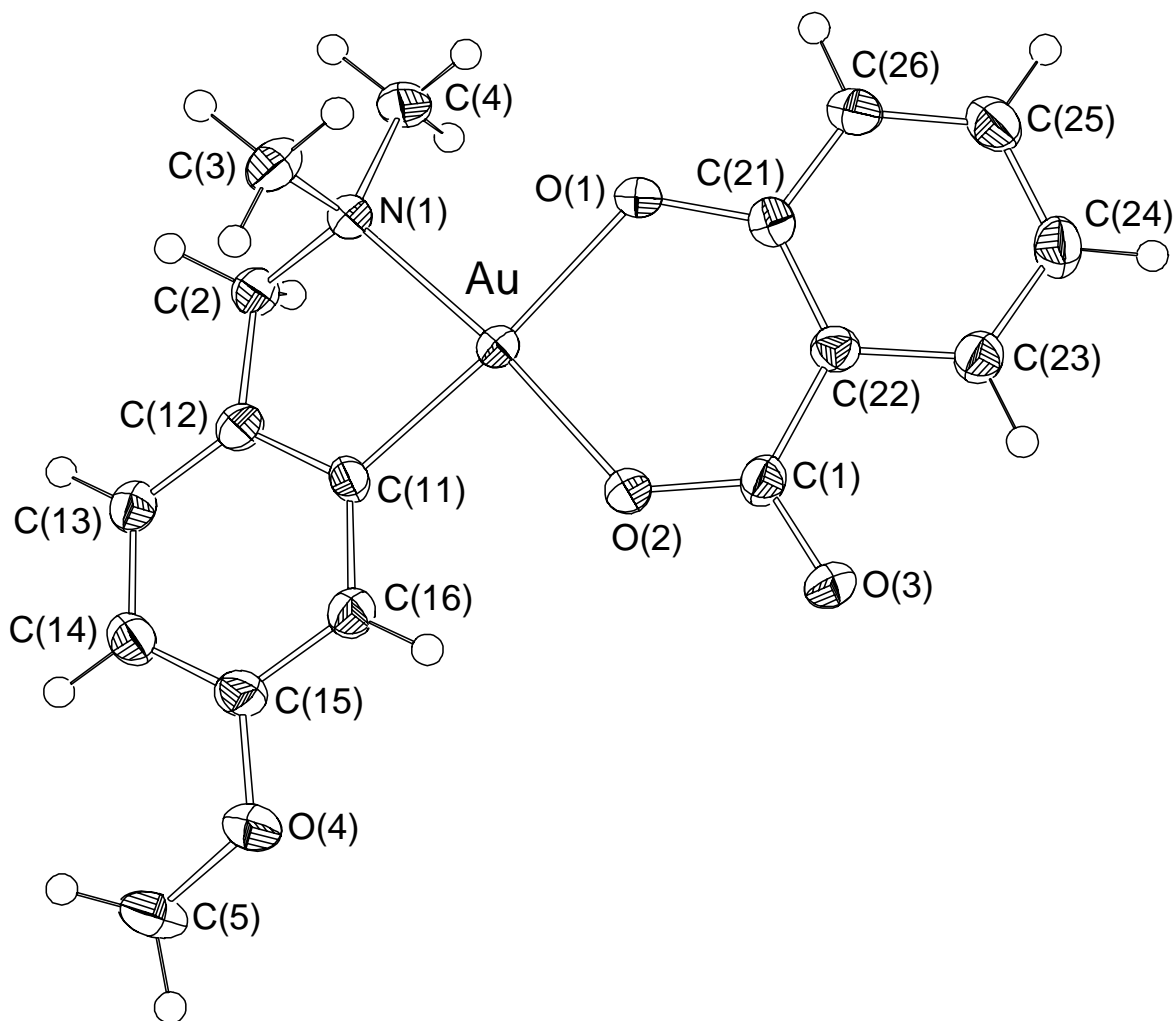


Figure 8.12: ORTEP perspective view of the molecular structure of the gold(III) salicylate complex $[\{C_6H_3(CH_2NMe_2)-2-(OMe)-5\}Au\{OC_6H_4(COO)-2\}]\cdot CH_2Cl_2$ **8.15b** showing the atom numbering scheme. The dichloromethane of crystallisation has been omitted. Thermal ellipsoids are shown at the 50% probability level.

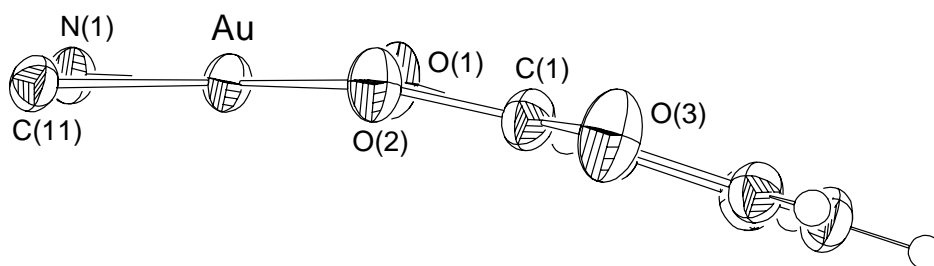


Figure 8.13: ORTEP side view of the molecular structure of the gold(III) salicylate complex $[\{C_6H_3(CH_2NMe_2)-2-(OMe)-5\}Au\{OC_6H_4(COO)-2\}]\cdot CH_2Cl_2$ **8.15b**, demonstrating the non-planarity of the gold-salicylate metallacycle. For clarity, only the Au-bonded atoms of the N,N-dimethylbenzylamine ligand are shown. The dichloromethane of crystallisation has been omitted. Thermal ellipsoids are shown at the 50% probability level.

Table 8.2: Selected bond lengths (Å) and angles (°) for the gold(III) salicylate complex **8.15b**·CH₂Cl₂ with estimated standard deviations in parentheses.

Bond	Length	Bonds	Angle
Au-O(3)	2.037(3)	O(3)-Au-O(1)	82.41(13)
Au-O(1)	1.985(3)	N(1)-Au-C(11)	92.45(11)
Au-N(1)	2.057(3)	N(1)-Au-O(3)	91.24(13)
Au-C(11)	2.001(3)	O(1)-Au-C(11)	122.0(2)
		Au-O(3)-C(21)	126.1(2)
		Au-O(1)-C(1)	
Salicylate ligand			
O(3)-C(21)	1.329(5)	O(3)-C(21)-C(22)	125.8(3)
C(1)-O(1)	1.315(4)	C(21)-C(22)-C(1)	126.2(3)
C(1)-O(2)	1.222(5)	C(22)-C(1)-O(2)	120.2(3)
C(1)-C(22)	1.497(5)	C(22)-C(1)-O(1)	122.6(3)
		O(2)-C(1)-O(1)	117.3(3)

As found in the thiosalicylate-gold system, the salicylate ligand is also non-planar with respect to the gold square-plane, although the degree of puckering [17.9(2)°] is considerably less than for the thiosalicylate complex **8.10b**. Unfortunately, no X-ray structure determinations of platinum(II) salicylate complexes exist to enable a comparison to be made. Indeed, an examination of the Cambridge X-ray Crystal Structure Database,²⁹ surprisingly revealed this to be only the second reported structure of a third row transition-metal mononuclear complex containing a chelating salicylate dianion, the other being Os(VI)³⁰, although a number of mononuclear salicylate dianion complexes derived from Mn(III),³¹⁻³³ Mn(IV),³⁴ Fe(III),³⁵ Co(III),^{36,37} Cu(II),^{38,39} and Mo(VI)⁴⁰⁻⁴² have been structurally characterised. The first row transition-metal salicylate complexes show essentially no puckering of the salicylate ring, whereas the molybdenum and osmium examples show significant puckering with fold angles of 24° and 12° for the two co-ordinated salicylate ligands in a molybdenum derivative,⁴¹ and 14.9° for the osmium system.³⁰ The former lends further evidence of the flexible nature of the salicylate ligand, since both ligands are bound to the same metal centre.

8.2.5 Spectroscopic and mass spectrometric characterisation

8.2.5.1 NMR spectroscopy

Proton and carbon NMR spectra for the complexes **8.10a**, **8.10b** and **8.15b** have been fully assigned using the COSY, HMBC and HSQC experiments (Appendix II), while **8.15a** was assigned by analogy with **8.15b**. The presence of only one resonance associated with N,N'-dimethylamino group indicates that in solution the gold-thiosalicylate moiety is either planar or undergoing rapid inversion, equilibrating the two N-bonded methyl groups which are clearly inequivalent in the solid state. The salicylate derivative **8.15b**, shows similar ^1H and ^{13}C NMR spectroscopic features to the thiosalicylate system **8.10a**, with only minor differences in resonance positions for the cycloaurated benzylamine ligand.

Table 8.3 shows the chemical shifts of quaternary carbon signals of the starting materials, thiosalicylic acid **8.1** and salicylic acid **8.2**, compared with those of the metallacyclic products **8.10a**, **8.10b** and the two salicylate isomers **8.15a** (initial) and **8.15b** (final). The positions of these carbons are identical for the complexes **8.10a** and **8.10b**, the methoxy group in **8.10a** being too far removed from the thiosalicylate moiety to elicit any effect. Surprisingly the carbonyl group undergoes only moderate changes in chemical shift on co-ordination, with the difference being more marked for the salicylate systems (~ 8 ppm). Additionally, the shift is *upfield*, indicating the availability of additional electron density on forming the metallacycle. Even smaller changes are seen for the C-X (X = S, O) aromatic carbons, with a slight upfield shift observed for the thiosalicylate complexes (4.9 ppm), and slight downfield shift for **8.15a** (3.6 ppm) and **8.15b** (1.0 ppm). However, for **8.10a** and **8.10b** very large changes are observed for the aromatic carbon bound to the carbonyl group, with a 27.1 ppm downfield shift. For **8.15a** and **8.15b**, the difference is less marked with downfield shifts of 7.2 and 10.1 ppm respectively. The $\underline{\text{C}}\text{-X}$ and $\underline{\text{C}}\text{-C(O)O}$ carbons seem to be perfectly superimposed for both **8.10a** and **8.10b**, and could not be resolved on the 400.13 MHz spectrometer used for the study.

Table 8.3: Comparison of selected ^{13}C NMR chemical shifts^a of **8.10a**, **8.10b** and **8.15b** compared to the respective thiosalicylic acid **8.1** and salicylic acid **8.2** starting materials.

Group	8.1	8.10a/8.10b ^b	8.2	8.15b
$\underline{\text{C}}=\text{O}$	171.7	168.8	175.0	167.8
$\underline{\text{C}}-\text{X}$ (X = S, O)	139.8	134.9	162.9	163.3
$\underline{\text{C}}-\text{C}(\text{O})\text{OH}$	107.8	134.9	111.3	121.4

^a All data acquired in CDCl_3 solvent and referenced to SiMe_4 (0.0 ppm)

^b The values observed for **8.10a** and **8.10b** are identical (refer main discussion)

8.2.5.2 Electrospray mass spectrometry (ESMS)

Positive-ion ESMS spectra of the complexes **8.10a**, **8.10b** and **8.15b** recorded in 1:1 MeCN- H_2O solution, yield the protonated $[\text{M} + \text{H}]^+$ ions as the base peaks, though the aggregate ions $[2\text{M} + \text{H}]^+$ were of almost equal intensity in the spectra recorded at cone voltages of 20 V. As suggested for the related platinum, palladium and nickel complexes,²² the carboxyl group is the major site for protonation for **8.10b** in the absence of other basic groups in the molecule. However, for the methoxy-substituted complexes, the MeO group would also be expected to play a significant role in the ionisation of the complex, as is the phenoxy O present in **8.15b**.

The $[\text{M} + \text{H}]^+$ ions showed exceptional stability when subjected to exceedingly high cone voltages (up to 200 V), which typically induces extensive fragmentation of parent ions. Undoubtedly, this stability is due to the presence of two chelate rings in the complexes, together with the absence of a facile decomposition pathway, such as cyclometallation of a phosphine ligand.²² It has been noted previously that thiosalicylate complexes containing phosphine ligands which do not readily undergo cyclometallation reactions [e.g. dppe and PTA (phosphatriaza-adamantane)] also show pronounced stability towards fragmentation at high cone voltages in ESMS experiments.²² This is in contrast to triphenylphosphine derived compounds, which often fragment to give cyclometallated complexes (see Chapter Four, Section 4.2.5.2.1). Thus, for the complexes **8.10a**, **8.10b** and **8.15b** at the maximum cone voltage possible for the instrument used (200 V), the $[\text{M} + \text{H}]^+$ ions remained the base peaks. This compares with the complex $[\text{Pt}\{\text{SC}_6\text{H}_4(\text{COO})_2\}(\text{PTA})_2]$ which also showed a comparable stability towards cone voltage-induced fragmentation.²²

8.2.6 Attempted reaction of **8.10a** with mercury(II) iodide

It has been previously found that several cyclic platinum(II) thiolate complexes, including the thiosalicylate complex **8.7a**, react with excess mercury(II) iodide, resulting in the formation of tetrametallic thiolate-bridged complexes with the thiolate sulfur atoms of the platinum complexes co-ordinated to the two mercury atoms of a $\text{IHg}(\mu\text{-I})_2\text{HgI}$ unit.^{43,44} These reactions are readily monitored by NMR spectroscopy, whereupon co-ordination of the thiolate sulfur induces chemical shift and coupling constant changes in the metalloligand. We have therefore investigated the reaction of one of the new gold(III) thiosalicylate complexes to see if the same general reaction holds.

Addition of excess red HgI_2 to a CDCl_3 solution of **8.10a** rather surprisingly resulted in no interaction, with the ^1H NMR spectrum of **8.10a** completely unchanged, and no visible colour change noted. Since the complexes **8.10a** and **8.10b** contain sterically unhindered sulfur atoms, it is speculated that the reluctance of **8.10a** to undergo co-ordination to mercury(II) is possibly related to the greater electronegativity of gold(III) compared to platinum(II), withdrawing electron-density away from the thiolate sulfur.

8.2.7 Biological activity of the gold(III) thiosalicylate and salicylate complexes **8.10a**, **8.10b** and **8.15b**

In light of the moderate to high biological activity shown by the gold(III) ureylene complex $[\{\text{C}_6\text{H}_3(\text{CH}_2\text{NMe}_2)\text{-2-(OMe)-5}\}\text{Au}\{\text{NACc(O)NAC}\}]$ **5.8b** (Chapter 5, Section 5.2.4), we have tested the biological activity of the complexes **8.10a**, **8.10b** and **8.15b**, and all three showed wide-spectrum biological activity, the results of which are summarised in Table 8.4.

Against P388 leukaemia cells, the complex **8.10a** gave an IC_{50} value (the amount required to inhibit 50% of cell growth) of 301 ng ml^{-1} , which is interpreted as having very high anti-tumour activity. Complex **8.10b** also showed significant activity ($\text{IC}_{50} 1937 \text{ ng ml}^{-1}$), although considerably less than that of **8.10a**. This is possibly the result of poorer solubility in biological media, with the absence of the solubilising methoxy group. The salicylate derivative **8.15b** showed only moderate anti-tumour activity ($\text{IC}_{50} 5056 \text{ ng ml}^{-1}$).

Table 8.4: Biological assay results for the gold(III)thiosalicylate complexes **8.10a**, **8.10b** and the salicylate complex **8.15b** (2 µg loaded on disc in each case).

Compd	Antitumour (P-388) and antiviral/cytotoxicity				Antimicrobial/antifungal ^g activities ^h					
	IC ₅₀ ^a	HSV1 ^b	PV1 ^c	Cyt ^d	Ec	Bs	Pa	Ca	Tm	Cr
8.10a	301	-	-	3+ ^e	2	6	3	5	4	7
8.10b	1937	-	-	4+ ^f	4	10	4	6	12	4
8.15b	5056	-	-	4+	8	12	7	8	13	1

^a The concentration of sample in ng/ml required to reduce the cell growth of the P-388 leukemia cell line (ATCC CCL 46) by 50%.

^b *Herpes simplex* type I virus (strain F, ATCC VR 733) grown on the BSC cell line (ATCC CCL 26)

^c *Polio* type I virus (Pfiser vaccine strain) grown on the BSC cell line.

^d Cytotoxicity to BSC cells.

^e 3+ denotes antiviral or cytotoxic zone 4-6 mm excess radius from the disc (75% zone).

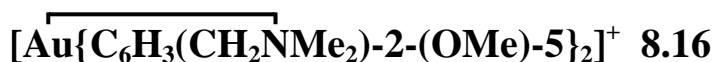
^f 4+ denotes antiviral or cytotoxic zone over whole well (100% zone).

^g Ec = *Escherichia coli*, Bs = *Bacillus subtilis*, Pa = *Pseudomonas aeruginosa*, Ca = *Candida albicans*, Tm = *Trichophyton mentagrophytes*, Cr = *Cladosporium resinae*.

^h Inhibition zone as excess radius (mm) from a 6 mm (diameter) disc containing 2 µg of complex.

For the antimicrobial assay, the complex **8.10a** showed moderate activity against the bacteria and fungi tested. Surprisingly **8.10b** and **8.15b** showed significantly higher activity against the microbes tested, and the reason for this is not obvious. The compounds show effectively no antiviral activity, since their high cytotoxicity killed the majority (or all) of the BSC-1 cell line used for test.

8.2.8 Attempted synthesis and characterisation of the cation



The ESMS spectrum of the crude reaction product of complex **8.10a** indicated an additional species at m/z 525, which was removed on recrystallisation. ESMS analysis of the starting dichloride complex **5.1a** revealed the presence of the same impurity species. This species was tentatively assigned as the cationic complex **8.16** (Figure 8.14), containing two cycloaurated N,N-dimethylbenzylamine ligands. Due to the cationic nature of **8.16** it is likely to have a very high ESMS ionisation efficiency. Other charged species such as metal complex cations and phosphonium salts typically yielded very intense parent ions.⁴⁵ In comparison, the complex **5.1a** ionises by loss of a chloride ligand, and, depending on the cone voltage, co-

ordinates a molecule of the solvent, similar to the ionisation observed for a range of other transition-metal halide and related complexes.⁴⁶ This ionisation process is likely to be far less efficient, resulting in detection of the cation **8.16** in ESMS, but not in the NMR spectra. Upon addition of pyridine to the solution of **5.1a** in MeCN/H₂O, the species [**5.1a** - Cl + py]⁺ was the major ion observed, and **8.16** was not observed in this experiment. This suggests that the added pyridine is more effective at forming positive ions than with the MeCN/H₂O solvent alone.⁴⁶ The cationic pyridine derivative of **5.1b**, **8.16** (Figure 8.14), has been isolated as its perchlorate salt.⁴⁷

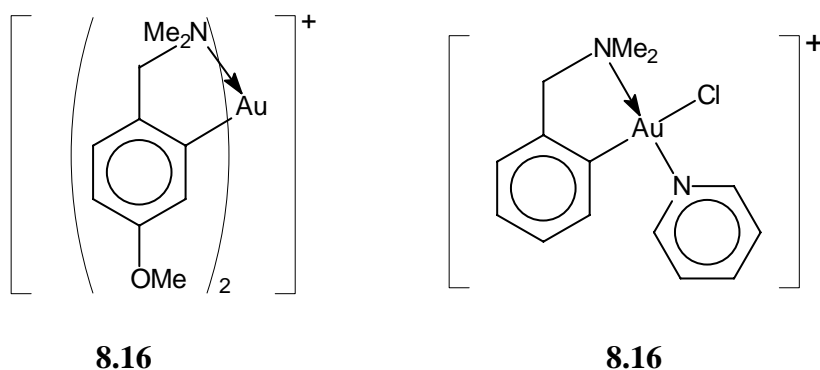


Figure 8.14

Modification of the synthesis of complex **5.1a**, by reaction of Me₄N[AuCl₄] with 2 mole equivalents of the organo-mercury precursor [Hg{C₆H₄(CH₂NMe₂)-2}Cl] in refluxing MeCN gave a very pale yellow solution. ESMS analysis revealed only the cation **8.16** at *m/z* 525. Addition of pyridine to the ESMS solution of **8.16** yielded no pyridine adducts, consistent with it being a bis(cyclometallated) species. Attempted isolation of complex **8.16** was not successful, since it appeared to be very light and/or air sensitive, decomposing even in the refrigerator, and so the nature of the anion remains unknown.

The complex **8.16** does not appear to have been described previously. The reaction of H[AuCl₄], Na[AuCl₄] or [AuLCl₂] with excess [{HgLCl}_n] (HL = 2-phenylpyridine) was unsuccessful in giving such a bis(cyclometallated) gold(III) cation.⁴⁸ However, several bis[(2-phenylazo)phenyl]gold(III) cationic complexes containing **8.12** (Figure 8.8) have been synthesised by reaction of [Hg(C₆H₄(N=NPh)-2)₂] with Me₄N[AuCl₄] followed by AgClO₄,²⁷ and the mixed cyclometallated ligand cation **8.11** (Figure 8.8) has been synthesised by reaction of **5.1b** with [Hg(C₆H₄(N=NPh)-2)₂].²⁶

8.2.9 Conclusions

The first gold(III) complexes containing the thiosalicylate and salicylate dianion ligands have been synthesised, and the structure of the thiosalicylate derivative **8.10b** bears resemblance to the isoelectronic platinum(II) complex **8.7a** structurally characterised previously, with both complexes containing markedly puckered metal-thiosalicylate metallacycles. The related salicylate system also contained a puckered ring system, although to a lesser degree. Electrospray mass spectrometry revealed that the gold-thiosalicylate complexes are very stable towards cone-voltage induced fragmentation. The compounds all displayed moderate to high biological activity, suggesting that further study of analogues of this class of compound could be useful.

8.3 Experimental

General experimental procedures and the instrumentation used are given in Appendices I and II. The synthesis of the gold(III) precursors $[\text{Au}\{\overline{\text{C}_6\text{H}_3(\text{CH}_2\text{NMe}_2)\text{-2-R-5}}\}\text{Cl}_2]$ **5.1a** (R = OMe) and **5.1b** (R = H) are described in Appendix I. Thiosalicylic acid, salicylic acid and red mercury(II) iodide were obtained from BDH, and used as supplied.

Positive-ion electrospray mass spectra were obtained in 1:1 MeCN/H₂O solution. Comparison of observed and calculated⁴⁹ isotope distribution patterns was carried out as an aid to species identification, but was of limited use due to the mono-isotopic nature of gold. However, the presence of heavier isotopomers (arising from contributions from ²H, ¹³C etc) at integral mass unit separation confirmed the unipositive charge on all the observed major ions.

All ¹H, ¹³C NMR and inverse 2D NMR spectra (used for unambiguous assignment) were recorded at 400.13 and 100.61 MHz for the proton and carbon channels respectively, with the exception of **8.15a** for which the ¹H and ¹³C spectra were recorded at 300.13 and 75.47 MHz. CDCl₃ was used as the solvent in all cases. The NMR experiments are detailed in Appendix II.

*Preparation of $[\{\overline{\text{C}_6\text{H}_3(\text{CH}_2\text{NMe}_2)\text{-2-(OMe)-5}}\}\text{Au}(\overline{\text{SC}_6\text{H}_4(\text{COO})\text{-2}})]$ **8.10a***

To a Schlenk flask containing dichloromethane (25 ml), was added **5.1a** (0.050 g, 0.116 mmol), thiosalicylic acid (0.018 g, 0.117 mmol) and silver(I) oxide (0.081 g, excess), and the resulting mixture refluxed under nitrogen in dark conditions for 2 hours. Without further

exclusion of air or light, the silver salts were filtered off, and the solvent evaporated under reduced pressure, to give a bright yellow oil which resisted crystallisation. However, rapid addition of hexane to a dichloromethane solution yielded **8.10a** as a yellow micro-crystalline powder (0.045 g, 76%).

m.p. 176-179 °C (melted with decomposition).

Found: C, 39.1; H, 4.0; N, 2.8%; C₁₇H₁₈NO₃SAu requires: C, 39.8; H, 3.5; N, 2.7%.

IR: ν (CO region) 1624 (s), 1598 (vs).

ESMS: (Cone voltage = 20V) m/z 1027 ([2M + H]⁺, 94%), 514 ([MH]⁺, 100%). (Cone voltage = 200V) m/z 1027 ([2M + H]⁺, 33%), 514 ([MH]⁺, 100%).

¹H NMR: δ 8.15 (1H, *dd*, ³J_{3",4"} = 7.22 Hz, ⁴J_{3",5"} = 2.18 Hz, H-3"), 7.47 (1H, *dd*, ³J_{6",5"} = 7.63 Hz, ⁴J_{6",4"} = 1.92 Hz, H-6"), 7.19 (1H, *td*, ³J_{5",4"/6"} = 7.91 Hz, ⁴J_{5",3"} = 2.43 Hz, H-5"), 7.16 (1H, *td*, ³J_{4",3"/5"} = 7.64 Hz, ⁴J_{4",6"} = 2.02 Hz, H-4"), 7.05 (1H, *d*, ⁴J_{6',4'} = 2.46 Hz, H-6'), 7.03 (1H, *d*, ³J_{3',4'} = 8.29 Hz, H-3'), 6.74 (1H, *dd*, ³J_{4',3'} = 8.29 Hz, ⁴J_{4',6'} = 2.46 Hz, H-4'), 4.16 (2H, *s*, CH₂), 3.81 (3H, *s*, OCH₃), 3.06 (6H, *s*, NCH₃).

¹³C NMR: δ 168.8 (*s*, C=O), 158.0 (*s*, C-5'), 137.3 (*s*, C-2'), 136.5 (*s*, C-1'), 134.9 (*s*, C-1"), 134.9 (*s*, C-2"), 133.3 (*d*, C-3"), 130.1 (*d*, C-5"), 129.7 (*d*, C-6"), 125.3 (*d*, C-4"), 124.7 (*d*, C-3'), 115.6 (*d*, C-6'), 114.0 (*d*, C-4'), 71.4 (*t*, CH₂), 55.6 (*q*, OCH₃), 50.0 (*q*, NCH₃).

[[C₆H₃(CH₂NMe₂)-2]Au(SC₆H₄(COO)-2)] 8.10b

Similarly, **5.1b** (0.051 g, 0.127 mmol), thiosalicylic acid (0.020 g, 0.130 mmol) and silver(I) oxide (0.083 g, excess), were added to dichloromethane (25 ml), and refluxed under nitrogen for 2 hours, during which time the solution changed from almost colourless to bright yellow. Work-up gave a bright yellow solid residue which could readily be recrystallised from dichloromethane-ether to yield yellow crystals of **8.10b** (0.048 g, 79%).

m.p. 165-170 °C (decomposed without melting).

Found: C, 39.5; H, 3.4; N, 2.9%; C₁₆H₁₆NO₂SAu requires: C, 39.8; H, 3.3; N, 2.9%.

IR: ν (CO region) 1621 (vs), 1604 (m), 1582 (m).

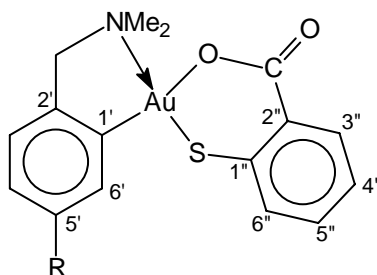
ESMS: (Cone voltage = 20V) m/z 967 ([2M + H]⁺, 97%), 484 ([MH]⁺, 100%). (Cone voltage = 200V) m/z 967 ([2M + H]⁺, 48%), 484 ([MH]⁺, 100%).

¹H NMR: δ 8.17 (1H, *dd*, ³J_{3",4"} = 7.50 Hz, ⁴J_{3",5"} = 1.91 Hz, H-3"), 7.50 (1H, *dd*, ³J_{6',5'} = 7.88 Hz, ⁴J_{6',4'} = 1.06 Hz, H-6'), 7.42 (1H, *dd*, ³J_{6",5"} = 7.49 Hz, ⁴J_{6",4"} = 1.60 Hz, H-6"), 7.22 (1H, *td*, ³J_{5",4"/6"} = 7.36 Hz, ⁴J_{5',3'} = 1.18 Hz, H-5'), 7.21 (1H, *td*, ³J_{5",4"/6"} = 7.22 Hz, ⁴J_{5",3"} = 1.84 Hz,

H-5"), 7.17 (1H, *td*, $^3J_{4'',3''/5''} = 7.36$ Hz, $^4J_{4'',6''} = 1.18$ Hz, H-4"), 7.15 (1H, *t*, $^3J_{4',3'/5'} = 7.66$ Hz, H-4'), 7.12 (1H, *d*, $^3J_{3',4'} = 7.47$ Hz, H-3'), 4.23 (2H, *s*, $\underline{\text{CH}_2}$), 3.11 (6H, *s*, NCH_3).

^{13}C NMR: δ 168.8 (*s*, C=O), 145.4 (*s*, C-1'), 135.9 (*s*, C-2'), 134.9 (*s*, C-1''), 134.9 (*s*, C-2''), 133.3 (*d*, C-3''), 130.4 (*d*, C-6''), 130.1 (*d*, C-5''), 129.7 (*d*, C-6''), 128.6 (*d*, C-5'), 127.9 (*d*, C-4'), 125.3 (*d*, C-4''), 124.1 (*d*, C-3'), 71.9 (*t*, $\underline{\text{CH}_2}$), 50.2 (*q*, NCH_3).

NMR numbering scheme for 8.10a (R = OMe) and 8.10b (R = H):



Preparation of $[\{\text{C}_6\text{H}_3(\text{CH}_2\text{NMe}_2)\text{-}2\text{-(OMe)\text{-}5}\}\text{Au}(\text{OC}_6\text{H}_4(\text{COO})\text{-}2)\text{-}2\}$ 8.15a and 8.15b

Similarly, **5.1a** (0.050 g, 0.116 mmol), salicylic acid (0.016 g, 0.116 mmol) and silver(I) oxide (0.087 g, excess) were refluxed in dichloromethane (25 ml), under nitrogen, for 4 hours. Work-up gave a pale yellow residue, which was revealed to be a mixture of the isomers **8.15a** and **8.15b** by preliminary ^1H and ^{13}C NMR spectroscopy, in a 1:3 ratio. However, standing a chloroform or dichloromethane solution of the mixture at room temperature for 24 hours, gave a pure product, this being the minor isomer initially formed. The almost pure residue crystallised readily by liquid-liquid diffusion of ether into a dichloromethane solution, to give **8.15b** as yellow needles (0.040 g, 70%).

m.p. 132-135°C.

Found: C, 39.6; H, 3.8; N, 2.6%; $\text{C}_{17}\text{H}_{18}\text{NO}_4\text{Au}$ requires: C, 41.0; H, 3.7; N, 2.8%.

IR: ν (CO region) 1599(*s*), 1576(*vs*).

ESMS: (Cone voltage = 20V) m/z 1017 ($[\text{2M} + \text{Na}]^+$, 32%), 995 ($[\text{2M} + \text{H}]^+$, 92%), 498 ($[\text{MH}]^+$, 100%). (Cone voltage = 200V) m/z 1017 ($[\text{2M} + \text{Na}]^+$, 28%), 995 ($[\text{2M} + \text{H}]^+$, 60%), 498 ($[\text{MH}]^+$, 100%).

Final Isomer 8.15b

^1H NMR: δ 8.10 (1H, *dd*, $^3J_{3'',4''} = 7.91$ Hz, $^4J_{3'',5''} = 1.58$ Hz, H-3''), 7.22 (1H, *td*, $^3J_{5'',4''/6''} = 7.61$ Hz, $^4J_{5'',3''} = 1.75$ Hz, H-5''), 7.05 (1H, *d*, $^4J_{6',4'} = 2.37$ Hz, H-6'), 6.99 (1H, *d*, $^3J_{6'',5''} = 8.26$

Hz, H-6''), 6.94 (1H, *d*, $^3J_{3',4'} = 8.32$ Hz, H-3'), 6.82 (1H, *t*, $^3J_{4'',3''/5''} = 7.69$ Hz, H-4''), 6.80 (1H, *td*, $^3J_{4',3'} = 8.29$ Hz, $^4J_{4',6'} = 2.42$ Hz, H-4'), 4.20 (2H, *s*, $\underline{\text{CH}}_2$), 3.85 (3H, *s*, $\underline{\text{OCH}}_3$), 3.14 (6H, *s*, $\underline{\text{NCH}}_3$).

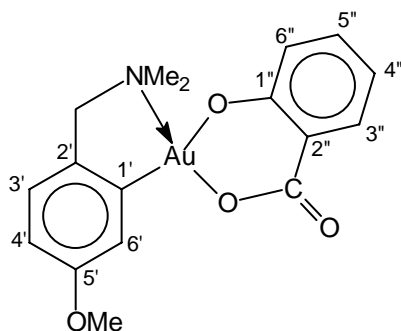
^{13}C NMR: (100.61 MHz) δ 167.8 (*s*, C=O), 163.3 (*s*, C-1''), 157.2 (*s*, C-5'), 138.6 (*s*, C-1'), 135.7 (*s*, C-2'), 133.3 (*d*, C-3''), 132.4 (*d*, C-5''), 123.5 (*d*, C-3'), 121.4 (*s*, C-2''), 120.0 (*d*, C-6''), 118.7 (*d*, C-4''), 114.8 (*d*, C-4'), 111.8 (*d*, C-6'), 74.0 (*t*, $\underline{\text{CH}}_2$), 55.5 (*q*, $\underline{\text{OCH}}_3$), 52.3 (*q*, $\underline{\text{NCH}}_3$).

Initial Isomer 8.15a

^1H NMR: δ 7.98 (1H, *dd*, $^3J_{3'',4''} = 8.00$ Hz, $^4J_{3'',5''} = 1.70$ Hz, H-3''), 7.22 (1H, *td*, $^3J_{5'',4''/6''} = 7.64$ Hz, $^4J_{5'',3''} = 1.86$ Hz, H-5''), 6.97 (1H, *d*, $^4J_{6',4'} = 2.14$ Hz, H-6'), 6.86 (1H, *d*, $^3J_{3',4'} = 8.32$ Hz, H-3'), 6.71 (1H, *d*, $^3J_{6'',5''} = 7.97$ Hz, H-6''), 6.68 (1H, *t*, $^3J_{4'',3''/5''} = 7.49$ Hz, H-4''), 6.59 (1H, *td*, $^3J_{4',3'} = 8.31$ Hz, $^4J_{4',6'} = 2.40$ Hz, H-4'), 4.23 (2H, *s*, $\underline{\text{CH}}_2$), 3.74 (3H, *s*, $\underline{\text{OCH}}_3$), 3.11 (6H, *s*, $\underline{\text{NCH}}_3$).

^{13}C NMR: δ 166.9 (*s*, C=O), 165.9 (*s*, C-1''), 157.3 (*s*, C-5'), 140.5 (*s*, C-1'), 135.6 (*s*, C-2'), 133.8 (*d*, C-3''), 133.3 (*d*, C-5''), 123.5 (*d*, C-3'), 121.4 (*d*, C-6''), 118.5 (*s*, C-2''), 116.7 (*d*, C-4''), 114.5 (*d*, C-4'), 112.2 (*d*, C-6'), 74.8 (*t*, $\underline{\text{CH}}_2$), 55.8 (*q*, $\underline{\text{OCH}}_3$), 52.6 (*q*, $\underline{\text{NCH}}_3$).

NMR numbering scheme for 8.15b (8.15a is analogous):



Preparation of $[\text{Au}\{\text{C}_6\text{H}_3(\text{CH}_2\text{NMe}_2)\text{-2-(OMe)-5}\}_2]^+$ 8.16

The orthomercurated complex $[\text{Hg}\{\text{C}_6\text{H}_3(\text{CH}_2\text{NMe}_2)\text{-2-(OMe)-5}\}\text{Cl}]$ (0.101 g, 0.267 mmol), $\text{Me}_4\text{N}[\text{AuCl}_4]$ (0.054 g, 0.131 mmol) and tetramethylammonium chloride (0.032 g, 0.292 mmol) were dissolved in acetonitrile (30 ml) which had been previously been degassed and purged with nitrogen. The yellow solution was refluxed for one hour, during which time the mixture became almost colourless. The solvent was evaporated under vacuum, and the residue

dissolved in dichloromethane. The insoluble material was filtered off, and the solvent removed from the supernatant, to give a white powder characterised by ESMS as containing cation **8.16**. Efforts at further purification and analysis were unsuccessful and resulted in rapid decomposition to gold metal, since the material was air and/or light sensitive.

ESMS: (Cone voltage = 20V) m/z 525 ($[M]^+$, 100%), 200 (unidentified, 57%). (Cone voltage = 50V) m/z 525 ($[M]^+$, 100%), 164 ($[C_6H_3(CH_2NMe_2)-2]^+$, 72%).

8.3.1 X-ray structure of $[\{C_6H_4(CH_2NMe_2)-2\}Au\{SC_6H_4(COO)-2\}]$ **8.10b**

Bright yellow blocks of **8.10b** suitable for an X-ray structure determination were grown by layering diethyl ether on a dichloromethane solution in a narrow tube at 4°C.

Data collection

Unit cell dimensions and intensity data were obtained on a Siemens CCD detector mounted on a P4 diffractometer at the University of Canterbury. Details regarding the collection methodology and configuration are described in Appendix II.

Collection Data: crystal size = 0.35 x 0.30 x 0.09 mm, total reflections = 16271, unique reflections = 5161, range = $1.29 < \theta < 24.99^\circ$, absorption correction $T_{max.,min.} = 1.00, 0.50$.

Crystal Data: $C_{16}H_{16}NO_2SAu$, $M_r = 483.34$, monoclinic, space group $P2_1/c$, $a = 17.560(1)$, $b = 12.418(1)$, $c = 15.608(1)$ Å, $\beta = 116.07(1)^\circ$, $U = 3057.3(1)$ Å³, $D_c = 2.100$ g cm⁻³, $Z = 8$, $F(000) = 1840$, $\mu(Mo-K\alpha) = 9.76$ mm⁻¹.

Solution and refinement

The structure was solved by the Patterson methods option of SHELXS-96,⁵⁰ and the gold positions determined. All further non-hydrogen atoms were located routinely (SHELXL-96).⁵¹ Building a model that successfully accounted for the observed electron density was thwarted by apparent twinning and/or disorder present in the crystals. This persisted despite two independent data collections on two different crystals. Significant electron density remained which could not be modelled in chemically sensible positions. The best refinement led only to an R_1 of 0.1555, therefore the determination can really only be taken to indicate atom

connectivity and overall conformation, and the numerical data presented in Appendix XIV should be treated with caution.

8.3.2 X-ray structure of

[{C₆H₃(CH₂NMe₂)-2-(OMe)-5}Au{OC₆H₄(COO)-2}] 8.15b dichloromethane solvate

Yellow needles of **8.15b** suitable for an X-ray study were grown by layering diethyl ether on a dichloromethane solution in a narrow tube at 4°C.

Data collection

Accurate cell parameters and intensity data were collected on Siemens SMART CCD diffractometer at Auckland University. Details regarding the collection methodology and configuration are described in Appendix II.

Collection Data: crystal size = 0.52 x 0.19 x 0.11 mm, total reflections = 9026, unique reflections = 4159, range = 1.99 < θ < 28.26°, absorption correction $T_{\max., \min.} = 0.54, 0.34$.

Crystal Data: C₁₇H₁₈NO₄Au.CH₂Cl₂, Mr = 582.22, triclinic, space group P $\bar{1}$ (no. 2), $a = 9.4172(2)$, $b = 9.9906(2)$, $c = 11.5903(2)$ Å, $\alpha = 67.993(1)$, $\beta = 69.561(1)$, $\gamma = 79.844(1)^\circ$, $U = 946.06(3)$ Å³, D_c = 2.044 g cm⁻³, Z = 2, F(000) = 560, $\mu(\text{Mo-K}\alpha) = 8.081$ mm⁻¹.

Solution and refinement

The structure was solved by the Patterson methods option of SHELXS-96,⁵⁰ and the gold position determined. All further non-hydrogen atoms were located routinely (SHELXL-96)⁵¹ and assigned anisotropic temperature factors, with all hydrogen atom positions determined by calculation. The refinement converged with $R_1 = 0.0223$ for 3960 data with $I \geq 2\sigma(I)$, 0.0237 for all data; $wR_2 = 0.0534$ { $w = 1/[\sigma^2(F_o^2) + (0.0161P)^2 + 2.2576P]$ where $P = (F_o^2 + 2F_c^2)/3$ }, and GoF = 1.079. No parameter shifted in the final cycle. The final difference map showed no peaks or troughs of electron density greater than +0.86 and -1.90 e Å⁻³ respectively, both adjacent to the gold atom.

References

- 1 J.R. Roberts, J. Xiao, B. Schliesman, D.J. Parsons and C.F. Shaw III, *Inorg. Chem.*, **35** (1996) 424.
- 2 S.J. Berners-Price and P.J. Sadler, *Coord. Chem. Rev.*, **151** (1996) 1.
- 3 P.J. Sadler, *Adv. Inorg. Chem.*, **36** (1991) 1.
- 4 D.H. Brown and W.E. Smith, *Chem. Soc. Rev.*, **9** (1980) 217.
- 5 S.J. Berners-Price and P.J. Sadler, *Structure and Bonding*, **70** (1988) 27.
- 6 C.F. Shaw III in *Metal Compounds in Cancer Chemotherapy*, Ed. S.P. Fricker, Chapman & Hall, (1994) Chapter 3.
- 7 A. Ulman, *Chem. Rev.*, **96** (1996) 1533.
- 8 *The Chemistry of Gold*, R.J. Puddephatt, Elsevier, Amsterdam, (1978).
- 9 M.D. Janssen, D.M. Grove and G. van Koten, *Prog. Inorg. Chem.*, **46** (1997) 97.
- 10 J.M. López-de-Luzuriaga, A. Sladek, and H. Schmidbaur, *J. Chem. Soc., Dalton Trans.*, (1996) 4511.
- 11 A. Sladek, K. Angermaier and H. Schmidbaur, *Chem. Commun.*, (1996) 1959.
- 12 A. Sladek and H. Schmidbaur, *Chem. Ber.*, **128** (1995) 907.
- 13 J. Vicente, M.-T. Chicote, P. González-Herrero and P.G. Jones, *J. Chem. Soc., Dalton Trans.*, (1994) 3183.
- 14 A. Sladek, W. Schneider, K. Angermaier, A. Brauer, and H. Schmidbaur, *Z. Naturforsch.*, **51b** (1996) 765.
- 15 W. Schneider, A. Bauer and H. Schmidbaur, *Organometallics*, **15** (1996) 5445.
- 16 P.D. Cookson and E.R.T. Tiekink, *J. Coord. Chem.*, **26** (1992) 313.
- 17 K. Nomiya, H. Yokoyama, H. Nagano, M. Oda, and S. Sakuma, *J. Inorg. Biochem.*, **60** (1995) 289.
- 18 K. Nomiya, Y. Kondoh, K. Onoue, N. C. Kasuga, H. Nagano, M. Oda, T. Sudoh, and S. Sakuma, *J. Inorg. Biochem.*, **58** (1995) 255.
- 19 D. Vlassopoulos, S.A. Wood, and A. Mucci, *Geochim. Cosmochim. Acta*, **54** (1990) 1575.
- 20 M.K. Koul, *Curr. Sci.*, **44** (1975) 426.
- 21 S.C.S. Rajan, and N.A. Raju, *J. Indian Chem. Soc.*, **52** (1975) 947.
- 22 L.J. McCaffrey, W. Henderson, B.K. Nicholson, J.E. Mackay, and M.B. Dinger, *J. Chem. Soc., Dalton Trans.*, (1997) 2577.
- 23 L.J. McCaffrey, W. Henderson and B.K. Nicholson, unpublished results.

- 24 T.G. Appleton, H.C. Clark and L.E. Manzer, *Coord. Chem. Rev.*, *10* (1973) 335.
- 25 R.G. Pearson, *Inorg. Chem.*, *12* (1973) 712.
- 26 J. Vicente, M.-T. Chicote, M.D. Bermudez and M.J. Sanchez-Santano, *J. Organomet. Chem.*, *310* (1986) 401.
- 27 J. Vicente, M.-T. Chicote, M.-D. Bermúdez, X. Soláns and M. Font-Altaba, *J. Chem. Soc., Dalton Trans.*, (1984) 557.
- 28 R.V. Parish, B.P. Howe, J.P. Wright, J. Mack and R.G. Pritchard, *Inorg. Chem.* *35* (1996) 1659.
- 29 F.H. Allen and O. Kennard, *Chemical Design Automation News*, *8* (1993) 131.
- 30 C.C. Hinckley and P.A. Kibala, *Acta Cryst., Sect. C*, *43*, (1987) 842.
- 31 X-S. Tan, J. Chen, P-J. Zheng and W-X. Tang, *Acta Cryst., Sect. C*, *51* (1995) 1268.
- 32 X-S. Tan, W-X. Tang and J. Sun, *Polyhedron*, *15* (1996) 2671.
- 33 M.L. Kirk, M.S. Lah, C. Raptopoulou, D.P. Kessissoglou, W.E. Hatfield and V.L. Pecoraro, *Inorg. Chem.*, *30* (1991) 3900.
- 34 P.S. Pavacik, J.C. Huffman and G. Christou, *J. Chem. Soc., Chem. Commun.*, (1986) 43.
- 35 M.R. McDevitt, A.W. Addison, E. Sinn and L.K. Thompson, *Inorg. Chem.*, *29* (1990) 3425.
- 36 Y. Kushi, T. Hosoo and H. Kuroya, *J. Chem. Soc., D.*, (1970) 397.
- 37 H. Sekizaki, E. Toyota and Y. Yamamoto, *Bull. Chem. Soc. Jpn.*, *66* (1993) 1652.
- 38 A. Pajunen and S. Pajunen, *Cryst. Struct. Commun.*, *11* (1982) 427.
- 39 H. Muhonen, *Acta Cryst., Sect. B*, *38* (1982) 2041.
- 40 C.F. Edwards, W.P. Griffith, A.J.P. White and D.J. Williams, *Polyhedron*, *11* (1992) 2711.
- 41 C.F. Edwards, W.P. Griffith, A.J.P. White and D.J. Williams, *J. Chem. Soc., Dalton Trans.*, (1993) 3813.
- 42 K. Boutilier, L.R. MacGillivray, S. Subramanian and M.J. Zaworotko, *J. Cryst. Spec. Res.*, *23* (1993) 773.
- 43 W. Henderson, B.K. Nicholson, and R.D.W. Kemmitt, *J. Chem. Soc., Dalton Trans.*, (1994) 2489.
- 44 L.J. McCaffrey, W. Henderson, and B.K. Nicholson, *Polyhedron*, *17* (1998) 221.
- 45 R. Colton and J.C. Traeger, *Inorg. Chim. Acta*, *201* (1992) 153.
- 46 C. Evans and W. Henderson, unpublished results.

-
- 47 J. Vicente, M.T. Chicote and M. Bermúdez, *J. Organomet. Chem.*, 268 (1984) 191.
- 48 E.C. Constable and T.A. Leese, *J. Organomet. Chem.*, 363 (1989) 419.
- 49 L.J. Arnold, *J. Chem. Educ.*, 69 (1992) 811.
- 50 G.M. Sheldrick, SHELXS-96, Program for Solving X-Ray Crystal Structures, University of Göttingen, Germany, (1996).
- 51 G.M. Sheldrick, SHELXL-96, Program for Refining X-Ray Crystal Structures, University of Göttingen, Germany, (1996).

Appendix I

General Experimental Procedure and Preparation of Inorganic and Organometallic Precursors

A.I.1 General experimental procedure

A.I.1.1 Solvents

Unless specifically stated the solvents used for preparation described in this thesis were either of analytical grade, or freshly distilled as described below.

Dichloromethane (drum grade) and X4 (drum grade petroleum spirits) were dried and purified by distillation from calcium hydride under nitrogen. THF (laboratory grade) and diethyl ether (analytical grade) were dried by distillation from sodium/benzophenone under nitrogen.

A.I.1.2 Glassware

All glassware used was clean, air dry, and free of grease prior to use. Oven dried glassware was only used if reactions were deemed water sensitive. Quick-fit joints were generally not greased.

A.I.1.3 Air sensitive reactions

All reactions deemed air sensitive were carried out under an inert atmosphere of dry nitrogen, using standard established Schlenk techniques. The reaction vessel to be used was purged of air, by at least three cycles of evacuation followed by filling with nitrogen. The solvent was then typically added to the vessel, and subsequently purged with nitrogen by three additional cycles of evacuation (boiling), followed by flushing with nitrogen.

A.I.1.4 Light sensitive reactions

The gold(III) precursors **5.1a** and **5.1b** were found to be moderately light sensitive, evidenced by purple colloidal gold formation on crystals after only a few hours of indirect sunlight

exposure, with direct sunlight inducing more extensive decomposition. For this reason all reactions involving gold complexes were undertaken in dark conditions, achieved by wrapping the reaction vessel with aluminium foil.

A.I.2 Preparation of inorganic and organometallic precursors

*[PtCl₂(COD)]*¹

Potassium tetrachloroplatinate (K₂PtCl₄, 5.0 g, 12.05 mmol) was dissolved in water (80 ml) and filtered (if required). To the deep red filtrate were added glacial acetic acid (80 ml) and 1,5-cyclooctadiene (5 ml, 40 mmol). The reaction mixture was heated, with stirring, to 90°C in an oil bath. Over 30 minutes the deep red solution slowly became pale yellow and fine crystals were deposited. The volume of the solution was reduced to 50 ml by evaporation under reduced pressure. The pale yellow to almost white needles were filtered and thoroughly washed in succession with 50 ml portions of water, ethanol and diethyl ether, and dried under vacuum to give [PtCl₂(COD)] (4.33 g, 96%). Any residual acetic acid or 1,5-cyclooctadiene could be removed by dissolving the product in the minimum quantity of dichloromethane and pouring this solution into petroleum spirits (200 ml) to induce precipitation.

¹H NMR: (300.13 MHz) (CDCl₃) δ 5.60 (4H, *s*, (*d*, ²J_{H,Pt} = 65.8 Hz), CH=CH), 2.73-2.69 (4H, *m*, CH₂-CH), 2.35-2.17 (4H, *m*, CH₂-CH).

¹³C NMR: (75.47 MHz) (CDCl₃) δ 100.1 (*s*, (*d*, ¹J_{C,Pt} = 152.3 Hz), CH=CH), 31.0 (*t*, CH₂-CH).

cis-[PtCl₂(PPh₃)₂]

This was readily prepared in quantitative yields by addition of two equivalents of triphenylphosphine to a dichloromethane solution of [PtCl₂(COD)] and the mixture stirred at room temperature for 5 minutes. Addition of petroleum spirits induced precipitation of *cis*-[PtCl₂(PPh₃)₂], which was subsequently filtered off, and thoroughly washed with diethyl ether.

³¹P NMR: δ 14.9 (*s*, (*d*, ¹J_{P,Pt} = 3689 Hz), PPh₃).

$[(\eta^6\text{-}p\text{-cymene})\text{RuCl}_2]_2$ ²

To a solution of hydrated ruthenium trichloride (1.0 g, 3.83 mmol based on $\text{RuCl}_3 \cdot 3\text{H}_2\text{O}$) in ethanol (50 ml) was added α -phellandrene (5 ml, excess), and heated under reflux for 4 hours. After cooling, the resulting red-brown micro-crystalline solid was filtered off, with further product being obtained by the removal of solvent from the filtrate (0.95 g, 82%).

 $[(\eta^6\text{-}p\text{-cymene})\text{RuCl}_2(\text{PPh}_3)]$ ³

$[(\eta^6\text{-}p\text{-cymene})\text{RuCl}_2]_2$ (0.101 g, 0.167 mmol) was dissolved in dichloromethane (50 ml). To this was added triphenylphosphine (0.088 g, 0.335 mmol) and the resulting mixture refluxed for 15 minutes. No colour change was observed. Removal of solvent and subsequent recrystallisation of the residue from dichloromethane and ether gave $[(\eta^6\text{-}p\text{-cymene})\text{RuCl}_2(\text{PPh}_3)]$ as orange micro-crystals (0.0180 g, 96%).

³¹P NMR: δ 24.9 (s, PPh_3).

¹H NMR: δ 7.82 (6H, t, $^3J_{3''} = 9.18$ Hz, C-3''), 7.37-7.32 (9H, m, C-2''), 5.19 (2H, d, $^3J_{2,3'} = 6.00$ Hz, C-2',6'), 4.99 (2H, d, $^3J_{3,2'} = 5.82$ Hz, C-3',5'), 2.84 (1H, quintet, $^3J_{4,1} = 6.90$ Hz, C-4), 1.86 (3H, s, C-3), 1.10 (6H, d, $^3J_{1,4} = 6.95$ Hz, C-1,2).

¹³C NMR: δ 134.4 (d, (d, $^3J_{\text{C,P}} = 9.36$ Hz), C-3''), 133.9 (s, (d, $^1J_{\text{C,P}} = 45.43$ Hz), C-1''), 130.2 (d, (d, $^4J_{\text{C,P}} = 1.51$ Hz), C-4''), 128.0 (d, (d, $^2J_{\text{C,P}} = 9.96$ Hz), C-2''), 111.2 (s, C-1'), 96.0 (s, C-4'), 89.1 (d, (d, $^3J_{\text{C,P}} = 2.79$ Hz), C-2',6'), 87.2 (d, (d, $^3J_{\text{C,P}} = 5.43$ Hz), C-3',5'), 30.3 (d, C-4), 21.9 (q, C-1,2), 17.8 (q, C-3).

 $[(\eta^6\text{-}p\text{-cymene})\text{OsCl}_2]_2$ ⁴

$\text{Na}_2[\text{OsCl}_6]$ (1 g, 2.223 mmol) and α -phellandrene (5 ml, excess) were added to ethanol (10 ml), and the mixture refluxed under nitrogen for 5 days. The resulting dirty yellow/orange suspension was concentrated to ~4 ml under reduced pressure, filtered, and washed with cold ethanol, followed by ether. The powder was subsequently rapidly recrystallised from dichloromethane/pentane to give $[(\eta^6\text{-}p\text{-cymene})\text{OsCl}_2]_2$ as a yellow powder (0.65 g, 74%).

$$[(\eta^6\text{-}p\text{-cymene})\text{OsCl}_2(\text{PPh}_3)]^5$$

$[(\eta^6\text{-}p\text{-cymene})\text{OsCl}_2]_2$ (0.65 g, 0.882 mmol) and triphenylphosphine (0.65 g, excess) were dissolved in dichloromethane (20 ml) and refluxed under nitrogen for 3 hours. The solvent was removed under reduced pressure, and the residue dissolved in a small amount of dichloromethane. On the solution, ether was carefully layered, and over 10 hours bright yellow crystals of $[(\eta^6\text{-}p\text{-cymene})\text{OsCl}_2(\text{PPh}_3)]$ formed (0.97 g, 89.7%).

^{31}P NMR: δ -12.4 (s, (d, $^1J_{\text{P,Os}} = 281.8$ Hz), $\underline{\text{PPh}}_3$).

^1H NMR: δ 7.80-7.73 (6H, m, Ar-H), 7.38-7.33 (9H, m, Ar-H), 5.40 (2H, d, $^3J_{2',3'} = 5.82$ Hz, C-2',6'), 5.18 (2H, d, $^3J_{3',2'} = 5.43$ Hz, C-3',5'), 2.74 (1H, *quintet*, $^3J_{4,1} = 6.91$ Hz, C-4), 1.97 (3H, s, C-3), 1.15 (3H, d, $^3J_{1,4} = 6.94$ Hz, C-1,2).

^{13}C NMR: δ 134.6 (d, (d, $^3J_{\text{C,P}} = 9.36$ Hz), C-3"), 133.4 (s, (d, $^1J_{\text{C,P}} = 52.23$ Hz), C-1"), 130.2 (d, (d, $^4J_{\text{C,P}} = 1.51$ Hz), C-4"), 127.9 (d, (d, $^2J_{\text{C,P}} = 10.26$ Hz), C-2"), 103.3 (s, C-1'), 88.6 (s, C-4'), 80.4 (d, (d, $^3J_{\text{C,P}} = 2.49$ Hz), C-2',6'), 79.9 (d, (d, $^3J_{\text{C,P}} = 4.91$ Hz), C-3',5'), 30.1 (d, C-4), 22.2 (q, C-1,2), 17.8 (q, C-3).

$$[\text{Cp}^*\text{IrCl}_2]_2^6$$

Hydrogen chloride gas (conveniently made *in situ* by adding, dropwise, concentrated H_2SO_4 to ammonium chloride) was bubbled into a solution of hexamethyldewarbenzene (0.5 ml, excess) in dichloromethane (10 ml) at room temperature for 1 hour. The resulting deep purple solution was stirred for a further 5 hours, after which the solvent was removed under reduced pressure to give crude 1-(1-chloroethyl)pentamethylcyclopentadiene. This was added to a suspension of $\text{IrCl}_3 \cdot 5\text{H}_2\text{O}$ (0.356 g, 0.88 mmol) in methanol (10 ml) and refluxed under nitrogen for 20 hours. After cooling to room temperature, the orange solid precipitated was collected on a filter, washed with methanol followed by ether, and dried in air to give $[\text{Cp}^*\text{IrCl}_2]_2$. Further product was collected by concentrating the filtrate under reduced pressure, total yield 0.19 g, 54%.

$$[\text{Cp}^*\text{IrCl}_2(\text{PPh}_3)]^6$$

A suspension of $[(\eta^5\text{-C}_5\text{Me}_5)\text{IrCl}_2]_2$ (0.210 g, 0.264 mmol) and triphenylphosphine (0.212 g, excess) in ethanol (12 ml) were refluxed under nitrogen for 2 hours. After cooling to room

temperature, the yellow/orange suspension was filtered and washed with ethanol and ether to give pure $[\text{Cp}^*\text{IrCl}_2(\text{PPh}_3)]$ as a yellow powder (0.210 g, 60%).

^{31}P NMR: δ 2.2 (*s*, $\underline{\text{PPh}}_3$).

^1H NMR: δ 7.74 (6H, *t*, $^3J_{3',2'} = 7.89$, C-3',5'), 7.36 (9H, *m*, br, C-2',4',6'), 1.35 (15H, *s*, (*d*, $^1J_{\text{H,P}} = 2.24$ Hz), Cp- $\underline{\text{CH}}_3$).

^{13}C NMR: δ 134.8 (*d*, (*d*, $^3J_{\text{C,P}} = 9.81$ Hz), C-3',5'), 132.2 (*s*, (*d*, br, $^1J_{\text{C,P}} = 56.68$ Hz), C-1'), 130.3 (*d*, C-4'), 127.8 (*d*, (*d*, $^2J_{\text{C,P}} = 10.41$ Hz), C-2',6'), 92.7 (*s*, Cp), 8.4 (*q*, Cp- $\underline{\text{CH}}_3$).

$[\text{Cp}^*\text{RhCl}_2]_2$ ⁶

A mixture of $\text{RhCl}_3 \cdot 3\text{H}_2\text{O}$ (2.4 g, 9.11 mmol) and hexamethyldewarbenzene (4.8 ml, excess) in methanol (60 ml) were refluxed under nitrogen for 15 hours. After cooling to room temperature the solvent was removed under vacuum, and the residue washed with ether to remove excess hexamethyldewarbenzene. The oily red crystals were extracted with dichloromethane, dried over anhydrous sodium sulfate, and evaporated under reduced pressure. The residue was recrystallised from dichloromethane-ether to give dark red crystals of $[\text{Cp}^*\text{RhCl}_2]_2$ (2.44 g, 87% based on $\text{RhCl}_3 \cdot 3\text{H}_2\text{O}$).

$[\text{Cp}^*\text{RhCl}_2(\text{PPh}_3)]$ ⁶

In the same fashion as that for the iridium complex, a suspension of $[\text{Cp}^*\text{RhCl}_2]_2$ (0.50 g, 0.81 mmol) and triphenylphosphine (0.44 g, 1.68 mmol) in ethanol (50 ml) were refluxed with stirring under nitrogen for 2 hours. The red solution was filtered and concentrated to ~10 ml under vacuum. After storing overnight at 4°C, the resulting orange powder was collected on a filter and dried under vacuum to give $[\text{Cp}^*\text{RhCl}_2(\text{PPh}_3)]$ (0.70 g, 76%).

^{31}P NMR: δ 30.0 (*d*, $^1J_{\text{P,Rh}} = 144.0$ Hz, $\underline{\text{PPh}}_3$).

^1H NMR: δ 7.82 (6H, *t*, $^3J_{3',2'} = 8.53$, C-3',5'), 7.37 (9H, *m*, br, C-2',4',6'), 1.36 (15H, *d*, $^1J_{\text{H,P}} = 3.48$ Hz, Cp- $\underline{\text{CH}}_3$).

^{13}C NMR: δ 134.8 (*d*, (*d*, $^3J_{\text{C,P}} = 9.81$ Hz), C-3',5'), 130.4 (*d*, C-4'), 128.0 (*d*, (*d*, $^2J_{\text{C,P}} = 9.74$ Hz), C-2',6'), 99.2 (*s*, (*d*, $^1J_{\text{P,Rh}} = 6.57$ Hz), Cp), 8.8 (*q*, Cp- $\underline{\text{CH}}_3$).

[Hg{C₆H₃(CH₂NMe₂)-2-(OMe)-5}Cl]⁷ and [Hg{C₆H₃(CH₂NMe₂)-2}Cl]⁸

In a Schlenk flask, under an inert nitrogen atmosphere, *p*-methoxy-N,N-dimethylbenzylamine (1.50 g, 9.08 mmol) or N,N-dimethyl benzylamine (1.22 g, 9.02 mmol) were dissolved in dry diethyl ether (40 ml) which had previously been degassed and flushed with nitrogen. *n*-Butyllithium (7.0 ml of 1.33 mol L⁻¹ in hexane, 9.31 mmol) was slowly added by syringe, and the resulting mixture stirred for 24 hours. After cooling the mixture to -84°C with an ethyl acetate slush bath, a solution of mercury(II) chloride (2.50 g, 9.21 mmol) in dry, degassed, THF (5 ml) was slowly transferred to the flask. The solution was warmed to room temperature and stirred for an additional 5 hours. With no further efforts at excluding air, the resulting dark grey precipitate was filtered off, and the supernatant evaporated to dryness. The residue was dissolved in a minimum quantity of dichloromethane, refiltered (if required) and pentane (50 ml) added. Shaking the solution induced precipitation of pure [Hg{C₆H₃(CH₂NMe₂)-2-(OMe)-5}Cl] (2.48 g, 68%) or [Hg{C₆H₄(CH₂NMe₂)-2}Cl] (2.10 g, 63%) which were collected by filtration, and washed with pentane.

Tetramethylammonium tetrachloroaurate(III), [Me₄NAuCl₄]

To an aqueous (50 ml) solution of tetrachloroauric acid, HAuCl₄ (5.0 g, 0.147 mol) was added tetramethylammonium chloride (1.8 g, excess), resulting in an immediate yellow precipitate. The solid was filtered and sequentially washed with water, ethanol and diethyl ether to give [Me₄NAuCl₄] as a yellow powder (5.75 g, 98%).

[Au{C₆H₃(CH₂NMe₂)-2-(OMe)-5}Cl₂]⁹ and [Au{C₆H₄(CH₂NMe₂)-2}Cl₂]¹⁰

Using a Schlenk flask and under a nitrogen atmosphere, the appropriate mercury precursor [Hg{C₆H₃(CH₂NMe₂)-2-(OMe)-5}Cl] (2.0 g, 5.0 mmol) or [Hg{C₆H₄(CH₂NMe₂)-2}Cl] (1.85 g, 5.0 mmol), [Me₄NAuCl₄] (2.0 g, 5.0 mmol) and tetramethylammonium chloride (0.55 g, 5.0 mmol) were dissolved in acetonitrile (40 ml) which had previously been degassed and flushed with nitrogen. The resulting mixture was stirred at room temperature in dark conditions for 2 days, during which time a white precipitate formed. The reaction mixture was filtered, and the solid washed with acetonitrile. The solvent was removed under reduced pressure and the residue extracted into dichloromethane (50 ml), and filtered. Evaporation of the solvent and recrystallisation of the resulting residue from dichloromethane and diethyl

ether gave $[\text{Au}\{\overline{\text{C}_6\text{H}_3(\text{CH}_2\text{NMe}_2)\text{-2-(OMe)-5}\}\text{Cl}_2]$ (1.80 g, 83%) or $[\text{Au}\{\overline{\text{C}_6\text{H}_4(\text{CH}_2\text{NMe}_2)\text{-2}\}\text{Cl}_2]$ (1.62 g, 81%) as yellow crystals.

$[\text{Au}\{\overline{\text{C}_6\text{H}_3(\text{CH}_2\text{NMe}_2)\text{-2-(OMe)-5}\}\text{Cl}_2]$: ^1H NMR: δ 7.33 (1H, *d*, $^4\text{J}_{6',4'} = 2.44$ Hz, H-6'), 7.06 (1H, *d*, $^3\text{J}_{3',4'} = 8.30$ Hz, H-3'), 6.80 (1H, *dd*, $^3\text{J}_{4',3'} = 8.31$ Hz, $^4\text{J}_{4',6'} = 2.47$ Hz, H-4'), 4.35 (2H, *s*, $\underline{\text{CH}_2}$), 3.81 (3H, *s*, $\underline{\text{OCH}_3}$), 3.30 (6H, *s*, $\underline{\text{NCH}_3}$).

^{13}C NMR: δ 157.9 (*s*, C-5'), 148.6 (*s*, C-1'), 135.5 (*s*, C-2'), 123.8 (*d*, C-6'), 115.7 (*d*, C-4'), 115.4 (*d*, C-3'), 75.5 (*t*, $\underline{\text{NCH}_2}$), 55.7 (*t*, $\underline{\text{OCH}_3}$), 53.7 (*q*, $\underline{\text{NCH}_3}$).

$[\text{Au}\{\overline{\text{C}_6\text{H}_4(\text{CH}_2\text{NMe}_2)\text{-2}\}\text{Cl}_2]$: ^1H NMR: δ 7.72 (1H, *d*, $^3\text{J}_{6',5'} = 8.47$ Hz, H-6'), 7.25 (1H, *td*, $^3\text{J}_{4',3'} = 7.43$ Hz, $^4\text{J}_{4',6'} = 1.10$ Hz, H-4'), 7.145 (1H, *d*, $^3\text{J}_{3',4'} = 7.75$ Hz, H-5'), 7.140 (1H, *t*, $^3\text{J}_{5',6'} = 7.56$ Hz, H-3'), 4.41 (2H, *s*, $\underline{\text{CH}_2}$), 3.32 (6H, *s*, $\underline{\text{NCH}_3}$).

^{13}C NMR: δ 148.1 (*s*, C-1'), 143.8 (*s*, C-2'), 131.3 (*d*, C-6'), 129.1 (*d*, C-4'), 128.1 (*d*, C-5'), 123.3 (*d*, C-3'), 75.9 (*t*, $\underline{\text{NCH}_2}$), 53.9 (*q*, $\underline{\text{NCH}_3}$).

$[\text{Au}\{\overline{\text{C}_6\text{H}_3(\text{CH}_2\text{NMe}_2)\text{-2-(OMe)-5}\}\text{Br}_2]$ and $[\text{Au}\{\overline{\text{C}_6\text{H}_4(\text{CH}_2\text{NMe}_2)\text{-2}\}\text{Br}_2]$ ¹⁰

To a flask containing $[\text{Au}\{\overline{\text{C}_6\text{H}_3(\text{CH}_2\text{NMe}_2)\text{-2-(OMe)-5}\}\text{Cl}_2]$ (0.130 g, 0.301 mmol) or $[\text{Au}\{\overline{\text{C}_6\text{H}_4(\text{CH}_2\text{NMe}_2)\text{-2}\}\text{Cl}_2]$ (0.120 g, 0.298 mmol) dissolved in acetone (20 ml), was added lithium bromide (0.2 g, excess) and the mixture stirred at room temperature for 2 hours. The acetone was removed under reduced pressure, and the residue extracted with dichloromethane. After filtration to remove the insoluble lithium salts, addition of ether precipitated pure $[\text{Au}\{\overline{\text{C}_6\text{H}_3(\text{CH}_2\text{NMe}_2)\text{-2-(OMe)-5}\}\text{Br}_2]$ (0.118 g, 75%) or $[\text{Au}\{\overline{\text{C}_6\text{H}_4(\text{CH}_2\text{NMe}_2)\text{-2}\}\text{Br}_2]$ (0.120 g, 82%) as yellow powders. The former complex had not been reported previously.

$[\text{Au}\{\overline{\text{C}_6\text{H}_3(\text{CH}_2\text{NMe}_2)\text{-2-(OMe)-5}\}\text{Br}_2]$: Found: C, 22.4; H, 2.7; N, 2.5%; $\text{C}_{10}\text{H}_{14}\text{NOAuBr}_2$ requires: C, 23.1; H, 2.7; N, 2.7%.

^1H NMR: δ 7.58 (1H, *d*, $^4\text{J}_{6',4'} = 2.17$ Hz, H-6'), 7.06 (1H, *d*, $^3\text{J}_{3',4'} = 7.78$ Hz, H-3'), 6.79 (1H, *dd*, $^3\text{J}_{4',3'} = 8.34$ Hz, $^4\text{J}_{4',6'} = 2.12$ Hz, H-4'), 4.34 (2H, *s*, $\underline{\text{CH}_2}$), 3.81 (3H, *s*, $\underline{\text{OCH}_3}$), 3.29 (6H, *s*, $\underline{\text{NCH}_3}$).

^{13}C NMR: δ 158.0 (*s*, C-5'), 150.8 (*s*, C-1'), 136.2 (*s*, C-2'), 123.8 (*d*, C-6'), 118.2 (*d*, C-4'), 114.8 (*d*, C-3'), 75.3 (*t*, $\underline{\text{NCH}_2}$), 55.7 (*t*, $\underline{\text{OCH}_3}$), 54.0 (*q*, $\underline{\text{NCH}_3}$).

$[\text{Au}\{\overline{\text{C}_6\text{H}_4(\text{CH}_2\text{NMe}_2)\text{-2}\}\text{Br}_2]$: Found: C, 22.2; H, 2.5; N, 2.8%; $\text{C}_9\text{H}_{12}\text{NBr}_2\text{Au}$ requires: C, 22.0; H, 2.5; N, 2.9%.

^1H NMR: δ 7.98 (1H, *d*, $^3J_{6',5'} = 8.33$ Hz, H-6'), 7.26 (1H, *t*, $^3J_{4',3'} = 7.34$ Hz, H-4'), 7.14 (1H, *d*, $^3J_{3',4'} = 7.11$ Hz, H-3'), 7.10 (1H, *t*, $^3J_{5',6'} = 7.25$ Hz, H-5'), 4.40 (2H, *s*, $\underline{\text{CH}_2}$), 3.31 (6H, *s*, NCH_3).

^{13}C NMR: δ 150.4 (*s*, C-1'), 144.4 (*s*, C-2'), 133.4 (*d*, C-6'), 128.8 (*d*, C-4'), 128.3 (*d*, C-5'), 123.3 (*d*, C-3'), 75.7 (*t*, $\underline{\text{NCH}_2}$), 54.1 (*q*, NCH_3).

*Silver(I) oxide*¹¹

To a stirred aqueous solution of silver nitrate or suspension of silver acetate (in water), was slowly added 1 equivalent of potassium hydroxide pellets (dissolved in water). A black precipitate formed rapidly, and the mixture was heated to 80-90°C, with additional potassium hydroxide added until no further precipitate formed, and in the case of silver(I) acetate, until no visible traces of the acetate remained. Heating with stirring was maintained for 1-2 hours. After allowing the black suspension to cool, the solid was filtered and thoroughly washed sequentially with water, ethanol and ether, and dried in an oven at 100°C overnight, to give silver(I) oxide in ~90% yield.

References

- 1 J.X. McDermott, J.F. White and G.M. Whitesides, *J. Am. Chem. Soc.*, 98 (1976) 6521.
- 2 M.A. Bennett, T.-N. Huang, T.W. Matheson and A.K. Smith, *Inorg. Synth.*, 21 (1982) 74.
- 3 A. Demonceau, A.F. Noels, E. Saive and A. J. Hubert, *J. Mol. Cat.*, 76 (1992) 123.
- 4 J. A. Cabeza and P.M. Maitlis, *J. Chem. Soc. Dalton Trans.*, (1985) 573.
- 5 H. Werner and K. Zenkert, *J. Organomet. Chem.*, 345 (1988) 151.
- 6 J.W. Kang, K. Moseley and P.M. Maitlis, *J. Am. Chem. Soc.*, 91 (1969) 5970.
- 7 P. A. Bonnardel, R.V. Parish, *J. Organomet. Chem.*, 551 (1996) 221.
- 8 A.F.M.G. van der Ploeg, C.E.M. van der Kolk and G. van Koten, *J. Organomet. Chem.*, 212 (1981) 283.
- 9 P. A. Bonnardel, R. V. Parish, and R. G. Pritchard, *J. Chem. Soc., Dalton Trans.*, (1996) 3185
- 10 J. Vicente, M. T. Chicote and M. Bermúdez, *J. Organomet. Chem.*, 268 (1984) 191.
- 11 H.L. Riley and H.B. Baker, *J. Chem. Soc.*, (1926) 2510.

Appendix II

Instrumentation and Analyses

A.II.1 NMR spectroscopy

All proton and carbon NMR spectra were recorded either on a Bruker AC300 spectrometer at 300.13 and 75.47 MHz for the proton and carbon channels respectively, or on Bruker DRX400 instrument at 400.13 and 100.61 MHz. All ^1H and ^{13}C NMR were referenced externally to tetramethylsilane (TMS, SiMe_4) at 0.0 ppm.

Phosphorus NMR spectra were recorded on either a JEOL FX-90Q at 36.23 MHz, or on a Bruker AC300 spectrometer at 121.49 MHz, referenced to 85% orthophosphoric acid (H_3PO_4) at 0.0 ppm.

Samples were generally run using deuterated chloroform solvent (CDCl_3). For compounds that failed to dissolve sufficiently in CDCl_3 , deuterated dimethyl sulfoxide [$\text{CD}_3\text{S}(\text{O})\text{CD}_3$] generally proved effective, and was used in these cases.

A summary of experiments used for the assignment of signals follows.

A.II.1.1 1D experiments

DEPT 135

This was routinely used for determining the multiplicity of the carbon signals, thus aiding assignment.

*NOE (Nuclear Overhauser Effect)*¹

Where appropriate, this ^1H NMR “through-space” experiment was the primary method used for assignment of the $\text{CH}=\text{CH}$ resonances of the cyclo-octa-1,5,-diene (COD) group (and those adjacent to it) of platinum(II) complexes. Figure A.II.1 shows the observed NOE enhancements for the platinum(II) ureylene complex **2.22d** (Chapter Two). The enhancements were typically 5-10% of the intensity of the irradiated signal.

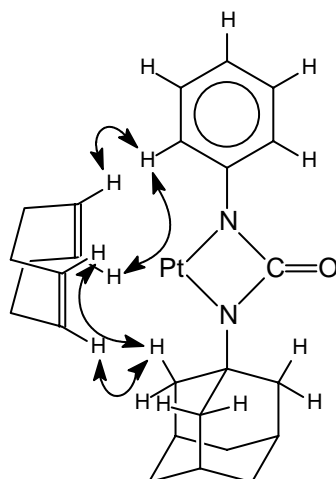


Figure A.II.1: $\underline{CH=CH}$ NOE enhancements for the complex **2.22d**. Enhancements also apply for magnetically equivalent protons (not depicted).

A.II.1.2 2D experiments

HOHAHA (HOmonuclear HArtmann-HAHn transfer)^{2,3}

The HOHAHA experiment, also known as TOCSY (TOtal Correlation SpectroscopY), was used on occasion to facilitate assignment of massively overlapping aromatic protons. The net result of the method is essentially a long-range COSY⁴ (COrrrelation SpectroscopY) experiment, and deconvolution of an entire ring is readily achieved, providing at least one resonance associated with that ring is sufficiently resolved from the remaining signals. An example ¹H spectrum is presented in Figure A.II.2 for the gold(III) biuret derivative **5.11** (see Chapter Five, Section 5.2.3), showing the highly overlapping resonances associated with four inequivalent aromatic rings. Assignment of the signals 2'''/6''' and 2'',6'' was achieved by use of the NOESY experiment (see below), and the doublet at 6.2 ppm showing ⁴J_{H,H} coupling can clearly only arise from 6'. The HOHAHA spectrum of **5.11** is shown in Figure A.II.3 (together with atom and ring labelling schemes), and the resulting fully resolved ¹H NMR spectra generated from the slices A-D taken therefrom, are shown in Figure A.II.4.

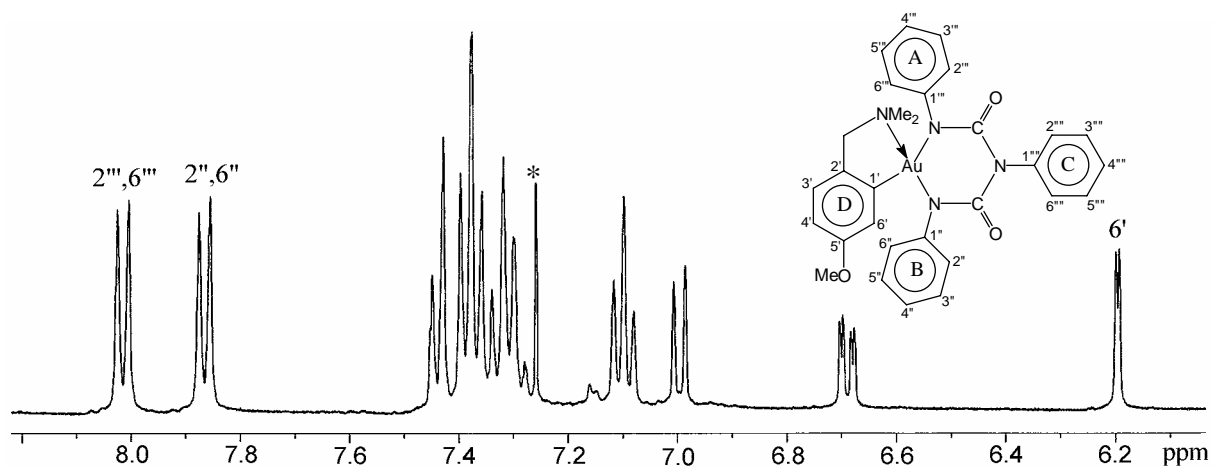


Figure A.II.2: ^1H NMR of the aromatic region of the gold(III) complex **5.11**, illustrating the large number of overlapping signals. The peak labelled * is from CHCl_3 in the solvent used, CDCl_3 .

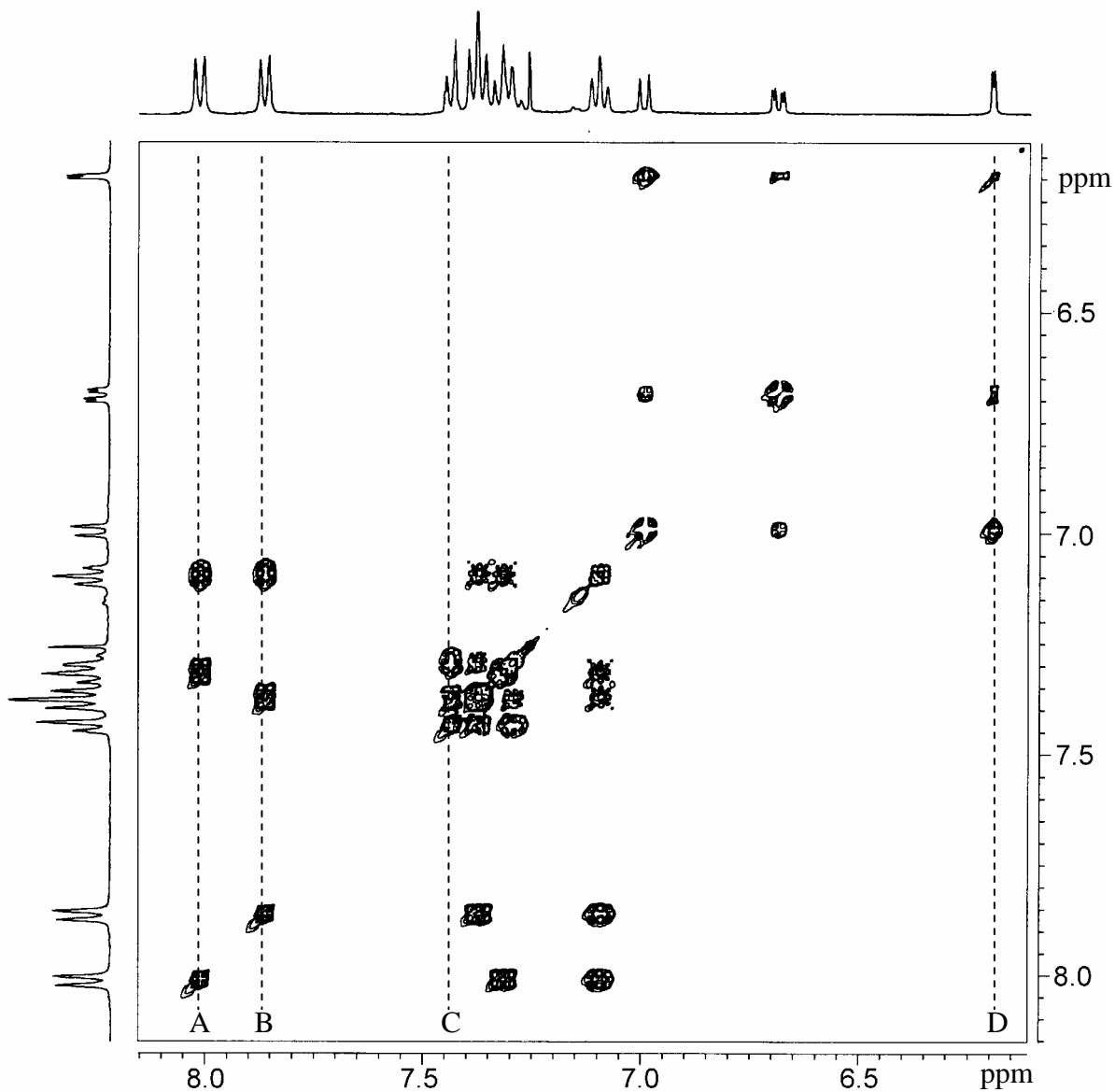


Figure A.II.3: HOHAHA spectrum of the gold(III) complex **5.11**, showing the slices A-D used to generate the corresponding ^1H spectra shown in Figure A.II.4.

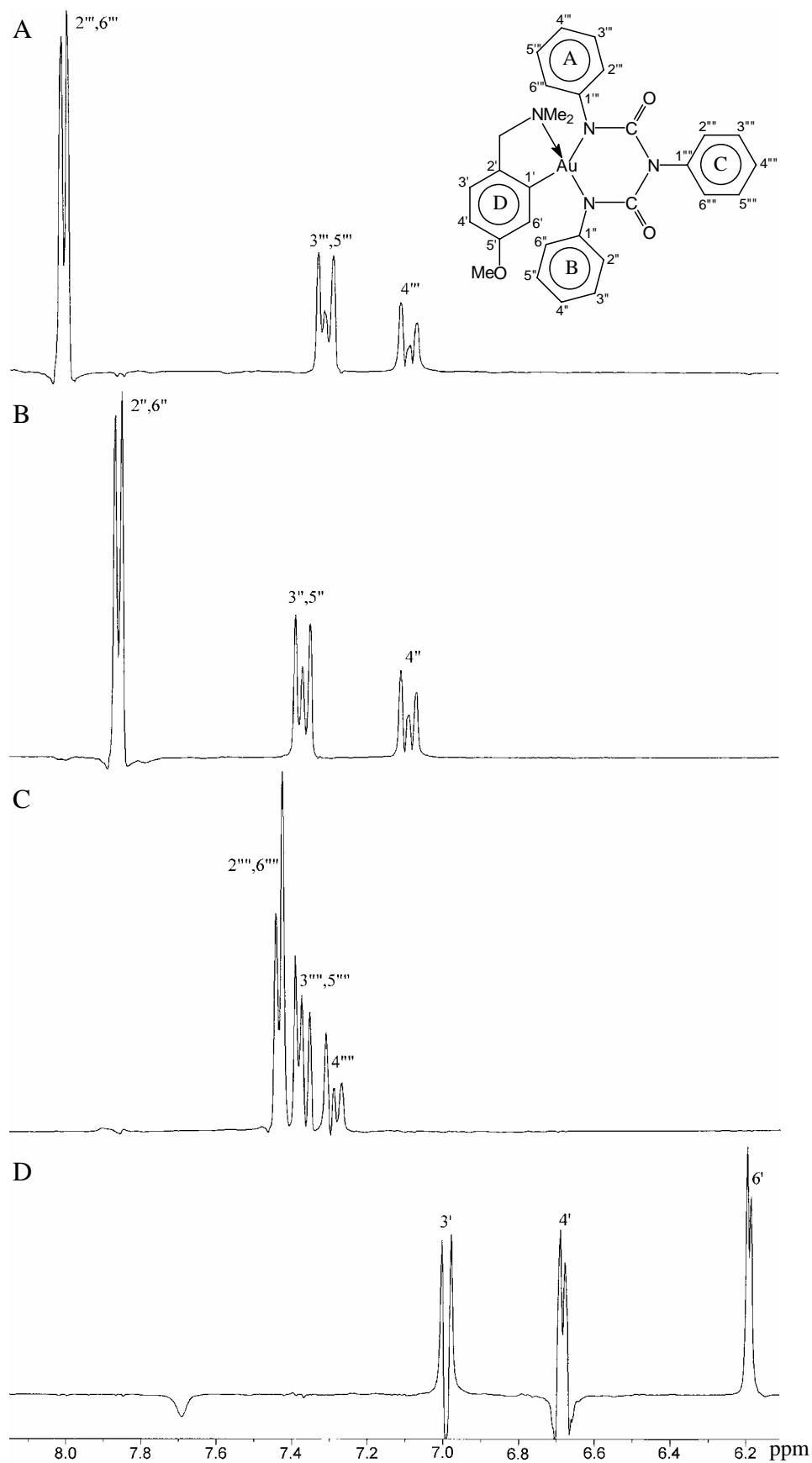


Figure A.II.4: Resolved ^1H NMR slices (for the gold(III) complex **5.11**) corresponding to those shown on the HOHAHA spectrum given in Figure A.II.3, together with the atom numbering scheme.

NOESY (Nuclear Overhauser Effect Spectroscopy)^{5,6} and *ROESY (Rotating-frame Overhauser Effect Spectroscopy)*⁷

The NOESY experiment, the 2D equivalent of the 1D NOE experiment described previously, was routinely used when the NOE enhancements for a number of signals was useful for assignment. The ROESY experiment, a variation of the NOESY experiment but with the homonuclear NOE effects measured under spin-locked conditions, was also used on occasion. The ROESY spectrum of the gold(III) thietane-3,3-dioxide complex **7.5** (Chapter 7) is shown in Figure A.II.5, and a diagram illustrating the observed enhancements is shown in Figure A.II.6.

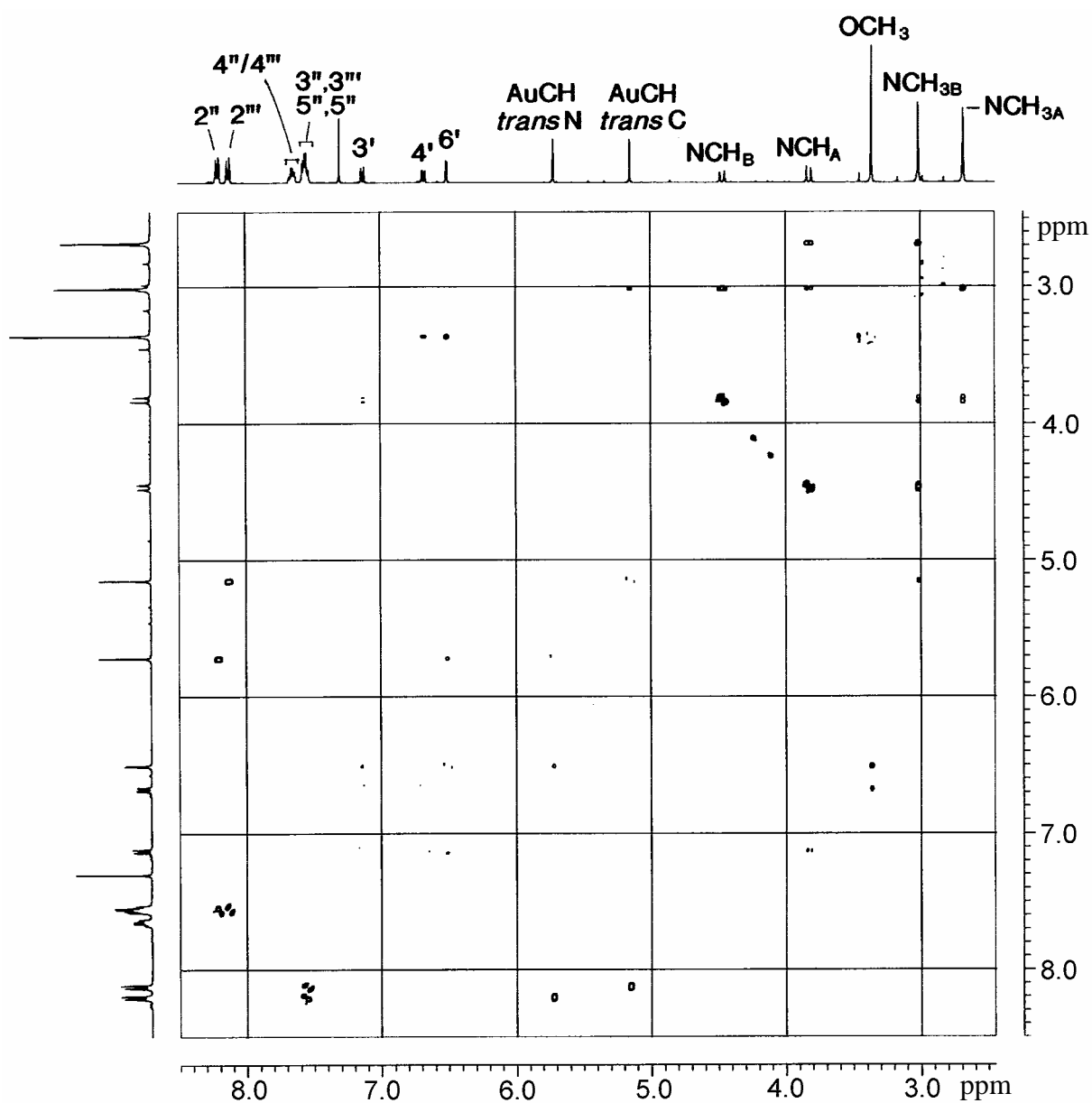


Figure A.II.5: ROESY spectrum of the gold(III) complex **7.5**.

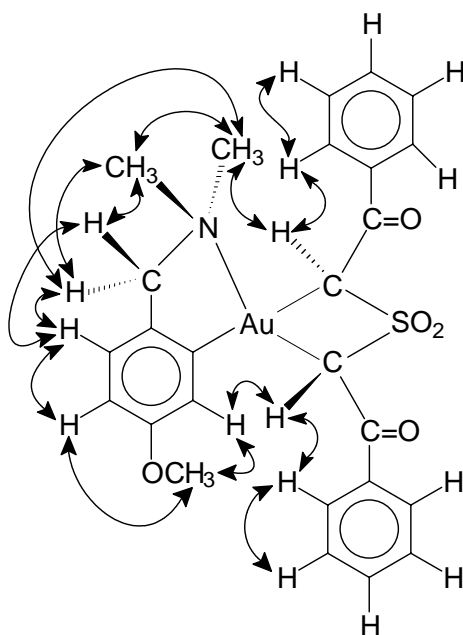


Figure A.II.6: Diagram illustrating observed NOE enhancements for the ROESY spectrum shown in Figure A.II.4.

¹H-¹³C COSY (normal-mode) and HMQC (inverse-mode, Heteronuclear Multiple Quantum Coherence)^{8,9}

The 2D ¹H-¹³C COSY experiment was routinely used to determine which ¹H's of a molecule are bonded to which ¹³C nuclei [based on ¹J (¹³C-¹H) coupling], thus facilitating assignment of ¹³C resonances. The normal-mode experiment was used for many of the compounds prepared in Chapters Two and Three, with assignment in subsequent chapters (Four-Eight) largely achieved by the superior HMQC experiment. The principle advantage of HMQC is that because it is an inverse-mode experiment and based around the *proton* nucleus (as opposed to carbon for the normal-mode experiment), signal to noise ratios over a given time-frame are vastly superior, since the proton nucleus has a much higher sensitivity than carbon.

BIRDTRAP (normal-mode) and HMBC (inverse-mode, Heteronuclear Multiple Bond Correlation)¹⁰

The BIRDTRAP experiment, an extension of the normal-mode long-range ¹H-¹³C COSY experiment, was primarily used for the assignment of quaternary carbons, but was often also useful for the assignment of other ¹H or ¹³C signals. The experiment differs from the

“standard” long-range ^1H - ^{13}C COSY experiment, in that an additional pulse sequence is applied that suppresses residual ^1J (^1H - ^{13}C) correlations, that otherwise complicate the spectra.

Use of the BIRDTRAP was superseded by the HMBC experiment. Since this is also a long-range chemical shift correlation experiment, HMBC provides basically the same information as the BIRDTRAP (normal-mode). However, because it is an inverse-mode experiment based on the proton nucleus, it, like HMQC, has a vastly superior signal to noise ratio, for the same reasons as described for HMQC above.

Despite both the BIRDTRAP and HMBC experiments being optimised for ^3J (^{13}C - ^1H) coupling, the predicted ^2J (^{13}C - ^1H) coupling was also generally observed, although with a much lower intensity.

A.II.2 X-ray diffractometer methodology and configuration

Siemens CCD SMART diffractometer at the University of Auckland

Unit cell dimensions and intensity data for the structures were obtained at 203(2) K, with monochromatic Mo- $K\alpha$ X-rays ($\lambda = 0.71073 \text{ \AA}$). The data collections nominally covered over a hemisphere of reciprocal space, by a combination of three sets of exposures; each set had a different ϕ angle for the crystal and each exposure covered 0.3° in ω . The crystal to detector distance was 5.0 cm. The data sets were corrected empirically for absorption using SADABS.¹¹

Siemens CCD diffractometer at the University of Canterbury

Unit cell dimensions and intensity data were obtained on a Siemens CCD detector mounted on a P4 diffractometer at 148(2) K, with monochromatic Mo- $K\alpha$ X-rays ($\lambda = 0.71073 \text{ \AA}$). The data collection nominally covered over a hemisphere of reciprocal space, by a combination of two sets of exposures. In the first, each exposure covered 0.3° for a total of 52° in ω . The second run covered 360° in ϕ (the mounting axis), also using 0.3° increments between frames. The crystal to detector distance was 4.0 cm. The data set was corrected empirically for absorption using SADABS.¹¹

A.II.3 Electrospray mass spectrometry (ESMS)¹²

Electrospray ionisation mass spectrometry was performed on a VG Platform II instrument. The sample to be analysed (generally one crystal) was dissolved in the same solvent used as the mobile phase (typically 1:1 (v/v) acetonitrile-water). All electrospray mass spectra data presented in this thesis were acquired in positive-ion mode, using MassLynx version 2.0 software. The sample was introduced via a 10 μ l sample loop fitted to a Rheodyne injector, and delivered to the mass spectrometer source by a SpectraSystem P1000 HPLC pump, at a flow rate of 0.1-0.2 ml min⁻¹. Nitrogen was employed as both the nebulising and drying gas, and the source temperature at the inlet capillary was 60°C. The cone voltage was typically adjusted between 20 - 80 V (although both higher and lower voltages were also occasioned), to examine any fragmentation reactions. To aid identification of peaks, higher resolution isotope patterns of major ions were also sampled, and compared with theoretical patterns using the Isotope¹³ program.

A.II.4 Elemental microanalysis and biological assays

Elemental analyses were obtained by the University of Otago Campbell Microanalytical Laboratory, and biological testing was carried out by the Marine Chemistry Group at the University of Canterbury.

A.II.5 IR spectroscopy

All infrared spectra for the final products were recorded as % absorbance spectra from KBr discs, on a Digilab FTS-45 FTIR instrument, with a resolution of 1 cm⁻¹.

A.II.6 Melting points

Melting points were determined on a Reichert Thermovar apparatus and are uncorrected.

References

- 1 D. Neuhaus and M.P. Williamson, *The Nuclear Overhauser Effect in Structural and Conformational Analysis*, VCH Publishers, New York, (1989).
- 2 L. Braunschweiler and R.R. Ernst, *J. Magn. Reson.*, *53* (1983) 521.
- 3 A. Bax and D.G. Davis, *J. Magn. Reson.*, *65* (1985) 355.
- 4 K. Nagayama, A. Kumar, K. Wüthrich and R.R. Ernst, *J. Magn. Reson.*, *40* (1980) 321.
- 5 J. Jeener, B.H. Meier, P. Bachmann and R.R. Ernst, *J. Chem. Phys.*, *69* (1979) 4546.
- 6 G. Wagner and K. Wüthrich, *J. Mol. Biol.*, *155* (1982) 347.
- 7 A. Bax and D.G. Davis, *J. Magn. Reson.*, *63* (1985) 207.
- 8 A. Bax, R.H. Griffey and B.L. Hawkins, *J. Magn. Reson.*, *55* (1983) 301.
- 9 A. Bax and S. Subramanian, *J. Magn. Reson.*, *67* (1986) 565.
- 10 A. Bax and M.F. Summers, *J. Am. Chem. Soc.*, *108* (1986) 2093.
- 11 R.H. Blessing, *Acta Cryst.*, *A51* (1995) 33.
- 12 *Electrospray Ionisation Mass Spectrometry*, Ed. R.B. Cole, John Wiley & Sons, Inc., New York, (1997).
- 13 L.J. Arnold, *J. Chem. Educ.*, (1992) *69*, 811.

Appendix III

Complete Bond Lengths, Bond Angles, and Thermal and Positional Parameters for $[\text{Pt}\{\text{NPhC}(\text{O})\text{NAd}\}(\text{COD})]\cdot\text{CH}_2\text{Cl}_2$ 2.22d

Table A.III.1: Complete Bond Lengths (Å) for 2.22d·CH₂Cl₂, with e.s.d.s in parentheses

Pt(1)-N(2)	2.021(8)	C(15)-C(16)	1.367(13)
Pt(1)-N(1)	2.048(8)	C(15)-C(14)	1.395(14)
Pt(1)-C(31)	2.177(9)	C(21)-C(22)	1.51(2)
Pt(1)-C(38)	2.178(9)	C(21)-C(26)	1.52(2)
Pt(1)-C(34)	2.185(9)	C(22)-C(23)	1.518(14)
Pt(1)-C(35)	2.191(9)	C(23)-C(24)	1.534(14)
Pt(1)-C(1)	2.558(10)	C(24)-C(25)	1.522(14)
O(1)-C(1)	1.244(11)	C(25)-C(26)	1.53(2)
N(2)-C(1)	1.387(12)	C(31)-C(38)	1.383(13)
N(2)-C(11)	1.408(12)	C(31)-C(32)	1.514(13)
N(1)-C(1)	1.374(12)	C(32)-C(33)	1.525(14)
N(1)-C(2)	1.471(11)	C(33)-C(34)	1.504(13)
C(2)-C(5)	1.527(13)	C(34)-C(35)	1.388(13)
C(2)-C(4)	1.535(12)	C(35)-C(36)	1.524(13)
C(2)-C(3)	1.540(12)	C(36)-C(37)	1.543(13)
C(3)-C(23)	1.526(13)	C(37)-C(38)	1.507(13)
C(4)-C(25)	1.545(13)	Cl(1)-C(41)	1.626(12)
C(5)-C(21)	1.536(13)	Cl(2)-C(41)	1.739(12)
C(11)-C(16)	1.399(13)	C(91)-C(92)	1.27
C(11)-C(12)	1.415(13)	C(91)-C(93)	1.75
C(12)-C(13)	1.374(14)	C(92)-C(93)	1.44
C(13)-C(14)	1.39(2)	C(92)-C(92')	1.88(3)

Table A.III.2: Complete Bond Angles (°) for 2.22d·CH₂Cl₂, with e.s.d.s in parentheses

N(2)-Pt(1)-N(1)	64.7(3)	C(16)-C(11)-N(2)	123.8(8)
N(2)-Pt(1)-C(31)	161.0(3)	C(16)-C(11)-C(12)	117.8(8)
N(1)-Pt(1)-C(31)	108.9(3)	N(2)-C(11)-C(12)	118.3(8)
N(2)-Pt(1)-C(38)	159.1(3)	C(13)-C(12)-C(11)	120.3(9)
N(1)-Pt(1)-C(38)	104.7(3)	C(12)-C(13)-C(14)	121.1(10)
C(31)-Pt(1)-C(38)	37.0(3)	C(16)-C(15)-C(14)	120.8(9)
N(2)-Pt(1)-C(34)	99.1(3)	C(13)-C(14)-C(15)	118.7(9)
N(1)-Pt(1)-C(34)	156.3(3)	C(15)-C(16)-C(11)	121.2(9)
C(31)-Pt(1)-C(34)	80.7(4)	C(22)-C(21)-C(26)	109.6(8)
C(38)-Pt(1)-C(34)	95.8(4)	C(22)-C(21)-C(5)	108.8(9)
N(2)-Pt(1)-C(35)	103.8(3)	C(26)-C(21)-C(5)	109.6(8)
N(1)-Pt(1)-C(35)	158.5(3)	C(21)-C(22)-C(23)	109.5(8)
C(31)-Pt(1)-C(35)	87.5(4)	C(22)-C(23)-C(3)	109.8(8)
C(38)-Pt(1)-C(35)	79.7(4)	C(22)-C(23)-C(24)	110.0(8)
C(34)-Pt(1)-C(35)	37.0(4)	C(3)-C(23)-C(24)	109.9(7)
N(2)-Pt(1)-C(1)	32.7(3)	C(25)-C(24)-C(23)	108.5(8)
N(1)-Pt(1)-C(1)	32.4(3)	C(24)-C(25)-C(26)	109.8(8)

C(31)-Pt(1)-C(1)	136.8(3)	C(24)-C(25)-C(4)	110.0(8)
C(38)-Pt(1)-C(1)	136.1(3)	C(26)-C(25)-C(4)	108.5(8)
C(34)-Pt(1)-C(1)	128.1(3)	C(21)-C(26)-C(25)	109.6(8)
C(35)-Pt(1)-C(1)	135.4(3)	C(38)-C(31)-C(32)	123.5(9)
C(1)-N(2)-C(11)	121.6(7)	C(38)-C(31)-Pt(1)	71.5(5)
C(1)-N(2)-Pt(1)	95.5(5)	C(32)-C(31)-Pt(1)	112.6(6)
C(11)-N(2)-Pt(1)	133.2(6)	C(31)-C(32)-C(33)	113.1(7)
C(1)-N(1)-C(2)	121.7(7)	C(34)-C(33)-C(32)	113.4(8)
C(1)-N(1)-Pt(1)	94.7(5)	C(35)-C(34)-C(33)	124.8(9)
C(2)-N(1)-Pt(1)	142.4(6)	C(35)-C(34)-Pt(1)	71.8(5)
O(1)-C(1)-N(1)	128.4(8)	C(33)-C(34)-Pt(1)	109.2(6)
O(1)-C(1)-N(2)	127.3(8)	C(34)-C(35)-C(36)	124.4(8)
N(1)-C(1)-N(2)	104.1(7)	C(34)-C(35)-Pt(1)	71.2(5)
O(1)-C(1)-Pt(1)	176.7(6)	C(36)-C(35)-Pt(1)	114.0(6)
N(1)-C(1)-Pt(1)	52.9(4)	C(35)-C(36)-C(37)	111.7(7)
N(2)-C(1)-Pt(1)	51.8(4)	C(38)-C(37)-C(36)	113.0(8)
N(1)-C(2)-C(5)	110.8(7)	C(31)-C(38)-C(37)	125.9(8)
N(1)-C(2)-C(4)	111.7(7)	C(31)-C(38)-Pt(1)	71.4(5)
C(5)-C(2)-C(4)	108.6(7)	C(37)-C(38)-Pt(1)	110.9(6)
N(1)-C(2)-C(3)	109.8(7)	Cl(1)-C(41)-Cl(2)	117.2(8)
C(5)-C(2)-C(3)	107.4(7)	C(92)-C(91)-C(93)	54.1
C(4)-C(2)-C(3)	108.4(7)	C(91)-C(92)-C(93)	80.4
C(23)-C(3)-C(2)	110.5(7)	C(91)-C(92)-C(92')	79.6(6)
C(2)-C(4)-C(25)	110.7(7)	C(93)-C(92)-C(92')	128.4(7)
C(2)-C(5)-C(21)	111.1(7)	C(92)-C(93)-C(91)	45.5

Table A.III.3: Final Positional (fractional co-ordinates) and Equivalent Thermal Parameters for 2.22d·CH₂Cl₂, with e.s.d.s in parentheses

Atom	X/A	Y/B	Z/C	U(eq)
Pt(1)	0.0176(1)	0.3286(1)	0.3615(1)	0.017(1)
O(1)	-0.3914(7)	0.2916(7)	0.3878(5)	0.026(1)
N(2)	-0.1498(8)	0.3206(8)	0.4516(5)	0.021(2)
N(1)	-0.1748(8)	0.3319(8)	0.2947(5)	0.021(2)
C(1)	-0.2563(10)	0.3085(9)	0.3783(6)	0.021(2)
C(2)	-0.2467(10)	0.3275(9)	0.1984(6)	0.019(2)
C(3)	-0.3122(11)	0.4418(9)	0.1930(7)	0.023(2)
C(4)	-0.3758(10)	0.1866(9)	0.1774(7)	0.025(2)
C(5)	-0.1310(10)	0.3547(10)	0.1184(7)	0.027(2)
C(11)	-0.1926(10)	0.2618(9)	0.5433(6)	0.021(2)
C(12)	-0.0862(10)	0.3082(9)	0.6217(7)	0.023(2)
C(13)	-0.1223(12)	0.2522(10)	0.7122(7)	0.032(2)
C(15)	-0.3670(11)	0.1012(10)	0.6513(7)	0.027(2)
C(14)	-0.2629(12)	0.1490(10)	0.7289(7)	0.032(2)
C(16)	-0.3328(11)	0.1565(9)	0.5610(7)	0.025(2)
C(21)	-0.2046(11)	0.3524(12)	0.0177(7)	0.033(2)
C(22)	-0.2679(11)	0.4656(11)	0.0152(8)	0.034(2)
C(23)	-0.3854(11)	0.4400(10)	0.0930(7)	0.028(2)
C(24)	-0.5157(11)	0.2993(11)	0.0742(7)	0.030(2)
C(25)	-0.4516(12)	0.1858(10)	0.0770(7)	0.031(2)
C(26)	-0.3323(13)	0.2114(11)	-0.0009(7)	0.037(3)
C(31)	0.1470(10)	0.2668(10)	0.2552(7)	0.025(2)
C(32)	0.2409(11)	0.1928(10)	0.3007(7)	0.029(2)

C(33)	0.2010(11)	0.1525(10)	0.4058(7)	0.031(2)
C(34)	0.1506(10)	0.2530(10)	0.4600(7)	0.025(2)
C(35)	0.2206(10)	0.3967(10)	0.4565(7)	0.024(2)
C(36)	0.3671(10)	0.4738(10)	0.4042(7)	0.026(2)
C(37)	0.3362(10)	0.5133(10)	0.3004(7)	0.027(2)
C(38)	0.1927(9)	0.4099(9)	0.2542(6)	0.020(2)
Cl(1)	0.1989(5)	0.0225(4)	0.6476(4)	0.091(1)
Cl(2)	0.3409(8)	0.2023(6)	0.8109(4)	0.120(2)
C(41)	0.2900(13)	0.1805(12)	0.6880(9)	0.106(7)
C(91)	0.0404(13)	0.9307(12)	0.0790(9)	0.089(8)
C(92)	-0.0761(13)	0.9397(12)	0.0390(9)	0.131(12)
C(93)	-0.1059(13)	0.9583(12)	0.1390(9)	0.137(12)

Table A.III.4: Final Positional (fractional co-ordinates) and Equivalent Thermal Parameters of Calculated Hydrogen Atoms for **2.22d**·CH₂Cl₂, with *e.s.d.s* in parentheses

Atom	X/A	Y/B	Z/C	U(eq)
H(3A)	-0.3887(11)	0.4267(9)	0.2436(7)	0.028
H(3B)	-0.2303(11)	0.5338(9)	0.2055(7)	0.028
H(4A)	-0.4521(10)	0.1679(9)	0.2285(7)	0.030
H(4B)	-0.3352(10)	0.1119(9)	0.1789(7)	0.030
H(5A)	-0.0864(10)	0.2829(10)	0.1201(7)	0.032
H(5B)	-0.0482(10)	0.4464(10)	0.1303(7)	0.032
H(12)	0.0107(10)	0.3784(9)	0.6118(7)	0.027
H(13)	-0.0499(12)	0.2846(10)	0.7643(7)	0.038
H(15)	-0.4628(11)	0.0294(10)	0.6613(7)	0.033
H(14)	-0.2876(12)	0.1117(10)	0.7918(7)	0.039
H(16)	-0.4057(11)	0.1227(9)	0.5092(7)	0.030
H(21)	-0.1270(11)	0.3694(12)	-0.0333(7)	0.040
H(22A)	-0.3149(11)	0.4660(11)	-0.0495(8)	0.041
H(22B)	-0.1851(11)	0.5574(11)	0.0267(8)	0.041
H(23)	-0.4264(11)	0.5154(10)	0.0911(7)	0.034
H(24A)	-0.5929(11)	0.2831(11)	0.1246(7)	0.036
H(24B)	-0.5645(11)	0.2986(11)	0.0099(7)	0.036
H(25)	-0.5352(12)	0.0932(10)	0.0647(7)	0.037
H(26A)	-0.2911(13)	0.1372(11)	0.0007(7)	0.044
H(26B)	-0.3793(13)	0.2094(11)	-0.0660(7)	0.044
H(31)	0.0865(10)	0.2183(10)	0.1961(7)	0.030
H(32A)	0.3493(11)	0.2540(10)	0.2984(7)	0.035
H(32B)	0.2258(11)	0.1077(10)	0.2618(7)	0.035
H(33A)	0.1191(11)	0.0590(10)	0.4064(7)	0.037
H(33B)	0.2906(11)	0.1469(10)	0.4401(7)	0.037
H(34)	0.1010(10)	0.2176(10)	0.5229(7)	0.030
H(35)	0.2100(10)	0.4452(10)	0.5174(7)	0.029
H(36A)	0.4271(10)	0.4144(10)	0.4008(7)	0.031
H(36B)	0.4277(10)	0.5593(10)	0.4417(7)	0.031
H(37A)	0.3292(10)	0.6059(10)	0.3027(7)	0.032
H(37B)	0.4226(10)	0.5202(10)	0.2593(7)	0.032
H(38)	0.1580(9)	0.4448(9)	0.1946(6)	0.024
H(41A)	0.2268(13)	0.2350(12)	0.6738(9)	0.127
H(41B)	0.3835(13)	0.2215(12)	0.6504(9)	0.127

Table A.III.5: Thermal Parameters for 2.22d·CH₂Cl₂, with e.s.d.s in parentheses

Atom	U11	U22	U33	U23	U13	U12
Pt(1)	0.0186(2)	0.0207(2)	0.0154(2)	0.0012(1)	-0.0004(1)	0.0120(1)
O(1)	0.021(3)	0.043(4)	0.020(3)	0.007(3)	0.002(3)	0.017(3)
N(2)	0.019(4)	0.027(4)	0.022(4)	0.004(3)	0.001(3)	0.013(3)
N(1)	0.021(4)	0.031(4)	0.017(4)	0.005(3)	-0.002(3)	0.015(3)
C(1)	0.029(5)	0.018(4)	0.019(5)	0.003(4)	0.001(4)	0.012(4)
C(2)	0.021(4)	0.023(5)	0.015(5)	0.004(4)	-0.004(3)	0.011(4)
C(3)	0.030(5)	0.020(5)	0.023(5)	0.001(4)	-0.001(4)	0.013(4)
C(4)	0.027(5)	0.022(5)	0.024(5)	0.001(4)	-0.007(4)	0.009(4)
C(5)	0.020(5)	0.038(5)	0.024(5)	0.001(4)	-0.004(4)	0.013(4)
C(11)	0.027(5)	0.025(5)	0.016(5)	-0.002(4)	-0.003(4)	0.017(4)
C(12)	0.024(5)	0.028(5)	0.022(5)	-0.002(4)	0.001(4)	0.016(4)
C(13)	0.044(6)	0.038(6)	0.021(5)	-0.003(4)	-0.003(4)	0.025(5)
C(15)	0.032(5)	0.024(5)	0.026(5)	0.003(4)	0.003(4)	0.010(4)
C(14)	0.051(7)	0.033(5)	0.024(5)	0.010(4)	0.011(5)	0.027(5)
C(16)	0.030(5)	0.021(5)	0.024(5)	-0.002(4)	-0.002(4)	0.011(4)
C(21)	0.026(5)	0.058(7)	0.018(5)	0.004(5)	0.003(4)	0.017(5)
C(22)	0.029(5)	0.042(6)	0.029(6)	0.010(5)	-0.003(4)	0.011(5)
C(23)	0.031(5)	0.030(5)	0.031(6)	0.009(4)	-0.001(4)	0.020(4)
C(24)	0.026(5)	0.046(6)	0.016(5)	0.007(4)	-0.004(4)	0.011(4)
C(25)	0.037(6)	0.031(5)	0.021(5)	-0.003(4)	-0.008(4)	0.008(4)
C(26)	0.052(7)	0.050(7)	0.019(5)	-0.008(5)	-0.008(5)	0.031(6)
C(31)	0.028(5)	0.035(5)	0.019(5)	-0.001(4)	0.005(4)	0.020(4)
C(32)	0.030(5)	0.035(5)	0.031(6)	-0.003(4)	0.000(4)	0.023(4)
C(33)	0.033(5)	0.035(6)	0.036(6)	0.008(4)	0.001(4)	0.026(5)
C(34)	0.027(5)	0.037(5)	0.019(5)	0.006(4)	-0.002(4)	0.021(4)
C(35)	0.028(5)	0.034(5)	0.016(5)	-0.002(4)	-0.008(4)	0.019(4)
C(36)	0.019(5)	0.030(5)	0.029(5)	-0.003(4)	-0.006(4)	0.010(4)
C(37)	0.021(5)	0.031(5)	0.032(6)	0.003(4)	0.000(4)	0.014(4)
C(38)	0.018(4)	0.032(5)	0.013(5)	0.005(4)	0.003(3)	0.011(4)
Cl(1)	0.096(3)	0.070(3)	0.093(3)	0.000(2)	-0.024(3)	0.017(2)
Cl(2)	0.191(6)	0.093(3)	0.072(3)	-0.011(3)	-0.029(3)	0.052(4)
C(41)	0.133(17)	0.120(16)	0.087(14)	-0.028(12)	-0.046(13)	0.074(14)
C(91)	0.062(12)	0.119(18)	0.121(20)	0.026(15)	-0.013(12)	0.074(13)
C(92)	0.158(25)	0.085(19)	0.119(21)	-0.054(16)	-0.087(19)	0.018(15)
C(93)	0.157(27)	0.177(28)	0.092(21)	-0.056(19)	-0.050(18)	0.086(22)

Appendix IV

Complete Bond Lengths, Bond Angles, and Thermal and Positional Parameters for $[\text{Pt}\{\overline{\text{NPhC(NPh)NPh}}\}(\text{COD})]\cdot\frac{1}{2}\text{C}_4\text{H}_{10}\text{O}$ **3.17a**

Table A.IV.1: Complete Bond Lengths (Å) for **3.17a**·½C₄H₁₀O, with e.s.d.s in parentheses

Pt(1)-N(2)	2.002(7)	C(21)-C(22)	1.409(12)
Pt(1)-N(1)	2.034(8)	C(22)-C(23)	1.386(14)
Pt(1)-C(45)	2.155(9)	C(23)-C(24)	1.38(2)
Pt(1)-C(41)	2.173(9)	C(24)-C(25)	1.392(14)
Pt(1)-C(48)	2.183(9)	C(25)-C(26)	1.380(13)
Pt(1)-C(44)	2.188(9)	C(31)-C(36)	1.376(13)
Pt(1)-C(1)	2.561(9)	C(31)-C(32)	1.406(13)
N(1)-C(1)	1.398(11)	C(32)-C(33)	1.378(14)
N(1)-C(11)	1.402(12)	C(33)-C(34)	1.42(2)
N(2)-C(1)	1.402(11)	C(34)-C(35)	1.36(2)
N(2)-C(21)	1.406(12)	C(35)-C(36)	1.395(14)
N(3)-C(1)	1.298(11)	C(41)-C(48)	1.407(13)
N(3)-C(31)	1.406(11)	C(41)-C(42)	1.496(12)
C(11)-C(12)	1.375(14)	C(42)-C(43)	1.511(13)
C(11)-C(16)	1.402(13)	C(43)-C(44)	1.540(12)
C(12)-C(13)	1.385(14)	C(44)-C(45)	1.379(13)
C(13)-C(14)	1.375(14)	C(45)-C(46)	1.510(13)
C(14)-C(15)	1.41(2)	C(46)-C(47)	1.529(13)
C(15)-C(16)	1.360(13)	C(47)-C(48)	1.518(13)
C(21)-C(26)	1.407(13)		
O(1)-C(2)	1.34(4)	C(2)-C(3)	1.19(4)

Table A.IV.2: Complete Bond Angles (°) for **3.17a**·½C₄H₁₀O, with e.s.d.s in parentheses

N(2)-Pt(1)-N(1)	65.9(3)	C(11)-C(12)-C(13)	122.2(10)
N(2)-Pt(1)-C(45)	100.6(3)	C(14)-C(13)-C(12)	120.7(10)
N(1)-Pt(1)-C(45)	154.4(3)	C(13)-C(14)-C(15)	117.4(9)
N(2)-Pt(1)-C(41)	157.9(3)	C(16)-C(15)-C(14)	121.4(10)
N(1)-Pt(1)-C(41)	102.5(3)	C(15)-C(16)-C(11)	121.1(10)
C(45)-Pt(1)-C(41)	96.7(4)	N(2)-C(21)-C(26)	118.7(8)
N(2)-Pt(1)-C(48)	159.4(3)	N(2)-C(21)-C(22)	122.9(9)
N(1)-Pt(1)-C(48)	103.6(3)	C(26)-C(21)-C(22)	118.4(9)
C(45)-Pt(1)-C(48)	81.6(3)	C(23)-C(22)-C(21)	119.5(9)
C(41)-Pt(1)-C(48)	37.7(3)	C(24)-C(23)-C(22)	121.1(9)
N(2)-Pt(1)-C(44)	105.1(3)	C(23)-C(24)-C(25)	120.1(9)
N(1)-Pt(1)-C(44)	163.4(3)	C(26)-C(25)-C(24)	119.3(9)
C(45)-Pt(1)-C(44)	37.0(3)	C(25)-C(26)-C(21)	121.4(9)
C(41)-Pt(1)-C(44)	80.9(4)	C(36)-C(31)-C(32)	119.1(9)
C(48)-Pt(1)-C(44)	89.0(3)	C(36)-C(31)-N(3)	123.6(9)
N(2)-Pt(1)-C(1)	33.0(3)	C(32)-C(31)-N(3)	117.0(8)
N(1)-Pt(1)-C(1)	33.0(3)	C(33)-C(32)-C(31)	120.1(10)
C(45)-Pt(1)-C(1)	129.9(3)	C(32)-C(33)-C(34)	120.1(10)
C(41)-Pt(1)-C(1)	133.3(3)	C(35)-C(34)-C(33)	119.2(9)
C(48)-Pt(1)-C(1)	133.9(3)	C(34)-C(35)-C(36)	121.0(10)
C(44)-Pt(1)-C(1)	136.9(3)	C(31)-C(36)-C(35)	120.5(10)

C(1)-N(1)-C(11)	125.1(8)	C(48)-C(41)-C(42)	124.8(9)
C(1)-N(1)-Pt(1)	94.7(5)	C(48)-C(41)-Pt(1)	71.6(5)
C(11)-N(1)-Pt(1)	129.2(6)	C(42)-C(41)-Pt(1)	111.1(6)
C(1)-N(2)-C(21)	124.8(7)	C(41)-C(42)-C(43)	113.7(7)
C(1)-N(2)-Pt(1)	96.0(5)	C(42)-C(43)-C(44)	114.3(8)
C(21)-N(2)-Pt(1)	133.5(6)	C(45)-C(44)-C(43)	124.2(8)
C(1)-N(3)-C(31)	122.1(8)	C(45)-C(44)-Pt(1)	70.2(5)
N(3)-C(1)-N(1)	133.0(8)	C(43)-C(44)-Pt(1)	111.5(6)
N(3)-C(1)-N(2)	123.7(8)	C(44)-C(45)-C(46)	125.1(8)
N(1)-C(1)-N(2)	103.3(7)	C(44)-C(45)-Pt(1)	72.8(5)
N(3)-C(1)-Pt(1)	174.7(7)	C(46)-C(45)-Pt(1)	109.2(6)
N(1)-C(1)-Pt(1)	52.3(4)	C(45)-C(46)-C(47)	113.4(8)
N(2)-C(1)-Pt(1)	51.0(4)	C(48)-C(47)-C(46)	112.8(8)
C(12)-C(11)-C(16)	117.0(9)	C(41)-C(48)-C(47)	122.1(9)
C(12)-C(11)-N(1)	123.8(9)	C(41)-C(48)-Pt(1)	70.8(5)
C(16)-C(11)-N(1)	119.1(9)	C(47)-C(48)-Pt(1)	111.8(6)
C(3)-C(2)-O(1)	125(5)	C(111 ^b)-O(1)-C(2)	180

Table A.IV.3: Final Positional (fractional co-ordinates) and Equivalent Thermal Parameters for **3.17a**· $\frac{1}{2}$ C₄H₁₀O, with e.s.d.s in parentheses

Atom	X/A	Y/B	Z/C	U(eq)
Pt(1)	0.2226(1)	0.0701(1)	0.0871(1)	0.014(1)
N(1)	0.3042(8)	-0.0580(5)	0.1128(4)	0.019(2)
N(2)	0.2096(8)	-0.0111(5)	-0.0071(4)	0.017(2)
N(3)	0.3009(8)	-0.1638(5)	0.0011(4)	0.019(2)
C(1)	0.2777(9)	-0.0871(6)	0.0343(5)	0.016(2)
C(11)	0.3004(9)	-0.1149(7)	0.1773(6)	0.018(2)
C(12)	0.2362(10)	-0.1996(7)	0.1710(6)	0.025(2)
C(13)	0.2323(10)	-0.2533(7)	0.2362(6)	0.023(2)
C(14)	0.2901(9)	-0.2221(8)	0.3109(6)	0.026(2)
C(15)	0.3517(10)	-0.1338(8)	0.3179(6)	0.027(2)
C(16)	0.3595(9)	-0.0832(7)	0.2534(5)	0.021(2)
C(21)	0.2012(10)	0.0065(6)	-0.0873(6)	0.021(2)
C(22)	0.3017(10)	-0.0247(7)	-0.1273(6)	0.021(2)
C(23)	0.2855(10)	-0.0051(7)	-0.2067(6)	0.027(2)
C(24)	0.1725(12)	0.0446(6)	-0.2474(6)	0.025(2)
C(25)	0.0725(10)	0.0764(7)	-0.2087(5)	0.024(2)
C(26)	0.0859(10)	0.0558(7)	-0.1301(6)	0.022(2)
C(31)	0.3928(9)	-0.2312(6)	0.0412(5)	0.015(2)
C(32)	0.3548(11)	-0.3239(7)	0.0254(6)	0.027(2)
C(33)	0.4452(12)	-0.3934(7)	0.0574(6)	0.030(2)
C(34)	0.5767(11)	-0.3718(8)	0.1060(6)	0.032(3)
C(35)	0.6125(10)	-0.2820(7)	0.1201(5)	0.025(2)
C(36)	0.5218(10)	-0.2112(8)	0.0875(6)	0.025(2)
C(41)	0.1865(9)	0.1157(7)	0.1996(5)	0.021(2)
C(42)	0.0552(9)	0.1707(6)	0.1887(5)	0.017(2)
C(43)	0.0229(10)	0.2263(7)	0.1136(6)	0.024(2)
C(44)	0.0805(9)	0.1847(6)	0.0461(5)	0.018(2)
C(45)	0.2101(10)	0.2043(6)	0.0328(5)	0.019(2)
C(46)	0.3161(10)	0.2674(7)	0.0828(6)	0.025(2)
C(47)	0.3341(10)	0.2513(7)	0.1712(6)	0.021(2)
C(48)	0.3155(9)	0.1509(7)	0.1914(5)	0.019(2)
O(1)	1.0000	0.5000	0.0000	0.210(19)
C(2)	0.9406(46)	0.5278(27)	0.0581(19)	0.249(25)
C(3)	0.9605(22)	0.6002(12)	0.0909(10)	0.084(6)

Table A.IV.4: Final Positional (fractional co-ordinates) and Equivalent Thermal Parameters of Calculated Hydrogen Atoms for **3.17a**·½C₄H₁₀O, with e.s.d.s in parentheses

Atom	X/A	Y/B	Z/C	U(eq)
H(12)	0.1930(10)	-0.2222(7)	0.1202(6)	0.030
H(13)	0.1893(10)	-0.3123(7)	0.2293(6)	0.028
H(14)	0.2887(9)	-0.2586(8)	0.3559(6)	0.032
H(15)	0.3886(10)	-0.1092(8)	0.3688(6)	0.032
H(16)	0.4057(9)	-0.0253(7)	0.2601(5)	0.025
H(22)	0.3801(10)	-0.0589(7)	-0.1001(6)	0.025
H(23)	0.3533(10)	-0.0262(7)	-0.2336(6)	0.032
H(24)	0.1629(12)	0.0571(6)	-0.3018(6)	0.031
H(25)	-0.0041(10)	0.1119(7)	-0.2362(5)	0.028
H(26)	0.0156(10)	0.0754(7)	-0.1043(6)	0.026
H(32)	0.2668(11)	-0.3386(7)	-0.0073(6)	0.033
H(33)	0.4192(12)	-0.4561(7)	0.0468(6)	0.036
H(34)	0.6392(11)	-0.4195(8)	0.1284(6)	0.038
H(35)	0.7006(10)	-0.2671(7)	0.1527(5)	0.030
H(36)	0.5494(10)	-0.1488(8)	0.0974(6)	0.030
H(41)	0.1944(9)	0.0654(7)	0.2396(5)	0.026
H(42A)	0.0627(9)	0.2131(6)	0.2340(5)	0.021
H(42B)	-0.0233(9)	0.1281(6)	0.1888(5)	0.021
H(43A)	0.0618(10)	0.2891(7)	0.1250(6)	0.029
H(43B)	-0.0794(10)	0.2325(7)	0.0958(6)	0.029
H(44)	0.0079(9)	0.1711(6)	-0.0027(5)	0.022
H(45)	0.2141(10)	0.2030(6)	-0.0240(5)	0.023
H(46A)	0.2874(10)	0.3322(7)	0.0706(6)	0.030
H(46B)	0.4070(10)	0.2583(7)	0.0687(6)	0.030
H(47A)	0.4281(10)	0.2720(7)	0.1987(6)	0.025
H(47B)	0.2653(10)	0.2893(7)	0.1905(6)	0.025
H(48)	0.3986(9)	0.1220(7)	0.2267(5)	0.023

Table A.IV.5: Thermal Parameters for **3.17a**·½C₄H₁₀O, with e.s.d.s in parentheses

Atom	U11	U22	U33	U23	U13	U12
Pt(1)	0.0201(2)	0.0102(2)	0.0130(2)	-0.0006(2)	0.0054(1)	0.0008(2)
N(1)	0.026(4)	0.015(5)	0.015(4)	-0.001(3)	0.004(3)	0.000(3)
N(2)	0.025(4)	0.020(5)	0.005(4)	0.000(3)	0.001(3)	0.001(3)
N(3)	0.034(4)	0.007(4)	0.016(4)	-0.002(3)	0.004(3)	0.001(3)
C(1)	0.027(5)	0.010(5)	0.012(5)	0.004(4)	0.004(4)	0.003(4)
C(11)	0.020(4)	0.020(5)	0.018(5)	0.000(4)	0.012(4)	0.008(4)
C(12)	0.030(5)	0.017(5)	0.028(6)	-0.005(4)	0.008(4)	0.001(4)
C(13)	0.028(5)	0.014(5)	0.032(6)	0.007(4)	0.013(4)	0.002(4)
C(14)	0.023(5)	0.029(6)	0.029(6)	0.008(5)	0.013(4)	0.006(4)
C(15)	0.024(5)	0.034(7)	0.021(5)	0.000(5)	0.004(4)	0.012(5)
C(16)	0.023(5)	0.021(6)	0.020(5)	0.002(4)	0.011(4)	0.007(4)
C(21)	0.032(5)	0.003(5)	0.027(6)	-0.004(4)	0.007(4)	-0.005(4)
C(22)	0.023(5)	0.017(5)	0.025(6)	-0.008(4)	0.012(4)	-0.006(4)
C(23)	0.035(6)	0.023(6)	0.027(6)	0.001(5)	0.017(5)	-0.004(5)
C(24)	0.051(6)	0.015(5)	0.013(5)	0.007(4)	0.013(4)	-0.005(5)
C(25)	0.036(5)	0.015(5)	0.015(5)	0.006(4)	-0.004(4)	0.003(4)
C(26)	0.027(5)	0.015(5)	0.024(5)	0.008(4)	0.005(4)	0.005(4)
C(31)	0.031(5)	0.008(5)	0.006(4)	0.003(3)	0.007(4)	0.004(4)
C(32)	0.043(6)	0.018(6)	0.018(5)	0.000(4)	0.001(4)	-0.001(5)
C(33)	0.055(7)	0.009(5)	0.028(6)	0.004(4)	0.013(5)	0.008(5)
C(34)	0.037(6)	0.022(6)	0.034(7)	0.013(5)	0.004(5)	0.017(5)
C(35)	0.031(5)	0.030(6)	0.014(5)	0.004(4)	0.004(4)	0.007(5)

C(36)	0.035(5)	0.023(6)	0.021(5)	0.003(5)	0.015(4)	0.003(5)
C(41)	0.024(5)	0.031(6)	0.010(5)	-0.003(4)	0.006(4)	-0.002(4)
C(42)	0.018(4)	0.013(5)	0.022(5)	-0.001(4)	0.008(4)	-0.002(4)
C(43)	0.025(5)	0.023(6)	0.023(5)	-0.012(4)	0.003(4)	-0.001(4)
C(44)	0.027(5)	0.009(5)	0.017(5)	0.000(4)	0.002(4)	0.006(4)
C(45)	0.037(5)	0.007(5)	0.014(5)	-0.002(4)	0.004(4)	0.000(4)
C(46)	0.030(5)	0.017(6)	0.031(6)	-0.001(4)	0.011(4)	-0.005(4)
C(47)	0.022(4)	0.016(5)	0.024(6)	-0.005(4)	0.003(4)	-0.003(4)
C(48)	0.027(5)	0.019(5)	0.010(5)	-0.003(4)	0.001(4)	0.004(4)
O(1)	0.102(17)	0.301(43)	0.225(34)	-0.196(34)	0.031(19)	0.014(21)
C(2)	0.353(54)	0.209(40)	0.121(28)	-0.054(27)	-0.083(30)	0.177(39)
C(3)	0.128(15)	0.046(10)	0.055(11)	-0.020(8)	-0.025(10)	0.017(10)

Appendix V

Complete Bond Lengths, Bond Angles, and Thermal and Positional Parameters for $[(\eta^6\text{-}p\text{-cymene})\text{Ru}\{\overline{\text{N}(\text{Ac})\text{C}(\text{N}(\text{Ac})\text{N}(\text{Ac}))}\}(\text{PPh}_3)]$ 3.21a

Table A.V.1: Complete Bond Lengths (Å) for 3.21a, with e.s.d.s in parentheses

Ru(1)-N(1)	2.042(17)	N(2)-C(1)	1.39(3)
Ru(1)-N(2)	2.100(16)	N(3A)-C(1)	1.46(4)
Ru(1)-C(16)	2.18(2)	N(3A)-C(6A)	1.47(6)
Ru(1)-C(12)	2.21(2)	N(3B)-C(1)	1.26(4)
Ru(1)-C(15)	2.22(2)	N(3B)-C(6B)	1.38(5)
Ru(1)-C(13)	2.22(2)	N(3B)-C(6A)	1.86(6)
Ru(1)-C(11)	2.228(17)	C(2)-C(3)	1.48(3)
Ru(1)-C(14)	2.29(2)	C(4)-C(5)	1.50(4)
Ru(1)-P(1)	2.347(5)	C(6A)-C(7)	1.29(5)
P(1)-C(31)	1.815(10)	C(6B)-C(7)	1.68(5)
P(1)-C(41)	1.830(12)	C(11)-C(12)	1.38(3)
P(1)-C(21)	1.836(10)	C(11)-C(16)	1.45(3)
O(1)-C(2)	1.24(2)	C(11)-C(17)	1.51(3)
O(2A)-C(4)	1.04(3)	C(12)-C(13)	1.37(3)
O(2B)-C(4)	1.54(4)	C(13)-C(14)	1.43(3)
O(2B)-C(6B)	1.71(5)	C(14)-C(15)	1.40(3)
O(3A)-C(6A)	1.25(6)	C(14)-C(110)	1.49(3)
O(3B)-C(6B)	1.17(4)	C(15)-C(16)	1.41(3)
N(1)-C(1)	1.36(3)	C(17)-C(19)	1.47(4)
N(1)-C(2)	1.37(2)	C(17)-C(18)	1.54(3)
N(2)-C(4)	1.36(3)		

Table A.V.2: Complete Bond Angles (°) for 3.21a, with e.s.d.s in parentheses

N(1)-Ru(1)-N(2)	62.4(6)	N(3B)-C(1)-N(3A)	41.5(19)
N(1)-Ru(1)-C(16)	95.6(8)	N(1)-C(1)-N(3A)	119(3)
N(2)-Ru(1)-C(16)	138.6(7)	N(2)-C(1)-N(3A)	137(2)
N(1)-Ru(1)-C(12)	121.2(8)	O(1)-C(2)-N(1)	118.6(16)
N(2)-Ru(1)-C(12)	94.5(8)	O(1)-C(2)-C(3)	120.0(17)
C(16)-Ru(1)-C(12)	66.1(8)	N(1)-C(2)-C(3)	121.4(19)
N(1)-Ru(1)-C(15)	120.9(7)	O(2A)-C(4)-N(2)	129(3)
N(2)-Ru(1)-C(15)	172.7(8)	O(2A)-C(4)-C(5)	109(3)
C(16)-Ru(1)-C(15)	37.5(7)	N(2)-C(4)-C(5)	116(3)
C(12)-Ru(1)-C(15)	78.2(8)	O(2A)-C(4)-O(2B)	45(2)
N(1)-Ru(1)-C(13)	157.2(8)	N(2)-C(4)-O(2B)	113(3)
N(2)-Ru(1)-C(13)	108.6(10)	C(5)-C(4)-O(2B)	128(2)
C(16)-Ru(1)-C(13)	77.7(9)	O(3A)-C(6A)-C(7)	114(5)
C(12)-Ru(1)-C(13)	36.1(7)	O(3A)-C(6A)-N(3A)	122(4)
C(15)-Ru(1)-C(13)	65.8(10)	C(7)-C(6A)-N(3A)	124(5)
N(1)-Ru(1)-C(11)	95.0(9)	O(3B)-C(6B)-N(3B)	126(4)
N(2)-Ru(1)-C(11)	105.0(7)	O(3B)-C(6B)-C(7)	123(3)
C(16)-Ru(1)-C(11)	38.5(7)	N(3B)-C(6B)-C(7)	108(3)

C(12)-Ru(1)-C(11)	36.2(8)	O(3B)-C(6B)-O(2B)	78(2)
C(15)-Ru(1)-C(11)	68.7(7)	N(3B)-C(6B)-O(2B)	98(3)
C(13)-Ru(1)-C(11)	66.0(9)	C(7)-C(6B)-O(2B)	111(3)
N(1)-Ru(1)-C(14)	156.7(8)	C(12)-C(11)-C(16)	115(2)
N(2)-Ru(1)-C(14)	141.0(8)	C(12)-C(11)-C(17)	124.6(19)
C(16)-Ru(1)-C(14)	66.1(8)	C(16)-C(11)-C(17)	120(2)
C(12)-Ru(1)-C(14)	66.1(8)	C(12)-C(11)-Ru(1)	71.2(11)
C(15)-Ru(1)-C(14)	36.1(8)	C(16)-C(11)-Ru(1)	68.9(10)
C(13)-Ru(1)-C(14)	37.0(9)	C(17)-C(11)-Ru(1)	130.3(16)
C(11)-Ru(1)-C(14)	79.6(8)	C(13)-C(12)-C(11)	123(2)
N(1)-Ru(1)-P(1)	85.2(5)	C(13)-C(12)-Ru(1)	72.3(12)
N(2)-Ru(1)-P(1)	90.3(5)	C(11)-C(12)-Ru(1)	72.6(12)
C(16)-Ru(1)-P(1)	124.3(5)	C(12)-C(13)-C(14)	122(2)
C(12)-Ru(1)-P(1)	152.2(5)	C(12)-C(13)-Ru(1)	71.5(13)
C(15)-Ru(1)-P(1)	96.4(5)	C(14)-C(13)-Ru(1)	74.1(12)
C(13)-Ru(1)-P(1)	116.7(6)	C(15)-C(14)-C(13)	116.9(19)
C(11)-Ru(1)-P(1)	162.8(5)	C(15)-C(14)-C(110)	119(2)
C(14)-Ru(1)-P(1)	93.4(5)	C(13)-C(14)-C(110)	124(2)
C(31)-P(1)-C(41)	99.5(7)	C(15)-C(14)-Ru(1)	69.3(12)
C(31)-P(1)-C(21)	103.4(7)	C(13)-C(14)-Ru(1)	68.9(12)
C(41)-P(1)-C(21)	102.9(7)	C(110)-C(14)-Ru(1)	133.6(15)
C(31)-P(1)-Ru(1)	118.4(5)	C(14)-C(15)-C(16)	120(2)
C(41)-P(1)-Ru(1)	118.1(5)	C(14)-C(15)-Ru(1)	74.7(14)
C(21)-P(1)-Ru(1)	112.3(5)	C(16)-C(15)-Ru(1)	69.7(11)
C(4)-O(2B)-C(6B)	123(3)	C(15)-C(16)-C(11)	122(2)
C(1)-N(1)-C(2)	127(2)	C(15)-C(16)-Ru(1)	72.9(12)
C(1)-N(1)-Ru(1)	99.4(15)	C(11)-C(16)-Ru(1)	72.6(11)
C(2)-N(1)-Ru(1)	133.4(13)	C(19)-C(17)-C(11)	112(2)
C(4)-N(2)-C(1)	124(2)	C(19)-C(17)-C(18)	112(3)
C(4)-N(2)-Ru(1)	140(2)	C(11)-C(17)-C(18)	116.0(19)
C(1)-N(2)-Ru(1)	95.6(13)	C(22)-C(21)-C(26)	120.0
C(1)-N(3A)-C(6A)	124(3)	C(22)-C(21)-P(1)	122.3(8)
C(1)-N(3B)-C(6B)	142(3)	C(26)-C(21)-P(1)	117.7(8)
C(1)-N(3B)-C(6A)	111(3)	C(32)-C(31)-P(1)	121.0(7)
C(6B)-N(3B)-C(6A)	65(3)	C(36)-C(31)-P(1)	119.0(7)
N(3B)-C(1)-N(1)	131(3)	C(42)-C(41)-P(1)	122.2(10)
N(3B)-C(1)-N(2)	117(3)	C(46)-C(41)-P(1)	117.6(10)
N(1)-C(1)-N(2)	103(2)		

Table A.V.3: Final Positional (fractional co-ordinates) and Equivalent Thermal Parameters for **3.21a**, with *e.s.d.s* in parentheses

Atom	X/A	Y/B	Z/C	U(eq)
Ru(1)	0.1912(1)	0.1965(1)	0.9561(1)	0.026(1)
P(1)	0.1042(2)	0.2470(3)	0.9335(3)	0.021(1)
O(1)	0.2132(5)	0.4095(8)	1.0211(7)	0.029(3)
O(2A)	0.1323(12)	0.0256(19)	1.1333(16)	0.029(7)
O(2B)	0.1638(13)	0.037(2)	1.176(2)	0.048(9)
O(3A)	0.0703(10)	0.148(2)	1.2137(18)	0.044(8)
O(3B)	0.2147(10)	0.0769(16)	1.2480(14)	0.022(6)
N(1)	0.1871(8)	0.2710(11)	1.0574(9)	0.040(5)
N(2)	0.1663(7)	0.1309(11)	1.0596(10)	0.045(5)
N(3A)	0.1473(14)	0.235(3)	1.1840(17)	0.025(8)
N(3B)	0.1778(14)	0.194(2)	1.180(2)	0.025(9)

C(1)	0.1691(12)	0.207(2)	1.1078(15)	0.071(9)
C(2)	0.2008(6)	0.3575(12)	1.0757(11)	0.020(4)
C(3)	0.1995(9)	0.3907(16)	1.1584(13)	0.055(7)
C(4)	0.1563(9)	0.0461(16)	1.086(2)	0.066(10)
C(5)	0.1573(10)	-0.0277(14)	1.025(2)	0.087(12)
C(6A)	0.115(2)	0.177(4)	1.235(3)	0.060(16)
C(6B)	0.1793(16)	0.126(2)	1.236(3)	0.028(10)
C(7)	0.1308(12)	0.146(3)	1.3027(18)	0.115(15)
C(11)	0.2794(7)	0.1852(16)	0.9566(14)	0.043(6)
C(12)	0.2582(8)	0.1036(14)	0.9340(13)	0.040(6)
C(13)	0.2228(9)	0.0942(18)	0.8727(15)	0.061(8)
C(14)	0.2067(8)	0.1690(17)	0.8249(13)	0.045(7)
C(15)	0.2261(8)	0.2537(17)	0.8465(10)	0.038(6)
C(16)	0.2621(7)	0.2623(14)	0.9102(12)	0.034(5)
C(17)	0.3187(8)	0.1977(17)	1.0232(12)	0.045(6)
C(18)	0.3090(15)	0.140(2)	1.098(2)	0.138(19)
C(19)	0.3740(11)	0.192(3)	0.996(2)	0.150(19)
C(110)	0.1717(8)	0.161(2)	0.7544(14)	0.076(11)
C(21)	0.1012(5)	0.3356(8)	0.8579(8)	0.026(5)
C(22)	0.0680(5)	0.3298(9)	0.7924(9)	0.071(10)
C(23)	0.0670(6)	0.3990(12)	0.7371(8)	0.075(10)
C(24)	0.0993(6)	0.4741(11)	0.7473(10)	0.115(16)
C(25)	0.1325(6)	0.4799(8)	0.8127(10)	0.062(9)
C(26)	0.1335(5)	0.4107(9)	0.8680(8)	0.042(6)
C(31)	0.0550(4)	0.1660(8)	0.9003(9)	0.027(5)
C(32)	0.0014(4)	0.1883(8)	0.8974(8)	0.042(6)
C(33)	-0.0357(4)	0.1246(11)	0.8731(9)	0.047(7)
C(34)	-0.0191(5)	0.0387(10)	0.8516(13)	0.098(13)
C(35)	0.0345(6)	0.0164(9)	0.8545(16)	0.21(3)
C(36)	0.0715(4)	0.0801(10)	0.8789(14)	0.121(17)
C(41)	0.0679(6)	0.2969(10)	1.0164(7)	0.037(5)
C(42)	0.0569(6)	0.3886(10)	1.0205(8)	0.043(6)
C(43)	0.0254(7)	0.4221(12)	1.0812(11)	0.108(15)
C(44)	0.0048(6)	0.3639(18)	1.1378(9)	0.18(3)
C(45)	0.0157(7)	0.2723(16)	1.1338(9)	0.107(16)
C(46)	0.0473(8)	0.2388(10)	1.0731(10)	0.082(10)

Table A.V.4: Final Positional (fractional co-ordinates) and Equivalent Thermal Parameters of Calculated Hydrogen Atoms for **3.21a**, with *e.s.d.s* in parentheses

Atom	X/A	Y/B	Z/C	U(eq)
H(3A)	0.1892	0.3425	1.1930	0.083
H(3B)	0.1744	0.4391	1.1627	0.083
H(3C)	0.2342	0.4119	1.1731	0.083
H(5A)	0.1788	-0.0094	0.9815	0.131
H(5B)	0.1217	-0.0394	1.0076	0.131
H(5C)	0.1718	-0.0814	1.0484	0.131
H(12)	0.2683	0.0523	0.9617	0.047
H(13)	0.2089	0.0375	0.8618	0.073
H(15)	0.2153	0.3047	0.8189	0.046
H(16)	0.2752	0.3191	0.9228	0.041
H(17)	0.3142	0.2602	1.0405	0.054
H(18A)	0.2726	0.1463	1.1138	0.208
H(18B)	0.3318	0.1606	1.1395	0.208

H(18C)	0.3164	0.0783	1.0861	0.208
H(19A)	0.3976	0.2003	1.0396	0.224
H(19B)	0.3804	0.2373	0.9567	0.224
H(19C)	0.3801	0.1333	0.9728	0.224
H(11A)	0.1619	0.0996	0.7468	0.114
H(11B)	0.1904	0.1827	0.7086	0.114
H(11C)	0.1404	0.1971	0.7623	0.114
H(22)	0.0464	0.2795	0.7857	0.086
H(23)	0.0448	0.3951	0.6934	0.090
H(24)	0.0987	0.5204	0.7103	0.138
H(25)	0.1541	0.5302	0.8195	0.075
H(26)	0.1557	0.4146	0.9118	0.051
H(32)	-0.0097	0.2458	0.9117	0.051
H(33)	-0.0715	0.1396	0.8711	0.057
H(34)	-0.0439	-0.0038	0.8354	0.118
H(35)	0.0455	-0.0410	0.8402	0.249
H(36)	0.1074	0.0652	0.8808	0.145
H(42)	0.0707	0.4275	0.9826	0.051
H(43)	0.0181	0.4834	1.0839	0.130
H(44)	-0.0163	0.3864	1.1784	0.218
H(45)	0.0019	0.2334	1.1716	0.128
H(46)	0.0546	0.1775	1.0703	0.099

Table A.V.5: Thermal Parameters for **3.21a**, with *e.s.d.s* in parentheses

Atom	U11	U22	U33	U23	U13	U12
Ru(1)	0.0273(8)	0.0189(8)	0.0328(9)	-0.0005(8)	-0.0091(8)	0.0045(8)
P(1)	0.027(3)	0.028(3)	0.010(2)	0.002(2)	0.003(2)	0.001(2)
O(1)	0.035(8)	0.020(7)	0.032(8)	0.001(7)	-0.003(6)	-0.018(6)
O(2A)	0.042(18)	0.040(19)	0.006(14)	0.019(14)	0.005(15)	-0.001(16)
O(2B)	0.042(19)	0.04(2)	0.06(2)	0.021(18)	-0.003(19)	0.026(17)
O(3A)	0.011(15)	0.06(2)	0.06(2)	-0.002(17)	0.004(15)	-0.001(16)
O(3B)	0.036(16)	0.016(14)	0.014(13)	0.006(12)	-0.019(12)	-0.010(13)
N(1)	0.063(12)	0.036(10)	0.022(9)	0.022(8)	-0.015(9)	-0.012(10)
N(2)	0.071(13)	0.029(10)	0.035(11)	0.023(9)	-0.030(10)	-0.036(10)
N(3A)	0.03(2)	0.05(3)	0.000(16)	0.001(16)	0.008(15)	-0.010(19)
N(3B)	0.03(2)	0.014(18)	0.04(2)	-0.022(19)	0.014(17)	-0.011(18)
C(1)	0.11(2)	0.06(2)	0.042(16)	0.022(16)	-0.031(15)	-0.053(19)
C(2)	0.006(9)	0.023(11)	0.030(11)	-0.013(10)	-0.014(8)	-0.004(9)
C(3)	0.041(15)	0.060(16)	0.063(16)	-0.010(13)	-0.030(13)	0.044(13)
C(4)	0.020(13)	0.037(17)	0.14(3)	0.060(19)	0.021(16)	0.008(11)
C(5)	0.050(17)	0.008(12)	0.20(4)	0.003(18)	0.04(2)	0.017(12)
C(6A)	0.06(4)	0.09(4)	0.03(3)	0.00(3)	0.01(3)	0.04(3)
C(6B)	0.03(3)	0.000(18)	0.05(3)	0.010(19)	0.02(2)	-0.008(18)
C(7)	0.07(2)	0.21(4)	0.07(2)	0.10(3)	0.017(17)	-0.02(2)
C(11)	0.012(9)	0.059(16)	0.059(14)	0.051(14)	0.001(11)	0.009(11)
C(12)	0.036(13)	0.020(12)	0.062(16)	-0.007(11)	-0.014(12)	-0.001(10)
C(13)	0.036(14)	0.064(18)	0.081(19)	-0.054(16)	-0.033(14)	0.038(14)
C(14)	0.034(13)	0.069(18)	0.034(13)	-0.019(13)	-0.007(10)	0.037(12)
C(15)	0.039(13)	0.067(17)	0.007(10)	-0.020(11)	0.005(9)	0.033(13)
C(16)	0.027(12)	0.029(12)	0.047(14)	0.014(11)	0.006(10)	0.012(10)
C(17)	0.038(13)	0.047(13)	0.050(14)	0.003(13)	-0.026(11)	-0.011(13)
C(18)	0.18(4)	0.10(3)	0.13(3)	0.07(2)	-0.13(3)	-0.08(3)
C(19)	0.038(17)	0.21(4)	0.21(4)	-0.06(4)	-0.05(2)	0.02(3)

C(110)	0.020(12)	0.16(3)	0.046(15)	-0.043(19)	-0.006(11)	0.027(16)
C(21)	0.014(10)	0.021(11)	0.042(12)	0.023(9)	-0.002(10)	0.008(9)
C(22)	0.020(12)	0.12(3)	0.075(18)	0.067(19)	-0.002(13)	-0.006(15)
C(23)	0.027(14)	0.11(2)	0.08(2)	0.06(2)	-0.020(14)	-0.025(16)
C(24)	0.024(13)	0.14(3)	0.18(4)	0.13(3)	-0.013(19)	-0.015(18)
C(25)	0.025(12)	0.060(19)	0.10(2)	0.061(17)	-0.013(14)	-0.016(12)
C(26)	0.026(12)	0.032(13)	0.070(17)	0.011(13)	0.003(12)	0.007(11)
C(31)	0.015(10)	0.039(13)	0.026(11)	0.003(9)	-0.012(8)	0.008(9)
C(32)	0.025(11)	0.055(15)	0.047(13)	-0.010(13)	0.013(10)	-0.029(13)
C(33)	0.024(12)	0.10(2)	0.019(12)	-0.011(13)	-0.007(10)	-0.010(13)
C(34)	0.046(17)	0.08(2)	0.17(4)	-0.08(2)	-0.02(2)	-0.013(17)
C(35)	0.06(2)	0.06(2)	0.50(9)	-0.12(4)	-0.15(4)	0.010(19)
C(36)	0.021(14)	0.052(18)	0.29(5)	-0.09(2)	-0.09(2)	0.045(14)
C(41)	0.036(12)	0.052(15)	0.023(11)	-0.019(12)	0.002(9)	0.008(13)
C(42)	0.038(13)	0.062(17)	0.028(13)	-0.016(12)	-0.001(10)	0.016(12)
C(43)	0.10(3)	0.16(4)	0.06(2)	-0.07(2)	-0.041(19)	0.10(3)
C(44)	0.05(2)	0.42(9)	0.07(3)	-0.11(5)	-0.01(2)	0.00(4)
C(45)	0.09(3)	0.18(4)	0.049(19)	-0.04(2)	0.029(18)	-0.09(3)
C(46)	0.071(19)	0.12(3)	0.053(18)	-0.043(19)	0.009(15)	-0.051(19)

Appendix VI

Complete Bond Lengths, Bond Angles, and Thermal and Positional Parameters for $[\{\text{Pt}(\text{SO}_3)(\text{PPh}_3)_2\}_2 \cdot 2\text{PhNHC}(\text{O})\text{NHMe}] \cdot 2\text{CHCl}_3$ 4.23

Table A.VI.1: Complete Bond Lengths (Å) for 4.23·2CHCl₃, with e.s.d.s in parentheses

Pt(1)-O(1)	2.084(2)	C(212)-C(213)	1.401(6)
Pt(1)-P(2)	2.2506(8)	C(213)-C(214)	1.378(8)
Pt(1)-S(1)	2.3273(7)	C(214)-C(215)	1.354(8)
Pt(1)-P(1)	2.3404(7)	C(215)-C(216)	1.383(6)
S(1)-O(2)	1.463(2)	C(221)-C(222)	1.386(5)
S(1)-O(3)	1.474(2)	C(221)-C(226)	1.388(5)
S(1)-O(1)	1.534(2)	C(222)-C(223)	1.388(5)
P(1)-C(131)	1.826(3)	C(223)-C(224)	1.375(6)
P(1)-C(111)	1.827(3)	C(224)-C(225)	1.384(6)
P(1)-C(121)	1.830(3)	C(225)-C(226)	1.391(6)
P(2)-C(231)	1.830(3)	C(231)-C(236)	1.386(5)
P(2)-C(221)	1.833(3)	C(231)-C(232)	1.387(5)
P(2)-C(211)	1.833(3)	C(232)-C(233)	1.385(6)
O(1)-S(1)	1.534(2)	C(233)-C(234)	1.360(7)
C(111)-C(116)	1.392(4)	C(234)-C(235)	1.379(6)
C(111)-C(112)	1.397(5)	C(235)-C(236)	1.388(5)
C(112)-C(113)	1.393(5)	O(4)-C(11)	1.233(5)
C(113)-C(114)	1.380(5)	N(1)-C(11)	1.355(6)
C(114)-C(115)	1.377(6)	N(1)-C(12)	1.446(6)
C(115)-C(116)	1.391(5)	N(2)-C(11)	1.367(5)
C(121)-C(122)	1.385(5)	N(2)-C(21)	1.395(6)
C(121)-C(126)	1.393(5)	C(21)-C(22)	1.398(6)
C(122)-C(123)	1.400(5)	C(21)-C(26)	1.399(6)
C(123)-C(124)	1.375(7)	C(22)-C(23)	1.378(7)
C(124)-C(125)	1.380(7)	C(23)-C(24)	1.383(8)
C(125)-C(126)	1.387(5)	C(24)-C(25)	1.379(9)
C(131)-C(136)	1.391(4)	C(25)-C(26)	1.390(8)
C(131)-C(132)	1.400(4)		
C(132)-C(133)	1.388(5)	C(1)-Cl(2)	1.743(5)
C(133)-C(134)	1.385(6)	C(1)-Cl(1)	1.748(6)
C(134)-C(135)	1.379(6)	C(1)-Cl(3)	1.761(5)
C(135)-C(136)	1.389(5)	C(2)-Cl(5)	1.734(8)
C(211)-C(212)	1.380(5)	C(2)-Cl(6)	1.751(8)
C(211)-C(216)	1.401(5)	C(2)-Cl(4)	1.755(8)

Table A.VI.2: Complete Bond Angles ($^{\circ}$) for **4.23**·2CHCl₃, with *e.s.d.s* in parentheses

O(1)-Pt(1)-P(2)	175.57(6)	C(135)-C(134)-C(133)	119.6(3)
O(1)-Pt(1)-S(1)	83.73(6)	C(134)-C(135)-C(136)	120.7(3)
P(2)-Pt(1)-S(1)	91.93(3)	C(135)-C(136)-C(131)	120.2(3)
O(1)-Pt(1)-P(1)	87.01(6)	C(212)-C(211)-C(216)	118.9(4)
P(2)-Pt(1)-P(1)	97.37(3)	C(212)-C(211)-P(2)	120.4(3)
S(1)-Pt(1)-P(1)	170.36(3)	C(216)-C(211)-P(2)	120.7(3)
O(2)-S(1)-O(3)	111.93(13)	C(211)-C(212)-C(213)	119.8(5)
O(2)-S(1)-O(1)	106.59(12)	C(214)-C(213)-C(212)	120.2(5)
O(3)-S(1)-O(1)	109.41(12)	C(215)-C(214)-C(213)	120.0(4)
O(2)-S(1)-Pt(1)	114.70(9)	C(214)-C(215)-C(216)	120.8(5)
O(3)-S(1)-Pt(1)	108.91(9)	C(215)-C(216)-C(211)	120.2(5)
O(1')-S(1)-Pt(1)	104.95(8)	C(222)-C(221)-C(226)	118.6(3)
C(131)-P(1)-C(111)	111.17(15)	C(222)-C(221)-P(2)	121.2(2)
C(131)-P(1)-C(121)	100.75(14)	C(221)-C(222)-C(223)	120.4(3)
C(111)-P(1)-C(121)	104.09(15)	C(224)-C(223)-C(222)	120.8(4)
C(131)-P(1)-Pt(1)	113.61(10)	C(223)-C(224)-C(225)	119.4(3)
C(111)-P(1)-Pt(1)	113.74(10)	C(224)-C(225)-C(226)	120.0(4)
C(121)-P(1)-Pt(1)	112.33(10)	C(221)-C(226)-C(225)	120.8(4)
C(231)-P(2)-C(221)	108.75(15)	C(236)-C(231)-C(232)	117.9(3)
C(231)-P(2)-C(211)	101.78(15)	C(236)-C(231)-P(2)	120.1(2)
C(221)-P(2)-C(211)	101.72(15)	C(232)-C(231)-P(2)	121.9(3)
C(231)-P(2)-Pt(1)	112.53(11)	C(233)-C(232)-C(231)	120.9(4)
C(221)-P(2)-Pt(1)	111.52(11)	C(234)-C(233)-C(232)	120.7(4)
C(211)-P(2)-Pt(1)	119.45(10)	C(233)-C(234)-C(235)	119.4(4)
S(1)-O(1)-Pt(1)	121.82(12)	C(234)-C(235)-C(236)	120.3(4)
C(116)-C(111)-C(112)	119.7(3)	C(231)-C(236)-C(235)	120.7(3)
C(116)-C(111)-P(1)	124.8(3)	C(11)-N(1)-C(12)	121.6(4)
C(112)-C(111)-P(1)	115.4(2)	C(11)-N(2)-C(21)	128.7(3)
C(113)-C(112)-C(111)	119.4(3)	O(4)-C(11)-N(1)	121.8(4)
C(114)-C(113)-C(112)	120.7(4)	O(4)-C(11)-N(2)	123.9(4)
C(115)-C(114)-C(113)	119.8(3)	N(1)-C(11)-N(2)	114.3(3)
C(114)-C(115)-C(116)	120.5(3)	N(2)-C(21)-C(22)	116.9(4)
C(115)-C(116)-C(111)	119.8(3)	N(2)-C(21)-C(26)	124.1(4)
C(122)-C(121)-C(126)	119.9(3)	C(22)-C(21)-C(26)	119.1(5)
C(122)-C(121)-P(1)	123.1(3)	C(23)-C(22)-C(21)	121.1(5)
C(126)-C(121)-P(1)	117.0(3)	C(22)-C(23)-C(24)	119.9(6)
C(121)-C(122)-C(123)	119.2(4)	C(25)-C(24)-C(23)	119.6(5)
C(124)-C(123)-C(122)	120.6(4)	C(24)-C(25)-C(26)	121.5(5)
C(123)-C(124)-C(125)	120.0(4)	C(25)-C(26)-C(21)	118.9(5)
C(124)-C(125)-C(126)	120.1(4)		
C(125)-C(126)-C(121)	120.1(4)	Cl(2)-C(1)-Cl(1)	110.1(3)
C(136)-C(131)-C(132)	118.9(3)	Cl(2)-C(1)-Cl(3)	109.1(3)
C(136)-C(131)-P(1)	118.5(2)	Cl(1)-C(1)-Cl(3)	110.0(3)
C(132)-C(131)-P(1)	122.2(2)	Cl(5)-C(2)-Cl(6)	109.2(4)
C(133)-C(132)-C(131)	120.3(3)	Cl(5)-C(2)-Cl(4)	109.7(5)
C(134)-C(133)-C(132)	120.3(3)	Cl(6)-C(2)-Cl(4)	109.5(4)
C(226)-C(221)-P(2)	120.1(3)		

Table A.VI.3: Final Positional (fractional co-ordinates) and Equivalent Thermal Parameters for $4.23 \cdot 2\text{CHCl}_3$, with e.s.d.s in parentheses

Atom	X/A	Y/B	Z/C	U(eq)
Pt(1)	0.6175(1)	0.6245(1)	0.5992(1)	0.019(1)
S(1)	0.5783(1)	0.4444(1)	0.5597(1)	0.022(1)
P(1)	0.6478(1)	0.7943(1)	0.6079(1)	0.023(1)
P(2)	0.7055(1)	0.6695(1)	0.7583(1)	0.023(1)
O(1)	0.5320(1)	0.5716(2)	0.4512(2)	0.023(1)
O(2)	0.6140(2)	0.4220(2)	0.6457(2)	0.029(1)
O(3)	0.6101(2)	0.3689(2)	0.4544(2)	0.030(1)
C(111)	0.6105(2)	0.9090(2)	0.7279(3)	0.027(1)
C(112)	0.5250(3)	0.8857(3)	0.7602(3)	0.036(1)
C(113)	0.4886(3)	0.9695(3)	0.8479(3)	0.045(1)
C(114)	0.5356(3)	1.0751(3)	0.9022(3)	0.045(1)
C(115)	0.6203(3)	1.0979(3)	0.8707(3)	0.040(1)
C(116)	0.6582(3)	1.0155(3)	0.7837(3)	0.033(1)
C(121)	0.5818(2)	0.7973(3)	0.4930(3)	0.029(1)
C(122)	0.5086(3)	0.8623(3)	0.5046(3)	0.037(1)
C(123)	0.4625(3)	0.8602(3)	0.4122(4)	0.049(1)
C(124)	0.4883(3)	0.7933(4)	0.3108(4)	0.057(1)
C(125)	0.5594(3)	0.7263(4)	0.2990(4)	0.056(1)
C(126)	0.6069(3)	0.7286(3)	0.3899(3)	0.042(1)
C(131)	0.7717(2)	0.8252(3)	0.5917(3)	0.026(1)
C(132)	0.8025(2)	0.9196(3)	0.5878(3)	0.034(1)
C(133)	0.8955(3)	0.9361(3)	0.5680(3)	0.043(1)
C(134)	0.9580(3)	0.8581(3)	0.5496(4)	0.046(1)
C(135)	0.9270(3)	0.7635(3)	0.5501(3)	0.046(1)
C(136)	0.8345(2)	0.7466(3)	0.5711(3)	0.034(1)
C(211)	0.7656(2)	0.8100(3)	0.8453(3)	0.032(1)
C(212)	0.8564(3)	0.8389(3)	0.8303(3)	0.046(1)
C(213)	0.9006(4)	0.9472(4)	0.8957(4)	0.069(2)
C(214)	0.8553(5)	1.0237(4)	0.9779(5)	0.077(2)
C(215)	0.7674(4)	0.9947(4)	0.9949(4)	0.071(2)
C(216)	0.7209(3)	0.8893(3)	0.9291(3)	0.048(1)
C(221)	0.6314(2)	0.6536(3)	0.8510(3)	0.029(1)
C(222)	0.5336(2)	0.6182(3)	0.8211(3)	0.034(1)
C(223)	0.4789(3)	0.6057(3)	0.8921(3)	0.042(1)
C(224)	0.5202(3)	0.6296(3)	0.9936(3)	0.047(1)
C(225)	0.6169(3)	0.6690(5)	1.0260(4)	0.064(1)
C(226)	0.6720(3)	0.6815(4)	0.9551(3)	0.056(1)
C(231)	0.8063(2)	0.5882(3)	0.7399(3)	0.028(1)
C(232)	0.8676(3)	0.6002(4)	0.8278(3)	0.055(1)
C(233)	0.9432(3)	0.5374(5)	0.8120(4)	0.062(1)
C(234)	0.9610(3)	0.4652(4)	0.7096(4)	0.051(1)
C(235)	0.9026(3)	0.4540(3)	0.6209(4)	0.050(1)
C(236)	0.8252(2)	0.5146(3)	0.6360(3)	0.036(1)
O(4)	0.1634(3)	0.8472(3)	0.4209(3)	0.076(1)
N(1)	0.2631(3)	0.7863(3)	0.5076(3)	0.053(1)
N(2)	0.2525(2)	0.7080(3)	0.3223(3)	0.046(1)
C(11)	0.2226(3)	0.7846(3)	0.4167(4)	0.049(1)
C(12)	0.2516(4)	0.8729(5)	0.6155(5)	0.079(2)
C(21)	0.2307(3)	0.6906(3)	0.2170(4)	0.046(1)

C(22)	0.2743(3)	0.6083(4)	0.1350(4)	0.054(1)
C(23)	0.2564(3)	0.5843(5)	0.0283(4)	0.064(1)
C(24)	0.1945(4)	0.6423(5)	0.0012(5)	0.076(2)
C(25)	0.1522(4)	0.7249(5)	0.0817(6)	0.078(2)
C(26)	0.1692(3)	0.7504(4)	0.1898(5)	0.061(1)
C(1)	0.7629(4)	0.3551(4)	0.3067(4)	0.064(1)
Cl(1)	0.7686(1)	0.4875(1)	0.3245(2)	0.111(1)
Cl(2)	0.6881(1)	0.2630(1)	0.1869(1)	0.064(1)
Cl(3)	0.8788(1)	0.3128(2)	0.2990(2)	0.109(1)
C(2)	0.9105(5)	0.7888(7)	0.2223(5)	0.104(2)
Cl(4)	0.8109(2)	0.8132(3)	0.2945(2)	0.184(1)
Cl(5)	0.9147(2)	0.8687(2)	0.1606(2)	0.145(1)
Cl(6)	0.9002(1)	0.6497(1)	0.1220(2)	0.093(1)

Table A.VI.4: Final Positional (fractional co-ordinates) and Equivalent Thermal Parameters of Calculated Hydrogen Atoms for $4.23 \cdot 2\text{CHCl}_3$, with *e.s.d.s* in parentheses

Atom	X/A	Y/B	Z/C	U(eq)
H(112)	0.4923	0.8140	0.7231	0.043
H(113)	0.4314	0.9539	0.8703	0.054
H(114)	0.5099	1.1314	0.9605	0.053
H(115)	0.6526	1.1697	0.9083	0.048
H(116)	0.7160	1.0316	0.7626	0.040
H(122)	0.4902	0.9074	0.5736	0.044
H(123)	0.4135	0.9050	0.4196	0.058
H(124)	0.4575	0.7932	0.2494	0.069
H(125)	0.5757	0.6790	0.2294	0.068
H(126)	0.6560	0.6838	0.3819	0.051
H(132)	0.7599	0.9720	0.5985	0.041
H(133)	0.9162	1.0005	0.5672	0.052
H(134)	1.0212	0.8696	0.5367	0.056
H(135)	0.9690	0.7099	0.5361	0.055
H(136)	0.8143	0.6818	0.5715	0.040
H(212)	0.8886	0.7861	0.7763	0.056
H(213)	0.9613	0.9678	0.8835	0.083
H(214)	0.8856	1.0961	1.0222	0.092
H(215)	0.7375	1.0469	1.0521	0.085
H(216)	0.6592	0.8708	0.9407	0.058
H(222)	0.5042	0.6025	0.7523	0.041
H(223)	0.4128	0.5806	0.8705	0.050
H(224)	0.4830	0.6192	1.0406	0.056
H(225)	0.6455	0.6872	1.0960	0.077
H(226)	0.7375	0.7093	0.9779	0.068
H(232)	0.8578	0.6517	0.8991	0.065
H(233)	0.9825	0.5447	0.8726	0.075
H(234)	1.0127	0.4232	0.6994	0.061
H(235)	0.9152	0.4052	0.5500	0.060
H(236)	0.7853	0.5057	0.5750	0.043
H(1)	0.2969	0.7341	0.5008	0.064
H(2)	0.2902	0.6642	0.3287	0.055
H(12A)	0.2847	0.8592	0.6696	0.118
H(12B)	0.1837	0.8745	0.6234	0.118

H(12C)	0.2787	0.9430	0.6259	0.118
H(22)	0.3166	0.5687	0.1529	0.065
H(23)	0.2861	0.5286	-0.0260	0.077
H(24)	0.1813	0.6256	-0.0716	0.091
H(25)	0.1110	0.7648	0.0629	0.093
H(26)	0.1398	0.8068	0.2438	0.073
H(1A)	0.7371	0.3555	0.3686	0.078
H(2A)	0.9689	0.8077	0.2723	0.129

Table A.VI.5: Thermal Parameters for 4.23·2CHCl₃, with e.s.d.s in parentheses

Atom	U11	U22	U33	U23	U13	U12
Pt(1)	0.0195(1)	0.0185(1)	0.0178(1)	0.0082(1)	0.0009(1)	0.0020(1)
S(1)	0.0233(3)	0.0190(3)	0.0211(3)	0.0090(3)	0.0003(3)	0.0029(3)
P(1)	0.0231(4)	0.0207(3)	0.0235(4)	0.0108(3)	0.0024(3)	0.0026(3)
P(2)	0.0218(4)	0.0242(4)	0.0203(4)	0.0100(3)	0.0000(3)	0.0026(3)
O(1)	0.0230(10)	0.0244(10)	0.0198(10)	0.0098(8)	-0.0014(8)	-0.0001(8)
O(2)	0.0307(12)	0.0269(11)	0.0309(12)	0.0172(10)	-0.0039(9)	0.0030(9)
O(3)	0.0337(12)	0.0254(11)	0.0273(11)	0.0092(9)	0.0070(9)	0.0064(9)
C(111)	0.0302(16)	0.0226(14)	0.0267(15)	0.0113(12)	0.0034(12)	0.0057(12)
C(112)	0.0329(18)	0.0285(16)	0.0376(19)	0.0094(14)	0.0078(15)	-0.0001(13)
C(113)	0.042(2)	0.041(2)	0.042(2)	0.0104(17)	0.0182(17)	0.0057(16)
C(114)	0.051(2)	0.0353(19)	0.037(2)	0.0083(16)	0.0138(17)	0.0147(17)
C(115)	0.049(2)	0.0242(16)	0.0372(19)	0.0078(14)	0.0007(16)	0.0039(15)
C(116)	0.0360(18)	0.0264(16)	0.0328(17)	0.0118(14)	0.0018(14)	0.0015(13)
C(121)	0.0302(16)	0.0277(15)	0.0304(16)	0.0179(13)	-0.0008(13)	-0.0029(12)
C(122)	0.0380(19)	0.0291(17)	0.043(2)	0.0190(15)	-0.0052(15)	0.0019(14)
C(123)	0.045(2)	0.040(2)	0.065(3)	0.035(2)	-0.019(2)	-0.0050(17)
C(124)	0.066(3)	0.067(3)	0.051(3)	0.045(2)	-0.019(2)	-0.014(2)
C(125)	0.062(3)	0.080(3)	0.037(2)	0.037(2)	0.004(2)	0.001(2)
C(126)	0.043(2)	0.055(2)	0.0322(18)	0.0248(18)	0.0063(16)	0.0060(18)
C(131)	0.0254(15)	0.0276(15)	0.0260(15)	0.0129(13)	0.0033(12)	0.0030(12)
C(132)	0.0318(17)	0.0301(16)	0.0434(19)	0.0197(15)	0.0096(15)	0.0050(13)
C(133)	0.038(2)	0.042(2)	0.052(2)	0.0249(18)	0.0117(17)	-0.0020(16)
C(134)	0.0277(18)	0.058(2)	0.057(2)	0.030(2)	0.0145(17)	0.0053(17)
C(135)	0.0325(19)	0.053(2)	0.058(2)	0.029(2)	0.0156(17)	0.0190(17)
C(136)	0.0334(17)	0.0323(17)	0.0363(18)	0.0173(15)	0.0075(14)	0.0064(14)
C(211)	0.0364(18)	0.0283(16)	0.0272(16)	0.0130(13)	-0.0105(14)	-0.0037(13)
C(212)	0.049(2)	0.049(2)	0.042(2)	0.0271(18)	-0.0104(18)	-0.0165(18)
C(213)	0.069(3)	0.068(3)	0.070(3)	0.045(3)	-0.032(3)	-0.039(3)
C(214)	0.104(5)	0.032(2)	0.069(3)	0.017(2)	-0.042(3)	-0.017(3)
C(215)	0.091(4)	0.030(2)	0.055(3)	0.0001(19)	-0.028(3)	0.011(2)
C(216)	0.053(2)	0.0341(19)	0.039(2)	0.0061(16)	-0.0069(18)	0.0120(17)
C(221)	0.0300(16)	0.0326(16)	0.0234(15)	0.0138(13)	0.0061(12)	0.0055(13)
C(222)	0.0341(18)	0.0386(18)	0.0237(16)	0.0122(14)	0.0023(13)	0.0012(14)
C(223)	0.0352(19)	0.049(2)	0.039(2)	0.0201(17)	0.0088(16)	-0.0015(16)
C(224)	0.056(2)	0.056(2)	0.040(2)	0.0290(19)	0.0213(19)	0.0132(19)
C(225)	0.051(3)	0.119(4)	0.040(2)	0.053(3)	0.009(2)	0.014(3)
C(226)	0.032(2)	0.107(4)	0.037(2)	0.042(2)	-0.0001(17)	0.003(2)
C(231)	0.0230(15)	0.0323(16)	0.0330(17)	0.0185(14)	0.0026(13)	0.0053(12)
C(232)	0.047(2)	0.080(3)	0.039(2)	0.029(2)	0.0036(18)	0.030(2)
C(233)	0.044(2)	0.098(4)	0.060(3)	0.050(3)	0.002(2)	0.029(2)

C(234)	0.034(2)	0.057(3)	0.074(3)	0.039(2)	0.011(2)	0.0213(18)
C(235)	0.039(2)	0.048(2)	0.054(2)	0.017(2)	0.0121(18)	0.0190(18)
C(236)	0.0279(17)	0.0356(18)	0.0376(19)	0.0138(15)	0.0026(14)	0.0085(14)
O(4)	0.082(2)	0.085(2)	0.103(3)	0.067(2)	0.043(2)	0.059(2)
N(1)	0.052(2)	0.0466(19)	0.069(2)	0.0324(19)	0.0168(18)	0.0225(16)
N(2)	0.0387(17)	0.0450(18)	0.068(2)	0.0374(18)	0.0107(16)	0.0167(14)
C(11)	0.044(2)	0.045(2)	0.078(3)	0.041(2)	0.021(2)	0.0180(18)
C(12)	0.090(4)	0.080(4)	0.079(4)	0.043(3)	0.033(3)	0.041(3)
C(21)	0.0272(18)	0.048(2)	0.077(3)	0.043(2)	0.0021(18)	-0.0024(16)
C(22)	0.043(2)	0.056(3)	0.072(3)	0.041(2)	0.007(2)	-0.0017(19)
C(23)	0.049(3)	0.075(3)	0.071(3)	0.042(3)	0.002(2)	-0.016(2)
C(24)	0.062(3)	0.098(4)	0.080(4)	0.061(4)	-0.013(3)	-0.025(3)
C(25)	0.054(3)	0.095(4)	0.113(5)	0.078(4)	-0.014(3)	-0.005(3)
C(26)	0.043(2)	0.067(3)	0.094(4)	0.058(3)	-0.003(2)	0.002(2)
C(1)	0.056(3)	0.070(3)	0.043(2)	0.011(2)	0.015(2)	-0.008(2)
Cl(1)	0.1034(12)	0.0465(7)	0.1218(14)	-0.0056(8)	0.0374(11)	-0.0064(7)
Cl(2)	0.0668(7)	0.0472(6)	0.0564(7)	0.0114(5)	0.0009(6)	0.0029(5)
Cl(3)	0.0583(9)	0.1658(19)	0.1281(16)	0.0939(15)	0.0020(9)	0.0063(10)
C(2)	0.073(4)	0.140(6)	0.066(4)	0.034(4)	-0.013(3)	-0.026(4)
Cl(4)	0.178(3)	0.269(4)	0.0756(13)	0.0594(19)	0.0392(16)	0.027(3)
Cl(5)	0.164(2)	0.0868(13)	0.177(2)	0.0657(15)	0.0159(18)	-0.0237(14)
Cl(6)	0.0955(11)	0.0822(10)	0.1000(12)	0.0524(9)	-0.0233(9)	-0.0120(8)

Appendix VII

Complete Bond Lengths, Bond Angles, and Thermal and Positional Parameters for $[\text{Pt}\{\text{SC}(\text{S})\text{NMeC}(\text{O})\text{NPh}\}(\text{PPh}_3)_2]\cdot\text{CHCl}_3$ 4.28

Table A.VII.1: Complete Bond Lengths (Å) for 4.28·CHCl₃, with e.s.d.s in parentheses

Pt(1)-N(2)	2.066(3)	C(122)-C(123)	1.400(6)
Pt(1)-P(2)	2.2686(10)	C(123)-C(124)	1.371(8)
Pt(1)-P(1)	2.2921(10)	C(124)-C(125)	1.378(8)
Pt(1)-S(2)	2.3358(10)	C(125)-C(126)	1.388(6)
P(1)-C(131)	1.819(4)	C(131)-C(132)	1.382(6)
P(1)-C(111)	1.823(4)	C(131)-C(136)	1.388(6)
P(1)-C(121)	1.825(4)	C(132)-C(133)	1.400(7)
P(2)-C(211)	1.819(4)	C(133)-C(134)	1.371(9)
P(2)-C(231)	1.827(4)	C(134)-C(135)	1.371(8)
P(2)-C(221)	1.833(4)	C(135)-C(136)	1.392(7)
S(1)-C(1)	1.672(5)	C(211)-C(216)	1.387(6)
S(2)-C(1)	1.736(5)	C(211)-C(212)	1.388(6)
O(1)-C(2)	1.232(6)	C(212)-C(213)	1.381(6)
N(1)-C(1)	1.360(6)	C(213)-C(214)	1.375(7)
N(1)-C(2)	1.454(6)	C(214)-C(215)	1.367(7)
N(1)-C(3)	1.470(6)	C(215)-C(216)	1.393(7)
N(2)-C(2)	1.323(6)	C(221)-C(226)	1.389(6)
N(2)-C(11)	1.441(6)	C(221)-C(222)	1.396(6)
C(11)-C(16)	1.382(7)	C(222)-C(223)	1.386(7)
C(11)-C(12)	1.389(7)	C(223)-C(224)	1.384(8)
C(12)-C(13)	1.382(8)	C(224)-C(225)	1.372(8)
C(13)-C(14)	1.369(10)	C(225)-C(226)	1.390(7)
C(14)-C(15)	1.394(10)	C(231)-C(236)	1.379(7)
C(15)-C(16)	1.395(8)	C(231)-C(232)	1.398(7)
C(111)-C(112)	1.381(6)	C(232)-C(233)	1.383(7)
C(111)-C(116)	1.406(6)	C(233)-C(234)	1.368(9)
C(112)-C(113)	1.393(6)	C(234)-C(235)	1.374(10)
C(113)-C(114)	1.381(7)	C(235)-C(236)	1.398(8)
C(114)-C(115)	1.380(7)		
C(115)-C(116)	1.381(7)	C(4)-Cl(1)	1.758(8)
C(121)-C(122)	1.385(6)	C(4)-Cl(2)	1.715(7)
C(121)-C(126)	1.396(6)	C(4)-Cl(3)	1.733(7)

Table A.VII.2: Complete Bond Angles (°) for 4.28·CHCl₃, with e.s.d.s in parentheses

N(2)-Pt(1)-P(2)	166.07(10)	C(115)-C(116)-C(111)	119.8(4)
N(2)-Pt(1)-P(1)	94.20(10)	C(122)-C(121)-C(126)	120.2(4)
P(2)-Pt(1)-P(1)	97.21(4)	C(122)-C(121)-P(1)	123.3(3)
N(2)-Pt(1)-S(2)	83.53(10)	C(126)-C(121)-P(1)	116.4(3)
P(2)-Pt(1)-S(2)	86.17(4)	C(121)-C(122)-C(123)	119.4(4)
P(1)-Pt(1)-S(2)	172.13(4)	C(124)-C(123)-C(122)	120.1(5)
C(131)-P(1)-C(111)	109.2(2)	C(123)-C(124)-C(125)	120.8(4)

C(131)-P(1)-C(121)	105.51(19)	C(124)-C(125)-C(126)	119.9(5)
C(111)-P(1)-C(121)	98.47(18)	C(125)-C(126)-C(121)	119.6(4)
C(131)-P(1)-Pt(1)	114.33(14)	C(132)-C(131)-C(136)	119.0(4)
C(111)-P(1)-Pt(1)	113.64(14)	C(132)-C(131)-P(1)	124.5(4)
C(121)-P(1)-Pt(1)	114.33(13)	C(136)-C(131)-P(1)	116.5(3)
C(211)-P(2)-C(231)	108.1(2)	C(131)-C(132)-C(133)	120.1(5)
C(211)-P(2)-C(221)	102.2(2)	C(134)-C(133)-C(132)	120.1(5)
C(231)-P(2)-C(221)	102.31(19)	C(133)-C(134)-C(135)	120.4(5)
C(211)-P(2)-Pt(1)	116.43(14)	C(134)-C(135)-C(136)	119.9(5)
C(231)-P(2)-Pt(1)	104.73(14)	C(131)-C(136)-C(135)	120.6(5)
C(221)-P(2)-Pt(1)	121.70(14)	C(216)-C(211)-C(212)	118.7(4)
C(1)-S(2)-Pt(1)	101.15(16)	C(216)-C(211)-P(2)	120.3(3)
C(1)-N(1)-C(2)	122.0(4)	C(212)-C(211)-P(2)	121.0(3)
C(1)-N(1)-C(3)	118.9(4)	C(213)-C(212)-C(211)	120.2(4)
C(2)-N(1)-C(3)	113.0(4)	C(214)-C(213)-C(212)	120.2(5)
C(2)-N(2)-C(11)	116.6(4)	C(215)-C(214)-C(213)	120.7(5)
C(2)-N(2)-Pt(1)	126.5(3)	C(214)-C(215)-C(216)	119.3(5)
C(11)-N(2)-Pt(1)	115.5(3)	C(211)-C(216)-C(215)	120.8(5)
O(1)-C(2)-N(2)	126.6(5)	C(226)-C(221)-C(222)	118.8(4)
O(1)-C(2)-N(1)	116.8(4)	C(226)-C(221)-P(2)	120.6(3)
N(2)-C(2)-N(1)	116.6(4)	C(222)-C(221)-P(2)	120.6(3)
N(1)-C(1)-S(1)	122.0(3)	C(223)-C(222)-C(221)	120.0(4)
N(1)-C(1)-S(2)	121.7(3)	C(224)-C(223)-C(222)	120.8(5)
S(1)-C(1)-S(2)	116.3(3)	C(225)-C(224)-C(223)	119.4(5)
C(16)-C(11)-C(12)	119.3(5)	C(224)-C(225)-C(226)	120.5(5)
C(16)-C(11)-N(2)	119.0(4)	C(221)-C(226)-C(225)	120.5(5)
C(12)-C(11)-N(2)	121.7(4)	C(236)-C(231)-C(232)	118.9(4)
C(13)-C(12)-C(11)	120.0(6)	C(236)-C(231)-P(2)	123.7(4)
C(14)-C(13)-C(12)	121.1(6)	C(232)-C(231)-P(2)	117.4(3)
C(13)-C(14)-C(15)	119.6(6)	C(233)-C(232)-C(231)	120.8(5)
C(14)-C(15)-C(16)	119.4(6)	C(234)-C(233)-C(232)	119.5(5)
C(11)-C(16)-C(15)	120.6(5)	C(233)-C(234)-C(235)	120.6(5)
C(112)-C(111)-C(116)	118.9(4)	C(234)-C(235)-C(236)	120.3(6)
C(112)-C(111)-P(1)	118.6(3)	C(231)-C(236)-C(235)	119.7(6)
C(116)-C(111)-P(1)	122.0(3)		
C(111)-C(112)-C(113)	120.8(4)	Cl(2)-C(4)-Cl(1)	107.8(4)
C(114)-C(113)-C(112)	119.7(4)	Cl(3)-C(4)-Cl(1)	110.8(4)
C(115)-C(114)-C(113)	120.0(4)	Cl(2)-C(4)-Cl(3)	108.3(4)
C(114)-C(115)-C(116)	120.6(5)		

Table A.VII.3: Final Positional (fractional co-ordinates) and Equivalent Thermal Parameters for 4.28·CHCl₃, with e.s.d.s in parentheses

Atom	X/A	Y/B	Z/C	U(eq)
Pt(1)	0.3395(1)	0.1011(1)	0.8205(1)	0.025(1)
P(1)	0.1718(1)	0.1215(1)	0.8494(1)	0.026(1)
P(2)	0.2993(1)	0.0100(1)	0.7402(1)	0.027(1)
S(1)	0.6695(1)	0.0034(1)	0.9002(1)	0.078(1)
S(2)	0.5151(1)	0.0731(1)	0.8055(1)	0.033(1)
O(1)	0.5184(3)	0.2410(2)	0.9604(2)	0.067(1)
N(1)	0.5273(3)	0.1076(2)	0.9353(2)	0.042(1)
N(2)	0.4031(3)	0.1928(2)	0.8787(2)	0.033(1)
C(3)	0.5712(5)	0.0946(4)	1.0031(3)	0.064(2)
C(2)	0.4812(4)	0.1867(3)	0.9250(2)	0.043(1)

C(1)	0.5681(4)	0.0661(3)	0.8861(2)	0.039(1)
C(11)	0.3745(3)	0.2725(3)	0.8572(2)	0.038(1)
C(12)	0.3346(4)	0.3281(3)	0.8992(3)	0.047(1)
C(13)	0.3052(4)	0.4032(3)	0.8762(4)	0.063(2)
C(14)	0.3149(5)	0.4243(4)	0.8123(4)	0.070(2)
C(15)	0.3569(4)	0.3698(4)	0.7699(3)	0.060(2)
C(16)	0.3873(4)	0.2941(3)	0.7932(3)	0.047(1)
C(111)	0.1114(3)	0.0322(2)	0.8811(2)	0.030(1)
C(112)	0.1741(3)	-0.0335(3)	0.8966(2)	0.033(1)
C(113)	0.1342(4)	-0.1002(3)	0.9271(2)	0.041(1)
C(114)	0.0300(4)	-0.1014(3)	0.9406(3)	0.045(1)
C(115)	-0.0331(4)	-0.0357(3)	0.9261(3)	0.048(1)
C(116)	0.0068(3)	0.0318(3)	0.8981(2)	0.038(1)
C(121)	0.1631(3)	0.1864(2)	0.9206(2)	0.029(1)
C(122)	0.0984(4)	0.2529(3)	0.9205(2)	0.038(1)
C(123)	0.0919(4)	0.2962(3)	0.9786(3)	0.047(1)
C(124)	0.1489(4)	0.2727(3)	1.0349(3)	0.051(1)
C(125)	0.2135(4)	0.2066(3)	1.0353(2)	0.045(1)
C(126)	0.2213(3)	0.1629(3)	0.9782(2)	0.037(1)
C(131)	0.0831(3)	0.1650(3)	0.7850(2)	0.032(1)
C(132)	-0.0148(4)	0.1346(3)	0.7647(3)	0.046(1)
C(133)	-0.0772(4)	0.1725(4)	0.7145(3)	0.063(2)
C(134)	-0.0408(5)	0.2393(4)	0.6847(3)	0.063(2)
C(135)	0.0573(5)	0.2689(3)	0.7032(3)	0.053(1)
C(136)	0.1193(4)	0.2321(3)	0.7536(2)	0.040(1)
C(211)	0.3346(3)	-0.0934(2)	0.7591(2)	0.033(1)
C(212)	0.3906(4)	-0.1133(3)	0.8178(2)	0.036(1)
C(213)	0.4120(4)	-0.1925(3)	0.8330(2)	0.046(1)
C(214)	0.3811(4)	-0.2519(3)	0.7891(3)	0.048(1)
C(215)	0.3276(4)	-0.2337(3)	0.7304(3)	0.051(1)
C(216)	0.3035(4)	-0.1541(3)	0.7156(2)	0.045(1)
C(221)	0.1656(3)	-0.0001(2)	0.7012(2)	0.031(1)
C(222)	0.0937(4)	-0.0518(3)	0.7272(2)	0.039(1)
C(223)	-0.0060(4)	-0.0608(3)	0.6961(3)	0.050(1)
C(224)	-0.0358(4)	-0.0189(4)	0.6392(3)	0.062(2)
C(225)	0.0341(4)	0.0328(4)	0.6140(3)	0.065(2)
C(226)	0.1347(4)	0.0421(3)	0.6444(3)	0.048(1)
C(231)	0.3729(3)	0.0425(3)	0.6720(2)	0.034(1)
C(232)	0.3652(4)	0.1230(3)	0.6537(2)	0.043(1)
C(233)	0.4129(4)	0.1511(4)	0.5999(2)	0.052(1)
C(234)	0.4710(5)	0.0998(5)	0.5652(3)	0.071(2)
C(235)	0.4832(5)	0.0212(5)	0.5839(3)	0.078(2)
C(236)	0.4337(4)	-0.0081(4)	0.6375(2)	0.054(1)
C(4)	0.2685(5)	0.6732(4)	0.0169(3)	0.073(2)
Cl(1)	0.1957(2)	0.7466(2)	0.0549(1)	0.115(1)
Cl(2)	0.2146(4)	0.5817(2)	0.0322(2)	0.208(2)
Cl(3)	0.2613(2)	0.6875(2)	-0.0673(1)	0.126(1)

Table A.VII.4: Final Positional (fractional co-ordinates) and Equivalent Thermal Parameters of Calculated Hydrogen Atoms for 4.28·CHCl₃, with e.s.d.s in parentheses

Atom	X/A	Y/B	Z/C	U(eq)
H(3A)	0.5343	0.1281	1.0325	0.097
H(3B)	0.6452	0.1084	1.0069	0.097
H(3C)	0.5629	0.0388	1.0148	0.097
H(12)	0.3276	0.3146	0.9432	0.056
H(13)	0.2781	0.4404	0.9049	0.075
H(14)	0.2933	0.4753	0.7971	0.084
H(15)	0.3647	0.3839	0.7261	0.072
H(16)	0.4168	0.2575	0.7650	0.056
H(112)	0.2446	-0.0333	0.8863	0.040
H(113)	0.1780	-0.1441	0.9384	0.050
H(114)	0.0021	-0.1470	0.9598	0.055
H(115)	-0.1041	-0.0370	0.9353	0.057
H(116)	-0.0357	0.0773	0.8905	0.045
H(122)	0.0593	0.2688	0.8818	0.046
H(123)	0.0483	0.3415	0.9790	0.056
H(124)	0.1439	0.3020	1.0738	0.062
H(125)	0.2524	0.1910	1.0743	0.054
H(126)	0.2654	0.1179	0.9782	0.044
H(132)	-0.0395	0.0884	0.7847	0.056
H(133)	-0.1441	0.1520	0.7011	0.075
H(134)	-0.0834	0.2651	0.6514	0.075
H(135)	0.0826	0.3139	0.6819	0.063
H(136)	0.1862	0.2528	0.7666	0.048
H(212)	0.4141	-0.0728	0.8474	0.044
H(213)	0.4477	-0.2059	0.8735	0.055
H(214)	0.3970	-0.3056	0.7995	0.058
H(215)	0.3073	-0.2745	0.7004	0.061
H(216)	0.2657	-0.1413	0.6756	0.054
H(222)	0.1130	-0.0805	0.7658	0.046
H(223)	-0.0541	-0.0957	0.7138	0.060
H(224)	-0.1033	-0.0258	0.6181	0.074
H(225)	0.0138	0.0622	0.5759	0.078
H(226)	0.1821	0.0772	0.6264	0.057
H(232)	0.3271	0.1585	0.6784	0.051
H(233)	0.4055	0.2050	0.5873	0.062
H(234)	0.5029	0.1186	0.5283	0.086
H(235)	0.5251	-0.0131	0.5605	0.093
H(236)	0.4419	-0.0620	0.6500	0.064
H(4)	0.3428	0.6747	0.0350	0.087

Table A.VII.5: Thermal Parameters for 4.28·CHCl₃, with e.s.d.s in parentheses

Atom	U11	U22	U33	U23	U13	U12
Pt(1)	0.0215(1)	0.0272(1)	0.0253(1)	-0.0020(1)	-0.0011(1)	0.0008(1)
P(1)	0.0234(5)	0.0272(5)	0.0279(5)	-0.0008(4)	-0.0006(4)	0.0012(4)
P(2)	0.0275(5)	0.0278(5)	0.0246(5)	-0.0004(4)	-0.0015(4)	0.0010(4)
S(1)	0.0642(10)	0.0902(12)	0.0746(11)	-0.0151(9)	-0.0263(8)	0.0449(9)

S(2)	0.0248(5)	0.0398(6)	0.0349(5)	-0.0039(4)	0.0012(4)	0.0029(4)
O(1)	0.054(2)	0.062(2)	0.079(3)	-0.037(2)	-0.027(2)	0.0054(19)
N(1)	0.041(2)	0.049(2)	0.034(2)	-0.0052(17)	-0.0091(16)	0.0036(18)
N(2)	0.0268(17)	0.0345(18)	0.0382(19)	-0.0099(15)	-0.0003(14)	-0.0024(14)
C(3)	0.068(4)	0.079(4)	0.042(3)	-0.006(3)	-0.021(3)	0.009(3)
C(2)	0.035(2)	0.050(3)	0.042(3)	-0.012(2)	-0.0012(19)	0.002(2)
C(1)	0.033(2)	0.042(2)	0.040(2)	0.0007(19)	-0.0074(18)	0.0018(19)
C(11)	0.026(2)	0.031(2)	0.055(3)	-0.0033(19)	0.0014(19)	-0.0049(17)
C(12)	0.030(2)	0.039(3)	0.072(3)	-0.013(2)	0.009(2)	-0.0052(19)
C(13)	0.040(3)	0.037(3)	0.112(6)	-0.012(3)	0.012(3)	0.001(2)
C(14)	0.046(3)	0.037(3)	0.126(6)	0.013(3)	0.000(4)	-0.001(2)
C(15)	0.046(3)	0.051(3)	0.083(4)	0.015(3)	-0.002(3)	-0.009(3)
C(16)	0.036(2)	0.044(3)	0.060(3)	0.003(2)	0.000(2)	-0.003(2)
C(111)	0.029(2)	0.033(2)	0.029(2)	-0.0025(16)	0.0003(15)	-0.0021(16)
C(112)	0.030(2)	0.036(2)	0.032(2)	0.0005(17)	-0.0015(16)	0.0003(17)
C(113)	0.049(3)	0.035(2)	0.039(2)	0.0031(19)	-0.004(2)	0.001(2)
C(114)	0.049(3)	0.042(3)	0.046(3)	0.004(2)	0.005(2)	-0.015(2)
C(115)	0.037(3)	0.051(3)	0.055(3)	0.003(2)	0.008(2)	-0.011(2)
C(116)	0.031(2)	0.039(2)	0.043(2)	0.0035(19)	0.0041(18)	0.0002(18)
C(121)	0.0282(19)	0.030(2)	0.031(2)	-0.0054(16)	0.0036(15)	-0.0020(16)
C(122)	0.037(2)	0.034(2)	0.045(3)	-0.0036(19)	0.0062(19)	0.0035(18)
C(123)	0.048(3)	0.035(2)	0.059(3)	-0.014(2)	0.013(2)	0.001(2)
C(124)	0.065(3)	0.050(3)	0.040(3)	-0.021(2)	0.015(2)	-0.015(3)
C(125)	0.056(3)	0.047(3)	0.031(2)	-0.006(2)	0.000(2)	-0.012(2)
C(126)	0.034(2)	0.038(2)	0.038(2)	-0.0016(18)	0.0017(18)	-0.0042(18)
C(131)	0.030(2)	0.033(2)	0.033(2)	0.0001(17)	0.0008(16)	0.0065(17)
C(132)	0.036(2)	0.049(3)	0.052(3)	0.008(2)	-0.010(2)	0.000(2)
C(133)	0.043(3)	0.072(4)	0.069(4)	0.013(3)	-0.023(3)	0.002(3)
C(134)	0.071(4)	0.061(4)	0.052(3)	0.009(3)	-0.023(3)	0.016(3)
C(135)	0.070(4)	0.045(3)	0.042(3)	0.007(2)	-0.004(2)	0.008(3)
C(136)	0.044(3)	0.038(2)	0.036(2)	0.0009(19)	-0.0013(19)	0.000(2)
C(211)	0.036(2)	0.027(2)	0.034(2)	-0.0008(16)	-0.0016(17)	0.0062(17)
C(212)	0.041(2)	0.034(2)	0.034(2)	-0.0025(17)	0.0016(18)	0.0099(18)
C(213)	0.055(3)	0.043(3)	0.040(3)	0.006(2)	0.000(2)	0.015(2)
C(214)	0.054(3)	0.034(2)	0.057(3)	0.003(2)	0.008(2)	0.010(2)
C(215)	0.061(3)	0.034(2)	0.057(3)	-0.010(2)	-0.005(3)	0.004(2)
C(216)	0.051(3)	0.037(2)	0.045(3)	-0.007(2)	-0.010(2)	0.007(2)
C(221)	0.032(2)	0.029(2)	0.031(2)	-0.0025(16)	-0.0048(16)	-0.0024(16)
C(222)	0.042(2)	0.036(2)	0.038(2)	0.0040(18)	-0.0021(19)	-0.0070(19)
C(223)	0.039(3)	0.052(3)	0.058(3)	0.008(2)	-0.003(2)	-0.018(2)
C(224)	0.039(3)	0.075(4)	0.068(4)	0.015(3)	-0.018(3)	-0.018(3)
C(225)	0.046(3)	0.084(4)	0.061(4)	0.034(3)	-0.023(3)	-0.012(3)
C(226)	0.040(3)	0.050(3)	0.051(3)	0.021(2)	-0.008(2)	-0.011(2)
C(231)	0.030(2)	0.048(3)	0.0239(19)	-0.0002(17)	-0.0018(16)	-0.0027(18)
C(232)	0.041(3)	0.050(3)	0.036(2)	0.002(2)	-0.0022(19)	-0.012(2)
C(233)	0.036(3)	0.073(4)	0.045(3)	0.017(3)	-0.008(2)	-0.019(2)
C(234)	0.040(3)	0.127(6)	0.048(3)	0.036(4)	0.011(2)	0.004(3)
C(235)	0.060(4)	0.127(6)	0.050(3)	0.024(4)	0.026(3)	0.047(4)
C(236)	0.048(3)	0.076(4)	0.037(3)	0.008(2)	0.006(2)	0.024(3)
C(4)	0.057(4)	0.081(5)	0.076(4)	0.014(4)	-0.013(3)	-0.007(3)
Cl(1)	0.1103(17)	0.157(2)	0.0790(13)	0.0393(14)	0.0210(12)	0.0604(16)
Cl(2)	0.275(5)	0.139(3)	0.190(4)	0.083(3)	-0.098(4)	-0.087(3)
Cl(3)	0.147(2)	0.150(2)	0.0765(14)	0.0036(14)	-0.0160(14)	0.0384(19)

Appendix VIII

Complete Bond Lengths, Bond Angles, and Thermal and Positional Parameters for [Pt{S₂C=NMe}(PPh₃)₂] 4.29a

Table A.VIII.1: Complete Bond Lengths (Å) for 4.29a, with e.s.d.s in parentheses

Pt(1)-P(1)	2.2804(17)	C(125)-C(126)	1.381(11)
Pt(1)-P(2)	2.2982(17)	C(131)-C(132)	1.372(9)
Pt(1)-S(2)	2.3209(17)	C(131)-C(136)	1.410(9)
Pt(1)-S(1)	2.3417(18)	C(132)-C(133)	1.378(10)
P(1)-C(131)	1.817(6)	C(133)-C(134)	1.366(11)
P(1)-C(111)	1.824(7)	C(134)-C(135)	1.380(11)
P(1)-C(121)	1.821(7)	C(135)-C(136)	1.383(9)
S(1)-C(1)	1.775(7)	C(211)-C(212)	1.383(9)
P(2)-C(221)	1.824(7)	C(211)-C(216)	1.404(10)
P(2)-C(211)	1.840(7)	C(212)-C(213)	1.384(10)
P(2)-C(231)	1.839(7)	C(213)-C(214)	1.358(12)
S(2)-C(1)	1.783(7)	C(214)-C(215)	1.370(12)
N(1)-C(1)	1.285(9)	C(215)-C(216)	1.375(10)
N(1)-C(2)	1.483(11)	C(221)-C(226)	1.400(10)
C(111)-C(112)	1.389(10)	C(221)-C(222)	1.412(9)
C(111)-C(116)	1.386(10)	C(222)-C(223)	1.373(11)
C(112)-C(113)	1.416(12)	C(223)-C(224)	1.371(12)
C(113)-C(114)	1.334(12)	C(224)-C(225)	1.403(11)
C(114)-C(115)	1.413(14)	C(225)-C(226)	1.368(11)
C(115)-C(116)	1.389(13)	C(231)-C(236)	1.372(10)
C(121)-C(122)	1.381(9)	C(231)-C(232)	1.395(10)
C(121)-C(126)	1.406(10)	C(232)-C(233)	1.379(10)
C(122)-C(123)	1.376(11)	C(233)-C(234)	1.391(12)
C(123)-C(124)	1.403(11)	C(234)-C(235)	1.393(13)
C(124)-C(125)	1.381(11)	C(235)-C(236)	1.371(11)

Table A.VIII.2: Complete Bond Angles (°) for 4.29a, with e.s.d.s in parentheses

P(1)-Pt(1)-P(2)	100.59(6)	C(122)-C(123)-C(124)	119.2(8)
P(1)-Pt(1)-S(2)	93.34(6)	C(125)-C(124)-C(123)	120.0(7)
P(2)-Pt(1)-S(2)	165.29(6)	C(124)-C(125)-C(126)	119.9(7)
P(1)-Pt(1)-S(1)	168.79(6)	C(125)-C(126)-C(121)	120.7(7)
P(2)-Pt(1)-S(1)	90.55(6)	C(132)-C(131)-C(136)	119.9(6)
S(2)-Pt(1)-S(1)	75.46(6)	C(132)-C(131)-P(1)	121.6(5)
C(131)-P(1)-C(111)	106.5(3)	C(136)-C(131)-P(1)	118.5(5)
C(131)-P(1)-C(121)	101.7(3)	C(131)-C(132)-C(133)	119.8(7)
C(111)-P(1)-C(121)	105.2(3)	C(134)-C(133)-C(132)	120.6(7)
C(131)-P(1)-Pt(1)	115.9(2)	C(133)-C(134)-C(135)	120.7(6)
C(111)-P(1)-Pt(1)	112.3(2)	C(136)-C(135)-C(134)	119.6(7)
C(121)-P(1)-Pt(1)	114.1(2)	C(135)-C(136)-C(131)	119.3(6)
C(1)-S(1)-Pt(1)	88.7(2)	C(212)-C(211)-C(216)	117.9(7)
C(221)-P(2)-C(211)	105.5(3)	C(212)-C(211)-P(2)	123.6(5)

C(221)-P(2)-C(231)	103.1(3)	C(216)-C(211)-P(2)	118.4(5)
C(211)-P(2)-C(231)	101.4(3)	C(213)-C(212)-C(211)	120.1(7)
C(221)-P(2)-Pt(1)	111.2(2)	C(214)-C(213)-C(212)	121.4(7)
C(211)-P(2)-Pt(1)	110.8(2)	C(213)-C(214)-C(215)	119.5(8)
C(231)-P(2)-Pt(1)	123.2(2)	C(216)-C(215)-C(214)	120.3(8)
C(1)-S(2)-Pt(1)	89.2(2)	C(215)-C(216)-C(211)	120.8(7)
C(1)-N(1)-C(2)	116.9(7)	C(226)-C(221)-C(222)	118.0(6)
N(1)-C(1)-S(1)	129.0(6)	C(226)-C(221)-P(2)	123.5(5)
N(1)-C(1)-S(2)	124.4(6)	C(222)-C(221)-P(2)	118.4(5)
S(1)-C(1)-S(2)	106.6(4)	C(223)-C(222)-C(221)	120.9(7)
C(112)-C(111)-C(116)	118.4(7)	C(224)-C(223)-C(222)	120.0(8)
C(112)-C(111)-P(1)	123.9(5)	C(223)-C(224)-C(225)	120.2(7)
C(116)-C(111)-P(1)	117.4(6)	C(226)-C(225)-C(224)	120.0(8)
C(111)-C(112)-C(113)	119.6(7)	C(225)-C(226)-C(221)	120.8(7)
C(114)-C(113)-C(112)	121.6(8)	C(236)-C(231)-C(232)	119.7(6)
C(113)-C(114)-C(115)	119.9(8)	C(236)-C(231)-P(2)	120.3(6)
C(116)-C(115)-C(114)	118.8(8)	C(232)-C(231)-P(2)	119.9(5)
C(115)-C(116)-C(111)	121.7(8)	C(231)-C(232)-C(233)	120.6(7)
C(122)-C(121)-C(126)	118.3(6)	C(234)-C(233)-C(232)	118.9(8)
C(122)-C(121)-P(1)	119.7(5)	C(233)-C(234)-C(235)	120.4(7)
C(126)-C(121)-P(1)	122.0(5)	C(236)-C(235)-C(234)	119.8(8)
C(121)-C(122)-C(123)	121.7(7)	C(235)-C(236)-C(231)	120.7(8)

Table A.VIII.3: Final Positional (fractional co-ordinates) and Equivalent Thermal Parameters for **4.29a**, with *e.s.d.s* in parentheses

Atom	X/A	Y/B	Z/C	U(eq)
Pt(1)	0.6956(1)	0.7496(1)	0.7577(1)	0.019(1)
P(1)	0.8061(2)	0.8648(2)	0.8603(1)	0.019(1)
S(1)	0.5534(2)	0.6153(2)	0.6682(1)	0.031(1)
P(2)	0.8114(2)	0.8407(2)	0.6681(1)	0.021(1)
S(2)	0.5367(2)	0.6433(2)	0.8222(1)	0.028(1)
N(1)	0.3446(7)	0.4889(7)	0.7313(4)	0.037(2)
C(1)	0.4540(7)	0.5661(7)	0.7374(4)	0.025(1)
C(2)	0.2863(9)	0.4395(10)	0.6556(5)	0.050(2)
C(111)	0.8099(7)	1.0585(7)	0.8476(4)	0.023(1)
C(112)	0.9245(8)	1.1433(8)	0.8710(4)	0.030(2)
C(113)	0.9200(9)	1.2914(8)	0.8541(5)	0.036(2)
C(114)	0.8085(11)	1.3517(9)	0.8152(5)	0.049(2)
C(115)	0.6906(9)	1.2677(12)	0.7911(5)	0.049(2)
C(116)	0.6950(8)	1.1219(8)	0.8067(4)	0.034(2)
C(121)	0.7278(7)	0.8380(7)	0.9433(4)	0.023(1)
C(122)	0.7565(8)	0.7150(8)	0.9848(4)	0.034(2)
C(123)	0.6978(8)	0.6889(10)	1.0472(5)	0.042(2)
C(124)	0.6065(8)	0.7898(9)	1.0692(4)	0.041(2)
C(125)	0.5743(8)	0.9123(9)	1.0277(5)	0.037(2)
C(126)	0.6341(8)	0.9366(8)	0.9653(4)	0.032(2)
C(131)	0.9826(6)	0.8097(7)	0.8920(4)	0.022(1)
C(132)	1.0556(7)	0.8599(8)	0.9572(4)	0.027(2)
C(133)	1.1923(7)	0.8235(8)	0.9768(4)	0.032(2)
C(134)	1.2550(7)	0.7350(12)	0.9327(4)	0.035(2)
C(135)	1.1818(8)	0.6771(8)	0.8689(4)	0.034(2)
C(136)	1.0450(7)	0.7136(6)	0.8478(4)	0.023(2)
C(211)	0.8411(7)	0.7007(7)	0.6014(4)	0.025(1)

C(212)	0.8416(6)	0.7263(8)	0.5268(4)	0.027(2)
C(213)	0.8742(8)	0.6171(9)	0.4813(4)	0.036(2)
C(214)	0.9045(8)	0.4831(10)	0.5080(5)	0.039(2)
C(215)	0.9057(8)	0.4556(8)	0.5818(5)	0.036(2)
C(216)	0.8743(8)	0.5622(8)	0.6284(4)	0.033(2)
C(221)	0.7101(7)	0.9782(7)	0.6133(4)	0.024(1)
C(222)	0.5700(7)	0.9934(9)	0.6206(4)	0.034(2)
C(223)	0.4883(9)	1.0933(10)	0.5798(5)	0.048(2)
C(224)	0.5432(9)	1.1826(9)	0.5324(5)	0.043(2)
C(225)	0.6819(9)	1.1692(9)	0.5237(5)	0.042(2)
C(226)	0.7631(8)	1.0681(8)	0.5632(4)	0.032(2)
C(231)	0.9831(7)	0.9228(8)	0.6891(4)	0.025(1)
C(232)	0.9961(8)	1.0657(8)	0.7114(4)	0.031(2)
C(233)	1.1243(8)	1.1252(9)	0.7337(4)	0.038(2)
C(234)	1.2406(8)	1.0410(11)	0.7325(5)	0.043(2)
C(235)	1.2274(8)	0.8991(10)	0.7088(5)	0.046(2)
C(236)	1.0990(7)	0.8419(8)	0.6872(4)	0.033(2)

Table A.VIII.4: Final Positional (fractional co-ordinates) and Equivalent Thermal Parameters of Calculated Hydrogen Atoms for **4.29a**, with *e.s.d.s* in parentheses

Atom	X/A	Y/B	Z/C	U(eq)
H(2A)	0.2048	0.3823	0.6579	0.075
H(2B)	0.3541	0.3822	0.6356	0.075
H(2C)	0.2619	0.5219	0.6239	0.075
H(112)	1.0046	1.1027	0.8978	0.036
H(113)	0.9973	1.3486	0.8708	0.043
H(114)	0.8085	1.4499	0.8039	0.058
H(115)	0.6105	1.3096	0.7650	0.059
H(116)	0.6181	1.0649	0.7891	0.040
H(122)	0.8176	0.6473	0.9702	0.041
H(123)	0.7187	0.6044	1.0747	0.050
H(124)	0.5673	0.7741	1.1123	0.049
H(125)	0.5117	0.9790	1.0419	0.045
H(126)	0.6119	1.0202	0.9371	0.039
H(132)	1.0125	0.9190	0.9884	0.032
H(133)	1.2428	0.8598	1.0209	0.038
H(134)	1.3489	0.7133	0.9460	0.042
H(135)	1.2247	0.6132	0.8399	0.041
H(136)	0.9942	0.6747	0.8044	0.028
H(212)	0.8197	0.8179	0.5070	0.032
H(213)	0.8754	0.6361	0.4308	0.043
H(214)	0.9244	0.4098	0.4760	0.047
H(215)	0.9282	0.3635	0.6007	0.044
H(216)	0.8751	0.5420	0.6789	0.039
H(222)	0.5322	0.9342	0.6540	0.040
H(223)	0.3946	1.1006	0.5843	0.057
H(224)	0.4878	1.2530	0.5057	0.051
H(225)	0.7189	1.2298	0.4907	0.051
H(226)	0.8557	1.0588	0.5567	0.038
H(232)	0.9168	1.1220	0.7112	0.038
H(233)	1.1329	1.2211	0.7495	0.045
H(234)	1.3286	1.0801	0.7477	0.051

H(235)	1.3063	0.8427	0.7077	0.055
H(236)	1.0902	0.7464	0.6708	0.040

Table A.VIII.5: Thermal Parameters for **4.29a**, with *e.s.d.s* in parentheses

Atom	U11	U22	U33	U23	U13	U12
Pt(1)	0.0172(1)	0.0224(1)	0.0180(1)	0.0008(2)	0.0048(1)	-0.0004(2)
P(1)	0.0187(8)	0.0211(8)	0.0175(8)	0.0007(7)	0.0038(6)	0.0032(6)
S(1)	0.0297(9)	0.0409(10)	0.0239(9)	-0.0034(8)	0.0058(7)	-0.0130(8)
P(2)	0.0182(8)	0.0256(8)	0.0193(8)	0.0011(7)	0.0056(6)	-0.0014(7)
S(2)	0.0266(9)	0.0354(9)	0.0249(9)	0.0005(8)	0.0108(7)	-0.0064(8)
N(1)	0.031(3)	0.039(4)	0.042(4)	-0.002(3)	0.010(3)	-0.007(3)
C(1)	0.028(4)	0.022(3)	0.027(4)	0.003(3)	0.008(3)	0.000(3)
C(2)	0.043(5)	0.053(5)	0.056(5)	-0.012(5)	0.012(4)	-0.025(4)
C(111)	0.029(4)	0.023(3)	0.019(3)	0.002(3)	0.009(3)	0.006(3)
C(112)	0.037(4)	0.025(4)	0.030(4)	-0.004(3)	0.007(3)	0.000(3)
C(113)	0.048(5)	0.023(4)	0.039(5)	0.001(3)	0.014(4)	-0.007(3)
C(114)	0.076(7)	0.025(4)	0.051(5)	0.007(4)	0.028(5)	0.004(4)
C(115)	0.055(5)	0.041(6)	0.054(5)	0.016(5)	0.018(4)	0.031(6)
C(116)	0.033(4)	0.034(4)	0.034(4)	0.007(3)	0.005(3)	0.008(3)
C(121)	0.019(3)	0.024(3)	0.025(3)	0.000(3)	0.006(3)	0.000(3)
C(122)	0.037(4)	0.035(5)	0.032(4)	0.008(3)	0.012(3)	0.005(3)
C(123)	0.040(5)	0.053(5)	0.035(4)	0.016(4)	0.012(4)	0.005(4)
C(124)	0.042(4)	0.055(6)	0.028(4)	-0.002(3)	0.016(3)	-0.011(4)
C(125)	0.036(4)	0.038(4)	0.043(5)	-0.010(4)	0.020(4)	0.000(4)
C(126)	0.035(4)	0.031(4)	0.034(4)	-0.002(3)	0.015(3)	0.000(3)
C(131)	0.018(3)	0.023(3)	0.024(3)	0.005(3)	0.003(3)	0.004(2)
C(132)	0.026(4)	0.031(3)	0.024(3)	-0.001(3)	0.005(3)	0.005(3)
C(133)	0.029(4)	0.039(4)	0.025(4)	0.005(3)	-0.001(3)	-0.006(3)
C(134)	0.019(3)	0.049(5)	0.036(3)	0.007(5)	0.000(3)	0.016(4)
C(135)	0.027(4)	0.037(4)	0.038(4)	-0.001(4)	0.006(3)	0.012(3)
C(136)	0.023(3)	0.026(4)	0.022(3)	0.002(2)	0.006(3)	0.003(2)
C(211)	0.018(3)	0.031(3)	0.026(3)	-0.001(3)	0.006(3)	-0.004(3)
C(212)	0.025(3)	0.031(5)	0.026(3)	0.002(3)	0.008(2)	-0.007(3)
C(213)	0.030(4)	0.055(5)	0.025(4)	-0.010(4)	0.010(3)	-0.001(4)
C(214)	0.030(4)	0.049(5)	0.039(4)	-0.016(4)	0.009(3)	-0.001(4)
C(215)	0.031(4)	0.031(4)	0.047(5)	-0.006(4)	0.006(4)	0.008(3)
C(216)	0.036(4)	0.035(4)	0.029(4)	-0.003(3)	0.009(3)	0.000(3)
C(221)	0.019(3)	0.030(3)	0.022(3)	0.002(3)	0.002(3)	-0.004(3)
C(222)	0.029(4)	0.047(5)	0.026(4)	0.010(3)	0.006(3)	0.000(3)
C(223)	0.024(4)	0.068(6)	0.048(5)	0.007(5)	-0.002(4)	0.016(4)
C(224)	0.043(5)	0.043(4)	0.038(5)	0.015(4)	-0.002(4)	0.007(4)
C(225)	0.045(5)	0.042(5)	0.038(5)	0.014(4)	0.002(4)	-0.004(4)
C(226)	0.026(4)	0.034(4)	0.035(4)	0.009(3)	0.005(3)	-0.003(3)
C(231)	0.017(3)	0.037(4)	0.022(3)	0.007(3)	0.006(3)	-0.006(3)
C(232)	0.026(4)	0.043(4)	0.025(4)	-0.001(3)	0.005(3)	-0.005(3)
C(233)	0.036(4)	0.045(5)	0.034(4)	-0.004(4)	0.008(3)	-0.018(4)
C(234)	0.022(4)	0.066(6)	0.040(5)	0.001(4)	0.004(3)	-0.016(4)
C(235)	0.019(4)	0.060(6)	0.060(5)	0.019(5)	0.008(4)	0.003(4)
C(236)	0.024(4)	0.033(4)	0.042(4)	0.011(3)	0.005(3)	0.001(3)

Appendix IX

Complete Bond Lengths, Bond Angles, and Thermal and Positional

Parameters for

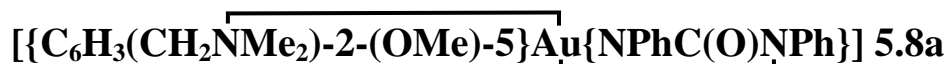


Table A.IX.1: Complete Bond Lengths (Å) for 5.8a, with e.s.d.s in parentheses

Au(1)-N(1)	2.003(6)	C(11)-C(12)	1.406(11)
Au(1)-C(31)	2.025(7)	C(12)-C(13)	1.395(11)
Au(1)-N(3)	2.088(6)	C(13)-C(14)	1.372(12)
Au(1)-N(2)	2.092(6)	C(14)-C(15)	1.371(13)
Au(1)-C(1)	2.584(8)	C(15)-C(16)	1.390(11)
O(1)-C(1)	1.219(8)	C(21)-C(26)	1.391(10)
O(2)-C(35)	1.375(9)	C(21)-C(22)	1.401(11)
O(2)-C(2)	1.433(10)	C(22)-C(23)	1.379(11)
N(1)-C(1)	1.387(10)	C(23)-C(24)	1.374(12)
N(1)-C(11)	1.404(9)	C(24)-C(25)	1.389(13)
N(2)-C(1)	1.383(9)	C(25)-C(26)	1.371(11)
N(2)-C(21)	1.421(9)	C(31)-C(36)	1.392(11)
N(3)-C(4)	1.470(9)	C(31)-C(32)	1.391(10)
N(3)-C(5)	1.505(8)	C(32)-C(33)	1.395(10)
N(3)-C(3)	1.519(9)	C(33)-C(34)	1.388(11)
C(3)-C(32)	1.474(10)	C(34)-C(35)	1.368(11)
C(11)-C(16)	1.398(10)	C(35)-C(36)	1.405(10)

Table A.IX.2: Complete Bond Angles (°) for 5.8a, with e.s.d.s in parentheses

N(1)-Au(1)-C(31)	106.3(3)	C(32)-C(3)-N(3)	107.9(6)
N(1)-Au(1)-N(3)	172.2(2)	N(1)-C(11)-C(16)	120.9(7)
C(31)-Au(1)-N(3)	80.9(3)	N(1)-C(11)-C(12)	120.7(7)
N(1)-Au(1)-N(2)	64.3(2)	C(16)-C(11)-C(12)	118.4(7)
C(31)-Au(1)-N(2)	169.9(3)	C(13)-C(12)-C(11)	120.6(8)
N(3)-Au(1)-N(2)	108.6(2)	C(14)-C(13)-C(12)	119.7(9)
N(1)-Au(1)-C(1)	32.1(2)	C(13)-C(14)-C(15)	120.5(9)
C(31)-Au(1)-C(1)	138.4(3)	C(14)-C(15)-C(16)	120.8(8)
N(3)-Au(1)-C(1)	140.6(3)	C(15)-C(16)-C(11)	120.0(8)
N(2)-Au(1)-C(1)	32.3(2)	C(26)-C(21)-C(22)	118.3(7)
C(35)-O(2)-C(2)	117.9(6)	C(26)-C(21)-N(2)	123.5(7)
C(1)-N(1)-C(11)	124.6(6)	C(22)-C(21)-N(2)	118.2(7)
C(1)-N(1)-Au(1)	97.7(5)	C(23)-C(22)-C(21)	120.0(8)
C(11)-N(1)-Au(1)	137.3(5)	C(24)-C(23)-C(22)	121.2(9)
C(1)-N(2)-C(21)	122.5(6)	C(23)-C(24)-C(25)	118.9(8)
C(1)-N(2)-Au(1)	93.9(5)	C(26)-C(25)-C(24)	120.7(9)
C(21)-N(2)-Au(1)	143.1(5)	C(25)-C(26)-C(21)	120.8(8)
C(4)-N(3)-C(5)	109.3(6)	C(36)-C(31)-C(32)	121.5(7)
C(4)-N(3)-C(3)	109.6(5)	C(36)-C(31)-Au(1)	125.1(6)
C(5)-N(3)-C(3)	109.8(6)	C(32)-C(31)-Au(1)	113.2(5)

C(4)-N(3)-Au(1)	111.9(4)	C(31)-C(32)-C(33)	118.3(7)
C(5)-N(3)-Au(1)	110.0(4)	C(31)-C(32)-C(3)	116.7(7)
C(3)-N(3)-Au(1)	106.2(4)	C(33)-C(32)-C(3)	125.0(7)
O(1)-C(1)-N(2)	128.9(8)	C(34)-C(33)-C(32)	121.0(7)
O(1)-C(1)-N(1)	127.1(7)	C(35)-C(34)-C(33)	119.9(7)
N(2)-C(1)-N(1)	103.9(6)	C(34)-C(35)-O(2)	115.5(7)
O(1)-C(1)-Au(1)	176.0(6)	C(34)-C(35)-C(36)	120.8(7)
N(2)-C(1)-Au(1)	53.9(4)	O(2)-C(35)-C(36)	123.6(7)
N(1)-C(1)-Au(1)	50.2(3)	C(31)-C(36)-C(35)	118.4(7)

Table A.IX.3: Final Positional (fractional co-ordinates) and Equivalent Thermal Parameters for 5.8a, with e.s.d.s in parentheses

Atom	X/A	Y/B	Z/C	U(eq)
Au(1)	0.8997(1)	0.7650(1)	0.1931(1)	0.023(1)
O(1)	0.9997(4)	0.9659(3)	0.2115(6)	0.044(2)
O(2)	0.5091(4)	0.7267(3)	0.0144(6)	0.043(2)
N(1)	0.8732(5)	0.8764(3)	0.1841(7)	0.030(2)
N(2)	1.0251(5)	0.8346(3)	0.2029(7)	0.028(2)
N(3)	0.9454(5)	0.6528(3)	0.2180(6)	0.027(2)
C(1)	0.9706(6)	0.9008(4)	0.2014(8)	0.029(2)
C(2)	0.5057(7)	0.8033(5)	-0.0374(10)	0.050(2)
C(3)	0.8601(5)	0.6112(4)	0.2866(8)	0.027(2)
C(4)	1.0348(6)	0.6461(4)	0.3156(8)	0.034(2)
C(5)	0.9652(6)	0.6191(4)	0.0690(8)	0.034(2)
C(11)	0.7902(6)	0.9243(4)	0.1807(8)	0.030(2)
C(12)	0.7082(6)	0.9080(5)	0.2661(9)	0.039(2)
C(13)	0.6246(7)	0.9543(5)	0.2589(10)	0.052(3)
C(14)	0.6217(8)	1.0157(6)	0.1660(11)	0.061(3)
C(15)	0.7012(8)	1.0330(5)	0.0827(10)	0.054(3)
C(16)	0.7858(6)	0.9882(4)	0.0893(8)	0.032(2)
C(21)	1.1299(6)	0.8338(4)	0.2246(8)	0.030(2)
C(22)	1.1838(6)	0.7813(4)	0.1442(9)	0.034(2)
C(23)	1.2852(6)	0.7762(5)	0.1672(10)	0.047(2)
C(24)	1.3353(7)	0.8225(6)	0.2667(11)	0.053(3)
C(25)	1.2822(7)	0.8756(5)	0.3446(10)	0.051(3)
C(26)	1.1814(6)	0.8813(5)	0.3235(8)	0.033(2)
C(31)	0.7664(5)	0.7135(4)	0.1662(7)	0.025(2)
C(32)	0.7670(5)	0.6389(4)	0.2151(7)	0.024(2)
C(33)	0.6811(6)	0.5960(4)	0.1921(8)	0.034(2)
C(34)	0.5965(6)	0.6271(5)	0.1242(8)	0.036(2)
C(35)	0.5969(5)	0.7008(5)	0.0782(8)	0.030(2)
C(36)	0.6826(6)	0.7454(4)	0.0961(9)	0.033(2)

Table A.IX.4: Final Positional (fractional co-ordinates) and Equivalent Thermal Parameters of Calculated Hydrogen Atoms for 5.8a, with e.s.d.s in parentheses

Atom	X/A	Y/B	Z/C	U(eq)
H(2A)	0.4402	0.8141	-0.0805	0.075
H(2B)	0.5546	0.8103	-0.1118	0.075
H(2C)	0.5198	0.8373	0.0451	0.075
H(3A)	0.8666	0.5566	0.2709	0.032

H(3B)	0.8606	0.6208	0.3935	0.032
H(4A)	1.0221	0.6677	0.4117	0.051
H(4B)	1.0890	0.6730	0.2721	0.051
H(4C)	1.0523	0.5932	0.3273	0.051
H(5A)	0.9062	0.6233	0.0046	0.052
H(5B)	0.9829	0.5663	0.0810	0.052
H(5C)	1.0193	0.6461	0.0254	0.052
H(12)	0.7098	0.8654	0.3286	0.047
H(13)	0.5704	0.9434	0.3174	0.062
H(14)	0.5647	1.0463	0.1595	0.073
H(15)	0.6984	1.0756	0.0204	0.065
H(16)	0.8401	1.0008	0.0323	0.038
H(22)	1.1510	0.7496	0.0747	0.040
H(23)	1.3206	0.7404	0.1136	0.057
H(24)	1.4043	0.8184	0.2819	0.064
H(25)	1.3157	0.9078	0.4125	0.061
H(26)	1.1467	0.9178	0.3765	0.040
H(33)	0.6805	0.5453	0.2232	0.040
H(34)	0.5391	0.5975	0.1098	0.043
H(36)	0.6834	0.7955	0.0616	0.039

Table A.IX.5: Thermal Parameters for 5.8a, with e.s.d.s in parentheses

Atom	U11	U22	U33	U23	U13	U12
Au(1)	0.0267(2)	0.0169(1)	0.0259(2)	0.0008(1)	-0.0003(1)	0.0008(1)
O(1)	0.040(3)	0.024(3)	0.066(4)	0.001(3)	-0.011(3)	-0.007(3)
O(2)	0.033(3)	0.043(4)	0.052(4)	0.010(3)	-0.009(3)	-0.003(3)
N(1)	0.042(4)	0.012(3)	0.036(4)	0.002(3)	-0.001(3)	-0.003(3)
N(2)	0.033(4)	0.017(3)	0.035(4)	0.002(3)	0.001(3)	-0.003(3)
N(3)	0.043(4)	0.013(3)	0.027(4)	0.000(2)	-0.002(3)	0.003(3)
C(1)	0.034(5)	0.022(4)	0.031(4)	0.002(3)	-0.001(4)	-0.006(4)
C(2)	0.043(6)	0.053(6)	0.054(6)	0.010(5)	-0.002(5)	0.007(5)
C(3)	0.035(5)	0.021(4)	0.024(4)	0.001(3)	0.005(4)	-0.006(3)
C(4)	0.031(5)	0.027(5)	0.043(5)	0.004(4)	-0.010(4)	0.004(3)
C(5)	0.049(5)	0.019(4)	0.035(5)	-0.004(3)	0.010(4)	0.001(4)
C(11)	0.033(5)	0.024(4)	0.033(5)	-0.001(3)	-0.003(4)	0.005(3)
C(12)	0.046(6)	0.031(5)	0.039(5)	-0.001(4)	-0.003(4)	0.002(4)
C(13)	0.051(6)	0.057(7)	0.049(6)	0.005(5)	0.017(5)	0.019(5)
C(14)	0.059(7)	0.050(7)	0.076(8)	0.019(5)	0.016(6)	0.032(5)
C(15)	0.078(8)	0.028(5)	0.056(6)	0.014(4)	0.002(6)	0.016(5)
C(16)	0.033(5)	0.032(5)	0.030(4)	0.000(3)	0.002(4)	0.007(4)
C(21)	0.033(5)	0.028(4)	0.028(4)	0.005(3)	0.000(4)	-0.004(3)
C(22)	0.037(5)	0.028(5)	0.036(5)	0.007(3)	-0.005(4)	-0.002(3)
C(23)	0.034(5)	0.043(6)	0.066(6)	0.014(5)	0.003(5)	0.012(4)
C(24)	0.029(5)	0.059(7)	0.071(7)	0.024(5)	-0.017(5)	-0.003(5)
C(25)	0.048(6)	0.049(6)	0.053(6)	0.010(5)	-0.017(5)	-0.014(5)
C(26)	0.036(5)	0.036(5)	0.027(4)	0.006(3)	0.003(4)	-0.003(4)
C(31)	0.029(4)	0.028(4)	0.020(4)	0.000(3)	0.016(3)	-0.002(3)
C(32)	0.024(4)	0.031(4)	0.019(4)	0.002(3)	0.001(3)	0.005(3)
C(33)	0.044(5)	0.020(4)	0.037(5)	0.003(3)	0.004(4)	-0.003(4)
C(34)	0.034(5)	0.034(5)	0.038(5)	0.000(4)	0.007(4)	-0.009(4)
C(35)	0.023(4)	0.034(5)	0.032(4)	0.000(4)	0.005(4)	0.001(3)
C(36)	0.030(4)	0.035(5)	0.034(4)	0.004(3)	0.004(4)	0.002(3)

Appendix X

Complete Bond Lengths, Bond Angles, and Thermal and Positional

Parameters for

$[\{\text{C}_6\text{H}_3(\text{CH}_2\text{NMe}_2)\text{-2-(OMe)-5}\}\text{Au}\{\text{NAcC(O)NAc}\}]\cdot\frac{1}{2}\text{H}_2\text{O}$ **5.8b**

Table A.X.1: Complete Bond Lengths (Å) for **5.8b**·½H₂O, with e.s.d.s in parentheses

Au(1)-N(1)	2.014(5)	N(2)-C(1)	1.390(9)
Au(1)-C(11)	2.021(6)	N(3)-C(6)	1.485(8)
Au(1)-N(3)	2.090(5)	N(3)-C(8)	1.488(8)
Au(1)-N(2)	2.092(6)	N(3)-C(7)	1.508(8)
Au(1)-C(1)	2.622(7)	C(2)-C(3)	1.495(10)
O(1)-C(1)	1.222(9)	C(4)-C(5)	1.513(10)
O(2)-C(2)	1.230(8)	C(6)-C(12)	1.500(9)
O(3)-C(4)	1.218(9)	C(11)-C(16)	1.391(8)
O(4)-C(15)	1.379(7)	C(11)-C(12)	1.414(9)
O(4)-C(9)	1.433(8)	C(12)-C(13)	1.383(9)
N(1)-C(2)	1.395(8)	C(13)-C(14)	1.408(9)
N(1)-C(1)	1.415(8)	C(14)-C(15)	1.396(10)
N(2)-C(4)	1.371(8)	C(15)-C(16)	1.394(9)

Table A.X.2: Complete Bond Angles (°) for **5.8b**·½H₂O, with e.s.d.s in parentheses

N(1)-Au(1)-C(11)	107.0(2)	O(1)-C(1)-N(1)	128.8(6)
N(1)-Au(1)-N(3)	171.1(2)	N(2)-C(1)-N(1)	102.0(6)
C(11)-Au(1)-N(3)	80.7(2)	O(1)-C(1)-Au(1)	177.7(6)
N(1)-Au(1)-N(2)	64.1(2)	N(2)-C(1)-Au(1)	52.6(3)
C(11)-Au(1)-N(2)	168.3(2)	N(1)-C(1)-Au(1)	49.5(3)
N(3)-Au(1)-N(2)	108.9(2)	O(2)-C(2)-N(1)	119.7(6)
N(1)-Au(1)-C(1)	32.3(2)	O(2)-C(2)-C(3)	122.3(6)
C(11)-Au(1)-C(1)	138.9(2)	N(1)-C(2)-C(3)	118.0(6)
N(3)-Au(1)-C(1)	140.4(2)	O(3)-C(4)-N(2)	121.4(7)
N(2)-Au(1)-C(1)	31.9(2)	O(3)-C(4)-C(5)	119.8(6)
C(15)-O(4)-C(9)	117.3(5)	N(2)-C(4)-C(5)	118.7(6)
C(2)-N(1)-C(1)	125.2(6)	N(3)-C(6)-C(12)	107.9(5)
C(2)-N(1)-Au(1)	133.8(4)	C(16)-C(11)-C(12)	119.6(6)
C(1)-N(1)-Au(1)	98.2(4)	C(16)-C(11)-Au(1)	126.2(5)
C(4)-N(2)-C(1)	127.1(6)	C(12)-C(11)-Au(1)	113.7(4)
C(4)-N(2)-Au(1)	133.4(5)	C(13)-C(12)-C(11)	119.7(6)
C(1)-N(2)-Au(1)	95.6(4)	C(13)-C(12)-C(6)	124.9(6)
C(6)-N(3)-C(8)	111.4(5)	C(11)-C(12)-C(6)	115.3(6)
C(6)-N(3)-C(7)	107.9(5)	C(12)-C(13)-C(14)	120.9(6)
C(8)-N(3)-C(7)	108.7(5)	C(15)-C(14)-C(13)	118.6(6)
C(6)-N(3)-Au(1)	107.9(4)	O(4)-C(15)-C(16)	115.5(6)
C(8)-N(3)-Au(1)	110.2(4)	O(4)-C(15)-C(14)	123.6(6)
C(7)-N(3)-Au(1)	110.7(4)	C(16)-C(15)-C(14)	121.0(6)
O(1)-C(1)-N(2)	129.1(7)	C(11)-C(16)-C(15)	120.0(6)

Table A.X.3: Final Positional (fractional co-ordinates) and Equivalent Thermal Parameters for **5.8b**·½H₂O, with e.s.d.s in parentheses

Atom	X/A	Y/B	Z/C	U(eq)
Au(1)	0.4853(1)	0.2754(1)	0.7548(1)	0.013(1)
O(1)	0.5791(7)	0.2905(8)	1.0854(5)	0.036(1)
O(2)	0.7963(6)	0.4377(6)	0.7563(4)	0.023(1)
O(3)	0.2322(7)	0.1109(7)	0.9568(5)	0.035(1)
O(4)	0.9692(5)	0.1915(6)	0.4665(5)	0.024(1)
N(1)	0.6347(6)	0.3075(6)	0.8748(5)	0.016(1)
N(2)	0.4186(7)	0.2470(7)	0.9370(5)	0.021(1)
N(3)	0.3032(6)	0.2609(6)	0.6443(5)	0.014(1)
C(1)	0.5481(8)	0.2823(9)	0.9814(7)	0.023(1)
C(2)	0.7583(7)	0.3805(8)	0.8609(7)	0.020(1)
C(3)	0.8419(9)	0.3834(10)	0.9755(7)	0.030(2)
C(4)	0.3200(8)	0.1665(8)	1.0053(7)	0.022(1)
C(5)	0.3190(9)	0.1502(9)	1.1432(7)	0.029(2)
C(6)	0.3209(7)	0.3467(8)	0.5143(6)	0.021(1)
C(7)	0.1490(8)	0.3411(8)	0.6827(7)	0.023(1)
C(8)	0.3055(8)	0.0914(7)	0.6559(6)	0.019(1)
C(9)	1.0334(8)	0.1766(9)	0.3515(7)	0.027(2)
C(11)	0.5928(7)	0.2780(7)	0.5952(6)	0.017(1)
C(12)	0.4901(7)	0.3083(7)	0.4908(6)	0.016(1)
C(13)	0.5488(7)	0.3062(8)	0.3765(6)	0.019(1)
C(14)	0.7098(8)	0.2696(8)	0.3632(6)	0.020(1)
C(15)	0.8097(7)	0.2313(7)	0.4684(6)	0.017(1)
C(16)	0.7520(7)	0.2347(7)	0.5838(6)	0.017(1)
O(5)	-0.0204(13)	0.0186(14)	0.8747(11)	0.039(3)

Table A.X.4: Final Positional (fractional co-ordinates) and Equivalent Thermal Parameters of Calculated Hydrogen Atoms for **5.8b**·½H₂O, with e.s.d.s in parentheses

Atom	X/A	Y/B	Z/C	U(eq)
H(3A)	0.7933	0.3327	1.0486	0.045
H(3B)	0.8367	0.4938	0.9747	0.045
H(3C)	0.9507	0.3255	0.9781	0.045
H(5A)	0.3965	0.2003	1.1671	0.043
H(5B)	0.3438	0.0372	1.1884	0.043
H(5C)	0.2160	0.2026	1.1633	0.043
H(6A)	0.2814	0.4628	0.5016	0.025
H(6B)	0.2611	0.3127	0.4563	0.025
H(7A)	0.1462	0.4528	0.6758	0.035
H(7B)	0.1352	0.2873	0.7688	0.035
H(7C)	0.0654	0.3353	0.6287	0.035
H(8A)	0.2944	0.0378	0.7426	0.029
H(8B)	0.4041	0.0387	0.6289	0.029
H(8C)	0.2196	0.0861	0.6039	0.029
H(9A)	1.1469	0.1488	0.3620	0.040
H(9B)	0.9981	0.2778	0.2878	0.040
H(9C)	0.9992	0.0929	0.3260	0.040

H(13)	0.4794	0.3298	0.3060	0.022
H(14)	0.7497	0.2710	0.2842	0.024
H(16)	0.8214	0.2075	0.6548	0.021

Table A.X.5: Thermal Parameters for **5.8b**·½H₂O, with *e.s.d.s* in parentheses

Atom	U11	U22	U33	U23	U13	U12
Au(1)	0.0117(1)	0.0193(1)	0.0108(1)	-0.0048(1)	0.0024(1)	-0.0077(1)
O(1)	0.037(3)	0.068(4)	0.015(3)	-0.015(3)	0.007(2)	-0.033(3)
O(2)	0.024(2)	0.034(3)	0.017(3)	-0.0063(19)	0.006(2)	-0.019(2)
O(3)	0.033(3)	0.052(3)	0.027(3)	-0.005(2)	0.004(2)	-0.030(3)
O(4)	0.015(2)	0.040(3)	0.018(3)	-0.009(2)	0.0050(18)	-0.010(2)
N(1)	0.018(2)	0.028(3)	0.002(2)	-0.0015(19)	0.0055(19)	-0.011(2)
N(2)	0.019(3)	0.036(3)	0.011(3)	-0.006(2)	0.001(2)	-0.013(2)
N(3)	0.018(2)	0.016(2)	0.007(3)	-0.0010(18)	0.0017(19)	-0.005(2)
C(1)	0.020(3)	0.035(4)	0.016(4)	-0.009(3)	0.001(3)	-0.011(3)
C(2)	0.014(3)	0.024(3)	0.027(4)	-0.012(3)	0.002(3)	-0.008(2)
C(3)	0.024(3)	0.050(4)	0.024(4)	-0.012(3)	-0.002(3)	-0.023(3)
C(4)	0.017(3)	0.025(3)	0.021(4)	0.000(3)	0.003(3)	-0.005(3)
C(5)	0.030(4)	0.033(4)	0.022(4)	-0.003(3)	0.008(3)	-0.010(3)
C(6)	0.017(3)	0.027(3)	0.018(4)	-0.001(3)	0.000(2)	-0.009(3)
C(7)	0.017(3)	0.031(3)	0.021(4)	-0.004(3)	0.001(3)	-0.009(3)
C(8)	0.024(3)	0.021(3)	0.015(3)	-0.003(2)	-0.002(3)	-0.011(3)
C(9)	0.025(3)	0.039(4)	0.019(4)	-0.012(3)	0.008(3)	-0.010(3)
C(11)	0.018(3)	0.021(3)	0.018(3)	-0.007(2)	0.009(2)	-0.011(2)
C(12)	0.017(3)	0.017(3)	0.014(3)	-0.003(2)	0.001(2)	-0.008(2)
C(13)	0.019(3)	0.026(3)	0.013(3)	-0.006(2)	0.000(2)	-0.009(3)
C(14)	0.025(3)	0.021(3)	0.016(3)	-0.008(2)	0.005(3)	-0.007(3)
C(15)	0.016(3)	0.022(3)	0.017(3)	-0.010(2)	0.006(2)	-0.010(2)
C(16)	0.016(3)	0.021(3)	0.017(3)	-0.005(2)	0.005(2)	-0.009(2)
O(5)	0.033(6)	0.048(7)	0.040(7)	-0.008(5)	0.001(5)	-0.022(5)

Appendix XI

Complete Bond Lengths, Bond Angles, and Thermal and Positional

Parameters for

$[\{(\{C_6H_3(CH_2NMe_2)-2-(OMe)-5\}Au\{\mu-S\})_2\}_3Ag_2Cl_2]^{1/2}AgCl_3$ **6.5a**

Table A.XI.1: Complete Bond Lengths (Å) for **6.5a**, with e.s.d.s in parentheses

Au(1)-C(11)	1.973(11)	S(3)-Au(3')	2.382(6)
Au(1)-N(1)	2.146(18)	O(1)-C(10B)	1.15(4)
Au(1)-S(2)	2.306(6)	O(1)-C(10A)	1.25(4)
Au(1)-S(1)	2.389(6)	O(1)-C(15)	1.42(4)
Au(2)-C(21)	2.030(11)	O(2)-C(25)	1.36(3)
Au(2)-N(2)	2.14(2)	O(2)-C(210)	1.50(3)
Au(2)-S(1)	2.302(6)	O(3)-C(35)	1.379(19)
Au(2)-S(2)	2.388(7)	O(3)-C(310)	1.47(2)
Au(3)-C(31)	2.034(8)	N(1)-C(19)	1.47(2)
Au(3)-N(3)	2.134(19)	N(1)-C(17)	1.49(2)
Au(3)-S(3)	2.293(6)	N(1)-C(18)	1.51(2)
Au(3)-S(3')	2.382(6)	N(2)-C(28)	1.46(3)
Ag(1)-S(2')	2.512(6)	N(2)-C(27)	1.48(3)
Ag(1)-S(2)	2.512(6)	N(2)-C(29)	1.49(3)
Ag(1)-Cl(1)	2.833(6)	N(3)-C(38)	1.50(2)
Ag(1)-Cl(1')	2.833(6)	N(3)-C(37)	1.51(2)
Ag(2)-S(1)	2.512(6)	N(3)-C(39)	1.54(2)
Ag(2)-S(3)	2.520(7)	C(12)-C(17)	1.40(2)
Ag(2)-Cl(1')	2.779(6)	C(22)-C(27)	1.49(2)
Ag(2)-Cl(1)	2.854(6)	C(32)-C(37)	1.49(2)
Cl(1)-Ag(2')	2.779(6)		
Ag(3)-Ag(3'')	1.430(16)	Ag(3)-Cl(2''')	2.54(2)
Ag(3)-Cl(2)	2.5389	Ag(3)-Cl(2''''')	2.899(12)
Ag(3)-Cl(2'')	2.90(3)	Ag(3)-Cl(2''''''')	2.899(12)
Ag(3)-Cl(2''')	2.54(2)	Cl(2)-Ag(3'')	2.90(3)

Table A.XI.2: Complete Bond Angles (°) for **6.5a**, with e.s.d.s in parentheses

C(11)-Au(1)-N(1)	80.8(6)	C(10B)-O(1)-C(15)	122(4)
C(11)-Au(1)-S(2)	93.9(3)	C(10A)-O(1)-C(15)	141(3)
N(1)-Au(1)-S(2)	174.3(6)	C(25)-O(2)-C(210)	124(2)
C(11)-Au(1)-S(1)	179.2(4)	C(35)-O(3)-C(310)	115.3(14)
N(1)-Au(1)-S(1)	100.0(6)	C(19)-N(1)-C(17)	109.1(15)
S(2)-Au(1)-S(1)	85.3(2)	C(19)-N(1)-C(18)	108.3(14)
C(21)-Au(2)-N(2)	83.1(7)	C(17)-N(1)-C(18)	112.2(14)
C(21)-Au(2)-S(1)	94.0(3)	C(19)-N(1)-Au(1)	109.9(12)
N(2)-Au(2)-S(1)	176.0(7)	C(17)-N(1)-Au(1)	105.8(11)
C(21)-Au(2)-S(2)	176.9(4)	C(18)-N(1)-Au(1)	111.3(13)
N(2)-Au(2)-S(2)	97.6(7)	C(28)-N(2)-C(27)	109.2(17)

S(1)-Au(2)-S(2)	85.4(2)	C(28)-N(2)-C(29)	108.7(17)
C(31)-Au(3)-N(3)	80.9(6)	C(27)-N(2)-C(29)	110.2(16)
C(31)-Au(3)-S(3)	95.0(3)	C(28)-N(2)-Au(2)	110.0(13)
N(3)-Au(3)-S(3)	175.7(6)	C(27)-N(2)-Au(2)	105.3(13)
C(31)-Au(3)-S(3')	179.5(3)	C(29)-N(2)-Au(2)	113.4(14)
N(3)-Au(3)-S(3')	98.6(6)	C(38)-N(3)-C(37)	110.8(14)
S(3)-Au(3)-S(3')	85.5(2)	C(38)-N(3)-C(39)	109.4(14)
S(2')-Ag(1)-S(2)	132.9(3)	C(37)-N(3)-C(39)	110.3(14)
S(2')-Ag(1)-Cl(1)	100.23(19)	C(38)-N(3)-Au(3)	108.7(12)
S(2)-Ag(1)-Cl(1)	113.08(18)	C(37)-N(3)-Au(3)	105.5(11)
S(2')-Ag(1)-Cl(1')	113.08(18)	C(39)-N(3)-Au(3)	112.1(11)
S(2)-Ag(1)-Cl(1')	100.23(19)	C(12)-C(11)-Au(1)	111.1(4)
Cl(1)-Ag(1)-Cl(1')	89.2(3)	C(16)-C(11)-Au(1)	128.8(4)
S(1)-Ag(2)-S(3)	129.6(2)	C(11)-C(12)-C(17)	122.1(10)
S(1)-Ag(2)-Cl(1')	113.8(2)	C(13)-C(12)-C(17)	117.8(10)
S(3)-Ag(2)-Cl(1')	101.09(19)	C(14)-C(15)-O(1)	126.7(17)
S(1)-Ag(2)-Cl(1)	98.09(19)	C(16)-C(15)-O(1)	113.2(17)
S(3)-Ag(2)-Cl(1)	117.9(2)	C(12)-C(17)-N(1)	106.3(8)
Cl(1')-Ag(2)-Cl(1)	89.8(2)	C(22)-C(21)-Au(2)	109.9(4)
Ag(2')-Cl(1)-Ag(1)	77.76(16)	C(26)-C(21)-Au(2)	130.1(4)
Ag(2')-Cl(1)-Ag(2)	73.12(16)	C(21)-C(22)-C(27)	119.9(10)
Ag(1)-Cl(1)-Ag(2)	76.54(15)	C(23)-C(22)-C(27)	119.3(10)
Au(2)-S(1)-Au(1)	94.7(2)	O(2)-C(25)-C(26)	114.3(12)
Au(2)-S(1)-Ag(2)	83.76(19)	O(2)-C(25)-C(24)	125.7(12)
Au(1)-S(1)-Ag(2)	99.8(2)	N(2)-C(27)-C(22)	108.1(10)
Au(1)-S(2)-Au(2)	94.6(2)	C(32)-C(31)-Au(3)	113.5(2)
Au(1)-S(2)-Ag(1)	83.47(19)	C(36)-C(31)-Au(3)	126.5(2)
Au(2)-S(2)-Ag(1)	98.6(2)	C(33)-C(32)-C(37)	122.6(10)
Au(3)-S(3)-Au(3')	94.4(2)	C(31)-C(32)-C(37)	117.1(10)
Au(3)-S(3)-Ag(2)	82.40(19)	O(3)-C(35)-C(36)	125.5(9)
Au(3')-S(3)-Ag(2)	100.6(2)	O(3)-C(35)-C(34)	114.5(9)
C(10B)-O(1)-C(10A)	94(2)	C(32)-C(37)-N(3)	108.8(9)
Ag(3'')-Ag(3)-Cl(2'')	89.3(8)	Cl(2'')-Ag(3)-Cl(2'')	63.7(3)
Ag(3'')-Ag(3)-Cl(2)	89.3(12)	Cl(2)-Ag(3)-Cl(2'')	150.5(6)
Cl(2'')-Ag(3)-Cl(2)	120.0(4)	Cl(2'')-Ag(3)-Cl(2'')	63.7(4)
Ag(3'')-Ag(3)-Cl(2''')	89.3(9)	Cl(2''')-Ag(3)-Cl(2'')	98.7(5)
Cl(2'')-Ag(3)-Cl(2''')	120.0(5)	Ag(3'')-Ag(3)-Cl(2''''')	61.1(8)
Cl(2)-Ag(3)-Cl(2''')	120.0(4)	Cl(2'')-Ag(3)-Cl(2''''')	150.5(3)
Ag(3'')-Ag(3)-Cl(2''''')	61.1(9)	Cl(2)-Ag(3)-Cl(2''''')	63.7(3)
Cl(2'')-Ag(3)-Cl(2''''')	63.67(17)	Cl(2''')-Ag(3)-Cl(2''''')	63.7(3)
Cl(2)-Ag(3)-Cl(2''''')	63.7(3)	Cl(2'''')-Ag(3)-Cl(2''''')	98.6(5)
Cl(2''')-Ag(3)-Cl(2''''')	150.5(2)	Cl(2'')-Ag(3)-Cl(2''''')	98.6(3)
Ag(3'')-Ag(3)-Cl(2'')	61.1(9)	Ag(3)-Cl(2)-Ag(3'')	29.5(4)

Table A.XI.3: Final Positional (fractional co-ordinates) and Equivalent Thermal Parameters for **6.5a**, with *e.s.d.s* in parentheses

Atom	X/A	Y/B	Z/C	U(eq)
Au(1)	0.0483(1)	0.6788(1)	0.1026(1)	0.047(1)
Au(2)	-0.0041(1)	0.7444(1)	0.1251(1)	0.052(1)
Au(3)	-0.0220(1)	0.7071(1)	-0.0299(1)	0.048(1)
Ag(1)	0.0743(1)	0.7500	0.0743(1)	0.064(1)
Ag(2)	-0.0071(1)	0.7298(1)	0.0454(1)	0.061(1)

Cl(1)	0.0563(2)	0.7068(1)	0.0204(2)	0.052(2)
S(1)	-0.0098(2)	0.6938(1)	0.0974(2)	0.051(2)
S(2)	0.0539(2)	0.7294(2)	0.1306(2)	0.053(2)
S(3)	-0.0526(2)	0.7433(1)	0.0032(2)	0.051(2)
O(1)	0.1738(7)	0.6836(11)	0.1537(10)	0.165(15)
O(2)	-0.1356(6)	0.7336(6)	0.0893(7)	0.119(9)
O(3)	-0.1089(5)	0.6269(5)	0.0439(5)	0.076(6)
N(1)	0.0475(5)	0.6301(4)	0.0790(5)	0.051(5)
N(2)	-0.0021(6)	0.7908(5)	0.1526(5)	0.070(6)
N(3)	0.0037(6)	0.6706(5)	-0.0600(5)	0.061(6)
C(11)	0.0964(3)	0.6670(3)	0.1072(3)	0.049(6)
C(12)	0.1046(3)	0.6393(3)	0.0873(3)	0.073(8)
C(13)	0.1369(3)	0.6258(4)	0.0885(4)	0.098(11)
C(14)	0.1610(3)	0.6400(4)	0.1097(5)	0.133(18)
C(15)	0.1528(3)	0.6676(4)	0.1296(4)	0.103(12)
C(16)	0.1205(3)	0.6811(3)	0.1283(4)	0.078(9)
C(17)	0.0817(3)	0.6253(3)	0.0642(3)	0.063(7)
C(18)	0.0201(4)	0.6278(4)	0.0528(4)	0.066(7)
C(19)	0.0416(4)	0.6039(4)	0.1044(4)	0.063(8)
C(10A)	0.1728(5)	0.7058(6)	0.1761(5)	0.15(4)
C(10B)	0.1970(4)	0.6702(7)	0.1651(6)	0.14(3)
C(21)	-0.0529(3)	0.7580(3)	0.1179(3)	0.069(8)
C(22)	-0.0580(3)	0.7908(2)	0.1289(3)	0.078(9)
C(23)	-0.0898(3)	0.8053(3)	0.1271(4)	0.100(12)
C(24)	-0.1167(3)	0.7869(3)	0.1141(4)	0.092(12)
C(25)	-0.1117(3)	0.7540(3)	0.1031(4)	0.093(11)
C(26)	-0.0798(3)	0.7395(3)	0.1049(4)	0.065(7)
C(27)	-0.0285(3)	0.8125(3)	0.1373(4)	0.074(8)
C(28)	-0.0104(4)	0.7849(5)	0.1880(4)	0.109(14)
C(29)	0.0313(3)	0.8078(5)	0.1506(5)	0.087(10)
C(210)	-0.1705(3)	0.7454(6)	0.0804(6)	0.19(3)
C(31)	-0.0430(2)	0.6645(2)	-0.0107(2)	0.048(6)
C(32)	-0.0255(2)	0.6353(2)	-0.0189(2)	0.055(6)
C(33)	-0.0361(2)	0.6044(2)	-0.0063(2)	0.058(7)
C(34)	-0.0642(2)	0.6027(2)	0.0145(3)	0.070(8)
C(35)	-0.0818(2)	0.6318(2)	0.0227(2)	0.057(7)
C(36)	-0.0712(2)	0.6628(2)	0.0101(2)	0.056(6)
C(37)	0.0065(2)	0.6395(2)	-0.0381(2)	0.063(7)
C(38)	-0.0171(2)	0.6636(3)	-0.0908(2)	0.074(8)
C(39)	0.0389(2)	0.6827(3)	-0.0707(3)	0.060(7)
C(310)	-0.1301(2)	0.6566(3)	0.0498(3)	0.082(9)
Ag(3)	0.4896(2)	0.4896(3)	0.0104(3)	0.092(3)
Cl(2)	0.4861(2)	0.4469(3)	-0.0371(3)	0.057(4)

Table A.XI.4: Thermal Parameters for **6.5a**, with *e.s.d.s* in parentheses

Atom	U11	U22	U33	U23	U13	U12
Au(1)	0.0604(6)	0.0397(5)	0.0395(5)	0.0005(4)	0.0104(4)	0.0028(4)
Au(2)	0.0705(7)	0.0363(5)	0.0507(6)	-0.0003(4)	0.0227(5)	0.0032(5)
Au(3)	0.0492(6)	0.0383(5)	0.0563(6)	-0.0060(4)	0.0027(4)	-0.0004(4)
Ag(1)	0.0687(12)	0.0543(16)	0.0687(12)	0.0058(9)	0.0240(15)	-0.0058(9)
Ag(2)	0.0740(14)	0.0527(11)	0.0556(12)	0.0054(9)	0.0030(10)	0.0023(10)
Cl(1)	0.061(4)	0.041(3)	0.055(3)	0.003(3)	0.013(3)	-0.002(3)

S(1)	0.055(4)	0.036(3)	0.061(4)	0.000(3)	0.016(3)	0.000(3)
S(2)	0.075(4)	0.039(3)	0.046(3)	-0.003(3)	0.008(3)	-0.004(3)
S(3)	0.048(3)	0.038(3)	0.066(4)	0.002(3)	0.006(3)	0.003(3)
O(1)	0.08(2)	0.22(4)	0.19(4)	-0.01(3)	-0.04(2)	0.00(2)
O(2)	0.078(16)	0.095(17)	0.18(3)	-0.011(17)	-0.005(17)	0.009(14)
O(3)	0.058(12)	0.081(13)	0.090(14)	-0.006(11)	0.007(10)	-0.027(10)
N(1)	0.072(14)	0.041(11)	0.040(11)	-0.001(9)	0.005(10)	-0.008(10)
N(2)	0.112(19)	0.040(12)	0.059(14)	0.004(10)	0.008(13)	0.022(12)
N(3)	0.078(15)	0.043(12)	0.061(13)	-0.016(10)	0.002(11)	0.001(10)
C(11)	0.055(15)	0.054(14)	0.037(13)	0.002(11)	0.003(11)	-0.004(12)
C(12)	0.067(19)	0.08(2)	0.069(19)	-0.002(16)	-0.004(15)	0.036(16)
C(13)	0.11(3)	0.11(3)	0.08(2)	-0.01(2)	0.00(2)	0.00(2)
C(14)	0.12(3)	0.11(3)	0.17(4)	0.04(3)	0.06(3)	0.07(3)
C(15)	0.06(2)	0.12(3)	0.13(3)	0.01(2)	-0.03(2)	-0.02(2)
C(16)	0.041(16)	0.10(2)	0.09(2)	0.005(18)	0.014(15)	0.018(15)
C(17)	0.058(17)	0.071(18)	0.061(17)	-0.011(14)	0.009(13)	0.023(14)
C(18)	0.09(2)	0.063(17)	0.047(15)	-0.010(13)	-0.015(14)	-0.018(15)
C(19)	0.12(2)	0.030(13)	0.043(14)	0.001(11)	0.018(14)	-0.004(13)
C(10A)	0.15(9)	0.21(12)	0.09(6)	-0.01(7)	-0.05(6)	-0.02(8)
C(10B)	0.15(9)	0.10(6)	0.15(9)	-0.02(6)	0.06(7)	0.00(6)
C(21)	0.077(19)	0.045(15)	0.09(2)	-0.001(14)	0.041(16)	0.017(14)
C(22)	0.062(18)	0.07(2)	0.10(2)	-0.016(17)	0.040(17)	0.011(15)
C(23)	0.09(2)	0.09(2)	0.12(3)	0.02(2)	0.06(2)	0.00(2)
C(24)	0.07(2)	0.051(17)	0.15(3)	0.032(19)	0.06(2)	0.033(15)
C(25)	0.06(2)	0.06(2)	0.15(3)	0.00(2)	0.04(2)	-0.003(16)
C(26)	0.058(17)	0.054(16)	0.08(2)	-0.022(14)	0.006(15)	0.011(13)
C(27)	0.10(2)	0.050(16)	0.074(19)	-0.003(14)	0.018(17)	0.017(16)
C(28)	0.23(4)	0.043(16)	0.049(17)	0.001(13)	0.02(2)	0.04(2)
C(29)	0.07(2)	0.09(2)	0.10(2)	-0.053(19)	-0.001(17)	-0.006(17)
C(210)	0.11(4)	0.12(4)	0.34(8)	-0.03(5)	-0.07(5)	0.03(3)
C(31)	0.047(14)	0.033(12)	0.064(16)	0.016(11)	-0.006(12)	0.011(10)
C(32)	0.062(16)	0.044(14)	0.059(16)	-0.008(12)	0.002(13)	-0.009(12)
C(33)	0.062(16)	0.032(13)	0.079(18)	-0.011(12)	-0.008(14)	-0.016(12)
C(34)	0.066(18)	0.046(16)	0.10(2)	-0.007(15)	0.014(16)	-0.014(14)
C(35)	0.045(15)	0.055(16)	0.071(17)	0.007(13)	-0.010(13)	-0.026(12)
C(36)	0.042(14)	0.049(15)	0.078(18)	-0.003(13)	-0.003(13)	-0.004(12)
C(37)	0.09(2)	0.028(12)	0.068(17)	0.001(12)	0.018(15)	-0.013(13)
C(38)	0.08(2)	0.10(2)	0.038(14)	-0.020(14)	-0.028(14)	-0.001(17)
C(39)	0.045(14)	0.048(14)	0.087(19)	-0.013(13)	0.030(13)	-0.013(11)
C(310)	0.065(19)	0.09(2)	0.10(2)	0.003(18)	0.012(17)	-0.007(17)
Ag(3)	0.092(3)	0.092(3)	0.092(3)	-0.003(3)	-0.003(3)	0.003(3)
Cl(2)	0.077(10)	0.065(9)	0.029(7)	0.008(6)	-0.010(6)	0.014(8)

Appendix XII

Complete Bond Lengths, Bond Angles, and Thermal and Positional

Parameters for

$[\{(\{C_6H_4(CH_2NMe_2)-2\}Au\{\mu-S\})_2\}_3Ag_2Br_2]Z$ 6.5d

Table A.XII.1: Complete Bond Lengths (Å) for 6.5d, with e.s.d.s in parentheses

Au(11)-C(111)	2.090(12)	Ag(21)-S(21)	2.543(8)
Au(11)-N(11)	2.14(2)	Ag(21)-Br(22)	2.893(4)
Au(11)-S(11)	2.298(7)	Ag(21)-Br(21)	2.909(5)
Au(11)-S(12)	2.393(8)	Ag(22)-S(22)	2.511(8)
Au(12)-C(121)	2.078(13)	Ag(22)-S(23)	2.553(7)
Au(12)-N(12)	2.09(2)	Ag(22)-Br(21)	2.959(5)
Au(12)-S(11)	2.303(7)	Ag(22)-Br(22)	2.960(5)
Au(12)-S(12)	2.404(7)	Ag(23)-S(24)	2.487(7)
Au(13)-C(131)	2.079(12)	Ag(23)-S(26)	2.549(8)
Au(13)-N(13)	2.17(3)	Ag(23)-Br(22)	2.845(6)
Au(13)-S(13)	2.304(8)	Ag(23)-Br(21)	2.897(4)
Au(13)-S(14)	2.410(8)	N(11)-C(119)	1.51(3)
Au(14)-C(141)	2.046(13)	N(11)-C(117)	1.53(2)
Au(14)-N(14)	2.12(3)	N(11)-C(118)	1.56(3)
Au(14)-S(13)	2.304(8)	N(12)-C(127)	1.53(3)
Au(14)-S(14)	2.411(8)	N(12)-C(129)	1.56(3)
Au(15)-C(151)	2.077(15)	N(12)-C(128)	1.61(3)
Au(15)-N(15)	2.11(3)	N(13)-C(139)	1.46(3)
Au(15)-S(15)	2.302(8)	N(13)-C(137)	1.54(3)
Au(15)-S(16)	2.403(9)	N(13)-C(138)	1.60(4)
Au(16)-C(161)	2.047(15)	N(14)-C(149)	1.43(4)
Au(16)-N(16)	2.18(3)	N(14)-C(147)	1.55(3)
Au(16)-S(15)	2.296(9)	N(14)-C(148)	1.56(3)
Au(16)-S(16)	2.398(8)	N(15)-C(158)	1.43(3)
Au(21)-C(211)	2.094(13)	N(15)-C(159)	1.50(3)
Au(21)-N(21)	2.18(2)	N(15)-C(157)	1.59(3)
Au(21)-S(21)	2.301(9)	N(16)-C(169)	1.47(4)
Au(21)-S(22)	2.391(8)	N(16)-C(168)	1.57(3)
Au(22)-C(221)	2.060(16)	N(16)-C(167)	1.58(4)
Au(22)-N(22)	2.17(3)	N(21)-C(217)	1.38(3)
Au(22)-S(21)	2.308(8)	N(21)-C(218)	1.44(3)
Au(22)-S(22)	2.395(9)	N(21)-C(219)	1.49(3)
Au(23)-C(231)	2.068(13)	N(22)-C(227)	1.48(4)
Au(23)-N(23)	2.16(3)	N(22)-C(229)	1.52(4)
Au(23)-S(23)	2.289(7)	N(22)-C(228)	1.53(3)
Au(23)-S(24)	2.393(9)	N(23)-C(237)	1.44(4)
Au(24)-C(241)	2.073(12)	N(23)-C(239)	1.51(3)
Au(24)-N(24)	2.17(3)	N(23)-C(238)	1.53(3)
Au(24)-S(23)	2.291(8)	N(24)-C(248)	1.47(3)
Au(24)-S(24)	2.405(8)	N(24)-C(249)	1.50(3)

Au(25)-N(25)	1.85(6)	N(24)-C(247)	1.55(3)
Au(25)-C(251)	2.030(13)	N(25)-C(258)	1.52(4)
Au(25)-S(26)	2.298(10)	N(25)-C(259)	1.62(5)
Au(25)-S(25)	2.408(8)	N(25)-C(257)	1.71(5)
Au(26)-C(261)	2.088(15)	N(26)-C(269)	1.46(3)
Au(26)-N(26)	2.10(2)	N(26)-C(268)	1.51(3)
Au(26)-S(26)	2.282(8)	N(26)-C(267)	1.53(3)
Au(26)-S(25)	2.391(9)	C(112)-C(117)	1.5071
Ag(11)-S(12)	2.494(8)	C(122)-C(127)	1.6044
Ag(11)-S(13)	2.520(10)	C(132)-C(137)	1.4830
Ag(11)-Br(11)	2.929(5)	C(142)-C(147)	1.5339
Ag(11)-Br(12)	2.952(5)	C(152)-C(157)	1.4547
Ag(12)-S(14)	2.497(9)	C(162)-C(167)	1.4922
Ag(12)-S(15)	2.534(8)	C(212)-C(217)	1.6217
Ag(12)-Br(11)	2.865(5)	C(222)-C(227)	1.6226
Ag(12)-Br(12)	2.889(5)	C(232)-C(233)	1.3900
Ag(13)-S(16)	2.465(7)	C(232)-C(237)	1.5512
Ag(13)-S(11)	2.523(8)	C(242)-C(247)	1.5065
Ag(13)-Br(11)	2.921(5)	C(252)-C(257)	1.4251
Ag(13)-Br(12)	2.932(5)	C(262)-C(267)	1.5017
Ag(21)-S(25)	2.481(8)		

Table A.XII.2: Complete Bond Angles ($^{\circ}$) for **6.5d**, with *e.s.d.s* in parentheses

C(111)-Au(11)-N(11)	82.3(7)	Au(23)-S(23)-Au(24)	98.0(3)
C(111)-Au(11)-S(11)	94.3(4)	Au(23)-S(23)-Ag(22)	93.5(3)
N(11)-Au(11)-S(11)	176.4(6)	Au(24)-S(23)-Ag(22)	88.3(2)
C(111)-Au(11)-S(12)	177.6(5)	Au(23)-S(24)-Au(24)	92.2(3)
N(11)-Au(11)-S(12)	98.0(7)	Au(23)-S(24)-Ag(23)	95.7(3)
S(11)-Au(11)-S(12)	85.4(3)	Au(24)-S(24)-Ag(23)	93.1(3)
C(121)-Au(12)-N(12)	83.6(8)	Au(26)-S(25)-Au(25)	91.8(3)
C(121)-Au(12)-S(11)	93.0(4)	Au(26)-S(25)-Ag(21)	95.6(3)
N(12)-Au(12)-S(11)	176.1(7)	Au(25)-S(25)-Ag(21)	96.7(3)
C(121)-Au(12)-S(12)	176.1(5)	Au(26)-S(26)-Au(25)	97.6(3)
N(12)-Au(12)-S(12)	98.5(7)	Au(26)-S(26)-Ag(23)	95.5(3)
S(11)-Au(12)-S(12)	85.0(3)	Au(25)-S(26)-Ag(23)	93.5(3)
C(131)-Au(13)-N(13)	81.0(7)	C(119)-N(11)-C(117)	110.1(16)
C(131)-Au(13)-S(13)	94.4(4)	C(119)-N(11)-C(118)	116.0(15)
N(13)-Au(13)-S(13)	175.3(7)	C(117)-N(11)-C(118)	104.3(15)
C(131)-Au(13)-S(14)	178.6(5)	C(119)-N(11)-Au(11)	113.4(13)
N(13)-Au(13)-S(14)	99.7(7)	C(117)-N(11)-Au(11)	104.1(12)
S(13)-Au(13)-S(14)	84.9(3)	C(118)-N(11)-Au(11)	107.9(14)
C(141)-Au(14)-N(14)	81.3(9)	C(127)-N(12)-C(129)	108.1(19)
C(141)-Au(14)-S(13)	93.9(4)	C(127)-N(12)-C(128)	106.9(16)
N(14)-Au(14)-S(13)	175.1(8)	C(129)-N(12)-C(128)	108.0(16)
C(141)-Au(14)-S(14)	175.8(5)	C(127)-N(12)-Au(12)	110.2(14)
N(14)-Au(14)-S(14)	100.0(8)	C(129)-N(12)-Au(12)	115.8(15)
S(13)-Au(14)-S(14)	84.8(3)	C(128)-N(12)-Au(12)	107.5(16)
C(151)-Au(15)-N(15)	82.0(9)	C(139)-N(13)-C(137)	110(2)
C(151)-Au(15)-S(15)	95.7(4)	C(139)-N(13)-C(138)	110.2(19)
N(15)-Au(15)-S(15)	177.2(8)	C(137)-N(13)-C(138)	113.2(18)
C(151)-Au(15)-S(16)	176.5(5)	C(139)-N(13)-Au(13)	113.2(17)
N(15)-Au(15)-S(16)	97.3(8)	C(137)-N(13)-Au(13)	103.9(15)
S(15)-Au(15)-S(16)	85.1(3)	C(138)-N(13)-Au(13)	106.4(16)
C(161)-Au(16)-N(16)	82.7(10)	C(149)-N(14)-C(147)	110(2)

C(161)-Au(16)-S(15)	94.2(5)	C(149)-N(14)-C(148)	111.8(18)
N(16)-Au(16)-S(15)	176.7(9)	C(147)-N(14)-C(148)	104(2)
C(161)-Au(16)-S(16)	177.0(5)	C(149)-N(14)-Au(14)	113(2)
N(16)-Au(16)-S(16)	97.8(9)	C(147)-N(14)-Au(14)	105.5(14)
S(15)-Au(16)-S(16)	85.3(3)	C(148)-N(14)-Au(14)	112.0(19)
C(211)-Au(21)-N(21)	81.2(7)	C(158)-N(15)-C(159)	111(2)
C(211)-Au(21)-S(21)	95.6(4)	C(158)-N(15)-C(157)	113(2)
N(21)-Au(21)-S(21)	176.6(6)	C(159)-N(15)-C(157)	101.8(18)
C(211)-Au(21)-S(22)	179.5(5)	C(158)-N(15)-Au(15)	119.0(18)
N(21)-Au(21)-S(22)	98.6(6)	C(159)-N(15)-Au(15)	108.4(16)
S(21)-Au(21)-S(22)	84.6(3)	C(157)-N(15)-Au(15)	102.3(15)
C(221)-Au(22)-N(22)	81.7(9)	C(169)-N(16)-C(168)	107(2)
C(221)-Au(22)-S(21)	95.2(4)	C(169)-N(16)-C(167)	110(2)
N(22)-Au(22)-S(21)	176.8(8)	C(168)-N(16)-C(167)	111.9(19)
C(221)-Au(22)-S(22)	177.1(5)	C(169)-N(16)-Au(16)	116.7(18)
N(22)-Au(22)-S(22)	98.8(8)	C(168)-N(16)-Au(16)	106.1(17)
S(21)-Au(22)-S(22)	84.3(3)	C(167)-N(16)-Au(16)	105.6(18)
C(231)-Au(23)-N(23)	78.9(9)	C(217)-N(21)-C(218)	107.9(19)
C(231)-Au(23)-S(23)	95.3(4)	C(217)-N(21)-C(219)	109(2)
N(23)-Au(23)-S(23)	173.3(9)	C(218)-N(21)-C(219)	106.2(15)
C(231)-Au(23)-S(24)	178.0(4)	C(217)-N(21)-Au(21)	106.4(13)
N(23)-Au(23)-S(24)	100.8(8)	C(218)-N(21)-Au(21)	112.7(17)
S(23)-Au(23)-S(24)	85.1(3)	C(219)-N(21)-Au(21)	114.2(16)
C(241)-Au(24)-N(24)	81.4(8)	C(227)-N(22)-C(229)	111(2)
C(241)-Au(24)-S(23)	95.2(4)	C(227)-N(22)-C(228)	109(2)
N(24)-Au(24)-S(23)	176.5(8)	C(229)-N(22)-C(228)	113(2)
C(241)-Au(24)-S(24)	177.3(4)	C(227)-N(22)-Au(22)	108.0(18)
N(24)-Au(24)-S(24)	98.6(8)	C(229)-N(22)-Au(22)	107.5(19)
S(23)-Au(24)-S(24)	84.8(3)	C(228)-N(22)-Au(22)	108(2)
N(25)-Au(25)-C(251)	82.5(11)	C(237)-N(23)-C(239)	113(2)
N(25)-Au(25)-S(26)	176.8(9)	C(237)-N(23)-C(238)	117.0(19)
C(251)-Au(25)-S(26)	94.8(5)	C(239)-N(23)-C(238)	104(2)
N(25)-Au(25)-S(25)	98.0(10)	C(237)-N(23)-Au(23)	108.7(17)
C(251)-Au(25)-S(25)	176.4(5)	C(239)-N(23)-Au(23)	109.8(16)
S(26)-Au(25)-S(25)	84.8(3)	C(238)-N(23)-Au(23)	103.7(16)
C(261)-Au(26)-N(26)	80.7(8)	C(248)-N(24)-C(249)	111(2)
C(261)-Au(26)-S(26)	95.9(4)	C(248)-N(24)-C(247)	107.3(16)
N(26)-Au(26)-S(26)	176.1(8)	C(249)-N(24)-C(247)	111(2)
C(261)-Au(26)-S(25)	178.5(4)	C(248)-N(24)-Au(24)	115.0(19)
N(26)-Au(26)-S(25)	97.8(8)	C(249)-N(24)-Au(24)	107.4(14)
S(26)-Au(26)-S(25)	85.5(3)	C(247)-N(24)-Au(24)	104.5(15)
S(12)-Ag(11)-S(13)	129.5(3)	C(258)-N(25)-C(259)	103(3)
S(12)-Ag(11)-Br(11)	105.1(2)	C(258)-N(25)-C(257)	102(3)
S(13)-Ag(11)-Br(11)	109.6(2)	C(259)-N(25)-C(257)	100(3)
S(12)-Ag(11)-Br(12)	103.3(2)	C(258)-N(25)-Au(25)	124(3)
S(13)-Ag(11)-Br(12)	112.4(2)	C(259)-N(25)-Au(25)	113(3)
Br(11)-Ag(11)-Br(12)	89.36(13)	C(257)-N(25)-Au(25)	112(2)
S(14)-Ag(12)-S(15)	125.3(3)	C(269)-N(26)-C(268)	111.9(18)
S(14)-Ag(12)-Br(11)	106.0(2)	C(269)-N(26)-C(267)	104.6(19)
S(15)-Ag(12)-Br(11)	112.0(2)	C(268)-N(26)-C(267)	108(2)
S(14)-Ag(12)-Br(12)	107.6(2)	C(269)-N(26)-Au(26)	110.7(17)
S(15)-Ag(12)-Br(12)	108.9(2)	C(268)-N(26)-Au(26)	115.8(17)
Br(11)-Ag(12)-Br(12)	91.91(14)	C(267)-N(26)-Au(26)	105.0(14)
S(16)-Ag(13)-S(11)	131.1(3)	C(112)-C(111)-Au(11)	109.7(4)
S(16)-Ag(13)-Br(11)	108.2(2)	C(116)-C(111)-Au(11)	130.2(4)

S(11)-Ag(13)-Br(11)	106.0(2)	C(111)-C(112)-C(117)	119.8
S(16)-Ag(13)-Br(12)	109.5(2)	C(113)-C(112)-C(117)	120.1
S(11)-Ag(13)-Br(12)	104.42(19)	C(112)-C(117)-N(11)	108.5(10)
Br(11)-Ag(13)-Br(12)	89.91(14)	C(122)-C(121)-Au(12)	110.2(4)
S(25)-Ag(21)-S(21)	132.8(3)	C(126)-C(121)-Au(12)	129.5(5)
S(25)-Ag(21)-Br(22)	106.2(2)	C(121)-C(122)-C(127)	120.8
S(21)-Ag(21)-Br(22)	107.6(2)	C(123)-C(122)-C(127)	119.2
S(25)-Ag(21)-Br(21)	106.8(2)	N(12)-C(127)-C(122)	104.6(11)
S(21)-Ag(21)-Br(21)	105.6(2)	C(132)-C(131)-Au(13)	113.6(5)
Br(22)-Ag(21)-Br(21)	89.20(13)	C(136)-C(131)-Au(13)	126.2(5)
S(22)-Ag(22)-S(23)	129.6(3)	C(133)-C(132)-C(137)	123.5
S(22)-Ag(22)-Br(21)	104.2(2)	C(131)-C(132)-C(137)	116.4
S(23)-Ag(22)-Br(21)	112.7(2)	C(132)-C(137)-N(13)	110.5(11)
S(22)-Ag(22)-Br(22)	106.7(2)	C(142)-C(141)-Au(14)	112.6(5)
S(23)-Ag(22)-Br(22)	108.32(19)	C(146)-C(141)-Au(14)	127.3(5)
Br(21)-Ag(22)-Br(22)	86.98(14)	C(143)-C(142)-C(147)	122.3
S(24)-Ag(23)-S(26)	127.3(3)	C(141)-C(142)-C(147)	117.6
S(24)-Ag(23)-Br(22)	108.9(2)	C(142)-C(147)-N(14)	104.9(12)
S(26)-Ag(23)-Br(22)	107.9(2)	C(152)-C(151)-Au(15)	114.2(5)
S(24)-Ag(23)-Br(21)	110.7(2)	C(156)-C(151)-Au(15)	125.6(5)
S(26)-Ag(23)-Br(21)	105.4(2)	C(153)-C(152)-C(157)	125.7
Br(22)-Ag(23)-Br(21)	90.37(14)	C(151)-C(152)-C(157)	114.2
Ag(12)-Br(11)-Ag(13)	73.38(12)	C(152)-C(157)-N(15)	112.0(11)
Ag(12)-Br(11)-Ag(11)	74.37(12)	C(162)-C(161)-Au(16)	109.0(6)
Ag(13)-Br(11)-Ag(11)	78.66(12)	C(166)-C(161)-Au(16)	130.8(6)
Ag(12)-Br(12)-Ag(13)	72.87(12)	C(161)-C(162)-C(167)	125.9
Ag(12)-Br(12)-Ag(11)	73.68(12)	C(163)-C(162)-C(167)	114.1
Ag(13)-Br(12)-Ag(11)	78.13(11)	C(162)-C(167)-N(16)	105.6(13)
Ag(23)-Br(21)-Ag(21)	76.42(12)	C(212)-C(211)-Au(21)	110.6(6)
Ag(23)-Br(21)-Ag(22)	73.64(12)	C(216)-C(211)-Au(21)	129.4(6)
Ag(21)-Br(21)-Ag(22)	78.05(13)	C(213)-C(212)-C(217)	123.7
Ag(23)-Br(22)-Ag(21)	77.48(13)	C(211)-C(212)-C(217)	116.3
Ag(23)-Br(22)-Ag(22)	74.36(13)	N(21)-C(217)-C(212)	109.6(11)
Ag(21)-Br(22)-Ag(22)	78.28(12)	C(222)-C(221)-Au(22)	111.0(6)
Au(11)-S(11)-Au(12)	97.3(3)	C(226)-C(221)-Au(22)	128.9(6)
Au(11)-S(11)-Ag(13)	95.8(3)	C(223)-C(222)-C(227)	120.4
Au(12)-S(11)-Ag(13)	93.4(3)	C(221)-C(222)-C(227)	119.2
Au(11)-S(12)-Au(12)	92.1(3)	N(22)-C(227)-C(222)	102.6(12)
Au(11)-S(12)-Ag(11)	97.7(3)	C(232)-C(231)-Au(23)	113.0(5)
Au(12)-S(12)-Ag(11)	95.2(3)	C(236)-C(231)-Au(23)	127.0(5)
Au(13)-S(13)-Au(14)	97.9(3)	C(231)-C(232)-C(237)	117.2
Au(13)-S(13)-Ag(11)	88.6(3)	C(233)-C(232)-C(237)	122.8
Au(14)-S(13)-Ag(11)	92.6(3)	N(23)-C(237)-C(232)	106.1(12)
Au(13)-S(14)-Au(14)	92.3(3)	C(242)-C(241)-Au(24)	112.1(5)
Au(13)-S(14)-Ag(12)	95.3(3)	C(246)-C(241)-Au(24)	127.9(5)
Au(14)-S(14)-Ag(12)	97.8(3)	C(243)-C(242)-C(247)	120.6
Au(16)-S(15)-Au(15)	97.4(3)	C(241)-C(242)-C(247)	119.1
Au(16)-S(15)-Ag(12)	93.3(3)	C(242)-C(247)-N(24)	107.7(11)
Au(15)-S(15)-Ag(12)	90.4(3)	C(252)-C(251)-Au(25)	113.8(6)
Au(16)-S(16)-Au(15)	92.1(3)	C(256)-C(251)-Au(25)	126.1(6)
Au(16)-S(16)-Ag(13)	94.0(3)	C(251)-C(252)-C(257)	118.0
Au(15)-S(16)-Ag(13)	95.7(3)	C(253)-C(252)-C(257)	121.7
Au(21)-S(21)-Au(22)	97.9(3)	C(252)-C(257)-N(25)	101.9(16)
Au(21)-S(21)-Ag(21)	94.2(3)	C(262)-C(261)-Au(26)	113.6(5)
Au(22)-S(21)-Ag(21)	92.2(3)	C(266)-C(261)-Au(26)	126.4(5)

Au(21)-S(22)-Au(22)	93.2(3)	C(261)-C(262)-C(267)	114.8
Au(21)-S(22)-Ag(22)	96.2(3)	C(263)-C(262)-C(267)	125.2
Au(22)-S(22)-Ag(22)	93.3(3)	C(262)-C(267)-N(26)	110.6(11)

Table A.XII.3: Final Positional (fractional co-ordinates) and Equivalent Thermal Parameters for **6.5d**, with *e.s.d.s* in parentheses

Atom	X/A	Y/B	Z/C	U(eq)
Au(11)	0.7237(1)	0.0573(1)	0.1415(1)	0.030(1)
Au(12)	0.6557(1)	0.1488(1)	0.0592(1)	0.032(1)
Au(13)	0.4667(1)	0.2637(1)	0.2607(1)	0.038(1)
Au(14)	0.3977(1)	0.3569(1)	0.1784(1)	0.039(1)
Au(15)	0.1429(1)	0.1471(1)	0.1271(1)	0.036(1)
Au(16)	0.2134(1)	0.0519(1)	0.2075(1)	0.039(1)
Au(21)	0.3784(1)	0.7125(1)	0.2765(1)	0.039(1)
Au(22)	0.4038(1)	0.8163(1)	0.3533(1)	0.043(1)
Au(23)	0.5521(1)	0.6020(1)	0.4664(1)	0.034(1)
Au(24)	0.5217(1)	0.4995(1)	0.3904(1)	0.033(1)
Au(25)	0.9163(1)	0.7161(1)	0.3379(1)	0.044(1)
Au(26)	0.8866(1)	0.6147(1)	0.2616(1)	0.038(1)
Ag(11)	0.5768(3)	0.2164(2)	0.1624(1)	0.061(1)
Ag(12)	0.2894(3)	0.2040(2)	0.1960(1)	0.064(1)
Ag(13)	0.4356(2)	0.0895(2)	0.1276(1)	0.062(1)
Ag(21)	0.6481(2)	0.7286(2)	0.3002(1)	0.054(1)
Ag(22)	0.4426(3)	0.6533(2)	0.3764(1)	0.067(1)
Ag(23)	0.7327(3)	0.6012(2)	0.3652(1)	0.063(1)
Br(11)	0.3981(3)	0.2236(2)	0.1121(1)	0.051(1)
Br(12)	0.4759(3)	0.1144(2)	0.2113(1)	0.047(1)
Br(21)	0.5958(3)	0.6007(2)	0.3009(1)	0.048(1)
Br(22)	0.6277(3)	0.7233(2)	0.3900(1)	0.056(1)
S(11)	0.6289(6)	0.0517(4)	0.0870(2)	0.032(2)
S(12)	0.7476(6)	0.1611(4)	0.1175(2)	0.036(2)
S(13)	0.5561(6)	0.3153(4)	0.2042(2)	0.043(2)
S(14)	0.2961(6)	0.3015(4)	0.2349(2)	0.043(2)
S(15)	0.1163(7)	0.1484(4)	0.1988(2)	0.042(2)
S(16)	0.2534(6)	0.0477(4)	0.1329(3)	0.041(2)
S(21)	0.4739(6)	0.7961(4)	0.2837(2)	0.041(2)
S(22)	0.3003(7)	0.7300(4)	0.3485(2)	0.041(2)
S(23)	0.4124(6)	0.5731(4)	0.4347(2)	0.033(2)
S(24)	0.6748(6)	0.5263(4)	0.4216(2)	0.040(2)
S(25)	0.8528(6)	0.7253(4)	0.2720(2)	0.042(2)
S(26)	0.9323(7)	0.6103(4)	0.3266(3)	0.047(2)
N(11)	0.8069(17)	0.0576(11)	0.1941(7)	0.031(6)
N(12)	0.670(2)	0.2367(12)	0.0322(7)	0.038(6)
N(13)	0.395(2)	0.2143(13)	0.3157(8)	0.047(7)
N(14)	0.261(2)	0.3990(15)	0.1507(9)	0.054(8)
N(15)	0.167(2)	0.1508(14)	0.0614(8)	0.045(7)
N(16)	0.306(3)	-0.0381(12)	0.2195(10)	0.058(9)
N(21)	0.2955(18)	0.6319(11)	0.2664(7)	0.031(5)
N(22)	0.342(3)	0.8399(14)	0.4183(10)	0.060(8)
N(23)	0.672(2)	0.6397(15)	0.4973(7)	0.051(8)
N(24)	0.616(2)	0.4277(12)	0.3479(7)	0.041(7)
N(25)	0.902(3)	0.800(3)	0.3502(11)	0.15(3)
N(26)	0.852(2)	0.6133(13)	0.2006(7)	0.042(7)

C(111)	0.7085(12)	-0.0348(6)	0.1607(4)	0.045(9)
C(112)	0.7253(9)	-0.0421(6)	0.2017(4)	0.039(8)
C(113)	0.7250(15)	-0.1005(6)	0.2205(5)	0.050(9)
C(114)	0.7079(16)	-0.1516(6)	0.1983(6)	0.059(11)
C(115)	0.6911(15)	-0.1444(6)	0.1573(6)	0.076(13)
C(116)	0.6914(16)	-0.0860(7)	0.1385(5)	0.049(9)
C(117)	0.7466(12)	0.0132(6)	0.2253(4)	0.037(8)
C(118)	0.9292(10)	0.0232(8)	0.1812(7)	0.055(10)
C(119)	0.7975(17)	0.1216(7)	0.2135(6)	0.046(9)
C(121)	0.5843(12)	0.1329(6)	0.0076(4)	0.036(8)
C(122)	0.5580(10)	0.1889(6)	-0.0124(4)	0.053(10)
C(123)	0.5176(15)	0.1888(9)	-0.0497(5)	0.076(14)
C(124)	0.5035(17)	0.1326(10)	-0.0669(5)	0.092(18)
C(125)	0.5298(15)	0.0766(9)	-0.0469(5)	0.063(11)
C(126)	0.5702(16)	0.0768(6)	-0.0096(5)	0.040(9)
C(127)	0.5774(15)	0.2541(6)	0.0062(5)	0.061(11)
C(128)	0.7891(14)	0.2319(10)	0.0006(7)	0.059(10)
C(129)	0.666(2)	0.2914(9)	0.0631(6)	0.057(10)
C(131)	0.6147(10)	0.2334(8)	0.2830(4)	0.042(8)
C(132)	0.6018(11)	0.1881(6)	0.3138(4)	0.047(9)
C(133)	0.6915(12)	0.1667(8)	0.3339(5)	0.062(11)
C(134)	0.7940(11)	0.1906(10)	0.3230(6)	0.055(10)
C(135)	0.8068(10)	0.2359(9)	0.2921(6)	0.058(11)
C(136)	0.7172(11)	0.2573(9)	0.2721(6)	0.056(10)
C(137)	0.4915(13)	0.1631(8)	0.3221(6)	0.063(12)
C(138)	0.3634(11)	0.2646(11)	0.3528(7)	0.054(10)
C(139)	0.2955(12)	0.1856(13)	0.3105(8)	0.080(15)
C(141)	0.4860(11)	0.4085(7)	0.1336(5)	0.074(14)
C(142)	0.4248(12)	0.4290(7)	0.1026(4)	0.065(12)
C(143)	0.4706(15)	0.4669(10)	0.0707(5)	0.103(18)
C(144)	0.5776(16)	0.4842(10)	0.0697(6)	0.081(14)
C(145)	0.6388(13)	0.4637(10)	0.1007(7)	0.072(12)
C(146)	0.5930(12)	0.4258(10)	0.1326(6)	0.067(13)
C(147)	0.3105(13)	0.4049(10)	0.1037(5)	0.046(9)
C(148)	0.1680(14)	0.3555(12)	0.1520(8)	0.071(13)
C(149)	0.2156(13)	0.4596(11)	0.1676(7)	0.063(11)
C(151)	0.0395(13)	0.2302(7)	0.1215(4)	0.069(13)
C(152)	0.0539(11)	0.2555(7)	0.0817(4)	0.063(12)
C(153)	-0.0167(16)	0.3082(8)	0.0728(5)	0.063(12)
C(154)	-0.1016(15)	0.3355(8)	0.1038(6)	0.088(15)
C(155)	-0.1160(14)	0.3102(9)	0.1437(6)	0.056(10)
C(156)	-0.0454(16)	0.2576(9)	0.1526(4)	0.046(8)
C(157)	0.1486(12)	0.2239(8)	0.0528(5)	0.049(9)
C(158)	0.2691(17)	0.1202(10)	0.0378(7)	0.070(13)
C(159)	0.0660(17)	0.1297(9)	0.0478(7)	0.094(17)
C(161)	0.1712(14)	0.0541(8)	0.2711(5)	0.061(12)
C(162)	0.2484(12)	0.0123(8)	0.2878(5)	0.071(13)
C(163)	0.2434(18)	0.0089(11)	0.3307(5)	0.101(19)
C(164)	0.161(2)	0.0472(12)	0.3569(5)	0.14(3)
C(165)	0.0837(17)	0.0891(10)	0.3403(6)	0.085(15)
C(166)	0.0888(16)	0.0925(9)	0.2974(6)	0.059(10)
C(167)	0.3410(13)	-0.0315(10)	0.2635(6)	0.067(12)
C(168)	0.2221(19)	-0.0875(10)	0.2201(8)	0.12(2)
C(169)	0.4074(19)	-0.0597(13)	0.1885(6)	0.074(13)
C(211)	0.4454(12)	0.6974(7)	0.2133(4)	0.034(7)

C(212)	0.4329(11)	0.6376(6)	0.2015(4)	0.040(8)
C(213)	0.4729(17)	0.6177(8)	0.1607(5)	0.069(12)
C(214)	0.5253(17)	0.6576(11)	0.1317(4)	0.13(3)
C(215)	0.5378(15)	0.7175(10)	0.1434(5)	0.052(10)
C(216)	0.4978(16)	0.7374(8)	0.1842(5)	0.051(9)
C(217)	0.3714(15)	0.5944(8)	0.2376(5)	0.058(11)
C(218)	0.1939(11)	0.6486(13)	0.2492(7)	0.13(3)
C(219)	0.2622(19)	0.5948(13)	0.3048(5)	0.058(11)
C(221)	0.4867(14)	0.8933(7)	0.3561(4)	0.047(9)
C(222)	0.4805(15)	0.9116(7)	0.3971(4)	0.072(14)
C(223)	0.527(2)	0.9646(10)	0.4056(5)	0.10(2)
C(224)	0.579(2)	0.9993(10)	0.3731(7)	0.15(3)
C(225)	0.5852(18)	0.9810(9)	0.3321(6)	0.059(11)
C(226)	0.5390(17)	0.9280(9)	0.3236(4)	0.055(10)
C(227)	0.4330(19)	0.8661(10)	0.4346(4)	0.078(14)
C(228)	0.317(2)	0.7799(10)	0.4423(8)	0.077(14)
C(229)	0.2386(14)	0.8881(12)	0.4202(9)	0.091(17)
C(231)	0.4461(10)	0.6652(6)	0.5068(4)	0.025(6)
C(232)	0.5033(11)	0.7082(6)	0.5229(4)	0.046(8)
C(233)	0.4441(14)	0.7533(7)	0.5510(5)	0.056(10)
C(234)	0.3278(14)	0.7554(8)	0.5631(5)	0.084(16)
C(235)	0.2706(11)	0.7124(9)	0.5470(5)	0.053(9)
C(236)	0.3297(10)	0.6673(8)	0.5188(5)	0.049(9)
C(237)	0.6324(11)	0.7046(7)	0.5068(5)	0.042(8)
C(238)	0.6814(12)	0.5957(9)	0.5342(6)	0.055(11)
C(239)	0.7875(11)	0.6304(11)	0.4705(6)	0.070(13)
C(241)	0.3884(11)	0.4733(6)	0.3657(4)	0.040(8)
C(242)	0.4252(12)	0.4387(6)	0.3293(4)	0.058(10)
C(243)	0.3471(16)	0.4186(8)	0.3078(5)	0.067(12)
C(244)	0.2320(15)	0.4329(9)	0.3228(7)	0.076(15)
C(245)	0.1952(11)	0.4674(8)	0.3592(6)	0.080(16)
C(246)	0.2734(11)	0.4876(8)	0.3807(5)	0.042(9)
C(247)	0.5495(13)	0.4296(9)	0.3111(4)	0.049(9)
C(248)	0.7325(11)	0.4383(13)	0.3304(8)	0.105(19)
C(249)	0.6131(14)	0.3664(10)	0.3707(7)	0.055(10)
C(251)	0.9800(12)	0.7077(8)	0.3916(5)	0.060(12)
C(252)	0.9594(11)	0.7620(8)	0.4153(4)	0.054(10)
C(253)	1.0009(18)	0.7634(11)	0.4523(5)	0.089(17)
C(254)	1.0631(18)	0.7106(12)	0.4655(5)	0.077(14)
C(255)	1.0838(14)	0.6563(10)	0.4418(6)	0.084(17)
C(256)	1.0422(15)	0.6548(8)	0.4048(6)	0.10(2)
C(257)	0.8857(14)	0.8129(9)	0.4028(5)	0.084(15)
C(258)	0.810(2)	0.8487(10)	0.3383(8)	0.083(15)
C(259)	1.016(2)	0.8315(10)	0.3343(6)	0.080(13)
C(261)	0.9148(12)	0.5184(7)	0.2511(4)	0.034(7)
C(262)	0.8670(10)	0.4998(7)	0.2184(4)	0.059(11)
C(263)	0.8775(16)	0.4369(7)	0.2082(6)	0.070(12)
C(264)	0.9358(16)	0.3926(6)	0.2307(7)	0.057(10)
C(265)	0.9836(14)	0.4112(8)	0.2633(6)	0.062(12)
C(266)	0.9731(15)	0.4741(9)	0.2735(5)	0.069(12)
C(267)	0.8031(13)	0.5518(8)	0.1976(5)	0.058(10)
C(268)	0.768(2)	0.6660(9)	0.1897(7)	0.059(10)
C(269)	0.9573(17)	0.6069(9)	0.1701(6)	0.068(12)

Table A.XII.4: Thermal Parameters for **6.5d**, with *e.s.d.s* in parentheses

Atom	U11	U22	U33	U23	U13	U12
Au(11)	0.0200(5)	0.0405(7)	0.0305(6)	-0.0030(5)	-0.0028(4)	-0.0098(5)
Au(12)	0.0246(6)	0.0424(7)	0.0292(6)	-0.0034(5)	-0.0035(4)	-0.0095(5)
Au(13)	0.0283(6)	0.0511(8)	0.0371(6)	-0.0086(6)	-0.0032(5)	-0.0106(6)
Au(14)	0.0261(6)	0.0485(8)	0.0423(7)	-0.0109(6)	-0.0008(5)	-0.0075(5)
Au(15)	0.0200(5)	0.0486(7)	0.0396(6)	-0.0026(6)	-0.0052(5)	-0.0102(5)
Au(16)	0.0194(6)	0.0529(8)	0.0474(7)	0.0059(6)	-0.0069(5)	-0.0115(5)
Au(21)	0.0205(5)	0.0579(8)	0.0371(6)	0.0140(6)	-0.0033(5)	-0.0065(5)
Au(22)	0.0329(6)	0.0546(8)	0.0361(6)	0.0114(6)	0.0001(5)	0.0004(6)
Au(23)	0.0265(6)	0.0534(8)	0.0248(5)	0.0028(5)	-0.0062(4)	-0.0167(5)
Au(24)	0.0297(6)	0.0435(7)	0.0259(5)	-0.0005(5)	-0.0006(4)	-0.0096(5)
Au(25)	0.0229(6)	0.0745(10)	0.0364(6)	0.0057(7)	-0.0096(5)	-0.0113(6)
Au(26)	0.0204(6)	0.0564(8)	0.0357(6)	0.0034(6)	-0.0018(5)	-0.0020(5)
Ag(11)	0.0604(19)	0.070(2)	0.0465(15)	-0.0143(15)	-0.0042(13)	0.0129(15)
Ag(12)	0.069(2)	0.069(2)	0.0664(19)	-0.0009(16)	-0.0285(16)	-0.0321(17)
Ag(13)	0.0241(13)	0.099(2)	0.0651(17)	0.0179(17)	-0.0065(12)	-0.0184(14)
Ag(21)	0.0277(13)	0.076(2)	0.0588(16)	-0.0042(15)	-0.0092(12)	-0.0046(13)
Ag(22)	0.080(2)	0.068(2)	0.0591(18)	0.0068(16)	-0.0330(16)	-0.0044(17)
Ag(23)	0.0558(18)	0.091(2)	0.0453(15)	0.0089(16)	0.0005(13)	-0.0346(17)
Br(11)	0.0336(18)	0.065(2)	0.053(2)	-0.0094(18)	-0.0025(15)	-0.0047(16)
Br(12)	0.0312(16)	0.065(2)	0.0476(18)	-0.0027(17)	-0.0063(14)	-0.0124(16)
Br(21)	0.0342(17)	0.064(2)	0.0481(18)	0.0065(17)	-0.0090(14)	-0.0092(16)
Br(22)	0.043(2)	0.079(3)	0.0471(19)	0.0125(19)	-0.0095(15)	-0.0111(19)
S(11)	0.024(4)	0.045(4)	0.030(4)	-0.009(3)	-0.005(3)	-0.011(3)
S(12)	0.022(4)	0.048(5)	0.039(4)	-0.005(4)	-0.005(3)	-0.012(3)
S(13)	0.025(4)	0.061(5)	0.043(4)	-0.002(4)	-0.002(3)	-0.016(4)
S(14)	0.025(4)	0.059(5)	0.043(4)	-0.011(4)	0.003(3)	-0.010(4)
S(15)	0.032(4)	0.055(5)	0.039(4)	0.001(4)	-0.010(3)	-0.007(4)
S(16)	0.022(4)	0.049(5)	0.053(5)	-0.005(4)	-0.006(3)	-0.014(3)
S(21)	0.024(4)	0.052(5)	0.043(4)	0.014(4)	0.006(3)	-0.003(3)
S(22)	0.032(4)	0.058(5)	0.032(4)	0.009(4)	-0.002(3)	-0.005(4)
S(23)	0.019(3)	0.051(5)	0.030(4)	-0.002(3)	-0.004(3)	-0.010(3)
S(24)	0.023(4)	0.068(6)	0.031(4)	0.008(4)	-0.002(3)	-0.015(4)
S(25)	0.023(4)	0.065(6)	0.040(4)	0.009(4)	-0.009(3)	-0.006(4)
S(26)	0.033(4)	0.064(6)	0.044(4)	0.016(4)	-0.008(4)	-0.012(4)
N(11)	0.009(10)	0.043(15)	0.037(13)	0.001(12)	0.001(9)	0.003(10)
N(12)	0.031(14)	0.046(16)	0.037(13)	0.001(12)	-0.001(11)	-0.013(12)
N(13)	0.033(15)	0.063(19)	0.051(16)	0.006(15)	-0.019(13)	-0.017(14)
N(14)	0.019(13)	0.08(2)	0.053(17)	-0.020(16)	0.001(12)	0.017(14)
N(15)	0.030(14)	0.068(19)	0.041(15)	-0.008(14)	-0.011(12)	-0.017(14)
N(16)	0.06(2)	0.030(15)	0.09(2)	0.039(16)	-0.036(18)	-0.013(14)
N(21)	0.012(11)	0.044(15)	0.036(13)	-0.007(12)	-0.001(10)	-0.005(10)
N(22)	0.06(2)	0.051(19)	0.07(2)	0.005(17)	-0.023(17)	-0.009(16)
N(23)	0.06(2)	0.08(2)	0.018(12)	-0.006(13)	-0.006(12)	-0.028(17)
N(24)	0.060(18)	0.040(15)	0.019(11)	0.001(11)	0.001(12)	-0.003(13)
N(25)	0.020(16)	0.33(7)	0.08(2)	0.13(4)	0.006(16)	0.03(3)
N(26)	0.050(16)	0.059(18)	0.017(11)	-0.023(12)	-0.006(11)	0.002(14)
C(111)	0.028(16)	0.022(16)	0.08(2)	0.041(17)	0.006(15)	-0.006(13)
C(112)	0.036(17)	0.043(18)	0.041(17)	0.036(16)	-0.006(13)	-0.018(14)
C(113)	0.031(18)	0.05(2)	0.07(2)	-0.021(18)	0.007(16)	-0.023(16)
C(114)	0.05(2)	0.06(3)	0.06(2)	0.03(2)	0.005(17)	-0.003(18)
C(115)	0.07(3)	0.05(3)	0.11(4)	0.00(3)	0.00(3)	-0.02(2)

C(116)	0.034(18)	0.04(2)	0.07(2)	-0.001(18)	-0.006(16)	-0.016(16)
C(117)	0.036(16)	0.05(2)	0.020(13)	0.021(14)	-0.013(12)	0.004(15)
C(118)	0.003(13)	0.08(3)	0.08(3)	-0.03(2)	-0.027(15)	0.011(15)
C(119)	0.030(16)	0.09(3)	0.033(16)	0.003(17)	-0.031(13)	-0.039(18)
C(121)	0.047(18)	0.049(19)	0.009(12)	0.017(13)	0.008(12)	-0.014(15)
C(122)	0.038(19)	0.08(3)	0.05(2)	-0.005(19)	-0.007(15)	-0.042(19)
C(123)	0.13(4)	0.08(3)	0.026(17)	0.013(19)	-0.03(2)	-0.02(3)
C(124)	0.002(14)	0.17(5)	0.11(4)	-0.08(4)	-0.018(18)	0.00(2)
C(125)	0.06(3)	0.08(3)	0.05(2)	-0.03(2)	-0.001(19)	-0.03(2)
C(126)	0.049(19)	0.050(19)	0.020(14)	-0.042(13)	0.030(13)	-0.043(16)
C(127)	0.033(19)	0.05(2)	0.10(3)	0.02(2)	-0.03(2)	-0.011(17)
C(128)	0.07(3)	0.05(2)	0.045(19)	0.007(18)	0.012(18)	-0.02(2)
C(129)	0.10(3)	0.031(19)	0.05(2)	0.004(16)	-0.03(2)	-0.03(2)
C(131)	0.019(15)	0.06(2)	0.051(19)	0.008(17)	-0.023(14)	-0.012(15)
C(132)	0.06(2)	0.05(2)	0.038(17)	0.003(16)	-0.014(16)	-0.020(18)
C(133)	0.07(3)	0.04(2)	0.07(3)	-0.014(19)	-0.01(2)	0.031(19)
C(134)	0.04(2)	0.06(2)	0.07(2)	-0.03(2)	-0.034(19)	-0.005(18)
C(135)	0.008(14)	0.06(2)	0.10(3)	-0.04(2)	-0.011(16)	0.009(15)
C(136)	0.037(19)	0.08(3)	0.05(2)	0.01(2)	-0.009(16)	-0.020(19)
C(137)	0.08(3)	0.05(2)	0.08(3)	0.03(2)	-0.05(2)	-0.03(2)
C(138)	0.06(2)	0.08(3)	0.020(15)	0.005(17)	0.002(15)	-0.02(2)
C(139)	0.05(2)	0.12(4)	0.09(3)	0.04(3)	-0.03(2)	-0.05(3)
C(141)	0.08(3)	0.03(2)	0.08(3)	0.01(2)	0.04(2)	0.006(19)
C(142)	0.04(2)	0.10(3)	0.036(18)	0.01(2)	0.014(16)	0.03(2)
C(143)	0.10(4)	0.07(3)	0.12(4)	0.04(3)	-0.02(3)	0.03(3)
C(144)	0.05(3)	0.10(4)	0.07(3)	0.03(3)	0.02(2)	-0.02(3)
C(145)	0.10(3)	0.07(3)	0.06(2)	-0.01(2)	-0.03(2)	-0.04(3)
C(146)	0.06(2)	0.04(2)	0.09(3)	-0.014(19)	0.05(2)	-0.034(18)
C(147)	0.030(17)	0.07(2)	0.046(18)	0.014(18)	-0.014(14)	-0.025(17)
C(148)	0.013(16)	0.14(4)	0.06(2)	-0.02(3)	-0.009(15)	-0.02(2)
C(149)	0.06(3)	0.04(2)	0.08(3)	0.00(2)	0.00(2)	0.015(19)
C(151)	0.05(2)	0.11(3)	0.06(2)	0.04(2)	-0.027(19)	-0.06(2)
C(152)	0.05(2)	0.10(3)	0.05(2)	-0.03(2)	0.004(17)	-0.06(2)
C(153)	0.031(19)	0.10(3)	0.06(2)	0.02(2)	-0.018(17)	-0.01(2)
C(154)	0.04(2)	0.12(4)	0.10(4)	0.02(3)	-0.02(2)	-0.03(3)
C(155)	0.029(18)	0.05(2)	0.09(3)	-0.02(2)	-0.021(19)	-0.003(16)
C(156)	0.038(18)	0.05(2)	0.042(18)	-0.042(16)	-0.005(15)	0.015(16)
C(157)	0.036(18)	0.040(19)	0.06(2)	0.020(18)	0.005(16)	-0.001(15)
C(158)	0.022(17)	0.10(3)	0.09(3)	0.04(3)	-0.015(18)	-0.009(19)
C(159)	0.06(3)	0.16(5)	0.06(3)	-0.02(3)	0.00(2)	0.00(3)
C(161)	0.04(2)	0.09(3)	0.06(2)	0.04(2)	-0.013(17)	-0.04(2)
C(162)	0.04(2)	0.12(4)	0.05(2)	0.01(2)	-0.021(17)	0.03(2)
C(163)	0.05(3)	0.16(5)	0.09(3)	-0.06(4)	-0.03(2)	0.03(3)
C(164)	0.09(4)	0.24(8)	0.10(4)	0.10(5)	-0.07(3)	-0.03(4)
C(165)	0.07(3)	0.12(4)	0.06(3)	0.01(3)	-0.03(2)	0.02(3)
C(166)	0.04(2)	0.09(3)	0.05(2)	0.01(2)	-0.012(17)	-0.01(2)
C(167)	0.04(2)	0.12(4)	0.04(2)	0.01(2)	-0.012(17)	-0.05(2)
C(168)	0.03(2)	0.07(3)	0.24(7)	0.09(4)	-0.01(3)	-0.01(2)
C(169)	0.04(2)	0.11(4)	0.08(3)	0.01(3)	-0.02(2)	-0.02(2)
C(211)	0.013(13)	0.046(18)	0.044(17)	-0.018(15)	-0.018(12)	0.007(12)
C(212)	0.028(16)	0.06(2)	0.045(18)	-0.006(16)	-0.021(14)	-0.024(15)
C(213)	0.05(2)	0.11(3)	0.06(2)	-0.01(2)	-0.004(19)	-0.03(2)
C(214)	0.04(3)	0.30(9)	0.03(2)	0.03(4)	-0.011(19)	-0.02(4)
C(215)	0.07(2)	0.07(3)	0.028(17)	-0.019(17)	-0.012(16)	-0.04(2)
C(216)	0.04(2)	0.08(3)	0.035(17)	0.013(18)	-0.015(15)	-0.014(19)

C(217)	0.06(2)	0.05(2)	0.06(2)	0.04(2)	-0.015(19)	-0.021(19)
C(218)	0.04(2)	0.28(8)	0.08(3)	0.06(4)	-0.01(2)	-0.06(4)
C(219)	0.038(19)	0.10(3)	0.038(18)	0.00(2)	-0.004(15)	-0.03(2)
C(221)	0.06(2)	0.04(2)	0.020(14)	-0.008(14)	0.005(14)	0.031(17)
C(222)	0.13(4)	0.05(2)	0.024(17)	-0.040(16)	0.03(2)	-0.01(2)
C(223)	0.18(6)	0.06(3)	0.06(3)	-0.05(2)	0.03(3)	-0.03(3)
C(224)	0.24(8)	0.11(4)	0.08(4)	0.06(3)	0.04(4)	-0.06(5)
C(225)	0.06(3)	0.04(2)	0.06(2)	-0.029(19)	0.02(2)	-0.014(19)
C(226)	0.05(2)	0.05(2)	0.05(2)	0.018(19)	-0.011(17)	0.006(18)
C(227)	0.09(3)	0.10(3)	0.04(2)	0.01(2)	0.02(2)	-0.03(3)
C(228)	0.10(3)	0.04(2)	0.07(3)	0.05(2)	0.02(2)	0.01(2)
C(229)	0.08(3)	0.10(3)	0.06(3)	0.01(3)	0.03(2)	0.05(3)
C(231)	0.046(17)	0.028(15)	0.007(11)	-0.015(10)	-0.017(11)	-0.012(13)
C(232)	0.05(2)	0.05(2)	0.031(16)	-0.021(15)	0.003(15)	-0.025(18)
C(233)	0.05(2)	0.06(2)	0.06(2)	0.01(2)	-0.022(19)	0.000(19)
C(234)	0.16(5)	0.06(3)	0.04(2)	0.01(2)	-0.05(3)	-0.03(3)
C(235)	0.07(3)	0.07(2)	0.017(14)	-0.025(16)	-0.003(15)	-0.01(2)
C(236)	0.07(2)	0.04(2)	0.040(18)	0.019(16)	-0.020(17)	0.003(17)
C(237)	0.06(2)	0.039(19)	0.023(14)	0.009(14)	0.004(14)	-0.010(16)
C(238)	0.024(16)	0.12(3)	0.025(15)	0.018(19)	-0.008(13)	-0.029(19)
C(239)	0.034(19)	0.14(4)	0.05(2)	0.02(2)	-0.009(16)	-0.07(2)
C(241)	0.07(2)	0.028(16)	0.031(15)	-0.011(13)	-0.020(16)	-0.036(16)
C(242)	0.06(2)	0.06(2)	0.06(2)	0.00(2)	-0.03(2)	-0.01(2)
C(243)	0.06(3)	0.07(3)	0.08(3)	0.02(2)	-0.04(2)	-0.01(2)
C(244)	0.14(4)	0.03(2)	0.09(3)	0.01(2)	-0.07(3)	-0.03(2)
C(245)	0.11(4)	0.015(17)	0.14(4)	0.02(2)	-0.08(3)	-0.05(2)
C(246)	0.026(15)	0.06(2)	0.053(19)	0.033(17)	-0.011(13)	-0.036(15)
C(247)	0.07(2)	0.06(2)	0.014(13)	-0.009(15)	-0.003(14)	-0.001(19)
C(248)	0.06(3)	0.19(6)	0.05(2)	-0.05(3)	0.04(2)	-0.01(3)
C(249)	0.06(2)	0.030(18)	0.07(2)	0.005(18)	-0.002(19)	-0.001(16)
C(251)	0.035(19)	0.11(3)	0.040(19)	0.04(2)	-0.014(15)	-0.02(2)
C(252)	0.04(2)	0.07(3)	0.06(2)	-0.02(2)	-0.035(18)	-0.01(2)
C(253)	0.06(3)	0.18(5)	0.04(2)	-0.01(3)	-0.001(19)	-0.06(3)
C(254)	0.05(2)	0.07(3)	0.12(4)	-0.02(3)	-0.05(3)	0.03(2)
C(255)	0.007(15)	0.18(5)	0.06(2)	0.05(3)	-0.003(15)	-0.02(2)
C(256)	0.030(19)	0.26(6)	0.04(2)	0.07(3)	-0.032(16)	-0.10(3)
C(257)	0.06(3)	0.09(3)	0.08(3)	-0.02(3)	0.04(2)	-0.01(3)
C(258)	0.07(3)	0.09(3)	0.10(3)	-0.09(3)	-0.05(3)	0.00(2)
C(259)	0.08(3)	0.07(3)	0.09(3)	0.02(3)	-0.02(3)	0.01(2)
C(261)	0.012(13)	0.038(17)	0.047(17)	-0.013(14)	0.007(12)	-0.004(12)
C(262)	0.014(15)	0.07(3)	0.09(3)	0.00(2)	-0.003(17)	0.002(16)
C(263)	0.03(2)	0.10(3)	0.07(3)	-0.01(3)	0.013(18)	0.00(2)
C(264)	0.04(2)	0.08(3)	0.06(2)	-0.01(2)	0.009(17)	-0.03(2)
C(265)	0.014(15)	0.06(2)	0.09(3)	0.02(2)	0.043(17)	0.005(15)
C(266)	0.03(2)	0.09(3)	0.08(3)	0.03(3)	0.001(18)	-0.03(2)
C(267)	0.04(2)	0.07(3)	0.06(2)	-0.03(2)	-0.025(18)	0.027(19)
C(268)	0.06(3)	0.07(3)	0.040(19)	0.007(19)	-0.009(17)	0.01(2)
C(269)	0.06(3)	0.09(3)	0.034(18)	0.00(2)	0.014(17)	0.03(2)

Appendix XIII

Complete Bond Lengths, Bond Angles, and Thermal and Positional

Parameters for



7.5

Table A.XIII.1: Complete Bond Lengths (Å) for 7.5·C₆H₆, with e.s.d.s in parentheses

Au(1)-C(31)	2.04(2)	C(6)-C(32)	1.54(3)
Au(1)-C(2)	2.06(2)	C(11)-C(16)	1.37(3)
Au(1)-C(1)	2.14(2)	C(11)-C(12)	1.41(3)
Au(1)-N(1)	2.14(2)	C(12)-C(13)	1.42(3)
Au(1)-S(1)	2.832(5)	C(13)-C(14)	1.32(3)
S(1)-O(4)	1.43(2)	C(14)-C(15)	1.40(3)
S(1)-O(3)	1.44(2)	C(15)-C(16)	1.41(3)
S(1)-C(1)	1.74(2)	C(21)-C(22)	1.35(3)
S(1)-C(2)	1.75(2)	C(21)-C(26)	1.40(3)
N(1)-C(8)	1.43(3)	C(22)-C(23)	1.38(3)
N(1)-C(6)	1.47(3)	C(23)-C(24)	1.36(3)
N(1)-C(7)	1.50(3)	C(24)-C(25)	1.38(3)
O(1)-C(4)	1.21(2)	C(25)-C(26)	1.39(3)
O(2)-C(3)	1.24(2)	C(31)-C(32)	1.37(3)
O(5)-C(35)	1.37(3)	C(31)-C(36)	1.44(3)
O(5)-C(5)	1.37(3)	C(32)-C(33)	1.40(3)
C(1)-C(4)	1.51(3)	C(33)-C(34)	1.40(3)
C(2)-C(3)	1.51(3)	C(34)-C(35)	1.36(3)
C(3)-C(21)	1.51(3)	C(35)-C(36)	1.43(3)
C(4)-C(11)	1.49(3)		

Table A.XIII.2: Complete Bond Angles (°) for 7.5·C₆H₆, with e.s.d.s in parentheses

C(31)-Au(1)-C(2)	101.1(9)	O(2)-C(3)-C(21)	118(2)
C(31)-Au(1)-C(1)	175.3(7)	C(2)-C(3)-C(21)	121(2)
C(2)-Au(1)-C(1)	74.2(8)	O(1)-C(4)-C(11)	119(2)
C(31)-Au(1)-N(1)	80.4(7)	O(1)-C(4)-C(1)	122(2)
C(2)-Au(1)-N(1)	177.4(8)	C(11)-C(4)-C(1)	119(2)
C(1)-Au(1)-N(1)	104.2(7)	N(1)-C(6)-C(32)	108(2)
C(31)-Au(1)-S(1)	137.9(6)	C(16)-C(11)-C(12)	118(2)
C(2)-Au(1)-S(1)	38.0(7)	C(16)-C(11)-C(4)	119(2)
C(1)-Au(1)-S(1)	37.7(5)	C(12)-C(11)-C(4)	123(2)
N(1)-Au(1)-S(1)	140.9(5)	C(11)-C(12)-C(13)	118(2)
O(4)-S(1)-O(3)	116.2(10)	C(14)-C(13)-C(12)	123(2)
O(4)-S(1)-C(1)	115.2(9)	C(13)-C(14)-C(15)	120(2)
O(3)-S(1)-C(1)	108.4(9)	C(14)-C(15)-C(16)	118(2)
O(4)-S(1)-C(2)	111.0(10)	C(11)-C(16)-C(15)	123(2)
O(3)-S(1)-C(2)	110.6(10)	C(22)-C(21)-C(26)	118(2)

C(1)-S(1)-C(2)	93.1(9)	C(22)-C(21)-C(3)	120(2)
O(4)-S(1)-Au(1)	136.0(8)	C(26)-C(21)-C(3)	122(2)
O(3)-S(1)-Au(1)	107.7(7)	C(21)-C(22)-C(23)	123(2)
C(1)-S(1)-Au(1)	48.8(6)	C(24)-C(23)-C(22)	119(2)
C(2)-S(1)-Au(1)	46.4(7)	C(23)-C(24)-C(25)	120(2)
C(8)-N(1)-C(6)	110(2)	C(24)-C(25)-C(26)	121(2)
C(8)-N(1)-C(7)	110(2)	C(25)-C(26)-C(21)	120(2)
C(6)-N(1)-C(7)	108(2)	C(32)-C(31)-C(36)	120(2)
C(8)-N(1)-Au(1)	110.0(12)	C(32)-C(31)-Au(1)	114(2)
C(6)-N(1)-Au(1)	105.9(13)	C(36)-C(31)-Au(1)	127(2)
C(7)-N(1)-Au(1)	112.6(12)	C(31)-C(32)-C(33)	122(2)
C(35)-O(5)-C(5)	119(2)	C(31)-C(32)-C(6)	117(2)
C(4)-C(1)-S(1)	116(2)	C(33)-C(32)-C(6)	121(2)
C(4)-C(1)-Au(1)	106.2(13)	C(34)-C(33)-C(32)	118(2)
S(1)-C(1)-Au(1)	93.4(8)	C(35)-C(34)-C(33)	122(2)
C(3)-C(2)-S(1)	116.2(14)	C(34)-C(35)-O(5)	118(2)
C(3)-C(2)-Au(1)	114(2)	C(34)-C(35)-C(36)	120(2)
S(1)-C(2)-Au(1)	95.6(10)	O(5)-C(35)-C(36)	122(2)
O(2)-C(3)-C(2)	121(2)	C(35)-C(36)-C(31)	117(2)

Final Positional (fractional co-ordinates) and Equivalent Thermal Parameters for 7.5·C₆H₆, with e.s.d.s in parentheses

Atom	X/A	Y/B	Z/C	U(eq)
Au(1)	0.0626(1)	0.0472(1)	0.3185(1)	0.017(1)
S(1)	-0.2130(5)	0.0563(2)	0.3505(4)	0.024(1)
N(1)	0.2793(19)	0.0778(7)	0.3827(13)	0.025(4)
O(1)	-0.1397(18)	0.1581(6)	0.2397(12)	0.042(4)
O(2)	-0.1065(16)	-0.0674(6)	0.3345(12)	0.031(4)
O(3)	-0.2137(17)	0.0214(6)	0.4411(13)	0.034(4)
O(4)	-0.3455(15)	0.0836(6)	0.2966(14)	0.039(4)
O(5)	0.1397(18)	-0.0963(7)	0.0015(14)	0.044(4)
C(1)	-0.0610(21)	0.0977(7)	0.3929(15)	0.016(4)
C(2)	-0.1489(23)	0.0213(9)	0.2547(19)	0.029(5)
C(3)	-0.1664(20)	-0.0396(9)	0.2521(15)	0.019(5)
C(4)	-0.0728(26)	0.1523(8)	0.3365(17)	0.030(5)
C(5)	-0.0045(27)	-0.1098(8)	-0.0352(19)	0.038(6)
C(6)	0.3752(23)	0.0307(9)	0.3899(17)	0.028(5)
C(7)	0.3105(24)	0.1012(10)	0.4969(18)	0.034(6)
C(8)	0.3056(23)	0.1178(8)	0.3089(18)	0.032(6)
C(11)	0.0184(25)	0.1980(8)	0.3970(17)	0.027(5)
C(12)	0.0672(22)	0.2014(8)	0.5137(19)	0.028(5)
C(13)	0.1549(24)	0.2464(10)	0.5633(20)	0.039(6)
C(14)	0.1973(25)	0.2837(8)	0.5056(21)	0.034(6)
C(15)	0.1514(27)	0.2812(9)	0.3895(22)	0.042(6)
C(16)	0.0622(28)	0.2372(9)	0.3381(22)	0.042(6)
C(21)	-0.2618(22)	-0.0685(8)	0.1505(17)	0.022(5)
C(22)	-0.2814(22)	-0.1226(9)	0.1525(18)	0.028(5)
C(23)	-0.3645(24)	-0.1517(8)	0.0620(21)	0.034(6)
C(24)	-0.4264(27)	-0.1249(9)	-0.0352(23)	0.043(7)
C(25)	-0.4107(23)	-0.0695(9)	-0.0402(17)	0.028(5)
C(26)	-0.3284(21)	-0.0408(8)	0.0516(15)	0.021(5)
C(31)	0.1648(22)	-0.0034(8)	0.2393(18)	0.025(5)
C(32)	0.3127(21)	-0.0043(8)	0.2859(15)	0.019(5)

C(33)	0.4025(21)	-0.0356(8)	0.2418(18)	0.023(5)
C(34)	0.3368(26)	-0.0672(9)	0.1483(21)	0.037(6)
C(35)	0.1913(25)	-0.0660(9)	0.0960(18)	0.032(6)
C(36)	0.0978(23)	-0.0354(8)	0.1419(19)	0.031(6)
C(41)	0.8706(25)	0.2274(11)	0.7157(16)	0.087(13)
C(42)	0.8801(28)	0.1711(11)	0.7117(21)	0.106(18)
C(43)	0.7935(37)	0.1427(7)	0.6206(29)	0.107(19)
C(44)	0.6975(27)	0.1707(14)	0.5334(22)	0.096(14)
C(45)	0.6881(24)	0.2270(15)	0.5374(19)	0.112(15)
C(46)	0.7746(33)	0.2554(8)	0.6286(24)	0.079(11)

Table A.XIII.3: Final Positional (fractional co-ordinates) and Equivalent Thermal Parameters of Calculated Hydrogen Atoms for $7.5 \cdot C_6H_6$, with *e.s.d.s* in parentheses

Atom	X/A	Y/B	Z/C	U(eq)
H(1)	-0.0190(21)	0.1000(7)	0.4752(15)	0.019
H(2)	-0.1931(23)	0.0367(9)	0.1789(19)	0.035
H(5A)	-0.0242(27)	-0.1313(8)	-0.1032(19)	0.057
H(5B)	-0.0631(27)	-0.0766(8)	-0.0502(19)	0.057
H(5C)	-0.0291(27)	-0.1312(8)	0.0218(19)	0.057
H(6A)	0.3808(23)	0.0091(9)	0.4570(17)	0.034
H(6B)	0.4740(23)	0.0430(9)	0.3946(17)	0.034
H(7A)	0.2922(24)	0.0735(10)	0.5466(18)	0.051
H(7B)	0.2476(24)	0.1326(10)	0.4946(18)	0.051
H(7C)	0.4121(24)	0.1126(10)	0.5241(18)	0.051
H(8A)	0.2412(23)	0.1489(8)	0.3048(18)	0.049
H(8B)	0.2869(23)	0.1019(8)	0.2350(18)	0.049
H(8C)	0.4066(23)	0.1298(8)	0.3364(18)	0.049
H(12)	0.0421(22)	0.1742(8)	0.5578(19)	0.033
H(13)	0.1842(24)	0.2497(10)	0.6417(20)	0.047
H(14)	0.2590(25)	0.3123(8)	0.5425(21)	0.041
H(15)	0.1795(27)	0.3082(9)	0.3467(22)	0.050
H(16)	0.0315(28)	0.2349(9)	0.2597(22)	0.050
H(22)	-0.2359(22)	-0.1417(9)	0.2192(18)	0.034
H(23)	-0.3784(24)	-0.1897(8)	0.0675(21)	0.040
H(24)	-0.4801(27)	-0.1445(9)	-0.0992(23)	0.052
H(25)	-0.4567(23)	-0.0507(9)	-0.1072(17)	0.033
H(26)	-0.3172(21)	-0.0026(8)	0.0474(15)	0.025
H(33)	0.5047(21)	-0.0353(8)	0.2744(18)	0.028
H(34)	0.3958(26)	-0.0903(9)	0.1202(21)	0.045
H(36)	-0.0044(23)	-0.0361(8)	0.1093(19)	0.038
H(41)	0.9298(25)	0.2467(11)	0.7780(16)	0.104
H(42)	0.9457(40)	0.1519(18)	0.7712(27)	0.127
H(43)	0.8000(56)	0.1042(7)	0.6178(43)	0.129
H(44)	0.6384(38)	0.1514(21)	0.4712(29)	0.115
H(45)	0.6225(35)	0.2462(21)	0.4779(25)	0.135
H(46)	0.7682(51)	0.2938(8)	0.6313(37)	0.094

Table A.XIII.4: Thermal Parameters for $7.5 \cdot C_6H_6$, with *e.s.d.s* in parentheses

Atom	U11	U22	U33	U23	U13	U12
Au(1)	0.0150(4)	0.0169(5)	0.0160(4)	0.0012(4)	-0.0015(3)	-0.0010(4)
S(1)	0.020(3)	0.027(3)	0.020(3)	-0.013(2)	0.001(2)	-0.010(2)
N(1)	0.035(10)	0.034(11)	0.011(9)	0.003(8)	0.016(8)	-0.006(9)
O(1)	0.053(10)	0.040(10)	0.016(9)	-0.006(7)	-0.016(7)	0.001(8)
O(2)	0.035(9)	0.027(8)	0.025(8)	0.011(7)	-0.001(7)	0.007(7)
O(3)	0.044(9)	0.026(8)	0.038(9)	-0.010(7)	0.020(8)	-0.009(7)
O(4)	0.015(8)	0.040(10)	0.054(10)	-0.037(8)	-0.001(7)	-0.002(7)
O(5)	0.051(11)	0.038(10)	0.042(10)	-0.022(8)	0.012(8)	0.000(9)
C(1)	0.033(12)	0.001(9)	0.011(10)	-0.006(8)	0.001(8)	-0.008(8)
C(2)	0.029(12)	0.027(12)	0.031(13)	0.007(10)	0.009(10)	-0.022(10)
C(3)	0.015(10)	0.040(13)	0.009(10)	0.012(10)	0.012(8)	-0.002(10)
C(4)	0.058(15)	0.017(11)	0.012(11)	-0.002(9)	0.007(11)	0.007(11)
C(5)	0.059(17)	0.009(11)	0.034(14)	-0.002(10)	-0.002(12)	-0.015(11)
C(7)	0.031(13)	0.037(14)	0.027(13)	0.001(11)	-0.003(10)	-0.002(11)
C(8)	0.030(12)	0.018(12)	0.035(13)	0.003(10)	-0.011(10)	-0.004(10)
C(6)	0.024(11)	0.035(13)	0.026(12)	0.019(10)	0.008(9)	0.012(10)
C(11)	0.045(14)	0.013(11)	0.023(12)	-0.007(9)	0.009(10)	-0.001(10)
C(12)	0.022(11)	0.018(11)	0.042(14)	-0.009(10)	0.007(10)	-0.005(9)
C(13)	0.032(13)	0.041(15)	0.038(14)	-0.022(12)	0.003(11)	-0.029(11)
C(14)	0.040(14)	0.007(11)	0.055(16)	-0.010(11)	0.014(12)	-0.014(10)
C(15)	0.053(16)	0.020(13)	0.059(18)	-0.001(12)	0.028(14)	-0.008(12)
C(16)	0.058(16)	0.013(11)	0.058(17)	0.002(12)	0.022(14)	0.007(12)
C(21)	0.034(12)	0.016(11)	0.024(12)	0.002(9)	0.021(10)	-0.009(9)
C(22)	0.024(11)	0.030(13)	0.032(13)	0.002(10)	0.011(10)	0.000(10)
C(23)	0.038(13)	0.007(11)	0.060(17)	-0.011(11)	0.021(12)	0.001(10)
C(24)	0.049(16)	0.025(14)	0.054(17)	-0.026(13)	0.015(13)	-0.031(12)
C(25)	0.029(12)	0.032(13)	0.017(11)	-0.001(10)	0.001(9)	-0.002(10)
C(26)	0.033(12)	0.013(10)	0.012(10)	-0.008(9)	-0.001(9)	0.003(9)
C(31)	0.025(12)	0.015(11)	0.037(13)	-0.005(10)	0.012(10)	-0.004(9)
C(32)	0.023(11)	0.022(11)	0.006(10)	0.000(8)	-0.005(8)	-0.003(9)
C(33)	0.015(10)	0.021(12)	0.034(13)	0.009(10)	0.007(9)	0.005(9)
C(34)	0.042(15)	0.014(11)	0.059(17)	0.014(11)	0.021(13)	0.008(10)
C(35)	0.042(14)	0.025(12)	0.027(13)	0.018(10)	0.005(11)	0.028(11)
C(36)	0.020(11)	0.016(12)	0.046(14)	0.001(10)	-0.008(10)	-0.006(9)
C(41)	0.113(31)	0.128(34)	0.047(20)	-0.044(23)	0.065(22)	-0.031(27)
C(42)	0.123(34)	0.127(36)	0.108(33)	0.086(30)	0.094(30)	0.102(31)
C(43)	0.224(56)	0.057(23)	0.089(29)	-0.028(24)	0.118(36)	-0.055(31)
C(44)	0.069(25)	0.137(41)	0.106(34)	-0.023(31)	0.063(25)	-0.052(26)
C(45)	0.083(30)	0.143(45)	0.097(34)	0.018(32)	0.006(25)	0.031(30)
C(46)	0.138(35)	0.040(18)	0.074(24)	-0.001(18)	0.056(25)	0.018(20)

Appendix XIV

Complete Bond Lengths, Bond Angles, and Thermal and Positional

Parameters for

$[\{\text{C}_6\text{H}_4(\text{CH}_2\text{NMe}_2)\text{-2}\}\text{Au}\{\text{SC}_6\text{H}_4(\text{COO})\text{-2}\}]$ **8.10b**

Table A.XIV.1: Complete Bond Lengths (Å) for 8.10b, with e.s.d.s in parentheses

Au(1)-C(11)	2.02(2)	Au(2)-C(31)	2.04(2)
Au(1)-O(1)	2.06(4)	Au(2)-O(3)	2.08(2)
Au(1)-N(1)	2.14(4)	Au(2)-N(2)	2.20(2)
Au(1)-S(1)	2.27(1)	Au(2)-S(2)	2.28(2)
S(1)-C(21)	1.77(2)	S(2)-C(41)	1.81(1)
O(1)-C(1)	1.24(6)	O(3)-C(2)	1.27(2)
O(2)-C(1)	1.14(5)	O(4)-C(2)	1.25(2)
N(1)-C(17)	1.50(4)	N(2)-C(38)	1.47(3)
N(1)-C(19)	1.52(4)	N(2)-C(37)	1.48(2)
N(1)-C(18)	1.53(4)	N(2)-C(39)	1.54(2)
C(1)-C(22)	1.60(5)	C(2)-C(42)	1.56(1)
C(12)-C(17)	1.54(4)	C(32)-C(37)	1.60(2)

Table A.XIV.2: Complete Bond Angles (°) for 8.10b, with e.s.d.s in parentheses

C(11)-Au(1)-O(1)	174.6(11)	C(31)-Au(2)-O(3)	172.7(5)
C(11)-Au(1)-N(1)	83.3(11)	C(31)-Au(2)-N(2)	83.4(4)
O(1)-Au(1)-N(1)	91.4(15)	O(3)-Au(2)-N(2)	90.0(4)
C(11)-Au(1)-S(1)	93.9(6)	C(31)-Au(2)-S(2)	93.3(4)
O(1)-Au(1)-S(1)	91.2(11)	O(3)-Au(2)-S(2)	93.2(3)
N(1)-Au(1)-S(1)	174.9(11)	N(2)-Au(2)-S(2)	175.4(3)
C(21)-S(1)-Au(1)	104.4(8)	C(41)-S(2)-Au(2)	101.1(3)
C(1)-O(1)-Au(1)	138(3)	C(2)-O(3)-Au(2)	128.1(5)
C(17)-N(1)-C(19)	109(3)	C(38)-N(2)-C(37)	112.8(15)
C(17)-N(1)-C(18)	111(3)	C(38)-N(2)-C(39)	114.7(11)
C(19)-N(1)-C(18)	110(2)	C(37)-N(2)-C(39)	109.6(15)
C(17)-N(1)-Au(1)	107(2)	C(38)-N(2)-Au(2)	105.1(12)
C(19)-N(1)-Au(1)	107(2)	C(37)-N(2)-Au(2)	105.5(7)
C(18)-N(1)-Au(1)	113(2)	C(39)-N(2)-Au(2)	108.5(12)
O(2)-C(1)-O(1)	127(5)	O(4)-C(2)-O(3)	120.4(15)
O(2)-C(1)-C(22)	114(4)	O(4)-C(2)-C(42)	112.8(6)
O(1)-C(1)-C(22)	118(4)	O(3)-C(2)-C(42)	126.7(6)
C(12)-C(11)-Au(1)	113.1(6)	C(32)-C(31)-Au(2)	111.8(6)
C(16)-C(11)-Au(1)	126.6(7)	C(36)-C(31)-Au(2)	127.9(7)
C(11)-C(12)-C(17)	118(3)	C(31)-C(32)-C(37)	118.1(15)
C(13)-C(12)-C(17)	122(3)	C(33)-C(32)-C(37)	121.7(15)
N(1)-C(17)-C(12)	109.0(16)	N(2)-C(37)-C(32)	107.7(8)
C(22)-C(21)-S(1)	129.0(7)	C(42)-C(41)-S(2)	128.9(6)

C(26)-C(21)-S(1)	110.6(7)	C(46)-C(41)-S(2)	110.9(5)
C(23)-C(22)-C(1)	115.6(18)	C(43)-C(42)-C(2)	118.9(6)
C(21)-C(22)-C(1)	124.4(18)	C(41)-C(42)-C(2)	121.0(7)

Table A.XIV.3: Final Positional (fractional co-ordinates) and Equivalent Thermal Parameters for **8.10b**, with e.s.d.s in parentheses

Atom	X/A	Y/B	Z/C	U(eq)
Au(1)	0.1098(1)	0.4714(2)	0.4569(1)	0.027(1)
S(1)	0.2131(8)	0.4250(10)	0.6021(8)	0.026(3)
O(1)	0.126(2)	0.330(3)	0.398(3)	0.035(9)
O(2)	0.1475(19)	0.165(3)	0.377(2)	0.021(7)
N(1)	0.019(2)	0.527(3)	0.321(3)	0.019(8)
C(1)	0.153(3)	0.237(4)	0.424(3)	0.021(10)
C(11)	0.0881(12)	0.6151(14)	0.5018(11)	0.019(9)
C(12)	0.0209(10)	0.6708(14)	0.4317(11)	0.015(9)
C(13)	0.0033(14)	0.7757(15)	0.4483(14)	0.029(11)
C(14)	0.0529(16)	0.8250(16)	0.5351(15)	0.023(10)
C(15)	0.1201(14)	0.7694(18)	0.6052(13)	0.024(10)
C(16)	0.1377(14)	0.6645(19)	0.5886(12)	0.019(9)
C(17)	-0.0344(11)	0.6099(18)	0.3388(13)	0.028(11)
C(18)	-0.0360(19)	0.438(2)	0.2563(18)	0.019(10)
C(19)	0.0684(19)	0.582(2)	0.2738(16)	0.028(11)
C(21)	0.2040(10)	0.2835(12)	0.6070(11)	0.024(10)
C(22)	0.1856(8)	0.2079(11)	0.5350(10)	0.016(9)
C(23)	0.1920(8)	0.0986(11)	0.5563(9)	0.029(11)
C(24)	0.2168(10)	0.0650(13)	0.6498(9)	0.043(14)
C(25)	0.2352(11)	0.1406(15)	0.7218(10)	0.042(14)
C(26)	0.2288(11)	0.2499(14)	0.7005(11)	0.014(8)
Au(2)	0.3860(1)	-0.0285(1)	0.3396(1)	0.009(1)
S(2)	0.2781(4)	-0.0745(5)	0.3759(5)	0.021(2)
O(3)	0.3706(4)	-0.1655(4)	0.2566(5)	0.017(6)
O(4)	0.3376(9)	-0.3324(6)	0.2094(11)	0.029(8)
N(2)	0.4860(4)	0.0291(5)	0.3020(5)	0.023(8)
C(2)	0.3429(7)	-0.2575(4)	0.2655(8)	0.013(8)
C(31)	0.4068(11)	0.1152(13)	0.4100(14)	0.018(9)
C(32)	0.4775(9)	0.1680(13)	0.4122(11)	0.015(9)
C(33)	0.4970(12)	0.2714(15)	0.4495(16)	0.019(9)
C(34)	0.4459(14)	0.3222(15)	0.4845(16)	0.018(9)
C(35)	0.3752(13)	0.2695(17)	0.4822(15)	0.022(10)
C(36)	0.3557(13)	0.1660(18)	0.4450(17)	0.011(8)
C(37)	0.5391(11)	0.1023(17)	0.3801(15)	0.026(11)
C(38)	0.4408(19)	0.085(2)	0.2102(13)	0.026(11)
C(39)	0.539(2)	-0.068(2)	0.299(2)	0.023(10)
C(41)	0.2963(7)	-0.2178(7)	0.3971(11)	0.010(8)
C(42)	0.3177(11)	-0.2933(10)	0.3456(11)	0.015(9)
C(43)	0.3214(8)	-0.4019(9)	0.3685(11)	0.017(9)
C(44)	0.3037(14)	-0.4351(8)	0.4429(16)	0.027(11)
C(45)	0.2823(16)	-0.3596(11)	0.4944(15)	0.021(10)
C(46)	0.2786(8)	-0.2509(9)	0.4715(7)	0.011(8)
Au(3)	0.1136(3)	0.0279(4)	0.4522(3)	0.008(1)
Au(4)	0.3965(10)	-0.4743(11)	0.3544(13)	0.149(8)

Table A.XIV.4: *Thermal Parameters for 8.10b, with e.s.d.s in parentheses*

Atom	U11	U22	U33	U23	U13	U12
Au(1)	0.0266(10)	0.0256(11)	0.0217(10)	0.0024(8)	0.0048(8)	0.0020(8)
S(1)	0.027(6)	0.015(6)	0.022(6)	0.006(5)	-0.003(5)	0.001(5)
Au(2)	0.0087(7)	0.0098(8)	0.0151(8)	0.0009(6)	0.0109(6)	-0.0023(6)
S(2)	0.023(6)	0.011(5)	0.044(7)	-0.001(5)	0.028(5)	-0.004(4)

Appendix XV

Complete Bond Lengths, Bond Angles, and Thermal and Positional Parameters for [{C₆H₃(CH₂NMe₂)-2-(OMe)-5}Au{OC₆H₄(COO)-2}]·CH₂Cl₂ 8.15b

Table A.XV.1: Complete Bond Lengths (Å) for 8.15b·CH₂Cl₂, with e.s.d.s in parentheses

Au(1)-O(1)	1.985(3)	C(17)-C(12)	1.496(5)
Au(1)-C(11)	2.001(3)	C(11)-C(16)	1.393(5)
Au(1)-O(3)	2.037(3)	C(11)-C(12)	1.400(5)
Au(1)-N(1)	2.057(3)	C(12)-C(13)	1.381(5)
O(3)-C(21)	1.329(5)	C(13)-C(14)	1.398(5)
O(1)-C(1)	1.315(4)	C(14)-C(15)	1.388(6)
O(2)-C(1)	1.222(5)	C(15)-C(16)	1.399(5)
O(4)-C(15)	1.373(4)	C(21)-C(26)	1.407(5)
O(4)-C(2)	1.422(5)	C(21)-C(22)	1.419(5)
N(1)-C(19)	1.493(5)	C(22)-C(23)	1.410(5)
N(1)-C(18)	1.501(5)	C(23)-C(24)	1.378(5)
N(1)-C(17)	1.514(4)	C(24)-C(25)	1.394(6)
C(1)-C(22)	1.497(5)	C(25)-C(26)	1.380(6)

Table A.XV.2: Complete Bond Angles (°) for 8.15b·CH₂Cl₂, with e.s.d.s in parentheses

O(1)-Au(1)-C(11)	91.24(13)	C(12)-C(11)-Au(1)	113.7(3)
O(1)-Au(1)-O(3)	93.88(10)	C(13)-C(12)-C(11)	118.9(3)
C(11)-Au(1)-O(3)	174.86(12)	C(13)-C(12)-C(17)	125.0(3)
O(1)-Au(1)-N(1)	173.50(11)	C(11)-C(12)-C(17)	116.0(3)
C(11)-Au(1)-N(1)	82.41(13)	C(12)-C(13)-C(14)	121.1(4)
O(3)-Au(1)-N(1)	92.45(11)	C(15)-C(14)-C(13)	119.4(3)
C(21)-O(3)-Au(1)	122.0(2)	O(4)-C(15)-C(14)	124.6(3)
C(1)-O(1)-Au(1)	126.1(2)	O(4)-C(15)-C(16)	114.9(3)
C(15)-O(4)-C(2)	117.0(3)	C(14)-C(15)-C(16)	120.5(3)
C(19)-N(1)-C(18)	109.0(3)	C(11)-C(16)-C(15)	119.0(3)
C(19)-N(1)-C(17)	109.6(3)	O(3)-C(21)-C(26)	115.7(3)
C(18)-N(1)-C(17)	109.4(3)	O(3)-C(21)-C(22)	125.8(3)
C(19)-N(1)-Au(1)	112.9(2)	C(26)-C(21)-C(22)	118.4(3)
C(18)-N(1)-Au(1)	107.9(2)	C(23)-C(22)-C(21)	118.3(3)
C(17)-N(1)-Au(1)	107.9(2)	C(23)-C(22)-C(1)	115.5(3)
O(2)-C(1)-O(1)	117.3(3)	C(21)-C(22)-C(1)	126.2(3)
O(2)-C(1)-C(22)	120.2(3)	C(24)-C(23)-C(22)	122.5(4)
O(1)-C(1)-C(22)	122.6(3)	C(23)-C(24)-C(25)	118.8(4)
C(12)-C(17)-N(1)	108.3(3)	C(26)-C(25)-C(24)	120.4(4)
C(16)-C(11)-C(12)	121.1(3)	C(25)-C(26)-C(21)	121.6(4)
C(16)-C(11)-Au(1)	125.2(3)		

Table A.XV.3: Final Positional (fractional co-ordinates) and Equivalent Thermal Parameters for **8.15b**·CH₂Cl₂, with e.s.d.s in parentheses

Atom	X/A	Y/B	Z/C	U(eq)
Au(1)	0.7495(1)	0.9143(1)	0.5113(1)	0.022(1)
O(1)	0.7860(3)	1.1185(3)	0.4733(3)	0.027(1)
O(2)	0.8151(4)	1.3008(3)	0.5197(3)	0.036(1)
O(3)	0.8345(3)	0.8365(3)	0.6649(3)	0.032(1)
O(4)	0.6184(4)	1.2715(3)	0.0789(3)	0.037(1)
N(1)	0.7075(3)	0.7107(3)	0.5304(3)	0.024(1)
C(1)	0.8134(4)	1.1696(4)	0.5524(4)	0.025(1)
C(17)	0.5776(4)	0.7249(4)	0.4775(4)	0.026(1)
C(18)	0.8476(4)	0.6512(4)	0.4493(4)	0.032(1)
C(19)	0.6686(5)	0.6099(4)	0.6688(4)	0.033(1)
C(2)	0.5342(6)	1.3090(5)	-0.0106(4)	0.044(1)
C(11)	0.6641(4)	0.9723(4)	0.3627(3)	0.022(1)
C(12)	0.5924(4)	0.8613(4)	0.3620(4)	0.024(1)
C(13)	0.5319(4)	0.8879(4)	0.2623(4)	0.027(1)
C(14)	0.5374(4)	1.0240(4)	0.1653(4)	0.030(1)
C(15)	0.6069(4)	1.1337(4)	0.1682(4)	0.028(1)
C(16)	0.6736(4)	1.1081(4)	0.2657(4)	0.027(1)
C(21)	0.8464(4)	0.9205(4)	0.7265(4)	0.025(1)
C(22)	0.8391(4)	1.0739(4)	0.6790(3)	0.023(1)
C(23)	0.8510(4)	1.1460(4)	0.7589(4)	0.027(1)
C(24)	0.8690(5)	1.0731(5)	0.8804(4)	0.034(1)
C(25)	0.8758(5)	0.9224(5)	0.9263(4)	0.034(1)
C(26)	0.8656(4)	0.8480(4)	0.8506(4)	0.030(1)
Cl(1)	-0.2848(2)	0.5531(2)	0.2098(1)	0.056(1)
Cl(2)	0.0448(1)	0.5570(1)	0.1299(1)	0.046(1)
C(3)	-0.1139(5)	0.4469(5)	0.2054(4)	0.039(1)

Table A.XV.4: Final positional (fractional co-ordinates) and equivalent thermal parameters of calculated hydrogen atoms for **8.15b**·CH₂Cl₂, with e.s.d.s in parentheses

Atom	X/A	Y/B	Z/C	U(eq)
H(2A)	0.5516	1.4080	-0.0687	0.066
H(2B)	0.4270	1.2995	0.0375	0.066
H(2C)	0.5667	1.2449	-0.0616	0.066
H(17A)	0.5811	0.6416	0.4511	0.031
H(17B)	0.4805	0.7280	0.5451	0.031
H(18A)	0.8732	0.7158	0.3592	0.048
H(18B)	0.8292	0.5567	0.4536	0.048
H(18C)	0.9311	0.6426	0.4829	0.048
H(19A)	0.5781	0.6478	0.7217	0.050
H(19B)	0.7522	0.6005	0.7023	0.050
H(19C)	0.6500	0.5158	0.6721	0.050
H(13)	0.4862	0.8132	0.2596	0.033
H(14)	0.4945	1.0411	0.0987	0.036
H(16)	0.7239	1.1813	0.2658	0.032
H(23)	0.8463	1.2476	0.7280	0.033
H(24)	0.8767	1.1242	0.9315	0.040
H(25)	0.8874	0.8712	1.0093	0.041

H(26)	0.8716	0.7464	0.8827	0.036
H(3A)	-0.1045	0.3823	0.1568	0.047
H(3B)	-0.1155	0.3870	0.2949	0.047

Table A.XV.5: Thermal Parameters for **8.15b**·CH₂Cl₂, with *e.s.d.s* in parentheses

Atom	U11	U22	U33	U23	U13	U12
Au(1)	0.0281(1)	0.0171(1)	0.0220(1)	-0.0062(1)	-0.0100(1)	-0.0022(1)
O(1)	0.0398(14)	0.0200(12)	0.0254(13)	-0.0039(10)	-0.0151(11)	-0.0064(11)
O(2)	0.0629(19)	0.0187(13)	0.0307(15)	-0.0036(11)	-0.0214(14)	-0.0068(13)
O(3)	0.0505(17)	0.0186(13)	0.0342(15)	-0.0070(11)	-0.0278(13)	0.0035(11)
O(4)	0.0541(18)	0.0283(15)	0.0281(14)	-0.0012(12)	-0.0185(13)	-0.0056(13)
N(1)	0.0287(15)	0.0204(14)	0.0238(15)	-0.0071(12)	-0.0111(12)	-0.0011(12)
C(1)	0.0305(18)	0.0230(18)	0.0231(17)	-0.0085(14)	-0.0065(14)	-0.0064(14)
C(2)	0.059(3)	0.036(2)	0.032(2)	0.0000(18)	-0.023(2)	0.004(2)
C(17)	0.0292(18)	0.0235(18)	0.0278(18)	-0.0063(14)	-0.0108(15)	-0.0076(14)
C(18)	0.0324(19)	0.0240(19)	0.041(2)	-0.0148(17)	-0.0115(17)	0.0016(15)
C(19)	0.051(2)	0.0200(18)	0.0263(19)	0.0022(14)	-0.0164(17)	-0.0097(16)
C(11)	0.0244(16)	0.0250(18)	0.0190(16)	-0.0092(13)	-0.0095(13)	0.0002(13)
C(12)	0.0229(16)	0.0220(17)	0.0254(17)	-0.0082(14)	-0.0061(14)	-0.0026(13)
C(13)	0.0287(18)	0.0267(19)	0.0300(19)	-0.0125(15)	-0.0098(15)	-0.0021(14)
C(14)	0.0329(19)	0.034(2)	0.0235(18)	-0.0103(16)	-0.0104(15)	-0.0003(16)
C(15)	0.0339(19)	0.0253(19)	0.0201(17)	-0.0047(14)	-0.0061(14)	-0.0016(15)
C(16)	0.0334(19)	0.0236(18)	0.0252(18)	-0.0078(14)	-0.0088(15)	-0.0058(15)
C(21)	0.0266(17)	0.0262(18)	0.0260(18)	-0.0097(14)	-0.0107(14)	-0.0013(14)
C(22)	0.0237(16)	0.0219(17)	0.0223(17)	-0.0058(14)	-0.0069(13)	-0.0022(13)
C(23)	0.0314(18)	0.0256(18)	0.0256(18)	-0.0088(15)	-0.0078(15)	-0.0051(15)
C(24)	0.040(2)	0.038(2)	0.0287(19)	-0.0160(17)	-0.0106(17)	-0.0061(17)
C(25)	0.040(2)	0.037(2)	0.0279(19)	-0.0079(17)	-0.0161(17)	-0.0020(17)
C(26)	0.0332(19)	0.0258(19)	0.0301(19)	-0.0056(15)	-0.0149(16)	0.0004(15)
Cl(1)	0.0488(7)	0.0629(8)	0.0549(7)	-0.0206(6)	-0.0187(6)	0.0057(6)
Cl(2)	0.0514(6)	0.0360(6)	0.0497(6)	-0.0071(5)	-0.0191(5)	-0.0089(5)
C(3)	0.047(2)	0.030(2)	0.033(2)	-0.0059(17)	-0.0072(18)	-0.0053(18)

Appendix XVI

List of Publications

The research described in this thesis is represented by the following publications:

1. "Synthesis and characterisation of platinum(II) ureylene complexes, and the X-ray structure of $[\text{Pt}\{\overline{\text{PhNC(O)NAd}}\}(\text{cod})]$ (Ad = 1-adamantyl, cod = cycloocta-1,5-diene)", M.B. Dinger, W. Henderson, B.K. Nicholson and A.L. Wilkins, *J. Organomet. Chem.*, 526 (1996) 303-312.
2. "The first mononuclear triazatrimethylenemethane metal complex, $[\text{Pt}\{\overline{\text{NPhC(NPh)NPh}}\}(\text{cod})]$ (cod = cycloocta-1,5-diene)", M.B. Dinger and W. Henderson, *Chem. Commun.*, (1996) 211-212.
3. "Organometallic complexes of platinum(II), rhodium(III), iridium(III), ruthenium(II) and osmium(II) containing substituted derivatives of the guanidine dianion (triazatrimethylenemethane) ligand", M.B. Dinger, W. Henderson and B.K. Nicholson, *J. Organomet. Chem.*, 556 (1998) 75-88.
4. "Insertion reactions of platinum(II) ureylene complexes", M.B. Dinger and W. Henderson, *J. Chem. Soc., Dalton Trans.*, (1998) 1763-1773.
5. "Organogold(III) Metallacyclic Chemistry. Part 1. Synthesis of the first auraxodimethylenemethane (auracyclobutan-3-one) and aurathietane-3,3-dioxide complexes", M.B. Dinger, W. Henderson, *J. Organomet. Chem.*, 547 (1997) 243-252.
6. "Organogold(III) Metallacyclic Chemistry. Part 2. Synthesis and characterisation of the first Gold(III) ureylene complexes", M.B. Dinger, W. Henderson, *J. Organomet. Chem.*, 557 (1998) 231-241.
7. "Organogold(III) Metallacyclic Chemistry. Part 3. Self-assembly of the nonametallic gold(III)-silver(I)-sulfido clusters $[\{\text{LAu}(\mu\text{-S})_2\text{AuL}\}_3\text{Cl}_2]^+$ (L = cycloaurated N,N-dimethylbenzylamine ligand), by thiourea desulfurisation", M.B. Dinger, W. Henderson, B.K. Nicholson and W.T. Robinson, *J. Organomet. Chem.*, 560 (1998) 169-181.
8. "Organogold(III) Metallacyclic Chemistry. Part 4. Gold(III) salicylate and thiosalicylate complexes", M.B. Dinger, W. Henderson, *J. Organomet. Chem.*, 560 (1998) 233-243.
9. "Synthesis and characterisation of the first auracyclobutane complex", M.B. Dinger, W. Henderson, *J. Organomet. Chem.*, 577 (1998) 219-222.